Technological solutions for steel-driven industrial symbiosis

Claudia Sergi, Matilde Breda

April 2026

Project funded by the Research Fund for Coal and Steel (RFCS)

G.A. 101156509

The information and views set out in this document do not necessarily reflect the official opinion of the European Commission. The European Commission does not guarantee the accuracy of the data included in this document. Neither the European Commission nor any person acting on the European Commission's behalf may be held responsible for the use which may be made of the information contained therein.

Table of content

Table of content 2

1. Introduction: Purpose and structure of the document 7
2. Steel sector EU driven initiatives which supported IS development: from ECSC to RFCS 8

2.1 ECSC 9

2.1.1 Economic advantages of integrated processing of steelworks EAF wastes, mainly containing Zn, Pb, Cd, FeO_x, Zn ferrite and others, with total recovery 9

2.1.2 The in-plant by-product melting (IPBM) process (1) 9

2.1.3 Improved cleaning of waste gases and recycling of BOF dusts (4) 15

2.1.4 Briquetting of self-reducing blending of waste iron oxide mixtures (8) 21

2.1.5 TREATDUST: Development of technologies for treatment of dusts and sludges containing zinc and lead to improve their recycle reuse (12) 23

2.1.6 High purity zinc and ferroalloys recovery from EAF dusts through a combined pyro-hydrometallurgical treatment (13) 30

2.1.7 Foaming of the slag and recycling of steel dusts by injection into the electric arc furnace for stainless steels (14) 31

2.1.8 Innovative use of iron and steel making by-products for the sealing and securing of steel industry deposits (16) 36

2.1.9 Characterization, modelling & validation of the impact of iron and steelmaking slags used in road construction on groundwater (17) 43

2.1.10 Efficient utilisation of waste products from secondary steelmaking as flux materials for electric arc furnace (18) 52

2.1.11 INQUISSS: In situ, quick sensing system for measurements of process-critical components in steelmaking slags (20) 59

2.1.12 Sustainable agriculture using blast furnace and steel slags as liming agents (21) 66

2.1.13 Alternative Processing of Sinter Plant Recycling Materials (22) 72

2.1.14 Hearth protection in BF operation by injection of TiO_2-materials (23) 77

2.2 RFCS 89

2.2.1 FULL-REC 2: Hydrometallurgical continuous treatment of ZnO enriched powders for metal zinc production (27) 89

2.2.2 SHOCOM: Short term CO_2 mitigation for steelmaking (28) 93

2.2.3 ACASOS: Alternate carbon sources for sintering of iron ore (29) 99

2.2.4 EPOSS: Energy and productivity optimised EAF stainless steel making by adjusted slag foaming and chemical energy supply (30) 106

2.2.5 URIOM: Upgrading and Utilisation of Residual Iron Oxide Materials for hot metal production (31) 110

2.2.6 FLEXINJECT: Flexible injection of alternative carbon material into the blast furnace (32) 117

2.2.7 GREENEAF: Sustainable Electric steel production (33) 123

2.2.8 SLASORB: Using slag as sorbent to remove phosphorus from wastewater (34) 130

2.2.9 INNOCARB: Innovative carbon products for substituting coke on BF operation (35) 137

2.2.10 OPTDESLAG: Increased yield and enhanced steel quality by improved de-slagging and slag conditioning (36) 144

2.2.11 PROTECT: Processes and technologies for environmentally friendly recovery and treatment of scrap (37) 149

2.2.12 SLAGFERTILISER: Impact of long-term application of blast furnace and steel slags as liming materials on soil fertility, crop yields and plant health (38) 153

2.2.13 REFFIPLANT: Efficient use of resources in steel plants through process integration (39) 160

2.2.14 SLACON: Control of slag quality for utilisation in the construction industry (40) 164

2.2.15 EIRES: Environmental impact evaluation and effective management of resources in the EAF steelmaking (41) 168

2.2.16 PSP-BOF: Removal of Phosphorous from BOF Slag (42) 172

2.2.17 ALTERAMA: Developing uses of alternative raw materials in cokemaking (43) 176

2.2.18 GREENEAF2: Biochar for a sustainable EAF steel production (44) 184

2.2.19 RIMFOAM: Recycling of industrial and municipal waste as slag foaming agent in EAF (45) 190

2.2.20 ACTISLAG: New Activation Routes for Early Strength Development of Granulated Blast Furnace Slag (46) 197

2.2.21 FINES2EAF: Cement-free brick production technology for the use of primary and secondary raw material fines in EAF steelmaking (56) 199

2.2.22 ECOSLAG: Eco-friendly steelmaking slag solidification with energy recovery to produce a high-quality slag product for a sustainable recycling (59) (60) 204

2.2.23 E-CO-Ladle Brick: Ecological and Economical waste management of the ladle refractory bricks by implementing circular economy criteria (62) 207

2.2.24 SLAGREUS: Reuse of slags from integrated steelmaking (64; 65) 209

2.2.25 TACOS: Towards A zero CO2 Sintering 213

2.2.26 iSlag: Optimising slag reuse and recycling in electric steelmaking at optimum metallurgical performance through on-line characterization devices and intelligent decision support system 217

2.2.27 OnlyPlastic: EAF working with polymers derived from plastic residue in substitution of fossil fuel (66) 221

2.2.28 BIOCODE: BIOmass for COkemaking DEcarbonization 228

2.2.29 BIORECAST: BIObased REsidues Conversion to Advanced fuels for sustainable STeel production 232

2.2.30 BIORESTEEL: Valorisation of wet biomass residues for sustainable steel production with efficient nutrient recycling 235

2.2.31 ZINCVAL: Valorisation of low zinc-containing residues 237

3. Further EU driven initiatives which fostered IS in the steel industry: 3rd to 6th FP and Horizon programs 240

3.1 FP3-FP4-FP5-FP6 240

3.1.1 FP3 - Recycling of zinc and lead containing dusts from the electric arc furnace (69) 240

3.1.2 FP4 - A new treatment process to recover magnetite, zinc and lead from iron and steel making dusts and sludges (70) 243

3.1.3 FP4 - Economical, technical and ecological utilisation of treated steel slag in civil engineering of high-quality demands (71) 244

3.1.4 FP5 - A new metallurgical route for the on-line conversion of by-products into valuable mineral and metallic products with a reduction of CO_2 emissions (72) 246

3.1.5 FP5 – REZIN: Elimination of zinc ferrite 250

3.1.6 FP6 – REDILP: Recycling of EAF dust by an integrated leach-grinding process 251

3.2 Horizon 2020 and Horizon Europe 256

3.2.1 FISSAC: Fostering industrial symbiosis for a sustainable resource intensive industry across the extended construction value chain (77) 256

3.2.2 RESLAG: Turning waste from steel industry into a valuable low-cost feedstock for energy intensive industry (78) 259

3.2.3 STEELANOL: Production of sustainable, advanced bio-ethANOL through an innovative gas-fermentation process using exhaust gases emitted in the STEEL industry (80) 263

3.2.4 CHROMIC: efficient mineral processing and Hydrometallurgical RecOvery of by-product Metals from low-grade metal containing secondary raw materials (81) 265

3.2.5 FRESME: From residual steel gases to methanol (89) 268

3.2.6 Recyclatrack: 100% recovery and RECYCLing of construction vehicle crAwler TRACKs into constituent rubber and steel for sustainable raw material supply (90) 272

3.2.7 Carbon4PUR: Turning industrial waste gases (mixed CO/CO2 streams) into intermediates for polyurethane plastics for rigid foams/building insulation and coatings (91) 273

3.2.8 TORERO: TORrefying wood with Ethanol as a Renewable Output: large-scale demonstration (92) 276

3.2.9 POLYINSPIRE: Demonstration of Innovative Technologies towards a more efficient and sustainable plastic recycling (93) 278

3.2.10 C2FUEL: Carbon Captured Fuel and Energy Carriers for an Intensified Steel Off-Gases based Electricity Generation in a Smarter Industrial Ecosystem (94) 280

3.2.11 RETROFEED: Implementation of a smart RETROfitting framework in the process industry towards its operation with variable, biobased and circular FEEDstock (96) 289

3.2.12 CORALIS: Creation Of new value chain Relations through novel Approaches facilitating Long-term Industrial Symbiosis (97) 292

3.2.13 INITIATE: Innovative industrial transformation of the steel and chemical industries of Europe (98) 295

3.2.14 REVaMP: Retrofitting Equipment for Efficient Use of Variable Feedstock in Metal Making Processes 299

3.2.15 H2STEEL: Green H2 and circular bio-coal from biowaste for cost-competitive sustainable Steel (99) 305

3.2.16 HEPHAESTUS: Heavy and Extractive industry wastes PHAsingout through ESG Tailings Upcycling Synergy (102) 312

3.2.17 RecHycle: Recycling renewable hydrogen for climate neutrality (103) 317

3.2.18 ReMFra: REcovering Metals and Mineral FRAction from steelmaking residues (104) 320

3.2.19 Carbon4Minerals: Transforming CO2 into added-value construction products (108) 326

3.2.20 GreenHeatEAF: Gradual integration of REnewable non-fossil ENergy sources and modular HEATing technologies in EAF for progressive CO_2 decrease (109) 328

3.2.21 FlexoFibers: Unlocking the potential of second life steel fibers from tire waste for the construction industry (110) 334

3.2.22 RESURGENCE: Industrial Water Circularity: Reuse, Resource Recovery and Energy Efficiency for Greener Digitized EU Processes (112) 335

3.2.23 Dust2Value: Pioneering Sustainable Recovery in Steelmaking: Hydrogen-Based Technology for Byproduct Management (113) 337

3.2.24 H2PlasmaRed: Hydrogen Plasma Reduction for Steelmaking and Circular Economy (115) 341

3.2.25 HURRICANE: Sector-coupling hub for circular use of thermal and industrial waste (116) 343

3.2.26 ZHYRON: Valorisation of iron-rich & Zinc-containing steelmaking by-products via HYdrogen-based ReductiON (117) 344
4. Other funded projects which assessed IS in the steel industry 346
4.1 C-CED: Carbon Cycle Economy Demonstration 346
4.2 USS2030: Underground Sun.Storage 2030 350
4.3 OSMET 3.0: Utilization of organic sludge in metal industry 353
4.4 CESAREF: Concerted European action on Sustainable Applications of REFractories (121) 358
4.5 ZEUS: Zero emissions through sector coupling 375
5. Main takeaways of actual IS scenarios and technologies 378
5.1 Upstream solutions 378
5.1.1 Secondary Carbon Carriers (SCCs) 378
5.1.2 Scrap 386
5.2 Downstream solutions 388
5.2.1 Slag 388
5.2.2 Dust 397
5.2.3 Sludge and Mill Scale 405
5.2.4 Off gas 407
5.2.5 Refractories 410
5.2.6 Others 413
List of Figures 415
List of Tables 418
List of acronyms and abbreviations 420
References 427

1. Introduction: Purpose and structure of the document

The present Deliverable D3.4 "Technological solutions for steel-driven industrial symbiosis" was generated in the framework of Task 3.2 "Technology screening for cross-sectorial replicability" of WP3 "Impact assessment" which is dedicated to the identification and monitoring of all relevant activities that the European Union (EU) steel sector is embracing to foster industrial symbiosis. Task 3.2 was designed with the primary goal of identifying and analyzing the technologies available in the framework of steel-driven industrial symbiosis and which may potentially enable a cross-sectorial replicability of best practices developed. In particular, the main idea was to provide a wide portfolio of technologies and technical solutions developed by the steel sector in collaboration with other relevant industrial sectors, e.g., construction and buildings, agriculture, and chemical, to support the implementation and development of new industrial symbiosis scenario on the EU area.

This goal was achieved by identifying and selecting the main national and EU-driven projects focused on steel industry decarbonization through circular economy and Industrial Symbiosis (IS) approaches and summarizing the main technical results and outcomes in the present deliverable. A total of 82 EU-driven projects among European Coal and Steel Community (ECSC), Research Fund for Coal and Steel (RFCS), Framework Program (FP), Horizon 2020, Horizon Europe and Klima und Energiefonds projects were selected and revised. In particular, 14 ECSC projects, 31 RFCS projects, 6 FP projects, 26 Horizon Europe and Horizon 2020, 3 Klima und Energiefonds and 1 Marie Skłodowska-Curie Actions (MSCA) were identified as suitable and significant to the final goal.

The present document was divided into four sections. Sections 2, 3 and 4 are dedicated to an in-depth analysis of the main technical and technological solutions investigated and developed in each project. In particular, section 2 is dedicated to ECSC and RFCS projects, section 3 to Framework Program and Horizon projects and section 4 to all other funding schemes. Finally, section 5 is going to provide an overview with the main takeaways for both steelmaking upstream and downstream material flows, involved in IS scenarios.

2. Steel sector EU driven initiatives which supported IS development: from ECSC to RFCS

On the 18th of April1951, six countries, i.e., France, Germany, Belgium, Italy, Luxembourg and Netherlands, signed the Treaty of Paris and founded the ECSC. The main idea behind this treaty was to establish a peaceful relation between the countries, based on common interests and political integration. This revolutionary treaty expired in 2002, but it set the basis for the Treaty of Rome and Maastricht which strengthened the institutional structure of the European Union (EU). Because of ECSC expiration, the RFCS was established in 2003 to continue supporting research in the coal and steel sectors and keep the related industry competitive and sustainable.

The policy instruments which guide RFCS are the EU Green Deal and Just Transition which aims to transform the EU into a resource-efficient and competitive economy ensuring no net emissions of greenhouse gases by 2050, the Circular Economy Action Plan which sets product sustainability principles to guide broader policy and legislative developments, Fit for 55 which targets the reduction of net greenhouse gas (GHG) emissions by at least 55 % by 2030, and RePowerEU which expects that around 30 % of EU primary steel production will be decarbonized with renewable hydrogen by 2030.

These new policy objectives were used to set up the new RFCS legal base to support breakthrough technologies. New, sustainable and low-carbon steel making and finishing products, and conservation of resources, protection of the environment and Circular Economy (CE) can be identified as cornerstones of the new research objectives of the RFCS program. Considering these guidelines, IS appears to be a powerful pathway. In light of this, many ECSC and RFCS projects were funded to develop this solution in the steelmaking sector.

2.1 ECSC

2.1.1 Economic advantages of integrated processing of steelworks EAF wastes, mainly containing Zn, Pb, Cd, FeO_x, Zn ferrite and others, with total recovery

The project was coordinated by Ferriere Nord and started on the 1st of July 1995, lasting almost three years until the 31st of December 1998. The overall project cost 1 M€ and the EU contributed almost 40 % with 400 k€.

This ECSC project was the first one to deal with CE and IS principles aiming to determine the optimum conditions for the total recycling of Electric Arc Furnace (EAF) dust through hydrometallurgical extraction by measuring the economic value of each element. The hydrometallurgical extraction system allowed separating the Fe, Zn, Pb oxides contained in the flue dust coming from EAF collecting almost pure metallic Zn at the cathode and separating lead and heavy metals in the form of cement. Beyond the extraction, separation and reclaiming of non-ferrous metals which can be conveniently readdressed to the non-ferrous alloy manufacturing sector in an IS perspective, ferrous residues were also obtained. The latter were conveniently recycled and reused in EAF to recover iron after being dried, mixed with reductants and converted into pellets. Experimental trials in EAF demonstrated the feasibility of this solution since no process or product anomalies were remarked thus ensuring also an internal exploitation of the wastes in a CE perspective.

2.1.2 The in-plant by-product melting (IPBM) process (1)

The project was coordinated by MEFOS (Foundation for Metallurgical Research) with CRM (Centre de Recherches Metallurgiques), CSM (Centro Sviluppo Materiali) and FEhS (Forschungsgemainschaft Eisenhuttenschlacken) participating as partners in the consortium. The project started on the 1st of July 1996 and lasted almost two years, ending on the 30th of June 1998. The overall project cost 1.78 M€ and the EU contributed 890.25 k€, i.e., half of the budget.

The main aim of the project was the development of a flexible process decoupled from the main metallurgical line to valorize steel industry by-products, e.g., slag, dust, and mill scale, with a view to achieve a zero-waste policy in the plant. EAF and Basic Oxygen Furnace (BOF) slags were mainly exploited as construction aggregates, but they had to deal with an increasing competition with other secondary materials proposed to the construction market and with the technical limitations resulting from the leaching of heavy metals and critical elements, e.g., Cr, V, Ni. Dust was an iron-rich residue attractive for internal recycling, but the main limitation to this approach was given by the presence of Zn. In light of this, different technologies were proposed for the treatment of this Zn-rich dust, but these processes were mainly oriented to Zn recovery and were less suitable for dust with low Zn-contents. Finally, another mineral by-product which was poor in valuable components and could hardly find internal or external utilization were refractory linings. The latter were in some cases considered as noxious due to Cr^{6+} presence and were often landfilled with high costs and environmental impact. In light of this, the present project evaluated two processing variants which were slag reduction to produce mineral products and hot metal, and vitrification to exploit the molten steel slag as

neutralization mass for noxious waste. Both processes were developed by using a smelting vessel to ensure the total transformation of steel slags and in plant by-products into added-value products. The process was required to be flexible to ensure the feasibility of both processing variants, must ensure the treatment of large amounts of slag in a continuous or semi-continuous mode and it was expected to ensure the treatment of all internal wastes/by-products, e.g., dust, mill scale, noxious spent refractories, etc. To this aim, the most suitable reactor identified was a Direct Current (DC) furnace with a hollow electrode which ensured the simultaneous treatment of slags and fine-grained products which were charged through the hollow electrode passing through the DC-plasma to be efficiently treated.

Project activities were divided among the partners following the two different treatment lines. In particular, MEFOS, CRM and FEhS focused on BOF-slags reduction while CSM dealt with by-products vitrification. CRM and FEhS provided basic experimental data and a mass-balance model for the design of the pilot scale trial performed at MEFOS targeting different degree of slag reduction. MEFOS investigated the technical feasibility and flexibility of the process at a pilot scale using a 3 MW DC furnace with a hollow electrode and provided process parameters optimization to ensure the total transformation of steel slags and other in plant by-products into added-value products. CSM developed a treatment process for the neutralization of wastes such as spent noxious refractory by using liquid steel slags with in-plant Zn containing dust and sludges to obtain inert products for glass and ceramic industries.

Focusing on the first development line, i.e., slag reduction, the by-products selected to be treated in the three pilot scale experimental campaigns were BOF-slag with high V content, BOF-slag with low V and MgO content and high P_2O_5 content, scrap residue from transportation and handling, BOF and Blast Furnace (BF) dust/sludge, EAF-dust from carbon and stainless steelmaking, mill scale, Fayalite slag from Cu smelter. Other supplementing materials used were iron-rich bauxite, sand and magnetite ore and reductants such as coke breeze, anthracite and petroleum coke.

Pre-investigations were carried out at the laboratory scale to perform the large-scale pilot plant test in the most efficient way. The measurement of slag viscosity was quite expensive, therefore FEhS developed a computer model based on Riboud (2) and Urbain (3) ones which exploited the Weymann equation whose constants accounted for temperature dependence and were calculated according to the basicity CaO/SiO_2 of the investigated materials. FEhS model was based on the $CaO\text{-}Al_2O_3\text{-}SiO_2$ system and model parameters were calculated by dividing the slag constituents into three categories, i.e., glass formers (SiO_2 and P_2O_5), amphoteric compounds (Al_2O_3, Fe_2O_3), and modifiers (CaO, MgO, Na_2O, CaF_2, FeO, MnO). The model was validated by measuring the experimental viscosity of the samples taken from the MEFOS campaigns and CRM tests. The results highlighted that viscosity was highly influenced by CaF_2 content which was able to decrease the melting range by 40 and 80 °C when added at 0.3 and 0.6 wt.%, respectively. On the contrary, CaO addition determined an increase in the melting range and in liquid slag viscosity. The results also reported that a decrease in the Fe content in the slag resulting from a better reduction process was responsible for an increase in slag viscosity. This effect must be compensated by the addition of a slag modifier, e.g., Al_2O_3, since the reduction reactions required a sufficient liquid slag to be optimized. The results also proved that it was almost

impossible to produce a cement clinker material starting from BOF-slag in a DC-furnace due to the high melting point of such materials and their high viscosity.

Preliminary reduction tests were also performed at CRM laboratory to study the reduction of the V_2O_5 contained in V-rich BOF slag and to investigate the properties of the resulting slag product which is a hydraulic binder. The results highlighted an increase in Fe and V recovery for increasing operating time, while no significant differences were observed when using coke and anthracite as reducing agent. Concerning slag products, their hydraulic properties were evaluated and compared with the one of the most common European granulated BF slags. A higher MgO, MnO and V_2O_5 content was detected, and the effect of cooling rate was investigated considering that hydraulic binder efficiency depends not only on the chemical composition but also by the content of the amorphous structure.

Moving to the pilot scale, a 3 MW DC furnace was used at MEFOS for the trial. This furnace with a hollow electrode was selected because it ensured the instantaneous melting of the charged materials and the occurrence of the chemical reactions within the plasma. This guaranteed that the reduction degree of oxides could be easily controlled by stoichiometric addition of the reducing agent thus minimizing gas volumes and dust amounts. The DC furnace also ensured a satisfying stirring of the metal bath while preventing the one of the slags thus safeguarding the refractories. The DC furnace was equipped with MEFARC, i.e., a dynamic process control system for EAF operations developed by MEFOS, for an on-line control of the process to produce heat and mass balances necessary for operation and later evaluation. A hydraulic sampling system was installed to collect slag and metal samples during the operations every 20-30 minutes. Bag-house filters were used to collect dust samples to estimate their amount and chemical composition. Three pilot campaigns were performed.

The main objective of the first pilot campaign was to test process considering different factors such as the feeding techniques, the feeding materials (slags and slag modifiers) and processability. The valuable products expected to be obtained were raw materials for cement clinker, hydraulic binders, metallurgical powder, reduced BOF-slag without addition for recycling back to BOF. The material used for the test are V-rich BOF-slag, i.e., 5 wt.% V_2O_5, as base slag material and coke breeze as reductant. Different slag formers were also used throughout the different tests, e.g., Fe-rich bauxite, fayalite from a Cu smelter and CaF_2. The experimental campaign demonstrated that it was quite easy to prepare mineral products with the desired chemical composition through smelting reduction of the BOF-slag by modifying the initial slag with oxides such as Al_2O_3 and SiO_2, but some major concerns arouse when it came to the physical properties of the reduced slag which proved to be very viscous. Further results showed that the control of FeO reduction degree was quite easy with FeO content being reduced to less than 2 %. More complex was the reduction of MnO and V_2O_5 with coke being apparently inefficient. Finally, all carbothermal reductions were coherently favored by high process temperatures.

The second pilot campaign aimed at identifying an efficient reducing agent to increase V recovery yield, i.e., >80 %, and the productivity in the furnace. High V-rich BOF slag were used as base material while coke, anthracite and pet-coke were tested as reducing agents and sand was used as only slag former. The effect of other process parameters such as gas stirring and slag size was also addressed. The results proved that anthracite is the most effective reductant ensuring a V recovery >80 %. Good results were also obtained with pet-coke which in turn was much more expensive. Gas stirring proved to be almost

ineffective since most of the reduction process occurred in the plasma region. Concerning the effect of slag size, most of the BOF-slag remained unreacted and floated on the slag surface when characterized by a coarse dimension. The floating was responsible for a progressive gathering of the unreacted slag towards the furnace wall and tapping hole. Therefore, it was concluded that DC-furnace was not suitable for melting of coarse material.

Finally, the last pilot campaign aimed to produce different slag products, e.g., clinker material, metallurgical powder and hydraulic binder, using normal, i.e., low vanadium, BOF-slag as base material. EAF-dusts from both carbon and stainless-steel mills, a mixture of BOF and BF-dust, and mill scale from an integrated steel plant were also treated. The results highlighted again that FeO and P_2O_5 reduction by anthracite was quite easy with residual FeO content <1 % and P_2O_5 content <0.2 %. Concerning the recovery of scrap residues, no significant problems were observed thus demonstrating that IPBM is an excellent solution for the destruction of this hazardous waste. Analogously, no specific problems were observed for the treatment of mixture of mill scale, BOF and BF-dust with over 95 % of the Fe recovered and a Zn-content in the slag <0.02 %. Concerning EAF-dust from stainless steelmaking, Cr-content in the treated dust was well reduced leading to a recovery of 94 % and a Ni recovery of 100 %.

In all campaigns, the amount of dust after each charge was weighed and the chemical composition analyzed. It was observed that dust amount was 1-5 % of the total fed and about half of it was caused by the evaporation of Mn, Mg, Zn, Pb and alkaline, while the rest was carry-over material. Concerning the effect of temperature, it was noticed that the evaporation rate of Mg and Mn increased rapidly when the temperature was higher than 1750 °C, but it did not seem to influence the evaporation of alkaline such as Na_2O and K_2O. In conclusion, the pilot trials allowed to conclude that the IPBM process was an excellent solution to treat fine grained by-products generated within steel plants including steel slags, EAF-dust from both carbon- and stainless steelmaking, BOF and BF-dust and mill scale from an integrated steel plant ensuring a recovery of Zn >99 %, of Cr >95 %, of Ni=100%, of Fe >95 % and of V almost 80 %. The process proved to be excellent also for slag products modification ensuring the achievement of the target products, such as raw material for metallurgical powder, glassy hydraulic binder, etc.

The quality of the materials obtained was also investigated. Slags were not as cement clinker material if their content of heavy metals remained high even after reduction. Indeed, Cr content in cement must be Cr^{6+} < 2 ppm while Cr^{6+} in the slag could reach values up to 1400-2500 ppm. If the heavy metals issue could be fixed, then it must be considered that cement was able to retain its strength and stability as a consequence of the hydration reactions resulting from mixing with water and hydraulic hardening was primarily due to the hydration of calcium silicates, but other chemical compounds, e.g., aluminates, may also participate in the hardening process. The sum of the proportions of reactive CaO and reactive SiO_2 must be at least 50 wt.%. For example, Portland cement clinker is a hydraulic material which consists of at least 2/3 by weight of calcium silicates and for the remaining part of Al_2O_3, Fe_2O_3 and other compounds with MgO not exceeding 5 wt.%. Considering all these aspects, the slag resulting from the last pilot campaign, which was characterized by Larnite, e.g., Ca_2SiO_4, as main mineralogical phase, could be conveniently exploited as cement clinker material but only after being mixed with

limestone (~70 %) and clay rock (~20 %). The low amount of slag used in the mix must be ascribed to the high Fe and Mn content. The mix obtained was burnt at 1460 °C for 2 hours and the mechanical and physical properties of the cement resulting from this mix, e.g., compressive and tensile strength, dynamic modules of elasticity, water demand, setting time, were evaluated and compared with the ones of ordinary Portland cement. All limiting values regarding the different requirements were met therefore a clinker cement material could be prepared starting from partial reduction of low vanadium BOF-slags.

Moving to the hydraulic binder application, when cement companies receive the granulated BF-slag, they control the chemical composition to be sure that FeO and MnO contents are sufficiently low, the hydraulic index which must be <1.65 and the glassy structure which must be higher than 95 %. The hydraulic binders obtained from IPBM in the present project satisfied all these requirements thanks to the rapid cooling obtained with the granulation device developed at FEhS which ensured the achievement of the required amount of glassy structure.

The metallurgical powders produced with the IPBM process were able to satisfy the three main requirements as desulfurizer, i.e., a correct chemical composition to ensure a high basicity and an Al_2O_3 content > 20, an autogenous disintegration resulting from the transformation of C_2S from ß to y phase which allows to remove crushing operations, and a high desulfurization capacity comparable with the one of synthetic slags in the market. The metallurgical powders produced were characterized by two compositions, one with an Al_2O_3 content between 20-25 % and the other one in the range of 25-30 %. This choice was a compromise to limit the addition of bauxite, which was not a by-product, to remove the crushing operation by keeping some dicalcium silicate and to produce a quick melting powder characterized by a low viscosity to keep a high potential for Al_2O_3 inclusions dissolution and for steel desulfurization.

Finally, the hot metal produced could not be recycled back to the main steel production line due to the high P content, i.e., ~2 % P_2O_5, unless it was conveniently lowered, but it could be exploited as cast iron for water pipe applications. The corrosion resistance of the proposed material was assessed by exposing the specimens to a 100-hour water-saturated and salty atmosphere and the results were compared with the one of a reference cast iron used for water distribution pipes displaying comparable results. From the mechanical performance perspective, the high P-content allowed to achieve a high tensile strength while endowing the material with a high brittleness which, however, was not considered as a negative factor for the proposed application.

Moving to the second treatment line, i.e., slag vitrification, the objective of the research program performed by CSM was the development of a process to vitrify wastes such as spent refractory, Zn containing dust and sludge, by using steel slags. This treatment would convert these wastes containing dangerous matters into inert products marketable for glass and ceramic industries. In particular, the glass produced should be a rigid and homogeneous amorphous mixture principally consisting of SiO_2 and at least two bases such as alkaline oxides and alkaline earth oxides or heavy metal oxides. It should display high resistance to water, chemical and atmospheric agents together with low thermal and electric conductivity. The materials investigated were steelmaking slag from EAF stainless steel

production, EAF dusts, BF sludges, silicon-alumina refractory containing Cr^{+6}, BOF slag, sinter plant dusts and mill scales.

Some preliminary laboratory tests were performed to ensure an adequate FeO removal by reducing the BOF slag and BF-sludge mixtures with char and Al. This also ensured the achievement of a white material for uncolored glass. The results reported a complete reduction of FeO, MnO and V_2O_5 with a clear separation of a metallic phase. Unfortunately, high ZnO losses were also observed, and this was extremely undesired since it was one of the compounds to entrap. In light of this, the best thermodynamic parameters to perform the inertization process needed to be identified to ensure a correct entrapment of Pb and Zn. It was discovered that a good Zn and Pb entrapment in a glassy matrix could be achieved working without reducing agents which caused ZnO reduction thus leading to a metal phase which volatilized at 911 °C. Moreover, it was necessary to work with temperatures lower than 1516 °C which was PbO boiling point.

The melting tests performed at the laboratory scale in a small induction furnace to obtain the inert products were carried out with 4 different mixtures: BF sludge 25 wt.%, 34 wt.%, 43 wt.% and 37.5 wt.%, steel slag 25 wt.%, 16 wt.%, 14 wt.% and 12.5 wt.%, refractories 50 wt.%, 50 wt.%, 43 wt.% and 50 wt.%, respectively. These mixtures were selected because their compositions allowed to obtain Tridymite or Wollastonite phases which were characterized by the lowest melting temperatures, i.e., <1400 °C. An insufficient presence of free silica proved to be responsible for the lasting presence of free lime in the product and for high Pb and Zn losses therefore the amount of silica was increased to avoid these problems by adding rejected glass coming from municipal solid wastes. A similar inertization campaign was carried out at the pilot scale on mixture number 3, i.e., BF sludge 43 wt.%, steel slag 14 wt.% and refractories 43 wt.%, characterized by a higher BF sludge content and therefore a higher Zn and Pb content. The initial batch was slightly modified by increasing the PbO and ZnO content to 5 % and part of the refractory material was substituted with waste glass to increase the silica content. This choice allowed to decrease considerably the free CaO-content as well as PbO and ZnO losses, i.e., PbO from 73 to 40 % and ZnO from 52 to 21%. The process was also optimized to further reduce Pb and Zn losses by introducing a preheating at 1000 °C for 2 hours to aid mixture softening and facilitate the formation of Zn and Pb silicates before reaching high temperatures.

The effect of cooling conditions was also investigated by performing both water- and air-cooling tests to verify the need for fast cooling conditions to obtain a glassy product. The leaching tests highlighted that Italian law limits were respected and that inertization of toxic-noxious metals was achieved in both cases while X-ray Diffraction (XRD) analysis highlighted a higher amorphous content of 80-90 % for the water-cooled product against the 65-75 % observed for the air-cooled one. Both structures also highlighted the presence of magnetite crystals while the air-cooled product also showed a second crystalline phase, i.e., anorthite, resulting from the slower cooling. Concerning element distribution, Zn was distributed between both crystalline and amorphous phases even if it prevailed in the crystalline structure of magnetite, Pb was exclusively entrapped and inertized in the amorphous matrix and Cr was only present in the crystalline phase. Considering the results obtained, water cooling was selected as the best cooling solution.

The optimized process was further extended to two other types of steelmaking wastes, i.e., sinter plant dusts and slag and dust from electric steelmaking. For sinter plant dust the mixture used was silicon- alumina refractory containing Cr (VI) 23 wt.%, sinter plant dust 33 wt.%, BOF slag 17 wt.% and Cullet (silica) 27 wt.%, while for electric steelwork wastes the mixture used was high SiO_2 refractory 20 wt.%, EAF dust 20 wt.% and EAF slag from stainless steel production 60 wt.%. The results for both mixtures proved that inertization of toxic-noxious metals was successful.

Concerning the costs of the vitrification route, they turned out to be high in Italy due to the high costs of electricity, i.e., almost 2/3 of operating costs, while they were significantly more competitive falling to half of the value in the Scandinavian countries thanks to the lower cost of electricity which accounted for only 1/3.

2.1.3 Improved cleaning of waste gases and recycling of BOF dusts (4)

The project was coordinated by Corus UK, i.e., former British Steel, with Corus NL, i.e., former Hoogovens, and RWTH (Rheinisch-Westfälische Technische Hochschule Aachen) as consortium partners. The project started the 1st of July 1996 and lasted more than three years, ending on the 31st of December 1999. The overall project cost 1.64 M€ and the EU provided half of the financing with 821 k€.

The project aimed to exploit the results obtained in previous research works, e.g., ECSC projects, which demonstrated that X-ray fluorescence (XRF) can be used for the continuous on-line monitoring of Fe and Zn content in the dust generated during BOF operation. In particular, the project wanted to make a step forward using the obtained data to improve the effectiveness of the waste gas cleaning system by identifying operational changes which could allow a reduction in the dust load. A further objective was the continuous monitoring of Zn levels in waste gas to investigate slurry diversion and ensure the correct separation of streams containing high and low Zn content. This would maximize the recycling potential of low-zinc slurry solids to the sinter plant. Indeed, the continuous and real time use of XRF to monitor Zn levels in BOF waste gas would provide a system to signal the optimum time to divert the Zn-rich slurry stream to minimize the landfill disposal. Going more into detail, the project pursued the following goals: reducing vessel fume losses by using XRF for cold end operation to improve cleaning, establishing the effect of recycling Zn-rich slurry via briquettes, and investigating the effect of top charging additions.

The activity connected with the reduction of vessel fume losses was undertaken by Corus UK and Corus Ijmuiden. In particular, Corus UK installed a XRF at Teesside plant which demonstrated excellent signal stability and provided an accurate measurement of the Fe emissions from the converter. The data collected was used to set up various trials to reduce Fe emissions via the systematic alteration of key steelmaking parameters. The results highlighted that the largest Fe losses occurred during the initial stages of the blow process while lower Fe losses were achieved for higher Si levels in the hot metal thus indicating that slag volume played a major role with a good slag coverage acting as a filter for fume particles generated from the bath. In particular, the trials conducted adding Si-rich sandstone reported a reduction of almost 10 % in fume losses, but in the longer term this

practice may result in increased refractory wear. In light of this, alternative methods for early slag generation were considered by substituting sandstone with recycled basic oxygen steel (BOS) slag. Trials with 2 tonne of fragmented recycled BOS slag with a size fraction of 10-30 mm as input were carried out charging the converter directly on top of the hot metal. This procedure allowed to reduce by 1 and 0.42 tonne the in-blow lime and dolomite additions without introducing any detrimental effects on refining, i.e., no differences in the end blow P, thus making the practice financially attractive with direct benefits from slag recycling. Moreover, BOS slag recycling exerted also a favorable effect on converter Fe losses increasing process yield with further financial benefits. In particular, a reduction of 11 % in Fe losses in the fume was identified switching from the standard practice to the recycled slag practice. The latter also led to an increase of 1.9 % in FeO level in the slag due to the reclamation of iron units from the recycled slag. All in all, a 0.2 % increase in yield was observed. It was concluded that the use of recycled BOS slag allowed a significant cost saving of £43 per heat thanks to a reduction in lime and dolomite consumption, but also to the avoidance of landfill tax. It was also found out that when slag experiences drying at mid-way of the blow, this resulted in an increase in Fe loss rate. The modification of lance height profiles and the increase of slag fluidity via the fluxing of small amounts of recycled BOS slag were two possible strategies to overcome this issue.

Similar trials were performed by Corus Ijmuiden which installed an energy dispersive X-ray spectrometry system (EDXS) in the plant at Hoogovens. Even these trials highlighted that an early formation of a fluid slag tends to reduce fume loss and to influence droplet formation behavior. The recycling of BOS slag with a size fraction of 25-80 mm reported a reduction in Fe losses between 4 and 15% depending on the level of Si in the hot metal. The effect of the weight of the recycled slag added was investigated and proved to be remarkable. Therefore, it would be an advantage to make the slag addition conditional on the hot metal Si level. Further efforts were made in the practical BOF trials to control foam and emulsion formation early in the process. It was found out that a lower basicity of the slag, a late ore addition and a lance pattern modification to a faster slope in the start of the process allowed to reduce significantly dry slag formation in the middle part of the blowing process.

The second goal of the project was to study the impact of lower levels of vessel particulate emissions on primary gas cleaning efficiency and to reach this goal, a form of dynamic stack particulate monitoring was required. In light of this, the potential use of XRF device already developed for monitoring vessel fume losses (hot end XRF) was also investigated for stack particulate monitoring (cold end XRF) by Corus UK. In this case, different XRF system demands were identified due to the much lower levels of fumes encountered after gas cleaning, i.e., 103 times lower in concentration, and to gas saturation with water resulting from the wet gas cleaning systems. At first, a feasibility study was carried out at the Corus Port Talbot BOS plant using an equipment like the one used in the previous work for vessel emissions. The analyzer was set up to measure only the Fe channel since it was a fair representation of the total material discharged to atmosphere based on the previous analysis performed on the dust sampled from the stack. Indeed, they showed that 70 % of the material passing through the waste gas cleaning plant was Fe. The work confirmed the ability of the XRF system to detect the Fe levels in the waste gas stacks after cleaning, but the liquid nitrogen cooled semi-conductor detector used was considered inappropriate for the cold end application due to the level of sophistication and the relatively high cost. In light of this and considering the need to measure only one element, i.e., Fe, a

proportional detector was considered as a suitable alternative and a subsequent trial at Scunthorpe was planned to test the new equipment, i.e., an argon filled sealed proportional counter X-ray detector. The latter proved to be fully capable of detecting the varying dust loading in the off-gas stack, but alternative filling gases were also investigated to improve detector sensitivity to iron and xenon became the preferred choice. Extensive laboratory work was carried out to optimize the system for Fe determination at low concentrations and completed this phase the modified XRF device was used on plant to monitor actual BOS primary gas cleaning plant performance and assess the practical application of XRF for monitoring fume levels which could be installed anywhere after the plant demister unit. Some preliminary plant tests were carried out using the cold end XRF device to monitor gas cleaning plant operation, but despite examining several BOS heats the results were inconclusive and some attempts were made to optimize the XRF equipment.

The activity was further developed at the Llanwer BOS plant with data monitoring the fume levels collected from both the hot end and the cold end XRF device. This was the first time that information indicating dynamic fume concentrations from both XRF systems was generated for BOS heats. This analysis disclosed some interesting outcomes on plant operation because the XRF device was able to identify and respond to abnormal operating conditions. For example, the hood pressure control loop became unstable during one of the BOS trials for part of the blow thus causing short term fluctuations in the waste gas flow and in the pressure drop across the main Bischoff scrubbing unit. This led to untypical short-term increase in the XRF counts resulting from the instability in the scrubber operation as proved by the signal registered between minutes 8 and 11 in graph A of Figure 1. In another trial, a sharp increase in XRF signal was registered at the end of the blow again due to a short-term loss of scrubber pressure drops resulting from an increased gas flows following vessel iron ore coolant addition. This resulted in a short-term increase in vessel emissions as shown in graph B of Figure 1from minute 12 to minute 13 minutes for the hot end XRF trace, the cold end XRF traces and the main scrubber pressure drop. These experiences proved that the cold end XRF device could be exploited to identify any scrubber dysfunctionality such as a healthy pressure drop but a poor water distribution which is responsible for a reduced cleaning capability.

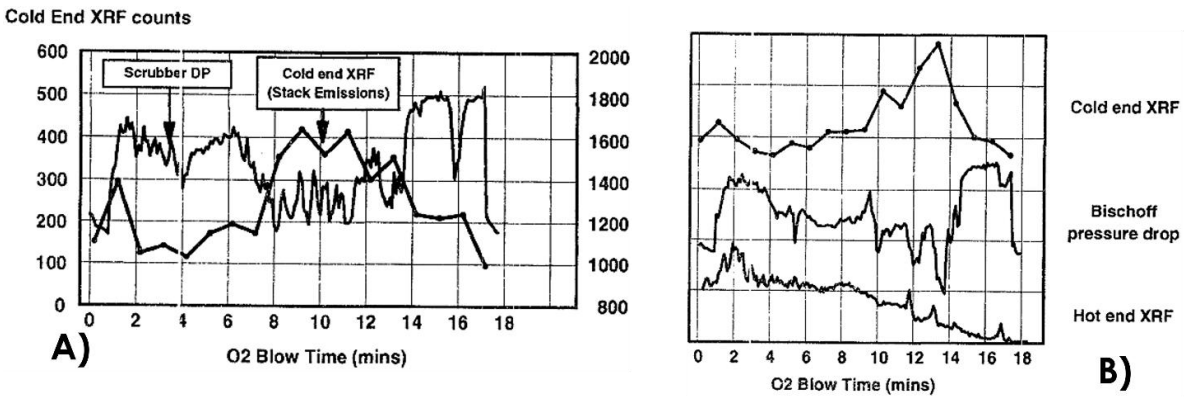

Figure 1: Hot end and cold end XRF traces, and scrubber pressure drops for two particular trials performed at Llanwern plant.

Some trials were also performed during the addition of briquettes in the vessel which further confirmed the strong relationship between the cold end XRF counts for Fe and the differential pressure across the Bischoff scrubber while no relationship was found between the gas cleaning efficiency of the system and ZnO recovery. Despite this, variation in Zn addition to the vessel resulting from low and high zinc level in the briquettes were clearly detectable in the cold end XRF signal. In particular, the absolute average count level for Zn was not significant but the relative level for the high Zn briquette heats was greater than that for the low Zn cases. This clearly indicated that for a given Bischoff pressure drop, there was more Zn passing to the stack for the higher Zn content briquettes which resulted in an increased concentration of fine Zn containing particles. In light of this, XRF could act as useful process control tool for monitoring vessel emissions and composition and in developing an effective slurry diversion route.

Further trials were conducted at Teesside Steelmaking site locating the cold end XRF device after the demister. Again, the preliminary plant trials indicated that the XRF device was able to monitor dynamically the current levels of fume encountered after the BOS primary gas cleaning plants and to register fault conditions and short-term fluctuations in gas cleaning efficiency.

A new X-ray detector system was acquired for assessment, i.e., a solid-state Si-PIN photodiode which did not require liquid nitrogen coolant since it had an integral thermoelectric cooler. Moreover, it was able to ensure an improved signal to background ratio thus ensuring an improved sensitivity and accuracy. This system was used to monitor the concentration of fume in the gas cleaning duct during a trial which involved comparing recycling of BOS slag with normal operation. The results indicated again that there is a higher concentration of fume at the start of all blows when the skirt was raised for the full combustion phase while a relatively stable period of operation followed for the rest of the blow. According to all the results obtained from the different trials, it was concluded that the use of XRF technique for monitoring cold end of the gas cleaning plants allowed to detect plant fault conditions which led to excessive atmospheric emissions, but it was not suitable for plant performance optimization at the design cleaning levels due to an insufficient sensitivity of the system.

The third goal of the project was the recycling of Zn-rich slurry by investigating operating practices which involved the addition of slurry briquettes to the vessel. In this perspective, a trial with a total amount of 45 tonnes of Zn containing briquettes was carried out by Corus UK at British Steel Llanwer by adding the briquettes in small batches of 3-5 tonnes over several heats. The briquetted material was a mix of EAF dust and mill scale to achieve the desired Zn contents. The first trial consisted of briquettes with a Zn content of 4.5 % while the second trial used briquettes with 11.8 % of Zn. Burnt lime was used to dry the material before briquetting and to provide a component of the binder. XRF was used to monitor vessel fume losses and fume levels after the gas cleaning plant. The results highlighted a good trend between the ZnO added to the BOS in the briquettes and the weight of ZnO collected in the slurry samples taken from the gas cleaning plant which also allowed for calibration of the hot end XRF system. The trial proved that from a practical perspective, it was better to divert Zn-rich slurry early in the blow even if the diversion duration was longer because the Zn derived from scrap additions would be missed if diversion occurred late in the blow. Moreover, it was observed that there were less problems in achieving a smooth steel refining and an optimized gas recovery if the

addition of Zn containing briquettes was made pre-blow or very early in the blow with the bulk flux additions because the addition of any oxygen containing materials in the middle or late blow affected adversely the control of the gas collection and of the gas cleaning system thus leading to slag foaming issues. The trial also indicated that XRF equipment could be used as useful process control tool for monitoring vessel emissions and composition to develop an effective slurry diversion route.

Considering the interest in achieving an effective recycling of Zn-rich slurry, it was necessary to establish an optimum agglomeration procedure for BOS slurry both through briquetting and extrusion to form a suitable feed stock. Various types of binders and different contents of binder and water were investigated. Considering the huge variability in the moisture content of BOS slurry and the need for strict control of moisture, the slurry was dried before agglomeration to provide consistent feed material. Briquettes were produced with a briquetting press, and their green strength was evaluated through crushing strength tests. The briquette mixes of the best quality were used as base for the extrusion process. The pre-drying step was not necessary for extrusion because higher moisture contents were a pre-requisite to ensure material extrudability. Indeed, a mix that was too dry for the extruder was generally too moist for briquetting and vice versa. In particular, an excessively dried mixture tends to block the rollers in the extruder. For extrusion, it was also found that an increase in the proportion of ordinary Portland cement was required to ensure sufficient green and subsequent strength. For both extrudes and briquettes, the resulting material must be left to air dry to allow the cement or lime to combine with the water, therefore the products were left for two weeks to allow for curing and hardening before handling. In the initial part of the study, crush strength was used to compare the performance of the different briquettes produced and to identify the more suitable mixes, but this technique was unsuitable for extrudes and tumble tests were identified as a suitable alternative. Samples of 15 kg were tumbled in a standard tumble drum for 200 revolutions, and the resulting material was passed over a 6.3 mm screen. The weight % greater than 6.3 mm was recorded as the tumble index. The results established that both extrusion and briquetting were useful techniques for agglomerating BOS slurry into a hard and durable feedstock for recycling if a suitable moisture control was developed. The moisture content of briquettes ensured a higher green strength and easier handleability of the product immediately after production thus making the commercialization of the briquetting route preferable.

In oxygen steelmaking, dust generation is caused by the ejection of metal and slag droplets from the vessel because of bubble bursting, metal evaporation and entrainment of solid fines. It is necessary to know the effect of each dust-forming mechanism to reduce the overall amount of dust by tailoring accurately the production parameters. Top charged additions of lime, scrap and fluxes proved to be one of the main factors affecting dust emission therefore RWTH performed a huge work to provide an improved understanding of the effect of this procedure on dust generation within the BOS process. Moreover, the top addition procedure which allowed a better concentration of Zn dust emissions to a narrow time period during the blow was also to be determined. The experimental campaign was carried out at Thyssen-Krupp Stahl (TKS) with a 200 tons BOF vessel using both steel scraps and hot metal from BF. Before adding both, lime was charged from a bunker at the beginning of the heat to reduce the impact of the 20 tons of scrap that were subsequently charged and the 180 tons of molten iron. Once completed the charging, pure oxygen was blown through a lance on the melt for 20 minutes

while nitrogen and argon were injected from bottom nozzles to improve mixing. The dust was collected in the gas cleaning system. The waste gas left the BOF vessel at a temperature of 1700 °C and experienced a reduction to 1000 °C on their way to the horizontal duct which was equipped with a sampling probe and further reduced their temperature to 700°C. Then, the washer was used to separate the bigger dust while the smaller ones were removed in a hydro cyclone. A laser diffraction spectrometer was used for particle size distribution examination, while dust batch-wise were collected on a filter to determine dust generation rate and to get information about the chemical composition. The chemical analysis was performed not only by XRF but also through Atomic Absorption Spectroscopy (AAS). Additional samples were investigated with Scanning Electron Microscope (SEM) for granulometry and with EDX for chemical analyses. The results highlighted that the highest dust generation rate was achieved during lime charging and it became progressively lower with a continuous decrease despite being constant the blowing rate and the lance height. The total Fe content rose during blowing from 60 to 70 %, CaO dust generation rate had its peak during and after lime charging and SiO_2 dust generation rate was nearly constant. Fe_2O_3 covered almost 80 % of the total dust at the beginning of blowing, coherently with the results reported in previous works (5) (6) (7), and its content increased to 90 % within 4 minutes and remained at this level. CaO experienced its peak with a content of 15 % at the beginning of blowing and progressively decreased to less than 10 %. The highest SiO_2 content was almost 3 % after the beginning of the blowing and the content decreased to less than 1 % at the end of blowing. The MgO content was nearly constant and relatively low, i.e., 1 %, Al_2O_3 content varied between 0.2 and 1 % and the average MnO content was 0.2 %. Zn was observed only in 3 heats and during them the highest ZnO level was detected at the beginning of the blowing time. Further studies were performed in this sense dividing the heats into two groups, i.e., heats with top charging of lime and heats with top charging of lime and of scraps and iron ore. As previously reported, dust generation rate steadily decreased for heats with the sole top charging of lime while the heats with additional top charging displayed an increase in dust generation rate every time that material top-charging was performed with the highest dust generation rate achieved again during lime charging. A possible reason could be the temporary collapse of the foaming slag due to the lumps falling upon the slag. Indeed, lime charging took place in an early stage before slag started to foam, and it was during this period that the increase in dust generation was particularly strong. Another possible explanation related to the property of the metal melt which became supersaturated with respect to dissolved carbon and oxygen. In the presence of highly siliceous slags the heterogeneous nucleation of CO bubbles became strongly retarded leading to definite super-saturation in dissolved carbon and oxygen and eventually to explosive CO formations. Concerning particle size distribution, particle size ranged between 0.7 and 180 μm and three main peaks at 1, 12 and 140 μm were always observed. Another maximum of around 50 μm was sometimes found. Four classes of particles sizes were formed around these maxima, i.e., Class I < 2.2 μm, Class II: 22-26.7 μm, Class III: 26.7-101.5 μm and Class IV > 101.5 μm. Concerning the effect of top-charging on particle size distribution and focusing on sole lime charging, the smallest particles proportion, i.e., Class I, was nearly constant at 6 % while Class II started from 40% and rose up to 59 %. Class III was nearly constant around 10 % and rose only at the end of blowing up to 20% while the biggest particles of Class IV started from 40 % and ended at 20 %.

2.1.4 Briquetting of self-reducing blending of waste iron oxide mixtures (8)

The project was coordinated by Profilarbed with CRM and BFI (Verein Deutscher Eisenhüttenleute) participating as consortium as partners. The project started on the 1st of July 1997 and lasted almost three years, ending on the 31st of December 2000. The overall project cost 1.26 M€ and the EU contributed almost 60 % with 756.9 k€.

EAF dust was characterized by a high Zn content up to 40 % (9), while oily mill scale and mill/BF/BOF sludge resulting from different water treatments were contaminated with oil and grease and all these elements made them hazardous waste. Concerning EAF dust, the main pyrometallurgical method for Zn recovery was the Waelz process which was based on a carbothermic reduction of ZnO and volatilization of metallic Zn in a rotary kiln. The process ensured a high Zn recovery, but it was also characterized by high energy consumption which made Zn recyclable at a cost of 75-125 €/ton depending on the total amount of Zn available in the waste. Analogously, oily mill scales and sludges could be recycled only after expensive de-oiling treatments. Considering these, the main goal of the project was the development of a technically and economically feasible recycling process of these iron-rich residues by using a low temperature briquetting process to produce self-reducing briquettes to be fed in existing melting facilities such EAF and/or cupola furnace.

At first, an experimental campaign was performed at the laboratory scale by CRM to determine the best configuration for the self-reducing briquettes containing mixtures of mill scales and sludges, EAF dust and the reducing agent to be sure of their complete reduction once loaded with the scrap into EAF. The briquettes were optimized in terms of binder type, composition, grain size and activator for the reduction reaction to ensure also satisfying mechanical properties comparable with the ones of anthracite which was already regularly loaded into EAF. Concerning binder type, tar pitch proved to be not idoneous due to the high content of polycyclic aromatic hydrocarbons which might cause severe environmental problems both at the briquettes manufacturing stage and at the briquettes use in EAF stage. Moreover, it proved to be extremely sticky thus complicating the cleaning phase and making necessary the use of sand blasting of the linear press after each manufacturing round. Finally, the briquettes produced with tar pitch turned out to be very heterogeneous with binder segregation occurring in some areas of the tablet thus resulting in mechanical performance lower than anthracite one. Analogous outcomes were achieved with bitumen in terms of mechanical properties. In light of this, molasses was selected as binder since the mechanical performance of the briquettes containing oily mill scales and sludges and also EAF dust proved to be higher than anthracite ones. The presence of the fine EAF dust allowed to fill in the interstices between scales grains, to dilute the oily matters which act as an anti-setting agent and provided a hydraulic binder thanks to the presence of lime. An increase in residues grain size distribution was detrimental for the metallization yield determining a worse degree of metallization for coarse grained briquettes. The addition of K_2CO_3 or Na_2CO_3 proved to be beneficial for metallization (10) (11), especially for coarse grained residues, determining an increase of 20 % in metallization yield. This was ascribed to the thermal decomposition of the carbonates at 850-900 °C into K_2O, Na_2O and CO_2 and to the following full conversion of CO_2 into CO at temperatures higher than 1000 °C and in absence of O_2 according to Boudouard's reaction. This mechanism allowed the release of a reducing gas inside the briquette and was at the origin of the boosting effect. The trials highlighted also the possibility to effectively extract Zn and Pb from the

briquettes and to recover them in a form which allowed their valorization thanks to a concentration in the dust.

Once completed the laboratory scale analysis, ProfilARBED carried out an industrial trial loading the briquettes containing mill and EAF by-products into its EAF. Two different types of briquettes were considered for the industrial trial: BB briquettes with an oily mill scale content of 80 % and an oily mill sludge content of 20 % of the total co-products and PB briquettes with an oily mill scale content of 40 %, an oily mill sludge content of a 10 % and an EAF dust content of 50 % of the total co-products. Both briquettes were produced by mixing the selected by-products with lime for moisture removal and briquettes cohesion, with coal in the form of petrol coke as reducing agent and molasses as main cohesive agent. The resulting products were cold pressed and then stocked for few days to ensure hardening. The mechanical strength and the magnetic properties of the two types of briquettes were conveniently tested before the industrial trial.

After validating their properties, 2 tons of briquettes were loaded in the first scrap basket of each melt and their effect on key process indicators such as productivity, energy consumption, liquid steel and slag quality was investigated. The EAF process parameters considered demonstrated that the quantity of briquettes loaded in the EAF had an influence on the furnace performance lower than other factors such as scrap quality or slag foaming. In particular, the electric energy consumption was expected to increase by 0.5 MWh per ton of briquettes loaded in the furnace due to the supplementary energy necessary for iron oxide reduction in the briquette, but no significant differences were observed between the reference campaign and the ones with self-reducing briquettes. Analogously, the percentage of iron in the liquid slag didn't increase significantly in comparison with the reference slag analyses thus proving that the carbon added to the briquette was sufficient for the reduction reaction. Overall, the industrial trial allowed to conclude that it was possible to recycle mill and EAF by-products in self-reducing briquettes in EAF.

During the same period, BFI focused on the recyclability in a cupola furnace of the sludge and dust resulting from the gas cleaning system of BF and BOF which could not be recycled within the usual iron and steel processes due to their high Zn, Pb and alkalis content. Therefore, this part of the project aimed to optimize briquettes production for their subsequent smelting in a cupola furnace to produce liquid iron from the iron oxides wastes and non-ferrous metals enriched product which accumulates in the cupola dust. At first the composition of the briquettes was investigated at the laboratory scale to optimize mechanical strength, reduction behavior and melting behavior. Binder selection was accurately investigated to ensure sufficient mechanical resistance to the briquettes and dolomitic lime, Portland cement, molasses and granulated BF slag were selected as potential candidates. The experimental results highlighted an enhancement of 100 % in breaking strength for increasing binder content, i.e., 10 wt.%, of cement or lime. On the contrary, the results obtained with molasses and BF slag proved to be unsatisfying. After that, various reduction tests were performed, and briquettes were adequately reduced displaying a grey color resulting from the metallization. Moreover, almost 60 % of the carbon proved to be converted. Concerning the other chemical components in the briquettes, slag formers such as Al_2O_3 were still present in unchanged form whereas Zn and Pb oxide were completely volatilized. This means that if the material was loaded in the cupola furnace, its gas would

probably be enriched with these components. These tests also demonstrated that briquettes bound with lime were characterized by sharp cracks whereas briquettes bound with cement displayed no cracks. Moreover, the briquettes bound with cement were characterized by a metallization degree 10 % higher than the ones bound with lime being equal the reduction conditions. In light of all these considerations, briquettes bound with cement proved to be the best choice with sufficient strength and the best degree of metallization.

Based on the results obtained at the laboratory scale, briquetting technical-scale trials were performed using Portland cement as binder and extrusion as manufacturing technique. The strength of the briquettes produced was somewhat lower than the one of the tablets produced at the laboratory scale due to different briquetting pressures. The mechanical tests also highlighted that the breaking strength increased with a decreasing moisture content. In light of this, the direct use of fresh sludge recovered from the filter with a water content of 40 % for briquetting was clearly too high since the optimum water content to be used with cement as binder was around 20 %. Based on the results obtained, briquette composition for cupola trials was set at 80 wt.% of BF gas sludge and 20 % Portland cement and they were stored for 30 days to harden prior to being used. The industrial scale tests were performed with 15 tons of self-reducing FeO_x briquettes in the cupola furnace and confirmed the feasibility of metallurgical residues recycling. No great differences in iron composition were identified except for a slight decrease in C and Si concentration which could be compensated by adding C and Si carriers. A change in cupola slag composition was observed with a slight increase in slag basicity and a significant increase in MgO concentration. This must be ascribed to the higher MgO of the briquettes compared with the usual components charged. Furthermore, the operating data obtained during the trials allowed to calculate material and energy balances and to have a direct comparison with normal operations. The material balance showed that in briquettes made from BF sludge alone only 1/3 of the carbon was used for iron oxide reduction while another 1/3 was used to support the water gas shift reaction resulting from the moisture present in the briquettes. Considering this, a lower water content would be desirable to minimize the water gas shift reaction and the related carbon consuming thus leading to a higher rate of reduction. Finally, the last 1/3 of carbon was lost due to briquettes fragmentation which led to dust formation and loss.

2.1.5 TREATDUST: Development of technologies for treatment of dusts and sludges containing zinc and lead to improve their recycle reuse (12)

The project was coordinated by CSM with CENIM (Centro Nacional de Investigaciones Metalúrgicas), British Steel plc and VASL (Voest-alpine Stahl Linz) participating as partners in the consortium. The project started on the 1st of July 1996 and lasted almost three years, ending on the 30th of June 1999. The overall project cost 1.05 M€ and the EU contributed 629.40 k€, i.e., 60 % of the budget.

Linz-Donawitz (LD) process and EAF dusts are considered polluting materials and different treatments such as pyro, hydro, pyro-hydrometallurgical and vitrification were developed to recover the metals contained in the dusts, e.g., Zn, Pb and Cd, and to make the dumping easier. The pyro-metallurgical route was the most attractive for the integrated cycle since the related equipment, e.g., rotary kiln, rotary hearth and transport bed furnaces, allowed to treat large amounts of waste resulting from this

manufacturing route. On the contrary, electric arc plasma furnaces proved to be more appropriate for waste arising from the electric cycle. Furthermore, great interest arose for the hydrometallurgical and the combined pyro-hydro processes. All these treatments must be optimized in terms of charge pre-treatment, reductant type, process parameters, energy requirements, final products, etc. Considering the huge number of technologies available for treating these dusts, the present project aimed at identifying at the laboratory scale the optimum combination of these treatments to maximize the recovery of metals and four different technologies were identified to treat EAF and BOF dusts. British Steel focused on a pyro-process performing an efficient Zn removal from highly metallized products, i.e., briquettes and pellets obtained from continuously recycled BOF dusts, by applying a rapid thermal treatment at 1300 °C in a furnace designed according to the rotary hearth model. This solution also allowed to obtain Zn-rich filtrate easily saleable to Zn manufacturing industry. VASL focused on another pyro-process performed in a facility based on a transport bed process and demonstrated that it was possible to achieve dusts dezincification from LD process when they were characterized by a size lower than 125 µm and applying high temperatures and low residence time. Analogously, CENIM showed that it was possible to recover all Zn contained in EAF dusts performing a long cycle treatment of the pellets including mixing and palletization, reducing heat treatment, magnetic separation, melting of magnetic fraction and steel cuttings in an induction furnace, treatment of effluents. Finally, CSM developed a hydrometallurgical solution to couple with the pyro line already available at the industrial steelwork site of Terni to treat ZnO-rich powders coming from an arc-plasma industrial furnace. In particular, the treatments proposed include alkaline washing, sulfuric leaching, coagulant oxidation, purifying treatment, electrolysis and Mg bleed off. Each treatment investigated allowed to convert EAF and BOF dust into different types of by-products acquiring knowledge on the main critical points. One of the main aims of the project was the improvement of the pyrometallurgical and hydro processes for the treatment of dusts and sludges, i.e., study of pre- and post-treatments of charges and intermediate products, to improve the recycling of the Fe fraction in steel operations and obtain richer Zn and Pb fractions. The second aim of the project was the development of purification processes intended for the Zn and Pb enriched materials resulting from pyrometallurgical and hydro processes with the goal of producing cleaner fractions to make them more suitable for metallurgical industries.

Focusing on British Steel activities, a pyro-processes, i.e., a high temperature solid state process like that expected for a rotary hearth furnace, was designed to treat briquettes and pellets produced with dusts and sludges combined with a reductant, which would volatilize Zn and Pb components when subjected to a rapid thermal treatment. This would allow to obtain a product with a high metallic Fe content which could be recycled as direct reduced iron (DRI) or scrap substitute in EAF, BOS or BF and a high ZnO by-product for sale or further processing. This pyrometallurgical treatment would play a paramount role because dust and slurries collected from BOF and EAF gas cleaning systems could not be recycled to BF via sinter plant due to the high levels of Zn and Pb which would exert a detrimental effect on both furnace operation and refractory life. The experimental campaign was designed to examine the effects of slurry type, reductant type and ratio, percent of volatile matter, level of S and ash contents and agglomerate type, i.e., briquettes and pellets.

Concerning slurry and dust type, samples containing 2.28 and 5.59 % of ZnO were collected from BOF plant at Llanwern and Port Talbot, respectively. With a view at increasing the Zn content in the slurry,

the influence of dust and slurry recycling back to the BOF process was examined by collecting further samples at Port Talbot after adding BOF slurry back to the process in the form of briquettes. In this way, ZnO content was increased up to 10.7%. Further samples with high ZnO content, i.e., approximately 20.4 %, were provided by VASL after applying several recycling loops. EAF dust samples were also collected from the filter baghouse at British Steel Engineering Steels. Concerning the reductant, two types of coals with different volatile, S and ash contents were used during the trials, and their content was varied on two levels according to the agglomerate type, i.e., 11 and 22 % in the briquettes and 12 and 25 % in the pellets. Concerning operating temperature, three different levels, i.e., 1100,1200 and 1300 °C, were considered to ensure both Fe reduction and Zn volatilization. The results proved that a temperature of 1300 °C should be used to ensure the maximum Zn removal and metallization degree. The agglomerates were produced using a Komerak press for briquettes and an Orthos pelletizing disc for pellets. Pellets were treated with a disc rotation speed of 60 revolutions per minute, and the obtained product was screened through appropriately sized sieves to send the undersize pellets back to the pelletizing disc for further growth while oversize ones were discarded. Both briquettes and pellets were subsequently left to air cure. All agglomerates were incorporated with a small amount of bentonite to act as a binder and were cured for 3 days before being thermally treated in the furnace, i.e., a ceramic fiber insulated cylinder endowed with 8 electrical heating elements and fluxed with nitrogen to maintain an inert atmosphere to ensure that reduction reactions were fully carried out by the reductant contained in the agglomerates. Moreover, agglomerates preheating at approximately 420 °C allowed to achieve maximum reduction potential from coal volatiles and therefore a high degree of metallization. In light of this, the general heating procedure included an initial preheating at around 400-600 °C for almost 20 minutes before heating to the maximum selected temperature at which a dwell time of 20 minutes was also required. A rapid cooling of almost 30 °C/min was applied under a nitrogen shroud to limit or avoid reoxidation phenomena. The strong dependency of the process on operating temperature allowed to obtain a versatile route which ensured the treatment of many different dust and sludge mixtures.

The results highlighted that pellets perform slightly better than briquettes in terms of metallization degree and Zn removal but were characterized by a greater degree of inconsistency in performance thus making briquettes the preferred choice for this treating route. Indeed, the control of reductant amount was easier in the briquettes rather than in the pellets where a greater variation was observed due to the tendency of the reductant to segregate in the pelletizing. Moreover, it was observed that briquettes were able to better retain their structure and integrity compared to pellets. Indeed, the higher porosity of the pellets made them more homogeneous in terms of metallization degree but decreased significantly their post-reduced strength. This characteristic of briquettes made them easier to store and transport prior to recycling. Furthermore, it was observed that except for ZnO, PbO, and K_2O, other elements present in the initial agglomerate persisted inside the reduced metallized product and this aspect must be considered when assessing a potential recycling route where selective addition of this material to BOF or EAF processes would be made. The Zn-rich filtrate obtained provided a further product exploitable to produce a high purity ZnO saleable to Zn manufacturing industry.

Moving to VASL, it was endowed with three LD converters equipped with a closed system for converter gas and dust recovery. The coarse dust was almost 40 % and was removed from the converter gas in the evaporation cooler while the fine fraction accounted for almost 60 % and was removed in the downstream electrostatic precipitator. These dust fractions were characterized by different Zn-contents and were hot briquetted to be recharged in the LD converter to enrich the Zn content until reaching values suitable for being returned to a smelting plant for reutilization. Therefore, VASL activities aimed at investigating a selective reduction process of the ZnO_n/FeO_n-rich dust to produce a fraction with a higher Zn-content for reutilization in a Zn-smelting plant and a fraction with a higher Fe-content for reutilization in the hot metal and steel production using a fluidized bed process. The work program included an initial physical and chemical characterization of the coarse and fine dust including flow tests to determine flow rate, turbulence and discharge behavior necessary to perform some preliminary considerations for the layout, design and construction of the reactor for high-temperature tests. After these tests, dust was separated into two fractions, i.e., Zn and Fe-rich, under a reduction gas atmosphere using a laboratory transport reactor. Parameters such as grain size, gas composition, temperature and residence time were considered. Focusing on the chemical, physical and mineralogical properties of the dust, fine dusts, i.e., diameter <180 µm, were more Zn-rich and were responsible for a higher oxidation of Fe to Fe_2O_3 while coarse dust, i.e., diameter >180 µm, contained a higher content of CaO particles from the burnt lime addition. Coarse dust was also characterized by a higher bulk density, but a lower apparent and absolute density due to the lower Fe and Zn content and the higher CaO content.

The fluidized bed process can be classified into three main groups depending on the relative velocity between gas and solids. Conventional fluidized bed is characterized by a relative low velocity between gas and solid and the gas-solid suspension in the reactor is limited. If gas velocity increases and the gas-solid suspension in the reactor expands, there is an increase in the discharge of solids and in the relative velocity. If the discharged material is separated via a cyclone and returned to the fluidized bed, the fluidized bed is defined as circulating. Finally, the region of pneumatic transport is reached when gas velocity exceeds particles discharge velocity. In this case, the relative velocity between gas and solids goes back to zero and the equipment is defined as transport reactor. The minimum fluidization velocity defines the boundary between the fixed and the fluidized bed. The experimental data obtained from the flow tests highlighted a minimum fluidization velocity of 0.11 m/s for coarse dust and 0.04 m/s for fine dust.

To evaluate dust discharge behavior, the portion of fluidized bed which was discharged at a predetermined gas velocity was evaluated using dried compressed air as fluidizing medium and a cyclone and a 5µm metal filter as discharged dust separators. After completing the test for each operating gas velocity, three fractions of dust, i.e., one remaining in the reactor, one separated by the cyclone and the last in the filter, were obtained, weighed and characterized. A direct connection between the gas velocity and the discharge together with the distribution of Zn in the different fractions was observed, but it was also concluded that separation of Zn-containing dust by this method was not possible. Therefore, the test equipment was converted into a transport reactor to avoid longer residence times of the dust particles in the fluidized bed and related phenomena such as particles agglomeration. The results proved that the amount of dust separated in the transport reactor decreased with increasing

gas velocity and the dust fraction separated in the transport reactor was characterized by an increase in the grain size and a decrease of the Zn-content compared with the used fine dust. This allowed to obtain a clear distinction between fractions with a high Zn-content and fractions with a high Fe-content. The results also highlighted that the quantity of dust discharged at the same gas velocity was smaller compared to the fluidized bed probably due to the shorter residence time.

Based on the preliminary characterization of dust samples and the different flow tests, the test plant layout was designed, constructed and commissioned resembling a transport reactor, where dust particles were transported due to gravity and a gas flow running from the bottom of the reactor controlled the residence time. This test plant allowed to investigate the selective reduction of ZnO_n/FeO_n-rich dust during the reduction process occurring in a very short time under temperatures up to 1600 °C. The reactor consisted of an inductive-heated graphite pipe inserted in a quartz glass cylinder fixed with two water-cooled holding devices which accommodate the facilities for the dust supply and discharge and the reduction gas guide. The supply system fed the dust directly in the high temperature zone of the graphite pipe whose dimensions together with the reduction gas velocity were designed to ensure that the dust was heated up in the shortest possible time. Both particles diameters and reduction gas velocity were considered as main operating parameters to optimize both residence and heating-up times. In particular, the residence time in the high temperature zone was controlled by the reduction gas velocity which in turn-controlled dust sinking speed which increased as a function of dust diameter. Furthermore, dust diameter also controlled the heating-up time of the particles with coarser dust requiring a higher heating-up time. For example, particles with a 20 µm diameter were heated after 0.15 s whereas particles with a 50 µm diameter needed 0.25 s. According to these data, a 0.6 s residence time in the high temperature zone should be sufficient to ensure the reduction of the ZnO compounds and the subsequent evaporation on Zn while preserving iron in its oxidized phase.

The optimization of this separation can be achieved only by going through an accurate analysis of the thermodynamic aspects of the reduction process considering that the residual degree of oxidation of the FeO_n component and the velocity of the Zn separation were strongly influenced by both operating temperature and CO/CO_2 ratio in the reduction gas. Indeed, the partial pressure of Zn was a function of both temperature and reduction potential of the gas and increased with them. Considering this, the residence time for an equivalent degree of dezincing was reduced with higher temperatures and an increasing CO/CO_2 ratio. Furthermore, it must be considered that when a selective reduction is targeted the CO/CO_2 ratio must be tailored to avoid FeO_n components reduction to metallic iron while ensuring the full conversion of ZnO phases in Zn. All these aspects were confirmed by the test campaign carried out. During the cold tests commissioning of the reactor, the best carriage properties were achieved with the fine dust sample of original size because superfine dust, i.e., diameter < 100 µm, promoted the formation of adhesive grains which caused clogging of the material supply line. It was not possible to identify a satisfactory constant carriage for coarse dust. In light of this, fine dust < 125 µm and fine dust of original size were selected as input material. Despite this care, agglomerates of metallic iron formed in the reactor during the preliminary reduction tests at 1300 °C in CO atmosphere due to the direct contact between the dust particles and the graphite layer of the walls.

These agglomerates affected negatively the process since they reduced the reactor section and the portion of material passing the reactor.

CENIM was the third partner involved in the project and its activities focused on facilitating EAF dust recycling to improve the current Waelz method technologies by Zn volatilization and Fe recuperation with a view at reducing costs in the use of the reducing agent, achieving energy savings by minimizing reduction time, and trying to reduce the volume of slag, recovering the Fe. The production of an ultra-depurated ZnO for subsequent treatment in the Imperial Smelting Process or in the production of Zn by electrowinning was also targeted. After selecting the EAF dust and performing their physical and chemical characterization, the charge was washed to eliminate chlorides and sulphates and was prepared by pellettization after being agglomerated with other high Fe content wastes and calcinated with petroleum coke, i.e., coke with little reactivity able to withstand high temperatures without burning, before undergoing thermal treatment. The latter was optimized in terms of operating conditions to guarantee the best reduction and volatilization of Zn, which was then further treated and depurated, while coke and iron fractions were recovered by pellets grinding and magnetic separation. The concentrated iron was also subjected to melting tests in induction furnaces and the treatment of secondary waste was also performed.

Pelletization was performed in a pelleting disc using EAF dust, 10 % calcinated petroleum coke and 10-15 % humidity. The green pellets were dried in an oven for 24 hours at 100 °C and were characterized by a 10-12 mm diameter. Reduction tests were performed in a muffle furnace working in a reducing atmosphere. Zn and Pb gases were collected in the upper part of the equipment and were washed with water after passing through a ceramic tube. The results highlighted that Zn volatilizes completely by increasing temperature and permanence time in the furnace thus allowing to obtain residues with low Zn content. The reduction process must be optimized not only to reduce as much as possible the residual Zn content in the final residue but also to recover the Fe contained in it. Indeed, the control of the operating temperature allowed to convert the largest part of iron into metallic Fe or Fe_3O_4 which can be recovered through magnetic separation thus allowing to obtain a highly saleable product. A temperature of 1200 °C and a residence time of 2 hours were able to ensure a good Zn volatilization with the production of a ZnO of greater quality, together with high quality residues in the pellets characterized by enriched metallic iron which could be conveniently separated by the fluorine residue through magnetic separation being fluorine accumulated in the nonmagnetic fraction together with Ca. The residual pellets after the reducing treatment were shredded to perform magnetic separation and to obtain the Fe-enriched fraction,. The magnetic fraction ranged between 75-85 % of the initial pellet and was characterized by an Fe content around 63 % which was higher than the initial Fe content in the pellet around 41 %. Other impurities like F, Si and Ca were mainly segregated in the non-magnetic fraction which could be repurposed in clinker manufacturing processes, as forming part of the bituminous binder in the asphalt layer in road surfacing and as platform, bases and sub-bases in road construction. To this aim, non-magnetic fraction must not exceed concentration limits of heavy metals such as Ba, Cd, Cr, Mo, Ni, Pb, Se, V and Zi, as well as sulphates and fluorides. The magnetic fraction could be recycled to EAF therefore melting tests were performed with commercial steel cuttings in a vertical furnace which reaching 1600 °C with a controlled atmosphere. The use of commercial steel cuttings was fundamental to ensure the dilution of elements such as Cu, Sn and Cr which tended to

concentrate in the magnetic fraction thus creating problems when recycled to EAF. The metallographic results highlighted the presence of significant amounts of globular non-metallic oxide inclusions in the steel which may pass into the slag during industrial pyrometallurgical treatment. The results also indicated that it was possible to obtain a ferritic steel with the recovered magnetic fraction homogeneously incorporated in the molten bath without segregations.

Finally, the project coordinator CSM investigated the best combination of hydrometallurgical and electrolysis treatments to clean the enriched ZnO and PbO fraction obtained from the pyro-metallurgical treatment performed with a DC plasma-arc furnace placed at the downstream of Acciai Speciali Terni bag house. The plasma-arc furnace allowed to convert the dusts into a ferroalloy to be re-used as a furnace charge, a fully inert slag to be dumped and a ZnO-rich dust with high trading potential for non-ferrous industry after being cleaned by optimized hydrometallurgical and/or electrolysis treatments. The work program proposed by CSM included a preliminary characterization of the dust before and after leaching with different reagents to setup a laboratory hydrometallurgical process fed with sludges coming from the arc-plasma furnace, the study of purification treatments to eliminate Cd, Cu and Ni contained in the dust and which may reduce Zn purity or cause Zn redissolution during electrolysis and finally a study to eliminate by dissolution in an appropriate time the fluorine present in the sludges with a particular treatment with Na_2CO_3.

At first, leaching pre-treatments were performed on the dry dust with different chemicals to identify the most performing one to eliminate hazardous elements. In particular, the effect of H_2O, Na_2CO_3, NaOH, H_2SO_4 on F, Fe, Ni, Ca, Mg, Pb, Zn and Cl removal was assessed. The treatment with water allowed to remove part of fluorine from the dust since CaF_2 is a soluble salt and the percentage of fluorine in the dust decreased from 0.5 to about 0.12 %. It cannot be excluded that repeated treatments with water may allow to remove completely the fluorine from the dust. The treatment with the H_2SO_4 acid solution caused a decrease of Zn concentration into the dust while the alkaline solution of NaOH brought Cr and large amounts of Pb and Zn in solution together with the same percentage of fluoride obtained with the treatment with simple water. The Na_2CO_3 solution was a solvent for both chromates and fluorides without bringing Zn in solution. It was concluded that the best initial treatment was the one with water forming sludges because it allowed to decrease the chlorides. Furthermore, chemical treatments of sludges were carried out to decrease the hazardous elements content to acceptable levels before reclaiming Zn via electrolysis. The sludges were chemically treated to obtain an acid solution suitable to perform electrolysis and verify the deposition of high purity Zn. In particular, the treatment included leaching with H_2SO_4 at pH 4.5 performing a cold stirring for 2 h and then H_2O_2 was added to oxidize Fe^{+2} to Fe^{+3} allowing the precipitation of Fe^{+3} as iron hydroxide. Then filtering in a bag filter was performed and a Zn containing solution and a cake were obtained. The Zn solution needed to undergo further purification treatment because the presence of Ni, Co, Cu, and Cd was dangerous to reclaim and clean Zn via electrolysis. The treatment was divided into two stages, the first one at a temperature of 60 °C and the second one at a temperature of 90 °C. In the first stage, Zn powders were added to the leached solution and stirred for 1 hour to promote Cu and Cd complete and Ni partial precipitation. After this cementation step, the solution was filtered to remove the cements precipitated and was subjected to the second step where $CuSO_4$ and Sb_2O_3 were added together with excess of Zn powders to remove Ni, Co and Sb.

After purification, H_2SO_4 was added again to obtain a solution with a pH of 2.5. The first residue filter cake was a toxic waste due to the high Pb content, and it was recycled at the plasma-arc furnace to further concentrate Pb to ensure that the final residue obtained could be finally sold to the Pb smelters, i.e., minimum Pb content 40 %. Concerning the second residue obtained, it was nontoxic and could be dumped. Finally, the Zn-rich solution was subjected to electrolysis to achieve Zn separation at the cathode, and it was obtained using a current density of 500 A/m^2 for 5.8 h ensuring a Zn recovery of 93.7 % with a degree purity of 99.49 %. The laboratory experiments demonstrated that the hydrometallurgical process was a feasible route to produce a high-grade metallic Zn by electrowinning starting from a by-product rich in ZnO and obtained from the DC plasma-arc furnace sludges.

2.1.6 High purity zinc and ferroalloys recovery from EAF dusts through a combined pyro-hydrometallurgical treatment (13)

The project was coordinated by CSM with Aso Siderurgica, Acciai Speciali Terni, Techint and TKS Nirosta participating as partners in the consortium. The project started on the 1st of July 1998 and lasted almost three years, ending on the 30th of June 2001. The overall project cost 2.52 M€ and the EU contributed 1.26 M€, i.e., half of the budget.

The present project was a demonstration project, namely a scaling up of the findings obtained in the TREATDUST project thanks to CSM experience. Indeed, the aim of the project was to develop and tests a combined pyro-hydrometallurgical technology for the treatment of dusts generated in EAF to fully recover by-products such as ferro alloy, metal Zn and inert slag to be recycled, sold or disposed without any danger. The pyrometallurgical treatment was performed in a pre-existing single electrode electric arc DC furnace located at Acciai Speciali Terni and equipped with a snorkel to feed EAF dust into the furnace at the slag level allowing to avoid fed material carry over. Two different feeding systems were considered to minimize particle carry-over with the fumes and the snorkel solution was preferred when materials were introduced in the powdered state while free falling when materials were fed as preformed briquettes. The snorkel consisted of a water-cooled duct built up by stacking cylindrical metal sections, arranged vertically, which guided the charge down to the upper liquid bath surface while briquettes were produced by means of a briquetting press adding 2 % of starch, 20 % of coal and EAF dust. Reducing conditions were generated inside the furnace to produce ZnO-rich powders and the process was run continuously by charging mixtures of EAF dust, flux as slag modifier and coal into the furnace filled with liquid metals and slag. With this working configuration, all metal oxides contained into the dust reacted quickly with coal and volatile metals, e.g., Zn, Pb and Cd, evaporated and gathered as oxides in the gas cleaning plant whereas nonvolatile metals collected as liquid at the bottom of the furnace. Concerning non reducible oxides, they dissolved in the slag. The products were ZnO enriched powders, i.e., ZnO > 80%, ferro-alloy and inert slag. The experimental campaign for the pyro process reported almost a complete recovery of ZnO and PbO since their percentage in the residual slag and metal was lower than 0.01 %. Temperature was modified between 1400 and 1700 °C and no appreciable influence was observed on the reduction kinetics, but it proved to strongly influence the final quality of the powder obtained. Indeed, the content of ZnO and PbO passed from 93 % at around 1400 °C to 66 % when the temperature exceeded 1650 °C due to Fe, Mn, Cr, Ni evaporating from

the metal bath. In light of this, an operating temperature lower than 1450 °C was strongly suggested together with the use of snorkel feeding to avoid the costs of briquetting operation since no significant differences were observed between the two methods.

The powders obtained were subjected to hydrometallurgical treatment to increase their economic value in a newly designed plant divided into three sections. At first, powders were washed in water at 50 °C to remove chlorines, fluorine and alkali reporting reductions with yields of 90 % for Na, 82 % for K, 96 % for chlorines and 31% for fluorine. After this step powders were leached with H_2SO_4 which was able to dissolve also zinc ferrites under stirring conditions at a temperature of 55 °C and pH 2.5. The leaching procedure lasted almost 90 minutes. The solution obtained underwent various purification treatments to remove the residues rich in Pb resulting by sulfuric leaching, residues rich in Fe resulting by coagulant oxidation, and residues rich in Ni, Cd, Cu before undergoing electrolysis to extract metallic Zn. The coagulation process allowed Fe ions oxidation from bivalent to trivalent by means of H_2O_2 and its consequent precipitation as $Fe(OH)_3$. A partial co-precipitation of fluorine like CaF_2 was also achieved. The treatment was performed at 80 °C and at pH 4.8 obtained by $CaCO_3$ addition. The cementation of Ni, Cu and Cd was conducted at 90 °C in one stage of 90 minutes and in a single reactor using $CuSO_4$ and Sb-tartrate as catalysts. The electrolysis was carried out with a current of 6000 A and a voltage of 3.55 V for a series of 10 Al cathodes and with a voltage of 10.7 V for 3 series of Al cathodes at 25 °C. The Zn plates obtained were easily separated from the cathodes by means of common mechanical techniques and the quality of the Zn was a purity of 99.96 % and a density of 7.01 g/cm^3. Focusing on the plant, the first section was dedicated to water washing, sulfuric leaching and coagulant oxidation, the second section to the first step of purification treatments in a single reactor after which the solution was stored in appropriate tanks for the subsequent continuous electrochemical treatment which took place in the third section, i.e., a single cell of industrial size, equipped with 30 cathodes, arranged in three stocks of 10. Concerning the residues obtained, they were considered as secondary raw materials. Pb-rich residues were recycled in the pyro furnace until a Pb enrichment of 40 % was achieved to sell it to Pb-smelting plants. Fe-rich residues were recycled in the pyro furnace for Fe recovery as metallic phase whereas Ni, Cd, Cu rich residues were recycled in metal alloys producing plants. The coupled pyro-hydro treatment was called Full-Rec.

2.1.7 Foaming of the slag and recycling of steel dusts by injection into the electric arc furnace for stainless steels (14)

The project was coordinated by Ugine-Savoie Imphy (USI) with Institut de Recherches de la Siderurgie Francaise (IRSID), Krupp Edelstahlprofile (KEP) i.e., actual ThyssenKrupp, and FEhS participating as partners in the consortium. The project started on the 1st of July 1999 and lasted almost three years, ending on the 30th of June 2002. The overall project cost 1.52 M€ and the EU contributed 762 k€, i.e., half of the budget.

The present project focused on stainless-steel industry trying to demonstrate the feasibility of stainless-steel dust recycling by pneumatic injection in EAF during slag foaming operation. KEP with FehS support assessed the feasibility of recycling dusts generated during stainless steelmaking to improve the recovery of alloying elements from dust and slag by using other reduction agents than

coal. USI and IRSID developed an efficient slag foaming process to improve EAF productivity, increase the valorization of its dust and improve the knowledge on slag foaming in stainless steelmaking EAF.

At first, the analysis of slag and dust, e.g., chemistry, XRD and environmental compatibility, performed at FEhS, USI and IRSID laboratories were crosschecked and validated by two Round-Robin tests to ensure a better comparison of the results. These analyses were fundamental to preliminary characterize the dust resulting from KEP and USI manufacturing processes. KEP production was devoted to both engineering and high-quality steel grades thus requiring different scrap qualities and periods with high amounts of engineering scrap qualities with high inputs of Zn and Pb into the furnace alternated with periods of high alloy steel scrap qualities characterized by high inputs of Cr and Ni. This clearly entailed the generation of different dust qualities and the need for an accurate characterization to get a statistical overview on dust composition evaluating the influence of the steelmaking program. The trials performed allowed to determine both the influence of scrap quality and the time required until dust composition reflected the used scrap quality completely thanks to the collection of dust samples over a period of 26 h during the turnover from high-alloyed steel to engineering steel qualities. Starting with a period of high-alloyed stainless steel, the amount of alloyed scrap placed in the furnace was high while engineering scraps ranged only between 14-46 %. In this case, Cr content in the dust varied between 9-16 wt.% moving from 54 to 84 % of alloyed scrap in the charge. Analogously, Zn content increased from 11 to 30 wt.% when using 100 % engineering scraps. Changes in the production program and in the related scrap quality induced a delay of 8 hours to obtain a uniform dust quality. Differences in dust qualities were also observed in their mineral composition with dust from high-alloyed steel being dominated by Cr-rich spinels, e.g., chromite, and low amounts of zincite, and dust from engineering steel qualities being characterized by high amounts of zincite and Zn-rich spinel, e.g., franklinite. This preliminary characterization also proved that scrap quality influenced dust grain size with a 3 µm d50 value for dust generated in melts with almost 80 % of stainless-steel scrap and 4-5 µm d50 value for dust generated in melts with 100 % engineering scrap.

Focusing on USI, the company produced different stainless-steel grades, i.e., austenitic and ferritic, by successive campaigns with different input qualities. The main constituents of the dust obtained were Fe, Zn, Cr and CaO with average concentrations for austenitic grades of 32 % of Fe_2O_3, 22 % of ZnO, 11 % of Cr_2O_3 and 7 % of CaO and average concentrations for ferritic grades of 24 % of Fe_2O_3, 28 % of ZnO, 8 % of Cr_2O_3 and 6 % of CaO. Further minor constituents were SiO_2, MnO, MgO, and Ni, Al, Na, K and Cl. For the sake of clarity, it must be underlined that no real separation of the dust generated from the austenitic and ferritic campaign was possible due to their short duration time compared to the response time of the de-dusting equipment thus allowing only average compositions considerations. In some cases, this may limit their recycling to avoid the pickup of certain elements such as Ni.

After this step, it was necessary to identify the most important properties, i.e., specific density and grain size, of the dust to optimize their storage, pneumatic transportation and injection. Focusing on KEP, they already had an injection system for the pneumatic handling of dust from engineering steelmaking, therefore it seemed straightforward to use the same equipment and the same operational conditions for the dust generated in stainless steelmaking after determining and checking the specific

density and grading curve of the dust. Specific density of both dust from engineering and stainless steelmaking was determined by pycnometer tests while grain size analysis was performed by laser granulometry. The results highlighted that the specific density of Zn-rich dust from engineering steelmaking was almost 0.1 g/cm^3 higher than those of Cr-rich dusts from stainless steelmaking and this was coherent with the main mineral composition observed. Indeed, dust from engineering steelmaking was mainly composed of franklinite ($ZnFe_2O_4$) with a density of 5.34 g/cm^3 whereas dust from stainless steelmaking was mainly composed of chromite ($FeCr_2O_4$) with a lower density of 5.09 g/cm^3. Concerning the grading curves, it was observed that dust from stainless steelmaking displayed a lower grain size compared to dust from engineering steelmaking, but these differences could be considered as marginally considering the range in grain size distribution and the comparably small shift of the grading curves. Considering the results obtained, stainless-steel dust should have been characterized by better or similar storage, pneumatic transportation and injection characteristics as engineering steel dust, therefore the same injection system and the same operational conditions used to handle engineering steel dust were applied.

Concerning USI practices, dust was injected into EAF after being blended with carbon and this clearly entailed the optimization of the dust/carbon ratio to ensure a reliable flow rate and good transportation control. The grain size of the EAF dust used was 125 µm < 82 % < 250 µm while three different coke types were initially considered, i.e., coke A with particles much smaller than EAF dust (60 % < 63 µm), coke B with a grain size of 40 % < 125 µm and 125 µm < 40 % < 250 µm, and coke C with particles size equivalent to EAF dust (125 µm < 70 % < 250 µm). The effect of different dust and coke ratios were also assessed, i.e., 10,15,25 and 30 % of coke. The flowing tests proved that the presence of coke was fundamental because dust alone could not flow through the funnel. Moreover, coke A blends could not flow whatever the coke ratio whereas coke B and C blends were able to flow fluently. It was finally concluded that coke grain size must be between 125 and 500 µm and the carbon ratio higher than 25 % and this encouraged USI to use a coke ratio of 30 % for its blend.

Focusing on the trials performed at KEP, the effects of dust from stainless steelmaking injection in EAF on slag chemical and mineral compositions together with their melting behavior were investigated. In particular, slags were reduced with carbon and with FeSi and were sampled in four different operational conditions: before injection of dust, after injection of dust and oxygen blowing, with injection of dust and after reduction and tapping, without injection of dust, after reduction and tapping. From the compositional and mineralogical perspective, it was observed that after reduction and tapping slags from melts with and without dust recycling were nearly identical. Indeed, despite an additional incorporation of heavy metals resulting from dust injection, most of the valuable elements were recovered during the reduction period by injection of carbon and FeSi, i.e., Fe > 90 %, Cr > 80 % and Ni > 95 %. Therefore, it can be concluded that dust injection did not play any negative effect on the chemical and mineralogical composition of the tapped slags. Concerning the melting behavior and the viscosity of the liquid slags, it was calculated by means of an improved Urban model (15) and it was observed that slags after the injection of dust and oxygen blowing were characterized by the highest softening, half sphere and flowing temperatures. These values were significantly decreased after reduction with slags produced both with and without dust recycling which were characterized by similar values. These results were further confirmed by viscosity analysis which confirmed that the

highest viscosity was achieved just after dust injection and oxygen blowing while the viscosity of the reduced and tapped slag did not display any significant difference with or without dust recycling. These results allowed to conclude that the injection of dust generated during stainless steelmaking could be performed without detrimental effects on the metallurgical process and with no significant changes in composition and technical properties of the solidified slags. Furthermore, it was also concluded that the reduction step should be performed very shortly after the blowing of oxygen and the injection of dust to shorten the period with higher concentrations of Cr and the resulting stiff slag.

After verifying that no failures of the injection equipment were experienced by injecting the dust generated in stainless steelmaking in a similar way as dust from engineering steelmaking, further tests were performed to improve the reduction for Cr and other alloying elements recovery from the slag. In particular, the use of carbon as reducing agent should be limited due to economic reasons connected with the subsequent VOD (Vacuum Oxygen Decarburization) treatment necessary for the high alloy steel qualities which, otherwise, would have been extended. In light of this, FeSi was selected as reducing agent to support the reduction of chromium oxide from the slag. The results demonstrated that the use of FeSi allowed to obtain EAF slags with CaO and SiO_2 contents comparable with the ones from the trials performed with carbon. Only MgO, Al_2O_3, and TiO_2 concentrations were somewhat lower, but still within the same range. No significant differences were observed even from the mineralogical perspective with merwinite and spinel type compounds being the dominant components. Furthermore, the partial substitution of C with FeSi allowed to improve the recovery of Cr, Mn and Fe with a rough increase from 73 to 81 % for Cr from 12 to 38 % for Mn and from 92 to 93 % for Fe. The introduction of FeSi injection in the operating practice made necessary the substitution of the injection equipment due to sticking problems that arouse in the pipes of the pneumatic transport system when increasing the reductant flow rate due to an unsuitable shape of the conveyor-screw. The influence of injected dust on Cr scorification, i.e., $(Cr_2O_3)/[Cr]$, was also investigated and despite a wide scatter in the data it was observed that an increase in injected dust causes a small increase of Cr scorification. It was also observed that the regression line for melts with FeSi co-injection was shifted towards lower ratios of $(Cr_2O_3)/[Cr]$ compared to those without co-injection. Therefore, it can be concluded that Cr scorification was counterbalanced by the co-injection of reducing agents. This was further confirmed by the fact that increasing amounts of reducing agents seemed to decrease Cr scorification. Concerning the effects of injection procedure on Cr scorification, it was observed that reference melts with injection of dust but without additional co-injection of reducing agents were characterized by an average ratio $(Cr_2O_3)/[Cr]$ of 0.636 while the co-injection of FeSi with air allowed to reduce of 13 % this ratio to 0.551. If early boiling and liquid slag were obtained some additional benefits were achieved with a $(Cr_2O_3)/[Cr]$ of 0.531, i.e., 17 % lower. Co-injection of FeSi with nitrogen was also beneficial providing a $(Cr_2O_3)/[Cr]$ of 0.522, i.e., 18 % lower. This effect became even more pronounced when early boiling and liquid slag were achieved providing a $(Cr_2O_3)/[Cr]$ ratio of 0.375, i.e., 41 % lower. The influence of the co-injection procedure on the scorification of other alloying elements was also investigated, but no systematic variations with respect to the different treatment procedures were observed for both concentrations in the slag and distribution ratio for Ni, Co, Mo and V.

Moving to the trials performed at USI, the studies performed in collaboration with IRSID allowed to address the ability of the slag to develop stable foam to completely cover the electric arc developed between the electrode and the metallic bath. Several trials with dust/carbon blend pneumatic injection and some benchmark trials with no blend injection were performed. A small decrease in the average basicity index, i.e., (CaO/SiO_2), from 1.4 to 1.2 was observed in slag because of dust injection. Furthermore, XRF compositional analysis and temperature data were used in the CEQCSI model used by IRSID to evaluate different characteristics of the resulting slags such as the liquid and solid phase proportions, the chemical composition and the viscosity of the liquid phase. The results highlighted that the proportion of solid phase was in the range of 10-70 % at the end of the melting period and just before slag foaming with blend injection while it was completely liquid after blend injection. Furthermore, a foaming index which described foaming intensity was estimated to evaluate the influence of the process and slag characteristics on slag foaming quality and its effect on EAF performance, e.g., energetic. The results highlighted that an increase in the chromite content of the initial slag jeopardized its ability to develop a good foaming and when the chromite content was higher than 13-15 % the development of the foam became very long, very poor and did not cover the electric arc. The foaming index also depended on the proportion of solid phase in the initial slag, and a good foaming was observed when the solid phase content was less than 35-40 %.

Concerning the development of slag foaming process at USI, the first part of the project was devoted to the development of the dust injection equipment. After creating the 70/30 mix of dust and carbon, the blend was loaded into a truck characterized by 3 tanks of 6.5 m^3 each. The blend was transferred into a silo close to the EAF and with a capacity of 8 m^3. About 25 minutes were necessary to drain each tank. After that, further efforts were necessary to optimize the new process, stabilize the injection and train the operators. Some of the problems encountered were clogging of blend injection or difficulty to initiate slag foaming depending on blend quality, location of the nozzles, blend and oxygen flowrate, etc. A first technical analysis showed that even if the average economic balance was good, an increase in electrodes wear was observed. This was ascribed to furnace door opening during the dust injection period necessary to allow the entrance of the injection lances which led to an important air intake due to the de-dust system. In light of this, an air curtain was built on the top of the furnace door to limit the air intake. Despite the effort, this modification did not lead to the expected decrease in electrode wear because, as the flowrate of the de-dusting device was not changed, new air intake occurred through the top of the furnace. Considering this, the next step of the procedure consisted in adjusting de-dusting device flowrate to limit the air intake and a compromise between a good efficiency of de-dusting device and a low electrode wear was reached.

Further trials were performed in collaboration with IRSID to evaluate the possibility of injecting dust without decreasing the high voltage set point and the effect of this procedure on the temperature of the cooled panels. The arc voltage was usually decreased from 374 to 324 V during the refining period to avoid an increase in cooled panels temperature, but it was observed that dust injection was able to ensure a good slag foaming which in turn resulted in a good thermal insulation. The latter allowed the arc voltage to be kept constant at the highest level thus reducing the power on time. To this aim, the control of slag foaming height was fundamental to ensure a sufficient coverage of the electric arc while preventing deslagging which would cause chromium oxide losses. The height of foaming slag could be

conveniently tailored by controlling the gas quantity generated in the slag which was mainly the CO resulting from the oxidation of carbon coming from the injected blend. Therefore, it could be tailored controlling blend and oxygen injection flowrate. The effect of slag foaming on electric power efficiency was also investigated and an increase in electric arc thermal efficiency with slag foaming was observed. In particular, an increase of this parameter from 22 to 40 % was registered when slag foaming entirely covered the electric arc.

2.1.8 Innovative use of iron and steel making by-products for the sealing and securing of steel industry deposits (16)

The project was coordinated by Dillinger Hüttenwerke with EKO Stahl, FehS, LECES (Laboratoire D'Etude et de Controle de L'Environment Siderurgique), Profilarbed and Verein Deutscher Eisenhüttenleute (VDEh) participating as partners in the consortium. The project started on the 1st of July 1999 and lasted almost three years, ending on the 30th of June 2002. The overall project cost 1.54 M€ and the EU contributed 769 k€, i.e., half of the budget.

Since 1999, one of the main aims of the steel industry was the achievement of zero-waste steel production by efficient exploitation of residues and by-products. Despite this ambitious goal, some mineral materials were still deposited, making necessary the sealing and restoration of the in-house landfills, as well as the existing deposits and abandoned sites. In light of this, the main goal of the project was to verify the feasibility of iron and steel industries by-products or residues as effective sealing materials for the capping of in-house landfills, i.e., iron and steel deposits. The first step of the project included the identification of the main requirements of the sealing systems in relation to the typical steel industrial landfills within the context of the legislative conditions in Europe. Once completed this step, a pre-selection of different by-products and residues was performed as regards a potential sealing function based on soil-physical properties. After this step, suitable techniques were developed to exploit the selected steel residues and by-products for the targeted application to provide evidence of their equivalence in terms of sealing performance with conventional solutions by means of field tests.

The preliminary definition of sealing system characteristics was based on legal specifications. The requirements of a sealing system identified as a landfill class 1 in the German Regulation for Landfills (DepV) were used as basis for the test design. In particular, the main general requirements included mineral single-layer sealing with drainage and restoration. According to these requirements, the use of fine-grained by-products and residues from the iron and steel industry proved to be the most promising alternative to standard top sealing systems, i.e., natural clay minerals. Standard mineral clay liners consisted of very fine-grained particles with an optimized compaction to ensure low pore volumes which could foster water permeation. This characteristic was further supported by the capability of most clay minerals to swell because of water intake. This swelling ability was also responsible for a certain elasticity of the material. Despite this, the main disadvantage of clay-mineral sealing system was their significant shrinkage resulting from water withdrawn which could induce crack formation. Considering this, natural clay minerals could be replaced with suitable fine-grained materials or mixtures if the elasticity of the sealing material was of minor importance due to the static properties of the landfill body. Considering all these aspects, dusts from gas purification facilities of in-house plants

of iron and steel industries, fine-grained dusts from the wet purification of BF Gas, residues from slag processing facilities from BOF and EAF steel plants were identified as feasible candidates for preliminary laboratory tests. Furthermore, the soil physical pre-assortment allowed to refine the selection of the potential residues for sealing mixes allowing to draft the following list: Ladle Slag (LS), EAF Slag, residues of processed steelwork slags, fine-grained dust of the wet purification of BF gas and BF sludge.

The sealing properties of these mixes of by-products and residues were amended with the following reference materials: processed kaolinitic claystone (Clay), polymer amended bentonite (TRISOPLAST®), silica gel and sewage sludge. All these innovative and benchmark configurations were subjected to laboratory trials for a thorough characterization and a supplementary risk assessment. Grain size distribution, water conductivity, shear strength, and proctor test were performed on the sealing materials, and the determination of the pF-Curves was performed for the restoration layers. Furthermore, dedicated experimental test procedures were developed to investigate the mobilization behavior of harmful substances under special environmental conditions. Indeed, the main criterion to evaluate the hazard potential of harmful substances was their concentration in the seepage rather than in the soil because in this way the hazard potential of the heavy metals depended mainly on the bioavailable and mobile proportion of the existing total concentration. In light of this, the harmful substances which could be released from the material together with the conditions under which maximum concentrations occurred in the seepage must be identified to estimate the hazard. For this reason, several kinds of residues were preliminary tested with the method of elution pH_{stat} to determine the mobilization of heavy metals as a function of different pH.

The results obtained from this preliminary characterization of soil and materials at the laboratory scale were fundamental to better focusing on the next step of the research program. The grading curves, i.e., the grain size distribution, of the different mineral sealing materials were obtained since the evaluation of Fuller curves was necessary to minimize the pore volume fraction after compaction and ensure the maximum possible stability. Despite this, increasing amounts of fine-grained fractions were preferred to promote sealing properties. This conclusion was further supported by the results obtained in the present project which confirmed that it was not advisable to follow exactly the Fuller equation, and it was better to use as much fine-grained material as acceptable from the static stability perspective, to achieve effective mineral sealing. Considering this, the Fuller equation was used just to identify the minimum level of fine grain sizes in the sealing materials. Besides the grain size distribution, the compaction degree and the remaining pore volume were influenced by the water content, therefore Proctor tests were performed to find the optimal compaction parameters. Furthermore, water permeability (k) was monitored from 60 up to 200 days and the results highlighted that the 1:1 ratio by weight of LS (ladle slag) and BF sludge mixture was one of the most promising alternative sealing materials presenting a steep decrease in water permeability in the first few days. In particular, the water permeability decreased from 6.2×10^{-7} m/sec to 2.74×10^{-10} m/sec after 10 days with hydraulic gradients of 1 and 10. Furthermore, a continuous decrease in water permeability up to 1×10^{-11} m/sec after 170 days was detected despite increasing hydraulic gradients up to values of 20 and 30. Analogously, the water permeability of the 2:1 ratio by weight LS and BF sludge mixture showed a continuous decrease from 3.17×10^{-8} m/sec to 2.56×10^{-11} m/sec under hydraulic gradients of 10 and 20. After the increase of the hydraulic gradient up to 30, the water permeability of the mixture increased

again up to 2.16×10^{-8} m/sec, but it reached a stable value of about 2×10^{-11} m/sec after 47 days even under a hydraulic gradient of 40.

Concerning the chemical composition of the by-products used in the most promising sealing systems, the LS by Dillinger Hütte was dominated by CaO (49 %) and Al_2O_3 (25 %) with SiO_2 (6 %), MgO (5 %), H_2O (11 %) and Fe_{tot} (4 %) completing the mixture. It must be considered that a huge part of CaO was still soluble and reactive thus being able to undergo hydration and carbonatation processes. BF sludge by Dillinger Hütte were characterized mainly by iron oxides (Fe_{tot} 34 %) and carbon (C 31 %) according to the main input material for BF, i.e., ore, lime and coke, with silicate, aluminum and magnesium minerals and sublimated metal vapor completing the mixture, i.e., CaO 2 %, MgO 1 %, SiO_2 5 %, Al_2O_3 2 %, H_2O 21%, S 1 %, Pb 1 % and Zn 2 %. Considering these data, the chemical composition of the 1:1 ratio by weight of LS and BF sludge mixture was calculated as: CaO 25 %, MgO 3 %, SiO_2 6 %, Al_2O_3 13%, H_2O 16 %, Fe_{ges} 19 %, C 16 %, S 1 %, Pb <1 % and Zn 1 %. This chemical composition and the related mineral changes after emplacement may explain the water permeability decrease observed for this mixture. In particular, the massive presence of Ca could lead to saturated soil water fluxes and the diffusive transportation of Ca from the soil cores to the fine macro pores could cause crystallization processes after the contact with CO_2. Finally, the results of the risk assessment through pH_{stat} test highlighted that heavy metal ions in BF sludge were highly soluble for $pH \leq 4$, but BF sludge were also endowed with a high acid neutralization capacity before reaching this pH range thus ensuring their ability to buffer proton input caused by acid rain for a very long time. Pb and Zn displayed an increased solubility and mobilization not only in strong acid environment, but also in strong alkaline conditions while being almost immobile in the wide range in between them. In particular, the minimum solubility for both elements was registered between pH 9 and 11.5. It was concluded that the threshold values given by the German Technical Advice of Municipal Wastes for landfill-class I would have been exceeded only under strong alkaline conditions, i.e., pH>12.5. Moving to the LS and BF sludge mixture, the worst-case scenario for heavy metals solubility was again registered under acid conditions, but with Pb and Zn mobilized also in a strongly alkaline medium. The concentrations beyond the threshold values provided by the German Technical Advice of Municipal Wastes for landfill-class I were reached by Pb for pH > 13.2 and by Zn for pH > 12.8. In light of this, it can be concluded that the use of the mixture allows to increase the pH range between with low solubility of heavy metals.

After this preliminary phase, pilot and demonstration plant scale test fields were created to compare the efficiency of the novel alternative sealing systems to those available on the market. At first the water balance parameters of sealing systems under in situ conditions were studied. In particular, the minimum information which was necessary to record to describe the hydraulic conditions and processes of the various sealing systems were the atmospheric precipitation (P), the surface run off (Q_{surf}) which could occur in sloping locations, the drainage flow lead off onto the sealing layer (Q_{dr}), drainage flow percolated through the sealing layer and forming the seepage rate (Q_{perc}), the soil-water and snow storage (ΔSB) and the real evapotranspiration (E_{Treal}) given by the summation of the evaporation of the Soil-Surface (E_s), leaf interception of the vegetation (E_i) and plant-physiological transpiration (T). Therefore, the simplified equation to describe the water balance of the sealing system in the field test was:

$$P = Q_{perc} + Q_{surf} + Q_{dr} + E_{Treal} \pm \Delta S_B \quad (mm)$$

The values of P, Q_{surf}, Q_{dr}, Q_{perc} could be measured with a lysimeter while E_{Treal} must be derived exploiting the following auxiliar parameters to record on site: wind velocity, air temperature at 200 and 5 cm over ground, soil temperature at 20 and 50 cm underground, air moisture, global radiation and estimated values as leaf area index (BI), range of effective root presence (W_{zreff}) and start/finish of the annual vegetation period. The field tests were carried out to evaluate the actual efficiency of the novel capping systems considering not only the technical sealing layer itself but also the water balance of all including cover system because the results obtained in previous investigations proved that the whole capping system including vegetation, restoration layer, technical sealing liner and the drainage layer could significantly affect the long-term sealing function.

The large-scale lysimeter test field was constructed at Dillinger Hüttenwerke on the north-west flank of the existing steelworks landfill characterized by an approximate elevation of 190 m above sea level and a slope gradient of approximately 23°. The annual average precipitation at the location between 1961 and 1990 was 780 l/m^{2}and the annual average temperature was 8.5 °C. The landfill body exhibited a Proctor density ratio between 98.8 and 105.5 % at 30 cm depth under soil. The basic structure of the 12 test fields with a hydraulic area of 202.8 – 214.5 m^2 and an effective hydraulic basis area of 188 - 199 m^2 is shown in Figure 2 A. The fields were spaced one another of 3 m and each field was endowed with its own measurement shaft to contain the equipment. The standard soil profile used consisted of a 30-70 cm vegetation layer made of grassland with herbs, a 10cm top soil made of humous soil of weathered red sandstone, a 90-190 cm soil made of weathered Red Sandstone, 30 cm drainage necessary to supply infiltration water (Q_{perc}) to the metrology, a 2-50 cm technical sealing layer, a 20-90 cm basis drainage, a 2.5 mm basis sealing flexible membrane liner, and a protection Layer, i.e., Landfill Body with 5 cm protection layer. An example of on-site sealing layer deposition during the project period is given in Figure 2 B. Sensors for surface run off (Q_{surf}), drainage flow (Q_{dr}) and the collected leakage through the technical sealing layer (Q_{perc}) were installed and continuous information on the fluxes were collected with a resolution of 2-30 s. Relevant climatic parameters were also monitored and weather data were collected after installing a weather station directly on the location of the landfill. Furthermore, constructive precautions were taken to avoid sidewall leakage effects based on the experience gathered in previous similar projects. The efficiency of the new alternative sealing systems proposed in the present projects was compared to the water balance of more traditional sealing systems used as benchmark under the same conditions at the same site. In particular, the reference systems selected were: 1) 2×25 cm compacted Claystone, 30 cm Drainage, 100 cm Restoration (Test Field 9) 2) 600 g/m^2 Geosynthetic Clay Liner, 30 cm Drainage, 100 cm Restoration (Test Field 2) 3) 10 cm TRISOPLAST®, 30 cm Drainage, 100 cm Restoration (Test Field 3).

The six alternative sealing systems investigated were: 1) 2×25 cm mixture of LS and BF sludge provided by EKO with a ratio by weight of 2:1, 30 cm drainage, 100 cm restoration (Test Field 4) 2) 10 cm mixture of polymer-amended bentonite with LS in substitution of sand according to the TRISOPLAST system deposited upon 40 cm of simulated landfill body, i.e., compacted LS and BF Sludge, 30 cm drainage, 100 cm restoration (Test Field 5) 3) 2× 25 cm mixture of LS and BF Sludge by Dillinger Hütte

with a ratio by weight of 1:1, 30 cm drainage, 100 cm restoration (Test Field 6) 4) 2× 25 cm mixture of LS and BF Sludge by Dillinger Hütte with a ratio by weight of 2:1, 30 cm drainage, 100 cm restoration (Test Field 7) 5) 2× 25 cm mixture of kaolinitic clay stone and BF sludge by Dillinger Hütte with a ratio by weight of 1:1, 30 cm drainage, 100 cm restoration (Test Field 8) 6) 2×25 cm mixture of silica gel-amended EAF Slag and sewage sludges by ProfilArbed, Luxembourg and additionally 10 cm infiltration layer of loess soil (Test Field 10). The influence of the restoration layer was also assessed and the mixture from Test Field 6 was used also in Test Field 1 applying a minimum restoration layer with a thickness of 30 cm to intensify and accelerate the negative effects resulting from drying out processes, temperature extremes and rooting damage. Furthermore, standard and qualified capping systems with 200 cm restoration layers using simulated landfill bodies were tested with (Test Field 12) and without (Test Field 11) drainage. A total of 12 soil profiles variations were used as summarized in Figure 3.

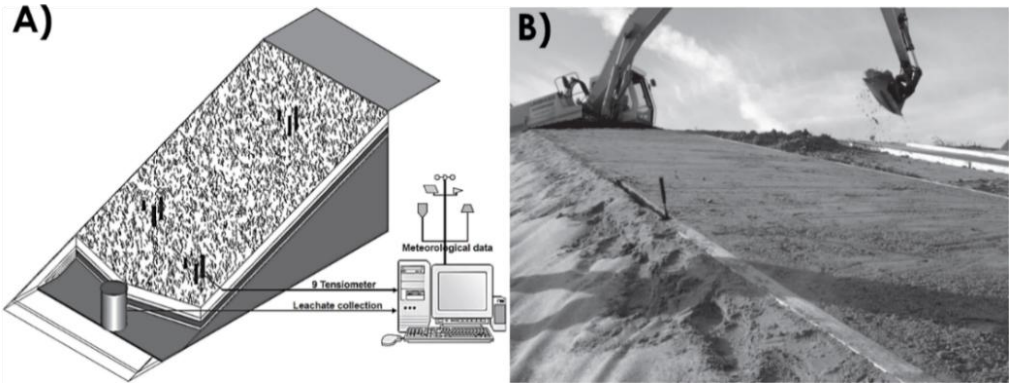

Figure 2: Schematization of the test field (A) and practical example of the sealing layer deposition procedure. (16)

Weather data of the investigated period reported a measured annual atmospheric precipitation of the test field of 754 l/m^2 in 2002, 605 l/m^2 for the first year of monitored water balance and 715 l/m^2 in the period from 1 April 2002 until 30 June 2003. Data regarding surface run off (Q_{surf}), real evapotranspiration and water flow in the upper and base-drainage, i.e., drainage Interflow upon the technical sealing layer (Q_{dr}) and basis drainage Interflow (Q_{perc}) which represent the potential infiltration water, were collected for a period of 15 months. The data were recorded every 2 s from each sensor and were then summed over each day to obtain the daily trend. In a second step, daily data were summed and condensed into curves. The results showed that surface run off was characterized by a good correlation to the precipitation in synchronous behavior for all variations, therefore it was concluded that the same behavior for the runoff could be expected for all variations with less than 1 % deviation related to the precipitation input. Concerning the drainage interflow, three different phases were detected for all variations under consideration. In the first phase, i.e., the first two months, the drainage water flow was characterized by a delivery from the soil water reserve of the restoration layer resulting from the melting of the previous snow and from the previous rainfall which saturated the restoration layer leading to a delayed delivery. This phenomenon almost stopped

at the latest end of May despite the continuous refill provided to the restoration layer by new rainfall. At this point the second phase started where real evapotranspiration (E_{Treal}) and field capacity-refill of the restoration (ΔSB) transcended the precipitation input. Indeed, almost no water reached the drainage layer from 237.3 l/m^2 rainfall during April until the end of August. After the end of the vegetation period the evapotranspiration effect decreased. Finally, conspicuous delivery of soil water into the drainage layer was observed in the third phase. The main differences between the variations investigated at the end of this first monitoring period depended mainly on the effectiveness of the sealing layer in combination with the water supply from the restoration. In particular, the three references F2, F3 and F9 with very low saturated water conductivities showed higher amounts of drainage water. Finally, the base drainage water flow, i.e., the potential infiltration of the landfill body covered with the tested sealing systems, was assessed. The behavior of the different variations investigated could be divided in three groups. The first group included variations 1, 3, 6, 9 and 10 which displayed very balanced curves. The second group included variations 2, 4, 8 and 12 and displayed a significant increase in leakage after the end of the vegetation period and of the increasing supply of drainage water. Finally, the last group included variations 5, 7 and 11 and was considered unreliable due to sensor defect. The highest amount of infiltration water was 47.8 l/m^2 and it was measured for Test Field 12. This value was followed by 42.7 l/m^2 of Test Field 2 and 34 l/m^2 of Test Field 4 after 15 month and 715 l/m^2 precipitation. Despite being the worst cases, these results remained beneath 7 % of the precipitation.

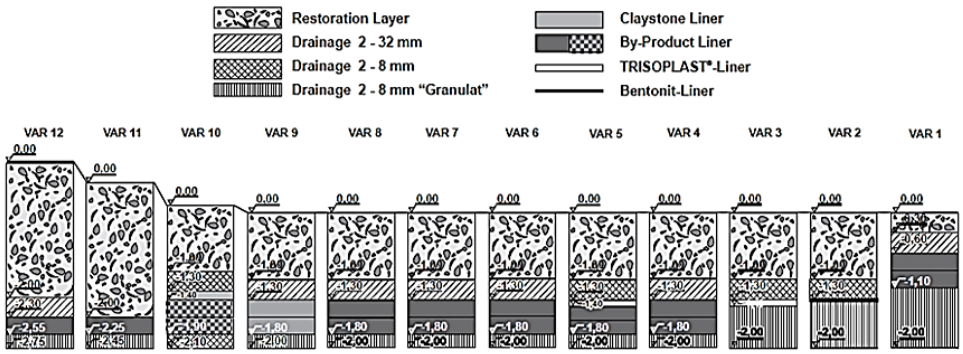

VAR 1	LS: BF Sludge = 1:1 with minimal restoration layer, 30 cm
VAR 2	Bentonite Geosynthetic Clay Liner with standard restoration layer, 1 m
VAR 3	Amended mineral liner TRISOPLAST® with standard restoration layer, 1 m
VAR 4	LS : BF Sludge = 2 : 1 by EKO with standard restoration layer, 1 m
VAR 5	Amended LS liner placed on a 2nd layer of Steel Work Slag : BF Sludge = 3 : 1 with standard restoration layer, 1 m
VAR 6	LS : BF Sludge = 1 : 1 with standard restoration layer, 1 m
VAR 7	LS : BF Sludge = 2 : 1 by Dillinger Hütte with standard restoration layer, 1 m
VAR 8	Clay : BF Sludge = 1 : 1 with standard restoration layer, 1 m
VAR 9	Standard TASi Claystone mineral liner with standard restoration layer, 1 m
VAR 10	Amended Mixture of LF Slag : EAF-Slag with standard restoration layer, 1 m
VAR 11	Capping System; hydraulically optimised Restoration Layer (2 m) on the compacted landfill-body without drainage
VAR 12	Capping System; hydraulically optimised Restoration Layer (2 m) on the compacted landfill-body with drainage

Figure 3: Soil profiles used in the 12 different test fields (16)

The registered data allowed calculating the water balance of the different systems. Considering the reference systems and in particular test field 2, i.e., GCL (Geosynthetic Clay Liner) Bentonite Mat, 100 cm Restoration, almost 60 % of the precipitation input was evaporated by surfaces, transpired by the vegetation or stored in the restoration soil, 32 % was drawn away by the drainage of the sealing and only less than 6 %, i.e., 42.7 l/m^2 of 715 l/m^2, permeated the sealing system. Comparing the results with the ones of test field 12, i.e., 2 m restoration layer, a decrease in strength of the restoration after each subsequent rain event was observed probably due to bentonite swelling after water intake. The results also highlighted that test field 12 was able to react to every precipitation event due to the 2 m-thick restoration layer thus resulting in an increased drainage flow and in relation to the resulting permeability of the entire sealing system. The best results in terms of sealing system penetration were achieved with test field 3 thanks to the TRISOPLAST® sealing layer which ensured a base drainage of only 0.1 l/m^2 from 715 l/m^2 precipitation. Good results were also achieved with test field 9, i.e., compacted clay with 100 cm Restoration layer, with only 0.25 l/m^2 from 715 l/m^2 precipitation. Moving to the alternative sealing systems, test field 4, i.e., the LS and BF sludge mixture sludge from EKO-Stahl, displayed a sealing efficiency comparable to the reference test field 2 with a penetration of 34.8 l/m^2 from 715 l/m^2, i.e., 4.9 % of the precipitation. Test field 6, i.e., the 1:1 LS and BF sludge mixture, and test field 10, i.e., EAF slag with silica gel and sewage sludge, also displayed very promising results with a high sealing efficiency and very low infiltration rate, i.e., < 1 % and equal to 0.2 % of precipitation, respectively. Finally, only 2.7 % of the rainfall, i.e., 19.05 l/m^2 from 715 l/m^2, penetrated the sealing system with test field 1, i.e., the 1:1 LS and BF sludge mixture with a thinner 30 cm restoration layer. Seal effect of test field 1 can be considered good compared with other variations, but it was significantly lower than test field 6 which differed only for the thicker restoration layer which resulted in a lower water balance effect.

The results obtained from the pilot and plant were used to calibrate a mathematical model aimed at providing water balance for other sites or under divergent climatic conditions. In particular, the Hydrologic Evaluation of Landfill Performance (HELP) model was selected by Dillinger Hütte while LECES used many different models like PLEFFIC (PLuie EFFICace), SWIM (Soil Water Infiltration and Movement), GMSFEMWATER (Groundwater Modelling System – Finite Element Water) and MARTHE (Modélisation d'Aquifère par un maillage Rectangulaire en régime Transitoire pour le calcul Hydrodynamique des Ecoulements). HELP was a semi-two-dimensional hydraulic model for landfill water balance able to process information relating to weather, soil physics and profile structures and to simulate surface run off (Q_{surf}), real evapotranspiration (ET_{real}), leakage, drainage flow (Q_{dr}) and percolation through sealing liner (Q_{perc}).

The project demonstrated that mixtures easily manufactured starting from different mineral by-products and residues from the iron and steel industries could be conveniently used as sealing materials in top capping systems of statically stable industrial mono-landfills. The efficiency achieved under the climatic conditions investigated was perfectly comparable with the one of the commercially available sealing materials selected as reference system, even if the monitoring time was relatively short. All the test fields created for the comparative efficiency test of the alternative sealing systems indicated that system permeability was significantly below 8 % of precipitation after 15 months of observation. It was concluded that compared with traditional sealing materials available on the market, the alternative

sealings solutions obtained from silica gel amended EAF-slag system using ProfilArbed materials, a clay-liner with a 50% substitution of natural clay by BF sludge using DH materials and a sealing from complete substitution through a mixture of LS – BF Sludge with 1:1 ratio using DH materials show comparable or better sealing efficiency. The identification of this new potential field of application for the by-products and residues of the steel industry clearly entailed some paramount economic and industrial benefits. For example, an evident cost reduction of the sealing systems for in-house landfills can be achieved by exploiting own by-products and residual materials in substitution to clay thus lowering the purchase costs. In particular, it was estimated that moving from the standard sealing system based on 2×25 cm clay-sealing layer to variation 6, a cost reduction of approximately 25 €/m^2, i.e., 2.5 M€ for 100.000 m^2.

2.1.9 Characterization, modelling & validation of the impact of iron and steelmaking slags used in road construction on groundwater (17)

The project was coordinated by LECES with Austrian Research Centers (ARC), FEhS, and Laboratoire central des ponts et chaussées (LCPC) participating as partners in the consortium. The project started on the 1st of July 2000 and lasted almost three years, ending on the 30th of June 2003. The overall project cost 860,5 k€ and the EU contributed 516 k€, i.e., 60 % of the budget.

In 2000, slag from steel production were already characterized by a long tradition as building materials in road construction and hydraulic engineering. Despite their technical suitability, the environmental compatibility of these aggregates was a major concern which required an in-depth analysis. In light of this, the present project aimed at completing and updating the existing data on slag environmental compatibility through laboratory and in situ experimental campaign, but also at developing a computer-aided hydro dispersive model to rate the impact of steelmaking slags on soils and groundwater. The results of the model were intended to be converted into a technical guideline summarizing the rules for the good use of these residues in the building sector. The research program was divided in five phases: 1) Slag selection and preparation 2) Characterization of the slags and their mixtures at laboratory scale to investigate paramount properties such as water response 3) Modelling the pollution transfer impact of the slags on soils and groundwater by using hydro dispersive models considering different hydro-geological and weather conditions 4) In situ validation by road investigation 5) Guidelines definition.

Slag selection focused on the four quantitatively most significant types of slags in the iron and steel sector, i.e., BF slag, Granulated blast furnace (GBF) slag, BOF slag and EAF slag. Furthermore, three mixtures typically used in road construction were selected because slag components were often mixed together to combine the characteristics of the single components and achieve optimized technical and environmental properties. Mixture 1 (M1) was produced with 15 % of GBF slag and 85 % of air-cooled BF slag, mixture 2 (M2) was produced with 25 % of BOF slag, 15 % of GBF slag and 60 % of air-cooled BF slag and mixture 3 (M3) was produced with 15 % of GBF slag, 84 % of air-cooled BF slag and was hardened with 1 % of CaO in a proctor-cylinder. The seven configurations were characterized at the laboratory scale through chemical and physical analysis, batch leaching tests, tank leaching test, up flow column percolation test, downflow lab-lysimeter test, climate chamber test, and hydrodynamic

characterization. Two types of percolation tests depending on temperature variations were performed, i.e., percolation tests under normal temperature conditions and percolation tests after drying-wetting cycles and freezing and thawing cycles. Furthermore, in situ percolation tests were performed at the pilot scale in Nantes with the pilot lysimeter. Chemical analysis performed with XRF, ICP-MS (Inductively Coupled Plasma-Mass Spectrometry) and AAS confirmed that the chemical composition of the slags investigated was representative of the different types of steelmaking slags selected. Physical analysis focused on the identification of the particle size distribution of the four base slags and the grading curves obtained were within the expected limits for each particle size interval: EAF and BOF 0/32 mm, BF 0/45 mm and GBFS 0/4 mm.

Considering that building materials are characterized by complex leaching mechanisms which strongly depend on construction design and environmental conditions, e.g., rainfall and temperature, this aspect was deeply analyzed performing two different laboratory leaching tests: compliance test EN 12457-4 and single German tank test EN1744-3. EN 12457 compliance test aimed at studying the short-term leachability of granular waste materials and sludges and was performed using a liquid/solid ratio of 10 and a maximum grain size of 10 mm to be consistent with the German standard DIN 38414-4 which was the base for the German legislation in the matter of waste avoidance and management. The single German tank test EN1744 was more suitable for coarse grained materials and allowed to perform the test circulating constantly the leaching medium with a motor thus avoiding the agitation of the entire container which could cause mechanical stresses on the material investigated. The tests were performed with almost the same conditions used for EN 12457, i.e., liquid/solid ratio of 10 for 24 hours. Both types of tests were good to speed up the long-term leaching of aggregates allowing to understand their response in contact with water and to point out potential differences between the selected building materials. Despite their utility, they could not reflect the real impact of aggregates on soil and ground water because they did not account for aspects such as the effects of adjacent soil and construction, emission of pollutants by air, the chemistry of the upstream runoff water, etc. The results highlighted low Cr concentrations below or at the determination limit of 10 mg/l. This was ascribed to the fact that the binding of an element in the mineral phases played a more significant role in its leaching behavior than its total content. This conclusion was further confirmed by the low concentration of heavy metals in the eluate. In this case, a strong influence of pH-value and ionic strength in the leachate was also observed. Indeed, the alkaline environment resulting from the presence of free lime and other calcium mineral phases in the steel slag can prevent heavy metals from leaching and their alkaline buffer could be strong enough to prevent the leaching of heavy metals over more than a road construction lifecycle. The results for M3 underlined a higher pH-value, electrical conductivity and Ca and Ba concentrations in the leachates together with a lower leaching of sulphates (SO_4) compared to M1. The lower SO_4 leaching was probably caused by a reduction of the available surface and determined an alteration of the equilibrium conditions of low soluble barium sulphate causing a higher leaching of Ba.

Up-flow percolation tests were also performed by pressing the leachant at the base of the column containing the slags to permit an up-flow stream. The results for the three mixtures displayed a fast decrease over time of the easily leachable elements such as SO_4 and Cl, but also NO_3 in M2 and M1. Slower leaching kinetics were observed for Ba which was present in small amount in the mixtures.

Downflow percolation tests, i.e., lysimeter tests, were also carried out to investigate the long-term leaching behavior of the aggregates spreading the leachant from the container on the surface of the sample. The results for GBF slag percolate reported a pH between 9.6 and 10.3, a decreasing electrical conductivity and a Ba concentration close to the 10 mg/l determination limit. The results for BF slag percolate highlighted increasing pH values from 9 to 10, a significant decrease in SO_4 with thiosulphate (S_2O_3) decreasing from 341 to 2 mg/l and a constant Ba leaching of 50 mg/l. Concerning BOF slag, high pH values of 12 were registered due to the leaching of Ca(OH) resulting from the presence of free lime. The results also reported a progressive decrease in percolate electrical conductivity, in Ba concentrations from 110 to 30 mg/l and in Cr concentration from 50 to 20-30 mg/l. Cu concentration was mostly below the 10 mg/l determination limit. Due to the absence of free lime, EAF slag percolates were characterized by lower pH, i.e., 11.3, and electrical conductivity values than BOF slag. Ba concentration decreased from 110 to 90 mg/L as well as Cr concentration which decreased from 30 to 10 mg/l. Again, Cu concentration was mostly below the 10 mg/l determination limit. M1 and M2 displayed a behavior like the one of the base slag, i.e., BF, with sulphate being the most significant parameter which experienced a decrease of the leaching of a factor of 4-5. Considering this, a negative effect of mixing the aggregates was not observed. Furthermore, the concentration of Cr and Cu in M1 proved to be below the determination limit while for M2 the presence of BOF slag allowed a detection of Cr leaching which decreased from 30 mg/l to 10 mg/l.

Climate chamber and leaching tests were also performed in percolation cylinders filled for 50 cm of their height with slag similarly to the sub-base thickness in road construction. Sample surface was constantly irrigated during the wetting operations, and the percolate was collected after 1-2 hours from the beginning of the wetting operation. The percolates of 40 wetting operations were analyzed and after the 8th and 33rd cycle the wetting operations were stopped for 3 and 5 months, respectively, to figure out the effect of longer drying periods on the quality of the percolates. At the end of the whole campaign three freezing/thawing cycles (FTC) were carried out by freezing the aggregates at –20 °C for 3 days in a climate chamber and then thawing them for 4 days under ambient conditions. After each FTC a wetting operation was performed, and the next FTC was started immediately after percolate sampling according to the normal wetting operations. The results of the wetting/drying cycles for BF slag highlighted the highest SO_4 concentrations at the beginning of the experiment and the lowest pH values compared to all base slags. A significant effect of the drying period was observed on BF slag because the percolate showed a significant drop in SO_4 concentration after both drying periods, even if a constant increase in this parameter was observed after the first drying period until reaching concentrations comparable to the initial ones. Afterwards a continuous decrease took place, and the final leaching presented a concentration of about 40-50 % lower than the initial value. Similar behavior was observed for Ca and conductivity. BOF slags were characterized by a high conductivity and a highly alkaline pH value (12-12.5) at the beginning of the tests due to the presence of Ca(OH) in the slag and contained high Cr concentrations between 10-15 µg/l which remained almost constant during the wetting-drying-cycles. Analogously, the initial high Ba concentrations up to 500 µg/l remained constant for most of the experiment decreasing visibly just in the last cycles after the second drying. Concerning EAF slag, Cr concentration was the most important parameter regarding environmental aspect because it was about 40 µg/l, i.e., about 4 times higher than BOF slag, during most of the wetting-drying cycles.

Also, Ba concentration was slightly higher than those of the other base slags except BOF slag. A continuous increase in this value was also observed for increasing numbers of wetting-drying cycles. To conclude the analysis of the base slags, GBF slag was characterized by initial high Cl concentrations, i.e., about 60 mg/l, which rapidly diminished to values comparable with the other base slags due to its quick release. Similarly to the evolution of Cr in EAF slag, the first percolates after the drying cycles displayed significantly higher Cl concentrations thus allowing to conclude that both EAF and GBF slag were the only ones with a clear reaction to drying regarding their characteristic parameters.

Moving to the mixtures, M1 displayed initial values of conductivity, pH, Ca and SO_4 concentrations comparable to the range of pure BF slag, but it also revealed a constant decrease of the major parameters in the percolates with values significantly lower than BF ones after the end of the wetting-drying cycles. Regarding M2, the lower portion of BF slag and the mixing with BOF ones allowed to achieve a higher pH value around 11-11.5 which did not change significantly during the wetting-drying cycles. Ca and SO_4 concentrations were quite low, i.e., 5 to 10 times lower than in the base slags, and their decrease for increasing wetting-drying cycles was only slightly detectable. This was ascribed to a fixation of these components within the slag resulting from the reaction between the constituents of M2. Furthermore, Cr concentration was not detectable despite BOF slag addition in the admixture. Finally, M3 displayed significant differences in its leaching behavior compared to M1. No initial maximum SO_4 and Ca concentrations were detected with initial values comparable with M2. Higher pH values of 11-11.5 compared to pH 10 of M3 were also observed due to the transformation of quicklime into Ca(OH). This difference in pH was probably responsible for the different leaching behavior of M1 and M3 since the higher pH value of M3 endorsed the reaction between the different slag components which resulted in the fixation of Ca and SO_4 from the very beginning. This caused Ca concentration to remain constant while SO_4 concentrations increased towards the end of the experiment. This was ascribed to recrystallization phenomena occurring in M3 which resulted in a higher SO_4 release at the later stages. For all slags and mixtures, except EAF and GBF slag, an increase in the concentration of the characteristic parameters was observed after FTC due to the formation of new fracture plains which made available new areas for the leaching. All mixtures and BF slag displayed a significant increase in Ca and SO_4 concentrations, BOF slag an increase in Ca and Cr concentration and in conductivity, while the effect on EAF and GBF slag was of minor importance interesting only a slight increase in conductivity. Overall, an increase in the characteristic percolate concentrations in the range of 150-200 % was achieved compared to the last percolate before the FTC. It was not possible to compare the results of laboratory lysimeter and FTC tests with the ones of practical conditions, but the impact of FTC on leachate concentrations was regarded as the worst-case scenario. Indeed, the frost event in FTC started with high amounts of residual water in the slag body while under practical conditions a much lower water content can be expected and the effect of freezing on the subsequent leaching would be much less pronounced than in the laboratory tests.

Moving to the pilot scale, downflow lysimeter tests were performed complementary to laboratory tests. Mixture M3 was not included in the campaign but a blank with natural quartzite aggregate was used as basic comparison. The boxes containing the aggregates were exposed to rainfall to trigger the leaching process and to ensure a correct comparison of the results obtained with laboratory ones. The effect of using rainfall rather than deionized water was considered by collecting and evaluating the

quality of the rainfall. All materials displayed alkaline pH with BOF slag presenting the higher pH value of 12.5-13, EAF slag and M2 of 11-12 and M1 from less than 10 to 11.5 due to the absence of BOF slags. Regarding SO_4, BOF slag released less than quartzite while M1, i.e., 85% of BF slag, released the most. Regarding Cl, BOF slag released less than quartzite while the higher release was from BF slag with a plateau value at 32 mg/kg and all other materials and mixtures being comprised in between them. Regarding F, the leaching from M1 and M2 was similar to quartzite one while BOF slag displayed the highest value of 15 mg/kg. Regarding Ca, all materials and mixtures released more than the blank with EAF slag releasing 90 mg/kg, M2 145 mg/kg and BOF slag 550 mg/kg at the final liquid-solid (L/S) ratio. Regarding Cu, all materials and mixtures released more than the blank with BOF slag releasing 2.6 mg/kg, BF slag 3.9 mg/kg, M1 3.5 mg/kg, EAF slag and M2 3.4 mg/kg. Regarding Ni, all materials and mixtures released concentrations similar or lower than the blank while regarding Cr all release were above the blank one with the most important of 78 mg/kg at final L/S ratio from EAF slag. All other materials and mixtures were between these two extremes, e.g., BOF slag 6.8 mg/kg, M1 and M2 6.2 mg/kg. Concerning Cd, its release was negligible for all materials and mixtures, i.e., < 0.1 mg/kg. Regarding Ba, fluxes from all configurations were far higher than blank ones. It was concluded that regarding the impact of BF and steel slag on the environment, alkalinity, high electric conductivity, Ca and Ba concentrations affected mainly BOF slag, SO_4 and S_2O_3 mainly affected BF slag, Cu concentration affected mainly BOF and EAF slags, Cr, V, B and Mo concentration affected mainly EAF slag, while Ni and Cd did not represent a problem.

The identification of BF and steel slag hydrodynamic properties was also fundamental because mechanical performance and pollutant release were strongly dependent on water content and moisture changes. Aggregates hydrodynamic properties were determined in water saturated and non-saturated conditions by measuring the permeability (K_{sat}) and establishing its relationship with water content (W) and water retention or suction (S), i.e., the strength that a material exerts to keep the water in its pores. Considering that the relation between these two parameters is not linear, it is advisable to draw the suction curve S=f(W) of a material using a pressure chamber to apply different pressures to a given material and measure its water content for each pressure. These tests were performed on all 4 base materials and on mixtures M1 and M2. After saturating samples with water, they were submitted to hydrodynamic tests to obtain water retention curve and saturated permeability. The results for the saturated hydraulic conductivity showed that GBF displayed a relatively high permeability due to its lower compaction rate of 97 % compared to the 100 % of other materials. BF slag displayed a hydraulic conductivity of one order of magnitude lower than GBF as well as M1 due to the addition of 15 % of smaller GBF slags which were able to enter the voids between the coarser particles of BF. BOF slag permeability was close to BF slag one while EAF slag permeability was one order of magnitude lower and comparable to M2 one. The retention curves composed of the hydration curve h and the drainage curve d were expressed as a function of water content. The results highlighted that all materials behaved more like sand rather than like silt and the retention curves of all materials showed the typical hysteresis phenomenon with the drainage curve (d) shifted with respect to the hydration curve (h). This is due to the drainage pressure of a pore which is inversely proportional to its entrance radius, r, while the re-hydration pressure of the same pore is inversely proportional to its radius, R, which is R > r. This allowed to conclude that the suction on the drainage

curve is always higher than the one on the hydration curve for a given water content and the hysteresis phenomenon is more marked with coarse aggregates. For example, coarse GBF slag were able to retain high amount of water (42.5 vol.%) under low suction pressures, but small changes in this parameter caused fast water drainage leading to only 7 vol.% under a pressure of 100 cm which was close to its residual water content of 5 vol.%. EAF slag behaved like a thinner material despite being coarser than GBF slag probably due to the high 100 % compaction achieved which significantly reduced the global volume of voids and the dimensions of the remaining ones. This clearly caused a reduction in the overall saturated water content (24 vol.%) and an increase in the retention strength of the small pores. BF slag and M1displayed a behavior comparable to EAF slag one. BOF slags were able to keep high water content at high pressures as EAF and BF slag and M1, but for low pressures they could not catch more water because the total void volume was lower than the one of the other materials. M2 showed a behavior like BOF slag with a slight shift on the right side of few percents due to higher void volume. It was concluded that BOF slag was the base material less prone to water content variations and that all base materials and mixtures, except GBF slag, presented a volume water content always higher than 14-21 % in the range of pressure generally observed in road layers. These values were fundamental to model water transfer under non-saturated conditions, i.e., the most common one in slag layers, and were useful to describe slag behavior in the short transient period after implementation in road construction. Indeed, the water content in the slag and the water potential of the structure in this period need to balance each other until equilibrium is reached. Indeed, if implemented slag water potential was higher than road structure one, the slag was excessively dry tending to re-hydrate while if the water content of the implemented slag has a water potential lower than road structure one, the slag is excessively wet and tend to release water. This aspect must be carefully controlled in this transition period because material mechanical properties and bearing capacity depend on its water content, even if slag seemed to be slightly affected by this phenomenon.

All laboratory and pilot tests allowed to calculate elements mobilization kinetics, i.e., curves which describe leached element concentration as a function of time, which were essential for modelling. Indeed, the MISP (Modèle d'Impact sur les nappes Souterraines) model selected required to impose the input signal of concentration over time. The form of this signal was determined for each element by sigmoid adjustment of the results because it was the one which best fitted the data displaying a correlation coefficient > 0.85. The slag and mixtures considered for modelling were BF_{air}, EAF, GBF and BOF slags plus M1 and M2 mixtures. The selection of the most appropriate data as input signal for the model was performed and it was concluded that rack lysimeter data should have led to realistic results while ensuring a safety margin. The modelling activity aimed to evaluate the incidence that steelmaking slags use as road materials could have on the quality of underground water. This was done through sensitivity tests which assessed the effect of large variations of several parameters and through modelling of some typical cases corresponding to possible European situations. The model considered cinematic dispersion and molecular diffusion while neglecting adsorption-desorption phenomena and chemical reactions between the elements dissolved in the water and the surrounding environment.

Sensibility tests assessed the effect of different parameters envisaging different configurations. The influence of input signal shape in the aquifer was assessed considering the effective rainfall, the possibility to set up a cover with low permeability on the slags, the thickness of the slag layer, the

nature of the chemical element considered and the unsaturated zone. The influence of the type of aquifer was assessed considering its nature, i.e., alluvial, crystalline or karstic, and its productivity while the influence of the road infrastructures geometry and position with respect to the main axis of ground water runoff were assessed considering highway and earthwork parallel or perpendicular to the main axis of the ground water flow. The reference data used for comparison were an effective rainfall of 406 mm/year, a highway infrastructure 50 m wide and 10 km long whose axis were parallel to the ground water runoff axis, the absence of a cover with low permeability on the slags, a slag layer 0.5 m thick, an unsaturated zone 5 m thick, a moderately productive alluvial aquifer 10 m deep and an initial concentration of the groundwater equal to zero for all elements. The time steps used followed a logarithmic progression according to 4 modules, i.e., 0.1 to 1 year, 1 to 10 years, 10 to 100 years and 100 to 1000 years, with each module presenting 75 steps. The parameters chosen to describe the morphology of the pollutant restitution curves and to compare the different scenarios were t_{peak}, i.e., the time necessary to reach the concentration peak in the aquifer, C_{peak}, i.e., the maximal concentration corresponding to t_{peak}, $t_{min.1/5}$, i.e., time necessary for exceeding the concentration value $C_{peak/5}$, $t_{max.1/5}$, i.e., time necessary to be located again below the concentration value $C_{peak/5}$. The legal limit values considered were 250 mg/l for SO_4 and Cl, no maximal admissible concentration just a recommended value of 100 mg/l for Ca, 1.5 mg/l for F, 0.7 mg/l for Ba, 2 mg/l for Cu, 50 mg/l for Cr.

The effect of rainfall proved to be determinant with an increasing impact on groundwater for increasing value of effective rainfall. The implementation of a cover proved to be beneficial, decreasing the impact on groundwater by 2-4 times in good condition up to 20-350 times in very good conditions. Increasing values of slag layer were responsible for higher impact on groundwater and the maximum authorized concentration in SO_4 would be reached for a slag layer 2 m thick. Concerning the unsaturated zone, adsorption-desorption phenomena and chemical reactions between the elements dissolved in the water and the surrounding environment were neglected but parameters such as tortuosity, dispersivity, thickness, volumetric water content were considered to model the unsaturated zone in MISP. The variations of these parameters did not influence significantly the results. The main aquifer types considered were alluvial, crystalline, and karstic and their main parameters, e.g., hydrodynamic, productivity, hydro dispersive, were taken from bibliography. Modelling results showed that pollutant restitution was faster, less spread throughout time and the concentration peak less important when the productivity of the aquifer increased and this phenomenon was more pronounced for alluvial and karstic aquifers. Finally, the effect of slag layer geometry was investigated and for an infrastructure parallel to the groundwater flow the concentration peak for a highway was 1.6 times higher than for an embankment. This difference reached a value of 4.3 times when the infrastructure was perpendicular to the aquifer flow. It was also observed that concentration peaks were higher for infrastructure parallel to the aquifer flow than for infrastructure perpendicular to the aquifer flow with proportionality factors of 3 for a highway and of 5.3 for an embankment.

Considering typical cases corresponding to possible European situations, the configurations considered are summarized in Table 1 and the reference values considered in this case were a rainfall of 800 mm/year, a highway infrastructure 5 km long whose axis was parallel to the groundwater runoff axis. The time steps chosen followed logarithmic progression according to 3 modules, i.e., from 0.1 to 1 year, from 1 to 10 years and from 10 to 100 years, with each module having 75 steps. The parameters

chosen to describe the pollutant restitution curves and make comparisons between different scenarios as well as the reference concentrations used were the same used for sensitivity tests.

The results for a fairly productive alluvial aquifer demonstrated that the dilution into the aquifer was quite important, allowing element concentration never reaching the reference values for all configurations tested. Embankment proved to cause a higher impact in terms of concentration in groundwater than highway and covered highway were more impacting than uncovered roads because the surface and the volume of the slag layer was much higher for a highway than for a road. Despite this, coverage of the slag layer significantly limited the infiltration rate through the slag layer thus reducing pollutant flux towards the groundwater. In summary, the quantity of pollutants was higher for a highway than for a road and the leaching of the elements for a highway was longer than for a road due to the lower infiltration rate. This meant that the maximum concentration and the time to resorb the pollution on groundwater was greater for a highway. Considering a poorly productive alluvial aquifer, the impact was much more important, and the maximum authorized concentration were reached for SO_4 with BF_{air} slag and for Cr with EAF slag in the case of a highway.

Table 1: Configurations tested in the typical cases modelling

Base Slag	Infrastructure	Alluvial aquifer	Ca	SO_4	Cr	Cu
BF_{Air}	Road	Fairly Productive	X	X		
	Highway	Fairly Productive	X	X		
		Poorly Productive		X		
	Embankment	Fairly Productive	X	X		
GBF	Road	Fairly Productive	X	X		
	Highway	Fairly Productive	X	X		
		Poorly Productive		X		
	Embankment	Fairly Productive	X	X		
BOF	Road	Fairly Productive	X		X	X
	Highway	Fairly Productive	X		X	X
		Poorly Productive			X	X
	Embankment	Fairly Productive	X		X	X
EAF	Road	Fairly Productive	X		X	X
	Highway	Fairly Productive	X		X	X
		Poorly Productive			X	
	Embankment	Fairly Productive	X		X	X

The results of the modelling were compared with the results of in situ measurements designed for testing element release from large slag volumes and under natural weather conditions. Two different cases were considered: a recent road to evaluate the short-term impact and an ancient road to study the long-term impact. Focusing on the recent road case, the investigation took advantage of the road construction close to Nancy in 2001-2002 establishing the experimental site in the town of Essey-les-Nancy on an agricultural track. A portion of this road was made with the EAF slag from the Neuves-

Maisons plant which already undergone a partial leaching by meteoric water during their storage. The experimental site was equipped with three successive test panels 4 m wide which were physically separated with small transversal shouldering wall in the underlying soil to avoid contamination risks. The first panel was 23 m long and was a benchmark made with limestone materials, the second panel was 6.5 m long and was made with a 0.5 m thick EAF slag layer placed on a geomembrane to recover the natural percolates, and the third panel was 23 m long made with a 0.5 m thick EAF slag layer placed directly on the natural soil. Rainfall was continuously monitored with a tipping-bucket rain gauge while the volumes of leachates coming from the second panel were monitored using a pressure sensor. Water analysis allowed to monitor conductivity, pH, Ca, SO_4, Cr, Cu, Ba, Mo, V over one year. No groundwaters were observed below the site therefore their monitoring was impossible. Concerning soil quality evolution, natural soil was sampled at the beginning of the campaign from each of the three panels at different depths and particle size distribution and chemical analysis in terms of pH, electric conductivity, Ba, Ca, Cd, Cr, Cu, Mo, SO_4, V concentrations were evaluated. After that, the potential of EAF slag as source of contamination was assessed sampling specimens from each panel after 20 months of exposure.

The analysis of the initial state of the soil revealed preexistent contamination with As, Ni and Cr because the site was initially used as farm soil, and As compounds were widely used in pesticides in agriculture. The analysis of the soil exposed for 20 months at the EAF slag highlighted that among Ca, Cd, Cu, Cr and Ni, Cr was the element with the most important effect. The results connected with EAF slag leachate reported a progressive decrease of electric conductivity with time with sporadic increases in summer after long dry periods. Despite this, it always remained below the European recommendation for drinking water. SO_4 contamination was particularly strong in the first month until decreasing around 100 mg/l. It reached another peak similar to the initial one of 300 mg/l in spring and this caused the leachate approaching the worst red quality class. Except for this episode, the concentration always remained between the orange and the blue (best quality) threshold. Similar trend was observed for Ca with 216 mg/l released in the first month and a subsequent decrease at 80-50 mg/l. A 100-150 mg/l spike which made exceed the blue quality, was observed in spring. Cu concentration in the leachate belonged to the orange quality class from the beginning ranging from 8 to 19 µg/l and exceeded the European recommendation of 2 µg/l for drinking water. More critical was Cr trend which displayed poor emissions at the beginning of the campaign thus entering the green quality of the French system, but increasing regularly until exceeding the red quality threshold with a concentration higher than 110 µg/l. V displayed initial concentrations of 400 µg/l until decreasing to 200 µg/l, Ba followed an opposite evolution moving from an initial 100 µg/l to 200–250 µg/l together with Mo which moved from 40 µg/l up to 180 µg/l.

The ancient road case in the Bouzonville site was selected to assess the long-term effects of slag application on underlying soil and groundwater. The site was constructed in 70' and the material supposed to be used for the construct was air-cooled BF slag. This site was selected because of the silty soil able to enhance pollutant accumulation, the thin unsaturated zone which allowed the aquifer to be as close as possible to the application site providing a chance for pollutants to transfer to the aquifer and finally for the small velocity of the aquifer to limit the dispersion of pollutants. Ground water was characterized by means of piezometers and through chemical analysis and a sample of slag

was collected to confirm its air-cooled BF nature. A drilling was also performed, and a slag layer thickness of 60 cm was observed. The results of the leaching laboratory test on the BF slag collected highlighted a pH ranging from 10.7 to 11.4, a decreasing electrical conductivity and decreasing values of SO_4 from 903 to 122 mg/l, typical for leachable salts. Analogously, Cl displayed the typical trend of leaching soluble salts, with concentrations of 33 mg/l in the beginning and 1 mg/l in the end. The leaching of Ba and Se was constant at 30-40 mg/l and 1-2 mg/l, respectively. Groundwater was characterized by an alkaline pH, by an electric conductivity relatively high but in accordance with the European recommendation for drinking water as well as SO_4 concentration while Ca concentration was not very high and fell into the green class quality of the French system. The groundwater also presented high level of Al, Ba, Fe and Mn probably resulting from the local natural geochemical foundation and low but not negligible level of As, Cr, Ni and Pb resulting from man-made origin such as demolition materials, scrap and various waste. The content of some trace-elements such as Cr, Cu, Zn, Ni, Pb, and Cd in the underlying soil analysis were far below the threshold values however their content was often above the highest values recorded in similar soils in France, but only the Zn transfer to the soil could be directly imputed to the presence of slag. The content of B, V and Ba in the analyzed soil was very similar to the one of reference soil contents while the influence of the slag on the Ca, Mg and Mn contents was much more evident.

The last phase of the project tried to provide some general guidelines for good practices when using steelmaking slags in road construction to keep the quality of water within acceptable limits for its subsequent use as drinking water. Considering that it is impossible to act on weather conditions or on the underlying aquifer, some general recommendations were made to limit as much as possible slag leaching by rainwater to minimize pollutant contents in the underlying aquifer by setting up a cover, e.g., asphalt-fines matrix or concrete surface course, on road or highway infrastructures, and/or a drainage system at the base of the surface course. Further recommendations concerned the reduction of lateral infiltrations, i.e., border effect, towards the subgrade and the use of hydraulic binders. Some conclusions were drawn thanks to the modelling activity which highlighted that the embankment configuration was the most disadvantageous infrastructure, the crystalline aquifer was the most vulnerable type, the infrastructure parallel to the aquifer flow would be the most disadvantageous configuration from the geometrical perspective, and finally BOF slag seemed to be the most disadvantageous one while GBF slag seemed to be the one which would generate the less impact on groundwater.

2.1.10 Efficient utilisation of waste products from secondary steelmaking as flux materials for electric arc furnace (18)

The project was coordinated by FehS with CENIM, Horn & Co., FQZ Brandenburg, KEP, and Riva Acciaio participating as partners in the consortium. The project started on the 1st of July 2000 and lasted almost three years, ending on the 30th of June 2003. The overall project cost 1.565 M€ and EU contributed 939 k€, i.e., almost 60 % of the budget.

The project fully incarnated the circular economy principles fostering the use of waste products from secondary steelmaking, e.g., slag and spent refractory, as flux material in EAF, i.e., primary steelmaking,

investigating different recycling paths. Indeed, secondary steelmaking slags, e.g., LS, and spent refractory were usually dumped while their high CaO and MgO concentrations would still ensure a high metallurgical potential in primary steelmaking to solve S and P and replace part of the virgin material. Therefore, the main targets of the project were decreasing waste from steelmaking to decrease dump space, improving EAF metallurgy by maintaining slag metallurgical activity, reducing the use of raw materials to protect natural resources and saving energy by recycling hot materials.

A broad range of materials, processing and recycling procedures were investigated. In particular, LS from both structural and alloyed EAF steelmaking and spent refractory from EAF, BOF and secondary steelmaking were selected as materials to be recycled. Selection of suitable fractions and agglomeration through briquetting and pelletizing were considered as processing aids and both liquid/hot materials and solid/cold materials, e.g., injections and big bags, recycling procedures were investigated. For liquid material recycling, RIVA Acciaio was endowed with the necessary infrastructure to perform this type of trial into EAF. For solid material recycling, Horn & Co. developed the technical prerequisites for recycling such as crushing, separation, mixing and pelletizing while CENIM developed the extrusion and briquetting processes by also adding molasses as binder and reduction agents for the recycling trials into the EAF performed at KEP. FEhS supported the campaign with analytical investigations of raw materials, recycling products and EAF slags and developing optimized fluxes. Furthermore, FQZ targeted the internal recycling of spent refractory into the BF-BOF line addressing all aspects of selection, processing, characterization and development of recycling strategies.

Focusing on LS liquid recycling into EAF, i.e., RIVA Acciaio contribution, the activity aimed at recycling the liquid LS slag while exploiting its melting heat to achieve significant energy savings. Two different steel qualities were selected to evaluate the effect of LS recycling on their characteristics and an average amount of 7.5 kg of LS at about 1500 °C per ton of raw steel was recycled. No increase in S content for both steel types nor significant differences in EAF slag chemical and mineral composition and melting behavior were observed because of LS recycling. Considering the positive outcomes obtained, the practice of liquid LS recycling became almost daily and a recycling rate of 80 % was achieved. The long-term campaigns confirmed that no significant differences in both steel and slag chemical composition were observed. The control of the most relevant EAF process parameters was performed and no relevant differences between periods with and without LS recycling were detected. The only difference was an increase of 2 minutes in the tap-to-tap time due to the power off time required for LS recycling which resulted in a partial energy loss by heat radiation, i.e., 310 kWh at 1500°C and 430 kWh at 1650°C, due to furnace roof opening. In addition, approximately 55 kWh/heat were necessary to reheat the slag up to 1670 °C considering the recycling rate of 7.5 kg/t raw steel. According to these calculations, the additional energy demand for slag recycling was < 0.8 % of the total melting energy and this data were coherent with the additional power consumption registered in the melts with LS recycling which ranged from 0 to 0.4% for the two different types of steel.

Moving to the recycling of solid materials into EAF, KEP collected different LS qualities using as separation criteria for collection the slag ratio $CaO/SiO_2>2$. CENIM also investigated LS from other Spanish EAF steelmakers, i.e., ACERALIA Perfiles, ACERALIA Redondos and SIDENOR, for comparison purposes while Horn & Co. processed and prepared the materials selected at KEP. Slag

chemical composition was investigated through XRF and wet chemical analysis, the mineral composition through XRD and the melting behavior through heating microscopy. LS collected at KEP always displayed a basicity CaO/SiO_2>2 coherently with the chosen selection criteria, a content of CaO> 50 %, SiO_2<20 %, MgO in the range 8-21 %, F in the range 2-7.5 % due to the use of fluorspar, Al_2O_3 in the range 10-20 % due to the killing operations on steel performed with Al, and S in the range 0.5-1.5 % with occasional concentrations up to 2.8 %. A start softening temperature between 1310 and 1400 °C and a liquid temperature between 1320 and 1490 °C were detected with higher temperatures resulting from increasing MgO and decreasing F contents. LS generated in Aceralia carbon steelmaking was characterized by a lower basicity with $CaO/SiO_2 \cong 2$ and lower Al_2O_3 concentrations around 3-4 %. LS by Sidenor did not fit these ranges with a content of MgO around 48 %, CaO around 31 % and SiO_2 around 5 % probably due to some contaminations with the refractories. Aceralia slags also displayed higher melting temperatures than KEP due to the liquefying influence of Al_2O_3 in the latter. Most LS were prone to disintegration during storage and cooling, and the resulting coarse and fine fractions were characterized by different chemical and mineralogical composition with fine grained material showing a lower basicity and a higher SiO_2 concentration.

The selection of appropriate LS and/or spent refractory to ensure satisfying metallurgical performance was made following these requirements, i.e., high CaO and/or MgO concentrations to successfully replace lime and/or dolomite, low melting temperature to ensure the formation of an early liquid slag and adjusted viscosity. FEhS focused on the determination and optimization of LS and spent dolomite mixtures assessing viscosity with improved Urban model, melting behavior and refractory consumptions. The optimization of the mixture highlighted that LS viscosity was typically lower than EAF slag one and could be increased to comparable values by adding spent dolomite, i.e., 20 % of spent refractory containing 40 % CaO and 60 % MgO. Furthermore, it was observed that concentrations of 25 % of MgO in mixture made up with 80 % LS and 20 % spent dolomite provided a satisfying protection of the refractory lining. The melting behavior confirmed these conclusions with 20 % spent dolomite addition increasing LS softening temperatures of 30-60 °C for high F contents and up to 20 °C for low F contents. Its addition also extended the softening range, i.e., the difference between softening and half sphere temperature, by 20 to 100 °C which was advantageous for the formation of a stable slag foaming. LS and its mixtures presented also a lower softening temperature than EAF slag. Concerning EAF refractory consumption and corrosion, the laboratory tests at 1600 °C showed that the recycling of LS rich in F and Al_2O_3 might be detrimental to furnace lining while a high basicity preserved it. Considering all these outcomes, it was concluded that the mixture of 80 % LS and 20 % spent refractory was suitable as synthetic flux.

Once identified the best slag composition, its pre-processing was investigated by Horn & Co and by CENIM. Indeed, LS from secondary steelmaking had the tendency to disintegrate during cooling thus leading to the formation of dust which might cause inadmissible annoyance in the neighborhood of the processing facilities. Therefore, different strategies were adopted for coarse and fine fractions to reduce this issue and achieve 100 % recycling. Lump material accounted for 15-40 % of the total slag production and could be conveniently recycled as aggregates via big bags or bunker adding separately the spent refractory. Fine grained materials accounted for up to 70 % and could be recycled by pneumatic injection thanks to a closed system which prevented inadmissible dusting or after

agglomeration or briquetting. Horn & Co considered four different agglomeration methods, i.e., briquetting of cylindrical bodies, briquetting on a rolling press, pressuring through a die body agglomeration with mixer and balling disk. All tested methods were suitable for agglomeration of LS fine fraction, but some agglomerates displayed a tendency to disintegrate again after about 7 days of storage similarly to the coarse fraction of 10 to 70 mm aggregates which disintegrated after 2-3 weeks of storage. This phenomenon was mainly ascribed to the hydration of free lime (CaO) and after longer periods of periclase (free MgO). Therefore, it was concluded that it was advisable to recycle coarse LS aggregates and the mixtures agglomerates shortly after their preparation. The four technologies selected for the laboratory trials were also investigated at the semi-technical scale to optimize them for industrial application, but the results showed that briquetting and pressuring through a die body were unsuitable due to the low performance of the available equipment while briquetting on a rolling press was economically unfeasible with costs 2 to 4 times higher than other methods. In light of this, LS and their mixtures with spent dolomite could be conveniently agglomerated by coupling mixer and balling disk. The best results were achieved by pre-mixing the 80 % LS and the 20 % spent dolomite with 10 % of cement and this solution was then recycled into the EAF at KEP.

Further briquetting tests were performed by CENIM to optimize the compositions and the physical properties of the aggregates produced with the Spanish LS slags applying a pressure of 200 bar and molasses as binder. Supply energy agents were also included in the briquettes with petrol coke used for Sidenor and Aceralia Perfiles slags and coke for Aceralia Redondos slag to compensate the additional energy demand necessary to heat the higher amount of secondary steel slags necessary to compensate the lower CaO content. Concerning Sidenor briquettes, the compression strength improved for increasing storage times and increasing molasses and petroleum coke content. For Aceralia Redondos briquettes optimization through experimental design was carried out and four operational parameters varied on two levels, i.e., compaction pressure (150- 200 kg), compaction time (45-75 sec), molasses (4-6 %) and coke (0-10%) content, were selected to optimize the manufacturing process. The results highlighted that the higher the pressure applied the higher the compressive strength achieved while no clear effect of agglomeration time and molasses content was observed. A positive effect of coke on agglomeration was also detected together with a decrease in compressive strength moving from 7 to 14 days. Further tests were performed after drying the slag for 24 hours at 110 °C. In this case an increase in compressive strength was observed for increasing percentage of molasses which became the most important parameter to achieve good agglomeration. The transition from the laboratory to the semi-industrial scale made necessary the use of a more liquid type of industrial molasses. The slag-molasses-coke mixture was homogenized in a concrete mixer and then briquetted in the cylindrical molds. The compressive tests displayed a two-step deformation mode for the briquettes with the first stage occurring at relatively low forces and the second stage achieving strong resistance until final disintegration. The results reported an increased strength of the briquette for increasing curing days whereas an increase in molasses from 10 to 15 % determined a reduction in compressive strength due to its high-water content. The briquettes were also subjected to tumbler tests and proved to perform well yielding indexes greater than 90.

Once completed this phase, the recycling tests at KEP were performed assessing both injection of the fine portion and introduction of the coarse portion as aggregates and of the fine portion as

agglomerates. Three different campaigns were performed for the injection trials. In the first campaign, LS fine portion was pneumatically injected in addition to the normal amount of lime determining an increase of 3 % in the amount of EAF slag. The procedure did not reveal any technical issue, but the maximum amount of LS recycled was limited to 0.3-0.4 tons/heat due to the maximum injection rate and the time available for the steelmaking operation. The second campaign was stopped due to some issues in the pneumatic transportation and injection resulting from the further LS disintegration during longer storage which caused an increase in the amount of fines < 1 mm. Considering this, the third campaign was performed using the same fine material but placing it through big-bags into the EAF together with the scrap baskets. In this campaign, 1 ton of LS/spent refractory mixture replaced 1 ton of lime to keep constant the amount of slag in the furnace, and this caused a decrease of CaO in the slag because LS contained only 50 % of CaO compared to the 100 % in lime. Despite this, no significant variation in furnace operation were observed with no criticalities in slag formation and foaming. The analysis of the chemical composition of the resulting EAF slag highlighted that the recycling of LS/spent refractory mixture up to 0.5 tons caused only a minor influence. On the contrary, the recycling of 1 tons of the mixture or the substitution of lime in a ratio 1:1 determined an increase in MgO concentration and in the basicity (CaO+MgO)/SiO_2 which might be responsible for the reduced concentrations of Cr_2O_3 (19). Further differences were observed in an increased concentration of F and a decreased liquefying temperature which ensured an early formation of liquid slag. Finally, none of the typical minerals of LS, i.e., Periclase, Fluorite, Mayenite, Jasmundite, Oldhamite, were detected in EAF slag thus proving that the recycled material was completely dissolved and transformed into the typical minerals of EAF slag, i.e., Gehlenite, Merwinite and Spinel.

Three further campaigns were performed for the recycling of the LS/spent refractory mixture in the form of pellets. The first campaign recycled 1-ton of pellets by placing them with a big-bag in the empty furnace together with the first scrap basket to study pellets thermal shock behavior. Despite the agglomeration with 10 % of cement containing 4 % of CO_2 and 10 % of H_2O, no bursting of pellets and additional dust formation were observed and positive outcomes were registered. The second campaign investigated pellets recyclability by injection after installing a hopper with fluidized bottom to ensure higher feeding rates and achieve amounts up to 1.3 tons within the available time. In the last campaign, the substitution of 0.5 tons of lime with 1 ton of pellets to ensure a replacement nearly 1:1 of CaO was investigated. The analysis of the resulting EAF slags highlighted a clear trend with an increase in Al_2O_3, CaO, MgO and F concentrations and a drop in SiO_2 and Cr_2O_3 which resulted in an increase in CaO/SiO_2 and (CaO+MgO)/SiO_2 basicity. Again, an extension of the softening range was observed which was beneficial for a stable foaming of the EAF slag and none of the typical minerals of LS were detected in the EAF slags thus confirming the complete dissolution of the recycled material. In conclusion, the positive results of the recycling procedures demonstrated the feasibility of recycling by pneumatic injection and via big-bags and that the selected mixture could be used as a partial substitute of lime without detrimental effects in metallurgy.

After these trials, the recycling of the coarse portion of LS slag, i.e., aggregates of fraction 10 to 70 mm, was investigated trying to recycle higher amounts to better evaluate their influence on the chemistry and melting behavior of EAF slags. About 1.5 and 2.0 tons per heat of aggregates were recycled together with the scrap baskets in stainless steelmaking thus the amount of lime introduced

into the furnace was reduced by a ratio of 1:1 compared to standards. The trend of EAF slag chemical composition reported an increase in Al_2O_3 and F concentrations, a decrease in CaO and MgO concentrations and in the basicity CaO/SiO_2 and $(CaO+MgO)/SiO_2$ with LS recycling. The latter caused and increased Cr scorification. No significant influences were observed on the softening range nor on the mineral composition thus confirming the complete dissolution of the recycled LS despite the higher amounts and the bigger particle size. In conclusion, the recycling up to 2 tons of coarse aggregates of LS proved to be possible and long-term trials were started for both stainless and engineering steelmaking. The coarse LS was not pre-mixed with spent refractory materials which were rather added simultaneously from a separate silo and lime substitution with was performed in a ratio 1:2 to prevent the basicity decrease observed for the 1:1 ratio. In this way there was just an acceptable increase in the total amount of EAF slag while the added CaO was constant. Concerning stainless steelmaking, a slight increase in CaO and SiO_2 content was detected while MgO remained constant leading to almost constant values of basicity CaO/SiO_2 and $(CaO+MgO)/SiO_2$. Furthermore, an increase in Al_2O_3 and F concentration was observed due to their higher intrinsic content in LS compared to normal EAF slags whereas Cr_2O_3 concentration was decreased from 9.0 % to 7.1 % probably due to the liquefaction of slag at lower temperatures which resulted in a higher reactivity. Finally, S concentration was slightly increased from 0.20 % to approximately 0.24 % because LS were intrinsically endowed with a S content 10 times higher than EAF slags for stainless steelmaking. It could be concluded that the substitution of lime by LS in a ratio 1:2 did not have any negative influence on steelmaking and steel quality in the case of stainless steel. The trials performed for engineering steelmaking reported a slight increase in Al_2O_3, F, MgO, S and SiO_2 concentrations and a slight decrease in CaO in EAF slag after LS recycling while the basicity CaO/SiO_2 and $(CaO+MgO)/SiO_2$ did not seem to be influenced as well as Cr_2O_3 concentration.

Considering the good outcomes of the long-term trials, paramount topics such as energy demand and S input were addressed. Indeed, LS/spent refectory mixture recycling required additional energy supply to heat up the material from ambient to steelmaking temperature, i.e., 1670 °C, and for their transformation from solid to liquid state. The calculation on energy consumption reported an additional energy demand of about 500 kWh/t for LS which was somewhat higher than the 440 kWh/t for lime. This led to an overall additional energy demand of 2.3 kWh/t of steel, i.e., 300 kWh/melt, for the substitution of lime by LS mixture in a ratio of 1:2. This contribution was quite low compared to the total EAF energy consumption at KEP. This conclusion was further confirmed by trial data which proved that energy consumption was much more influenced by other operational conditions such as scrap quality. Analyzing desulphurization aspects, the recycling of 1 ton of LS containing approximately 0.2 % of S caused a higher input of approximately 2 kg of S which induced higher S concentration in EAF slags, i.e., 0.04 % in stainless steel and 0.07 % in engineering steelmaking. Despite this, the sulfur capacity of EAF slags was not decreased for engineering steelmaking, and it was improved for stainless steelmaking.

The last experimental activity of the project was performed by FQZ and focused on the recycling of spent refractory with high MgO contents as substitute for olivine and soft burnt dolomite in the integrated steel work of EKO Stahl. The refractories were obtained from the four EKO Stahl converters which were renewed every year leading to an overall amount of 800 t of unused magnesite

refractory with a MgO content of 97 %, and from the relining of the 100 ladles which provided about 2500 t-spent magnesite refractory per year. The spent refractories were subjected to crushing, magnetic separation and sieving to achieve the desired sizes for recycling, i.e., 10 – 32 mm for use in BOF converter, 10 – 40 mm for BF charging, and 0 - 3 mm for the sinter plant. Concerning sintering recycling, 50 t of magnesite spent refractory with a MgO content of 43.3 % were added to the sinter feed as olivine substitution and the results proved the feasibility of the procedure since all examined parameters, i.e., CaO, FeO, SiO_2 and MgO concentration and basicity (CaO+MgO)/SiO_2 in the sinter, productivity and dust generation of the sintering plant, waste gas temperature, sinter characteristics (ISO T, ISO A), remained constant with no deviations compared to the reference condition. For BF recycling, the 25 kg of olivine per ton of hot metal normally charged to adjust the MgO content of the slag at 10-11 % were replaced with spent magnesite refractory. The experience proved that it was fundamental to know the real MgO content in the spent refractory to perform a correct estimation of the material to feed in the BF to achieve the desired slag composition. Indeed, incorrect estimations would lead to a deficit or an excess of MgO in the slag detectable only after 12 hours. Finally, spent magnesite refractories recycling in BOF was assessed trying to replace 0.5 t of soft-burnt dolomite (MgO> 30 % and CaO equal to 50 %) normally charged for each heat in the BOF converter to decrease slag viscosity and protect the magnesite lining. This procedure would allow to reduce the costs for dolomite and for spent refractory disposal. In the first trial, 60 tons of spent magnesite refractory with an average MgO concentration of 90 % were recycled allowing dolomite replacement. The average MgO content with dolomite was 3.9 % while it reached values of 3.5 % in heats with magnesite refractory. These values were perfectly within the normal range considering that MgO content alternated between 2.5 and 6.0 % in both converters. In the second trial, 30 tons of spent refractory material were recycled using a fraction with less fines and a MgO content lower than in the first trial, i.e., <30 %. Again, the comparison with reference dolomite conditions did not reveal any significant difference and XRD analysis did not detect any visible concentrations of free MgO allowing to conclude that the dissolution of recycled spent magnesite refractory was not an issue. The concentration of MgO in BOF-slag without refractory recycling was investigated as a function of lining lifetime and it was observed that it increased after 1500 heats and more drastically after 2000 heats. According to these results, it was recommended to recycle spent magnesite refractory materials within the first 2000 heats after relining the converter to prevent difficulties on MgO concentration control. The last trial was performed with 700 kg of spent magnesite refractory from steel ladles which contained a MgO concentration of 56 % and a lower slag content which made them easier to process. Even in this last case, the results highlighted no significant differences compared to normal operation. The three trials allowed to conclude that the substitution of dolomite by spent magnesite refractory in the BOF process was possible, but good preparation of the material in terms of grain size was recommended.

In conclusion, the recycling strategies developed did not display negative impacts on steelmaking and steel quality and provided distinct economic and/or ecological benefits. At Riva Acciaio, it was not possible to include the recycled liquid LS in burden calculation thus preventing any economic advantage resulting from material savings, but the ecological benefits, e.g., less dusting, perfectly justified the recycling. At KEP, LS recycling permitted to save lime, but to estimate the real economic benefits the additional processing required must be considered. It was proved that the economic benefit was high

when the amount of coarse material was high and tended to decrease when fine fractions were recycled due to the preparing costs of grinding, sieving, drying, pneumatic injection, etc. Nevertheless, the ecological benefits were high for recycling both the coarse and the fine fractions.

2.1.11 INQUISSS: In situ, quick sensing system for measurements of process-critical components in steelmaking slags (20)

The project was coordinated by RWTH with Aceralia Corporacion Siderurgica, Acerinox, Helliniki Halyvourgia, Instituto de Soldadura e Qualidade (ISQ), Universidad de Malaga and University of Patras participating as partners in the consortium. The project started on the 1st of July 2001 and lasted almost three years, ending on the 30th of June 2004. The overall project cost 1.46 M€ and the EU contributed 878 k€, i.e., almost 60 % of the budget.

The INQUISSS project aimed to investigate and adapt a laser-based sensing system, i.e., Laser-Induced-Breakdown-Spectroscopy (LIBS), with an online analytical tool for in-situ detection of pre-defined elements of steel slags, e.g., Fe, Ca, Si, Al, Mg, Cr, Mn, during plant operations such as EAF, BOF and ladle furnace. Steel quality is strongly dependent on slag quality and on the optimization of their interaction to remove harmful impurities or undesired dissolved elements. In this perspective, the formation of a slag with desired composition and proper thickness plays a major role thus a quick and online determination of slag chemical composition and the simultaneous calculation of its main properties, e.g., oxidation potential and basicity, could significantly improve metallurgical process control ensuring an immediate reaction in case of slag chemical composition deviation. This control can in turn ensure a better metallurgical yield and better refractories performance. Furthermore, slag control can enable determination of slag recycling capacity already during the metallurgical operations allowing to deliver valuable information to other industries, e.g., road construction or cement industry, in a much shorter time. In consideration of this, the project aimed to achieve a fast and reliable online analysis of the slag to make its use more effective both in the production and recycling phases. The main goal was to support process control and optimization while contributing to environmental strategies to support recycling measures.

The main operative parameters of slag processing were determined by integrating sensing and advanced process modelling, to ensure representativity of measurements and transferability of results. LIBS was selected for qualitative and quantitative multi-element analysis because the more traditional AAS and ICP endowed with low detection limits, great analytical variety and high accuracy over a wide concentration range could be used only at laboratory level requiring also large-scale sample preparation. All these features made them unsuitable for rapid on-site monitoring. On the contrary, LIBS was a technique based on simple principles already used for microanalysis in mineralogy, forensic science, archaeology, medicine, etc. It required minimal sample amount, no sample preparation and was able to work in hostile environment. Limits of detection varied for individual elements around 10-100 ppm with accuracy between 2-10 %. The main parts composing the system were generally a laser, an optical system to focus the beam, an optical system to collect the emission of the laser induced plasma, a method of spectral resolution and detection, and an evaluation and control unit. An

inspection machine was set up and integrated into a production line and approximately 30,000 inspections were performed demonstrating the industrial maturity of the technique.

LIBS analyzers had to work in particularly harsh environments, including poor sample accessibility, high temperatures and high dust levels. For this reason, two different solutions encompassing LIBS were investigated. The first solution included the use of a Galilean telescope able to ensure remote sensing, remote light collection and the ability to work in adverse analytical conditions. The second solution allowed molten slag analysis thanks to an optical lance in direct contact with the slag. Despite being based on the same technique, the results obtained with the two solutions were not directly comparable.

The first set up activity using the Galilean telescope was performed by University of Malaga using an apparatus like the one schematized in Figure 4. The produced laser was sent to a telescopic resonator to produce a multimode beam output with high energy and low beam divergence, a more uniform spatial intensity distribution, a more constant beam profile and a decreased risk of optical damage as a consequence of reduced hot spots. The laser beam was then focused on the sample at normal incidence at room temperature and atmospheric pressure using the Galilean telescope built to focus the laser beam to the far field. A coaxial collection configuration was achieved thanks to a toroidal mirror which ensured both laser beam and returned plasma light travelling in the same optical path. The plasma light resulting from the specimen was then reflected by the mirror into a Newton telescope to avoid chromatic aberration. Finally, the plasma dispersed light was spatially and temporally resolved by a solid-state two-dimensional intensified charge couple device iCCD. The acquisition was synchronized to the laser event because the TTL (transistor–transistor logic) signal from the pulse was guided to the CCD camera whose internal electronics allowed generating a programmable delay and gating the intensifier.

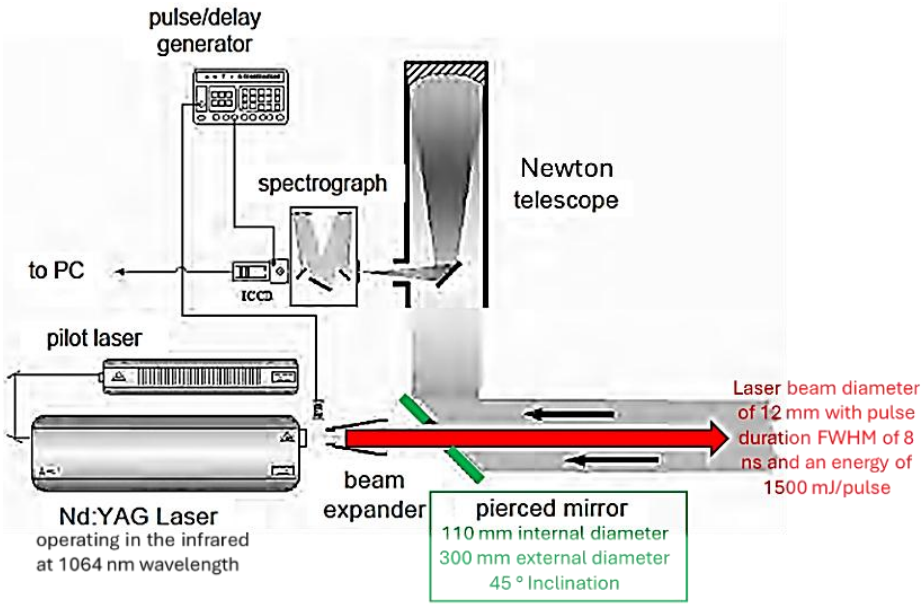

Figure 4: Schematic diagram of the instrumental set-up used with the Galilean telescope

The slag used for the analysis were EAF, ladle and AOD (Argon Oxygen Decarburization) slags and were located 10 m away from the laser beam. The analytical wavelength for the best reproducibility and signal to background ratio was accurately investigated and the best spectral windows identified was between 284 and 318 nm because it allowed the unequivocal identification of Si, Mg, Ti, Cr, Al and Ca. Ti and Cr were not characterized by the strongest emission lines in this region, but their concentration in the slag was relatively high and no detection problems were observed. Signal reproducibility was improved by averaging several laser shots, i.e., the signal increased with accumulated number of laser shots. Indeed, the precision calculated as RSD (Relative Standard Deviation) decreased from 15.6 to 12.2 % for Ca (II) 393.366 nm and from 16.9 to 10.7 % for Al (I) 394.401 nm increasing the laser shots from 1 to 30. This was ascribed to increasing number of measurements allowing to better mitigate and averaging compositional heterogeneities of the sample resulting from the analysis of different points throughout its depth due to ablation phenomena occurring, i.e., 1.5-3 ng of ablated material per pulse. Other sources of heterogeneity were steel nodules in the slag matrix, analysis of different points on slag surface, and a higher spot size. It was also observed that emission signal increased only for the first 50 pulses, subsequently reaching a plateau which remained constant for about 150 pulses before decaying again.

Considering the effect of energy per pulse, the amount of energy deposited on the sample affected the SBR (Saturable-Bragg-Reflector) and the higher the laser energy the better the SBR. The effect of sample temperature on slag analysis was also investigated and the higher the temperature the higher the emission probably due to an increase in ablation yield as proved by the increased crater volume for increasing temperature also observed through SEM analysis.

The basicity index (B.I.), i.e., %(CaO)+%(MgO)/%(SiO_2), plays a major role in steelmaking to tailor desulfurization and dephosphorization processes which are fostered by basic slags. In light of this, B.I. needed to be conveniently determined during the production process and the data obtained by LIBS were used to calculate (B.I.) exploiting the calibration curves of the elements of interest. The spectral lines chosen to obtain the calibration curves were Mg (II) 297.55 nm emission normalized to Ca(I) 299.49 nm, and Si (I) 288.16 nm emission normalized to Ca(I) 300.68 nm. In this way, it was possible to isolate all the necessary information using only two calibration curves by using Ca as an internal standard. B.I. values predicted with LIBS and plotted against the nominal value measured by XRF proved to be in good agreement with a slope close to 1 and an acceptable correlation of 0.986. The next step of the procedure focused on the identification of a suitable equivalence between the quantitative results obtained at high temperatures with those obtained at room temperature. The mathematical model designed to transform the intensity of the peak of the element of interest measured at high temperature in that intensity expected at low temperature was:

$$I_{Transferred\ (RT)} = factor * I_{Measured\ (HT)} + offset$$

The calibration curves must be linear both at room and high temperatures to use conveniently the mathematical model and to this aim the calibration range was restricted to the range of typical

concentrations used in the steelmaking. The normalized concentration ratio measured by LIBS at room temperature and that transferred from hot temperature were compared to that measured by XRF. The results related to Si and Mg concentration transferred from 800 °C to room temperature proved to be in good agreement with those obtained directly at room temperature and with XRF. Indeed, the correlation between the transferred concentration and the XRF normalized concentration displayed a slope and a correlation coefficient close to 1. Same conclusions could be drawn for B.I. where a slope close to unity and a satisfactory correlation coefficient of 0.983 were observed.

The second set up activity was performed by RWTH Aachen University and a moveable measurement unit with all necessary utilities was developed for both lab and plant scales according to the schematization shown in Figure 5. The laser and the spectrometer were placed in an aluminum box properly cooled and equipped with a filter system for dust protection. The adjustable table allowed the correct movement of the optical lance ensuring the flexibility necessary to perform both laboratory and industrial trials. A water supply system was also considered to cool the lance and the additional pyrometer. The lens on the bottom of the measuring lance was also cooled by an argon flux directed onto the lance. The laser beam was guided through a variable tube system which could be adjusted to all necessary positions providing a safety guide and was focalized to induce a plasma spot on the surface of the liquid slag. The radiation of the plasma was subsequently guided through the optical lance to reach the glass fiber optic connected with the spectrometer. A pyrometer placed at 1.5 m over slag surface was selected to measure the temperature since thermocouples were excessively fragile and unsuitable for long term measurements. The time delay between the laser pulse and the beginning of the acquisition was again selected to maximize the signal to noise ratio. Detector resolution allowed to separate the characteristic lines of a wide range of atomic elements, even in complex samples. The first step of the set-up activity concerned the identification of the exact wavelength position of the spectral lines of each critical element, i.e., Ca, Mg, Si, Cr, Al, Fe and Mn.

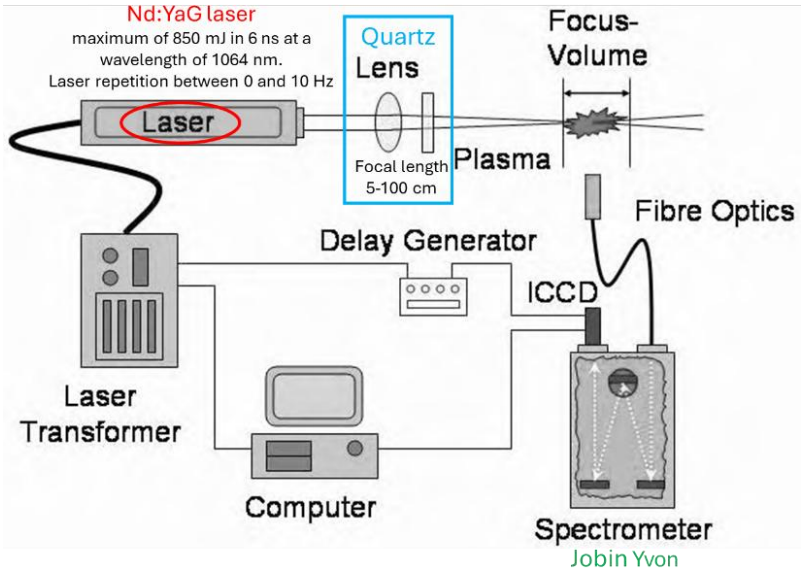

Figure 5: Schematic diagram of the instrumental set-up used with fiber optics

At first optimal laser power to excite all relevant elements was investigated and it was observed that the use of a spectrometer mirror with an 11 mm drill hole allowed to obtain a higher efficiency than a mirror with 9 mm drill hole. In light of this, the plasma scrapper with the bigger drill hole was selected for the following tests. After laser power, laser energy on liquid slag was also investigated and lower energy levels proved to save the lenses and the lifetime of the laser. Concerning the delay time for each element, 800 ns was identified as an adequate value to get clear spectral peaks while still receiving relatively high intensities. For the integration time, a 2000 ns value was selected. Subsequently, the shot-to-shot stability on solid slag was tested using the wavelength of Ca at 393.366 nm and a strong intensity increase was observed in the first 10-20 shots. After that, a short plateau and a low and continue decrease in plasma intensity was registered due to laser beam progressively digging a deeper hole into the sample which shielded the reflected plasma. For the shot-to-shot stability on hot liquid slag the same operating conditions were considered, and the results highlighted a constant plasma intensity opposite to solid slag. This was ascribed to liquid slag surface being able to close the gap after each laser shot. A further parameter considered was laser beam focus which was investigated considering three different scenarios, i.e., laser focus exactly on sample surface delivering an extremely high laser power, laser behind the focus and laser before the focus ensuring a much higher laser intensity than the previous case. Considering these three cases, it was better to hold the sample before or in the focus rather than behind it to perform quantitative measurements. This aspect was of primary importance considering that focus volume was slowly crossed during several plasma spots and that slag bath level would vary significantly during plant trials.

A special graphite nozzle was developed to level continuously slag surface into the focus to enable the same measurement conditions during lab scale and plant scale trials. It also allowed to cover completely the class 4 laser beam to improve safety. Graphite was selected as manufacturing material because it was a good refractory and ensured no reaction with slag. The effect of the diving depth of the nozzle into the slag on LIBS intensity was investigated and it was observed that it was able to stabilize the intensity for distances from 480 to 500 mm before the exact focus. A preheating time of 90 s was selected after dipping to ensure the graphite body reaching the same temperature of the liquid slag. For an accurate quantitative analysis, the effect of phase change from solid to liquid on signal intensity was also investigated, therefore the intensity of Al and Ca was tested in the temperature range of 1250-1600 °C with LIBS measurements taken every 25 °C. The intensity increased with increasing temperatures passing from 1250 °C to the melting point at 1350 °C where an abrupt decrease in intensity was observed. A further decrease was detected up to 1475 °C when the intensity curve returned to increase again. The initial increase in intensity at the solid state was ascribed to the decrease in laser beam reflection which resulted in a higher laser power getting into the solid thus evaporating higher amounts of material and increasing the breakdown of atoms. After reaching the melting point, the physical effect of viscosity became predominant. At the beginning of the melting, the slag was characterized by a high viscosity and when the laser beam hit the soft target a deep and huge hole formed. The viscosity of the slag became lower for increasing temperatures and the slag had the opportunity to close the hole faster determining the intensity increase at 1475 °C. After all this investigation, the calibration of the measurement system was performed in view of the plant trials.

The third set up activity was performed by University of Patras which developed the measurement system schematized in Figure 6. The conditions chosen for the best acquisition and signal/noise ratio for Fe, Ca, Mn, Cr and Mg were 3000 and 1000 ns for the delay time and the gate width, respectively. The energy of the applied beam was 20 mJ. The experimental campaign performed at the laboratory scale on standard samples was fundamental to create the calibration curves through the preparation of different stoichiometric samples. At first, the variation of element concentration was determined using the data analysis form the slag production line of the three industrial partners Helliniki Halyvourgia, Aceralia and Acerinox. After that, a proper spectrum area for each element used as calibration standard, i.e., Fe, Ca, Si, Al, Mg, was chosen and a spectrum area from 250 to 700 nm was mapped. Each individual spectrum corresponding to a different spectrum area and to one laser pulse was stored in the random-access memory of the computer during the measurement. The third step referred to the accumulation of ICP data for each element. In a first stage, the reference samples produced were analyzed with LIBS at room temperature and the elaboration of the obtained spectrums allowed to obtain a proper signal line to be used for the quantitative analyses of the reference standards and slag samples. During the experimental analysis process of multi-element samples, calibration curves for Al, Fe, Mn, Si, Cr and Ca were obtained. Helliniki Halyvourgia provided six samples from EAF and six samples from ladle furnace while Aceralia provided three samples from BOF and the chemical composition was estimated by AAS. The second stage of the calibration focused on the reference molten samples using an induction furnace and a temperature of 1450 °C to perform liquid slag analysis with LIBS. The number of 50 accumulations was chosen, as the lower limit where the ratio Fe/Ca became stable while the pulse energy was selected as 25 mJ to allow the emission lines to show minimal interference with other lines and to avoid breakdown in air. Generally, the interaction between a laser beam and a liquid generates weaker emissions than on a solid surface. In light of this, the distance of the focusing lens from the liquid surface was investigated and it was observed that when this exact distance, i.e., 500 mm, was reached the resulting plasma was not stable. The latter proved to be more stable when the lens-to-liquid surface distance was slightly longer than the focal length.

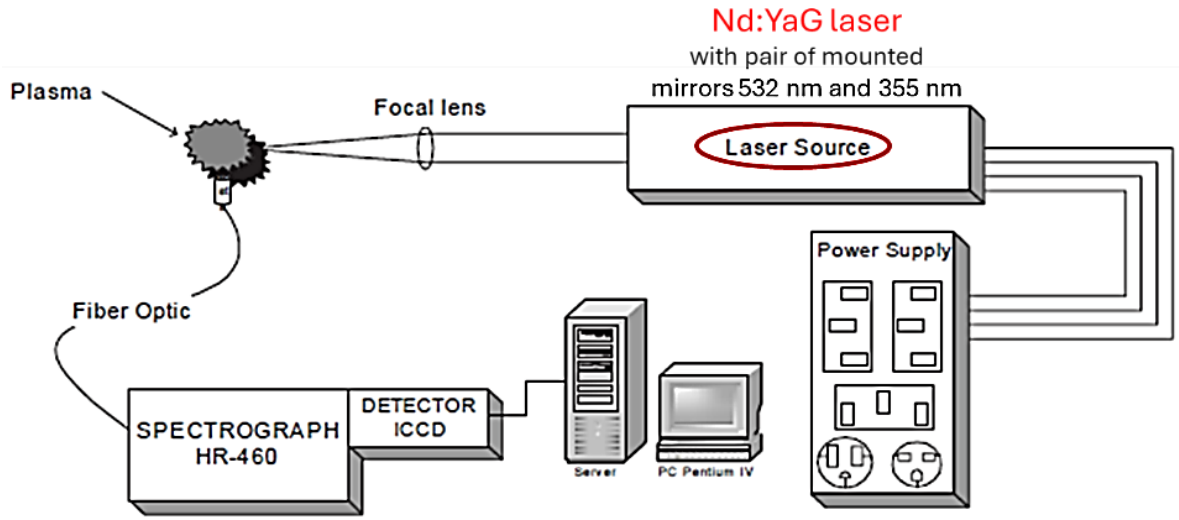

Figure 6: Schematic diagram of the instrumental set-up used by University of Patras

Once completed the set-up phases, plant scale tests with LIBS were performed at Helliniki Halyvourgia EAF. LIBS apparatus was placed in a room located 20 m from the EAF to be protected from the hostile environment. Slag samples were placed in cylindrical copper crucibles and were transferred to the laser room for analysis. Three campaigns of four heats each were performed considering Fe, Mn, Si and Al as elements of interest, using an energy pulse of 40 mJ, a pulse duration of 5 ns, a delay time of 1000 ns, 50 accumulated shots, and a focal length of the lenses of 100 mm. The experimental analysis presented some issues connected with laser focusing and emitted light collection due to slag surface roughness. In light of this, the on-line application of LIBS in the steel industry for in-situ quantitative analysis of the slag required much more efforts even if, the results were able to detect the progressive decrease in Fe concentration in the slag during the process. Concerning solid slag analysis, the parameters selected were a pulse duration of 5 ns, an energy per pulse of 15 mJ, a delay time of 1000 ns, 50 accumulated shots and a focal length of the lens of 500 mm. Again, the main difficulties arose in beam focusing due to the poor stability of sample surface during its transition from the liquid to the solid form. The analysis of the same slag samples through LIBS technique was repeated under laboratorial conditions to determine the influence of the surface to the data acquisition.

The main goal of ISQ in the project was to investigate steelmaking slags behavior to assess their recycling capacity for environmental purposes. To this aim, several leaching tests were performed, i.e., down flow through test and standard batch test DIN 38414-S4, to obtain information on the short and long-term leaching behavior. All tests were fundamental to investigate the potential environmental impact of the slags and to assess their reuse and recycling in the construction sector especially if application envisaging structures exposed to rainwater or watercourses must be foreseen. Indeed, the reuse of slag in cement industry for limestone partial substitution ensured important economic and ecological benefits like energy savings and flue gas emissions reduction during clinker production, but the potential contamination of soil and underground water with toxic elements must be considered. Trials with down flow through test were performed with fresh BOF, EAF and ladle slags at three different ageing levels with each sample being monitored for 30 weeks. Samples were watered every week with 1 l of demineralized water, and the leachate was collected 3 days later and was monitored in terms of Cr, Ca, Mg, Mn, Ti, Fe, Al concentrations, pH and electrical conductivity. The values of pH ranged from 7 to 10 for EAF slags, from 8 to 12 in LS and from 11 to 13 in BOF slags. The chemical analysis for all slags also underlined an increase in heavy metal release with ageing. The results after more than one year highlighted very low leaching levels with Ca an Mg being the most extracted elements probably due to the free calcium and magnesium oxides not completely solved into the slag. In particular, Ca and Mg leached from solid slags were below 0.5 wt.% and all other metals below 0.04 wt.%.

Test method DIN 38414-S4 was also used to evaluate heavy metals leachability assessing the presence of potentially toxic heavy metals such as As, Pb, Hg, Cd, Cu, Zn and Ni, but also Fe, Mn, Ti, Al, Ca, Mg, Cr concentrations, pH and electrical conductivity. Samples were exposed to pure agitated water for 24 h and to a further 24 h resting period. After that, the leachate was filtered and analyzed while the solid residue was submitted to additional agitation cycles, i.e., up to 8. Metals mobility in the residue was related to their extractability in fact samples with higher metal contents in the residue were potentially less hazardous due to a presumable lower mobility. As reference limit values were

considered the ones provided by Council Decision 2003/33/EC which established criteria and procedures for the acceptance of waste at landfills. The results reported leaching limit values (LLV) below LLVs for inert wastes, except for total Cr in ladle and BOF which were although much lower than the LLV for non-hazardous waste. This low solubility was ascribed to the mineral components being bounded within stable crystalline phases. Even if the leaching of heavy metals from slags might not be relevant in terms of environmental impact high final density of these materials may result in accumulation effects for long exposing periods as well as other factors influencing solubility and mobility of chemical species such as local leaching pH and temperature or slags and soils properties such porosity and permeability. DIN 38414-S4 showed higher leaching values than down flow test with 6 wt.% of Ca and 0.7 wt.% of the other elements. LIBS was identified as a suitable online analytic solution to monitor slag chemical composition and the related environmental impact already during the process trying to reduce as much as possible the Cr content thus also providing economic benefits. Cr content control would also allow to tailor slag foaming as increasing Cr content determines an increase in slag viscosity.

The possibility to implement LIBS measurement at Aceralia BOF was carefully checked and the main problems found were the dusty atmosphere in the converter vessel during blowing and the long distance between lens and slag surface where dust disturbed the beams heavily. The second problem to overcome was the protection of the employees against main laser beams and unwanted reflections in the plant. After finalizing the whole research project, it was concluded that LIBS methods were able to solve measurement problems of liquid and solid slags in steel plants.

2.1.12 Sustainable agriculture using blast furnace and steel slags as liming agents (21)

The project was coordinated by FEhS with Bundesamt und Forschungszentrum für Landwirtschaft (BLW), CENIM, Thomasdünger and TKS participating as partners in the consortium. The project started on the 1st of July 2001 and lasted almost three years, ending on the 30th of June 2004. The overall project cost 1.04 M€ and the EU contributed 622 k€, i.e., almost 60 % of the budget.

The main target of the project was to prove that steel slags could be advantageously exploited as liming materials with no harmful effects on soil and groundwater. To this aim, the research project was divided in two main lines: the investigation of the origin of heavy metals in the BF–BOF metallurgical cycle and the actual effects of steel slags as fertilizers in agriculture. The project was of great relevance since the use of BF and steel slag as fertilizer in agriculture could be a viable solution to ensure their 100 % reuse and recycling in some European countries. Indeed, previous studies showed that coarse BOF slag grained with 12 % of humidity were able to provide higher efficiency than natural coarse liming materials ensuring also less dust development. Despite this, fertilizers had to comply with the more restrictive regulations promulgated by the European Commission which aimed to limit the emission of some heavy metals such as Cr and V. This aspect was one of the most critical to ensure the further use of steel slag as a fertilizer. Considering this, the project tried to demonstrate through practical tests on plant and soils that steel slag fertilizers were not harmful to environment and men. In particular, long period test fields were performed on different lands, e.g., arable land, green land,

meadows, and forestry, trying to disclose the effect of heavy metals and toxic elements on plant growth, plant uptake, soil conditions and their harmfulness to groundwater. Further parameters considered were the pH-values and the behavior of other elements such as P, Ca, Mg, Zn and Pb in soils and plants. Furthermore, the evolution of Cr and V concentrations into the different steps of the metallurgical circuit from the BF to the BOF converter were studied analyzing the composition of the main input materials used in BF.

The first input material under investigation was iron ore characterized by variable quality depending on the exporting country, e.g., Australia, Brazil, India, South Africa, Sweden and Mauritania. Besides iron ores, scrap was considered as the second main variable affecting steel quality and steel slag composition. This aspect was fundamental since often data on scrap composition were not available thus complicating the planning of the scrap burden to be added to the hot metal in the BOF for a total amount around 10-20 %. The effect of reducing agents such as coal and coke was not considered in the analysis of heavy metal in the slag as they played only a marginal role due to their organic origin which influenced mainly S and P content. Analogously, fixing agents like sand, bauxite, dolomite and lime did not provide any noticeable heavy metal contents and their influence was neglected.

A burden normally used at TKS for hot metal production was taken as reference for the calculation and only the chemical influence of the different ores was examined at first. After that the high utilization of recycled materials coming from the production lines was also considered since this was an essential economic factor for the competitiveness of the primary products. For the analysis, the ores with the highest and lowest content of Cr and V were selected and their influence on hot metal, BF slag, crude steel and BOF slags was investigated. The ores coming from the Southern hemisphere, i.e., Brazil and Australia, were characterized by lower level of heavy metals compared to those from the Northern hemisphere. Indeed, Scandinavian ores displayed a relatively high V content, while pellets from Canada showed a relatively high Cr level. The results also underlined that the heavy metal content remaining in BOF slag was considerably high despite selecting iron ores with initial low contents. This was ascribed to the overall metallurgical treatment of iron ore. Heavy metals mainly concentrated in the hot metal after reduction in BF thus being conveyed into BOF where they accumulated into the slag after being oxidized by top-blowing. In particular, V can be oxidized up to about 95 % into BOF slag and Cr was scorified only about 40 % while a considerable amount remained solved into the crude steel.

V input was also influenced significantly by the amount of recycled material in the BF burden and the lower this amount the lower V content. This practice must be carefully balanced considering that recycled materials contain high amounts of metals and an eventual reduction of their content in the BF burden would affect the economic return of hot metal production. Finally, Cr input was mainly influenced by scrap, therefore the use of low Cr scarp could allow better control of this heavy metal. Considering the effect of scrap on heavy metal concentration in the slag and considering that EAF route used to produce stainless steel can envisage the use of 100 % scrap burden, the slag resulting from these operations cannot be used as fertilizers due to their higher concentration of Cr, Ni and V. It can be concluded that BF slag can be conveniently used as raw material to produce fertilizers being almost free of heavy metals thanks to the reducing conditions in BF. On the contrary, Cr content in

BOF slag could not fulfill the requirements of a liming material from natural stone even using the cleanest possible burden thus making necessary to investigate the effect of this element on soil and plants to exclude any risks for the environment.

Moving to the evaluation of slag feasibility as liming agent, the first camping was performed in different German sites investigating the impact of Cr and V contained in BF and steel slags and of Cd contained in phosphate fertilizer on plants growth, soil fertility and men and animals health. Seven static long-term fields, i.e., five arable lands and two grasslands, were selected for the liming tests. The first one was the grassland of St. Peter from 1954 to 2004 comparing the results without P fertilizers to the ones obtained with Thoms slag, i.e., industrial phosphate rich slag, and converter slag. Two liming tests were performed in Arzdorf and Sommerland considering four liming treatments, i.e., carbonate limestone, BF and BOF slags. The tests were temporarily interrupted after running 21 years from1975 to 1995 and 16 years from 1979 to 1993 and were reopened again for this research project from 2002 to 2004, respectively. Two further liming tests were performed in Rösrath on arable land from 1989 to 2004 and on pasture from 1990 to 2004 using two different amounts of two liming materials, i.e., carbonate limestone and disintegrated LD converter slags. Further liming tests were performed from 1993 to 2004 in the Essershausen fields using five different liming materials, i.e., burnt lime, carbonate limestone, milled converter slag, disintegrating converter slag and milled BF slag. Finally, the last field analyzed was in Kasseburg from 1993 to 2004 employing two different liming agents, i.e., carbonate limestone and disintegrated LS. The first general outcome was the significant increase in yield of experimental crops in long-term field when using BF, LD and ladle slag compared to burnt lime and carbonate limestone.

The results obtained at Azdorf reported a strong increase in plant yields after liming with BF and converter slag although the increase of soil reaction with BF lime was slightly lower. No significant differences were observed between burnt lime and converter lime pH values while the pH values with BF lime were almost 0.1 – 0.2 units lower. Furthermore, pH of the non-limed soil was the lowest. Cr content was mostly higher when using the converter lime treatments, but no clear increase was detected over the years. This was ascribed to the fact that Cr added through converter lime may transform into compounds that are not soluble in aqua regia, i.e., the solvent used to perform the analysis. Similarly, a clear increase in V content was observed with converter lime treatment during the last five years of the first period while it remained on a constant level with the other treatments.

During the experimental trial on the clay-rich marsh soil in Sommerland, significant increases in yields and pH-values affected by liming were detected but the additional yields were comparatively small on this site with mean yield increases of about 3 % in the first period. In particular, BF and converter lime provided higher yields than burnt lime while no significant differences were observed in pH by using the different treatments. Even in this case, the use of converter lime caused an increase of Cr content in the soil during the first five years. In particular, the Cr content in the soils treated with converter lime was 10 mg Cr/kg higher than in the soils treated with the other liming materials. The development of V concentration was like Cr one. At beginning of the experiment V content increased about 20 mg V/kg within the first three years and remained on this level until the end of the first period of trial.

Rösrath field tests reported no significant differences in arable and grassland soil pH performing the treatments with both liming materials, i.e., carbonate limestone and disintegrated converter slags. It was also observed that liming was generally responsible for an increase in soil pH leading to an increase from 5.8 to 6.5 in grassland. Again, the application of converter lime led to higher yields in both arable lands and pasture. The analysis of Cr and V content in Rösrath field highlighted an increase of these elements in the top layer when using disintegrated converter slag as liming agent. Grassland seemed to be more affected than arable land displaying a steady increase of this variable probably ascribable to the sampling of unsolved converter lime on soil surface. Cr and V migration in the subsoil of grassland went no further than 25 cm depth after 44 years of annual basic slag application.

Essershausen test fields reported significantly higher mean additional yields when performing the treatment with slag rather than with burnt lime and carbonate limestone. By annual liming, soil pH-values steadily increased from 4.9 to 6.5 and no significant differences were observed between the different liming treatments even if the highest pH-values were reached with carbonate limestone. In this test field, the aqua regia extractable Cr in the soils treated with converter lime increased during the experiment. In particular, Cr values in converter lime treated soils increased over the 11-year period of the field experiment to about 10 mg Cr/kg soil compared to the non-limed treatment. Cr input caused by BF lime application was considerably lower than by converter lime. Again, V concentration developed similarly to Cr one with the highest levels being achieved with converter lime. In particular, aqua regia extractable V in the soil treated with converter lime increased of 8 mg V/kg compared to non-limed soils. Furthermore, higher Cr and V contents were observed when using milled BOF converter lime rather than disintegrated converter BOF lime due to the abrasion of milling objects during grinding.

Kasseburg test field reported similar results with LS being more effective than carbonate lime in increasing plant yields. An increase of pH in the soil up to 6.6 was observed with all liming materials and it proved to be slightly too high for this sandy soil. LS treatment determined Cr levels in the soils about 2 mg Cr/kg higher than limestone treatment. Because of the low V input with the liming materials a clear change of V content in dependence of liming and time was not expected.

Concerning plant V an Cr uptake, huge deviations of these parameters were observed in field experiments with significantly higher Cr and V contents observed on the treatments with converter lime in the shoot of winter wheat in Sommerland in 2002 and in grassland cuts in Rösrath in 2002. Only higher Cr contents were found in stems of maize in Rösrath in 2002 and in grains of rape in Essershausen in 2002. To overcome the uncertainty deriving from these huge deviations, pot experiments under controlled conditions with soils from two long-term field trials with different Cr and V contents were performed. Wessenstedt soil limed with carbonate limestone and BF slag, and Schillhofen soil limed with carbonate limestone and converter lime were considered. On Wessenstedt soil, nearly all crops produced higher yields on the soil subjected to the liming treatments. BF and BOF limed soil displayed significantly higher values than carbonate limestone treated soils. On Schillhofen soil, yield differences were less evident yet still statistically significantly higher for the converter lime treatment. Schillhofen soil displayed and increase in Cr and V content after the treatments with converter lime and Wessenstedt soil also displayed higher soil V contents when liming with BF slag.

Despite this, Cr and V uptakes by all crops did not show any dependence on the contents of both elements in the soil. As in the plant samples of the field experiments, V contents in the plants were lower than Cr ones.

In Austria three long term field were selected for the investigation, i.e., Fuchsenbigl, Rottenhaus and Zwettl. Fuchsenbigl soil was classified as a sandy silt with a medium texture characterized by an alkaline nature with a pH >7.3. Rottenhaus soil was classified as a silty loam with a heavy texture and higher contents of organic matter than Fuchsenbigl. Furthermore, the highest filter and buffer capacity among all three investigated sites was detected. Zwettl soil was classified as a loamy sand with an acidic light texture and was characterized by the lowest organic C content of all three sites. All relevant crops for the specific sites, e.g., cereals, root crops, legumes, were tested since 1956. The chemical composition of the P-fertilizers used in the Austrian field test is reported in

Table 2 and two different fertilizers rates, i.e., 44 kg P/ha yr medium rate and 175 kg P/ha yr high rate, were considered. Four of the six basic slags used overcame the V threshold of 4000 mg/kg and one of them overcame the Cr threshold of 2500 mg/kg according to the Austrian Fertilizer Ordinance of 2004.

The results highlighted that BF slags ensured higher yields of rye in Fuchsenbigl, potato in Rottenhaus and Zwettl, and winter wheat in all three sites compared to superphosphate when using the medium rate. The use of basic slag for 48 years did not modify significantly soil parameters such as soil texture or content of organic matter which may influence heavy metal mobility and availability. However, significant increases were observed in pH on neutral or slight acidic soils. Concerning V concentration in the soil, the use of medium rates of basic slag caused an accumulation of V in the topsoil of +11 % in Zwettl and +68 % in Fuchsenbigl while high basic slag rates caused an accumulation of +74 % in Zwettl and +167 % in Fuchsenbigl. Concerning Cr, considerable amounts of Cr VI could be detected in BF slag fertilizers, but it did not seem to be stable in the soil displaying values below 0.30 mg/kg. Furthermore, basic slag medium rates also determined higher Cr and V contents until 40 cm in Fuchsenbigl and Rottenhaus and 35 cm in Zwettl thus indicating a downwards translocation of about 10 cm below the plough layer. Concerning Cd, significant accumulation in the soil was observed only with high rates of superphosphate, with +57 % in Fuchsenbigl, +106 % in Rottenhaus and +133 % in Zwettl. Despite this, Cr and Cd contents of all investigated soil were far below the limit values. Finally, the presence of these trace elements, i.e., Cr, V and Cd, in different crops, i.e., rye, rape, spring barley, potatoes and winter wheat, was investigated. Cr proved to be near or below the detection limit of 0.035 mg/kg in rye, rape and winter wheat because it was quite immobile in the soil. Analogously, V could not be measured in rye, rape, spring barley and winter wheat while significantly high contents were detected in potatoes when using basic slag compared with the control. Concerning Cd, significant accumulation in the potatoes was observed when using the superphosphate variant, i.e., 3 times higher than control plots in Fuchsenbigl and Rottenhaus, while its content in rye and spring barley was far below the EU limit. Overall, these results demonstrated the low risk of accumulation of potential toxic heavy metals in the investigated food plant with long term usual amounts of the tested fertilizer.

Table 2: Chemical analysis of the fertilizer used in Austrian Fields

	P_2O_5 %	CaO %	MgO %	SiO_2 %	Cu mg/kg	Zn mg/kg	Pb wt.%	Cd mg/kg	Cr mg/kg	Ni mg/kg	V mg/kg
Fuchsenbigl											
Basic Slag 1999	18.2	51.8	1.8	9.7	39.5	56	8.8	0.33	2100	1.2	6473
Basic Slag 2000	18.8	52.1	1.8	9.2	40.7	47	9.0	0.25	2200	1.6	6972
Superphosphate 2000	23.7	34.6	0.3	4.5	12.4	145	2.2	5.20	99	7.7	76.1
Rottenhaus											
Basic Slag 1999	17.0	50.7	1.9	8.6	39.2	51	6.1	0.21	2100	1.3	6433
Basic Slag 2000	22.1	42.5	5.7	4.2	37.7	648	23.0	10.0	990	11	25.88
Superphosphate 2000	25.4	33.2	0.9	3.4	11.5	145	3.8	5.40	96	8.4	83.1
Zwettl											
Basic Slag 1999	16.6	48.2	2.0	8.6	39.4	47	8.1	0.32	2500	1.5	6616
Basic Slag 2000	18.5	35	5.6	6.7	17.3	395	5.8	12.0	230	33	290
Superphosphate 2000	19.9	31.8	0.6	5.0	11.8	127	2.2	4.20	88	9.0	68.9

Finally, some experiments were performed in Spain on arable land in Cepeda and Villarrobejo, pastureland in Abadiano and Derio and in forest. The arable land and the pastures were fertilized for 10 years with BOF slag from 1980 to 1990 and were then limed with other agents. The forest test field was fertilized by BOF slag from 1994 to 1996 and was divided in two areas: a forest module without any additional planting and an agricultural forest module. Concerning the forest module, the application of BOF slag caused a moderate increase in soil pH and Mn content with an increase from 35.8 to 70.5 mg/kg. Similarly, an increase of approximately 1 pH unit in the first 5 cm of soil was detected in the agricultural forest module as a consequence of BOF slag application. A positive pH trend was also found in the layer from 5 to 25 cm. Again, the Mn content increased by adding BOF slag every year and its accumulation was mainly recorded in the first 5 cm of soil. Mn increased from 26.7 mg/kg to 475.7 mg/kg, but these values were well below the 1500 mg/kg threshold considered for toxicity. BOF slags also influenced positively wood production expressed in terms of plant height. In particular, the differences in height would involve an average difference at the end of a 25-year period of 1.70 m compared to those with any slag applications. The application of BOF slag also determined an increase in P, Ca, Mg and K concentrations in the plants with K increasing from 8.39 to 9.23 g/kg.

The results of the project proved that fertilizers and liming materials produced from BF and steel slags may contribute significantly to a sustainable agriculture by improving plant yields. The enrichment of Cr and V elements seemed to have no negative effects on crop development and soil fertility. The results showed no risk in using fertilizers from iron and steel slags on soil, soil fertility, groundwater and health of men and animals. These outcomes were of primary importance considering that fine grained slag cannot be used in the building sector and dumping must be avoided to reach the European environmental strategic targets of a waste free steelmaking.

2.1.13 Alternative Processing of Sinter Plant Recycling Materials (22)

The project was coordinated by BFI with DK Recycling & Roheisen and Voestalpine Stahl participating as partners in the consortium. The project started on the 1st of July 2002 and lasted almost three and a half years, ending on the 31st of December 2005. The overall project cost 1.15 M€ and the EU contributed 692 k€, i.e., almost 60 % of the budget.

Sinter plants were often used to recycle residues rich in iron oxides resulting from different steelmaking processes. The different raw materials were premixed together with auxiliary materials such as coke breeze, lime and return fines from the sinter process itself. This mix was treated in a pelletizing drum with water and then fed on the sinter strand where it was ignited with natural gas burners. Normally, the amount of recycled residues exploitable in the sinter plant was limited to about 5 % due to productivity drop, sinter quality and emissions. Indeed, the experience demonstrated that some materials in the sinter mix, e.g., BF dust and sludge or mill scale, were responsible for significant sinter quality loss and could be used only to a limited extent. For example, the C content of BF dust and sludge in the sinter raw mix components allowed to lower coke breeze demand, but if their content was excessively high sinter reducibility was compromised due to the high FeO content. This effect became worse when using higher amounts of mill scale. To overcome these drawbacks, the production and use of cold bonded briquettes as additional raw material for BF was identified as a suitable alternative route for the co-processing of sinter plant recycling materials. Considering this, the present project aimed at developing an alternative industrial process for material recycling to reduce the quality drop of the sinter plant, assessing also the potential reduction in sinter plant emissions resulting from the reduced use of recycling materials in the sinter mix. In particular, the production of self-reducing briquettes from sinter plant recycling material to be exploited in BF was investigated.

Different briquetting processes were examined but agglomeration via vibration compacting press, i.e., the one used for concrete bricks production, was considered the best choice. Indeed, briquetting through stamp press provided high density and strength but resulted in high costs and low performance whereas pelletizing with added binders allowed the costs to decrease significantly but led to insufficient strength. On the contrary, vibration compacting press ensured very high performance and moderate strength when using fines together with moderate costs. Additionally, it ensured a strength similar to stamp press one when fine materials were agglomerated with coarse ones. In light of this and considering that recycling materials for briquetting were characterized by both fine, e.g., BF sludge and BOF dust, and coarse fractions, e.g., BF dust and mill scale, briquetting via vibration compacting was the best choice. The material charged in the mold was vibrated to ensure maximum particles rearrangement and self-compaction. Further compaction was provided by a stamp falling on the mold. Green bricks were then transported to curing.

BFI and DK characterized the main components of the sinter mix considered responsible for the quality and productivity drop at DK sinter plant, i.e., BF dust and sludge and mill scale. In particular, the chemical composition and the grain size distribution of these briquetting materials were determined. Furthermore, BFI carried out laboratory briquetting and strength tests to identify the most suitable recipes to be used in the technical scale trial. Particle size distribution confirmed the fine nature of Fe-rich BOF dust characterized by mean size between 0.1-0.25 mm and the coarse nature of the Fe-rich

mill scale and iron ore with a mean size of about 1.5 mm. BF dust was characterized by a moderate mean particle size of 0.4 mm and a high carbon content around 30 %. BF sludge displayed even a higher carbon content of 40 %. It was concluded that the recycling mixtures for briquetting should have been characterized by a size distribution with about 30 % of particles smaller than 1 mm, and 60 % smaller than 5 mm and a maximum upper size of 10 mm. Beside particle size distribution, the optimization of the chemical composition of the mixture was of primary importance to ensure a proper iron oxide-carbon ratio to ensure briquette self-reduction. To this aim, iron oxide rich components, e.g., mill scale, iron ore or BOF dust, were added to BF dust and sludge as their C content was higher than the reductant demand corresponding to their iron oxide content. Great amounts of BF dust and sludge and a binder content not higher than 20 % were used to produce the 18 different mixtures with the laboratory scale hydraulic stamp press. Portland cement was selected as binder applying a pressing pressure of 5 MPa and a pressure time of 30 sec. The curing time of the tablets was also varied and its effect on the breaking force was assessed. In most cases no curing effect was detected and curing time higher than one week was considered useless. Breaking tests proved that the use of 20 % cement binder ensured a higher breaking strength than 10 % and the highest value was achieved when using mixtures of coarse iron ore or mill scale together with BF dust, i.e., breaking force higher than 3000 N. This value dropped significantly to 2000 N when using BF sludge rather than BF dust.

Hot disintegration and melting tests were also performed on the 10 mixtures identified as the most suitable ones for the technical scale trial. These mixtures were selected because they were able to ensure high breaking strength while using high percentage of BF sludge and dust. This aspect was fundamental since they were largely available in the plant and contained the C necessary for reduction. Disintegration tests were performed at 550 °C for 90 minutes and all tablets almost retained their initial shape demonstrating good stability with just minor signs of material disintegration on the surface. This led to a reduced bonding strength in the subsurface area to a maximum depth of 2 mm. No major differences were observed in chemical composition between the original material and the post-test specimens. Melting tests were performed at 1750 °C and significant differences in melting behavior were observed between the different mixtures. Three different melting trends were observed: 1) complete iron and slag melting with the formation of an iron regulus and a solid slag layer, 2) complete iron and slag melting with formation of individual iron globules and powdered disintegrating slag, 3) incomplete iron and slag melting which prevented the separation of iron and slag constituents. Despite this, no significant discrepancies were observed in slag chemical analysis for all mixes displaying approximately 60 % of CaO, 30 % of SiO_2, and 10 % of Al_2O_3.

According to the laboratory scale results, some mixtures were selected to produce the bricks for the technical scale trial at DK using a concrete brick press to achieve high packing densities and strength. All ingredients were mixed with a concrete mixer and subsequently placed in the press mold to be compressed by vibration of mold walls. After that, a stamp plate was dropped onto the mold cavity to provide the final compression. Preliminary trials were conducted to identify the most suitable press parameters. Vibration time varied between 15 and 30 s, and it was concluded that cycles longer than 20 s did not provide any improvement in shape stability. The mixtures selected for the technical scale trial were those characterized by high strength and high concentrations of BF dust and sludge and are summarized in Table 3. Bricks breaking strength was tested to ensure their ability to withstand handling

and storage maneuvers without damage. Strength evolution was monitored over 1 month. Tests at Voestalpine were performed with a system of 2 balls or of one ball and a wedge and provided information on brick behavior in a pile whereas tests at BFI were performed with a universal hydraulic testing machine with a wedge as compression tool and allowed to simulate brick handling during charging. All mixtures strength increased with storage time and mixtures containing BF dust exhibited the highest strength coherently with laboratory tests. M1 displayed the highest breaking force of 1900 N at BFI and 3000 N at Voestalpine whereas M6 showed the worst breaking force around 600 N. Considering that the minimum breaking force identified as suitable for industrial trials was 1000 N, M1, M2, M5 and M7 proved to be suitable for the next steps.

Reduction tests were performed to simulate bricks behavior in the furnace since adhesion forces responsible for brick integrity may be affected during heating. The latter should remain high enough to minimize abrasion and maintain bricks strength and shape up to 500 °C. Previous research reported a full neutralization of cement and lime bonded bricks at 700-900 °C therefore tests were conducted in a reducing atmosphere at 1000 °C for 4 hours. All bricks mixtures displayed signs of disintegration over the entire surface. After reduction, bricks were subjected to ISO standard tumbler strength. M6 and M7 were completely unsuitable, being completely disintegrated after tumbler tests whereas M1, M3 and M5 exhibited good resistance to mechanical stresses assuming a spherical shape with diameters up to 5 cm. The remaining brick-balls still displayed the initial strength levels.

Based on these results, the best batch composition, i.e., M1, was selected to produce a 300-t industrial batch of residual-material bricks to be tested in the BF of DK. The effects of bricks on BF operation, in terms of production rate, coke consumption, gas utilization, blast pressure, slag amount and basicity and BF dust amount and chemical composition, were the main output of the trial. After pressing, bricks were stored for 5 days without further handling to allow cement to set and were then stored for 3 weeks in loose pile before use. Their chemical analysis showed high iron oxide and C contents which were well balanced to ensure the complete reduction of the iron oxide in the bricks. Relatively high Zn contents were also detected due to the use of BF dust. Bricks were also tested for their compression strength and reduction behavior before being charged in BF to ensure their compliance with the results previously obtained. Breaking strength was monitored over 3 weeks and increasing values of 35, 47 and 55 MPa were observed after 7, 14 and 21 days, respectively. Considering that the breaking strength required to withstand the charging processes without undergoing disintegration was 40 MPa, this value was easily obtained after a 2-week storage period. Shatter tests were also performed and bricks displayed high inherent stability with 85 % of the bricks retaining a size of at least 20 mm. Reduction tests performed at 1050 °C for 4 hours highlighted a significant reduction in C content due to the consequent transformation of oxidic iron into metallic Fe with a metallization degree of 94 %. Bricks displayed high inherent stability after reduction and were subjected to tumbler test. Almost 34 % of the bricks retained a size higher than 25 mm after the test allowing to conclude that bricks were able to arrive intact in the melting zone of the furnace not being discharged as dust. BF trial assessed the use of residual-material bricks accounting for up to 10 % of the input and lasted 1 week. The bricks were initially added to the charge at a rate of 30 kg/t hot metal, but this rate was increased up to 60 kg/t hot metal after 2 days. The results demonstrated that bricks charging did not have any direct negative influence on BF operating behavior. No impacts on hot metal composition were detected and

all sporadic fluctuations in C, Mn, P and S contents were operation related and not directly attributable to bricks charging. Similar conclusions were drawn for slag composition and basicity. Also, slag balance calculation proved that basicity would potentially increase only by 0.02 by charging the bricks at a rate of 60 kg/t hot metal. Analogously, BF dust analysis did not reveal any notable changes given the low input of 6 %.

Table 3: Composition of the mixtures used for the technical scale investigation expressed in wt.%

	BF Sludge	Mill Scale	BF Dust	BOF Dust	Iron Ore	Cinder	Binder (Portland Cement)
M1	0	40	30	10	0	0	20
M2	0	0	30	10	40	0	20
M3	0	30	30	0	0	20	20
M4	0	0	30	0	30	20	20
M5	0	40	40	0	0	0	20
M6	40	40	0	0	0	0	20
M7	40	0	0	0	40	0	20

A second test batch trial was performed using a 240-t lot of residual-material bricks consisting mainly of coke breeze, high amounts of mill scale and some BF dust. Larger brick dimensions were selected for this campaign to improve gas circulation in the furnace and to achieve better productivity in brick making. Furthermore, a better adjustment of grain size distribution of brick batch was performed to improve the cold crushing strength. A maximum cold crushing strength of 102 MPa was registered which was twice the strength of the bricks of the first trial. Shatter tests were also conducted and 95 % of the bricks retained a dimension of at least 20 mm after the test thus demonstrating a high inherent stability which was further confirmed after the reduction. Indeed, bricks after reduction tests were subjected to drum testing and the results were consistent with those of the first lot confirming their ability to reach intact the BF melting zone. This second BF trial lasted one week and was performed using a charging rate of 40 kg/t hot metal. The quality of the hot metal produced corresponded to that normally produced by DK with Si content varying between 1.3 and 3.1 wt.%. Also, C, Si, Zn and P concentrations did not seem to be affected by brick charging and oscillations in their values could be ascribed to production-related variations. In particular, C content averaged around 3.9 wt.%, P content was kept constant around 0.12 wt.% and Mn ranged between 0.5 and 0.6 wt.%. Also, S and Zn contents stayed at normal levels with little variation. Similar findings were made regarding slag composition with CaO, MgO and SiO_2 concentrations did not displaying any noticeable changes.

A further activity performed during the project concerned the evaluation of sinter input materials to improve and optimize sintering rate and quality and to reduce environmental emissions by varying the amount of recycled materials. Environmentally relevant emissions normally increased with growing amounts of recycled residual materials and for this reason their use in the sinter mix was around only 10 %. Considering this, tests were planned to estimate the alleviating effect played by the alternative

processing of the recycled materials on the sinter plant in terms of sinter quality and plant performance and emissions. The basic sinter mixture at DK was characterized by a medium size D50 of 27.1mm, a bulk density of 1690 kg/m^3, a Fe content of 55.3 wt.%, a SiO_2 content of 8.5 wt.%, a CaO content of 8.2 wt.% and a Zn content of 2.4 wt.%. Three different DK sinter specimens were considered, i.e., sinter basic, neutral and acidic, and all of them were mainly characterized by hematite and various Ca silicates, i.e., CS, C_2S, C_2S_3, rankinite, as slag phases. Dendritic Ca ferrites were more predominant in alkaline specimens and were easier to reduce than the iron bonded in slag phase which was present in the acidic specimens.

Sinter pot tests were performed by Voestalpine using an equipment with a 0.16 m^2 suction area and an ignition unit consisting of a natural gas burner. Pressure drop was controlled by adjusting the frequency of the fan motors and waste gas temperature, amount and pressure drop were measured online, as well as their composition in terms of O_2, CO_2, CO, SO_2 and NO. The burning through procedure included 2 minutes of sucking with decreased pressure drop, after that the sinter cake was discharged and chopped into several coarse pieces, cooled down for at least 1 hour and then treated in an ISO-drum. The particles still coarser than 50 mm were crushed in a jaw crusher and then the material was screened with a Mogensen sizer into several size fractions from 40 to 4mm. Five tests were performed: 2 with the basis mix with 1.2 % of flue dust and 3.7 % mill scale, 1 without mill scale, 1 without flue dust and 1 with none of them. Grain size distribution of sinter mix played a marginal effect as well as the related void fraction and cold permeability. Unsubstantial differences were registered with and without flue dust and mill scale and this allowed to conclude that small amounts of recycling materials in a sinter mixture did not have any negative influence as long as the amount of sinter-feed ore was high enough to bear these recycling materials. Also, the burn-through-time was in the same range for all tests. Sinter productivity proved to be the highest with both flue dust and mill scale and the lowest without both due to the different grain size distribution of the sinter cake after mechanical treatment. Indeed, the mixture without recycling materials was characterized by the finest grain size with a smaller portion of coarse sinter product and the highest portion of return fines. The use of flue dust seemed to have more substantial influence while mill scale behaved rather indifferently and this was ascribed to dust carbon content. Indeed, the carbon content of the flue dust seemed to contribute significantly to the heat in the flame front under the investigated conditions. Coke breeze content was increased by 0.43 % in tests without flue dust to substitute the carbon provided by it, but this action did not seem to cover the full substitution. This could be the main reason for a higher return of fines, a smaller sinter yield and specific productivity, a finer size distribution of the sinter and a higher low-temperature breakdown. Sinter pot tests allowed to conclude that small amounts of recycling materials did not affect significantly specific sinter productivity and could rather exert a positive effect on sinter quality in terms of strength, grain size distribution and return of fines, therefore the most efficient utilization of fine iron bearing recycling materials was still sintering. Nevertheless, an increase in specific emissions and an adverse alteration of sinter waste gas composition was observed depending on the composition of the recycled materials. Indeed, C content of the flue dust acted as fuel in the same way as C in normal coke breeze, but flue dust used in the tests also contained 0.3-0.35 % of S which despite being smaller than S content of normal coke breeze, i.e., 0.5-0.6 %, led to

higher specific S input and specific emission due to the compensation ratio between flue dust and coke breeze which was about 2.5.

A comparison between sinters with different basicity and bricks was also performed in terms of softening temperature, softening time and degree of reduction, assessing also mixtures of 85 wt.% of acidic sinter and 15 wt.% of bricks. BF conditions were simulated up to a softening point for a defined pressure differential across the packed bed. In particular, a heating of 50 minutes up to 950 °C in N_2 atmosphere was followed by 15 minutes holding time, after that reduction at 950 °C was performed for 75 minutes in a 60 % N_2 and 40 % CO atmosphere, finally softening up to 200 mbar fixed pressure differential in the bed with a further temperature increase in a 60 % N_2 and 40 % CO gas atmosphere was carried out. The results highlighted an increase in the softening temperature and time and in the degree of reduction with the basicity of the sinter.

2.1.14 Hearth protection in BF operation by injection of TiO_2-materials (23)

The project was coordinated by TKS with BFI, CSM, EKO Stahl, MEFOS, Ruukki (Rautaruukki) and Voestalpine Stahl participating as partners in the consortium. The project started on the 1st of July 2002 and lasted almost three and a half years, ending on the 31st of December 2005. The overall project cost 2.01 M€ and the EU contributed 1.2 M€, i.e., almost 60 % of the budget.

The protection of BF hearth by charging ilmenite, i.e., $FeTiO_3$, with the burden was a well-established practice to shield the refractories thanks to the formation of a solid high melting scaffold of solid titanium carbonitride (TiCN) at the carbon brick/hot metal interface (24) (25). Scaffold formation started with TiO_2 dissolution in the slag which was then reduced to Ti and dissolved into the hot metal. Once the Ti-enriched hot metal reached a cold worn area at hearth walls, it experienced a rapid thermal energy loss which caused a drop in Ti, C and N solubility which resulted in the formation of the TiCN scaffold (26). These scaffolds acted as protective layers precipitating in the most worn areas of the furnace. Despite the positive effect of ilmenite on hearth protection, some disadvantages such as poor efficiency in terms of amount of raw material used, increased reductant consumption, poor slag tapping, and unstable furnace operation due to ilmenite charging arouse from this practice. Indeed, ilmenite addition determines an enrichment of hot metal with Ti and of slag with TiO_2, but the distribution of Ti between metal and slag was quite poor with Ti content in the hot metal being significantly lower than in the slag, i.e., lower than 10 %. This caused a poor efficiency of the ilmenite charged, together with a raise in TiO_2 content in the slag which resulted in a higher viscosity and a reduced quality of the granulated BF-slag.

It must be also considered that ilmenite charging with the burden caused significant time delay from charging to carbonitride precipitation at the hearth refractory due to burden residence time. This problem was completely overcome by using ilmenite sand injection at tuyere, but its strong abrasive nature allowed to apply this solution only if acute problems in the hearth occurred. Alternative TiO_2 materials such as synthetic Rutile were developed to avoid wear problems while still ensuring BF elongate campaign life. The first injection tests in BF showed promising results, but few information was available at the time of the project on the metallurgical reactions occurring. The preliminary

information available from TiO_2 injection trials displayed an initial Ti-enrichment of the slag and only with a certain time delay hot metal Ti-enrichment allowing to conclude that TiO_2 reduction and its mass transfer from slag to metal were the rate determining steps. TiO_2 is much more difficult to reduce than FeO and its carbothermic reduction led to the formation of solid TiC with a melting point above 3000 °C which required dissolution in liquid iron. Considering this, the present project aimed to optimize the injection of Ti materials at BF tuyeres to ensure a fulfilling hearth protection while reducing the costs connected with hot metal enrichment in Ti and lowering TiO_2 content in the slag to keep good its quality for granulation processes.

Thermochemical calculations on TiCN formation were performed with FactSage by BFI and a simplified melt flow pattern was developed to evaluate Ti time dependent behavior in BF hearth. At first, the calculations considered only a single component system with hot metal alone and only at a later stage the complete system of slag and hot metal was assessed. A temperature of 1550 °C and a pressure of 2.6 bar were applied to predict Ti distribution in slag and hot metal. Hot metal composition was simplified as 4.8 wt.% C, 0.006 wt.% N and rest Fe while slag composition was schematized as 42.1 wt.% CaO, 36.6 wt.% SiO_2, 12.6 wt.% Al_2O_3 and 8.7 wt.% MgO. The first step of the analysis evaluated the dependence of hot metal saturation with Ti as a function of temperature and other components. The results showed that TiCN separation occurred at higher Ti content in the hot metal for increasing temperatures due to the higher Ti dissolution. Furthermore, TiCN composition depended strongly on hot metal temperature with TiN content decreasing from 70 to 45 wt.% and TiC content increasing from 10 to 40 wt.% for temperatures rising from 1350 to 1700 °C. The effect of accompanying elements such as Mn, Si, S and P was also evaluated. Si and Mn did not influence Ti solubility in the hot metal whereas P and S exerted a negative influence decreasing rapidly Ti solubility. This phenomenon was more exacerbated at low temperatures.

The second step of the investigation was performed considering both hot metal and slag and an addition of 6 kg/t hot metal TiO_2 to the system. Increasing S content in the hot metal determined increasing Ti content in the slag and decreasing Ti content in the hot metal itself thus allowing to conclude again that S content must be kept low to enhance Ti enrichment in the hot metal. Opposite effect was exerted by Si because increasing content in the hot metal determined increasing Ti content in the pig iron and decreasing Ti content in the slag thus exerting a positive effect on hot metal Ti-enrichment. The effect of hot metal temperature demonstrated that increasing values were responsible for increasing Ti content in the hot metal as the content in the slag grew only up to 1570 °C and then started to decrease. The trend of the ratio of Ti content in the hot metal to the Ti content in the slag could be divided in 3 zones, i.e., a decreasing Ti distribution up to 1510 °C, a smooth growth up to 1570 °C followed by a steeper one. The calculations reproduced quite faithfully the tendencies of the Ti content as a function of the operating parameters observed in real BF operations.

BFI also developed a simplified melt flow pattern using a statistical reactor model evaluation method thanks to a commercially available mathematical simulation tool. Injection trials were performed at the BF of EKO using a Ti-rich waste material to tailor and verify the melt flow pattern. During the trial, 1 ton of the material was injected in 3.5 hours and the residence time distribution (RTD) of the trials allowed to develop the zone model and to calculate the mean residence time of Ti in BF. The trial

allowed to investigate RTD and mean residence time of the injected material as a function of the injection point, i.e., angles of 90 and 180 ° between tuyere and tap hole. The results highlighted a maximum TiO_2 content in the slag 4 hours after injection start. This value decreased continuously until reaching normal levels after 10 hours from injection end for the 90° configuration. For the 180° configuration, the maximum TiO_2 content in the slag was achieved after 5 hours from injection start and the normal TiO_2 content was reached after 16 hours from injection end. The mean residence time for the 90° configuration was 3.4 hours whereas the one for the 180° configuration was longer and equal to 6.4 hours. A good consistency between the RTD resulting from the simulation and the one obtained from the injection trials was observed for both configurations.

Once validated the RTD model, different injection regimes were simulated. Continuous and discontinuous injection regimes were analyzed considering equivalent total amounts of injected Ti and an injection with a 90° angle to the tap hole. Small Ti rates were injected with the continuous regime over a period of 36 hours while three injection intervals with high Ti rates were selected for the discontinuous regime applying a 12 hours interval periods between the different injections. The simulation demonstrated that a discontinuous regime was more favorable for protective layer formation since Ti concentration increased constantly when applying a continuous injection regime until reaching a steady state where Ti input and output were the same. In this case, Ti concentration in both slag and hot metal remained on comparable low levels. On the contrary, Ti concentration reached very high values, i.e., 5 times higher than during continuous injection, shortly after injection when using the discontinuous regime. This scenario made the approach of Ti saturation limit in hot metal more likely to be exceeded, leading to the formation of the TiCN protecting layer.

Beyond the modelling activity, many injection campaigns at various BFs were performed at TKS, EKO, Ruukki, Voestalpine and MEFOS. TKS focused on both short- and medium-term injection trials using BFs with single and multiple tap holes and investigating different TiO_2-containing materials assessing also the co-injection with reductants. EKO Stahl performed injection trials using TiO_2-rich waste material both as pure substance and as a mixture with plastic wastes. Ruukki analyzed the efficiency of charging TiO_2 materials with the burden performing also injection trials with ilmenite clay. Furthermore, it determined scaffold formation during mid-campaign repair of BF. Analogously, Voestalpine studied the long-term effect of TiO_2-input into BF with the burden and investigated scaffold formation after BF blow down. MEFOS investigated TiO_2-materials injection in an Electric Blast Furnace (EBF) analyzing again scaffold formation after hearth dissection. Finally, CSM studied the use of TiO_2-enriched clay for tap hole production making laboratory tests on clay properties.

Ruukki and Voestalpine provided experimental evidence on the effect of TiO_2 charging with the burden on scaffold formation and on hot metal and slag quality. Sinter was the main Ti source for Ruukki BFs contributing for more than 80 % to the overall Ti load as titano-hematite with a 4 % Ti content was used. The results highlighted that Ti load did not have a verifiable correlation with Ti mass distribution whereas a much stronger effect was exerted by BF heat levels and by BF hearth activity which was conveniently described by S distribution. Indeed, a very strong correlation between Ti content in the hot metal and S distribution was observed as they were directly correlated by slag oxygen potential. The experimental campaign at Voestalpine assessed the long-term input of TiO_2 into BF by charging

ilmenite lump ore and TiO_2 for almost 10 years. A total amount of 234,499 t of ilmenite lump ore was charged in BF and a total amount of 64,860 t of Ti passed through the furnace but only 21 % was picked up by the hot metal. In 1996, a significant increase in Ti content in both hot metal and slag was observed due to the increase in ilmenite lump ore rate to average 15 kg/t hot metal. Voestalpine BF was often operated at production levels exceeding its nominal capacity of 5500 t/24 h and this accelerated hearth wearing rate which was investigated by monitoring hearth temperatures evolution. Preliminary signs of hearth wear phenomena were detected in 2000 after almost 5 years from starting blow in BF, but real hot spots occurred only 3 years later in 2003. The first attempt to stop temperature rising was made by lowering oxygen rate, but it failed displaying a further temperature increase in the next days. Considering this, one of the tuyeres was plugged and blast oxygen enrichment was shut down again. Furthermore, ilmenite lump ore was raised from 15 to 20 kg/t hot metal leading to a higher TiO_2 content in the slag. After 3 days of tuyere plugging, the temperature went down significantly for few weeks before rising again to a new peak within 3 days. Again, two of the tuyeres were plugged, blast oxygen rate was shut down, and ilmenite lump ore rate was increased to 25 kg/t hot metal. This procedure allowed to drop down hearth temperature immediately, but further information was not available as the thermocouple failed after experiencing the temperature peak.

In summary, the actions undertaken at Voestalpine to face temperature peaks in hearth were the decrease of blast oxygen enrichment, the lowering of oil injection rate, the plugging of the tuyeres on the affected area, and the change of tapping management. All these countermeasures aimed at reducing the heat flow along the furnace wall. The rate of ilmenite lump ore in the burden was also increased when hot spots became critical, but this procedure was only a preventive action considering that it was unlikely that its temporary increases may have any influence when temperature peaks were already evident. TiO_2 injection into BF hearth could be considered as a preferred method to fight directly hot spots formation. Despite this, TiO_2 materials both in the burden and injected must be limited due to the negative effect exerted on slag viscosity and quality for reuse in road construction and cement industry. Considering this, the long-term rate of ilmenite lump ore was limited to 22 kg/t hot metal to meet slag quality specification.

Trials assessing TiO_2 injection were performed by Ruukki, TKS and EKO. The trials at Ruukki were performed just before BFs mid-campaign repair when the hearth was protected by injecting Rutile. Injection position and duration, injected material mass flow rate and the overall amount of injected material were registered. During the first injection campaign, 500 kg of rutile were injected in 45 minutes, and the injection started 30 minutes after tapping start. The injection was performed at the tuyeres around the tap hole as the hot spot was located there at 2.6 m below tuyere level. Rutile injection seemed to be successful in decreasing side wall temperatures probably due to the extra material injected into the hot conditions. This effect was more evident when hearth temperature was higher. Hearth temperature decrease started 45 minutes after injection started and the biggest drop was almost 200 °C, but it was only temporary since operating temperature went back to ordinary level after 12 hours from injection. In the second trial, the amount of injected Ti ranged from 300 and 700 kg and took about 20-90 minutes to be completed using a maximum load of 3.5 kg/t hot metal. Injection was performed mainly through tuyeres 11 and 12 which were near the hot spot located below tuyeres 13 and 15 at +6.6 m level. This choice was made because practical experience

demonstrated that the tuyeres used for injection should be close to the hot spot to maximize the effect. For comparison, an injection was carried out also on the opposite side of the hot spot and, in this case, Ti injection did not exert a clear lowering effect on hearth temperatures in worn areas. After injection, the formation of a hard skull around the tap hole was observed and its chemical analysis pointed out the poor efficiency of the process highlighting a C content lower than 4.0 %, i.e., 0.33-0.45 %, and a S content higher than 0.1 %, i.e., 0.38-0.39. Ti content in the hot metal proved to be the major factor affecting the injection process as injected Ti must circulate in the hot metal to get in contact with hearth wall refractories. Indeed, mass flow rate of Ti-material was modified between 2.5-25 kg/min during the injection trials and increasing values proved to be positive in providing more protective conditions. It can be inferred that increasing amounts of injected material intensify the efficiency of the process. Furthermore, injection seemed to be more effective when started simultaneously with slag delay because the liquid level in the hearth decreased and it was easier for the injected Ti to reach the surface of the hot metal and the duration of injection could be shorter.

Further short- and long-term injection trials were performed at TKS. Local short-term injections of TiO_2 materials were performed after the formation of a hot spot where temperature rose from 150 to 350 °C at the transition zone between ring and bottom layer close to tap hole. TKS injected Rutile with a Ti content of 80-85 % to counteract this phenomenon with the production of a local Ti enrichment close to the worn area in addition to the standard ilmenite charging with the burden. Both tap holes were in operation when the hot spot was generated therefore Rutile was injected directly above the worn area. During the 4 days of injection, stagnation of hearth temperature at the worn area was achieved, but it rose again to 400 °C after a 2-day delay. A temperature decrease was achieved only after performing the tapping at the tap hole opposite to the worn area. The injection trial proved that local short-term injection of Rutile was able to arrest critical temperature increases in BF hearth, but long-term injections were necessary for a more durable effect. To this aim, local long-term injection trials were carried out after identifying a new temperature increase in the transition zone between the ring and the bottom layer. Local injections of 2-2.5 t/d of Rutile were performed for 2 days and allowed to decrease or keep constant the hearth temperature in the affected regions. The following days the injected material was progressively reduced until stopping and temperatures began to rise again therefore it was necessary to reperform local injection to arrest temperature increase and allow for temperature decrease in the upcoming days. Approximately 22 t of Rutile were injected during the campaign. The same year, a further temperature increase was observed, and another injection campaign was started using an injection rate of 1.5 t/d. In the first period of the campaign, Rutile was injected through one of the tuyeres affected by the temperature increase thus allowing it to stop. With the change of tap hole, the injection position was slightly switched to reach further on the affected area. The injection campaign lasted 26 days until all hearth temperatures tended downward. Approximately 37 t of Rutile were injected during the campaign. The local injection during both campaigns was performed discontinuously for about 30 minutes during tapping and it was carried out additionally to the standard ilmenite charging with the burden of 20 kg/t hot metal.

The results pointed out that local injection of Ti-rich materials caused only low increase of Ti in the hot metal and in the slag, but a significant enrichment was achieved locally at the worn areas. Furthermore, increasing temperatures were responsible for increasing Ti content in the hot metal and

decreasing content in the slag. It was also concluded that worn areas occurred mainly near tap holes therefore switching the tapping from the hole close to the worn area to the opposite one resulted in a change of flow condition which caused a decrease of hearth temperature due to the building of a TiCN layer. Finally, it was observed that a bad coke quality may hinder the formation of the TiCN layer in the hearth.

Further long term campaign were performed by TKS in Hamborn where the BF operated since 1987 without relining and two worn areas in the hearth were detected, i.e., below tuyeres 3 and 4 close to the tap hole in the transition area between ring and bottom layer and at tuyeres 17 and 21. In particular, an increase in temperature from 110 to 290 °C was observed below tuyere 21. The scheduled shutdown of 80 hours allowed the temperature to go back to 180 °C, but it rose again after the furnace was restarted. Therefore, rutile injection was applied at tuyere 21 allowing to stop temperature rising at 300 °C after 9 days and to decrease it to 210 °C after 14 further days. During the whole trial, ilmenite charging varied between 17 and 20 kg/t hot metal. Again, one of the main factors ensuring the formation of a protective layer was a high Ti content in the hot metal which should be higher than 0.09 % to see a reaction. It was also noticed that hot metal temperature should be higher than 1480 °C to get the best outcome.

A last long-term trial was performed in Schwelgern where temperatures above 400 °C were detected in the area below tuyeres 22 and 24 in the transition area between ring- and bottom-layer and below tuyeres 13 and 35. Charging 10 kg/t hot metal of lump ilmenite was the first attempt to control the situation. It allowed the temperature to go back to normal values during the scheduled shut down of 52 hours, but the temperatures increased again to more than 100 °C below the previous level after restart. This phenomenon was counteracted by Rutile injection which started at tuyere 24 due to the highest temperature observed below tuyeres 22 and 24. The injection was performed 30 minutes before closing the tap hole placed almost at the opposite side. After 4 days the injection position was changed to tuyere 26 and the procedure was performed 30 minutes before closing the tap hole considered before. Material was injected when hot metal temperature was above 1480 °C to ensure the best outcomes. After this first step, rutile was injected at tuyeres 34 and 11 in the successive months due to the rising temperature below tuyeres 13 and 35. In particular, 1.5 and 2 t of Rutile were injected per tap while ilmenite load was increased to 15 kg/t hot metal, respectively. This ensured a Ti level in the hot metal of 0.09 % and thus stopping temperature increase and leading progressively to temperatures below 300 °C. Again, Ti oversaturation in hot metal was fundamental to detect a reaction and a daily average Ti content of 0.09 % in hot metal was the lower limit for a successful injection of TiO_2 materials. The importance of hot metal temperature was again underlined, but its dependence on Ti input was also disclosed. Indeed, 1480 °C was identified as limit for Hamborn BF characterized by a Ti input of 4.5 to 5.5 kg/t hot metal whereas 1500 °C was necessary for Schwelgern BF as its Ti input was lower and equal to 3.0 to 3.5 kg/t hot metal. If sufficient hot metal temperatures cannot be ensured Ti input must be increased at slag quality expenses.

After completing the preliminary trials necessary to get a deeper knowledge of the injection process, further trials were scheduled at Schwelgern to determine the residence time of injected Ti in the BF when no ilmenite in the burden was used, and an alternating tapping technique was applied. Two

different Rutile types with a TiO_2 content of 50 and 85 % were considered for injection. At tuyere 21, 3 t of Rutile 50 were injected when opening the tap hole just below the tuyere. After 55 minutes the Ti content in hot metal reached the maximum value while a time delay of 30 minutes was observed for the content in the slag. Approximately 90 % of the additional Ti was discharged after 2.5 hours at tap hole just below the tuyere and the rest after 5.5 hours at the opposite tap hole. Another trial was performed with both Rutile types starting injections just after closing the tap hole below tuyere 21. Ti was not transported to the tap hole opposite to the injection tuyere during the trial when using Rutile 50 thus accumulating at the tap hole below the tuyere where it was discharged after 5 hours. During tapping the Ti content in the hot metal increase to 0.14 % while the TiO_2 content in the slag reached the maximum value of 1.8 %. Analogous trends were observed with Rutile 85, but the lower hot metal temperature determined Ti discharge mainly in the slag and the residence time increased to 10 hours because two taps were needed to reach the previous Ti level.

Residence time was also investigated selecting another tuyere, i.e., tuyere 30, which was exactly in the middle between the two tap holes previously considered. This condition allowed to investigate the maximum distance for the alternating tapping technique. Rutile injection started with the opening of the tap hole on the left side of the tuyere and Ti content in the hot metal and slag reached the maximum value at the tap hole after 65 minutes. This time was 20 minutes shorter compared to test with Rutile injection directly above the tap hole. Ti was discharged at both tap holes in 7 hours. These trials focused on residence time allowed to point out how the conditions occurring in large BFs with alternating tapping technique were totally different compared to smaller furnaces with a single tap hole. The main conclusion drawn was that Rutile injection above a straight closed tap hole led to Ti accumulation in that area and was discharged only after opening that tap hole again.

Once completed these preliminary trials on small and big BFs aimed at identifying TiO_2 injection effects in traditional conditions, TKS assessed the injection of TiO_2 materials mixed with reductants, i.e., Rutile 50 and coal. BF was normally charged with 16 kg/t hot metal of ilmenite, but this value was reduced to 12 kg/t hot metal during the injection campaigns to keep constant the total Ti input as the missing Ti amount was added by injection. The injection trial was performed at tuyere 21 where raising hearth temperatures were detected in the transition zone between ring and bottom layer. At the beginning of the campaign, hearth temperature at the worn area still increased slightly, but its stagnation was reached after few days, and a constant decrease was observed by the end of the injection campaign. This decrease continued even after stopping Ti and coal injection, thus indicating that Ti and coal co-injection was a suitable solution to build protective layers at worn areas in BF hearth. During the campaign, additional raceway temperature measurements were performed with a pyrometer considering different injection conditions. At first, no coal and no rutile injection was considered as reference and a mean temperature of 2000 °C was measured with variation between 1900 and 2300 °C. The next condition investigated was the injection of 1.4 t/h of coal with an oxygen enrichment of the hot blast of 400 m^3/h. In this condition, temperature rose to 2400 °C as expected and its variation decreased rapidly thanks to the good conversion ensured by oxygen enrichment. After that, the effect of Rutile injection was investigated with a 0.8 t/h flow rate, and the pyrometer reported a slightly decreasing raceway temperature about 30 minutes after starting the measurement. The last three conditions examined addressed the simultaneous injection of coal and rutile increasing progressively

their amount, i.e., 0.21 t/h of coal and 0.49 t/h of rutile, 0.3 t/h of coal and 0.7 t/h of rutile, and 0.39 t/h of coal and 0.91 t/h of rutile. The mean raceway temperature with low injection rates reached 2000 °C, but it was characterized by high variations with temperature peaks up to 2400 °C at the end of the trial probably due to pulsating combustion of the injected coal. Analogously the mean temperature with the medium flowrates was kept nearly constant at 2000 °C while a slightly decreasing raceway temperature was measured during the injection with high flowrates. It was concluded that Rutile and coal co-injection was a suitable measure for local wear protection.

Other interesting trials were carried out by EKO which investigated the injection of TiO_2-rich waste materials in their BF characterized by 15 tuyeres and a single tap hole. TiO_2-rich wastes from the chemical industry with high TiO_2 content, i.e., 75 wt.%, were mixed with plastic wastes which acted as additional reductants into the furnace. Different attempts were made by injecting both materials through different tuyeres and performing a multi-tuyere-injection. The first multi-tuyere-injection trial exploited 5 tuyeres for the injection of waste materials while the second trial used all tuyeres except the two near the tap hole. The first campaign was performed with TiO_2-rich waste powders alone and lasted 13 hours injecting 210 kg/h of wastes. The Ti content in the hot metal remained nearly constant during and after the trial. The Ti content in the slag increased strongly already after short times from injection start reaching a maximum value at the end of injection. After injection, Ti content in the slag decreased rapidly achieving ordinary level after 24 hours, but these values raised again displaying a delayed response. This phenomenon was ascribed to a certain amount of slag remaining in the hearth after tapping, to the enrichment of pig iron with Ti and to the possible precipitation and dissolution of TiCNs. The second trial failed due to massive problems regarding mixture conveyance. Choking of the conveying lines and nozzles together with bridging phenomena and arch formation in the hopper system were caused by the plastic wastes which formed woolen structures. Possible causes of these technical issues were the change of plastic waste composition resulting from the change of plastic waste supplier or the higher humidity of the agglomerated plastic. The latter trial proved that the injection of a mixture of plastic wastes and TiO_2-rich powder did not guarantee sufficient operational reliability thus requiring a separate injection of TiO_2-rich powder into BF hearth.

Further trials assessed the injection of ilmenite sand. The first campaign was proposed by TSK using both Rutile 50 and ilmenite sand to study the efficiency of the latter in forming a protective layer at worn areas of BF hearth. The chemical analysis of the raw materials pointed out a lower Ti content of ilmenite sand, i.e., almost 44 wt.%, compared to Rutile 50. Further differences were found in the grain size and in the mineralogical structure. Ilmenite sand displayed a grain size between 5 and 150 µm and contained mainly $FeTiO_3$ while Rutile displayed a grain size between 5 and 50 µm and contained mainly TiO_2. Further differences were observed in the bulk density with ilmenite sand displaying values in the range of 2.4-2.7 t/m^3 and Rutile presenting a density of 0.9 t/m^3. The higher bulk density and the larger grain size of ilmenite made necessary the use of more gas for pneumatic transportation thus causing higher mechanical wear in the injection system. This issue was partially fixed by grinding ilmenite sand to the same size as Rutile.

The injection campaign was performed in the 4-tap hole BF working with an alternating tapping regime when hearth temperature increased in the area of tuyere 22, 24 and 35. Ilmenite was injected in the

area of tuyere 35 while no Ti injection occurred at tuyeres 22 and 24 to identify potential temperature decrease resulting from TiO_2 rich material introduction. The injection was performed additionally to the charging of 10 kg/t hot metal of lumpy ilmenite in the burden. Ilmenite injection was a suitable measure to form local protective layers at worn areas in BF hearth allowing to arrest temperature increase around tuyere 35 and keeping it constant even when injection was stopped while hearth temperature around tuyeres 22 and 24 continued to increase. Ti content in the hot metal was significantly higher when injecting Rutile rather than ilmenite due to the inherent higher Ti content. It also depended strongly on temperature with an increasing trend for increasing temperatures. On the contrary, TiO_2 content in the slag displayed a slight decrease when hot metal temperature increased. Furthermore, it was observed that TiO_2 content in the slag was nearly the same when injecting both rutile and ilmenite sand. Overall, ilmenite sand injection proved that protective layers were built at worn areas in BF hearth even if Ti content in the hot metal was much lower than during Rutile injection.

Ilmenite injection was also investigated at Ruukki using ilmenite clay as injection material and comparing the results with Rutile F ones. Significant differences were observed in TiO_2, Fe_2O_3, SiO_2 and MgO contents with rutile displaying a TiO_2 content of 54.5 % against the 21.2 % of ilmenite. Fe_2O_3, SiO_2 and MgO were higher in ilmenite clay. Some differences were also observed in grain size and shape which determined a higher probability for tuyere refractory damage when using ilmenite as injection material. For this reason, the lance was imposed right to the middle of tuyere and easy material flowing should be secured during injection. Furthermore, blowing pressure of the lance should be adjusted properly. Almost 200 kg of ilmenite clay were injected during the trial with a rate of 520 kg/h. Injection started 9 minutes after the end of tapping and was stopped before the start of the next one. The amount of ilmenite injected, and its inherent Ti-content were so low that a strong effect on the analysis was not detected, but some important lessons were learnt. The small diameter of the injection lance caused some problems when injecting ilmenite because the blowing of materials with small particle size and high pressure produced some kind of arching effect to the discharge hole while blowing the material only with tube ran smoothly to the dust catcher.

All injection trials performed at TKS, EKO, Ruukki and Voestalpine allowed to gather a lot of experience and to provide a list of recommendations. First of all, TiO_2 materials injection must be performed at high temperature in BF hearth to increase Ti content in the hot metal and decrease its content in the slag to support the formation of a protective TiCN layers. The use of discontinuous injections with high injection rate must be preferred to continuous injection with low intensity. Indeed, this solution allowed to achieve higher Ti content in the hot metal close to the injection position for a limited period thus locally resulting in a more protective condition for BF hearth. TiO_2 injection start was recommended to the mid or end of tapping. At the latest, local injection must be stopped shortly after tap hole closing, because during tapping Ti loaded in the hot metal flows from the local injection position to the tap hole in operation and passed the worn area. A fourth recommendation regarded the injection of TiO_2 materials in the area or directly through the tuyere upstream of the hot spot to achieve local higher Ti content in the hot metal close to the worn area. Indeed, the worn area must be located in the flow direction between the local injection position and the tap hole in operation. Some recommendations were given also regarding the length of the injection period. A minimum of one week was recommended to reach durable hearth protection at worn areas. Local short-term

injections for a few days allowed only stagnation of the temperature for the injection period at best, but only local long-term injection were able to provide a more or less durable temperature decrease resulting from the formation of a protective TiCN layer. High injection rates of TiO_2 materials were also recommended to get high Ti content in the hot metal. They must be clearly tailored according to Ti input in the burden to assure the building of the protective layers at the worn area. Finally, it was observed that Ti residence time in the hearth was influenced by both injection and drainage positions. Indeed, it was almost impossible to build a protective layer of TiCN in BFs with drainage problems. For this reason, the first step should be always the elimination of the permeability and drainage problems, and afterwards preventive measures can be tackled to protect the hearth wall.

Further activities were undertaken by CSM which evaluated the potential enrichment of BF tap hole clay with TiO_2 materials. The main idea was to develop and characterize a new generation of tap hole clay containing TiO_2 able to create a protective scaffold on the inner face of the refractory near the tap hole zone. CSM focused on thermomechanical, chemical and physical characterization of these new tap hole clays and on the study of their interaction with the liquid hot metal and the refractory in BF hearth. The first point investigated was the formation of the TiCN protective layer starting from the TiO_2 contained in the tap hole clay under chemical and physical conditions, e.g., temperature, similar to those expected in the BF. The second point addressed regarded the chemical reactions that intervened between the new tap hole clay and the refractory in BF hearth.

The first experimental campaign was performed by filling a graphite crucible with various layers of tap hole clay and prefixed TiO_2 amount and by pouring pig iron in the upper part. The crucible was heated up to 1600 °C and kept at this temperature for different time. After cooling, the crucible was dissected for mineralogical and structural examination to study the reaction products. Five different trials were performed: 1) tap hole clay and pig iron at 1600 °C for 6 h 2) tap hole clay, 5 % of TiO_2 dust and pig iron at 1600 °C for 6 h 3) tap hole clay, 15 % of TiO_2 dust and pig iron at 1600 °C for 6 h 4) tap hole clay, 15 % of TiO_2 dust and pig iron at 1600 °C for 12 h 5) tap hole clay, 15 % of TiO_2 dust and pig iron at 1600 °C for 3 h. The main components of the tap hole clay were corundum, graphite and SiC while the binder was tar. Petrographic analysis was used to study the chemical composition of Ti neoformation phases resulting from the reaction among TiO_2, carbon and nitrogen under the catalytic action of metallic iron. The reference sample from trial 1 showed the typical texture of pig-iron and tap hole clay with no TiN, TiC or TiCN crystals formation. The samples from the other trials showed again the typical constituents of tap hole clay observed in trial 1, but pig-iron displayed neoformations of grey TiN crystals especially at the interfacial zone with tap hole clay. TiN amount varied according to the quantity of TiO_2 added to the tap clay in the trial whereas increasing holding time did not seem to affect crystal quantity.

The second experimental campaign focused on the industrial production and characterization of tap hole clay enriched in TiO_2 thanks to the help of a European tap hole clay producer which made the mixtures with different materials, i.e., pure TiO_2 (98.5 %), screened ilmenite ore (TiO_2 31.4 %) and rutile sand (TiO_2 93.5 %). The different blends made with resin bonded tap hole clay are summarized in Table 4 and were compared with the reference tap hole clay A and C. At the end of the preliminary experimental cycle, only blends 1B, 3B, 1C and 2C were selected to continue the campaign together

with the reference materials A and C. The tendency of these blends to form carbides and nitro carbides of Ti when in contact with hot metal was investigated by applying the same set up used in the previous experiments applying a temperature of 1600 °C and a residence time of 6 h. The results highlighted that pig-iron and crucible graphite were always in contact or rather separated by a gap but in all cases no tap hole clay presence between them was observed. This was ascribed to the inherent difference in density between tap hole clay and pig iron which made tap hole clay slag in liquid pig iron. Microanalysis further demonstrated that slag came from tap hole clay. Reference sample A displayed some preliminary TiCN grey crystals formations at the pig-iron interface probably due to Ti compounds already present in the tap hole clay whereas no neoformations of Ti were detected in reference sample C. Samples 1B and 3B displayed increasing amounts of TiCN grey crystal neoformations compared to previous samples thanks to the higher amount of TiO_2 added to the tap hole clay. The TiO_2 content in the tap hole clay was even higher in samples 1 C and 2C, but the amount of TiCN crystals observed did not differ largely compared to samples 1B and 3B. Both experiments proved that rutile sand was the best TiO_2 containing material and 1B mixture, i.e., 12 % of rutile sand with about 15 % of TiO_2, was the best because TiO_2 percentage higher than 25 % gave a deterioration of physical characteristics. The good results obtained at the laboratory scale were promising in view of an extension of the work to an industrial scale.

Table 4: Composition of the blends and the reference materials considered in the preliminary campaign

	A	1A	2A	1B	2B	3B	C	1C	2C
TiO_2 %	0.0	10.0	10.0	-	-	-	0.0	49.8	10.0
Rutile sand %	-	-	-	12.0	12.0	22.0	-	-	29.5
Ilmenite %	-	-	-	-	46.5		-	-	-
Resin %	Yes	Yes	No	Yes	Yes	Yes	No	No	No
Oil %	Yes	Yes	Yes	Yes	Yes	Yes	Yes	Yes	Yes

The last part of the project focused on the determination of scaffold formation and deformation. MEFOS investigated this aspect by injecting two different TiO_2-rich materials, i.e., ilmenite powder (TiO_2 50.9 % and Fe tot 33.8 %) and Ti powder (TiO_2 40-47 % and Fe tot 30-37 %), into LKAB EBF via one tuyere during two campaigns and monitoring hearth temperature, Ti yield and distribution, and other operational parameters. The hearth was excavated after the injection periods to analyze samples of the formed hearth scaffold. The analysis from the first campaign displayed TiN in all samples taken from the scaffold together with a mixture of Fe and different slag phases. The scaffold was characterized by a thickness of 5-10 cm and TiN was found at different depths in the scaffold thus indicating that it was formed during the whole campaign. Furthermore, the formation of a scaffold with high melting Ti-containing oxides, e.g., Ca titanate, was observed in front of tuyere 2. It was concluded that an injection rate of 40 kg/h at the end of the injection period was too high. For this reason, a lower injection rate of 20 kg/h was used in the second campaign where injected TiO_2 powders seemed to reduce more easily into the hot metal and TiCN to be formed to a greater extent. The analysis of the samples

showed that TiC formed together with TiN and two different TiCN phases were identified, i.e., Ti (0.7C, 0.3N) and Ti (0.3C, 0.7N). The high carbon TiCN was predominant in the area between the injection tuyere and the tap hole while the low carbon TiCN was found in other areas. Nitride/carbide formation was controlled by N content in the iron and only when N was completely consumed TiC formation occurred.

Scaffold formation was also investigated by EKO exploiting heat flux data. Heat flux is given by the product of gradient temperature ΔT with thermal resistivity, i.e., the ratio between wall thickness and thermal conductivity s/λ. The installation of a flat thermal resistivity into a wall allowed to derive heat flux density from the temperature difference measured at this resistivity. Five heat flux meters were installed in EKO BF refractory at two levels during the shut-down. The heat flux meters on the upper level were located in the transition zone between ring and bottom layer at a distance of 4 m at the right and the left side from the tap hole. The heat flux meters on the lower level were installed 2 meters below the elements of the upper level. The heat flux in the upper level of BF hearth was higher than the heat flux in the lower level and a decrease in heat flux was observed during the intensified Ti input by ilmenite charging. This effect lasted for few days before heat flux density rose again. The formation of scaffolds in the period of high Ti input and its deformation after decreasing Ti input could be the reasons for this progression of the heat flux.

Further investigations on scaffold formation were undertaken by Voestalpine after BF blow down to perform relining. Several samples of carbon bricks, scaffolds and parts of the salamander body were obtained from the hearth, and their chemical composition and microstructure were analyzed. No signs of TiCN formation were identified at the hot face of defined carbon bricks while TiN and TiCN crystals were detected in the metal rich area of the scaffold and at the salamander body. This confirmed the formation of TiCN not only at the surface of the refractory lining but also in those positions where Ti, C and N can react with each other. According to these results, TiO_2 injection proved to be more effective than TiO_2 addition in the burden as it allowed the formation of TiCN phases directly at the hot spot area.

Finally, scaffold formation was also assessed by Ruukki during the mid-campaign repair. A skull band was found, and it was characterized by a thickness of 0.2-0.3 m at the center of the bottom before increasing significantly when approaching hearth walls where a thickness of 0.9 m and a width of 1.5 m were achieved. The measurements also highlighted that hearth refractories were almost completely worn out due to erosion around the tap hole where the thickness of the bricks was locally less than 0.2 m. The main phases of the skull band near hearth walls were Fe, Mg-Ca aluminate, Ca-Al-silicate ($CaAl_2Si_2O_8$), Ca-Mn sulfide ((Ca,Mn) S), melilite final slag ($Ca_2(Mg\ Al)(Al\ Si)_2O_7$) and carbon. These phases created a mixture with TiCN crystals. Ti content was up to 17 % in some samples and the highest contents were found near the hot spot. The main phases of the skull band at the center of the bottom were Fe, melilite final slag ($Ca_2(MgAl)(AlSi)_2O_7$) and carbon. In addition, some dicalcium silicate (Ca_2SiO_3) and potassium aluminum silicate, leucite ($KAlSi_2O_6$) were detected. The melting points of the components at the bottom of hearth were so high that it was almost impossible for the skull to dissolve.

2.2 RFCS

2.2.1 FULL-REC 2: Hydrometallurgical continuous treatment of ZnO enriched powders for metal zinc production (27)

The project was coordinated by CSM with ASO Siderurgica, Acciai Speciali Terni (AST), and Techint participating as partners in the consortium. The project started on the 1st of September 2003 and lasted almost two years ending on the 31st of August 2005. The overall project cost 1.46 M€ and the EU contributed 0.58 M€, i.e., almost 50 % of the budget.

FULLREC2 was the continuation of the previous demonstration ECSC project 2.1.6 "High purity zinc and ferroalloys recovery from EAF dusts through a combined pyro-hydrometallurgical treatment" where a new integrated pyro-hydrometallurgical process called the Full-Rec technology was developed and tested at demonstrative plant scale. This technology allowed the treatment of EAF dusts with a wide range of composition to obtain products of commercial value such as inert slag, metal alloys and ultrapure ZnO for the further recovery of high-grade metal Zn (>99.95%) in the subsequent electrowinning phase. Concerning the pyro-metallurgical plant section, the Full–Rec process resulted in a technologically reliable and economically valid solution ready for industrial application. Indeed, the pyro-metallurgical reactor has been applied in two industrial Italian plants. Concerning the hydrometallurgical process, the results from batch operation proved the technological feasibility of this solution even though additional experiments proved to be necessary to design an industrial plant, define the most appropriate annual capacity, explore financial needs and economic return.

At the time of the project, examples of other hydrometallurgical treatment available for EAF dust were the EZINEX process and REZADA process. The EZINEX process was developed by ENGITEC IMPIANTI and was based on the direct leaching of EAF dust with ammonium chloride to exploit the non-dissolution of Fe and, as consequence, of the zinc ferrites. This process allowed to obtain low Zn yields compared to the sulfuric leaching which allowed also the dissolution of Zn ferrite thus increasing significantly Zn yield. Furthermore, the treatment with ammonium chlorine caused problems of alkali accumulation in the solution thus requiring purification treatment to eliminate the salts. The REZADA process was developed by a consortium of French Steelmaker and was based on the direct leaching of EAF dust with sodium hydroxide but displayed the same problems of the EZINEX process.

Despite many processes under development, neither hydrometallurgical nor pyro-hydrometallurgical processes for the treatment and valorization of EAF dusts was characterized by industrial maturity. Considering this, the present project aimed to demonstrate the industrial feasibility of a continuous hydrometallurgical process for metallic Zn recovery from ZnO enriched EAF dust. In principle, there were no conceptual obstacles to the industrial exploitation of the hydrometallurgical technology developed in the previous project, but some aspects needed further investigation since they were not considered in the previous pilot plant experimentation due to the discontinuity of the phases preceding the electrolytic recovery of Zn. In particular, eventual accumulation of impurities in the recycled leaching solution, the reusability of secondary solid and liquid fluxes deriving from solution purification treatments and the conditions to improve Zn purity to values >99.99 % needed to be addressed. The project was divided into different phases. ASO and AST were responsible for the collection of EAF dust arising from the production of carbon and stainless steel, respectively. Furthermore, they carried out the preliminary pyrometallurgical treatment to enrich the dusts in ZnO up to 80 %. ASO Siderurgica treated the EAF carbon steel dust with the Wealz furnace to obtain enriched ZnO material while AST treated the EAF dust from stainless steel production with a plasma arc furnace of ILSERV

plant located at AST steelworks to obtain ZnO enriched powders. In the meanwhile, CSM and Techint focused on the design and realization of modifications of the hydro-metallurgical plant designed and built during the previous demonstration project to make it suitable for continuous operation in the solution purification section. This redesign of the plant was accompanied by an experimental campaign in fully continuous operation mode at the hydro-metallurgical pilot plant to get data for plant scaling up and to develop a new control system for the process. Finally, all partners contributed to the evaluation of the technical feasibility and the economic convenience of the whole process for the development of a business plan with a view to transfer it to an industrial scale

The transformation of the hydro-metallurgical plant for continuous operation entailed the introduction of some new components. The first component was a continuous feeder made of a screw conveyor with a material flow rate ranging from 60 to180 kg/h to feed the ZnO-rich powders washed with water. In particular, the powder coming from the washing treatment performed with water for chlorides, fluorides and alkali removal was stored in a tank and charged in a reactor for sulfuric leaching with the continuous feeder. The second type of component added to operate the pilot plant in a continuous way was a set of continuous batchers for additives and reagents. In particular, the batchers were added for the reagents used before coagulant oxidation to decrease Fe ion and precipitate F as CaF_2 and before the final purification treatment. The reagents before coagulant oxidation were the flocculating agent (400-1200 g/h), H_2O_2 (120-1200 cc/h) and $CaCO_3$ (600-1800 g/h) while the reagents before final purification treatment were Zn powder (2000-12000 g/h), Sb tartrate (0.01 g/l of solution) and $CuSO_4$ (360-1080 cc/h). The flow rates of the batchers were calculated considering a minimum process solution flow rate of 500 l/h. The third component was a gravity separator to remove the $Fe(OH)_3$ precipitates after the coagulant oxidation since in the previous project it was identified as a critical step due to the colloidal nature of this type of precipitate. Indeed, it was not possible to make a filtration and the only procedure exploitable was the sedimentation. The last component added was a set of continuous filters to obtain a purified solution without suspended solid material before electrolysis to collect metal Zn with a very high purity (99.99%). The filtering system consisted in two sets of filters that worked alternately thanks to a valve switching system which intervened when there was an increase in the internal pressure due to a high amount of solid residue. Each set was composed of four filters. The first two were filters with metallic baskets characterized by a pore diameter of 50 and 25 mm, respectively while the third and fourth were filters with six fiber cartridges with pore diameters of 10 and 1 mm, respectively. Another important modification concerned the type of anodes used in the electrolytic cell since in the previous project they were made of Pb while for the continuous experimentation they were made of Pb/Ag(10 %) to produce Zn 99.99 % of purity. Process control was also upgraded to monitor the status of the process in the single tanks. In particular, the existing control and regulation system of the process was based on a supervisor computer connected to a PLC (Process Logic Control) where all the signals, e.g., pH, temperature, liquid levels, etc., from the different reactors were present. This system architecture enabled the acquisition of process parameters data, the consequential control of different phases of the process, the online visualization of the alarms and the analysis of the alarms trend.

Concerning EAF dust collection and storage for the pilot campaigns, 360 t of stainless steel from AST EAF were stored and treated in the plasma arc furnace and 70 t of dry ZnO enriched dust were obtained. Chlorides and fluorides were decreased through water washing of the Zn enriched powders performed at the industrial dust washing treatment plant of AST. Furthermore, 100 t of carbon steel dust from ASO EAF were stored and then treated at Waelz furnace to obtain almost 20 t of dry ZnO enriched dust. After the pyrometallurgical treatment, hydrometallurgical treatment was developed to

reduce and control the concentration of some impurities in the solution and ensure the production of high-quality metallic Zn through electrochemical deposition. F^- and Cl^- concentrations should be <150 mg/l since high concentration of F^- made difficult the detachment of the Zn deposit from the cathode and high concentration of Cl^- led to the formation of soluble $PbCl_2$ thus resulting in Pb anode dissolution. The use of Pb/Ag anode decreased this phenomenon. Fe^{++}concentration must be <5 mg/l, Cu^{++} concentration must be <10 mg/l and Ni^{++} concentration must be <1 mg/l since higher concentrations would promote H_2 discharge due to the decrease of H_2 over voltage thus resulting in a lower current utilization. Cd^{++} concentration must be <1 mg/l because otherwise it would co-deposit with Zn thus impairing the quality of the metallic Zn. Finally, Mn concentration must be controlled because MnO_2 was used for oxidation of Fe(II) to Fe(III) in the coagulant oxidation step to eliminate iron and the remaining Mn in solution was oxidized at the anode where it precipitated again as MnO_2. To achieve the targeted values, the continuous hydrometallurgical process was designed including four different operations. The first step was sulfuric leaching aimed at dissolving the ZnO and zinc ferrite contained in ZnO enriched powders using a sulfuric acid solution. The resulting suspension was pumped in the filter press to separate the filtered residue composed by $PbSO_4$, $CaSO_4$, Fe_2O_3, SiO_2, and Al_2O_3. The solution was then sent to the second step, i.e., coagulant oxidation, aimed at decreasing Fe ions in the solution at value lower than 5 mg/l. The removal consisted in the oxidation of Fe ions from bivalent to trivalent form by means of H_2O_2 and the consequent precipitation of $Fe(OH)_3$ at pH 4.8 obtained by $CaCO_3$ addition. After that, a purification treatment was included to reduce Ni^{++}, Cd^{++} and Cu^{++} to metals and separate them from the solution as cement. The reducing agent selected was fine Zn metallic powder. After this last step, the solution was filtered and stored in tanks for subsequent electrolysis. The latter aimed to deposit metallic Zn from the purified solution. Electrolysis was performed at constant potential, and the cell was arranged in three stocks of 10 cathodes with each stock having a shunt connection. The exhausted electrolytic solution was then reused in the first step of the process. The entire workflow of the hydrometallurgical process is summarized in Figure 7.

The experimental campaign was performed in three periods of 10 days using the fully continuous mode and considering daily working time of 12 hours. During Zn deposition in electrolysis, the formation of dendritic structures which formed when Zn content in the solution was low must be avoided since they prevented the deposition of other Zn on the electrode. Considering this, pH and current intensity were monitored and measured during electrolysis while Zn content was analyzed by sampling periodically the solution. At the beginning of electrolysis, Zn concentration was around 90 g/l, pH around 2.5 and current density at around 2500 A. During the first 6 hours, Zn concentration experienced a progressive decrease until reaching values around 75 g/l as well as pH which reached a value of 1.14. At the same time, current density experienced an increase up to 6000 A. After that, current density stabilized around 6000 A value while Zn concentration and pH went on decreasing until reaching values of 40 g/l and 0.78 after 10 hours. At the end of electrolysis, the cathodes were extracted to strip the metallic Zn deposit whose thickness was not uniform for all electrodes depending on the movement of the solution in the cell during the deposition process. At the end of the experimental campaign, it was concluded that the continuous hydrometallurgical procedure tested in the project was suitable to produce metallic Zn with a purity of 99.98% thus confirming the technical feasibility of the FULL-REC solution. A higher degree of purity could have been reached using a solution with lower impurities levels, for example applying a double purifying treatment to further decrease Ni to the exhausted electrolytic solution. It must be also considered that the main impurities in the exhaust solution were Pb coming from the dissolution of anodes and this further problem could be overcome by substituting Pb anodes with a new generation of Ti anodes. The experimental campaign

also reported a Zn yield in the deposit around 74 and 87 % and no accumulation of impurity was detected.

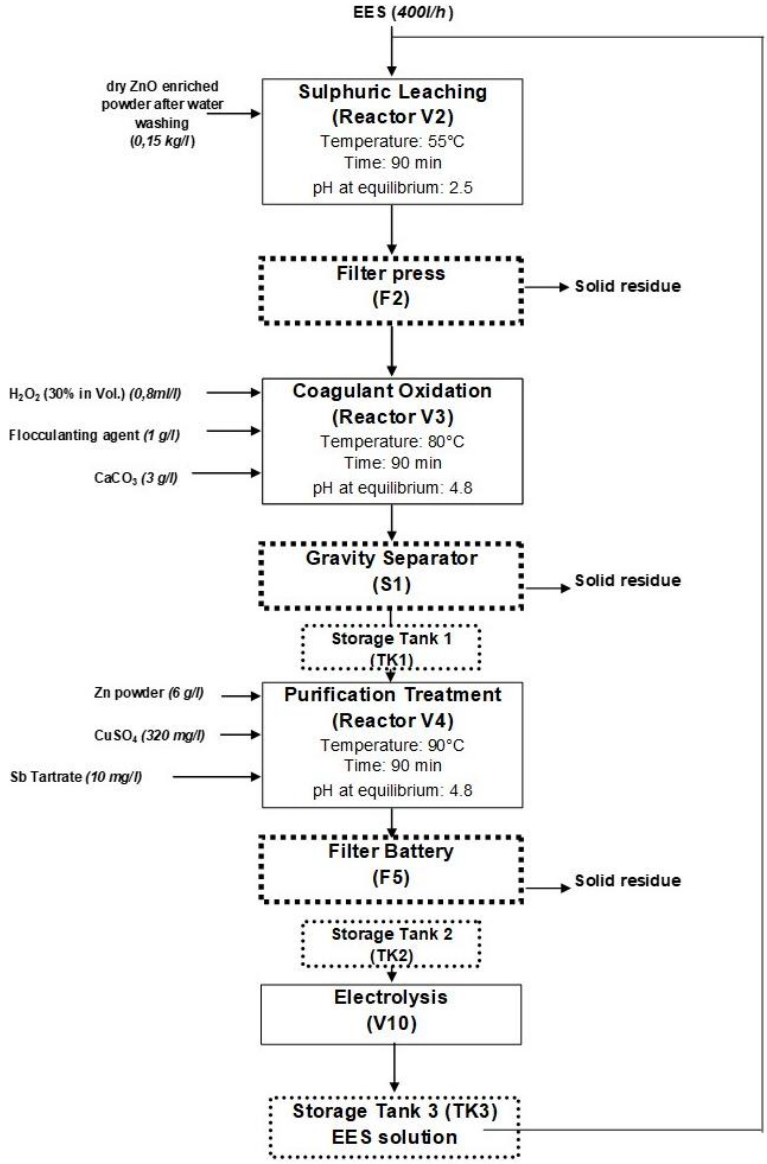

Figure 7: Flow diagram of the hydrometallurgical treatment

Concerning the reuse of the solid residues produced during the process, the PbO-rich residues coming from sulfuric leaching and the Fe-rich residues coming from coagulant oxidation should be charged in the pyro-metallurgical furnace. The Zn-rich solid material coming from the purification treatment could be recycled in the hydrometallurgical plant for selective Zn recovery. The calculation about the accumulation phenomena of the solid residues demonstrated that after the first three cycles a steady state of accumulation phenomena was reached. This allowed to conclude that the recycling of the solid residues did not have any significant effect on the mass balance of the process and on the economic evaluation. The cost analysis estimated that the total operational cost for the hydrometallurgical

treatment of 1 t of ZnO enriched powder was 916.31 €. The economic evaluation of the whole treatment process of 5t of stainless-steel EAF dust including also energy and personnel costs reported a margin of 1519-3499 € depending on the composition of the ferro-alloy produced during the treatment at plasma arc furnace. In the case of carbon steel EAF dust, the economical evaluation demonstrated that the pyro-hydrometallurgical cycle was not advantageous due to the Waelz treatment where no recovery of metals was possible and the slag produced must be disposed.

Full-Rec technology proved to be a radical contribution to sustainable growth allowing to minimize electric steelmaking waste, preserving natural resources, enhancing recycling, recovery and valorization of solid by-products and reducing pollution load. The techno-economical evaluation of the hydrometallurgical process was referred to an industrial plant for the treatment of 20.000 t/y of ZnO enriched dust from stainless steel EAF dust and reported operating result of 10,500 k€/year considering the investment cost. Finally, the application of this technology was available in different treatment capacity ranges which may meet specific requirements in different areas and/or conditions. This guaranteed the maximum transferability of the project results to other applications throughout the European steel industry.

2.2.2 SHOCOM: Short term CO_2 mitigation for steelmaking (28)

The project was coordinated by ArcelorMittal with BFI, CSIC (Consejo Superior de Investigaciones Científicas), RWTH and Voestalpine participating as partners in the consortium. The project started on the 1st July 2005 and lasted three years, ending on the 30th June 2008. The overall project cost 2.4 M€ and the EU contributed 1.44 M€, i.e., 60 % of the budget.

The main goal of the project was the substitution of conventional fossil carbon with sustainably secondary carbon carriers (SCC) both biogenic, i.e., charcoal, and non-biogenic, i.e., plastic wastes, to enable carbon recovery and waste valorization while reducing the demand for primary fossil fuels. At first, the incorporation of pyrolyzed biomass, i.e., charcoal, into coal blends and its subsequent impact on coke quality and BF operation was assessed with the dual objective of introducing CO_2-neutral carbon and lowering the thermal reserve zone temperature (TRZT) by enhancing coke reactivity. The biogenic SCC selected were two charcoals produced from Brazilian eucalyptus and French hardwood fines which were compared with pyrolyzed miscanthus. Both charcoals were characterized by a good grindability allowing to obtain very fine particles, but their addition into coke blend led to a clear decrease in fluidity and a slight reduction in bulk density. These effects were more pronounced with Brazilian charcoal due to its higher volatile matter and the lower carbonization temperature. Indeed, Brazilian charcoal was characterized by a 22.9 % volatile matter and by a 300-350 °C coking temperature while French charcoal was characterized by a 12.4 % volatile matter and by a 550-600 °C coking temperature.

Pilot-scale coking trials were performed in a 400 kg condensable particulate matter (CPM) rotary klin using three representative industrial coal blends with low, medium and high fluidity and incorporating charcoal with different grain sizes at 3 and 6 %. Charcoal addition reduced coke median size and impaired mechanical strength due to fluidity loss, although acceptable fragmentation (I40) and abrasion (I10) resistance were maintained when charcoal was added to highly fluid blends. Coke reactivity increased systematically with charcoal incorporation leading to a reduction of about 100 °C in the threshold temperature of the Boudouard reaction. This was ascribed to the intrinsic reactivity of charcoal and to its ash chemistry. In contrast, miscanthus char caused severe deterioration of coke

quality due to its very low density and high P content, i.e., 0.4 %, thus making it unsuitable for this application.

The effect of charcoal on BF performance was further assessed through laboratory gasification tests, reduction tests in Boris furnace, and through mathematical modelling using Mogador and MMHF (Model-Driven Mobile HMI Framework) models. Gasification tests confirmed that charcoal reacted at significantly lower temperatures than conventional coke, i.e., a gasification temperature 100 °C lower, thus validating the reduction in TRZT. Reduction kinetics became slower when TRZT was lowered therefore Boris tests were necessary to determine at which extent the kinetics were impaired. Sinter reduction kinetics remained acceptable down to 870 °C while some loss of shaft efficiency appeared at 750 °C requiring additional coke to compensate. Nevertheless, the net balance indicated a potential coke saving when TRZT was lowered with modelling predicting substantial reductions in coke consumption and CO_2 emissions at constant or near-constant shaft efficiency. Finally, heat and mass balance demonstrated that lowering TRZT reduced overall BF heat requirements and coke rate without altering substantially shaft gas and temperature profiles. Charging small amounts of highly reactive charcoal, either via coal blend or at BF top proved to be sufficient to control TRZT without creating multiple thermal reserve zones.

The second scenario focused on charcoal injection into BF via the tuyeres. Combined laboratory and pilot-scale tests and modelling activities were performed to investigate different charcoal production routes, the resulting material properties, combustion and gasification behavior under raceway conditions, and the technological and ecological impact on BF operations. Different charcoals were produced from three different types of dry wood, i.e., oak, olive and eucalyptus. At laboratory scale, carbonization was performed in a vertical tubular muffle furnace at three temperature ranges, i.e., 360–400 °C, 450–460 °C and 550–570 °C. In particular, oak was carbonized at 400 °C for 60 minutes (oak1), at 450 °C for 50 minutes (oak2), at 445 °C for 60 minutes (oak2.b) and at 570 °C for 40 minutes (oak3), olive was carbonized at 360 °C for 65 minutes (olive1), at 460 °C for 70 minutes (olive2), at 455 °C for 80 minutes (olive2.b) and at 560 °C for 60 minutes (olive3) and eucalyptus was carbonized at 500 °C for 162 minutes. Carbonization temperature demonstrated a strong influence on charcoal properties, especially volatile matter content and carbon concentration with higher carbonization temperatures decreasing significantly the volatile matter and increasing the fixed carbon content. Furthermore, all samples displayed very low S content typically around 0.02-0.04%, and the resulting ashes consisted mainly of basic components, i.e., 35-50 % CaO and 5-10 % MgO. BET surface area revealed an exceptionally high specific surface ranging from 150 to 350 m^2/g compared with the 1.0–2.6 m^2/g of reference pulverized coals. This corresponds to a factor of 60 to 350 which explained the extremely high reactivity potential of charcoal. Increasing carbonization temperature led to higher increases in surface area thanks to enhanced devolatilization and pore development. SEM analysis confirmed these findings highlighting a highly porous structure with vessels and fiber-like pores of the charcoal particles in contrast to the dense and compact structure of mineral coals. The shape factor of pores ranged between 0.5 and 0.7, indicating irregular but well-developed pore shapes. Charcoals produced at higher temperatures contained a higher fraction of large pores exceeding 100 μm^2.

Charcoal reactivity under simulated raceway conditions was also investigated through Simultaneous Thermal Analysis (STA) to determine mass loss, reaction rates, characteristic temperatures and enthalpy changes during combustion-like conditions. Five charcoals and two reference coals were tested, i.e., oak 1, oak 2.b and oak 3, olive 2.b and eucalyptus. Charcoal combustion behavior proved to be comparable or better than the one of high-volatile pulverized coal while low-volatile coal

exhibited significantly poorer conversion. Despite a lower volatile matter content than some coals, charcoals achieved higher conversion degrees thanks to a highly porous structure and a large reactive surface area. Differential thermal analysis (DTA) indicated that charcoal combustion was dominated by exothermic processes even during heating under inert conditions likely due to oxygen trapped within the pore structure. Charcoals produced at lower temperatures showed rapid initial mass loss due to higher volatile matter, while the charcoals carbonized at higher temperatures reacted faster at elevated temperatures and reached complete burnout earlier. At moderate temperatures, reaction rates were almost independent of carbonization temperature. Tests on mixtures of 50 % charcoal/ 50 % coal showed intermediate reactivity between the two components thus indicating additive behavior. Grain size effect was limited and mainly observed during final stages of combustion. Injection trials in a small-scale injection rig demonstrated that charcoal achieved high conversion degrees in the tuyere and oxygen-rich raceway zone. Conversion increased for both coal and charcoal with increasing O/C atomic ratio, but charcoal showed a flatter dependence thus reporting a lower sensitivity of conversion to oxygen availability. At typical coal injection rates of 150–180 kg/t of hot metal, charcoal conversion became increasingly favorable thanks to the oxygen stored in its pores which compensated local oxygen deficits.

For larger-scale testing at RWTH and CENIM, a modified pyrolysis plant was used to produce approximately 94 kg of charcoal by carbonizing around 285 kg of dry eucalyptus wood without bark at an average temperature of 415 ± 13 °C for 2 hours. This resulted in an average charcoal yield of 32.8 % with a C content of 82.3 %, a H content of 3.1 %, extremely low S content of 0.005 %, a volatile matter of 30.5 %, a ash content of 0.42 %, and a P content in ash of approximately 0.8 %. These values confirmed the very low impurity level of charcoal compared with conventional pulverized coal for BF injection. Large-scale investigations were carried out in a combustion pilot plant at CENIM and in an injection coke bed simulator in RWTH. In the combustion pilot chamber, ten charcoal injection tests and three reference coal tests were performed under comparable conditions. Charcoal combustion efficiency reached 60 % like coal while average charcoal efficiency was around 18 % higher when accounting for lower injection rates. In the coke-bed simulator, two tests with reference coal and four tests with charcoal injection were performed under the same conditions and temperature profiles and gas compositions along the raceway showed very similar behavior for both charcoal and coal with peak temperatures reaching approximately 1700 °C in both cases. Oxygen consumption was slightly faster and CO_2 peaks somewhat higher for charcoal. Charcoal behavior outside the raceway was also examined through gasification tests simulating solution loss reactions in BF shaft between 900 and 1300 °C. Both STA and Tamman furnace experiments were performed and demonstrated that charcoal reacted faster than mineral coals even when coal volatile matter was higher. Furthermore, reaction rate differences tended to diminish with increasing temperature, indicating that the main advantage of charcoal lied in lower temperature regions of the shaft. Interestingly, it was observed that coke reactivity towards CO_2 at 1300 °C decreased by 18–20 % when fine charcoal particles were attached to coke surfaces and SEM observations attributed this trend to a thin ash layer rich in CaO forming on coke surface thus partially protecting it from solution loss reactions.

A techno-ecological assessment using BF modelling showed that pulverized coal replacement with low-ash, high-basicity charcoal at an injection rate of 200 kg/t hot metal allowed to reduce blast volume, slag volume and coke rate, while increasing productivity and lowering heat losses. A decrease in top gas volume and calorific value was also observed. Carbon balance calculations showed that direct CO_2 emissions decreased up to 1.8 % when charcoal replaced coal. Furthermore, when charcoal was

considered CO_2-neutral, total CO_2 input decreased by 36–45 % for full substitution of pulverized coal, depending on charcoal quality.

The third goal of the project was the generation and use of reducing gases from CO_2-neutral secondary and waste raw materials, with a particular focus on mixed plastic waste. The objective was to develop a simple gasification-based process able to produce reducing gas suitable for ironmaking applications, either in BF or shaft furnace. The reducing gas generated must fulfil specific requirements of the iron ore reduction process reported in Table 5 and the secondary raw materials selected must had an availability of at least 100,000 t/y. Among the secondary and waste raw materials considered dry sewage sludge, waste wood, plastic waste and used tires, mixed plastic waste from packaging recycling was selected as feedstock thanks to its availability, favorable reactivity and low content of tramp elements especially Cl. The average composition was 1% moisture, 75 % C, 11 % H, 0.1 % N, 7 % O, 3.5 % ash, a bulk density of 300 g/l and a calorific value of 35 MJ/kg.

Table 5: Reducing gas requirements

		Midrex		BF tuyere	
		Desired	Acceptable	RWTH	Voestalpine
Temperature	°C	900	25-1480	1000-1200	30
Pressure	bar	3-4	20	3-4	3-4
H_2/CO Ratio		0.5-inf.	0-inf.	0.3-3.3	2.2-9.8
$(CO+H_2)/(H_2O+CO_2)$		>10	>2	>30	11-34
Nitrogen	%	<1	<6	Low	3.9-10.6
Methane	%	3-4	0-5	3	18.1-25.0
Sulphur	ppm	<100	<3000	Low	-
Soot	Mg/Nm^3	<100	<100	-	-

Reducing gas generation was based on an entrained flow gasification process analogous to pulverized coal or plastic injection at the tuyere but operated at lower temperatures. Trials were conducted using plastic particles <3 mm, residence times of 0.6–0.9 s, mass flows of 1–3 kg/h, gas flows of 21–37 Nm^3/h and oxygen contents of 4.5–9.5 vol and the main parameters controlled were carbon yield, reducing gas ratio $(CO+H_2)/(H_2O+CO_2)$, gas volume and calorific value. An increase in the specific oxygen input increased carbon conversion but decreased the reducing gas ratio. The maximum reducing gas ratios achieved at 900 °C was 2 with typical values near 1.1. These values were within the range of BF shaft gas quality but below Midrex target. Furthermore, the specific reducing gas volumes decreased from 2 to 1.5 m^3/kg plastic with decreasing oxygen input due to lower conversion. Hot gas cleaning with $Ca(OH)_2$ was also investigated since secondary raw materials introduce S and halogens. Thermodynamic equilibrium at 800–900 °C with S input of 90 ppm and Cl input of 200 ppm showed retention rates of 91% for H_2S and 85% for HCl. This was confirmed by the experimental trials performed using $Ca(OH)_2$ with d_{50} = 6 µm, a specific surface area of 45 m^2/g and a pore volume of 0.22 cm^3/g which achieved S reductions up to 92% at a Ca:S ratio of 4:1, gas temperatures of 900 °C and residence times of 1–2 s.

A detailed substance flow analysis was carried out at Linz facility for the BF process with plastic injection of 35 kg/t hot metal over three months with daily sampling of input and output streams to evaluate element flows. Additional Zn input from plastics was insignificant since more than 90 % left the process with hot metal and slag before oxidizing into dust. Pb and Cd predominantly exited with uncleaned top gas and were captured in scrubber solids, while Hg was largely retained in scrubber residues with only 5 % emitted in gaseous form. Since the one-step process analyzed before displayed significant limitations, a two-step industrial concept was evaluated by equilibrium calculations. In the first step, secondary raw materials were gasified using recycled top gas as carrier and oxidant and, in the second step, the gas was conditioned and reformed at 1100 °C with the addition of natural gas to achieve the required quality. Compared with the reference Midrex case achieving a reducing gas ratio of 10.1, the two-step process allows partial substitution of natural gas by secondary fuels and results in a CO_2 mitigation of about 43 kg/t DRI. Feasibility study for BF gas injection was performed

The last goal of the project was the incorporation of post-consumer plastic waste as minor additives in industrial coal blends for coke making. The investigation covered the selection and characterization of representative plastic wastes, the analysis of their influence on the thermal and thermoplastic behavior of coal blends, the development of coking pressure during carbonization, and the quality of the resulting cokes. In addition, mass and carbon balances of coal–plastic blends were assessed through Gray–King co-pyrolysis experiments to quantify the redistribution of carbon among coke, gas, and tar products.

The plastic wastes selected were multi-component streams representative of municipal packaging residues with the main restriction that PVC (Polyvinyl chloride) content was below 2 wt.% to avoid chlorine-related operational and environmental issues. Four principal wastes were examined. The first one was a reference mix with 73 wt.% HDPE (High-density polyethylene), 20 wt.% PP (Polypropylene), 5 wt.% PET (Polyethylene terephthalate) and 2 wt.% cellulose and particle size <10 mm. the second mix had a similar composition with 70 wt.% HDPE, 5 wt.% LDPE (Low-density polyethylene), 20 wt.% PP and 5 wt.% PET. The third mix derived from films and laminates smaller than 10 mm and contained more than 55 wt.% polyolefins, about 35 wt.% PET and PS (Polystyrene), 1 wt.% PVC, 1.2 wt.% cellulose and 6.9 wt.% of unclassified plastics. The last mix was a compacted multi-component plastic with higher inorganic content. In addition, compost precursors were included to represent organic-rich residues present in unwashed waste streams. Single plastics such as HDPE, LDPE, PP and PET were also studied as references, along with synthetic binary and ternary mixtures prepared to explore compositional effects systematically. Elemental analyses showed that polyolefin-rich wastes exhibited atomic C/H ratios close to 0.5 typical of HDPE, LDPE and PP, whereas the third mixture had a significantly higher atomic C/H ratio of 0.79 and an oxygen content of 16.6 wt.% on a dry ash-free basis. The last mix was distinguished by a relatively high inorganic fraction of 7.4 wt.% dry basis and a very high oxygen content in the organic matter close to 29 wt.%, with S and N contents of about 0.3 and 0.7 wt.%, respectively. Compost showed the most extreme composition, with 35.4 wt.% inorganic matter, 40.6 wt.% oxygen and low C and H contents of around 50 and 6 wt.%.

Thermogravimetric analysis (TGA) demonstrated that thermal degradation behavior of the wastes was strongly governed by polymer composition with DTG (Derivative Thermogravimetry) curves revealing three main stages during pyrolysis. The first stage below 375 °C corresponded to decomposition of minor PVC traces, cellulose from labels and compost-derived organic matter. The second main devolatilization stage occurred between 375 and 525 °C and was associated with degradation of HDPE, LDPE, PP, PS and PET. A final stage at higher temperatures reflected decomposition of residual organic

matter in complex wastes. Most volatile matter was released between 375 and 500 °C. Mix four also left a notably higher solid residue at 800 °C due to its ash content, reaching 16.5 wt.% compared to 2.9 wt.% for mixture 1 and 5.9 wt.% for mixture 3. Coal–plastic mixtures were also examined and combined plastic wastes were prepared by mixing mixture 3 or mixture 2 with compost in a 4:1 weight ratio. At 1000 °C, coke yields from coal–plastic mixtures were consistently lower than that of the reference coal blend due to enhanced formation of gas and condensable products. The addition of plastics generally increased the maximum pyrolysis rate (DTG_{max}). The temperature of maximum volatile release shifted slightly to lower values with the magnitude depending on plastic type and loading. Comparison between experimental DTG curves and those calculated using additivity laws indicated only minor deviations, confirming that thermal degradation reactions of coal and plastics occurred largely independently, with negligible chemical interaction at low plastic addition rates. Combustion TG experiments in air showed that oxygen significantly altered polymer degradation behavior, shifting mass loss to lower temperatures and reducing residual carbonaceous material. During combustion of coal–HDPE mixtures, oxygen adsorption by coal overlapped with polymer degradation, suggesting possible temporary retention of volatile products within the coal matrix before their release at higher temperatures.

Thermoplastic properties of coal blends were evaluated by plastometry and the addition of plastics proved to reduce maximum fluidity consistently with previous studies. The extent of the modification depended on polymer type, addition rate and base coal fluidity. Polyolefins caused similar and relatively moderate reductions, whereas PET and PS produced much stronger effects due to their aromatic structure. A fluidity loss of approximately 23, 31and 42% was measured for base coal blends produced with mixture. A predictive approach was developed by correlating coal blend fluidity with the relative proportions of polyolefins, PS and PET in the waste. The model was less accurate for low-fluidity blends, indicating that its applicability is limited to coal blends with sufficient plasticity.

Gray–King carbonization tests at 900 °C were used to establish mass and carbon balances for coal blends containing 2 wt.% of HDPE, PET, mixture 2 and mixture 3. The reference coal blend yielded 78.5 wt.% of coke whereas blends containing plastics produced slightly less coke and more gas and tar. Polyolefins were mainly recovered as oils, waxes and light hydrocarbons, contributing less than 0.6 % to the solid residue. PET behaved differently, increasing both coke and gas yields. Gas chromatography revealed that the gas fraction consisted mainly of hydrogen (36–50 vol%) and methane (33–45 vol%), with CO, CO_2 and C2–C4 hydrocarbons forming the remainder. Gas densities ranged from 0.52 to 0.62 kg/Nm^3, and gross calorific values from 21 to 26 MJ/m^3 with higher values for polyolefin-rich wastes.

Coking pressure development was assessed under controlled bulk density conditions of approximately 800 kg/m^3 dry base. The reference coal blend exhibited a coking pressure of about 20 kPa, i.e., a moderate-risk level. Addition of polyolefin-rich waste at 2 wt.% increased coking pressure to approximately 44 kPa while the same waste mixed with compost produced around 36 kPa. In contrast, waste containing significant proportions of PET and PS generated coking pressures like the reference blend. Binary HDPE–PET mixtures confirmed an exponential decrease in coking pressure with increasing PET content. For example, pure HDPE or LDPE+PP mixtures produced pressures near 37 kPa, whereas mixtures containing 50 wt.% PET reduced pressure to around 16 kPa. These results demonstrate that plastic waste composition can be tailored to control coking pressure.

Coke quality was also evaluated through mechanical strength, CO_2 reactivity and post-reaction strength (CSR). Semi-pilot cokes produced with plastic additions showed mechanical strength

comparable to or slightly better than reference coke. For example, the use of mixture 2 allowed to improve CSR by approximately three points. Wastes rich in PET and PS also increased coke reactivity as well as compost-containing wastes which in turn reduced CSR due to catalytic effects of inorganic constituents. Total coke porosity was only slightly affected, increasing from about 49–50% in the reference coke to 51–52% for cokes produced with mixtures 2 and 3. Pilot-scale carbonization confirmed these trends and mixtures richer in PET reduced coking pressure while maintaining coke quality, confirming the scalability of the semi pilot observations.

Finally, a comparative assessment of the main technological routes investigated with respect to their effectiveness in reducing CO_2 emissions and their economic impact was conducted. The highest CO_2 mitigation potential was achieved through massive charcoal injection in BF with a reduction of up to 28 % although this option entailed a productivity loss of about 10 % and a moderate cost increase. Lowering the TRZT was also effective achieving CO_2 reductions between 9 and 12% depending on the target temperature with more limited productivity penalties at moderate TRZT reduction. The combination of charcoal injection and TRZT reduction showed an almost additive effect in terms of CO_2 mitigation. Routes involving plastics provided smaller but still significant benefits. The incorporation of about 2 % plastics in the coal blend led to almost 2 % CO_2 reduction, while plastic gasification routes achieved 5–7 % mitigation. From an energy perspective, low-TRZT scenarios generate savings in total energy demand but increase electricity consumption due to reduced blast furnace gas availability, whereas gasification-based routes increase overall energy consumption because of conversion losses. From an economic perspective, charcoal-based routes were more expensive than the reference case with cost increases up to 7 % while plastic-based routes generally reduce operating costs, even when plastics were assumed to have a positive purchase price.

2.2.3 ACASOS: Alternate carbon sources for sintering of iron ore (29)

The project was coordinated by BFI with ArcelorMittal Bermen, Corus Technology, i.e., Tata steel, Corus UK, ILVA and Voestalpine participating as partners in the consortium. The project started on the 1st July 2007 and lasted almost 3 and a half years, ending on the 31st of December 2010. The overall project cost 1.55 M€ and EU contributed 929 k€, i.e., 60 % of the budget.

The main goal of the project was the reduction of coke breeze consumption in iron ore sintering by introducing and optimizing the use of a broad spectrum of alternative carbon sources. In particular, renewable biogenic carbon sources were evaluated by TATA, carbon-rich dusts and wastes were investigated by BFI and ArcelorMittal, conventional alternative fossil carbons such as anthracite, petroleum coke and coke dust were studied at ILVA and carbon-rich in-house BF sludges were assessed by Voestalpine. The project focused on the systematic identification, characterization and pre-processing of alternative carbon sources, evaluating their chemical and physical properties, availability and costs as a basis for comparison with conventional coke breeze. Processing routes were developed to adapt these materials to the specific requirements of the sintering process with the aim of increasing substitution rates while maintaining high productivity, sinter quality and low emissions. A comprehensive database was established to allow direct comparison between different alternative carbon sources and conventional coke breeze in terms of physical, chemical, thermal and economic properties.

Anthracite and petroleum coke were identified as technically suitable fossil alternative carbons thanks to their high fixed carbon content, low volatile matter and high calorific value. Anthracite was

characterized by very high fixed carbon of 95 %, very low volatile matter of 1.9 %, very low S content of 0.9 % and low ash content of 3.3 %. It was also characterized by good grindability and by calorific values exceeding 30 MJ/kg. Petroleum coke displayed a similar behavior with a high fixed carbon of 87 %, a moderate volatile matter of 11 % and comparable calorific value 32 MJ/kg whit higher S content of 1.9 %. Both materials were globally available, although their use was constrained by market price and S specifications.

C-rich in-house residues such as BF dust and sludge represented important internal resources with BF dust being already used as a supplemental fuel in sinter plants to reduce coke breeze consumption even if its effectiveness was low with a low replacement factor of 0.5. This poor efficiency was traced back to the addition of BF dust via the blending beds and its behavior during granulation since its small particle size caused the C content to be mainly embedded within the quasi-particles formed during sinter mix preparation which reduced its combustion efficiency. Considering this, the investigation focused on optimizing BF dust pelletizing to improve the use of its C content during sintering. Over the sampling period, the C content of the BF dust varied between 20 and 56 % with an average value of 41.2 %. The average ash content was approximately 55 % consisting mainly of iron oxides, the average volatile matter content was about 2.3 % and the average calorific value was 11.3 MJ/kg. Median particle diameter D50 of BF dust was about 0.2 mm, compared to approximately 1.2 mm for conventional sinter fuel. Bulk density was in the range of 0.8-0.9 t/m^3.

The study at Voestalpine focused on BF sludge obtained from two types of BF, i.e., one with top pressure and an older one without top pressure. The chemical composition of the two sludge types was similar with C contents around 30 % for the newer BF and 34 % for the older one while the Fe_2O_3 contents were roughly 55 and 48 %, respectively. The slag components were comparable and within normal variation ranges. A key difference was observed in the heavy metal content with Zn being 10–15 times higher in sludge from old BF without top pressure making carbon recovery more challenging. In terms of physical properties relevant to sintering, both sludge types had a maximum particle size of about 400 µm, but the mean particle diameter of sludge from the new BF was considerably coarser. The bulk density was around 2000 kg/m^3, and the calorific value ranged from 11 to 13 MJ/kg.

Biological carbon sources were also investigated with the aim of partially replacing coke breeze with renewable materials. Biomass generally exhibited significantly lower calorific values than coke breeze thus implying higher mass requirements for equivalent energy input. While sufficient agricultural land could theoretically supply the required quantities, availability, price volatility, and competition with food production represented major constraints. Many biomass types, including crops, agricultural residues and by-products of biofuel production, were rejected due to excessive volatile matter, low energy density, handling difficulties, etc. The most promising biomass candidates identified were residues from food processing, such as olive pits, sunflower residues and bagasse pellets. These materials were characterized by lower S content, lower ash levels, higher P contents, higher CaO and MgO levels compared to coke breeze. They also exhibited high volatile and oxygen contents which must be carefully managed in sintering.

The pre-processing of alternative carbon sources was governed by the requirements of sintering in which coke breeze was normally blended with the sinter mix prior to granulation. The fuel particle size should typically be in the range of 1–3 mm to achieve high sinter productivity and good quality. Therefore, pre-processing aimed to minimize harmful components and to optimize grain size distribution to maximize utilization of the C content. For example, BF sludge recycling limiting values were 0.5 % for Pb and 1% for Zn and their very fine particle size required agglomeration to fit into a

conventional sinter mix. Focusing on the straight substitution of coke breeze with biomasses, the pre-processing options were quite limited with the biomass which must be correctly sized. Biomass could not be milled in the same way as coke breeze due to its soft and fibrous nature and size reduction could be achieved using a cutter mill operating with both cut and shear forces. In particular, biomass passed into a grinding chamber where it was crumbled between 3 high-speed rotating blades operating at more than 1200 rpm and stationary ledges arranged around about 80 % of the chamber circumference. Material residence time increased with decreasing mesh size and discharge occurred once particles pass through the bottom screen. For initial laboratory sinter pot tests, biomass was milled below 2 mm and then screened to a size range of −2 mm +0.85 mm to achieve particles predominantly between 1-2 mm. Coke breeze used for comparison was screened to the same size range. Laboratory sinter pot tests were carried out using crushed refractory alumina chips as an inert bed to facilitate direct comparison between coke breeze and biomass fuels. Thermal profiles showed that biomass fuels produced broader time–temperature response than coke breeze thus indicating a mismatch between flame front speed and heat front speed probably ascribable to differences in reactivity. The effect of particle size was assessed by milling and screening sunflower husk pellets into four fractions, i.e., −4 +2 mm, −2 +0.85 mm, −0.85 +0.6 mm and −0.6 +0.2 mm. The highest peak temperature of 1313 °C was achieved with the 0.6–0.85 mm fraction compared with the 1370 °C of 2-4 mm coke breeze thus indicating that biomass must be finer than the coke it replaced.

Concerning BF sludge pre-processing, a combination of hydro cyclone separation, filter pressing and crushing was investigated. A pilot-scale hydro cyclone was installed at the BF sludge dewatering station with a characteristic separation size in the range of 10–20 µm consistently with laboratory results. Mass balance showed that 70 % of BF sludge mass was recovered in the underflow fraction containing almost 73 % of the total C. Heavy metals such as Pb, Zn, Cd and Hg were enriched in the overflow to be landfilled. Sludge from older BF without top pressure produced lower underflow yields due to the finer grain size distribution. The hydro cyclone underflow was subsequently dewatered using a chamber filter press and laboratory pressure filtration tests showed that moisture contents of 18 % could be easily achieved, but crushing was required for the filter cake to obtain a particle size suitable for sintering, i.e., <10 mm. Field tests with an adapted blade crusher led to the development of a prototype capable of in-situ crushing of filter cake from an industrial chamber filter press and the resulting material had a grain size distribution suitable for sinter mixing with chemical and thermal properties comparable to BF dust. Magnetic separation was also investigated as alternative or complementary method for BF sludge treatment. A laboratory high-intensity magnetic separator was adapted for wet operation using a steel wool matrix to enhance magnetic field gradients. Tests showed that no effective separation between carbon and heavy metals, e.g. Pb and Zn, could be achieved with this method even though Fe was concentrated in the magnetic fraction. The poor separation was not ascribed to intergrowth of C and heavy metals but to insufficient differences in magnetic properties.

The optimized and combined process including separation, dewatering and crushing allowed to produce enough pre-treated BF sludges for sinter pot testing and thermal evaluation. Briquetting and pelletizing were investigated to recycle fine BF dust and sludge and to substitute coke breeze. Die pressing, continuous roller pressing and disc pelletizing were evaluated to produce C-rich agglomerates with the coke breeze size range and to improve the replacement factor. Various binders and additives were tested, and process parameters were scaled up from laboratory to semi-technical and technical levels. Laboratory scale tests were performed to investigate mixture composition and evaluate pellet strength as a function of binder type and content, as well as moisture and C content. Moisture varied between 0 and 15 % but pelletizing without water proved to be unsuccessful while 10 % moisture

allowed the strength to increase significantly with no further benefit at 15 %. The effect of binder type showed that aluminate cement provided the highest strength and calcium hydrate gave a strong increase after one day while Portland cement and water glass resulted in lower strengths. Adding sinter coke slightly increased pellet strength with similar trends for all binders. Based on these results, a basic mixture of 60 % BF dust, 30 % sinter coke and 10 % binder at about 10 % moisture was selected, with calcium hydrate selected as binder for cost reasons and using a curing time of three days. Pilot pelletizing tests were conducted using a ring die press achieving throughputs of 400–500 kg/h and producing stable pellets of 3 mm diameter using the basic mixture. Further tests performed at the laboratory scale were roller press tests, briquettes extrusion and disc pelletizer. Roller press tests showed that briquette yield decreased significantly for volumes below 9 cm^3 and extrusion resulted in low production rates which limited the feasibility of this technique to an industrial scale since an annual production of about 100 kt of briquettes for a sinter plant producing 10 Mt per year was targeted. Disc pelletizer tests were performed using mixtures of BF dust, BF sludge, mill scale and cast house dust and moisture contents of 12%. After curing for 48 hours, pellets with size range of 3–8 mm and C contents between 23 and 32% were used in sinter pot tests. Abrasion resistance tests showed that pellets from both die press and disc pelletizer produced less fines below 1 mm than conventional sinter fuel thus indicating sufficient strength to withstand handling and sinter mix preparation, with disc-pelletized material showing the best performance at high stress levels.

Thermal evaluation of pre-treated alternative carbon sources aimed at determining reactivity and sinter performance to evaluate the C replacement factor when substituting coke breeze. Pet coke, anthracite, anode coke, BF dust, BF sludge, and mixtures of BF dust and sludge containing cast house dust and binder, as well as biomass in the form of olive pits and wood pellets were tested. A carbon replacement factor of 1 with coke breeze being fully substituted by alternate carbon sources was selected for most sinter pot trials with some additional tests performed at Voestalpine considering a replacement factor of 0.5 and 1 to evaluate the influence on sintering performance. Characteristic parameters assessed included flame front propagation, sintering temperature, sintering speed, efficiency, and sinter quality metrics according to ISO standards, e.g., tumbler and shatter tests, reduction degradation index, and grain size distribution. Laboratory thermal tests performed in a laboratory tube furnace at 1200 °C allowed to determine the combustion reactivity of the pellets produced with both die press and disc pelletizer using different fuels. Off-gas components CO_2, CO, and O_2, along with volume flow and temperature, were measured continuously to calculate the combustion reactivity using a mass balance and reaction model. BF dust pellets reactivity was between that of sinter coke and that of pet coke and anthracite. A clear influence of sinter coke content on BF dust pellets reactivity was not observed leading to the conclusion not to add of sinter coke in the pellet raw mixture thus reducing the volume of material to be mixed and pelletized. Laboratory sinter pot tests on pre-treated biomass were also carried out. The reference mix contained 4 wt.% of coke breezes on a wet basis and 4 wt.% of moisture. For the trials, a quarter of the coke breeze was replaced on a carbon basis with biomass materials, including hazelnut shells, almond shells, and crushed sunflower husk briquettes. The mix components were dry mixed in a rotating drum for 10 minutes and moisture was then added before proceeding with wet mixing for additional 10 minutes. Thermal profiles and off-gas compositions, i.e., CO, CO_2, O_2, and SO_2, were recorded together with NO_x emissions. Coke breeze thermal profile reached the highest temperature, and sunflower husk produced the next highest peak approximately 150 °C lower and occurring slightly earlier. Almond and hazelnut shells exhibited much lower peak temperatures with post-peak curves displaying shapes deviating from that of coke breeze thus reflecting differences in structural composition and loss of heating potential. This indicated that the C replacement factor

for biomass must be considerably lower than 1. Average combustion efficiencies calculated as $CO_2/(CO_2+CO)$ differed little among the fuels but were marginally lower for the sunflower husk material. Peaks near the end of the tests appeared earlier for biomass materials compared to coke breeze. SO_2 emissions were significantly lower for biomass, reflecting their lower S content, i.e., 0.14 wt.% against 0.6 wt.% of coke breeze. NOx emissions showed no significant differences.

Technical-scale sinter pot tests were carried out at Tata Steel, ILVA and voestalpine to evaluate the influence of alternate carbon sources on sintering performance, product quality and flame front behavior. At Tata Steel, biomass in the form of olive pits was used to partially replace coke breeze on an equivalent carbon basis using a standard Scunthorpe ore blend. The most promising result was obtained with the substitution of 15 % of the carbon from coke breeze combined with a small additional coke input, which led to the best compromise between productivity, cold strength and coke consumption. The results demonstrated the high sensitivity of the sintering process to small variations in moisture content, ignition conditions and blend composition. Despite the generally positive trends, the overall performance of biomass remained below that of the base case, indicating a carbon replacement factor lower than 1 due to reduced combustion efficiency and lower bed temperatures.

The sinter pot tests at ILVA were performed to evaluate the impact of non-briquetted and briquetted BF dust and sludge mixes, as well as alternate carbon sources such as anthracite and pet coke, on the sintering process. Standard sinter pot trials used a controlled mix of five iron ores, fluxes, and circulating materials, targeting a self-fluxing sinter with an IB2 index of 1.8–2, FeO content of 4 %, and a return fines ratio of 0.95–1.05. Mechanical properties including shatter index, ASTM tumble index, reducibility, and reduction degradation index were monitored. The substitution of 50 % of coke breeze with pet coke increased sinter productivity thanks to higher volatile matter that promoted combustion ignition and to the increased permeability that allowed a faster cooling. Chemical and mechanical properties were unaffected. The substitution of 30 % of coke breeze with anthracite slightly reduced yield but improved ignition thus decreasing the sintering time thanks to the higher volatile content that supported combustion. This mixture also caused an increase in fine fraction thus reducing productivity. Moving to the substitution of coke breeze with untreated sludge mix (47 % BOF sludge, 32 % BF dust, 16 % BF sludge, 5 % Dredging sludge) and with BF dust and sludge mix in the range of 10–20 % sinter yield decreased when 10 % was substituted while it increased when 20 % was substituted. Sludge and dust mixture also caused an increase in the sintering time and in the fine fraction formation as well as a decrease in the shatter index and in reducibility. The carbon replacement factor proved to be significantly lower than 1. Concerning the study of temperature profile, the replacement of coke breeze with pet coke determined a flame front temperature around 1250–1350 °C depending on the volatile content. Flame front speed was not influenced by pet-coke addition, but sinter productivity raised because of the higher volatile matter which supported combustion ignition and because of the increased permeability that allowed a faster cooling. Concerning the use of anthracite, a slight increase in maximum gas temperature and in flame front average speed was observed as well as a higher cooling speed thanks to the higher sinter permeability. Analogous results were also obtained with the BF sludge and dust mixture. Concerning the substitution of 10–20% coke breeze with pellets containing 23–32 % C, 12 % moisture, and with a size of 3–8 mm or with briquettes produced with a mixture of 20 % BF dust, 40 % sludge, 40 % lame scales, and 5 % bentonite, minor changes in shatter index, reducibility, and permeability were observed while chemical composition was mainly influenced by briquette content with decreasing wüstite and increasing Zn. Waste gas analyses indicated no deterioration in emissions.

Comparative sinter pot tests were conducted at voestalpine to evaluate pre-treated alternative carbon sources provided by other project partners. The reference sinter mix composition included ores, recycling materials, basicity, coke breeze, and return fines and was based on average EBFC sinter plant data with return fines being reduced from 360 to 300 kg/ ton of sinter. The alternative carbon sources considered were pre-processed BF sludge, briquetted in-house dust mixes and pet coke. Initially, a carbon replacement factor of 1 was assumed thus meaning that 10 % of the carbon from coke breeze was replaced by 10 % of carbon from the alternative carbon source. After that, a carbon replacement factor of 0.5 was selected thus meaning that 10 % of the carbon from coke breeze was replaced by 20 % of the carbon from the alternative carbon source. All tested materials showed that when carbon replacement factor was equal 1, the balance of return fines output and input was close to 1, but when carbon replacement factor was equal to 0.5 the mass of output return fines was significantly lower than 1 and this led to the conclusion that there was more effective fuel in the mixture than in the basis mix, and therefore the carbon replacement factor for all three tested materials is closer to 1 than to 0.5. Additional tests included olive pits, wood pellets, anode coke, and pet coke under the same conditions. Both biomasses showed a return fines higher than input. This difference was quite small for olive pits thus indicating a noticeable contribution to fuel effect while wood pellets produced much higher return fines thus suggesting a carbon replacement factor far below 1. Crushed anode coke achieved a return fines balance near 1 at a replacement factor of 1 thus confirming high fuel effectiveness, while assuming a factor of 0.5 resulted in lower return fines thus indicating that the actual factor was significantly higher. Concerning the reduction degradation index, anode coke and pre-treated alternative carbon sources from BF sludge and dust displayed values around 23–33% comparable to the standard reference while both biomasses exhibited reduction degradation index around 36–40 % with higher low-temperature breakdown further indicating a lower effective carbon replacement factor. Thermocouple measurements also showed that biomass fuels produced lower maximum temperatures and a broader flame front compared to the reference mixture while BF dust pellets and pet coke exhibited flame front propagation and temperature profiles similar to those of coke breeze. Off-gas emissions in terms of CO, CO_2, SO_X and volatile organic carbon were measured and the results showed that sulfur dioxide emissions were strongly influenced by the S content of the substitute. Pre-treated BF sludge and pet coke produced higher average SO_2 concentrations than the reference mixture, reflecting their elevated S levels. Volatile organic carbon (VOC) emissions for pre-treated BF sludge and dust pellets remained comparable to those of the reference mixture whereas pet coke generated markedly higher VOC levels, i.e., 5 times higher. Industrial-scale dust emission measurements confirmed that replacing coke breeze with alternate carbon sources did not cause any detectable adverse effects on particulate emissions. Sinter pot tests with anode coke reported a S content like pet coke thus resulting in increased SO_2 emissions, while biomass fuels particularly olive pits significantly reduced SO_2 concentrations. Besides their favorable CO_2 balance, this reduction in S emissions represented a key environmental advantage of biomass-based fuels. However, biomass substitution consistently led to higher VOC emissions due to the higher content of hydrogen-rich organic compounds. The increase was especially pronounced for wood pellets probably due to their higher volatile matter and lower fixed carbon content compared with olive pits. Despite the high volatile content of biomass, a comparison between olive pits and pet coke showed similar VOC and CO emission levels, even though the volatile matter in olive pits was several times higher. This indicated that a substantial fraction of the volatile components released from biomass participated in the sintering reactions partially mitigating their negative impact on off-gas quality.

Field tests were carried out at the sinter plants to transfer laboratory and pilot-scale results to industrial operation. Pelletized BF dust was applied at ArcelorMittal, pre-processed BF sludge was used at Voestalpine, and anthracite was employed to replace coke breeze at ILVA. These trials demonstrated the technical feasibility of substituting conventional coke breeze with alternative carbon sources under real plant conditions. Concerning material pre-treatment, BF sludge was pre-treated with a hydro cyclone, with dewatering in a chamber filter press and subsequent crushing. This process allowed to recycle almost 65-70 % of the sludge while achieving sufficient separation of fine particles and heavy metals. The dewatered material with moderate moisture content did not show any handling problem even under winter conditions and did not lead to any enrichment of Zn or Pb in the sinter. BF dust was agglomerated at industrial scale using an intensive mixer and applying a mixture with 70 % BF dust, 10 % cast house dust, 20 % of calcium hydrate and about 9 % of water.

Industrial trials at Voestalpine showed that substituting a significant amount of coke breeze with pre-treated BF sludge resulted in a corresponding reduction in coke consumption indicating a carbon replacement factor close to 1. Waste gas CO levels remained unchanged thus confirming the complete combustion of the alternative carbon source while sinter quality and productivity were almost unaffected. The replacement of high levels of coke breeze with anthracite at ILVA caused a slight decrease in sinter yield and productivity consistently with sinter pot trials. Nevertheless, sinter quality remained stable, and emissions showed only moderate changes with slightly higher SO_x and lower NO_x levels. Considering the acceptable performance and the lower S content, anthracite was adopted as main sinter fuel at ILVA. The use of BF dust pellets at ArcelorMittal showed clear benefits compared with untreated dust. Indeed, pelletized BF dust achieved a significantly higher carbon replacement factor close to 1 while untreated dust required additional carbon input and did not improve productivity. Therefore, pelletizing proved to enhance carbon utilization stabilizing sinter operation. No negative impacts on sinter chemistry and emissions were detected although optimization of binder content was identified as a requirement for long-term application.

From an emissions perspective, S and VOC emissions were the key limiting factors. Pet coke and anthracite grades often contained more S than coke breeze and BF dust and sludges can also show a higher S-to-C ratio. This could become critical in sinter plants equipped only with electrostatic precipitators which have limited desulphurization capability. Biomass fuels, while beneficial in terms of S reduction, tended to increase VOC emissions due to their high volatile matter which was released early during sintering thus confirming that VOC emissions may restrict the extent to which biomass can be applied in sintering. Life cycle assessment (LCA) was used to quantify the environmental impact of substituting coke breeze with biomass comparing a reference case with conventional coke breeze and a scenario with 15 % replacement by olive pits. The models indicated a total CO_2 emissions reduction of the steelwork of 1% corresponding to a 10 % of CO_2 reduction at the sinter plant itself thus confirming the relevance of biomass substitution from a life-cycle perspective.

Project results were already implemented at industrial scale. ILVA adopted a full anthracite sinter strand thanks to its low S content of 0.9 %, its limited impact on sintering performance and anthracite costs 60–70 % lower than coke breeze. Voestalpine implemented a full-scale pre-processing of BF sludge including hydro cyclone separation, dewatering in a chamber filter press and crushing of filter cake which allowed about 70 % of the sludge from one BF to be recycled ensuring a recovery of 3,350 tons of C and 4,050 tons of Fe demonstrating both economic and environmental benefits.

2.2.4 EPOSS: Energy and productivity optimised EAF stainless steel making by adjusted slag foaming and chemical energy supply (30)

The project was coordinated by BFI with Acroni, BGH, Gerdau (current Sidenor), SWEREA (Current SWERIM), and Outokumpu Stainless participating as partners in the consortium. The project started on the 1st of July 2007 and lasted almost 3 and a half years, ending on the 31st of December 2010. The overall project cost 1.47 M€ and EU contributed 885 k€, i.e., 60 % of the budget.

In stainless steel EAF operations, electricity is a dominant cost driver and a major source of indirect emissions, while productivity is tightly linked to melting and refining duration, i.e., time-on and tap-to-tap time, as well as to unplanned process disturbances. In addition, oxidation of Cr and other alloying elements generates slag losses that must be compensated with additional ferroalloys thus affecting both costs and slag environmental performance. Slag foaming is a key lever because a stable, foamable slag can shield the arc, improve electrical efficiency, enhance bath stirring and reduce refractory wear. However, slag foaming and chemical energy input, i.e., oxygen, fuel, reductant oxidation, must be balanced with Cr yield, slag properties and emission-related constraints. In light of this, the EPOSS project aimed to increase energy efficiency and productivity during EAF high-alloy stainless steelmaking by developing innovative slag conditioning techniques for slag foaming and by adjusting the use of all available energy sources.

Three plant-specific optimization routes were designed, developed and trialed. The first route concerned Acroni steelwork and focused on the development of an EAF slag conditioning technique through the injection of CaC_2 mixtures as reductant recover the oxidized Cr from slag reduction. The second route concerned Gerdau Sidenor and addressed the development of an optimized EAF slag conditioning technique through the injection of carbon/oxygen and addition of FeSi to make the slag foamable and to recover oxidized Cr by slag reduction. The last route concerned BGH and was dedicated to the development of an optimized EAF slag conditioning technique through the coherent-jet injection of Al granules as main additive and as chemical heating technique to reduce electrical energy demand. Carbon/oxygen injection and additional oxyfuel burner operations to improve the exploitation of chemical energy to reduce electric energy consumption and to improve productivity were also investigated.

Initial project activities were dedicated to the identification of the baseline condition, i.e., the reference operations, for each steelwork to have a benchmark against which validate or discharge the new proposed solution. In particular, material and heat balances were performed as well as slag analysis to investigate slag chemistry including Cr_2O_3 and other paramount slag properties such as the leaching behavior. Knowledge of Cr_2O_3 content was essential since higher amounts caused higher slag viscosity thus jeopardizing foamability. In this first part of the project, BFI supported the activities by performing some thermodynamic and kinetic assessments by performing laboratory test to investigate Cr_2O_3 reduction kinetics at 1550 °C. In particular, two slags with high and low-Cr content and FeSi, Al and CaC_2 as reductant were selected to perform the tests. The influence of FeSi and Al on slag Cr_2O_3 content proved to be similar determining a Cr_2O_3 content of 4 – 6 % for the high chromium slag after 30 min and of 8 – 11 % for the lower chromium slag thus being less effective. Opposite was the effect of CaC_2 which proved to be more effective in reducing Cr from the low chromium slag with a resulting

Cr_2O_3 content of 5 % compared to the resulting Cr_2O_3 content of 9 % of the high chromium slag. With the best suited reductants for each slag a final chromium oxide content in the range of 4 % was obtained. The analysis of the produced gas volume and the heat supply by each additive were then subjected to thermodynamic calculations. Al was the most effective additive for heat supply to EAF providing an average heat supply of 1.6 kWh/kg Al and being effective in the range of 0 – 40 kg/t of liquid steel. On the contrary, FeSi was not effective for heat supply with an average heat supply < 0.1 kWh/kg FeSi. CaC_2 proved to be effective in the range of 20 – 40 kg/t of liquid steel providing an average heat supply of 0.7 kWh/kg CaC_2. This allowed to conclude that Al was the best additive to supply chemical energy.

Focusing on the first route, the best practice for slag foaming by combined CaC_2 injection and FeSi addition at Acroni included CaC_2 injection into the melt through one submerged slag door lance, the use of an average CaC_2 amount of 5 kg/t of steel applying a mass flow rate around 60 kg/min. This CaC_2 amount allowed to comply with the stoichiometric requirement for a target Cr reduction of 8 kgCr/t of steel while the mass flow allowed to prevent CaC_2 powder carryover into EAF off gases. CaC_2 injection was also delayed as much as possible in the flat bath melting period and slag mixing was provided by C injection during this period but reducing as much as possible the C content needed to minimize the subsequent decarburization step. FeSi and SiMn addition were performed according to the normal melting practice according to each steel composition while natural gas/oxygen burner operation was abandoned to minimize Cr oxidation. The industrial trials demonstrated that increasing CaC_2 content increased Cr reduction ensuring average Cr values of 1.6 kg/ton of liquid steel, i.e., a 22 % reduction compared to normal practice, corresponding to an estimated average Cr reduction efficiency of 27 %. Despite this improvement in Cr reduction, a critical outcome was that CaC_2 use did not provide an energy benefit under the conditions investigated. Actually, heat-balance comparisons showed electrical energy consumptions between 549 and 597 kWh/t for CaC_2 injection trials which were significantly higher than the reference value of 519 kWh/t for normal operation. This was associated with the longer melting time during CaC_2 trials and as evidence that injected CaC_2 did not contribute measurable net energy to the process. Despite this, the cost analysis demonstrated a certain balance of the different effects as proved by the cost allocation data in Table 6 where additional costs and savings are reported against the normal practice and highlights an overall cost change close to zero, i.e., −0.22 €/t. From an environmental perspective, slag leaching tests indicated that reducing Cr_2O_3 content in the slag did not necessarily lead to a reduction of Cr leaching emphasizing that the optimization must consider also slag mineralogy and oxidation state and not only bulk Cr content. Indeed, Cr in the leachate mainly in the form of Cr(VI) reported higher values of 2.2 mg/kg for the CaC_2 route against the 1.6 mg/kg for the reference slag.

Table 6: Cost allocation example for the CaC_2 injection route at Acroni.

Cost category	Δ consumption/saving	Unit price	Δ cost (€/t)
CaC_2 addition	+4.7 kg/t	0.8 €/kg	+3.8
Cr addition (as FeCr)	−1.6 kg/t	2.7 €/kg	−4.32
FeSi addition (Si 75%)	−1.5 kg/t	1.4 €/kg	−2.10
Electric energy	+30 kWh/t	0.08 €/kWh	+2.4
Total			−0.22

Moving to the second route at Gerdau Sidenor, the optimization of the operating conditions focused on the injection of oxygen and carbon as well as FeSi addition to increase chemical energy contribution and improve slag foaming without disproportionate oxidation losses. Three process variants, i.e., A, B and C, were compared against standard operation in terms of production costs and operational performance. Process A entailed a good slag foaming practice with high oxygen injection and high Cr recovery, process B included a good slag foaming practice with low oxygen injection and intermediate Cr recovery and process C was developed with a bad slag foaming and a small Cr recovery. The main parameters used in the standard practice and for the practices of processes A, B and C are summarized in Table 7. From an operational perspective, process B proved to be the best practice Table 1combining slightly higher oxygen consumption, i.e., 15 versus 11 Nm^3/t, and a longer injection time, i.e., 11 versus 6 minutes, compared to the standard practice with reduced lime addition, i.e., 57 versus 70 kg/t, and reduced FeCr addition, i.e., 5 versus 12 kg/t. Electrical consumption also decreased from 546 to 503 kWh/t and tap-to-tap time was reduced from 123 to 104 minutes, i.e., −15%, while steel output per heat increased slightly from 111 to 113 t in the reported comparison. The slag at tapping changed from thick to fluid thus indicating modified slag condition. Process B proved to be the best choice even from a cost analysis perspective where the penalty for Cr process losses was explicitly included and calculated from Cr introduced into the EAF as scrap and ferroalloys and Cr contained in steel at tapping. This penalty was converted into an economic term to reflect additional alloy demand. The results of the analysis are summarized in Table 8 and reported a total production cost of 162.87 €/t for standard practice, 166.77 €/t for process A, 138.47 €/t for process B and 156.31 €/t for process C with process B being the most economic route. This was mainly due to a substantially lower penalty for Cr process losses of 33.14 €/t against the 42.57 €/t for standard practice. It can be concluded that the best-practice procedure identified in process B allowed significant cost savings of 24 €/t and electrical energy savings of almost 8% for the plant-specific comparison compared to the previous operational procedure. Finally, from an environmental perspective, particle emission peaks were identified during discrete operational actions such as scrap basket charging and start of the foaming slag phase when injecting oxygen and carbon. Higher peaks were detected for the process variant with higher injected carbon, i.e., 50-100 kg more than process B, thus highlighting significant dust emission constraints when intensifying chemical energy input.

Table 7: Comparison of the standard practice with the practices of processes A, B and C at Gerdau Sidenor.

Parameter	Standard	Process A	Process B	Process C
Lime (kg/t)	70	48.6	56.9	57.1
Oxygen (Nm^3/t)	11	27.9	14.5	23.4
Injection time (min)	6	15	11	22
FeSi (kg/t)	3	3.47	2.2	2.2
FeCr (kg/t)	12	9.1	5	4.4
Carbon (kg/t)	3	4.44	3.55	2.21
Basicity	1.41	1.51	1.30	1.41
Electrical consumption (kWh/t)	546	491	503	487
Tap-to-tap time (min)	123	100	104	118

Table 8: Comparison of the production cost (€/t liquid steel) of the standard practice with the cost of processes A, B and C at Gerdau Sidenor.

Cost item (€/t)	Standard	Process A	Process B	Process C
Electrical consumption	39.85	35.84	37.12	35.58
Cost of time process	66.49	54.41	55.57	62.65
Carbon consumption	0.69	1.00	0.77	0.50
Lime consumption	5.61	3.89	4.58	4.57
O_2 consumption	3.36	8.36	4.39	7.04
FeSi	4.30	4.51	2.90	2.88
Penalty for Cr process losses	42.57	58.75	33.14	43.09
Total	162.87	166.77	138.47	156.31

The last route was developed at BGH trying to validate an innovative chemical heating practice based on coherent-jet injection of Al granules. Heat and material balances performed for a ferritic grade clearly underlined that Al injection increased the chemical energy input by about 54 kWh/t thus enabling an average electric energy saving of 45 kWh/t, i.e., 9 % of the normal electric input. For austenitic grades, chemical energy input increased by ~44 kWh/t and the average electric energy saving

was 32 kWh/t, i.e., about 6 %. The trials also indicated higher thermal energy carried by the output slag of 16 kWh/t and a higher heat removal in cooling water of 16-17 kWh/t thus confirming that operational control such as start time of Al injection, C injection and oxygen practice was essential to translate chemical heating into net electrical savings.

Overall, EPOSS showed that meaningful improvements in stainless EAF efficiency were achievable through plant-specific optimization of slag conditioning and chemical energy utilization, but those benefits and trade-offs depended strongly on the process route and on local constraints. The CaC_2 route at Acroni was effective for Cr recovery but introduced energy and leaching-related limitations, whereas the Gerdau Sidenor and BGH approaches yielded clear reductions in electrical energy and improvements in productivity.

2.2.5 URIOM: Upgrading and Utilisation of Residual Iron Oxide Materials for hot metal production (31)

The project was coordinated by BFI with Böhler Edelstahl GmbH and CSM participating as partners in the consortium. The project started the 1st of July 2007 and lasted almost three and a half years, ending on the 31st of December 2010. The overall project cost 1.56 M€ and the EU contributed 938 k€, i.e., almost 60 % of the budget.

In the framework of the URIOM project, two new technologies for the recovery of Fe and Cr containing residues from stainless steelmaking were developed. The first technology was an inductively heated coke bed reactor process developed by Böhler and BFI while a new briquetting technology using vegetable binders and direct recycling in EAF was the second technology developed by CSM. In particular, Böhler developed a concept for an inductively heated coke bed reactor (ICBR) preceded by a flash smelter process step to pre-melt the oxidic residues. This process allowed to collect Fe and other valuable alloying components in the hot metal, while Zn was separated into a ZnO product obtained at the inductively heated coke bed reactor. Böhler performed extensive lab scale and technical scale experiments to develop the process. In addition, BFI worked on an additional concept, i.e., an inductively heated coke bed reactor process preceded by a cupola furnace for melting and pre-reduction of the oxidic residues. In this case, the main product was the hot metal containing valuable alloying components such as Cr. BFI exploited liquid flow modelling and carbothermic reduction trials to develop a software-based process model for simulation of the overall process. The basic design of the coke bed reactor unit was carried out in cooperation between Böhler and BFI and the different processes variants were finally evaluated and compared. All technologies proved to be key processes for an economic and environmentally friendly on-site recycling of stainless steelmaking residues with a complete recovery of alloying elements for steelmaking, Zn for nonferrous metal use and a product slag usable for building applications.

The first step of the project included an extensive characterization performed by all partners to obtain representative data from the different waste iron oxides for further process development. BFI analyzed a set of high Cr EAF dusts and of hot rolling scale from stainless steel production while Böhler performed a comprehensive investigation of EAF dust properties. CSM analyzed both hot and cold collected residues from stainless steelmaking. The first group included EAF and AOD slag while the second group included oil containing materials, refractory materials, scale, dust and sludge. The waste

materials rich in metals were sludge, scale and dust, whereas EAF and AOD slag and refractory materials were low metal materials.

Dust analysis reported significant variation in the chemical composition, especially regarding Fe_3O_4, Cr_2O_3, ZnO, CaO, MgO and SiO_2. WDX (Wavelength-dispersive X-ray) analysis revealed that Fe, Cr and Zn were the main components and appeared mainly as combined complex oxides in the form of $(Fe, Zn)O{\cdot}(Fe, Cr)_2O_3$) compounds. Nevertheless, Fe and Cr, as well as Mn and Ni, were partially found in the metallic form always surrounded by an oxide layer. The melting behavior was also investigated with a high-temperature heating microscope and with thermochemical melting point calculations. It was almost impossible to melt any of the samples at temperatures <1650 °C under oxidizing conditions even when significant amounts of slag-forming agents such as SiO_2 were added. However, the main dust components, i.e., Fe_3O_4, Cr_2O_3 and ZnO, were reduced to metal under strong reducing conditions like the ones of ICBR thus allowing either the slag formers or the formed alloy to determine the melting point. Grain size analysis revealed that the dust was very fine displaying for 57 % a dimension < 1 µm and for 100 % a dimension < 12 µm. A low bulk density of 0.70-0.91 g/cm^3 was also detected thus indicating that the dust was formed via evaporation and condensation/sublimation processes. BFI also performed initial calculations with FactSage thermochemical software to select suitable slag forming additives and ensure both liquid slag and metal phases during chromium oxide reduction. The calculations were based on a typical high-Cr EAF slag from which Cr recovery was a suitable option. The results showed that untreated high-Cr EAF slag was not sufficiently liquid at 1600 °C due to the high fraction of solid compounds and the addition of SiO_2 was able to increase the proportion of liquid phase in the slag at lower temperatures. Indeed, the addition of 15 wt.% SiO_2 ($CaO:SiO_2$ = 1.1) to typical high-Cr EAF slag allowed for a sufficient fraction of liquid slag phase to be obtained at relatively low temperature of 1400 °C. Therefore, the mass relation of $CaO:SiO_2$ should be in the range of 1 to obtain a low viscosity of the slag at 1600 °C.

All materials composing the briquettes, i.e., iron residues, vegetable binders and reducing agent, were analyzed to produce suitable briquettes for Fe recovery. Suitable vegetable binders must be good filling agents and absorbents for eventual oily residues and different potential materials were considered such as starch, sawdust and flour. Flour was selected by CSM among them for briquettes preparation thanks to its good binder characteristics resulting from both starch gelatinization and gluten formation. Both mechanisms help stability and compactness of briquettes. The selection of the appropriate reducing agent was performed thanks to accurate chemical and energy balances, as a function of the percentage of the constituents of the mixtures involved in the chemical reactions and energy exchange and FeSi was finally selected. Briquettes recipes included 80-90 % of waste materials in the form of residual iron oxides, 8-10 % of expired wheat flour as binding agent and 2-3 % of water.

After the preliminary characterization and selection of materials, BFI built a full-scale physical coke bed reactor model to investigate the melt flow of an ICBR. The reactor had a diameter of 60 cm and a height of 120 cm appropriate to guarantee a slag input of 300 kg/h. The reactor model allowed to estimate the pressure loss occurring in a coke bed reactor, to visualize the slag flow and measure the mean residence time, dead time and maximum tracer concentration as a function of the different operating parameters, i.e., gas flow, coke particles diameter, slag flow rate, slag viscosity and type of slag feeding, e.g., the feeding point. The trials performed with the model revealed that the mean residence time decreased with increasing slag flow rate and viscosity while it was nearly independent from coke particles diameter and gas flow rate. Concerning the type of feeding, it was proved that mean residence time increased when circumferential slag feeding was applied in comparison to point

feeding. Circumferential slag feeding to the coke bed reactor was the reference state when a cupola furnace was the preceding process while point feeding referred to liquid slag charging e. g. from a flash reactor.

Based on the results of the melt flow investigations, kinetic investigations on carbothermic reduction of chromium oxide were performed by BFI in a high-temperature laboratory furnace to assess the performance of the chromium oxide reduction in the new designed coke bed reactor. The high-Cr EAF stainless steel slag was heated up in the furnace to 1600 °C and a rotating graphite rod acting as reductant for chromium oxide was immersed in the slag to simulate the slag flow conditions on the coke surface inside the coke bed reactor. The rotational speed of the graphite rod was varied to simulate different flow velocities in the coke bed reactor and slag samples were frequently taken for chemical analysis. The chromium oxide reduction capability of the new designed coke bed reactor was estimated to be around 4-7 kg Cr_2O_3 per minute depending on coke size. Considering a typical input slag flows of 100-300 l/h and a chromium oxide mass percentage of 14 %, a complete Cr reduction was ensured for all investigated operational parameters because the chromium oxide reduction capability was always significantly higher than the amount of chromium oxide in the slag. The reduction kinetic of Zn and Fe in the ICBR was also investigated by Böhler using a high-temperature muffle furnace and a laboratory ICBR. ZnO reduction proved to be significantly faster, i.e., almost double, than Fe reduction and this was coherent with the thermodynamic principles for which ZnO reduction was preferred to that of FeO and Cr_2O_3 at 1600 °C. Considering this, ZnO reduction proved to be very fast and started immediately when the slag got in contact with the hot coke. This rapid reduction of ZnO was accompanied by the sudden formation of a large volume of Zn and CO gases which emerged directly at the top of the ICBR, and this aspect must be considered when charging the ICBR to avoid ejections of slag and dust. It was also noticed that reduction kinetics was accelerated by using smaller coke size.

The next step of the project included the generation of a basic layout of an ICBR pilot plant considering aspects like geometry, the design of the induction coil, the power of the generator, the required induction frequency, the electric-thermal conversion efficiency, etc. In this framework a further intensive campaign was performed to investigate the induction-heating behavior of different coke types assessing the influence of coke grain size and induction frequency. Three coke grain size classes of 10-20 mm, 20-40 mm and 40-60 mm were systematically tested with three different frequencies of 75, 105, and 150 kHz. Coke induction heating proved to be very fast reaching velocities of 25 - 45 K/min up to a maximum of 55 K/min while the required induction frequency laid between 75 and 105 kHz. The conversion efficiency of electric energy to coke heat was about 60 % with very high temperature levels mainly limited by the refractory materials. A sharp skin effect was observed due to small penetration depth of induction into the coke and to poor thermal conductivity of coke itself. This resulted in a large temperature gradient between the margin and the center of the coke bed, but the use of lower frequencies and larger grain sizes allowed to reduce this temperature gradient.

The RecoDust process proposed by Böhler for the pyrometallurgical treatment of steel mill dust consisted on a first flash-smelting of steel mill dust under oxidizing conditions to evaporate impurities like Pb, alkalis and halogens and in a second ICBR step where the pre-melt produced and containing Zn, Fe, Ni, V, W, Cr, Ca, Si, Al in oxidic form was reduced on the inductively heated coke bed. In this context, it is necessary to consider the extremely corrosive nature of the pre melt on ICBR refractories due to its high content of dissolved iron oxide and its relatively high temperature of 1600 °C. Considering this, the interface between the Flash Reactor and the ICBR required a special focus it

must also prevent slag freezing and ensuring an optimal melt distribution on the coke bed. In light of this, an appropriate ICBR feeding concept had to be found and the solutions investigated were cold feeding, tundish feeding, spray feeding and snorkel feeding. Each feeding and interface concept demonstrated specific advantages and disadvantages, but the spray feeding system was selected among them because it seemed to fulfil the requirements in the best way. Furthermore, it was preferred because it allowed dispersing the melt into fine droplets and directly feeding them into the energy rich area of the coke bed cross section thus also accelerating reduction kinetics. Another aspect to consider was the need to separate the gas phases from the Flash Reactor and the ICBR to get a high purity ZnO from the ICBR reduction process. In light of this, extensive experimental work was carried out on a continuously working and gas tight tapping system for the Flash Reactor pre-melt. The only system which proved to be successful was an indirectly water-cooled tuyere (tapping hole), installed at the bottom of the Flash reactor.

Some trials were also performed to generate basic data to set-up a rough mass and energy balance for treating EAF dust from stainless steel production with the RecoDust process. In the coupled trials, the Flash Reactor demo-plant was used to smelt the stainless-steel mill dust under oxidizing conditions at a temperature of 1600°C to supply the liquid pre-melt to the ICBR reactor placed directly underneath the Flash Reactor. Several test runs were performed to calculate the mass balance. In the Flash reactor a significant amount of material was carried over by the filter dust, i.e., up to 9.5 %, due to the partial reduction of ZnO which caused Zn vaporization and final reoxidation. Apart from Zn, Pb, F and Mo also concentrated in the filter dust. Oxides reduction in the ICBR reactor was almost complete and the slag produced was almost free of reduceable metals with just a residual 1.5 % of Cr_2O_3 and 1.2 % of FeO, i.e., 3.7 and 0.5 % of the amount contained in EAF dust. The reduction rate of Co, Mn, Ni, V, W and Cu was also high and above 90 % allowing to obtain a slag almost free from heavy metals and characterized by a very good leaching behavior. The iron alloy produced was rich in C and displayed a high Cu content together with high amount of Cr, i.e., 10.2 %, and Mn, i.e., 7.6. This mixed composition made it difficult to use the iron alloy as scrap substitute even for high alloyed steels although it contained a lot of expensive alloying elements. In conclusion, the combination of the flash reactor with ICBR allowed to process flue dusts from stainless steelmaking, transforming them from hazardous waste into valuable products.

A coke feeding and pre-heating system was also developed by Böhler to exploit the sensible heat from the CO and Zn off gases resulting from the ICBR to preheat the coke required as reductant in the ICBR itself taking into account that the gas should not be cooled below 1000 °C in the pre-heater to avoid Zn-condensation. Several coke charging and preheating concepts were developed and evaluated, but a horizontal coke pushing unit and an inclined coke feeding tube was estimated to fulfil the requirements in the best way. A laboratory scale prototype of this system was built and tested to check the functionality of the proposed equipment and to gain layout data for the industrial pilot plant. The parameters investigated were the inclination angle, coke grain size and interface design on the coke distribution in the ICBR. The best results were achieved without using any interface for distributing the coke in the reactor and applying an inclination angle of the coke feeding tube of 60°. In the end, the feeding unit was redesigned into a vertical feeder with a horizontally moving feeding plate considering the high pushing force required. Apart from the mechanical feeding unit, thermal engineering of the pre-heater was performed remembering that CO and Zn vapor off gas entered the pre-heater at 1600 °C and could only be cooled to 906 °C, i.e., Zn boiling point, to avoid Zn condensation on the coke in the pre-heater. The maximum length of the pre-heater was identified

around 0.5 m by heat balance calculations and under these specifications. Longer pre-heating zone would cause off-gas cooling below 900 °C and Zn condensation would arise.

A reforming concept was selected to recover Zn and water was injected into the Zn-CO off gas to form H_2 and ZnO. Thermochemical equilibrium calculations were performed to predict the amount of reaction products and to design and build a laboratory scale testing facility for the treatment of the Zn-CO containing off-gas evolving from the ICBR reactor. The tests were performed considering a reforming temperature from 700 – 1000 °C, a Zn-contents in the CO-Zn mixture of 10-20 % and steam amounts 3 - 9 times the stoichiometric amount of Zn contained in the off-gas. A good conversion efficiency >90 % was obtained in the temperature range from 700 to 950 °C proving that a wide process window was available for the operation while the amount of water and the Zn content in the off-gas had minor importance with respect to the conversion degree achieved. Analogously, the amount of CO converted into CO_2 proved to be almost constant, varying between 16-18 % of the original CO volume. The reforming solution allowed to simultaneously generate a marketable ZnO product while conserving the chemical energy of the off-gas during the cooling process thus being the perfect solution for the Flash Reactor-ICBR process. Indeed, the ZnO produced could be sold as valuable raw material to hydrometallurgical Zn winning, while the cold CO and H_2 rich gases from the reforming unit could be used as fuel in the Flash Reactor. Furthermore, the direct link with the coke pre-heater was an ideal solution since the optimal reforming temperature was around 800 °C and the off gas left the preheater at around 900 °C.

Moving to the concept proposed by BFI, i.e., an ICBR process preceded by a cupola furnace for melting and pre-reduction of oxidic residues, the first step concerned the modelling of the carbothermic reduction of the molten stainless-steel wastes in the inductive heated coke bed using the Fact Sage Software. Initially, the model was based on the thermochemical equilibrium calculation performed in one single reaction volume until the inductive heating trials performed at Böhler revealed a concentric heat distribution in the inductively heated coke bed. At this point, the highest temperatures at the outer part near the induction coil and lowest temperatures in the center of the coke bed were considered for model optimization and an optimized mass and energy balancing model was developed with FactSage and HSC software exploiting two different reaction units representing the different reaction temperatures. The temperature in the outer area was set to 1600 °C and the one in the inner area to 1400 °C. Element distribution in the main reaction units was calculated according to different element distribution models developed by thermochemical equilibrium calculations with reference residual materials by use of the FactSage Software.

After modelling the ICBR, BFI developed a new element and component distribution model including heat and material balances with the HSC software and based on initial calculations by the SimuSage software and on the existing BFI cupola furnace model. This model was able to predict successfully the chemical composition and the amount of products for given input materials for the cupola furnace process. The specific amount of the different materials streams and the composition of the output streams was calculated for a standard cupola furnace process by use of this model. The feasibility of the new cupola furnace process model was proven since the results of the calculation were similar to operational cupola furnace process data. The adapted cupola furnace model was the basis for the combination with the inductively heated coke bed reactor model obtained in the previous step.

The combination of the inductively heated coke bed reactor with the cupola furnace was performed thanks to the link of the two models. The cupola furnace was used to pre-melt and pre-reduce the residues considering 15 % of metallic input and the resulting slag was treated in the coke bed reactor

for the final reduction of metal oxides. Two different high Cr residues were considered for the model calculations, i.e., a spray roasting residue and a high-Cr EAF slag. Overall material balances and chemical composition of the final product slag and product iron were calculated for both residues. In both cases the final slag was nearly free from chromium oxides and iron oxides and contained only slag formers to a large extent. The metallic product was a cast iron with C and Si content around 3 % and elevated Cr content around 2.5 %. High Ni content of 1.1 % were also observed for the spray roasting residue scenario. The energy and consumables demand for processing both types of residues and resulting from the modelling activity allowed to perform an economic assessment for both residues. Coke consumption of the coke bed reactor unit was 2.5 higher for the high-Cr EAF slag compared to the spray roasting residue for processing 1 t of residue. Furthermore, the thermal energy feed and the electric energy consumption was significantly higher for processing EAF slag compared to spray roasting residue, i.e., a factor of 1.8. These outcomes must be ascribed to the higher amount of input slag when processing EAF slag. The electric energy consumption of the coupled process proved to be very high with 2905 kWh for processing 1 t of the EAF slag and 1635 kWh for processing 1 t of spray roasting residue. The electric power demand of the coke bed reactor unit related to 300 kg input slag per hour was higher for the spray roasting residue, i.e., 962 kW, than high-Cr EAF slag, i.e., 677 kW, because the spray roasting residue contained a higher amount of Fe- and Ni-oxide which required higher energy demand for oxide reduction.

Böhler calculated the mass and energy balance of the whole process chain to evaluate the performance of the coupled flash reactor and ICBR process basing on the results of the coupled trials and on few theoretical and thermochemical calculations. The calculated mass and energy balances of Flash reactor and ICBR referred to 1 ton of EAF dust. The main products of the coupled process were 185 kg of inert slag, 455 kg of liquid metal phase and 171 kg of Zn vapor. The addition of 176 kg of water in the gas reforming step allowed to turn the off gases from CO and gaseous Zn into 213 kg of pure ZnO and 203 Nm^3 of CO and 100 Nm^3 of H^2 and 42 Nm^3 of CO_2. The slag did not contain any harmful heavy metals and showed a stable elution behavior therefore it was not considered as a waste product but as a raw material for further applications.

Finally, the third route proposed by CSM, i.e., a new briquetting technology using vegetable binders to recycle directly residues from stainless steelmaking into EAF, was assessed. Preliminary briquettes were produced at a laboratory scale to identify the principal operational parameters considering that a suitable density around 2.7-3.1 g/cm^3 to prevent floating on slag surface and a good mechanical resistance to ensure handling without fragmentation or pulverization are the main requirements. First, the binding behavior was analyzed, and no reducing agent was added in these tests. Briquettes preparation passed through various steps: 1) Mixing of the solid components to facilitate the homogenization of the materials, 2) Water addition to activate the binding effect, 3) Charging of the mixture into the cylindrical shape mold with selected specific dimensions, 4) Mechanical pressing, 5) Drying and storage of the obtained briquette. Mechanical pressing aimed to reinforce the bonds between the different materials due to the increase of the surface contact between the units made by gel surrounded particles which reinforced the mutual entanglement of molecules. In addition, pressure compacted briquettes were characterized by a reduced number of pathways for water entry thus meaning that the briquettes were protected by high humidity content of the environment.

The briquetting procedure was tested with three different types of residuals iron oxides: briquettes type A were made packing the blast grinding residual from austenitic steel, briquettes type B were packed using the fine metals residual from the slag treatment and briquettes type C were build-up

using very fine residual blast grinding from ferritic stainless steel. Only A and B briquettes proved to be sufficiently compact and solid after fall test and long storage therefore only these two types were used in melting tests. The melting behavior of A and B briquettes was investigated during pilot plant tests with a VIM (Vacuum Induction Melting) furnace using a 10-l crucible, an Ar atmosphere and applying a maximum pressure of 350 mbar during the melting phase to hamper bubble formation in the metal bath. Melting temperatures were measured by both pyrometer and thermocouple. No problems were observed during the melting of type A briquettes while a dense black fume was generated during the melting of type B briquettes. At the end of the trial, carbon residues were detected on the wall, and a pungent smell arose at the opening of the furnace. These phenomena was ascribed to binder reaction in reducing atmosphere. Indeed, type A briquettes contained high contents of metal oxides whose oxygen was consumed by the wheat flour carbon to produce CO/CO_2 while type B briquettes contained mostly not oxidized metal and slag residues thus preventing the oxy-reduction reaction and leading to binder pyrolysis and gasification. In light of this, a new melting test was performed with type B briquettes in air atmosphere for better simulation of EAF conditions and a high metal yield > 90 % was achieved.

After these preliminary tests, a suitable quantity of briquettes for pre-industrial trials was prepared. This phase was fundamental to evaluate the difference between laboratory and pilot plant scale briquettes production. Wheat flour and water content were optimized during briquettes production operations, and some problems were encountered due to the water quantity in the final product. Indeed, the machine showed operative difficulty during the preparation of the first group of briquettes due to the formation of a plastic water-flour-iron residual mixture that blocked part of the machine. Moreover, the briquettes produced were weak, wet and with a high tendency of crumbling and this was ascribed to the excessive content of water in the residual iron used, i.e., H_2O >5 %. Moreover, the importance of a dry environment for briquettes storage was confirmed. The main conclusions on the briquetting process were that an excess of water with contents >3 % caused a weak and crumbling briquettes as well as a content of wheat flour >13 % resulted in a lack of mechanical resistance although it had the function to absorb excess of iron residual water. Briquettes at the exit of the machine needed to be stored in aerated and dry location to promote the drying of the binding agent and the achievement of a material more resistant to traction and flexion.

A minimum number of 15 stainless steel briquettes for each type was produced for the pre-industrial trials which were performed in a 1-ton capacity furnace. Two different trials were conducted to test briquette charging mode into EAF. The first test was carried out by charging briquettes in a preformed bath of scrap using a continuous charge and the second test was performed by charging in batch together a suitable quantity of briquettes and scrap. A Fe yield >90 % was achieved in both cases. Fume analysis in terms of temperature, CO, NO_2, O_2 and dioxins concentration was performed during the experimentation, and some peaks of CO were detected due to the partial oxidation of the carbon within the briquettes. Melting tests allowed also to establish a relation between melting time and chemical composition of iron residues with lower melting time when iron residues were essentially metallic and not oxides. Furthermore, briquettes were able to remain at the interface between slag and steel thanks to their suitable density. Finally, preservation of briquettes characteristics for long time > 3 months was possible if they were properly stored in a dry environment and the leaching of the produced slags respected Italian Law limits for inert materials. From a process management point of view, it was suggested to introduce briquettes together with the second or third bucket to have better melting conditions and optimize Fe recovery. Indeed, briquettes were heavier than the slag so during the charge of the second bucket they went directly in the melted bath. In addition, the second

bucket was added to melted bath at ambient temperature and this procedure avoided dioxins formation during the pre-heating normally performed with the first bucket. A preliminary economical evaluation of the process was performed to estimate the advantages in the internal reuse of Fe residue by means of briquettes preparation. The economical evaluation was favorable with about +130 € for each ton of used iron residues considering only the briquettes production, but it is important to define costs referring to additional energy consumption and slag disposal.

2.2.6 FLEXINJECT: Flexible injection of alternative carbon material into the blast furnace (32)

The project was coordinated by Swerea, with LKAB (Luossavaara-Kiirunavaara Aktiebolag), SSAB, BFI and Voestalpine participating as partners in the consortium. The project started on the 1st of July 2008 and lasted almost three and a half years, ending on the 31st of December 2011. The overall project cost 1.87 M€ and the EU contributed 1.12 M€, i.e., almost 60 % of the budget.

The primary objective of the Flexinject project was to enhance operational flexibility and promote a more sustainable use of carbon resources through an increased exploitation of alternative carbon materials (ACMs). The main idea was to reduce the demand for conventional carbon sources by enabling high injection levels of ACMs. e.g., plastics, dust, and sludges. Furthermore, the return of dust and sludge would allow to increase the efficiency of charged virgin materials since collected and returned off gas dust mainly contained fines of coke and ferrous materials. To achieve these objectives, a novel pre-treatment approach for ACMs was evaluated to make them suitable for BF injection. Various treatment methods for BF flue dust, sludge, and waste plastics were investigated with the aim of improving their transportation behavior and reaching high availability of the injection system necessary for high injection rates. Furthermore, it was essential to understand the effects of ACMs on fluidized bed mixing behavior and pneumatic conveying during BF injection to ensure a successful co-injection with pulverized coal using existing injection equipment, as the physical and flow properties of these materials differ significantly from those of pulverized coal.

The first step in the project concerns the characterization of different ACMs, i.e., BF flue dust, BF sludge, and four different types of plastics, to assess their suitability for BF injection and partial substitution of conventional reductants. Detailed chemical and physical analyses were performed on selected BF flue dusts from different plants, various pulverized coals, plastics, and sludge in combination with Tornado treatment. The characterization included elemental composition, ash content and composition, calorific value, particle size distribution, bulk density, repose angle, moisture content and thermal behavior and aimed to determine the correlation between the fluidization behavior and physical properties of these materials thus providing input data for fluidization, dense-phase conveying, CFD simulation and raceway modelling.

The analysis of pulverized coals reported different properties according to the origin. Pulverized coal from hard coal was characterized by a higher C content around 80 %, a higher fixed C content of 62 %, a lower volatile content of 31 % and a lower moisture content of just 1 % compared to the pulverized coal from lignite characterized by a C content around 57 %, a fixed C content of 38 %, a volatile content of 46 % and a moisture content of 10 %. BF flue dust compositions varied according

to furnace operation, e.g., type of burden used or BF parameters selected, and dust separation method with coarser dust from dust catchers generally containing higher C than finer cyclone dust. Concerning particle sizes, BF flue dust displayed values of d50 ≈ 0.1 mm to 0.2 mm which were higher than pulverized coal ones, i.e., 0.05–0.08 mm. The bulk density of BF flue dust and BF sludge were around 1000 kg/m^3 and was considerably higher than pulverized coal one, i.e., 600 kg/m^3, due to their higher mineral content. Even lower was the density of the four plastics selected with values ranging from 290 to 460 kg/m^3. The repose angles were similar for BF flue dust and pulverized coal but higher for BF sludge due to a higher fraction of fine particles and a higher surface roughness. Thermal analyses of BF flue dust revealed a release of free water at 100–200 °C, a removal of the chemically bound water at 330–450 °C, and endothermic reactions around 800 °C with a a total mass loss of about 40 % at 1200 °C. These results were similar to those of Tornado-treated BF sludge, as will be shown later in the summary, even if Tornado-treated sludge released more water and showed higher total mass loss due to a higher C content. A mixture of 2/3 pulverized coal and 1/3 BF flue dust was also investigated, and it displayed a release of volatiles at 400-600 °C, a mass loss of 76 % at 1200 °C and a limited moisture content exhibiting dominant C conversion behavior.

As largely demonstrated, chemical and physical properties of ACM and pulverized coal differed significantly thus generally leading to the requirement of separate injection systems. Injection of ACM and coal mixtures required careful adjustment of the pneumatic conveying and injection conditions. For example, operational problems such as plugging could occur when plastics were industrially injected, or pipe wearing could occur due to the highly abrasive nature of BF flue dust. To improve handling and injection, a preliminary metallurgical Tornado treatment was selected as potential alternative to other traditional treatment methods such as grinding, agglomeration, fragmentation, screening and drying. It also allowed to overcome the excessive energy intensity of conventional drying systems. Preliminary trials were performed using the Tornado process since this technology allowed to obtain metallurgical sludge with 20–40% moisture at 40 °C and with an energy consumption of 0.7 kWh/kg of evaporated water. The process simultaneously dried, grinded, classified and modified particle shape improving transport and fluidization behavior. The process was based on an air grinder with a high-velocity stream generated by a specially balanced fan delivering 28,000–30,000 Nm^3/h. The mixture of air and material entered a cyclone where rapid changes in velocity and pressure induced strong particle vibrations and disintegration. Fine particles and moisture were removed with the exhaust gas through the top of the cyclone and separated in a baghouse filter, while the treated product was discharged at the bottom. Further improvements could be achieved by preheating the incoming process air exploiting the low-grade waste heat streams below 100 °C available in the metallurgical industry. This waste heat would allow to raise the inlet air temperature to about 50–60 °C thus increasing the moisture absorption capacity of the air and the drying performance. A temperature increase of 10 °C normally enhances the moisture absorption capacity by more than 40 %, making air preheating especially beneficial when processing wet materials with high drying requirements.

Considering this, the effect of Tornado pretreatment on ACMs was investigated and it proved to significantly modify material properties. The automotive shredder residue (ASR), i.e., one of the four plastic types selected, reported an increase in the mass fraction <2.8 mm and a decrease in the coarser fractions from 4 to 6.3 mm. A decrease in the C content of the fraction <2.8 mm from 50.1 % to 46.1

% was observed as a consequence of the Tornado treatment with a consequent decrease in the net calorific value from 29.9 to 26.4 MJ/kg. The overall carbon content decreased from 63.79 % to 57.01 % as well as the net calorific value from 29940 to 26410 kJ/kg while the ash content increased from 17 to 23 % and heavy metals and tramp elements remained largely unchanged. For BF sludge and the related mixtures with pulverized coal and flue dust, the Tornado treatment proved to be effective in drying the material as well as in comminuting and classifying the material concentrating particles <10 µm in the filter dust. Furthermore, Tornado-treated improved the handling properties of both BF sludge and flue dust making their sharp-edged smoother and more uniform thus reducing abrasiveness.

The next phase of the study focused on the determination of the limits for ACM addition to pulverized coal and on assessing the influence of ACM type and concentration on the fluidization behavior of the resulting mixtures. Laboratory scale fluidization tests were performed using a pressurized fluidized bed mixer to evaluate the mixing stability and homogeneity under conditions representative of BF injection systems. Fluidization experiments were carried out on both individual ACMs, i.e., BF flue dust and Tornado-treated BF sludge, and mixtures with pulverized coal at gauge pressures of 5 bar. Minimum fluidization conditions were determined experimentally using pressure-drop and bed-expansion measurements. The fluidization velocity for all materials fall within a narrow range of 0.017 to 0.027 m/s and was higher than theoretically predicted values probably due to the formation of gas drains within the bed. Overall, the experiments did not show a correlation between fluidization velocity and the physical properties of the investigated BF flue dust, BF sludge, and pulverized coal. Mixtures with a pulverized coal/BF flue dust ratios up to 3:1 were tested and demonstrated stable fluidization and homogeneous mixing with no evidence of segregation across the bed height. This was confirmed by the C-content analysis. The results showed that fluidization was an effective method to homogenize ACM and pulverized coal mixtures for BF injection and no operational limits were identified for ACM addition up to 25 %. For practical application, a minimum fluidization velocity of 0.03 m/s was recommended to ensure stable operation and consistent mass flow in industrial injection systems.

The influence of Tornado process conditions on the treatment of ACMs for BF injection was further investigated with the main objective of identifying suitable operating parameters to upgrade the selected ACMs. The experimental included a one-week campaign at the large-scale plant Airgrinder in Skelleftehamn (Sweden) where ASR, BF sludge and two mixtures, i.e., 70% BF sludge with 30% pulverized coal and 70% BF sludge with 30% BF flue dust, were tested which was accompanied by additional pilot-scale trials at Swerea on BF sludge for EBF tests and ASR with intermediate wet fraction. The mixtures selected were the result of a laboratory campaign performed to define the optimal mixing ratios to reduce stickiness and improve handling properties. Indeed, excessively sticky materials impaired reactor flow promoting wall adhesion and reducing vacuum efficiency therefore the desired properties were a dry material with granular surface to enable stable feeding and efficient dispersion within the Tornado reactor. Process conditions were adjusted for each material with particular emphasis on damper setting to control the airflow and the balance between the product and the filter dust. Indeed, the damper gap represented a compromise between drying efficiency and product yield since a larger gap increased airflow and moisture removal but also raised filter dust generation. For BF sludge, an optimal damper setting of 100 mm cone lift was identified and used while process air temperature remained stable between 50 and 60 °C.

A reference test with pure BF sludge was performed to provide reference feed rate, product moisture content and product/filter dust distribution. Approximately 900 kg of wet material were treated with a capacity slightly below 400 kg/h and the resulting distribution of product and filter dust was about 60% and 40%, respectively. Material balance discrepancies were mainly attributed to a moisture content higher than expected material adhesion to reactor walls, and retention in the filter system. A special material handling technology for BF sludge was developed consisting of a feeding screw with the outlet end modified to extruder-type. Mixing BF sludge with other additives allowed to improve process performance. A mixture of 70 % BF sludge and 30 % pulverized coal ensured higher throughput, lower feed moisture, and improved product yield, i.e., 65 % product and 35 % filter dust. The use of the mixture of 70 % BF sludge and 30 % BF flue dust led to a higher moisture content in the product and caused increased wall adhesion resulting in a 55% product and 45% filter dust distribution. ASR trials demonstrated good drying performance with high product yield of 83 %, but some feeding limitations were observed with wet plastic fluff. Indeed, the plastic fluff tended to get stuck in the funnel above the cell feeder for increasing feeding rate thus causing interruptions in the process. This problem started to occur at a feeding rate of about 120kg/hour. Energy consumption of the Tornado process, excluding feeding, was about 150 kW with an airflow of 13,000 m^3/h, corresponding to approximately 3.5 kWh per kilogram of water removed under the tested conditions. The Tornado process proved effective for drying fine, moisture-rich materials such as BF sludge and plastics. The main treatment effect was moisture removal, and drying efficiency could be further enhanced by increasing air temperature.

After this step, technical scale material processing and handling trials were conducted to define suitable conditions for continuous pneumatic conveying of ACMs and their mixtures with BF injection coal to ensure high solid loading ratio and low conveying velocity. A modified dense phase conveying system was operated in both dilute- and dense-phase modes, enabling systematic evaluation of conveying behavior, mixture stability, and wear under conditions representative of industrial injection systems. Initial trials focused on optimizing plant configuration, including nozzle size, conveying line diameter, and operating mode. Preliminary dilute-phase tests were performed to simulate the conditions of the EBF injection system. These tests confirmed stable and continuous conveying of pulverized coal/ACM mixtures at constant mass flow without clogging or segregation. Carbon content analyses of samples taken during conveying showed that mixture homogeneity was maintained throughout fluidization and transport. Subsequent dense-phase trials targeted industrially relevant mass flows of approximately 500 kg/h corresponding to a single BF tuyere. Conveying lines with an inner diameter of 19 mm were used, and solids loading ratios above 30 kg/kg N_2 were achieved for all tested materials. Mixtures of pulverized coal with BF flue dust or Tornado-treated BF sludge were conveyed reliably at solids loading ratios up to about 100 kg/kg N_2 at gas velocities around 12 m/s. Pure BF flue dust reached even higher loading ratios due to the higher bulk density. These results demonstrate that high-load, low-velocity conveying was feasible, allowing to reduce conveying gas consumption. Conveying lines and critical components must be equipped with highly wear-resistant materials to ensure reliable plant operation. Indeed, materials with a Vickers hardness above 600 HV were adequate for standard pulverized coal transport, but hardness above 1000 HV were necessary for bends and high-stress sections handling BF flue dust. For high-rate transport of very abrasive solids, cast basalt, corundum, Al_2O_3, or SiC ceramics were typically used with Al_2O_3-based ceramics normally outperforming the others thus making them ideal for heavily loaded sections. This was confirmed by abrasion tests where Al_2O_3 ceramics sustained

virtually no damage, whereas cast basalt and Zr corundum suffered significant surface wear under intensified abrasion with BF flue dust thus emphasizing the importance of selecting appropriate lining materials for long-term reliability.

Another key objective of the study was to investigate the industrial injection of ACMs. A first step in this analysis consisted in the introduction and evaluation of advanced measurement techniques for BF raceway to improve understanding of injection related phenomena during ACM use since they were expected to replace up to 15 % of the total reducing agents. The understanding of their impact on raceway conditions and overall BF operation was fundamental to ensure reliable monitoring of raceway temperature and depth essential. To this aim, a fiber-optic–based system for temperature measurement was developed and adapted for BF application. The radiant emission from the raceway was guided through fiber optics to spectrometers for spectral analysis. Early laboratory calibration using heated tungsten foils demonstrated that assuming constant emissivity over a wide wavelength range led to significant temperature uncertainty and the raceway measurements performed in LKAB BF confirmed that accurate temperature evaluation required a careful selection of narrow wavelength intervals, compensation for wavelength-dependent detector efficiency, and exclusion of alkali emission peaks. Adequate nitrogen cooling and purging of the optical fibers was essential to prevent thermal damage and ensure stable signal quality in the harsh raceway environment. Measured raceway temperatures were consistently lower during pulverized coal injection or mixed pulverized coal/BF flue dust injection due to several physical effects, including heating of injected cold materials, volatilization of injected carbonaceous matter, endothermic reactions such as iron oxide reduction and carbonate decomposition, and changes in the extent and location of oxidation and reduction zones within the raceway. A less pronounced oxidation zone prior to the onset of the Boudouard reaction contributed to lower local temperatures. Raceway depth measurements were also performed at SSAB using a microwave radar-based system operating at a nominal frequency of 10 GHz and a wavelength of 0.03 m. The instrument was normally not susceptible to dust and smoke and thus not the injection of coal and residues. The measurements showed that raceway depth variations were primarily driven by changes in blast pressure and temperature in the hot stove cycles since short-term reductions in raceway depth were observed toward the end of hot stove cycles as blast temperature and pressure decreased.

Once identified the measurement techniques for BF runaway, the effects of ACMs injection on raceway conditions in LKAB BF were investigated. In particular, BF flue dust and ACMs treated by the Tornado process both alone and mixed with pulverized coal were considered and the effect of their injection on raceway temperature, coke conversion rate, tramp elements accumulation etc. under conditions representative of industrial operation were assessed. Raceway conditions were examined through core-drilling campaigns conducted before and after operational trials. One reference core was taken after conventional pulverized coal injection operation, while a second core was collected after injection of a mixture corresponding to 110 kg pulverized coal and 40 kg BF flue dust per tonne hot metal. This injection level reflected the specific tuyere rates used at the full-scale BF at SSAB where ACM is injected at alternating tuyeres. Macroscopic and granulometric analyses of the raceway cores showed clear differences between the two injection modes. Injection of pulverized coal alone resulted in increased coke disintegration, higher amounts of fine material, and a significant presence of rounded metallic droplets, particularly in the early raceway region. In contrast, injection of pulverized coal mixed with BF flue dust led to a higher proportion of coarse coke particles with sharper edges, more evenly distributed along the raceway length, and a reduced amount of fines below 1 mm. Chemical analyses

revealed higher bulk densities and elevated metallic content in the pulverized coal injection core due to the abundance of fine metallic droplets. In the mixed pulverized coal /ACM core, injected iron oxide from BF flue dust was shown to be substantially reduced within the raceway, although residual wüstite was still present in the early raceway region. The presence of residual FeO may contribute positively to slag fluidity and melting behavior at the tuyere level. Alkali and Zn contents were notably higher in the beginning of the raceway after PC/ACM injection, suggesting incomplete reaction of injected dust or accumulation due to lower temperatures and oxidation–condensation phenomena. These findings highlight potential operational limitations at higher ACM injection rates related to pressure drop, scaffold formation, and tramp element accumulation. XRD analyses of coke and fines supported the chemical and macroscopic findings. Indeed, the graphitization degree of coke was significantly higher after pulverized coal injection, particularly in the first part of the raceway, thus indicating higher historical temperatures. In contrast, coke from the mixed pulverized coal/ACM core exhibited lower graphitization degrees in the initial raceway region, with temperatures increasing further downstream. Estimated raceway temperatures based on calibrated laboratory heat-treatment experiments ranged from approximately 1920–2085°C for pulverized coal and 1750–1965°C for pulverized coal/ACM thus confirming that flue dust injection delays ignition and lowers the initial flame temperature due to reduced volatile content and energy-consuming reactions.

The next step of the project concerned the evaluation of the technical feasibility of partially substituting pulverized coal with ACMs at high injection rates by performing coordinated trials at LKAB experimental BF and industrial scale trials at SSAB. The trials at SSAB focused on injection of BF flue dust and pulverized coal in separate lances at moderate amounts and the approximate injection rates corresponded to recycling of BF flue dust produced in a BF to the same BF. At LKAB ACMs, i.e., Tornado treated sludge and BF flue dust, were premixed with pulverized coal and were injected at four levels from 20 to 60 kg/t hot metal per tuyere. The trial started with a reference period using pulverized coal only at 150 kg/t hot metal, after that 20 kg of pulverized coal was replaced with Tornado treated sludge and by 20 kg/t hot metal of BF flue dust. In the following periods BF flue dust was then increased in steps from 20 to 60 kg/t hot metal. The expected C-content of the mixture was estimated in advance based on chemical compositions and the ratios of each material to be included in the mix. Samples taken from the coal injection line were analyzed and showed that BF flue dust closely matched expected values, while Tornado sludge exhibited significant deviations due to the high bulk density resulting from the high content of iron oxide and the fine particle size which resulted in segregation phenomena occurring in storage and transportation with pulverized coal. This resulted in a lower C input and a slightly reduced thermal level in the furnace. Another issue arose from a material moisture content higher than expected. Overall, the results demonstrate that carbon contained in injected BF flue dust effectively replaces carbon from pulverized coal and coke at a ratio close to 1:1. For extended test periods, the total carbon rate was comparable to the reference operation without ACM. These findings indicate high energy efficiency of BF flue dust carbon, comparable to conventional reducing agents. However, due to limited residence time in the raceway and the relatively low reactivity of coke fines, there is a potential risk of fine carbon accumulation above the raceway at higher injection levels. Based on the trials, injection rates up to approximately 40 kg/tHM were feasible, although long-term operation is required to fully assess accumulation effects. The utilization efficiency of Tornado-treated BF sludge was less certain. Lower carbon content, higher moisture uptake during storage, and segregation during handling led to reduced effective carbon input and temporary low heat levels. The carbon in BF sludge also differed in quality compared to BF flue dust, with higher moisture, volatile

release, and limestone decomposition consuming additional energy. These factors contributed to a lower apparent carbon efficiency during the trials.

Industrial-scale pneumatic conveying trials were performed at AMEh and confirmed that pulverized coal/BF flue dust mixtures (4:1 ratio, total 7.5 t/h) could be transported without segregation or clogging, validating conditions determined in technical-scale trials. The use of separate injection systems minimized the risk of abrasion and allowed reliable transport of highly abrasive BF flue dust. Overall, the injection of 15–20 kg/tHM per tuyere had no adverse short-term effects on the BF process, while higher BF injection rates (40–60 kg/tHM) caused moderate increases in pressure drop and alkali accumulation. The trials demonstrated that technical fluidization and conveying results can be transferred to industrial scale, enabling reliable, low-velocity, high-loading transport, reduced energy and gas consumption, minimal wear, and cost-effective recycling of BF flue dust. Long-term operation requires targeted wear protection at critical positions in the injection system to ensure consistent performance and durability.

Based on the extensive technical-scale and industrial trials, a set of practical rules for stable and reliable conveying and injection of pulverized coal/ACM mixtures was established and validated for BF operation. The main purpose of the guidelines was the identification of the relevant parameters for processing and handling and defining threshold values applicable to typical BF injection systems. Uniform dense-phase conveying without clogging was identified as a key requirement for high injection plant availability. This required the exclusive use of dry conveying gas and nitrogen for inertisation, fluidization, and conveying. All storage bins, pressure vessels, and conveying lines must be purged with nitrogen prior to start-up after downtime. Stable BF operation further depends on supplying the injection system with a homogeneous mixture. Controlled feeding using rotary feeders was shown to be essential, as screw feeders do not provide sufficient dosing accuracy. Technical-scale trials demonstrated that homogeneous mixtures were formed in the fluidized bed of the pressure vessels and that subsequent pneumatic transport occurs without segregation. These results were confirmed during industrial trials. Low energy consumption and reduced wear were achieved by operating under dense-phase conditions with high solids loading ratios and low conveying velocities. Stable conveying was demonstrated at solids loading ratios of up to 100 kg/kg N_2 with gas velocities around 12 m/s. Because wear increases strongly with velocity, with a doubling of velocity leading to approximately sixfold higher wear, dense-phase operation at low velocities was critical. For an expected conveying capacity of about 500 kg/h per tuyere, corresponding to approximately 150 kg/t hot metal and BF flue dust contents of up to 50%, conveying line diameters of 18–20 mm were recommended. Under these conditions, stable operation was achieved at a conveying velocity of about 12 m/s and solids loading ratio of approximately 35 kg/kg N_2, with good results confirmed in industrial practice. Abrasion testing showed that ceramics based on Al_2O_3 were particularly suitable for wear protection when conveying abrasive materials such as BF flue dust. All bends in the conveying system should be lined with Al_2O_3-based ceramics, and straight pipe sections of approximately 2 m downstream of each bend should also be protected to account for erosion caused by particle deflection.

2.2.7 GREENEAF: Sustainable Electric steel production (33)

The project was coordinated by Ferriere Nord with CSM, while Tecnocentro, Imperial College, RWTH, Deutsche Edelstahlwerke (DEW), Stahl- und Walzwerk Marienhütte participated as partners in the consortium. The project started on the 1st of July 2009 and lasted almost three years, ending on

the 30th of June 2012. The overall project cost 2.11 M€ and the EU contributed 1.27 M€, i.e., almost 60 % of the budget.

In modern EAF, more than 40 % of the energy was from chemical sources based on fossil fuels with natural gas being used in dedicated burner during scrap melting while lump coal mainly in the form of anthracite were inserted in the basket or pulverized and used through wall injector as foaming agent. The main goal of the GREENEAF project was to increase EAF process environmental sustainability by replacing coal with char and natural gas with syngas produced by biomass pyrolysis. In particular, char was both injected as powder and charged into the basket while syngas was planned to be used in EAF burners. The project was divided into different steps, and the first one concerned the selection and classification of the biomasses according to their origin as well as their characterization. After that, biomasses pyrolysis was optimized at laboratory scale to identify pyrolysis kinetics and obtain sufficient knowledge to design the subsequent industrial pyrolysis. This part of the activity was supported by chemical and physical analysis of the char produced to define the best pyrolysis plant process parameters being sure that the characteristics of char and biogas were matched EAF requirements. Based on these results about 15 tons of char were produced for both EAF pilot plant experimentation and industrial trials. Finally, the use of syngas produced by biomass pyrolysis in EAF burner was investigated by calculation based on Computational Fluid Dynamics (CFD) due to the difficulty of having syngas available close to the EAF steel plant.

The analysis of biomass availability was performed considering the proximity to the steel plant of Ferriere Nord (Italy), DEW (Germany) and MH (Austria). In general, biomass was collected from agricultural residues, forest residues, and wood industry or can be cultivated either. In the framework of the GREENEAF project the biomass species selected for characterization activities were forest residues including ligneous species such as saw dust for pellets or pulp, grape wine and corn stalk as agricultural residues and mischantus and sorghum as biomass from cultivation. Samples of these biomasses were subjected to a physio-chemical characterization to identify the chemical composition, the ash content, composition and properties and the heating value. Furthermore, thermogravimetric tests were performed. The selected biomasses displayed similar elemental analysis in terms of C/H/O content with C values between 44 and 51 %, H values between 5.4 and 7.3 % and O values between 38 and 44 %. Analogously, similar volatile matter content between 76 and 82 % and comparable heating values around 18500 kJ/kg were observed. The main differences were observed in minor elements such as N, S and Cl and in ash content with values ranging from 0.8 % in wood to 6.8 % in sorghum.

After this preliminary characterization, biomass pyrolysis was tailored and optimized investigating the influence of different parameters such as temperature, residence time, heating rate, material size and atmosphere on char and biogas yields and quality. Char and syngas yield, char chemical composition, porosity, low heating value (LHV) and reactivity and syngas composition and heating value. A comparison of char reactivity with coal reactivity was also performed. The tests were performed in a thermobalance to follow weight variation as a function of time and temperature using also different atmosphere and low heating rates around 1-20 °C/min, but also in a Wire Mash Reactor to achieve higher heating rates. The results proved that biomass initial particle size did not affect the general yield of char, tar and syngas. Furthermore, char yield was almost stable after 500 °C independently on the

biomass type after experiencing an initial drop. Also tar and gas yield proved to be stable after 500 °C independently on the biomass. The chemical and physical properties of the char obtained after testing four biomasses at 500 °C for 700 s are summarized in Table 9. Char porosity and density were affected by operating temperature test with increasing porosity and decreasing density obtained for increasing temperatures. Typical values of coal density were 2-3 times higher than the low-density values observed for all char and this may cause problems during injection since large dispersion of char particles may occur into fumes instead of penetrating into steel bath. Char heating value proved to be lower than coal one, but in any case, comparable. Among the different types of char the one with highest heating value was the one produced from forest residues. It was also observed that LHV showed increasing trend with increasing temperature of pyrolysis. Syngas composition was also determined by connecting a mass spectrometer to the equipment and the resulting chemical composition is reported in Table 10 for mischantus treated at different temperatures. Contrary to char, the LHV of syngas proved to decrease for increasing pyrolysis temperature therefore process conditions can be optimized to have higher LHV for char or syngas. If both products were required a good compromise was obtained at temperature of 500°C. The reactivity of the chars was also assessed through TGA and the chars produced at higher temperatures presented lower reactivities. Marked differences were observed between the behavior of the 300 °C char characterized by a high volatile content and that of the chars produced between 325-450 °C. There were as well significant differences between the latter and those generated at 500-600 °C which presented the same reactivity among themselves. Furthermore, a progressive increase in the amount of fixed carbon in the chars was observed for increasing pyrolysis temperature thanks to proximate analysis.

Table 9: Chemical and physical properties of the char produced after test at 500°C for 700s of the four biomasses

	Corn	Grape wine	Forest Residues	Mischanthus
C %	70	70-81	75	73
H %	2	2	3	2
N %	1.8	2	0.3	1.2
S %	0.2	0.2-0.9	0	0.1
P %	-	0.48	-	-
Ash %	23	10-16	3	10
LHV (kJ/kg)	23000	23000	27000	25000
Density (kg/m^3)	280	270	300	270

Table 10: Composition (%) and LHV of the syngas produced as a function of temperature, for mischantus

	C_2H_6	C_3H_8	CH_4	CO	CO_2	H_2	Calc. LHV MJ/Nm^3
400 °C	10	10	21	21	23	15	27
500 °C	9	9	19	24	21	17	26
600 °C	9	8	17	27	19	20	24

Overall, 500 °C proved to be a good compromise for pyrolysis temperature and validation of these results was performed by Tecnocentro which designed a small-scale demonstrative pyrolysis plant composed of a horizontal electric furnace working in nitrogen atmosphere. The tests were performed with ligneous biomass and agricultural residues. Char, tar and gas percentage produced after different pyrolysis campaigns, were measured to study their characteristics by varying process parameters to define and confirm the best operative conditions. In particular, the effects of the main process parameters, e.g., heating rate, treatment time, rotation speed of pyrolysis reactor were considered. For example, the continuous rotating movement of the reactor contributed to the degradation of biomass into powder. The demonstrative pyrolysis plant consisted of a pyrolysis reactor, a gas cleaning system and a microturbine and could be fed with 200 kg/h of fuel while the necessary heat energy for pyrolysis was supplied by a gas burner with a maximum power of 500 kW. During the tests, the pyro gas was burnt in the torch and sampled, the tar which accounted for 7-11 % of the biomass was eliminated from the gas in the treatment section and collected in the tank with cooling and washing water. Finally, the char was conveyed by a screw and discharged from the reactor at 500 ° C and the yields was sampled, weighed and analyzed for each test to highlight the correlation between product characteristics and process parameters. The main pyrolysis parameters monitored were pyrolysis temperature through optical pyrometer, gas temperature and pressure out from the reactor, internal reactor pressure, rotation speed of the reactor and therefore residence time, feeding speed varying the rate of the feeding metering screw, chemical and physical properties of the feeding fuel and chemical and physical characteristics of the char and gas obtained. The main pyrolysis parameters vaired during the campaign were pyrolysis temperatures with values of 450°C, 550°C, 650°C and residence time with values of 30, 40, 50 minutes. The gas product was typically a mixture of CO_2 (9-55 vol.%), CO (16-51 vol.%), H_2 (2-43 vol.%), CH_4 (4-11vol.%) and small amounts of higher hydrocarbons. Char composition proved to be affected by temperature with higher temperatures ensuring higher C contents both total- and fixed- but leading to lower char yield. Feedstock humidity was another paramount parameter to control for optimizing process efficiency because higher levels increased the heat necessary for pyrolysis of the biomass since a part was for evaporating the water in the fuel. For good process performances, fuel moisture contents of 15-20 % were typical.

The next step of the project concerned the definition of EAF operating practices and preliminary laboratory tests were carried out to have a first evaluation of char foaming behavior compared to coal one using slag sampled from the DEW EAF right before slag foaming. Slag foaming was performed into an alumina crucible filled with a mixture of pulverized charcoal from Tecnocentro or coal and put into a furnace at 1600 °C. In this way, the increasing volume of the foaming slag was freezed onto the inner crucible wall up to a height indicative of the maximum volume increase during the trial. The achieved volume increases showed the general suitability of char for slag foaming. Similar experiments were performed with MH EAF slag using again charcoal from Tecnocentro compared with petroleum coke. The investigation was performed with sessile drop test whose results are shown in Figure 8. The first picture of each row shows the melting beginning of the slag at about 1300 °C and the subsequent formation of a spherical shape due to the no wettable nature of carbon. The next pictures show the reaction of FeO in the liquid slag with the C of the substrate with increasing temperature. The intensity of the reaction differs depending on the type of carbonaceous material which results in varying CO bubble formation and therefore slag foaming. Petroleum coke formed very rapidly a foamed slag due to a fast slag-carbon-reaction which remained stable for a long time period. The charcoal from Tecnocentro allowed to obtain only slight foaming at the beginning which also collapsed faster.

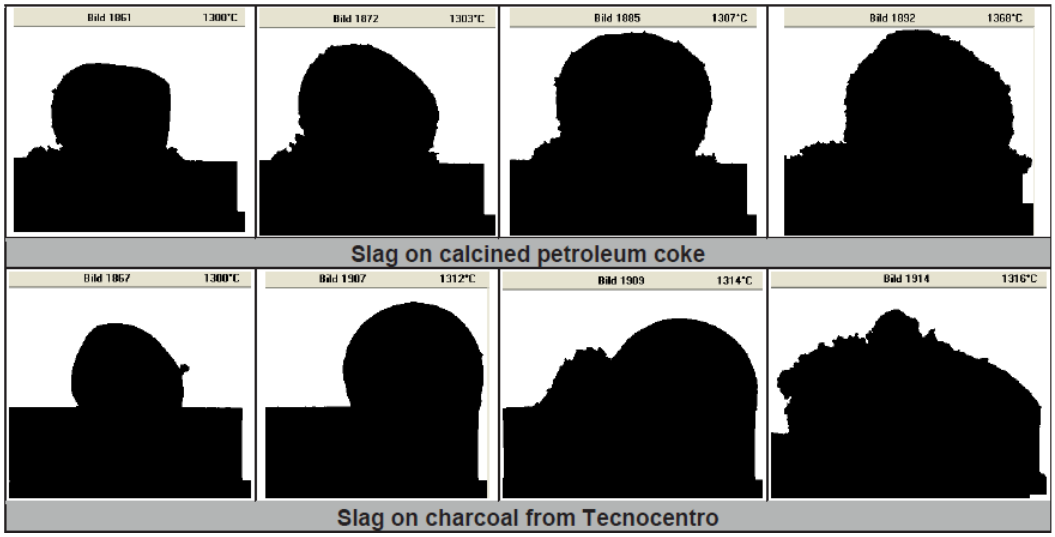

Figure 8: Sequence of the slag-carbon-reaction with different carbonaceous materials as a function of temperature.

After the preliminary laboratory scale tests, pilot plant tests were performed at RWTH investigating the slag foaming capability of the charcoal delivered by Tecnocentro and comparing it to conventionally used fossil coals. Actually, a second type of biochar, i.e., biochar from wood gasification, was tested in the pilot plant both as charge and as injection. Anthracite coal and petrol coke were used as reference materials. The reference trials used 1 kg of anthracite coal and 50 kg of scrap while 1.6 kg of charcoal from Tecnocentro and from wood gasification plants were charged to compensate for their lower heating value. A melt sample was taken for chemical analysis just before tapping at 1650 °C to obtain information about possible negative effects of biochar use. No negative effects regarding steel and slag analysis were detected. Some differences were detected in terms of Ni and Mn content, but they were mainly ascribed to fluctuations in scrap composition rather than to pollution from the char. The reference trial also showed a higher C content in the steel bath than the two biochar trials thus implying a better carburization of the melt by anthracite. Considering the S content in the steel, lower contents were obtained with the biochar compared to the reference materials, i.e., about half S content. Despite the higher P concentration in the biochar, the P content in the steel was the same for all trials. In conclusion, the use of biochar instead of fossil coal did not show any negative impact on steel composition as well as on slag composition which was not affected by the higher ash content.

Once legitimated the use of biochar at the pilot scale, its feasibility was tested on an industrial scale by the performing the tests at the EAF of the three industrial partners, i.e., Ferriere Nord (FENO), DEW and MH. The EAFs of the three partners differed significantly in terms of size, capacity, and amount of chemical energy and their main characteristics are summarized in Table 11. Char industrial testing with these three furnaces allowed to exploit a wide range of operational variability assessing both charging and injection. Indeed, FENO used coal charged for bath carburization and injected for foaming, DEW used coal mainly for bath carburization and it was manly charged with injection occurring only in small amounts and MH used coal only for foaming therefore coal was only injected. Substitution of charged coal with char was tested at FENO and DEW to carburize the steel bath and to substitute electrical energy by chemical energy when oxygen was used to decarburize the melt and C was burned to CO and CO_2. The substitution trials at FENO highlighted the fine nature of char as the main difficulty in

charging since it resulted in a very high reactivity. Significant powder dispersions were noticed during handling and charging operations as well as intense flame emissions were observed during trials with char. This problem was solved by performing preliminary material briquetting with 90 % char, 5 % flour, and 5 % bentonite. New industrial tests were performed with charcoal briquettes and no modification in steel and slag characteristics nor in process parameters were observed as well as the intense flame emissions during char charge in bucket disappeared. Similar trials were performed at DEW and again a rapid combustion of the biochar fines was observed. Considering this, it was only possible to replace partially the 1320 kg of anthracite with biochar fines, i.e., 800 kg anthracite and 720 kg biochar from wood gasification. The average of steel and slag chemical composition from five heats charged with char were compared with the average of five standard heats and the results obtained are shown in Figure 9. No significant differences for both steel and slag were observed for standard and biochar trials.

Table 11: Main characteristics of the EAFs of the industrial partners participating to the project

	FENO	DEW	MH
Charge weight (TLS)	140	130	40
N° buckets/heat	3	2	3
Electrical energy input [kWh/TLS]	341	417.2	375
CH_4 [Nm^3/TLS]	6	0	7
O_2 [Nm^3/TLS]	42	21.8	45
Coal lump [kg/TLS]	4	10.7	0
Injected Coal [kg/TLS]	8	1.53	12
Power on [min]	38	54	31
Tap to tap [min]	45	69	45

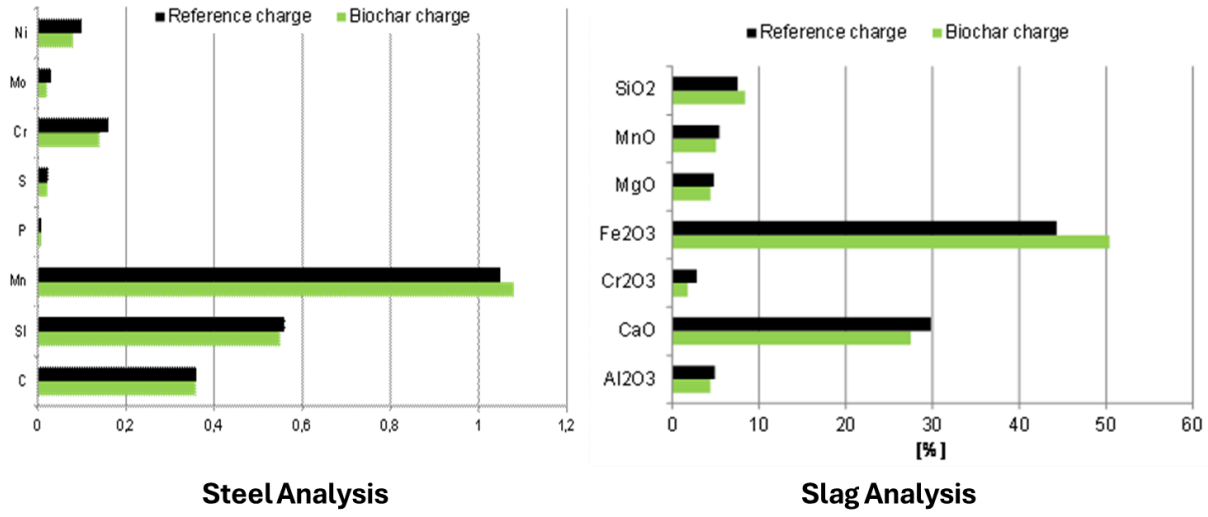

Figure 9: Comparison of steel and slag analysis of standard and biochar charges measured at DEW

After injection trials, foaming trials were performed by all three industrial partners since slag foaming was a very complex equilibria depending on slag properties, e.g., viscosity and surface tension, amount of injected coal which affected the amount of gas necessary to promote foaming and coal reactivity. In light of this, both the energetic input and the foaming behavior were considered for industrial testing of char. The test performed at FENO employed 500 kg of char with a mass flow rate of 12-16 kg/min. The first results showed that the injected char could not penetrate efficiently inside the slag therefore two possible solutions were proposed, i.e., injection below the slag level and use of a double jet to improve with one lance for oxygen and one lance for pulverized char with a gas carrier. The trials at DEW with wood from gasification were performed after installing a secondary coal injection system and proved to be successful with a satisfying foaming, without any negative effect on both slag composition and basicity. Environmental monitoring at stack was carried out both by FENO and DEW and confirmed that char did not introduce any modification respect the historical plant trends. Finally, the foaming tests performed at Marienhütte were developed together with Vatron to improve process control by using an Optical Foaming Slag Management System (OFSM). Slag height was continuously monitored by a camera placed close to the slag door and a special image processing software calculated the slag index to be used for the injection of the C amount required. Indeed, the real-time monitoring of the slag level allowed to adjust the C-contents by injection of the optimal quantity of carbon. The result of charcoal injection showed that charcoal could not cause any foaming of the slag probably due to a low wettability by the liquid slag which prevented a reaction of its C with the FeO of the slag to form enough CO bubbles. Furthermore, the low bulk density of charcoal bore a risk of floating on the slag thus reducing its penetration. Only moist charcoal was able to induce the formation of an acceptable slag foaming since the water vapor at temperatures >1500 °C resulted in the formation of high quantities of gas due to the water-shift equilibrium. Of course, this effect was not accompanied by any reducing of FeO and this was of course undesirable. Furthermore, high humidity in combination with liquid metal and/or slag had the high risk of explosive gas formation.

The last step of the project concerned the potential use of syngas in EAF burners which were simulated through CFD modeling due to the difficulty to produce syngas close to the steel plant for industrial trials. Considering the complexity of syngas composition, the simulation was carried out defining a quantitative criterion to compare natural gas burning with syngas burning. A bidimensional domain with a diameter of 250 cm and a length 600 cm surrounded on three sides by the furnace atmosphere at temperature of 1100 °C was set. The composition of the atmosphere was taken from the off-gas analysis system of FENO while the composition of the syngas was measured during industrial char production. The criteria selected to compare natural gas and syngas burning was the efficiency defined as the ratio of the kW provided to the scrap and the kW provided from the burner. The results of flames temperatures with natural gas and syngas as well as the efficiency of the burners are reported in Figure 10. Natural gas and syngas flames were characterized by different shapes as well as by different temperatures with the syngas flame being characterized by a lower temperature than natural gas. This is also reflected in a lower burner efficiency of 8-15 %. The following actions were proposed to recover the gap of efficiency namely increase the amount of CH_4 in the mix, increase burner size and syngas flow rate or modify burner geometry to increase combustion efficiency. In light of this the design of new burner was simulated and an increase in efficiency of about 10 % was achieved.

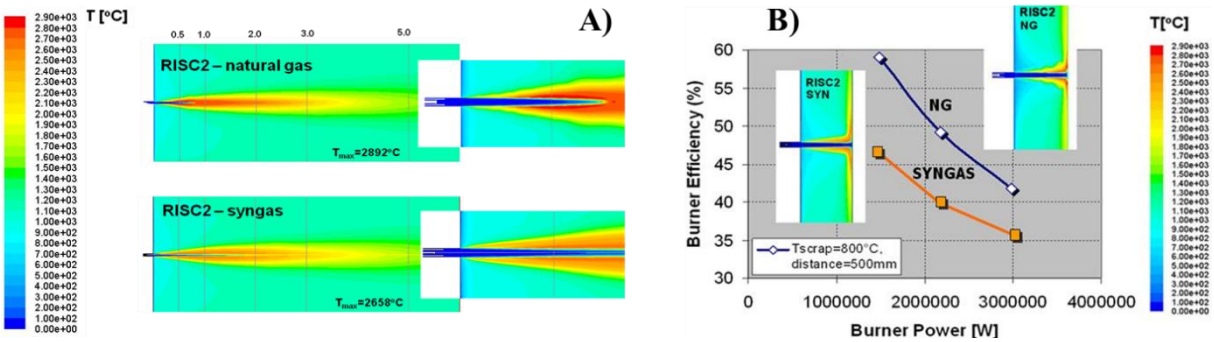

Figure 10: Calculated flame temperature for natural gas and syngas burning (A) and comparison of efficiency between syngas and natural gas (B).

The overall objective of the project was to assess the partial or total substitution of coal and natural gas with charcoal and syngas produced from biomass pyrolysis. The characteristics of the char and syngas and the related pyrolysis process were tailored to match the requirements for their utilization in EAF. The tests performed both at the pilot and the industrial scale showed that coal could be replaced by char both in charging and injection to promote foaming. In case of charging, char reactivity should be considered to avoid burning during charging. Considering that this aspect was strongly dependent on surface area, volatile content and powders dispersion, a briquetting pre-treatment was proposed as solution. Concerning injection, some trials showed good foaming behavior while others were not satisfactory, and the solutions proposed were an improvement of the injection system to ensure char injection below the slag as well as the utilization of additives to increase char/slag wettability and promote reaction of char with iron oxide.

2.2.8 SLASORB: Using slag as sorbent to remove phosphorus from wastewater (34)

The project was coordinated by the Département Systèmes Energétiques et Environnement of Armines with Epur Nature SARL, FEhS, AKUT Umweltschutz Ingenieure Burkard und Partner, ArGe Arbeitsgemeinschaft Hüttenkalk, and ArcelorMittal participating as partners in the consortium. The project started on the 1st of July 2009 and lasted approximately three and a half years, ending on the 31st of December 2012 after a six-month extension. The overall project cost 1.26 M€ and the EU contributed 632 k€, i.e., almost half of the budget.

Considering the EU legislation on phosphorus discharged into the surrounding environment including the Water Framework Directive [2000/60/EEC], it was evident that additional filter systems filled with reactive materials such as sand filters, constructed wetlands or waste stabilization ponds represented a valuable solution to remove P in small wastewater treatment plants (WWTPs) with a capacity of less than 2000 People Equivalent (p.e.). The main objective of the SLASORB project was to demonstrate the use of iron and steel slag as a sorbent material for P removal from wastewater. The project was structured in three main phases with the first phase devoted to the selection of relevant slag types available in Europe and the design of demonstration-scale slag filters. The second focused on the construction and operation of two demonstration-scale filter systems, one in France and one in

Germany, to assess the technical feasibility of P removal under real conditions. The third and last part addressed the economic feasibility including the potential of recycling P-saturated slag as fertilizer and the market analysis comparing slag filters with conventional coagulation-flocculation technologies.

European iron and steel industry produces a large number of slag qualities therefore the first step of the project concerned slag characterization and selection. Slag samples were collected from ten different steel production sites in four countries, i.e., France, Luxembourg, Germany and Spain, with 7 slags generated in BOF and 3 in EAF. Several analyses were performed including XRF for chemical composition, inductively coupled plasma optical emission spectroscopy (ICP-OES) for trace elements, and batch isotherms to estimate maximum P removal under static conditions. The main component of BOF-slag was CaO with values around 46–60 % while the main component of EAF-slag was Fe_2O_3 with values around 28–51 %. Availability as coarse aggregates, assured future availability on the market, comparably high concentration of CaO in the solid slag, comparably high concentration of total Fe, comparably high release of Ca^{2+} ions in aqueous solutions, and comparably low concentration of other components with environmental relevance were identified as key parameters for the selection of suitable slag qualities with respect to efficient P removal from wastewater. Based on these criteria, several slag types were excluded from further consideration. For example, granulated BF slag had a strong market position in the cement industry and was available only in grain sizes below 5 mm while air-cooled BF slag might become a scarce raw material due to its strong market value in road construction, and its CaO and Fe concentrations were low compared to BOF- and EAF-slag. Table 12 presents the selection criteria established for slag to be used in P removal.

Table 12: Main parameters for selecting slag for P removal in wastewater.

Parameter	Test method	EAF threshold	BOF threshold
Particle size	mm	5-40 (optimal 15)	5-40 (optimal 15)
Volume increase	Stem test EN 1744-1	< 5 % (opt. < 2 %)	< 5 % (opt. < 2 %)
P removal capacity	Batch test 7 days (Pin 10 mgP/L)	> 0.10 (opt. 0.20) mgP/g slag	> 0.10 (opt. 0.20) mgP/g slag
CaO content	XRF composition	> 20 % (opt. 25 %)	> 40 % (opt. 45 %)
Fe_2O_3 content	XRF composition	> 25 % (opt. 30 %)	> 40 % (opt. 50 %)
Leaching	EN 12457-2	Below limits 2003/33/EC	Below limits 2003/33/EC

After this preliminary characterization, a lab-scale column was designed to perform experiments in a dynamic reactor under controlled conditions. Furthermore, a first design of both French and German demonstration-scale systems was performed. EAF and BOF slag were tested in continuous flow column

experiments to determine their capacities to remove P from a synthetic wastewater containing initially 10 mg P/L. The influences of various parameters were studied, including the ratio of width to length of the column, i.e., 0.21 and 0.42, slag type, i.e., EAF and BOF, slag size, i.e., 5–16 mm, 6–12 mm, 20–40 mm and 20–50 mm, and slag composition, i.e., CaO content. P removal mechanisms were also investigated through chemical and mineralogical analyses of the slag surface before and after use. It was confirmed that P removal occurred predominantly via CaO-slag dissolution followed by calcium phosphate precipitation. Over a period of 100 weeks of column experiments, small-size slag, i.e., 5–16 mm EAF-slag and 6–12 mm BOF-slag, removed more than 98 % of the inlet total P, reaching retention levels of 1.71 g P/kg for EAF slag and 1.98 g P/kg for BOF slag. On the contrary, big-size slag, i.e., 20–40 mm EAF slag and 20–50 mm BOF-slag, showed lower P removal efficiencies since they were negatively affected by massive releases of previously accumulated P precipitates. Treatment performance and hydraulic properties improved with decreasing the aspect ratio of the column and with decreasing slag size, most probably because filtration of P precipitates was more efficient with smaller particles providing greater specific surface area for CaO dissolution.

The second phase of the project started by addressing the behavior of an intensive slag filter under real dynamic conditions through the German demonstration-scale filter (DSF) system. The German SLASORB DSF-system was located at Kappe a small village about 60 km north of Berlin where a 190 people equivalent treatment system based on sequenced batch reactor technology was in operation. The latter technology was typical for newly constructed small-size biological WWTPs in Germany: wastewater was fed discontinuously to the reactor and the discharge of treated water occurred at the end of each treatment cycle. The slag filter was implemented as a post-treatment step. Two different kinds of slag were tested in parallel with two lines of filter containers containing BOF slag with a size of 8–32 mm and EAF slag with a size of 5–10 mm. Each treatment line consisted of 3 parallel filters with a volume of 0.31 m^3 each, i.e., height 0.7 m, and diameter 0.75 m, giving a total volume of about 1.9 m^3. The liquid-to-slag ratio was 190 kg water per 500 kg of slag. The containers were highly equipped with pumps and valves for operation control, and a heated enclosure was built to prevent frost and improve working conditions. Both filter lines were equipped with acidification facilities using CO_2 injection to reduce the pH of the outlet water. The total performances of the six reactors were controlled against their P mass loadings allowing comparison of all reactors although not being operated at identical conditions. Results from tracer tests showed lower hydraulic efficiencies for the upstream containers, with short-circuit flows possibly caused by clogging of the inlet structure. The results clearly demonstrated the different reactions of BOF and EAF slag and gave valuable information for optimum operation and reactor design. An optimum hydraulic design was found to be essential for good P uptake since short circuits and dead volumes within the slag filter reduced the average reaction time. A minimum reaction time of 6 hours was recommended with a design reaction time of 8 hours being reasonable considering hydraulic efficiencies down to 80 %.

Based on the German results, a new design concept was proposed, i.e., a Submerged Slag Revolving Reactor (SSRR). This was a circular reactor placing big bags of slag in chambers arranged around a central neutralization tank. The chambers were connected to each other for cascading operation. The first charged reactor was switched to the next one clockwise when breakthrough of P concentration was detected at the last reactor in the circle. The bag with the highest P concentration was exchanged

against fresh slag, followed by a resting period for commissioning. The standard size of a SSRR with 6 big bags would use 5 bags at a time, summing up to approximately 4.5 m^3 of slag. The total reactor volume would be 10 m^3 with the water volume being 2.2 m^3 pore volume plus 5.5 m^3 supernatant resulting in a water-to-slag ratio of 0.95. Considering an average retention time of 8 hours referring to pore volume, the design flow would be 6.6 m^3/day which should be sufficient to serve about 50 p.e. An exchange of one big bag every two months was estimated.

A further step in the project was undertaken by addressing the behavior of extensive slag filters under real dynamic conditions through the French DSF system. In particular, two DSF-systems with selected BOF and EAF slag were designed and operated at La Motte d'Aigues a small village about 70 km east of Avignon where local domestic wastewater was treated by a two-stage vertical flow constructed wetland with a capacity of 1200 p.e. and an actual load of about 800 p.e. The slag filters with a volume of 6 m^3 each, were added as a third stage of treatment designed as sub-horizontal flow filters to remove P from the constructed wetland effluent. The containers were designed to be transportable thus enabling the reactors to be taken to other locations for additional scientific research in the future. The influences of slag composition, void hydraulic retention time (HRT_v), temperature and wastewater quality on filter performance were studied. EAF-slag removed 36 % of the inlet total P reaching a retention level of about 0.26 g P/kg while BOF-slag removed 59 % of the inlet total P reaching a retention level of about 0.47 g P/kg over a period of 85 weeks of filter operation. P removal efficiency improved with increasing temperature and HRT_v, most probably because these factors affected the rate of CaO-slag dissolution and calcium phosphate precipitation. It was observed that at long HRT_v higher than 3 days, slag filters may produce high pH in the effluents (> 9) because of excessive CaO-slag dissolution. However, at shorter HRT_v of 1–2 days, pH values were elevated only during the first 5 weeks of operation and then stabilized below pH 9. The kinetics of P removal was investigated employing a first-order equation, and a model for filter design was proposed based on the results.

Significant differences in P removal were observed between the column experiments and the field experiments. Overall, column experiments showed higher outlet pH and higher P removal than field experiments. The rate of CaO-slag dissolution was identified as the main parameter controlling pH and hence P removal efficiency. Several factors were identified to explain the differences. The first one was the effect of loading mode since column experiments were performed with continuous horizontal flow with a HRT_v of about 1 day, while field experiments used discontinuous sub-horizontal flow with batch loads with a HRT_v of 1–2 days though tracer tests suggested the different loading rates probably did not significantly affect CaO dissolution. The second effect was temperature since column experiments were performed at a constant temperature of about 20 °C whereas field experiments were conducted under field conditions with air temperatures ranging from below 0 °C to above 30 °C and seasonal fluctuations in treatment performance were observed. The third and most important effect was wastewater composition since column experiments used a synthetic P solution, i.e., tap water and KH_2PO_4, while field experiments treated the effluent of a constructed wetland. The constructed wetland effluent had a mean total alkalinity of 282 mg $CaCO_3$/L which was a very hard water compared to 140 mg $CaCO_3$/L for the synthetic solution and this higher alkalinity may have buffered the pH increase due to CaO dissolution thus limiting calcium phosphate precipitation. In addition, the higher Ca^{2+} concentration of the real wastewater may have limited the dissolution rate

of CaO, and the presence of organic colloids and humic acids may have further affected calcium phosphate nucleation and recrystallisation.

A further fundamental step of the project concerned the valorization of P-saturated slag as fertilizer with the aim to determine whether the phosphate retained in slag filters led to an increase of plant-available phosphate. Slags from lab-scale columns as well as from the full-scale system near Avignon were analyzed for their mineral acid soluble and citric acid soluble phosphate content. Vegetation experiments were then carried out under climate chamber conditions with wheat in small vegetation pots and subsequently in larger Mitscherlich cultivation pots under more realistic field conditions, using an experimental soil (Vörden). The results showed that yields and P concentrations in both cultures, i.e., spring rape and winter rye, were significantly increased by P fertilization with slag materials. Both BOF and EAF slags in finely milled texture increased the P uptake of the plants to a similar extent as the fully solubilized P fertilizers triple superphosphate and Thomas phosphate, and significantly more than soft ground rock phosphate. There was a clear close relationship between the applied lime amount and the achieved soil pH values. Doubling the P fertilization amount led to an additional increase of P uptake especially on the soils treated with BOF slags from both field-scale experiments. However, EAF slag required considerably higher lime amounts due to its lower P content and caused soil pH to increase above 8.0 which was combined with a decrease of yields. A comparison of untreated slag and P-enriched slag showed that there was a slightly lower efficacy of the enriched P fraction particularly in water and CAL extractable soil phosphate fractions, but yields were equal. No phytotoxic effects of the wastewater-treated slag were detected, even at high application rates. The vegetation experiments confirmed that BOF and EAF slag used as phosphate filters in wastewater treatment could be successfully reused as liming materials and phosphate fertilizers after appropriate conditioning.

Concerning the environmental safety of slag filters, the mineralogical and leaching behavior of fresh and saturated slag was thoroughly investigated. Leaching tests according to EN 12457-2 and DIN 19528 were performed on all slag types before and after use in both the column and field-scale filters. The results showed that the leachate concentrations of heavy metals remained generally very low and below the limit values for waste acceptable at landfills for inert waste according to EU Council Decision 2003/33/EC. The pH of fresh slag leachates was very high around 11–12 but decreased after saturation in the filters. The total content analysis showed that P was indeed accumulated in the slag during operation thus confirming the retention mechanism. The mineralogical investigation by XRD identified that P was retained mainly as calcium phosphate precipitates. The volume expansion tests, i.e., steam test according to EN 1744-1, showed that both EAF and BOF slag fulfilled the requirement of less than 5 % volume increase which is important for the structural stability of the filter over time.

The socio-economic and environmental evaluation of slag filters were also evaluated. A design tool and a cost simulator were developed to estimate the investment and operating costs of implementing a slag filter compared to the conventional alternative of coagulation-flocculation with $FeCl_3$. The study was conducted primarily for the French market where regulations in sensitive areas imposed a discharge limit of 2 mg/L total P for small WWTPs below 5000 p.e.. In France, 29,343 rural communities with a total of approximately 13.9 million inhabitants were identified as potential clients

for slag filter systems. It was noted that small towns of less than 10,000 inhabitants represent a growing demographic trend in France with data showing faster population growth in rural areas compared to large cities. The economic model considered a slag volume of 2 m^3 per p.e., a filter lifetime of 5 years with one renewal over the 30-year tool lifetime, slag density of 1.8 t/m^3, and transport distances of 100 and 200 km from the steel plant. Road transportation appeared the most suitable, fastest and most cost-effective for delivery. The results of the case study at 100 km transport distance showed that slag filter option was more expensive in initial investment than the coagulation-flocculation solution regardless of station size. However, the slag filter was always less expensive during the operational phase. When combining investment and operating costs, the slag filter option became competitive for wastewater treatment stations with a capacity below 400 p.e. at 100 km distance, and below 200 p.e. at 200 km distance. Interestingly, it was noted that in France municipalities received more subsidies for investment when they modernized their wastewater treatment systems, which paradoxically made them more attracted by solutions requiring higher initial investment. The cost difference between the two solutions at higher capacities was relatively small, i.e., about 3 € per p.e. per year, and the slag filter offered additional advantages including simplicity and rusticity of operation, no overproduction of sludge from chemical precipitation, and a subsequent valorization of the P content. Table 13 summarizes the main comparative advantages and drawbacks of each technology.

Table 13: Comparison of slag filter and coagulation-flocculation for P removal

Criterion	Slag filter	Coagulation-flocculation ($FeCl_3$)
Investment cost	Higher	Lower
Operating cost	Lower (no reagents, minimal maintenance)	Higher (reagents, qualified manpower, sludge disposal)
Competitiveness	Below 400 p.e. (100 km) or 200 p.e. (200 km)	Above 400 p.e. (100 km) or 200 p.e. (200 km)
Sludge production	No additional sludge	Additional sludge from chemical precipitation
Slag end-of-life	Reusable as fertilizer/ liming material	Not applicable
Operational complexity	Simple, no qualified labor needed	Requires qualified and regular manpower

An important aspect of the socio-economic analysis was the consideration of P as a critical non-renewable resource. Researchers estimated a peak in P production around 2030 and, while this estimation remains debatable, the reduction of high-quality natural phosphate reserves was expected

to continue. In a context where the global population is projected to reach 9 billion people by 2050 and P requirements will increase accordingly, the price of phosphate rock has been moving upward continuously. SLASORB was therefore innovative because it offered a way to capture a significant proportion of phosphate from wastewater of small towns and return the phosphorus back into the agricultural cycle. The P_2O_5 content observed in the P-saturated slag after filtration was around 2 % which was still below the minimum level of 3 % P_2O_5 typically required for commercial agricultural fertilizers. However, the primary economic value of the used slag after its end-of-life as a filter would be its remaining lime content rather than its P_2O_5 content, since converter slag was already widely used and appreciated as a liming agent to correct soil pH across European countries. If the slag did not accumulate external pollutants, i.e., heavy metals, from wastewater during its use as a filter, the steel supplier could potentially rent the slag to municipalities managing material lifecycle from delivery to recovery as fertilizer.

Regarding environmental and social acceptance, the study noted that slag was already locally known and recognized for various uses in regions with steel industry presence. Building companies consider slag as a noble material able to replace natural aggregates such as porphyry stone or limestone for construction purposes. Converter slag was used as a liming agent in agriculture across European countries and was highly appreciated by farmers who used it as a pH corrector. In contact with water, converter slag was also widely used in Germany to protect riverbanks against erosion, and in France it was employed in road construction under specific environmental regulations. The levels of heavy metals released by the slag in the filter systems were measured during the project and found to comply with existing standards applied to constructed wetlands. The pH of discharged water needed to respect a maximum level of 8.5 and this could be achieved through CO_2 injection for pH neutralization, as demonstrated in both the French and German pilot systems. Transparency about the technical results and the environmental impact was identified as essential for social acceptance of this new water treatment process.

In conclusion, the SLASORB project demonstrated that the use of filters filled with EAF and BOF slag was an efficient technique to upgrade P removal in small wastewater treatment plants. Two demonstration-scale filters were successfully built and operated in France and in Germany, showing that slag was able to remove P from wastewater in very different treatment environments without any environmental issues and with the problem of high outlet pH being easily solved using CO_2 injection. The large number of steelmaking plants in Europe represented a diffuse and low-cost source of steel slag for wastewater treatment, with an estimated 2 to 3 Mtons/year of suitable material available. The socio-economic study showed that the potential for slag filters was substantial, especially around existing large steel sites where social acceptance was likely to be more favorable due to the long-standing culture and history around the steel industry. The study highlighted that the most interesting areas to develop the market were those closest to the production sites. However, P removal performance of slag filters may vary depending on the design and system operation, i.e., batch load, downflow, residence time, the temperature and wastewater composition, which affected the rate of CaO-slag dissolution and hence calcium phosphate precipitation. The need for more full-scale field applications to confirm the working hypothesis and strengthen the reliability of the process was identified, to evaluate treatment performance under different climates and wastewater compositions,

and to determine the full P-loading capacity of the slag over periods of 10 years or more. The effect of different loading strategies on P removal should also be studied by altering feeding periods and resting periods which may give important information to enhance the phenomena of calcium phosphate precipitation and crystallization. The results obtained, combined with the successful reuse of P-saturated slag as fertilizer pointed towards a circular economy approach where an industrial by-product of the iron and steel industry was first used as a reactive material to remove P from wastewater, and then valorized as liming material and phosphate fertilizer in agriculture thus contributing to the recovery of a critical non-renewable resource.

2.2.9 INNOCARB: Innovative carbon products for substituting coke on BF operation (35)

The project was coordinated by BFI with DK Recycling & Roheisen, LKAB, Swerea, TKS, Uniwersytet Śląski and Voestalpine participating as partners in the consortium. The project started on the 1st of July 2010 and lasted almost three and a half years, ending on the 31st of December 2013. The overall project cost 2.57 M€ and the EU contributed 1.54 M€, i.e., almost 60 % of the budget.

At the time of the project, primary steelmaking through BF was the dominant route, accounting for 72 % of worldwide steel output. However, this pathway was one of the most carbon-intensive industrial processes relying on metallurgical coke for structural support for the burden, chemical reduction of iron oxides, and primary fuel for generating the high temperatures required. Coke consumption was directly linked to CO_2 emissions thus making the decarbonization of BF a critical challenge for the steel sector. To this end, the INNNOCARB project tried to develop and investigate two different pathways to reduce metallurgical coke usage in BF ironmaking process. The first pathway entailed the substitution of coke with cold bonded carbon briquettes made of carbon usually not suitable for BF to broaden reductant base. The second route measured the influence of activated nut coke on coke consumption, and the indirect reduction were investigated. In particular, the nut coke was selected and activated to increase reactivity and lowering the TRZT in the BF shaft.

Focusing on the first strategy, i.e., the substitution of a portion of coke with cold-bonded briquettes, a variety of C-bearing materials such as coke breeze, coke dust, anthracite, petroleum coke, lignite coke and charcoal were evaluated to determine whether they could meet the functional requirements of BF coke while contributing to lower fossil-carbon consumption. The mechanical and physical properties of this carbon material are summarized in Table 14. The thermal behaviour of the different carbon materials was also analysed through TGA and DTA by heating up the samples up to 1100 °C in a CO_2 atmosphere with a 5 °C/min heating rate. Charcoal weight loss started from the beginning of the analysis reaching its degradation peak at 922 °C while lignite coke decomposed at about 861 °C. Pet coke and anthracite decomposed at higher temperatures of 1050-1080 °C as well as BF-coke which did not display any loss up to 1000 °C reaching the maximum decomposition at about 1070 °C. The tests showed that lignite coke and charcoal had the highest reaction rates in the temperature range between 850-920 °C while the highest reaction rates of pet coke, anthracite and hard coal coke occurred about 120 °C later. The reaction rate of hard coke was lower than pet coke and anthracite one.

Table 14: Physical and chemical properties of the different carbon materials considered

	C (%)	Moisture (%)	Volatile (%)	Ash (%)	Calorific Value (MJ/kg)
Coke Breeze	85.7	14.6	0.7	11.9	28.9
Anthracite	85.9	17.9	2.2	10.0	30.3
Pet Coke	90.0	7.9	13.7	0.3	36.0
Lignite Coke	87.4	0.5	3.0	10.5	29.9
Charcoal	90.0	2.5	17.2	2.7	33.1
Coke dust	85.7	14.6	0.7	11.9	28.9

After selecting the carbon materials, laboratory scale agglomeration tests were performed using Portland cement as binder and varying the type and content of the different C bearing material as well as operating pressure. In particular, all the mixtures had a 15 % of binder and a 60 % of coke breeze as basis and 25 % of anthracite, lignite coke, pet coke and charcoal. The results reported that the mixture of BF coke and binder alone led to the highest cold strength around 8.5 MPa and satisfying results above the minimum cold strength of 6 MPa required were achieved with pet coke and lignite coke mixtures. The cold strength of anthracite mixture was lower than the imposed threshold but was still of interest while the charcoal mixture reached an excessively low value not being suitable for the final purpose. The compression tests also showed that tablets strength was not influenced by the production pressure and that a binder content of 12-15 % was sufficient to obtain the cold strength necessary for briquette making, after an appropriate curing time of 3 days. Considering the results obtained, four different brick recipes were considered for the next step, and they are summarized in Table 15. Agglomeration trials were carried out using a manual vibrating compaction press and the resulting briquettes were then subjected to a quality assessment. Recipes R1 and R4 exhibited superior high-temperature stability and the highest mean cold strengths of 3.64 and 4 MPa, respectively. Additional Refractoriness Under Load (RuL) testing were performed to investigate the effect of thermal, mechanical and chemical stress on bricks by applying a temperature of 1040 °C, a load of 0.5 kp/cm^2 and a gas atmosphere with 58 % N_2, 30 % CO, 10 % CO_2 and 2 % H_2. The tests confirmed that briquettes from R1 and R4 performed better under this simulated BF conditions with recipe R4 being the best choice. Based on their superior cold strength and high-temperature behaviour, R1 and R4 were selected as the most suitable formulations for further evaluation and testing in experimental BF trial where baskets filled with R1 and R4 briquettes were charged into the furnace.

Another objective of the study was to investigate the feasibility of using agglomerated petroleum coke as a substitute for nut coke in BF by applying press and growth agglomeration techniques. The mechanical and metallurgical properties of the produced agglomerates were assessed. Petroleum coke is characterized by a high fixed C content and by a slightly higher volatile matter and significantly higher combustion reactivity than coke breeze. Moreover, most pet coke grades contained higher S levels around 1.5 % which is the main factor influencing its market price. Despite these marginal discrepancies,

the large quantities of fine pet coke (0–1 mm size) available at relatively low cost were not suitable for direct BF use due to their size. In light of this, two pet coke grades were selected for agglomeration trials to make them suitable as nut coke alternatives. The first pet coke was a coarse grade with a maximum particle size of 1 mm while the second one was a very fine grade with a maximum size of 70 µm. Both grades were characterized by C contents above 95 %. Press agglomeration process was selected to treat the coarse pet coke using Portland cement and alumina cement and applying a drying period of 21 days. A cold crushing strength of 5-8 MPa was achieved thus satisfying the required minimum of 5 MPa. Granulation process was applied to the fine pet coke using alumina cement and bentonite as binders. These trials resulted in a much lower strengths with about 40 N per pellet for alumina cement and about 10 N per pellet for bentonite which were far below the strength of conventional nut coke. Based on these results obtained, press agglomeration was selected for further trials including the production of larger batches for abrasion resistance and cold crushing and CSR testing. Pet coke agglomerates showed much higher reactivity than conventional BF coke and therefore lower CSR, but their high reactivity indicated that they could contribute effectively to CO generation in the thermal reserve zone, where conventional coke showed limited reactivity according to the Boudouard reaction.

Table 15: Composition of the four recipes selected for the next step of the agglomeration trials

Recipe	Binder (%)	Coke Breeze (%)	Anthracite (%)	Lignite coke (%)	Petrol coke (%)
R1	15	85	-	-	-
R2	15	60	25	-	-
R3	15	60	-	25	-
R4	15	60	-	-	25

Once completed the laboratory campaign, pilot tests were performed in experimental BF by charging various baskets filled with carbon briquettes from recipes R1 and R4 according to the sequence reported in Figure 11. The furnace was quenched, cooled, and excavated after the campaign and the recovered baskets were examined. Briquettes showed a clear decreasing trend in mechanical integrity with increasing depth with samples from layer 2 still being compact and samples from layer 12 being strongly disintegrated. This deterioration was attributed to binder-related phase transformations at elevated temperatures. Indeed, dehydration led to the formation of cracks and to the appearance of new phases such as Tobermorite which weakened the binding matrix. Also, calcite was detected in the binder matrix of the lower layers thus indicating the exposure to higher temperatures, although the lack of slag formation suggested that temperatures did not exceed 950–1000 °C. The thermal analysis of the carbon briquettes R1 and R4 was carried out before and after the campaign and allowed to study the influence of the thermal process on briquettes reaction behavior and stability. Tests were performed up to 1200 °C in a CO_2 atmosphere using a heating rate of 2 °C/min. Despite hard coal and pet coke being characterized by similar reaction temperature range, hard coal coke displayed a

lower activation energy, i.e., 100 kJ/mol, than pet coke, i.e., 144-202 kJ/mol, and therefore a higher reactivity. Furthermore, R4 briquettes containing pet coke showed a distinctly lower reaction temperature range than R1 despite the reaction ranges of the individual raw materials that fell within the interval observed for R1 and R1 activation energy was lower and aligned with that of hard coal coke. This indicated that briquetting process modified the apparent reactivity of the components. The reaction temperature ranges of both briquette types after the trial remained largely unchanged in the upper layers, but the range for R1 shifted downward to match that of R4 at Layer 12. Nevertheless, thermal exposure did not significantly affect activation energy, suggesting that the basic reaction kinetics remained stable. The basket samples recovered revealed a pronounced brick disintegration even in cooler shaft zones well before reaching temperatures high enough to initiate solution loss reaction. Estimated exposure temperatures ranged from approximately 500–600 °C in the upper layers to 750–850 °C in the lower layers thus being still insufficient for substantial CO_2–carbon gasification. This confirmed that the deterioration of R1 and R4 bricks was not driven by chemical reaction but by mechanical or structural degradation occurring at relatively low temperatures. This underlined an intrinsic weakness in brick formulation or bonding mechanisms rather than thermochemical instability thus highlighting the need to improve the cold strength performance of the briquette itself.

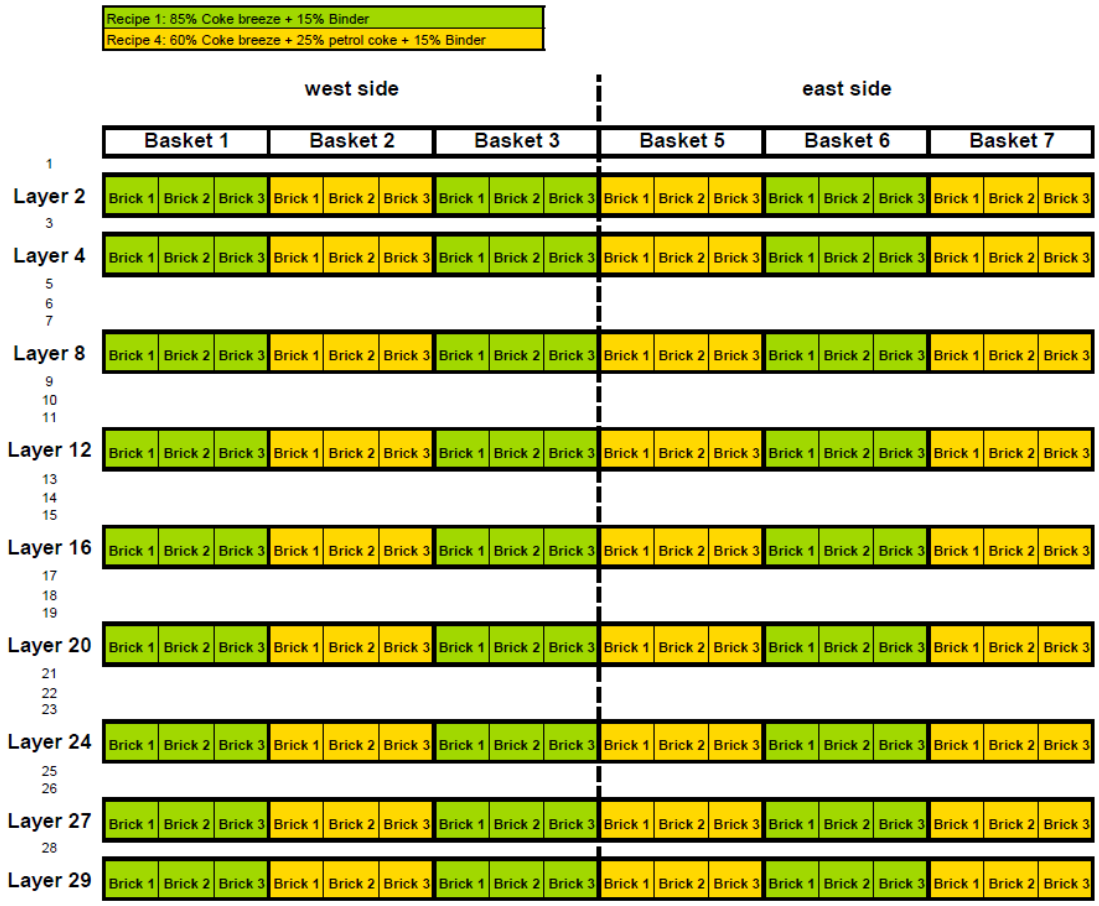

Figure 11: Basket charging schedule used to perform experimental BF trial

The adjustment of R1 and R4 recipes was performed by replacing part of the coke breeze with coke dust. In particular, 8.5 % of coke dust was substituted to coke breeze in R1 and 6 % was substituted in R2 thus resulting in the modified recipes $R1_{new}$ and $R4_{new}$. This addition resulted in an increase in cold strength reaching values higher than 5 MPa for both new recipes, i.e., 5.4 MPa R1 and 5.3 MPa R2. After that, carbon briquettes behaviour under simulated furnace conditions was compared to standard BF coke exposing the materials to increasing temperatures up to 1100 °C, to increasing pressure, decreasing CO_2 and increasing CO content. $R4_{new}$ briquettes showed a steady weight loss up to 900 °C with a final weight loss around 12.1–13.5 %. $R1_{new}$ displayed a consistent behaviour with a total weight loss of 6.8-8.5%. the comparison of these results with the ones of BF coke indicated that both $R1_{new}$ and $R4_{new}$ briquettes were significantly more reactive than BF coke which showed only a 1–1.5 % weight loss. Additional laboratory tests were conducted to evaluate the disintegration risk during the hot stage by heating the carbon bricks in a 100 % CO_2 atmosphere up to 1100 °C. A weight losses of 21.3 % for $R1_{new}$ brick and of 26.1% for the $R4_{new}$ brick was observed thus confirming the trends previously observed. The higher reactivity of the $R4_{new}$ bricks due to the addition of PC resulted in abrupt disintegration of the brick once the temperature of 1100 °C was reached. The reaction behaviour of $R1_{new}$ and $R4_{new}$ was further studied and compared to coke breeze and pet coke one using TG and DSC (Differential Scanning Calorimetry) under controlled Ar/CO_2 and Ar/CO_2/CO atmospheres. Under CO_2-rich atmosphere, petrol coke showed the earliest mass loss due to degasification of volatiles up to 680 °C after that strong solution-loss reaction were observed. Coke breeze reacted much slower due to the lack of volatile and remained almost inert until 850 °C displaying a 5 % mass loss only while a strong increase in reaction rate arose above 950 °C after. $R4_{new}$ reacted at an early stage with a 5 % weight loss already at 630 °C due to the 25 % pet-coke content which caused the degasification of volatiles. $R1_{new}$ consisting of coke and cement binder showed unexpectedly a high low-temperature reactivity probably due to the catalytic action of the binder which was rich in CaO which in turn accelerate C gasification. Both briquetted materials reached almost complete C conversion under the CO_2-rich atmosphere. Reducing the CO_2 content by half reduced significantly the reactivity of both coke breeze and pet coke while this effect was smoother in both recipes due to the catalytic effects of CaO which made the dependence on CO_2 concentration less pronounced. DSC measurements in the CO_2-rich atmosphere revealed an exothermic signal around 600–700 °C likely caused by residual oxygen in the samples reacting with C. Petrol coke also showed a strong additional endothermic peak at around 600 °C linked to volatile evaporation. When CO was added to the gas mixture, this signal disappeared, exposing only the true endothermic solution-loss reaction arising for all materials. Overall, carbon reactivity was shaped by volatile content, CO_2 concentration, and especially catalytic effects from cement in the briquette formulations.

Successive BF trials were conducted at DK to evaluate the suitability of carbon bricks as partial substitute for coke. The required quantity of carbon bricks for each test was calculated considering a C contents of 89 % for coke and 66 % for the carbon bricks and substitution rates between 2 and 15% were investigated. During the 12 % substitution trial with $R4_{new}$ bricks and the 15 % substitution trial with $R1_{new}$ bricks, oil injection was additionally applied. The impact of coke replacement was assessed considering both product quality and process parameters and comparing the results with reference periods. Each trial included a first reference period during which BF operated without C-brick input

and a second test phase in which a defined amount of coke was replaced by C-bricks. The Fe content of the sinter used in the trials ranged from 55.8 to 57.2 % while the FeO content varied between 14.0 and 16.3 %. BF operational mode strongly depended on the required pig-iron quality and the conditions used in the trials are summarized in Table 16.

Table 16: Average BF-data from DK for Reference periods and Trials

		Ref.1	Trial	Trial	Ref.2	Trial	Ref.3	Trial	Ref.4	Trial
C-brick			$R4_{new}$	$R4_{new}$		$R4_{new}$		$R1_{new}$		$R1_{new}$
Coke substitution		-	2%	5%	-	12%	-	12%	-	15%
Length	d	9	8	7	8	8	14	8	8	1
Hot metal	t/d	810	891	911	716	709	639	626	900	810
Coke	kg/t_{HM}	707	693	671	719	650	697	645	670	607
C-bricks	kg/t_{HM}	0	15	32	0	87	0	84	0	103
Oil	kg/t_{HM}	0	0	0	23	32	0	0	45	42
O_2	Nm^3/t_{HM}	23	26	23	2	2	0	0	5	47
Steam	kg/t_{HM}	30	26	17	0	0	2.8	1.1	5	6
Blast	$1000Nm^3/h$	60	67	67	60	57	49	48	61	56
Pressure	bar	0.79	0.88	0.86	0.63	0.56	0.52	0.51	0.63	0.65
Form T	°C	2245	2244	2250	2196	2181	2226	2241	2246	2196

C-brick charging proved to exert a minor influence on BF operation with slight variations in furnace permeability, and no significant effects on hot-metal Si content or tapping temperature. Dust emission revealed a modest increase in total dust amount with somewhat higher C and Ca contents. Nevertheless, the increase of C emission was rather low thus indicating that C bricks possessed adequate mechanical strength and that most of their C was successfully consumed inside the furnace. No operational differences were detected between $R1_{new}$ and $R4_{new}$ bricks thus suggest that C-bricks could substitute coke at levels up to 10 % without compromising process stability or product quality.

Focusing on the second objective of the project, i.e., nut coke activation, nut-coke samples original and activated were characterized through reaction-rate measurements of CO_2 gasification process, using both fluidized-bed reactor and TGA analyses. The tests enabled a direct comparison between untreated and activated nut-coke types assessing the effects of activation on reactivity and gasification behaviour. Nut coke activation was performed using slurries of magnetite (Fe_3O_4), hematite (Fe_2O_3) and hydrated lime ($Ca(OH)_2$) selected as activation agents since Fe and Ca were known to catalyze

the gasification reaction. Additionally, a solution of iron nitrate ($Fe(NO_3)_3$) was selected. Four different nut coke types were considered and the effectiveness of the activation treatments varied according to the nut coke considered. Nut coke type 2 was intrinsically characterized by a high content of catalytically active Fe and Ca in the ash, and their uniform distribution contributed to a diffusion-limited behaviour. In this case the hematite slurry treatment caused the blockage of the pores thus hindering mass transfer and reducing the apparent reaction rate. On the contrary, hematite activation proved to be beneficial increasing the reaction rate for all nut coke type with the best results being achieved with type 1. The latter was characterized by an increased reactivity with all activation agents with $Fe(NO_3)_3$ treatment producing the strongest effect by increasing the gasification rate by a factor of 3 in fluidized-bed reactor tests. This was attributed to a deeper penetration of dissolved Fe into the coke structure. $Ca(OH)_2$ slurry produced the second most effective response. In TGA tests, hematite and magnetite treatment increased the gasification rate by 33 % while $Ca(OH)_2$ and $Fe(NO_3)_3$ more than doubled its value. The high effect of $Ca(OH)_2$ in TGA was partially due to mass loss from lime calcination and water release enhancing gasification.

Activated nut coke was then tested in a BF simulated test both separately and in mixtures with MPBO (Magnesium-rich Pelletized Blast Furnace Olivine) pellets to verify the eventual reduction improvement of the ferrous material. In mixed samples, 19-20% of nut coke was mixed with the MPBO pellets. The test included an initial 45-minute heating up to 500 °C in N_2 atmosphere, after that a further heating up to 850 °C was performed in 70 minutes in a 21-23 % CO, 20-18 % CO_2 and 59 % N_2 atmosphere, then heating up to 950 °C was achieved in 95 minutes in a 23-39 % CO, 18-2 % CO_2 and 59 % N_2 atmosphere. The final heating step up to 1100 °C was achieved in 55 minutes in a 39-41 % CO, 2-0 % CO_2 and 59 % N_2 atmosphere followed by the cooling phase. A positive effect of nut coke addition to pellets reduction degree was observed and the activation on nut coke type 1 with $Ca(OH)_2$, and $Fe(NO_3)_3$ proved to be even more beneficial. Chemical analyses of the activated nut coke before and after the test showed that the activation agents containing Fe or Ca remained detectable both before charging and after testing thus confirming their persistence during the simulation. Strength evaluations through CSR test demonstrates that simulated BF conditions did not weaken the nut coke.

The next step of the project consisted in full operational trials at LKAB experimental BF to determine the impact of activated nut coke on BF operations, i.e., stability, C consumption, gas utilisation, reduction behaviour of ferrous materials, energy efficiency, etc. Based on the pre-tests conducted in laboratory, nut activation with magnetite and lime containing slurry was selected for the study. The trial consisted in three experimental periods with Zr-traced nut coke, Zr-traced and magnetite activated nut coke and Zr-traced hydrated lime activated nut coke compared against a reference campaign without nut coke in the ferrous burden. Zr-tracing was fundamental to monitor coke behaviour and consumption. The furnace operated stably during all campaigns with consistent descent rate and normal BF thermal behaviour. Operational evaluation showed generally stable furnace conditions during all nut coke charging periods with increased gas efficiency of about 1.5 % during periods with magnetite or lime-activated nut coke, based on both top-gas and upper-probe measurements indicating improved gas distribution. Higher tap temperatures and slightly elevated Si levels were observed when nut coke was charged though slag composition remained comparable to the reference. Heat and mass-balance calculations demonstrated that activated nut coke reduced C

consumption by roughly 4–6 kg/t hot metal compared with the reference. This improvement was linked to a 25–40 °C decrease in TRZT thus enhancing indirect reduction.

The study demonstrates that C-bricks produced from low-cost carbon materials such as coke breeze, coke dust and petroleum coke, using standard cement binders, could partially replace metallurgical coke in BF. Industrial trials confirmed that vibration-compacted carbon bricks met BF operational requirements and enabled coke substitution rates of about 10 % with economic benefits strongly dependent on coke market prices. Cold strength was sufficient for handling and charging, higher mechanical stresses in large BF required cautious scale-up supported by preliminary trials. In addition, nut coke activation and the catalytic effect of lime showed clear potential for lowering TRZT, reducing carbon consumption and CO_2 emissions, provided the process is carefully optimized for industrial application.

2.2.10 OPTDESLAG: Increased yield and enhanced steel quality by improved de-slagging and slag conditioning (36)

The project was coordinated by BFI while Swerea, Saarschmiede and SSAB participated as partners in the consortium. The project started on the 1st of July 2010 and lasted almost three years, ending on the 30th of June 2013. The overall project cost 1.03 M€ and the EU contributed 618 k€, i.e., almost 60 % of the budget.

The OPTDESLAG project focused on a critical and often underestimated steelmaking operation, i.e., deslagging. In both primary and secondary steelmaking, incomplete or poorly controlled deslagging can lead to the carry-over of reactive slag into subsequent process steps thus compromising steel quality, e.g., affecting desulphurization performance, re-oxidation and inclusion behavior, and increasing consumption of slag-forming agents and deoxidants. This also generates direct yield losses through entrained metal in the removed slag. Considering this, the project aimed at increasing yield and enhancing product quality by improving deslagging control and monitoring as well as slag conditioning at industrial scale. The central concept was to combine permanent camera instrumentation, online image analysis and process modelling to support reproducible deslagging decisions thus reducing excessive metallic losses and quality risks from remaining slag. The project aimed also to complement the process this with dynamic online process models to track slag condition throughout key steelmaking steps so that subsequent operations can be adapted to the actual amount of residual slag.

Project objectives were pursued through the development and installation of imaging-based sensors, i.e., CCD (charge-coupled device) and Infrared (IR) cameras, image analysis tools and associated process-data acquisition. Based on this enhanced monitoring capability, deslagging schemes for optimum operation were established. In parallel, dynamic slag balancing models and online set-point calculations for slag conditioning were developed to support online slag control. Finally, the sensor systems and model-based control approaches were implemented and validated at two industrial steelmaking plants representing two distinct deslagging contexts. The first one concerned ladle deslagging of liquid steel after EAF tapping at Saarschmiede while the second one concerned deslagging of hot metal after desulphurization and before charging the BOF at SSAB. In particular, deslagging at

Saarschmiede was performed by tilting and stirring and was controlled by an operator standing near the deslagging station at the height of the ladle lip who positioned the ladle over a slag pit and performed the tilting of the ladle by pulling up a chain attached to the ladle. The operator also controlled the flow rate and pressure of the purging gas. Different was the procedure at SSAB were a mechanical deslagging with a ceramic slag rake was performed by an operator who controlled the slag rake through a joystick and with the help of a camera which allowed the correct positioning. Both slag raking and tilting in the two deslagging processes were carried out by different operators thus meaning that both procedures would vary in terms of deslagging rate and the efficiency.

The first step of the project was dedicated to the identification of robust imaging hardware and mounting solutions suitable for the harsh environment of the deslagging station. After preliminary tests, housing design and installation were completed and the imaging system was prepared to be combined with additional sensor signals, e.g., stirring gas flow rate and pressure, and with data from the process control system. This combined image-and-process dataset provided the backbone for subsequent tool development and plant-trial evaluation. A CCD camera for permanent installation and an IR camera for complimentary mobile installation were selected for Saarschmiede and SSAB exemplificative images resulting from these tools are shown in Figure 12. The main problems at the beginning of the project concerned the correct positioning of the cameras to have a view almost perpendicular to the bath surface of the ladle and to have a full view of the bath. In the case of SSAB, it was also necessary to design protective gas-cooled housing. Early plant trials with combined CCD and IR image sequences and process data were performed to collect data to develop image analysis tools for online assessment of deslagging. Indeed, a strategy was established to monitor the remaining slag area on the melt bath surface as shown in Figure 13. Over the last two years of the project, longer-term data acquisition expanded the dataset substantially; representative data from two steel grades collected over two months were analyzed to identify influencing parameters and to develop deslagging schemes. In addition, extensive slag sampling campaigns were executed to validate the slag balance model developed in parallel.

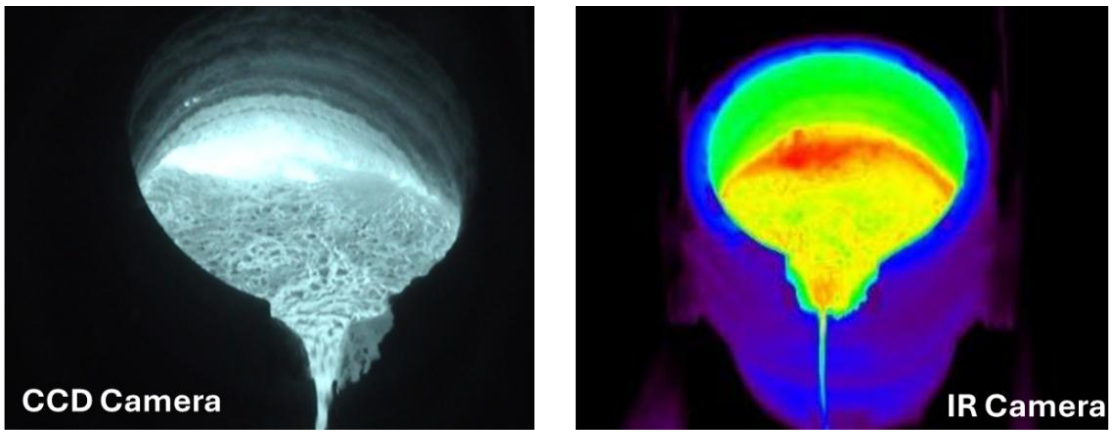

Figure 12: Example of images from deslagging operations at Saarschmiede recorded with both a CCD camera and an IR camera

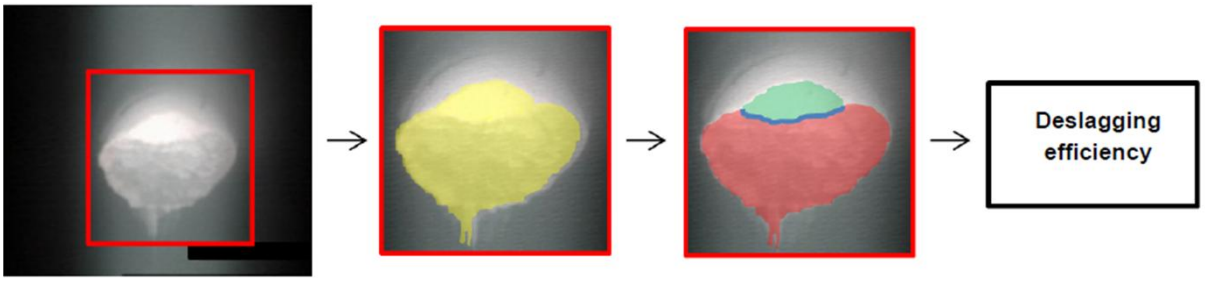

Figure 13: Strategy used by the image analysis software to estimate deslagging efficiency at Saarschmiede

The study of the influence of the main operating parameters at Saarschmiede revealed that several intuitive operator parameters such as the duration of deslagging, tapping weight and tilting angle did not show a significant influence on the deslagging rate and efficiency in the studied range while the purging gas flow rate and the slag temperature proved to be key influencing variables visible in the quantifying results from the image analysis. Slag thickness was also identified as a significant factor since it affected the grey-scale signature of the slag area and the evaluation of deslagging efficiency from camera images. On this basis, an automated monitoring function was developed and implemented to detect cold slag, which can become stiff and cause problems during deslagging. When cold slag is detected and stiffness is expected, liquefying the slag by emulsification and/or addition of slag modifiers was recommended as an operational countermeasure.

Beyond monitoring, OPTDESLAG developed a dynamic process model for slag balancing. After specifying and collecting the necessary process input data, a model to calculate both composition and amount of slag throughout the liquid steelmaking route was developed. The model accounted for all slag former additions and relevant material pick-ups, e.g., from refractory wear or from slag remaining in the ladle from the previous heat, including explicit representation of deslagging steps, and incorporating the effects of key metallurgical operations such as deoxidation, reduction and desulphurization on slag status. The model was adapted to the specific processing routes for lower-alloyed and higher-alloyed grades recognizing that high-alloy production can involve more complex metallurgy such as slag reduction after decarburization under vacuum and multiple deslagging steps and larger alloy additions. Validation of the slag balancing model relied on intensive plant trials with slag sampling at specific processing steps. Comparisons between analyzed slag samples and model calculations showed that the model was able to reproduce the major slag components with satisfactory accuracy. In particular, the agreement of CaO, MgO, Al_2O_3 and SiO_2 was reported as good and sufficiently accurate for practical slag conditioning decisions. Higher deviations were observed for MnO, FeO and Cr_2O_3, but these oxides were considered less critical for the slag conditioning required to ensure good desulfurization performance because their contents were typically low already at the beginning of the relevant ladle refining operations. This validation step was essential for the subsequent online implementation, because it established trust that the model could provide reliable guidance for the most influential slag property targets.

The project defined the metallurgical aims and the corresponding optimum slag properties mainly in terms of basicity and lime saturation and extended the model with online set-point calculations to translate the slag balance calculations into actionable process control. These set-point functions compared the calculated slag state to the optimum properties and determined optimized target amounts for the addition of slag-forming agents considering the actual slag amount and composition at the relevant process stage. The combined slag balance and set-point calculations were implemented online within the control system at Saarschmiede, enabling a more consistent and data-driven approach to slag conditioning after deslagging.

In the final phase, an online automated control system for deslagging was developed and validated. The image analysis software was enhanced to provide operators with a real-time display of the melt bath surface, the evaluated slag area, the estimated remaining slag amount, and warnings such as slag chunk formation or cold slag. A dedicated campaign using combined IR and CCD cameras evaluated the influence of tilting the ladle back to the upright position on slag re-emulsification, and these data were used to refine threshold values within the image analysis algorithms. In long-term operational trials, the remaining slag estimated by the system was compared with operator evaluations and a good agreement was reported thus leading to validation of the monitoring approach and broad acceptance by operators. Overall, a reduction of the scattering throughout the project became obvious and the analysis of the mean values of steel losses at the beginning of the project, i.e., 579 kg, and at the end of the project, i.e., 413 kg, highlighted that steel loss was reduced by 29 %. The standard deviation was also reduced from 773 to 316.

Moving to SSAB, an important enabling step in the preliminary set up phase concerned the installation of sensors on the deslagging machinery to record slag rake position, i.e., x, y and z directions. These signals allowed raking movements to be restricted in semi-automatic mode or, in principle, controlled automatically if actuators were present. The implemented setup included a working hatch and camera mounting on the off-gas hood. The image analysis software developed for SSAB was able to process both IR and CCD images and to return the slag area as a percentage of the whole hot metal surface. The remaining slag amount could be calculated if slag height was known and this parameter was estimated in the project by the operator at the end of deslagging because no robust automatic thickness measurement method was available. Attempts were made to categorize the type of slag, e.g., firm, heavy, viscous or liquid, but it was concluded that camera images did not provide sufficiently detailed information for reliable categorization under the thermal constraints that limited camera proximity and achievable resolution. Based on the trials, slag thickness and bottom purging were identified as the two main parameters affecting deslagging rate and efficiency at SSAB.

The SSAB route tried to develop a predictive model to link the remaining desulphurization slag to S outcomes after BOF processing but due to the limited slag sample availability the S content in the slag was predicted rather than directly measured. It was noted that hot metal desulphurization quality could vary between 10 and 200 ppm of S in steel after BOF processing. Within this framework, multivariate data analysis models were developed to predict S amounts in the desulphurization slag and in the produced steel, and to estimate permissible slag carry-over into the BOF without steel-quality decrease. Separate models were developed for low-S steel (S < 0.0044%) and high-S steel (S >

0.0044%) recognizing that multiple steel grades with different S demands fall into the latter category. The model was deliberately not implemented as a full mass and heat balance model, because not all required input and validation data were available. Instead, the multivariate approach placed relevant process variables, i.e., hot metal analysis, temperature, desulphurization agent additions and other significant signals, into a multi-dimensional coordinate system and fitted the variables of interest. Set-point calculations were then developed to provide target values for permissible remaining slag after desulphurization, supporting the selection of suitable deslagging schemes and helping determine when deslagging was accomplished. Validation against additional campaign data showed that predicted S amounts in produced steel were higher than actual values which in turn yielded conservative and lower permissible slag amounts. Conservative guidance may be acceptable for quality protection, but it also indicated the importance of continuous model improvement and data enrichment. The project quantified model uncertainty through error estimation. For example, the total error for the low-S models expressed as ±2 times the root mean squared error of estimation was reported as S in slag (%) ±2·0.24%, S out (%) ±2·0.00019%, and S in steel (kg) ±2·0.26 kg. For the high-S models, total errors were approximately S in slag (%) ±2·0.29%, S out (%) ±2·0.0019%, and S in steel (kg) ±2·0.90 kg. These values gave a practical indication of expected prediction spread and could be used by operators to interpret advisory outputs with an appropriate safety margin.

In long-term trials, the combined use of semi-automatic restricted slag raking based on rake position sensors with recommendations from the image analysis system and the slag/S models resulted in reduced hot metal losses, i.e., from 19.1 kg/t hot metal of metallic loss in manual operation to 18.2 kg/t hot metal when switching to semi-automatic mode, while also noting that the database was too small to confirm the effect with high statistical confidence. This demonstrated both the potential value of the approach and the practical need for extended monitoring to separate systematic improvements from normal production variability.

A concluding comparison across both plants highlighted that the same overall concept including image-based slag area monitoring with process models and advisory/online control integration must be implemented in a plant-specific way. At Saarschmiede, a CCD camera was permanently installed, and IR was used for campaigns. The online system continuously monitored purging gas flow, slag area and remaining slag amount during ladle deslagging of liquid steel after EAF tapping. At SSAB, CCD monitoring and IR campaigns were combined with rake position sensing. The estimation of remaining slag amount relied on operator input for slag height, and full automation was limited by missing actuators for rake control and the lack of an online slag thickness measurement method. Despite these constraints, both implementations improved deslagging performance, enabled the definition of optimized deslagging schemes, and provided a pathway towards reproducible operation and yield improvements through data-supported decision making.

Overall, OPTDESLAG demonstrated that robust imaging systems and tailored image analysis could deliver actionable indicators for deslagging efficiency, e.g., slag area evolution, warnings for cold or stiff slag, and visualization of operator-relevant parameters. When coupled with dynamic slag balancing and set-point calculations as at Saarschmiede or with multivariate S/slag carry-over forecasting as at SSAB, these indicators could be used to control subsequent steelmaking steps and reduce losses. The project

also clarified the main limitations for wider deployment, notably the need for reliable online estimation of slag thickness to convert area to mass, durable automation hardware for mechanical deslagging equipment where applicable, and sufficient high-quality datasets for model calibration and continuous improvement.

2.2.11 PROTECT: Processes and technologies for environmentally friendly recovery and treatment of scrap (37)

The project was coordinated by Swerea MEFOS with SSAB, Engitec Technologies SPA, Stena Metall, SiCon, Universität Siegen, IVL Svenska miljöinstitutet, Scuola Superiore Sant'Anna (SSSA), and Stena Recycling as partners in the consortium. The project started on the 1st of July 2010 and lasted almost three and a half years, ending on the 31st of December 2013. The overall project cost 3.27 M€ and the EU contributed 196 k€, i.e., almost 60 % of the budget.

The PROTECT project aimed at developing a new method to promote synergetic use of low-value energy wastes with cleaning and preheating of Zn-containing steel scrap. Indeed, low-carbon galvanized steels normally used in automotive bodies and appliances were a source of high-quality scrap feed for both BOF and EAF steel production. Despite this, recycling of coated scrap was limited by the formation of problematic by-products, such as Zn containing dust and hazardous air emissions. PROTECT proposed an innovative stand-alone process for the preheating and surface cleaning of scrap by decoupling scrap preheating from the off-gas streams from the melting furnace. This solution was expected to significantly improve the recyclability of these scrap sources thus widening the scrap base, simplifying recycling of in-house byproducts and reducing hazardous emissions. The process allowed to use Cl containing waste, e.g., ASR, in separate oxygen combustion thus enabling minimisation of flue gases. Scrap coatings were removed in gas phase and collected in dedicated recovery system rendering the possibility for recovery of valuable metals. PROTECT focused on developing a de-zincing process that could fit into the economic realities, i.e., loss of yield, inability to recycle the iron units in the dusts/sludges, increasing costs to meet new tighter limits for water and exhaust gas treatment, furnace delays to manage charging emissions. This process concept was carried on by performing experiments and tests to derive methods for separating and refining waste streams thus proving the technologies in pilot scale to achieve design data and environmental impact in industrial scale.

At first, pre-treatment and refining methods to separate the feed waste material into valuable resources were developed. In particular, two techniques for separating and treating energy containing waste streams were developed and assessed. The Volkswagen-SiCon modular process, i.e., an innovative technology to recycle end-of-life (EoL) vehicles to transform complex shredder residues into valuable secondary raw materials like plastic granulate and fibres, was adapted according to the requirement for separation of non-complex fractions, e.g., tyres, and complex fractions, e.g., ASR and WEEE (Waste of Electrical and Electronic Equipment). After that, the possibility to transform these energy containing wastes into valuable resource through thermochemical recycling was studied, to generate a suitable fuel for the downstream preheating and surface rinsing application. Two thermo-chemical conversion methods were studied, i.e., pyrolysis (conversion of solid fuels in absence of an oxidant) and gasification (use of an oxidizer), to produce combustible syngas to be used as fuel in the

preheating concepts. The remaining solid residue such as inorganics and metals of both processes could also react with Cl. After that, a combined scrap preheating and surface cleaning process which could use the energy containing waste as primary fuel was developed. Pilot testing of scrap preheating showed the possibility to remove organic and metallic coatings while reaching a high preheating degree. A dedicated scrubber and recovery system was derived for the exhaust gases from the scrap preheating system. The gas leaving the scrap cleaning system through the stack were in the range of 80 Nm^3/ton scrap, showing a substantial reduced gas volume compared to the industrial gas cleaning systems. This resulted in efficient and cost-effective gas treatment. Furthermore, the recovery of valuables removed from the scrap was performed exploiting the EZINEX process which was designed to recover the valuables from the wet scrubber. The concept proved to be positive from an environmental and economic point of view, but some technological and metallurgical questions still remain opened thus requiring more research to validate and improve them before the large-scale demonstration and implementation of the preheating concept.

Focusing on the first step of the project, the thermal processes to create suitable combustible and halogen-rich syngas to be used in the scrap surface cleaning process were developed. In particular, two different thermal treatment methods were tested and evaluated. The advantages related to pretreatment and refinement of the incoming material, e.g., ASR etc., with two different technologies was also investigated. As previously mentioned, the Volkswagen-SiCon modular process was adapted to the requirement for separation of non-complex fractions such as tyres and complex fractions such as ASR and WEEE. A new module T was designed for the pre-treatment of non-complex fractions, i.e., tyres, and allowed to produce successfully two materials streams one with tire cords and one without. Furthermore, the existing modules B and C were adapted and modified to improve the separation of the waste into low Cl fractions and high Cl fractions. Module B was dedicated to plastic and metal mixture separation which was performed with a magnet drum to remove ferrous metals, with an eddy current separator and with an air fluidizing step to separates from plastics by density. The metal-free plastics were then transported to a washing centrifuge and were then sent to a floating unit to separate plastics based on their density. In Module C the fibers got their final treatment by additional vibration screen to separate the raw dust. In addition, the Plastsep process was evaluated and used as further pre-treatment concept to produce and separate different plastic fractions at the pilot scale by exploiting floating and plastic density differences. The process allowed to separate residual metals from ASR thus producing simultaneously a metal free light plastic fraction and one or two metal free heavy plastic fractions and the recovery of about 8-10 % of metals would increase the overall recycling degree for cars.

Pyrolysis tests of ASR proved to be a viable method for producing combustible and Cl containing gas for scrap cleaning and de-zincing process. The gas obtained from each of the pyrolysed materials presented variable composition and energy content. Heating values ranged from 19.4 to 55 MJ/m^3, CH_4 content varied from 8.5 to 15.2 %, C_2H_4 from 4.3 to 19.9 %, C_2H_6 from 2.4 to 8.5, C_3H_6 from 3.8 to 16.9 %, C_3H_8 from 0.7 to 4.2 %, hydrogen from 5.9 to 14.3 %, etc. Analogously, gasification of tyre fractions and ASR fractions at different temperatures, i.e., 700, 800 and 900 °C, and with different gasification agents, i.e., steam and air, led to different gas compositions, gas-yields, residual carbon and cold gas efficiency. In particular, tyres gasification with steam proved that gas yield increased with

increasing temperatures with H_2 and CO concentration increasing while CO_2 remaining nearly constant. Furthermore, lower residual carbon contents were observed for increasing temperatures. Analogous results were observed for ASR both with steam and air as gasification agent. The comparison of pyrolysis and gasification underlined fundamental differences between the two methods regarding the resulting products. Gasification process provided higher process gas and Cl yields with higher energy content of the fuel being converted in gaseous products. The residual coke or a partial oxidation of the syngas produced could be used to cover the energy demand of the gasification process thus not requiring any additional energy sources necessary. However, a higher energy demand was required to produce steam for the steam gasification process. Pyrolysis process led to higher amounts of coke and oils which could be sold if sufficiently clean. It was possible to use the pyrolysis oils together with the gas for incineration to improve the energy and Cl yield of the fuel. For the pyrolysis an additional energy source like propane was needed since pyrolysis was an endothermic process. Due to the reducing conditions of both processes, the metals in ARS were preserved and un-oxidized and could be recycled. Results showed that both pyrolysis and gasification could be used to produce the energy needed for pre-heating and surface cleaning and the selection depended on different parameters, such as capacity needed, composition of waste for heat generation, type and form of metal in waste fraction, operational reliability of commercial plants, cost for external energy, value of oil and coke from pyrolysis, etc.

A scrap pre-treatment method was developed with pilot trials that allowed preheating of scrap and removal of organics and metallic coatings in real BOS production at SSAB. Concerning scrap preheating, cold and hot tests were performed showing that the concept could successfully be regulated and controlled. Much of the harmful elements generated from melting of scrap contaminated by organic and other metal coatings were reported in the gas volume. In addition, other metals in the scrap which evaporated at low temperatures, e.g. Hg, were found in the gas flow thus making the separation of these impurities easier. Zn removal efficiency was evaluated by analysing scrubber fluid. Results showed that controlling the pCl_2/pO_2 in the preheating gas was an important parameter for successful operation and a significant improvement in Zn removal efficiency was observed. In particular, when the pCl_2/pO_2 ratio was controlled within the favourable region significantly increased Zn removal efficiency was observed. Furthermore, the preheating temperature in the steel scrap proved to be high ~600 °C in average. One important conclusion from the trials was the concept of removable shafts (scrap buckets) which would simplify the handling of the preheated scrap. It is important that the vessel did not act as chimney due to convection in transport of preheated material. It was also concluded that it was possible to achieve a low exhaust gas flow to the stack by a combination of gas recirculation and oxy combustion. This gas stream was treated in a wet scrubber system capturing dust. Concerning the recovery of valuables, a Zn recovery plant based on modified EZINEX® technology was considered and compared with the existing process, considering the cost of steel production and the management of the metal containing dust. One solution to make this metals recovery unit more economically attractive could be to operate the metals recovery unit through a consortium. This would result in reducing the specific CAPEX and the impact of manpower. In addition, as the water coming from the scrubber must be evaporated, for this purpose some waste energy could be used. This approach was environmentally friendly, as it reduced waste and produced a commodity easily marketable as Zn metal

instead of landfilling dust and sludge. In addition, it reduced other environmental issues, such as organics and leaching of metals from landfill sites.

During the industrial trials, sampling and analysis of Zn in the primary and secondary dust were carried out. After charging the scrap to the converter, Zn started to evaporate and more Zn was reported to the secondary gas cleaning dust when blow start was delayed and the converter was on hold before hot metal charging. On the other hand, the generated dust was found in the primary gas cleaning system when the converter was in start position but blow start was delayed. Using shredded scrap did not influence the process negatively and no changes in steel quality were observed. Consequently, charging of shredded material did not influence the amount of scrap. As results from the last industrial campaign were contradictory to the results from the scrap cleaning tests, more trials were needed to understand the mechanisms needed for the removal of Zn coatings on scrap.

Modelling and holistic evaluation of the technical innovations within the PROTECT project started to review the project needs in terms of models for the holistic simulation/optimisation tool to achieve a common understanding on the modelling environment and methodology. The PROTECT processes were modelled in the Aspen+ software to allow detailed dynamic optimisation of the individual processes and of a network of processes set up in Aspen+. The steel plant was modelled in reMind as a modification of the previously developed steel plant model. Preparations were carried out for the conversion of Aspen models into Matlab models to be integrated with the simulation and optimisation tool. The models developed in Aspen+ were highly non-linear and different approaches for integration were explored. The latter included linearization of Aspen+ models, use of look-up table, a "two-steps" optimization approach and the use of Aspen+ optimization routines. In the last solution integrated in the simulation and optimisation tool, Zn removal and recovery model was merged with the steel plant model and then optimised by a multi criteria optimisation algorithm developed in MatLab, including the following steps: merger of the two models, specification of optimisation problem via used input, the optimiser solves the problem in three nested steps, making use of Non-linear, Linear and Integer parts of the defined problem. Concerning CFD simulations, there were several important parameters to achieve high Zinc removal efficiency. The results showed that for a scrap preheating shaft to be energy efficient and efficient for Zn removal, the inlet gas should have a high temperature and a low flow rate. A user-friendly Graphical Use Interface for simulating and optimising the PROTECT processes was developed.

PROTECT processes, i.e., pyrolysis, gasification, scrap heating for zinc removal and zinc recovery, were also modelled in the LCA tool KCL-ECO, and the results were used to perform one model for the gasification route and another for the pyrolysis route. From an energetic and environmental point of view, the results indicated that the new Zn recovery methods allowed to recover the Zn contained in the steel scrap without increasing energy and environmental load. The extra energy required was recovered in the steel process and the energy and Cl used for the Zn recovery could be obtained from waste plastics. The new technologies seemed to be economically viable and feasible and in all the analysed cases since the incomes were higher than the benchmark. In addition, extra selling, such as the Zn sales, could produce a further benefit. A further reduction in the operating costs was due to savings on the landfill cost and other savings such as EAF energy savings resulting from scrap preheating.

2.2.12 SLAGFERTILISER: Impact of long-term application of blast furnace and steel slags as liming materials on soil fertility, crop yields and plant health (38)

The project was coordinated by FEhS with Dillinger Hüttenwerke, Arbeitsgemeinschaft Hüttenkalk, Voestalpine, AGES (Österreichische Agentur für Gesundheit und Ernährungssicherheit GmbH), SSSA, ILVA s.p.a., and SSAB participating as partners in the consortium. The project started on the 1st of July 2011 and lasted almost four years, ending on the 30th of June 2015. The overall project cost 1.90 M€ and the EU contributed 1.14 M€, i.e., almost 60 % of the budget.

The objective of the SLAGFERTILISER project was to evaluate the effects of iron and steel slag fertilizers and liming materials on crop yields and quality, as well as on selected biological and chemical soil parameters. Special attention was placed on the contents and the availability of trace elements in the soil, in particular Cr and V. The research also addressed specific concerns encountered in each partner country, i.e., accumulation of Cr and V in German soils, high Cr content in slag fertilizers in Austria, and soil salinity combined with lack of fresh water in Italy. The project pursued several specific objectives including the influence of long-term liming with iron and steel slags on soil fertility and structure, the difference between Cr and V accumulated by long-term liming compared to soils with naturally high Cr and V contents of geological origin, and the effects of regular liming on Cr and V immobilization in the soil. Furthermore, the uptake of Cr and V by plants in sprouts and roots with special regard to potatoes, tomatoes and winter wheat, the effects of Si content in slags on plant health and resistance against disease attacks, the effects of liming on acid soil structure and potato plant disease especially scab, the effects of high Cr and V content in P-rich soil on crop yields and soil microbiology under consideration of the Cd balance, the effects of steel slag on soil and crop growth combined with saline water irrigation, the effects of conservation liming of forest soils on chemical, physical and biological soil properties and on phytosociology, and the behavior of Cr and V on acidic forest soils were also addressed.

Different field trials were installed across four European countries to enable comparison of the effects of silicate liming materials under different climatic and soil conditions. In particular, four new field trials by AGES, Arbeitsgemeinschaft Hüttenkalk, SSAB and Dillinger Hüttenwerke, five long-term field trials by AGES and Arbeitsgemeinschaft Hüttenkalk, 24 lysimeter trials by ILVA and SSSA and a new forest trial by Dillinger Hüttenwerke were started or continued in this project. Concerning the new test field, one was selected in each country, i.e., A1 at Schönfeld in Austria managed by AGES, F1 at Siikajoki in Finland managed by SSAB, and G1 at Mülheim an der Ruhr in Germany on arable land managed by Arbeitsgemeinschaft Hüttenkalk. The 24 lysimeter tests I1 performed in Italy by SSSA and ILVA employed the soil and water mimicking conditions around the ILVA steel plant in Taranto which was characterized for salinity. Finally, the long-term field experiments which were continued in this project were two long-term trials in Austria, i.e., A2 at Fuchsenbigl and A3 at Rottenhaus, performed by AGES with Thomas phosphate basic slag and which had been running since 1956 (almost 60 years of continuous slag application). Three further long-term field experiments managed by Arbeitsgemeinschaft Hüttenkalk were continued in Germany, i.e., G2 at Rösrath which was a permanent grassland limed since 1990 (almost 20 years of slag application), G3 at St. Peter in the Black

Forest which was a permanent grassland fertilized since 1954 (almost 60 years), and G4 at Essershausen which was an arable land limed since 1993 (almost 20 years). Finally, the forest test (GF) conducted by Dillinger Hüttenwerke near Dillingen included analysis of soil, vegetation and Douglas fir trees. All new test fields and lysimeters were fertilized with BOF slag while the long-term fields continued with their historical fertilization regimes. Slag fertilizers were collected from the steel companies in the consortium, i.e., Voestalpine, SSAB, Dillinger Hüttenwerke and ILVA, and were characterized by FEhS.

The new test fields presented different initial soil conditions. A1 site had a light-texture, very acid soil wit pH $CaCl_2$ = 4.5 (loamy sand) with a high liming demand and initial Cr and V concentrations of 20.6 and 37.7 mg/kg, respectively. F1 site featured a Podzol soil typical for the Ostrobothnia region with medium fine sand with 3–6 % organic matter, pH=5.6–6.4, at only 4 m altitude with a mean rainfall of 541 mm and mean temperature of 2.6 °C. G1 site presented a loess-derived Argic Luvisol (loamy sand) at 107 m altitude, with mean rainfall of 745 mm and mean temperature of 10.2 °C. The Italian lysimeter trials used soil and water characterized for salinity, reflecting the specific Mediterranean problem of exchangeable Na in coastal soils. All fields were limed and fertilized according to local practice, with slag limes and fertilizers compared to natural limes and fertilizers. A1 trial compared ladle furnace slag with 37.9 % CaO and 7.8 % MgO, with carbonate magnesium limestone with 30.8 % CaO and 7.2 % MgO at two dosage levels, i.e., 750 and 1500 kg CaO/ha/y, each with 4 replicates. F1 trial compared disintegrated BOF slag with carbonate limestone at a low dose of 370 kg CaO/ha/y and high dose of 740 kg CaO/ha/y following Finnish maintenance liming practices. G1 trial compared disintegrated BOF slag with carbonate magnesium limestone at two levels, i.e., 250 and 500 kg CaO/ha/y. The Italian lysimeters compared milled BOF slag (<1 mm) with carbonate limestone. Cultivation crops were chosen based on the most appropriate crop in each area thus making direct comparisons between countries difficult but ensured realistic growing conditions. In A1, the rotation included spring barley, winter wheat and potato, in A2 the rotation was potato, winter wheat and carrot and in A3 it was potato, winter wheat and pea. In F1, potatoes were the selected crop for all three years, in G1 the rotation followed was winter wheat, winter barley and winter rape while G2 and G3 were permanent grassland and G4 rotated through oats, triticale and maize. In Italy, the lysimeters grew tomato and potato in the first year, followed by tomato and durum wheat in subsequent years. Liming and fertilization, sowing and planting, harvesting, analysis of harvest and soil analysis after harvest were undertaken by each partner during each year of the project, covering three cultivation periods.

The slag fertilizers used in the project were characterized by FEhS. They had the added benefit of containing high amounts of Ca and Mg with higher solubility than magnesium carbonate in natural limestone and dolomite, as well as the presence of Cu, Zn, B and Co needed for good plant growth and animal health. However, the presence of heavy metals, in particular Cr and V, in the slag remained a topic of concern and long-term research was needed to show the effects of currently produced slag on soil and plants. The BOF slags used in the project contained significant amounts of Cr, e.g., 1123–1700 mg/kg in German BOF slags and 998–1021 mg/kg in ILVA BOF slag, and V, e.g., 1217–1350 mg/kg in German BOF slags and 623–661 mg/kg in ILVA BOF slag. Cr was present predominantly in the trivalent form Cr(III) with Cr(VI) levels below 1.0 mg/kg. This was fundamental since Cr(III) was far less toxic and considered a micronutrient in plants and animals. BOF slags also contained notable amounts of Fe, e.g., 17.2 % in the German slag, Mn (1.76–2.23 %), and other elements. The reactivity

and neutralization values of the slags were assessed according to European standards UNI EN 13971 and EN 12945 and were found to fulfil the requirements of the foreseen EU legislation for liming fertilizers in most cases. Despite not fully meeting the grain size distribution requirements of German slag fertilizer regulations, ILVA finer slag (< 1 mm) was judged suitable for lysimeter trials as its reaction in the soil might be higher than with the coarser product.

Concerning soil investigations, soil samples were collected from all test fields before the first fertilization and after each harvest over the three-year project period. The impact of liming materials of iron and steel slag origin was compared with that of carbonate limestone or burnt lime. Additional tests were done in pot experiments with soils from original locations and soils with naturally high contents of Cr and other heavy metals to obtain better comparable results. Special investigations on the leaching of elements from slag-treated soils and the probable pathway to groundwater were carried out using the lysimeter trials in Italy. The results showed that after three years of slag application according to normal fertilization and liming practices, there was a small increase at most test fields in Cr and V concentration in the soil, but this increase was small and not statistically significant in most cases. Indeed, it was very difficult to analyze the impact of heavy metal accumulation after only three fertilization seasons due to the heterogeneity of element concentrations in soils. Table 17 summarizes the Cr and V composition in selected test fields. The results for the long-term fields were more revealing at the A2 and A3 fields after about 60 years of basic slag application and at G3 also about 60 years where the "before" values already show the effect of long-term fertilization with slag. For comparison, the German limiting value for Cr in soil for residential areas is 400 mg/kg and for playgrounds is 200 mg/kg, while the measured values after slag treatment remained well below these thresholds.

On the long-term G2 trial with 25 years of annual BOF slag application, a detailed soil profile investigation was performed. Significantly higher Cr contents could only be detected in the first 10 cm of soil depth. At 5 cm depth, Cr was 73.8 mg/kg in the high-dose BOF slag treatment compared to 44.5 mg/kg in the unlimed control, while at 25 cm depth the values converged to about 42–46 mg/kg across all treatments. The distribution of V in the soil profile was similar, with considerable accumulation in the topsoil at 5 cm depth with values of 92 mg/kg in the high-dose treatment compared to 60.8 mg/kg in the control. Beneath 25 cm depth, V concentration in all treatments was similar. This demonstrated that even after decades of slag application, Cr and V remained immobilized in the upper soil layers and did not migrate to the groundwater.

The liming effect of slag fertilizers on soil pH was clearly measurable across all test fields. BOF slag significantly increased soil pH in all countries. At grassland trial after 25 years of annual application, BOF slag maintained consistently higher pH values compared to the control and even to carbonate limestone treatments. The soil microbial activity was generally positively influenced by liming with both slag and natural materials with no detrimental effects attributable to the higher Cr and V contents. In the pot experiments with soil naturally high and low in Cr and V, the basalt-weathered soil from Freiensteinau contained much higher levels of Cr, V and Ni than the comparable soil from Bellersen, but the very high heavy metal contents had no significant influence on plant growth, confirming that Cr(III) and V in the soil are largely immobile and non-toxic to plants. Italian lysimeters showed that

BOF slag application on saline conditions, i.e., sodic soil and saline irrigation water, significantly reduced the exchangeable Na percentage in the soil, which is beneficial for soil structure and crop growth in Mediterranean conditions. Concerning crop yields, the results across all test fields and crops showed a clear pattern with the addition of fertilizer, whether slag or natural, increasing the yield of all crops compared to the unfertilized control. The yields were most of the time not statistically different between slag and natural fertilizer treatments, but the positive trend was consistent. Table 18 summarizes the average yields for selected crops and test fields. Spring barley both at A1 and G1 test fields had a slightly better yield with ladle and BOF slag compared to the control, but natural fertilizer had the highest yield. Winter wheat had better yield most of the time with slag fertilizer compared to control or natural fertilizers at A1, A2, A3 and G1 test fields. Winter wheat yield was 49.5 dt/ha with the higher dose of ladle slag compared to 47.1 dt/ha for the control at A1 site in 2013, though this difference was not statistically significant. Winter rape had higher yield with slag and natural fertilizer compared to control at G1. Potato had higher yield with ladle and BOF slag compared to basic slag fertilizers and control at A1 and F1. However, at the Finnish site the third-year potato yields were significantly lower regardless of treatment due to poor quality seed, a two-week cold period in midsummer, and an exceptional dry season followed by about 90–100 mm of rain in one day which contributed to potato scab. Grass had consistently higher yield at G2 and G3 test fields with BOF and basic slag compared to carbonate magnesium limestone. Yields on all plots with annual basic slag were still the highest with better fodder qualities at G3 site after about 60 years of basic slag application, although significant Cr and V accumulations in the topsoil occurred. Tomato yield was higher with BOF slag than control at I1 and the positive effect was related to the significant decrease of exchangeable Na percentage observed with slag application. No positive effects of slag were observed on durum wheat grown in the Italian lysimeters.

Regarding the uptake of Cr and V in grain, plant or fruit, the results showed that Cr and V concentrations remained very low regardless of the fertilizer treatment in most crops. A small amount of Cr uptake was observed with slag fertilization in some crops, but the differences were not consistent and always very low. Spring barley had a small increase in Cr uptake with ladle and BOF slag compared to the control. Winter wheat had no clear pattern with Cr uptake since sometimes Cr in the grain was even higher in control than with fertilizers. Potato had a higher Cr uptake due to slag fertilization only twice out of six times it was planted. Grass did not show increased Cr concentrations with BOF slag at G2 but showed some increase with basic slag at G3 likely because the higher soil life attracted moles, voles and mice, leading to higher contamination of plant samples with soil particles. There was higher Cr concentration with BOF slag than with the control at I1 in the tomato fruit. Concerning V, no significantly consistent uptake was detected in any crop with slag fertilization. The investigation of Cr and V accumulation into edible organs of tomato and potato showed that the risk of accumulation in edible organs is very low with higher accumulation observed in the root, scarce effect induced by slag and very low translocation levels in fruits. It must be considered that Cr(III) is a micronutrient in plants and animals and small amounts are needed, so slightly higher Cr contents in food would actually be beneficial.

Table 17: Summary of Cr and V composition in soil before and after 3 years of fertilization.

Test field	Fertiliser	Cr before (mg/kg)	Cr after (mg/kg)	V before (mg/kg)	V after (mg/kg)
A1	Control	20.6	19.7	37.7	34.7
A1	LF slag	20.6	22.6	37.7	36.1
A1	Carb. Mg limestone	20.6	20.6	37.7	36.3
F1	Control	12.0	8.9	18.0	12.8
F1	BOF	10.0	10.1	16.0	19.8
F1	Carb. limestone	12.0	9.1	18.0	13.8
G1	Control	40.6	35.3	68.3	58.4
G1	BOF (*disintegrated*)	36.9	37.8	61.3	61.5
G2	Control	46.4	40.5	58.5	63.0
G2	BOF (*disintegrated*)	47.6	52.7	61.4	77.1
G3	Control	27.0	29.0	59.0	57.0
G3	Basic slag	49.0	53.0	136.0	106.0
I1	Control	50.3	44.3	16.8	17.0
I1	BOF (milled)	51.5	68.7	18.2	33.0

The phytosanitary effects of slags on plants were investigated through pot experiments focused on the Si content of slags and its potential to enhance plant resistance against fungal infections, particularly mildew. A pot trial was installed using the acid, nutrient-poor sandy soil "Lavesum" with spring wheat as experimental crop. The tested silicate liming materials included sieved and milled BOF slags, granulated BF slag, and a phosphate-enriched milled BOF slag, all applied at two levels, i.e., 5.5 and 11 g CaO/pot. Sodium silicate and carbonate limestone served as reference materials with all treatments doubled with and without fungicide application. Liming had a significant effect on soil pH increase for all BOF and phosphate-enriched slags, while the effect of carbonate lime was lower. Natural mildew infestation was observed during the growth period. In an early stage, i.e., 41 days after installation, a certain improved resistance could be observed. However, within two weeks the mildew infestation reached 70–80 % of the leaf surface with little differences between the higher-yielded treatments. The yields of spring wheat increased significantly by liming and fungicide application. There was a high correlation between the water-soluble Si content in soil and the uptake of Si by the plants with the

phosphate-enriched BOF slag showing particularly good plant availability of Si. The granulated BF slag led to the lowest soluble Si content in the soil due to its reduced solubility despite bringing the highest Si amount. Despite relatively good Si solubilities and good Si uptake by wheat, the effect on better mildew resistance was limited.

Table 18: Average yield of selected crops after 3 years of fertilization (dt dry matter/ha)

Test field	Fertiliser	Year 1	Year 2	Year 3
A1	Control	19.9 (barley)	47.1 (wheat)	488.2 (potato)
A1	LF slag	20.6 (barley)	49.5 (wheat)	504.7 (potato)
A1	Carb. Mg limestone	21.3 (barley)	48.7 (wheat)	488.4 (potato)
F1	Control	50.7 (potato)	44.2 (potato)	36.4 (potato)
F1	BOF	52.5 (potato)	41.1 (potato)	39.7 (potato)
G1	Control	102.8 (wheat)	55.0 (barley)	50.3 (rape)
G1	BOF (disintegrated)	108.4 (wheat)	56.4 (barley)	51.5 (rape)
G2	Control	137.6 (grass)	117.1 (grass)	130.0 (grass)
G2	BOF (disintegrated)	144.2 (grass)	113.7 (grass)	135.9 (grass)
I1	Control	36.7 (tomato)	25.7 (tomato)	36.4 (tomato)
I1	BOF (milled)	42.5 (tomato)	36.2 (tomato)	50.2 (tomato)

The forest field trials were conducted by Dillinger Hüttenwerke planting 250 Douglas fir trees in 2012 as one-year seedlings in "Jiffy" starter pellet propagation to ensure equal starting conditions. The trial tested different dosages of BOF and ladle slag, i.e., 4 and 8 t/ha, compared to untreated controls. Forest soil is mostly more acidic than agricultural soils and liming is a prerequisite for good growth of young trees. Soil investigations yielded the clearest results with a clearly visible positive effect of liming on base saturation increasing from 68.5 % to 77.8–92.6 % and on pH(H_2O) increasing from 4.65 to 4.80–5.35, depending on the liming agent and dosage. There was also an effect on the content of Cr and V in the topsoil, but the values remained well below German threshold values even for playground soils. The ground vegetation, dominated by bracken and Canadian goldenrod had overgrown the planted Douglas firs since 2013 with a close cover of more than 1 m in height. The biodiversity and spatial distribution of the species were independent of treatment. Cr and V average contents in the leaves seemed slightly increased two years after liming, but the spread of values did not allow a significant proof of any uptake into the biomass of the ground vegetation. The potential liming effect on tree size

showed a slight increase of growth, but this was not significant. Soon after mowing and measurements towards the end of 2014, game animals rooted off many of the remaining Douglas firs, but the test field was reconstructed to enable future measurements. It was concluded that liming resulted in better pH levels and cation saturation of the forest topsoil without significant pollution caused by Cr and V although no significant increases of biological production were found. Forest liming in Germany aims not at accelerating tree growth but rather at long-term stabilization of forest ecosystems against progressive soil acidification and loss of bases due to atmospheric acid deposition, including buffering acidification, regeneration of base saturation on clay minerals and stabilization of the nitrogen cycle.

The economic evaluation highlighted that the prices of liming materials for farmers in Germany were in an average ratio of 1:1 for slag and carbonate limestone or dolomite, and between 1:2 and 1:3 for slag and burnt lime. In Austria, farmers had some concerns regarding Cr in the slag however, the slag was sold as liming material and the prices were comparable. In Finland, BOF slag was about 33 % cheaper than natural lime based on the neutralization price. In all three countries, the slag was prepared to be sold as liming material, with high costs to farmers being mainly due to transportation. The use of slag as liming material had also the added benefit to contain a high amount of Si and other trace elements beneficial to plant growth. The current Italian legislation did not allow the use of BOF slag in agriculture. However, lysimeter tests showed significant achievements, in particular the reduction of exchangeable Na percentage in sodic soils representing a potential alternative to mined gypsum traditionally used for neutralizing alkaline and saline soils. BOF slag could be produced with less effort, and its use would allow saving natural resources while reducing energy-intensive mining activities for gypsum extraction. Concerning the social and environmental impact, the negative perception related to slag use is mainly linked to the common idea that industrial by-products used in agriculture could release pollutants into the environment and the food chain. The Italian word for slag had a negative connotation often linked with nuclear waste, while volcanic lava which presented a similar composition was perceived as a natural material. ILVA proposed the term "BOF inert" as alternative. Transparent technical and environmental communication was identified as key to increasing public acceptance.

In conclusion, the SLAGFERTILISER project demonstrated that Cr and V accumulation into soil was a consequence of slag application only over long periods, but the risk for groundwater pollution was very low, as these elements remained confined to the top 30 cm of soil even after 60 years of fertilization. Slag use as fertilizer was as beneficial in increasing crop yield as natural fertilizers, and always better than unfertilized controls. No significant uptake of Cr and V was observed in most crops except for potatoes, where half the time it was planted the increase in V was statistically significant, but this was partly attributable to the untypically high V content in BOF slag due to the use of Swedish iron ore. Further tests are needed to confirm these findings, with emphasis on what factors might increase the bioavailability of Cr and V in the soil. Informing farmers about which crops might take up Cr or V at higher levels will increase the confidence in slag use. The project provided valuable data supporting the sustainable use of currently produced slag fertilizers and liming materials, e.g., BF, BOF and ladle slag, across different European soil and climate conditions, contributing to a circular economy approach for the iron and steel industry, potentially decreasing the amount of slag sent to landfill.

2.2.13 REFFIPLANT: Efficient use of resources in steel plants through process integration (39)

The project was coordinated by SSSA with ILVA, Tata Steel UK, Swerea MEFOS, SSAB, and Process Integration Limited participating as partners in the consortium. The project started on the 1st of July 2012 and lasted almost three and a half years ending on 31st of December 2015. The overall project cost 2.35 M€ and EU contributed 1.41 M€, i.e., almost 60% of the budget.

The ReffiPlant project aimed at improving resources efficiency in terms of materials, water and energy in integrated steelmaking plants by minimizing them at source and by introducing new integrated solutions for recycling, reuse and treatment of wastewater, slag, sludge and dust. ReffiPlant aimed at undertaking investigations to provide information for developing novel Process Integration (PI) solutions for resource efficiency. It aimed at investigating solutions to improve water efficiency at source and available PI options for water systems, evaluating the impacts on energy minimization and CO2 footprint, and potential savings. Furthermore, it wanted to investigate solutions to improve material efficiency at source through reuse, recycling, and/or treatment of slag, dust and sludge, to identify PI options for a more flexible steelmaking system through low cost and higher secondary raw materials utilization. Finally, it aimed at developing new design frameworks for generating alternative process solutions leading to the implementation of PI measures and practical decision-support tools exploiting multi-objective optimization techniques for evaluating the feasibility of different solutions. The project also intended to assess the engineering, practical aspects and resource efficiency improvements associated with the implementation of the proposed PI solutions by undertaking on-site experimental activities at pilot scale and identifying the constraints for different EU sites. It can be summarized that ReffiPlant aimed at showing how to exploit PI methods and techniques with multi-criteria optimization to identify overall solutions that point at minimizing the steelmaking ecological footprint.

An analysis of the by-products and wastes flows including water networks of the involved steelworks, i.e., ILVA, TATA, SSAB, was carried out to develop solutions for resources efficiency. This analysis resulted in an inventory of the main flows and lists of key processes and factors affecting water and material efficiency, respectively. After the definition of the key parameters and performance indicators, each industrial partner identified the potential main directions of investigation related to their facilities to improve the management and the exploitation of water and by-products. In addition, two lists of practical and technical constraints affecting water networks and by-products and wastes reuse and recycling in the steelworks, and also affecting the PI solutions, were identified. Furthermore, the non-technical constraints that could affect the PI-based solution were analyzed and a common list of all the industrial partners was produced, representing the general situation of the European steelworks. Industrial partners carried out analysis to provide parameters related to water streams and water treatment processes for modelling work and data collection. In this regard, lists of measurement points and common lists of relevant contaminants and main process variables were produced for ILVA, TATA Steel and SSAB for the modelling work. In addition, an analysis of the most relevant parameters related to by-products and wastes fluxes and treatment processes was carried out as well as lists of the main contaminants related to each by-product or waste and of the main process variables. They were considered in the modelling of processes of by-products treatments and reuse.

A comparative study of the selected simulation tools available was carried out. This resulted in choosing Aspen Plus and Aspen Hysys as more generic and flexible tools. In addition, the WATER tool was preferred due to its holistic approach. On the other hand, the reMIND optimization framework for by-products and waste management, which embeds MASMOD and TOTMOD to calculate mass balances on specific processes, was preferred. The data from the three industrial sites were deeply analyzed and reconciled and a unified approach was developed and applied to a case study on each of the three industrial sites to carry out mass, energy and contaminant balances. In addition, the analysis for identifying the main water treatment processes to model was carried out and the most relevant ones were modelled by developing a general model template to allow a unified development of the models. This template could be treated as a black box communicating with the incoming and outgoing water streams only the most relevant information, e.g., water temperature, flowrate, pH, contaminants properties such as concentration, density, particle diameter. Process knowledge collection, modelling and simulation work allowed identifying a list of potential solutions and technologies for water and energy efficiency at industrial partner sites.

The variables relevant for process modelling were identified and relevant process data were collected at ILVA and SSAB industrial sites. In particular, the analysis was focused on possibilities for a more efficient recovery and treatment of some by-products or waste flows. These procedures aim at reducing the volume of waste for disposal, the amount of hazardous waste and the recovery of some raw material for internal or external reuse, according to principles of circular economy. To identify potential solutions/technologies for waste recycling, two processes, i.e., the R1 process and non-thermal washing, were investigated at ILVA for the recovery of oily scale after oil removal. The application of fine grained BOF sludge to produce briquettes and the use of steel LS as slag former or as complementary binding agent in agglomerates were investigated at SSAB. In addition, fine-grained materials such as BF flue dust and fine scrap were recycled via cold bonded briquettes. Finally, the potential utilization of BOF slag for agriculture purposes was considered. To investigate and evaluate the two waste treatment processes at ILVA some models were developed by SSSA in Aspen Plus®. In addition, simulations with the Excel-based TOTMOD model for BF, hot metal desulphurization and BOF were carried out for SSAB for the recycling into BF of BF flue dust through direct injection, of BOF fine sludge through palletization, and of steel LS as slag former. Simulations showed major cost savings for the first two solutions, while the third one implied minor or no cost savings. Despite this, all solutions proved to be relevant from an environmental perspective showing potential reductions in landfilling.

Some optimization studies on water networks were carried out to develop holistic models suitable for multi-objective optimization. In particular, some holistic models aiming at the simplified representation of common unit operations of resources utilization to predict the main properties of products flows, were developed. These models were inserted into a general-purpose tool for preliminary simulation and optimization of industrial water networks. A superstructure approach was chosen to carry out the integrated water network optimization studies, considering water re-use, water regeneration and re-use, water regeneration and recycling, local recycling around process and treatment units and pre-treatment of feed-water streams. The mathematical model of water network consisted of mass balance equations for water and contaminants for every unit in the network. The

model was suitable for studying in new designs and retrofits, i.e., fixed topology studies, re-use studies involving re-piping opportunities or regeneration & reuse studies involving distributed treatments. A model for the water network at SSAB plant in Luleå was developed with a mass and heat balance to compare available measured values for sources and sinks, to calculate consumption and the flow or quality of the discharge water temperature and chemical composition affected by a change in the system.

Optimization studies on material flows were used in the modelling for recycling of secondary materials at ILVA and SSAB plants. It is mixed-integer linear programming (MILP) by using the software reMIND. The developed model made possible to perform total analysis assessing effects from changes in operations. The analysis could be performed as multi-objective/multi-criteria analysis and could be made with different time steps. In this context, the objective function included different variables which could be minimized or maximized, such as landfill, cost, CO_2 and energy. The developed system optimization model was used by MEFOS and SSSA to investigate recycling strategies for secondary materials for SSAB and ILVA, respectively. Optimization was made regarding the different recycling options of dusts, sludges and slag, minimizing the landfilled amounts, while constraining the energy consumption.

Concerning the implementation of Multi-Objective Optimization techniques, a module was developed within the WATER software wherein two optimization objectives can be selected at a time. One of the optimization objectives needed to be cost-based, e.g. minimize capital cost, minimize operating cost, or minimize total cost, while the other need to be flow based, e.g., minimize freshwater flowrate, minimize treatment flowrate, or minimize discharge flowrate. A series of optimization runs were executed with different target value boundaries for flow based optimization objective function. Some cases-study related to water efficiency were investigated and some solutions/technologies were selected. Their viability was investigated in detail through process modelling and simulations. On the other hand, concerning the case studies related to Tata Steel water network, a 3 steps systematic work process identifying the improvement opportunities and carrying out further optimization work for 11 case studies was performed.

Some cases-study related to by-products and wastes were analyzed. For ILVA wastes and by-product related issues, some potential solutions included the distillation and pyrolysis for sludge/scale recovery, a mill scale washing process for not oily scale recovery, the use of BOF slag as fertilizing material and for internal reuse, e.g., pellets for sinter plant. For the last case study, simulations were carried out by using the holistic models developed by SSSA for material treatment units. Promising results were achieved about potential benefits related to the reduction of waste amount and cost saving due to external use for agriculture purpose although Italian regulations did not allow treat its industrial wastes without a special permission. On the other hand, SSAB developed a model to carry out MEFOS process simulations on preliminary case studies. The model included element distribution between slag and metal to be used for process simulation and analysis of various operating conditions as well as the influence of specific process parameters.

The MIND method was first developed to model industrial energy systems, but an upgrade including the development of ad-hoc superstructures allowed its Java-based version to be used as a powerful

decision support tool also in the steelmaking field. The analyses carried out by MEFOS and SSSA respectively for SSAB and ILVA under different conditions and related to different scenarios represented an assessment of the applicability of reMIND also for analyses to improve by-products and waste re-use and recycling.

Concerning the application of the selected novel solutions for water efficiency, ILVA assessed the possibility to treat and reuse the wastewater of the coke making area. For this purpose, indications coming from SSSA simulation were followed and tests were carried out in a pilot plant including chemical and physical treatments, including Ultra Filtration and Reverse Osmosis. The results highlighted contaminants removal by using the global treatment scheme of Reverse Osmosis in series to Ultra Filtration resulting in high quality water to be reused. Tata Steel carried out magnetic filter trials at the BF gas wash area to investigate the recycling of the overflow water with suitable treatment to improve the Lagoon water quality, lower the cost of running the existing dewatering plant, lower the pumping energy costs, improve cooling tower water quality and associated costs and provide substantial water conservation. However, water recycling increased water concentrations within the BF was wash water system thus requiring suitable water treatment such as filtration of suspended solids and treatment of the water for reducing ammonia and chlorides. A commercially available magnetic separation unit was assessed for the filtration of suspended solids in the water overflow and SSAB pursued a trial campaign on the BF gas cleaning system to investigate the correlations between increased recirculation and conductivity, ammonia nitrogen, chlorides, as well as to find out the behavior of other substances affecting the process, e.g., o the risk of fouling. During a few days the sludge flow was reduced, thereby increasing the degree of recirculation.

Concerning resource efficiency related to by-products and waste, experiments were carried out at ILVA to produce Fe-rich pellets maximizing the BOF slag fraction. Following indications obtained by SSSA through reMIND simulations, ILVA laboratory produced good pellets in terms of amount and quality with a mixture of pretreated BOF slag and sludge. BF dust, BOF dust and LS were considered in the preliminary case studies at SSAB. Almost half of the produced BF dust was injected into BF and the rest was recycled through briquettes and BOF sludge was used in BF via briquettes. In addition, on-site tests on the addition of LS as slag former in the BF were carried out.

PI-based solutions for water efficiency investigated through the on-site trials in the steelworks involved, were assessed by considering contaminants in water streams, investment and operating costs and savings of fresh water according to the preliminary analysis. Then, the selected PI-based solutions for resource efficiency through enhanced material recycling, investigated through the on-site trials at ILVA and SSAB, were assessed by considering the overall amount of wastes and by-products that were recovered and not landfilled as well as the overall amount of saved primary raw materials, according to the preliminary analysis. This allowed to evaluate the improvements made by implemented solutions. Finally, technological and economical constraints of the recommended implementation of considered case studies for ILVA, Tata Steel and SSAB were analyzed and assessed. It was highlighted that recycling was common practice in the steel sector, depending on plant layout, legal restrictions and physical conditions the level of efficient material use.

To sum up, ReffiPlant developed a methodological approach to elaborate and preliminarily assess PI-based solutions and technological improvements to increase resource efficiency based on data analysis and holistic simulation tools for several case studies. This approach proved its efficiency with different general-purpose and specific simulation tools, and it was fully transferable to other case studies and to other companies. One of these tools was developed inside the project and was dedicated to holistic simulation and multi-objective optimization of water networks. The application of multi-objective optimization proved to be valid in the case studies and different solutions could be found depending on the constraints. Simulation could not replace the development of on-site trials but were a powerful support to plan the useful ones. Results of the on-site trials confirmed in most cases the outcomes of the preliminary simulations, showing the efficiency of the adopted simulation frameworks as well as the validity of the pursued approach. The results showed that it was possible to improve resource efficiency in the steelworks through PI by increasing the reuse of water and the recycling of by-products and waste as well as saving energy consumption. Major cost savings could be achieved if internal recirculation could replace raw material such as iron ore, coke and limestone. These benefits were coupled to environmental impact reduction through virgin material and freshwater savings, smarter material handling and reduction of disposal. However, investment costs were not always negligible and could represent a barrier. Most of the analyzed and achieved solutions showed a good potential for exploitation to improve resource efficiency in integrated steelworks through the full-scale implementation in the future.

2.2.14 SLACON: Control of slag quality for utilisation in the construction industry (40)

The project was coordinated by FEhS with BFI, RINA (Registro Italiano Navale)-CSM, Sidenor and Riva Acciaio participating as partners in the consortium. The project started on the 1st July 2012 and lasted almost three and a half years ending on the 31st December 2015. The overall project cost 1.83 M€ with EU contributing 1.09 M€, i.e., almost 60 % of the budget.

The SLACON project was developed to address the growing need for sustainable management of EAF slag which was a major by-product of steel production in Europe. EAF slag represented both an environmental challenge and an opportunity as a secondary raw material for construction considering the Mtonnes generated annually. However, its reuse is limited by inconsistent quality and concerns over the leaching of potentially hazardous elements such as Cr, Mo, V, and others, often exceeding regulatory limits by factors of 1.5-5 depending on the element and test conductions. The project investigated how to improve the environmental and technical performance of EAF slag with the goal of increasing its safe utilization in construction applications. This involved the development of treatment methods that could reduce leaching up to 90 % for certain elements, stabilize chemical composition, and be realistically implemented at an industrial scale. A broader objective was to support industrial synergy by transforming steelmaking residues into valuable resources for the construction industry, while also addressing the lack of harmonized regulatory frameworks across Europe.

To achieve these objectives, the project investigated slag treatment at two key stages namely at the liquid phase and after solidification. In the liquid phase, the focus was on modifying slag chemistry

through metallurgical control including the addition of specific mineral phases and adjustment of process parameters such as temperature and cooling conditions. These interventions aimed to influence the formation of stable mineral phases capable of immobilizing problematic elements before slag solidification with targeted phase fractions, e.g., spinels and Ca-rich silicates, increasing by approximately 20–40 % depending on additive dosage.

In parallel, post-solidification treatments were studied to further improve environmental performance. These included controlled cooling strategies, mechanical processing, and washing techniques designed to remove or reduce the mobility of contaminants. Controlled slow cooling reduced the amorphous phase content by approximately 15–30 % enhancing mineral stability. The combination of these approaches provided a comprehensive strategy in which both primary in-process and secondary post-process treatments were used to optimize slag properties.

A central aspect of the project concerned the understanding and controlling of EAF slag leaching behavior by tailoring basicity, i.e., CaO/SiO_2 ratio, typically adjusted in the range 1.5–2.5, FeO content, and Al_2O_3 additions up to 5-10 wt.%. The results showed that targeted modifications during slag formation can significantly influence the release of specific elements. For example, the addition of Si-rich materials such as sand reduced Ba leaching by 30-60 % without negatively affecting V behavior. Similarly, the incorporation of Ca-rich additives helped reduce V mobility by 20-50%, while Al oxide promoted the formation of stable spinel structures that effectively immobilized Cr achieving reductions of 70-90% in leaching concentrations.

These findings demonstrated that controlling mineralogical composition is a powerful tool for improving slag stability. However, the effectiveness of such strategies is highly element specific. Indeed, significant reductions were achieved for some elements while others such as Mo and Se proved to be difficult to stabilize through liquid-phase treatment alone, with reductions typically limited to values <10-20% for Mo and negligible for Se. This highlighted the inherent limitations of thermodynamic control and the need for complementary treatment approaches.

The project also explored post-treatment and water treatment techniques given the limitations observed in stabilizing certain elements during slag formation. Washing processes were investigated to remove soluble contaminants from solid slag. Although this approach showed some potential, it was generally insufficient to reduce significantly the leaching of elements like V, i.e., reductions of only 10-25%, indicating that most V remains structurally bound or slowly released from the matrix.

More promising results were obtained in the treatment of process water generated during slag handling and washing. The use of Fe hydroxide-based absorbents proved to be effective in removing dissolved contaminants including Mo, V, and F-, from industrial wastewater, with removal efficiencies up to 80-95% for Mo, 70-90% for V, and 60-85% for F-. This indicated that liquid-phase treatment of leachates could provide an effective complementary solution to ensure overall environmental compliance while solid-phase stabilization may be challenging for certain elements.

The project included pilot-scale trials to validate laboratory findings under more realistic industrial conditions. These trials confirmed the feasibility of several treatment strategies, particularly those involving additive-based control during the liquid phase and adsorption-based water treatment. At the

same time, they highlighted practical challenges, especially in scaling up washing processes and ensuring consistent performance across different slag compositions.

Pilot-scale results showed slightly reduced efficiencies compared to laboratory conditions with Cr leaching reductions of approximately 70-85% and V reductions ranging between 15-40%, depending on slag composition and process stability. The results underlined that while technical solutions exist, their successful implementation depends on careful adaptation to specific plant conditions. Variability in raw materials, furnace operation, and slag composition means that no single treatment method can be universally applied, reinforcing the need for site-specific optimization.

A major barrier to the widespread reuse of EAF slag is the regulatory framework governing its classification and use. The project emphasized that leaching behavior is the key factor determining whether slag can be considered a waste, a by-product, or a secondary raw material. However, the absence of harmonized European standards leads to significant differences in acceptance criteria between countries. As a result, the same slag material may be suitable for use in one region but not in another, limiting market opportunities and discouraging investment in treatment technologies. The findings of the project therefore support the need for more consistent and science-based regulations at the European level, which would facilitate the broader adoption of improved slag management practices.

The SLACON project demonstrated that the environmental performance of EAF slag could be significantly improved through a combination of metallurgical control and targeted treatment processes, achieving up to 90 % reduction in Cr leaching, 60 % in Ba leaching, and 50 % in V leaching under optimized conditions. Adjustments made during the liquid phase are particularly effective for stabilizing certain elements, while water treatment technologies offer viable solutions for managing contaminants that cannot be immobilized in the solid phase, with removal efficiencies up to 95 %.

Despite these advances, challenges remain for elements like Mo and Se with stabilization typically <20% in solid phase and in the scaling and standardization of treatment methods. Future work should focus on developing more robust stabilization techniques, improving process integration, and advancing regulatory harmonization across Europe.

The project provides technical management guidelines summarized in Figure 14 for increasing the utilization of EAF slag in construction, contributing to resource efficiency, waste reduction, and the transition toward a more circular industrial economy. Ba leaching can be reduced by adding silica, e.g., sand, though care is needed to avoid increasing V leaching. Liquid-phase composition control promotes formation of less soluble phases like gehlenite and can be implemented directly in the slag pot. However, crushing and sieving are still required for reuse. V leaching can be decreased by adding ladle furnace slag, increasing Ca content and alkalinity. Fast cooling and washing were not effective at industrial scale. Mo and Se leaching could not be mitigated therefore the main option is controlling scrap input. Mo appears linked to metallic phases and particle size. Storage and washing showed no significant effect. Process water treatment is necessary to prevent cross-contamination. A filtration system was developed to remove Mo, V, Se, and F^- from recirculated water.

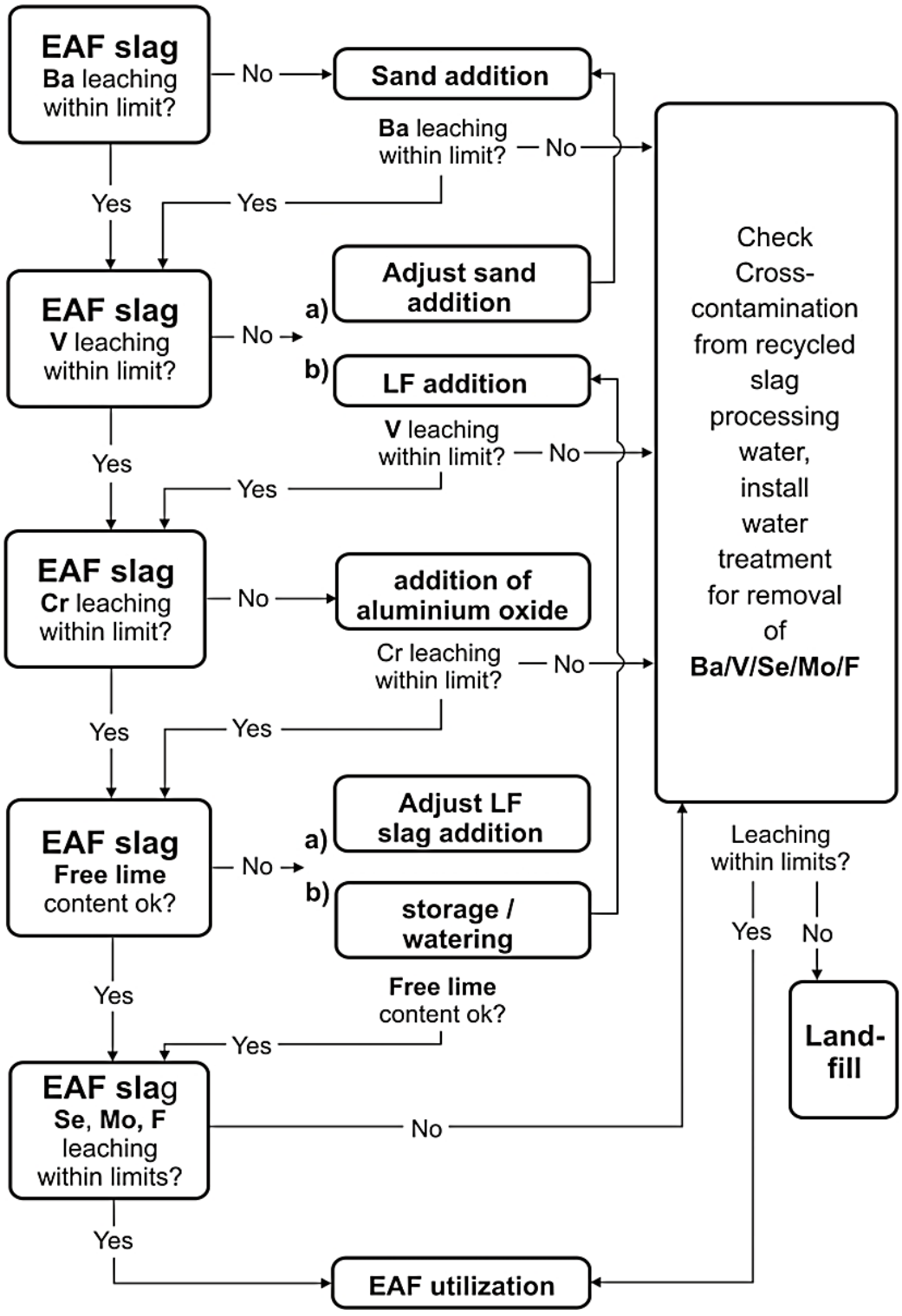

Figure 14: Guidelines developed for EAF slag management

2.2.15 EIRES: Environmental impact evaluation and effective management of resources in the EAF steelmaking (41)

The project was coordinated by SSSA with Riva Acciaio, Sidenor, BFI, DEW, CSM, Fundación Tecnalia, O.R.I. Martin, and Tenaris participating as partners in the consortium. The project started on the 1st of July 2013 and lasted almost three and a half years ending on the 31st of December 2016. The overall project cost 2.84 M€ and EU contributed 1.70 M€, i.e., almost 60 % of the budget.

The EIRES project provided plant managers and technicians with a consolidated and understandable metric to quantify and monitor the overall environmental impact of the production route with a view at reducing the environmental impact of EAF steelmaking. This objective was achieved by building up a data inventory for EAF steelmaking route based on historical industrial databases, available on-line specific plant database and data of dedicated acquisition campaigns. Based on data inventory, metrics to quantitatively assess the environmental impact of a specific electric steelmaking plant were defined and implemented in a metrics tool to monitor the evolution of the metrics over time. The metrics and Key Performance Indicator (KPI) were also developed by exploiting recognized techniques, such as LCA. After that, a process modelling tool was set up using the data inventory as input for an integrated modelling of the energy and mass flow of a specific EAF steelmaking plant and it was used to investigate different scenarios for potential reduction of the environmental impact of the process. This allowed to develop an integrated decision support tool to access and track the current environmental impact of the process and to assess the potential effect of modifications of process operating conditions on the environmental footprint of the whole production cycle. Finally, the effectiveness and reliability of the integrated decision support tool was validated with case studies related to specific aspects at the industrial partners sites.

Different tools and methodologies were developed during the project to reach these goals trying to provide practical and understandable tools for monitoring and simulating operational scenarios. The main results achieved included the creation of a data inventory through the collection of historical and specific data related to steel production based on EAF steelmaking including energy consumption, materials, emissions, and waste, the definition of 30 KPIs to quantify energy efficiency, air emissions, by-products and waste management, and water consumption, the development of simulation models to analyze energy and mass flows, emissions, and waste management using different software such as Aspen Plus and Matlab/Simulink and the development of a decision support tool combining process simulation, KPI assessment, and LCA to monitor and improve the environmental performance of specific electric steelmaking plants. Industrial case studies focused on industrial partners plants, i.e., Riva Aciaio, Sidenor, Tenaris, ORI Martin, and DEW, were considered to assess the effectiveness of the developed tools and identify measures to reduce their environmental impact.

The preliminary process inventory related to analyzed steelmaking plants included facilities, products, input materials, by-products (slag, refractories, etc.), waste flows, energy consumption (electricity, natural gas, etc.), and emissions including direct and indirect CO2 emissions, dust, and dioxins for different process phases. A review of existing tools and techniques for environmental impact assessment including standards ISO 14001 and ISO 14004 for CO2 emissions calculation, CEN/TC 264 for energy and mass balances and Green House Gases (GHG) emissions, and ISO 14040 and ISO 14025

for LCA, was carried out. In addition, the best available technologies for energy efficiency, emissions control, waste handling, and water management were identified by analyzing different Best Available Technology Reference Documents. Furthermore, some software tools for KPI evaluation, process simulation tools (Aspen Plus and Matlab/Simulink), and LCA were selected. The 30 KPIs were developed to measure energy efficiency, atmospheric emissions, waste/by-product management, and water usage and the KPI Evaluation Tool was developed to calculate and visualize the selected KPIs, enabling analysis of trends and environmental performance.

Process models were developed to calculate energy consumption, main atmospheric emissions and water consumption and the main streams of solid by-products and wastes, useful to evaluate the selected KPIs. Mass and energy models related to EAF steelmaking process were developed using Aspen Plus and Matlab/Simulink. Concerning Aspen® Plus simulation, each stage of EAF process could be thought as the sum of the effects in terms of material and energy streams. The model allowed to compute products, by-products and off-gases composition and monitor energy consumption. It included an EAF simplified model, EAF melting phase, EAF deslagging and refining phase, ladle furnace treatment, vacuum degassing and continuous casting treatments. Matlab simulation included a complete EAF steelmaking model based on Matlab/Simulink process model to calculate mass and energy balance and freshwater consumption, but also to calculate the relevant KPIs, single KPIs, offering several possibilities for selection and filtering, e.g. steel grades, process routes. A complete model of the fumes network to compute the main atmospheric emission and dust production was performed according to RIVA plant. Analogous work was performed with water emissions where a complete model of the water network to compute water consumption was developed according to RIVA plant. Furthermore, concerning by-products and wastes, the main streams of solid by-products and wastes were calculated through the mass and energy, water and fumes networks models. As in the real plant, EAF and LF slags were produced also in the models during the main production process and dusts were collected by fumes treatment while scales and sludges were the output of the wastewater treatment.

A Life Cycle Inventory (LCI) was organized and data for LCA were collected to identify and characterize processes and sub-processes involved in steel making plants. Tecnalia developed the LCI using the data provided by the industrial partners allocating them an environmental load using the Ecoinvent database 3.1. Life Cycle Impact Assessment (LCIA) was developed using the Ecoinvent database and CML 2001 methodology to assess environmental impacts. CML 2001 impact assessment method and ISO 14025 standard indicators were applied to obtain units of environmental impacts. The impact assessment categories selected were: 1) Climate change in kg CO2-eq, 2) Stratospheric ozone depletion in kg CFC-11, 3) Photochemical oxidation in kg ethylene, 4) Acidification potential in kg SO2-eq, 5) Eutrophication potential in kg PO4-eq, 6) Non-renewable fossil in MJ-eq. Furthermore, an Excel-based tool for LCA studies was developed independently of licensed software. The tool consisted of various work sheets, and the output included numerical and graphical presentation of results by impact category of the different products/services (EAF, ladle furnace, continuous casting and others).

An integrated decision support tool combining KPI evaluation, process simulation and LCA tools was designed and two global indexes GIKPI and GILCA to represent overall plant environmental performance were defined. A software tool was implemented to compute and aggregate KPIs and LCA indicators. Software architecture included different modules, e.g., LCA tool, KPI tool, and Process Simulation tool. The aggregation of KPIs into a single GIKPI provided a fast overview of the overall environmental behavior of the process and did not replace a detailed analysis of all indexes. The GI was expressed as dimensionless number and a percentage calculated over the possible maximum value of the GI itself. Different aggregation methods could be used such as simple addition of the scored KPIs, sum of the KPIs scores weighted against sampling frequency with a factor n/12 with n being the number of samplings per year, sum of the KPIs scores weighted against family coefficient inversely proportional to the number of components of the family (i.e. energy efficiency, CO2, other emissions, waste, water) and sum of the KPIs scores weighted against sampling frequency and "family", i.e., method 2 and 3 coupled. The comparison between scoring and aggregation methods suggested that the 4 aggregation methods gave similar trend of GI with standard method being the most different. Fixed scoring allowed the definition of plant historical trend and could overestimate the variation of the index, resulting in a useful diagnostic tool. BAT scoring allowed a more reliable calculation of GI to have a common recognized scoring of the recorded value and allowed the comparison among facilities of the same company. BFI also included the computation of some KPIs within a software tool for Statistical Process Control which was already available at the DEW steelworks. It allowed displaying the evolution of selected KPIs and filtering this display for certain time periods, steel grades or process routes.

Case studies at industrial partner sites were carried out to evaluate the effectiveness of some plant modifications and to identify efficient measures to reduce environmental impact, to test the integrated simulation tool in different industrial scenarios, and to develop general guidelines for the exploitation of the metrics and of the integrated simulation tool. The RIVA Acciaio case study aimed at evaluating potential pathways for the reduction of electric energy consumption, the control of steel quality during process changes, and the improvement of the environmental impact. In particular, they considered a modification of the normal production route that included a first stage of Fe-alloy addition in the ladle during EAF tapping and maintaining the addition of Fe-alloys only at ladle furnace station. This practice resulted in the achievement of the desired composition for each steel family tested and a negligible change in Fe-alloys content in the steel. A significant reduction between 5 and 12 % in ladle furnace slag production for each tested steel family was observed thanks to the minimization of Fe-alloy oxidation resulting from the lower time and oxygen to react. This, in turn, resulted in a higher electric energy consumption of 1-2 % per ton of steel since reduced oxidation provided a lower chemical energy to the system and higher electric energy is required to keep the desired temperature value. Overall, the reduction of direct CO2 emission was negligible around 0.2-1 %. Another modification considered for the Riva Acciaio case study concerned the internal reuse of slags. In particular, the standard route made a negligible reuse of slags while the modified route proposed a partial replacement of lime and dolomite with the total ladle furnace slag internal recovery and by the partial internal recovery of EAF slag (70 %). In particular, the analyzed case studies were characterized by different percentages of EAF and ladle furnace slags recovered or landfilled. The study demonstrated that the

final composition of the desired steel was not affected by the internal recovery of the slags as well as the metallic yield. EAF Energy distribution remained almost equal in all analyzed scenarios with only electric energy consumption directly increasing with the amount of internal recovered slag. In particular, required electric energy increased by around 2.5-7 %. The partial replacement of lime and dolomite resulted in a reduction around 18-55 % of specific non-metallic charged materials but also in a significant increase of EAF slag, i.e., 15-41 %, and ladle furnace slag, i.e., 9-27 %. This modification of the practice also resulted in a modification of EAF slag composition with higher Al2O3 and SiO2 and FeO content and lower CaO content. Analogously, ladle furnace slag composition resulted in a higher Al2O3 and FeO content and in a lower CaO and SiO2 content. Overall, only the ladle furnace slag recovery proved to be a good compromise as the use of EAF slag significantly increased the required electric energy and the production of other slags.

SIDENOR case study assessed the impact of Basauri plant considering different operating scenarios. The first case study aimed at identifying the categories with the highest impact in terms of Global Warming Potential (GWP) and photochemical oxidation (kg C2H4 eq) and acidification potential (kg SO2 eq) demonstrated to be the most relevant ones. The second case study analyzed the raw materials to identify the ones with the highest impact on GWP and FeSiMn proved to be the most affecting one. The third case study was dedicated to the eco-design of the product, disclosing the importance of considering life cycle considerations during product development. In particular, the effect of FeSiMn replacement with SiC was analyzed considering a replacement rate of 30 and 50 %. In both cases, an increase of GWP impact was observed and it was associated with the direct emissions of SiC combustion and with the indirect emissions of the energy necessary to melt more quantity of material. The fourth case study investigated the influence of raw materials on CO2 direct emissions. In particular, the evolution of CO2 direct emissions related to EAF and the impact of the emission produced by the coal and pig iron on the total quantity were investigated. Coal and pig iron were removed from the scrap mix given their impact to the total CO2 emissions. The last two case studies evaluated the influence of selection of different electric mixes and the influence of raw materials on process KPIs.

TENARIS case study aimed at assessing the impact of some process modifications on the overall environmental impact of Tenaris Dalmine production process. The first case study assessed the effect of the installation of an activated carbon injection system in the off-gas treatment plant of the steel shop to reduce dioxins emission in atmosphere. The installation of this system ensured a reduction of about 70 % in dioxins emission but caused an increase in electricity consumption of 0.03% and in waste generation of 0.4%. Despite this, the global index pointed out an improvement thus confirming that the two secondary effects could be considered negligible. The second case study assessed the use of rolling mill scale in EAF as scrap substitute. This solution produced an increase of 13 % in energy consumption, no carry over in slag or dust occurred and all the scale was reduced to iron in the EAF. From the environmental perspective, the advantages in terms of increased efficiency in material reuse substantially overcame the negative effect of the increased energy consumption. The third case study concerned the reuse of ladle slag in EAF as lime replacement. The energy required for this practice would be higher than in standard practice because 40 % more materials must be heated. Material efficiency would improve as the total amount of waste and by products would be lower. The specific

non-metallic charge would decrease because the process used fewer virgin resources and there would be a negligible variation in the CO2 mass balance, due to compensation between all the variations in input and output. GIKPI showed a slight improvement in the environmental performance, considering all these aspects together thus meaning that LS recovery should be convenient from an environmental point of view.

ORI Martin case study aimed at evaluating and controlling gaseous emissions with special emphasis on dioxin and dust assessing the effects of the installation of the I-recovery system after the Consteel tunnel. Results showed that the stack values of dust emissions were not affected, no new dioxin was formed, and reduction of energy consumption and CO2 emission was considered considering the typical energetic performances of I-recovery system. In this context, the increase of the GIKPI showed improvement in the overall environmental performance.

The DEW case study aimed at optimizing energy and resource efficiency to improve the environmental impact of the production of selected stainless-steel grades via the EAF route in the Siegen steel plant considering also the ladle furnace and VOD. The first case study analyzed the effects of different process routes on the environmental impact of different stainless-steel grades. For instance, direct specific power consumption for production of selected steel grades along different process routes demonstrated that Ruhrstahl Heraeus operations or return of heats showed significantly higher values of Direct Specific Power Consumption. The second case study analyzed the effect of different EAF charge material mixes on the environmental impact of production of selected stainless-steel grades. The properties of used scrap types were determined with multi-linear regression calculation for 1100 stainless steel heats in terms of metallic yield and composition, specific electric meltdown energy requirement, specific requirement of oxygen input and slag formers, direct CO2 emissions, and recycling /depositing costs for yield losses via dust and slag. After that, determination of optimal scrap mix for selected stainless steel grades was performed considering as optimization criterion the minimization of the cost function defined by properties such as purchase costs, metallic yield, element-wise composition, specific meltdown energy requirement, specific requirement of oxygen input, specific requirement of slag formers, direct CO2 emissions, costs for yield losses via dust and slag. Furthermore, weighing between the different contributions to overall costs allowed to consider environmental impact in the optimization calculation. Compared to standard scrap mix all KPIs could be improved and also scrap purchase costs were lower. However, impact on secondary metallurgy must be considered.

2.2.16 PSP-BOF: Removal of Phosphorous from BOF Slag (42)

The project was coordinated by Swerea MEFOS with BFI, Voestalpine Stahl, SSAB MEROX, FEhS, ILVA SPA and SSSA participating as partners in the consortium. The project started on the 1st of July 2013 and lasted almost three and a half years ending on the 31st of December 2016. The overall project cost 2.41 M€ and EU contributed 1.44 M€, i.e., almost 60 % of the budget.

The PSP-BOF (Removal of Phosphorus from Basic Oxygen Furnace Slag) project focused on solving a persistent challenge in steelmaking namely the limited recyclability of BOF slag due to its P content.

Indeed, conventional BOF slag contains approximately 1.5–3.0 wt.% of P_2O_5 which hinders internal recycling due to P accumulation in steel which affects product quality. At the same time, BOF slag contains valuable resources including 10–25 wt.% of total Fe and high levels of calcium oxide which make it a potential secondary raw material if the P content can be controlled. The PSP-BOF project aimed to develop efficient processing methods to selectively concentrate Fe-rich and P-rich phases to create distinct material streams suitable for internal reuse and external applications.

No correlation was found between the P content in BOF slag and steel grades. Furthermore, P content was almost constant in the BOF slag therefore no special selection was conducted. Two main processing routes were explored to achieve selective P removal. The first one was solid-state processing based on controlled cooling and mechanical separation while the second one was liquid or semi-liquid slag treatment with chemical modification. Both approaches relied on the principle of phase segregation enabling either Fe or P to concentrate in specific mineral phases rather than being uniformly distributed in the slag. The solid-state route involved engineered cooling profiles to generate a heterogeneous microstructure that enabled efficient physical separation. Controlled cooling facilitated the crystallization of distinct mineral phases including Fe-rich wüstite or metallic iron droplets and P-rich calcium silicate phases. Subsequent comminution and separation techniques, i.e., magnetic separation and particle classification, allowed recovery of Fe-rich fractions with 30–60 wt.% of Fe and a magnetic separation efficiency of 70–90 % depending on particles size and slag composition. The P content in the remaining slag fraction dropped below 1 wt. % thus making it suitable for internal recycling in sinter or BF operations. In the liquid-state route, molten BOF slag was modified with secondary P containing materials such as sewage sludge ash to enhance the formation of P-enriched phases during controlled cooling and solidification. Phase enrichment factors of 2–4 times for P were achieved with P_2O_5 content in the separated fraction reaching 5–10 wt.% compared with the original slag levels of 1.5–3 wt.%. This approach leveraged thermochemical control to create discrete P-rich domains that could later be separated.

First, separation techniques were investigated at the laboratory scale. Dry magnetic separation tests were performed on both slag samples from industrial partners used as reference material as well as on slag samples which were slow cooled in the laboratory. Grain size fractions <1 mm did not display any separation effect due to the metal sticking to the slag fractions while fraction between 1 and 2 mm showed a decrease in metal Fe. Dry-magnetic separation provided an increase of Fe in the slag from 33 to 38.5 % and was the highest achieved when the sample was milled below 1 mm. Air sorting was also assessed, but the separation obtained was low going from a Fe content of 24.8 % to 25.7 % when using coarse fraction. Wet-magnetic separation had a better separation rate resulting in increased Fe content in the Fe-rich fraction with Fe yield in the slow cooled slag being about 55 %. Fe yield increased to 77 % in samples which were produced with blown oxygen and to 92 % when sewage sludge was added. Concerning P yield in the P-rich fraction, i.e., the non-magnetic fraction, it went up to 5.7 % of P_2O_5 in sample with added sewage, but it proved to be high also in the magnetic Fe-rich fraction reaching values of 3.8 % of P_2O_5 thus being unsuitable for internal recycling. The non-magnetic fraction could be suitable for fertilizer use as it resulted in 9.3 % of P_2O_5 in the slag and Austria P-fertilizer must contain at least 5 % of P_2O_5. Thermal treatment was also investigated but found not to improve the separation of Fe.

Laboratory tests were validated at pilot scale covering the full chain from slag treatment to separation and material application testing. Slag samples were produced with slow cooling in a 16-tonne slag pot used for differential solidification trials. After 16 hours of controlled cooling, a solid layer formed at the outside of the slag pot with a thickness exceeding 20 cm, while the remaining liquid fraction was reported at approximately 27 wt.%. The liquid phase was enriched in Fe and was poured off while the solidified shell concentrated the P-rich dicalcium silicate–tricalcium phosphate (C2S–C3P) solid solution phases near the top and side walls of the pot. For the dry solid separation route, the slag was subjected to standard pre-treatment including metallic Fe recovery followed by fine grinding to achieve phase liberation. P enrichment was consistently observed near the top interface of the solidified slag pot with higher P_2O_5 concentration in the upper and side regions of the pot compared to the inner Fe-rich core. The liberation efficiency of the C2S phase was found to be a critical parameter since a coarse grinding left C2S locked within the magnetic RO/spinel matrix, while fine grinding below ~30 µm was required to achieve sufficient liberation for effective magnetic separation. The non-magnetic fraction after magnetic separation was thereby enriched in P_2O_5 and depleted in FeO while the magnetic fraction retained most of the Fe-bearing phases and returned a low-P product suitable for internal steel plant recycling.

The different slag fractions emerging from the separation were evaluated for distinct downstream applications. Process routes for each fraction were assessed from economic, environmental, and technical perspectives. The Fe-rich fraction, i.e., the magnetic fraction, was characterized by a low P_2O_5 content and by a significant metallic and oxidic Fe fraction and was identified as a suitable substitute for primary raw materials in integrated steelmaking. Its valorization as sinter plant or BF burden component was evaluated positively thanks to its high CaO content around 40–50 % and the good FeO content around 16–20% which ensured both fluxing and Fe units, partially replacing primary iron ore, manganese ore, and limestone. The introduction of this fraction into the current steelmaking process flow showed to yield significant improvements, including savings in primary iron ore, manganese, limestone, CO_2 emissions, and energy consumption. The P-rich fraction was investigated through fertilizer experiments which were carried focusing on BOF slag samples enriched in P through addition of sewage sludge ash containing approximately 23 wt.% of P_2O_5. The original P_2O_5 content of the untreated slags ranged between 0.14–1.92 wt.%. The target threshold of P_2O_5>5 wt.% was achieved in all samples after re-melting at 1600 °C in a Tamman furnace under nitrogen atmosphere and subsequent slow cooling at 1 °C/min. The mineralogical transformation was critical since during re-melting, the whitlockite phase ($Ca_{2.86}Mg_{0.14}(PO_4)_2$) from the sewage sludge ash reacted with larnite (Ca_2SiO_4) from BOF slag to form a calcium-phosphate-silicate ($Ca_{15}(PO_4)_2(SiO_4)_6$) which exhibited near-complete solubility in citric acid, i.e., a standard indicator of high plant-available P. Plant availability of P_2O_5 was confirmed analytically at 5.6 wt.% and 5.3–4.6 wt.%, matching the total P_2O_5 content. Greenhouse pot trials were conducted with sandy "Lavesum" soil with three replicates per treatment. The P-enriched BOF slag samples were benchmarked against triple superphosphate, rock phosphate, and a previously tested P-enriched slag. Despite not being water-soluble, results demonstrated that the sewage sludge ash-enriched BOF slags achieved statistically equivalent yields and P uptake in spring rape compared to triple superphosphate across all applied P levels. This performance was not replicated at all by rock phosphate. CAL-extractable soil phosphate increased nearly linearly with P

application and showed no significant difference between sewage sludge ash -enriched slags and triple superphosphate at 54 days after trial installation thus confirming sustained plant availability. The neutralizing liming value of the enriched slags was also confirmed since the highest slag treatment delivered 12.37 g of CaO equivalent per pot with reactivity values around 29–36 wt.% CaO-equivalent demonstrating a beneficial dual function as both phosphate fertilizer and liming agent.

The suitability of the Fe-poor non-magnetic BOF slag fraction as a supplementary cementitious material (SCM) or clinker substitute was evaluated after wet magnetic separation. Two sub-samples were blended at a 50/50 ratio with CEM I 42.5R Portland cement and subjected to isothermal heat of hydration calorimetry over 168 hours. The measured specific heat of hydration of the 50 % slag blends was 214 J/g and 223 J/g, respectively. These values were closely comparable to those of an inert quartz sand–cement mix, and far below the approximately 320 J/g measured for 100 % CEM I 42.5R over 7 days. Since reactivity in cementitious applications is primarily evaluated through heat of hydration driven by the hydraulic reactions of tricalciumsilicate (C_3S), dicalciumsilicate (C_2S) and calcium-alumoferrite, the near-inert behavior of the slag mixture confirmed that the slag fraction contributed negligible cementitious activity. The root cause was identified in pre-hydration since the slag already experienced contact with water during the wet magnetic separation process. This caused its reactive mineral phases to be consumed prior to the cement test thus leaving a material with no residual hydraulic potential. In light of this, slag subjected to wet magnetic separation proved to be not suitable as cement clinker or SCM, and any future valorization route targeting cement applications would need to employ dry separation processes to preserve slag mineralogical reactivity.

The PSP-BOF project demonstrated that selective separation of P and Fe from BOF slag is technically feasible across both the solid and liquid slag separation routes, though neither route achieved a fully complete zero-waste concept under the tested industrial conditions. The solid separation route comprised slag modification through slow cooling at 1 °C/min, standard pre-treatment with metallic Fe removal, fine grinding, and high-intensity magnetic separation. Its primary limitation was the intergrowth of Fe- and P-bearing mineral phases which could not be entirely overcome by slag modification and controlled cooling alone. The best achieved magnetic product carried approximately 32 wt.% of Fe and 0.6 wt.% of P_2O_5 falling short of the initial target of 45 wt.% Fe and 0.3 wt.% P_2O_5. Nevertheless, industrial application of this route at industrial conditions demonstrated meaningful resource savings including substitution of at least 50,000 t/year of sinter feed ore valued at 4 M€/year, along with reductions in limestone and manganese carrier consumption. For the liquid slag partial solidification route, system analysis indicated that a 63/37 blended recirculation of PSP-BOF-treated and landfilled slag at a total rate of 59.1 kg/t of hot metal could achieve annual savings of 8.0 kt of iron ore pellets, 17.5 kt of limestone, 3.9 kt of Mn carrier, and 1.7 kt of coke corresponding to 12.7 kt CO_2 abatement, 12.9 GWh reduction in energy consumption, and an economic saving of approximately 18 MSEK/year, while increasing the BOF slag recirculation rate by 19 kt/year. Regarding external valorization, greenhouse experiments confirmed that sewage-enriched BOF slag with P_2O_5 values >5 wt.% performs comparably to triple superphosphate as P fertilizer, while cement application was ruled out for slag processed via wet magnetic separation due to loss of hydraulic reactivity upon water contact. The project concluded that a combination of FeV recovery from the liquid fraction, BF recirculation of P-depleted slag, and targeted agricultural use of P-enriched fractions represents the

most promising pathway toward a zero-waste BOF slag management strategy at the European integrated steelmaking scale.

2.2.17 ALTERAMA: Developing uses of alternative raw materials in cokemaking (43)

The project was coordinated by University of Nottingham, with CSIC, Instytut Chemicznej Przeróbki Węgla, Tata Steel and Voestalpine participating as partners in the consortium. The project started on the 1st of July 2014 and lasted almost three and a half years, ending on the 31st of December 2017. The overall project cost 1.97 M€ and the EU contributed 1.18 M€, i.e., almost 60 % of the budget.

The ALTERAMA project addressed two recurrent constraints of coke production. The first one was the need to increase charge bulk density and operational stability while reducing reliance on industrial oils. The second one was the progressive scarcity and cost of high-quality coking coals which motivated partial substitution with alternative raw materials, e.g., low-rank coals, biomass-derived materials, and secondary carbon resources, and the use of briquetting routes. The project evaluated both charge preparation indicators and carbonization/coke-quality indicators. Concerning charge preparation, bulk density and flowability/handleability were emphasized. Concerning carbonization behavior, internal gas pressure (IGP) and wall pressure and carbon-deposit observations were considered. Coke quality was assessed via cold-strength indices (M40/I40 and I10-type indices) and hot-performance indicators such as CRI/CSR. ALTERAMA combined laboratory characterization and pilot-scale carbonization trials to evaluate alternative raw materials, binders, and process strategies to be realistically integrated into existing coke-oven practice. The activities covered raw material selection, renewable C maximization, utilization techniques, e.g., surfactant-based densification and briquetting, carbonization behavior and coke quality as well as industrial feasibility.

Concerning materials selection and characterization, different classes of materials were considered. The first class concerned renewable or waste-derived materials that could potentially be converted into coal-like carbon through hydrous pyrolysis, the second class focused on plasticizers and additives intended to modify coal blend thermoplasticity, the third class addressed surfactants as alternatives to conventional blend oils for charge densification and the last class evaluated binders and associated process concepts for coal briquetting. Focusing on the first class of materials three Kraft lignin samples produced as wastes in pulping and isolated via the Kraft alkali process were selected for hydrous pyrolysis tests. Additional biomass types such as sugar beet roots, eucalyptus wood, olive stones and olive cake were included as comparators with olive cake specifically used to probe the effect of higher ash/mineral content on hydrous pyrolysis products. Concerning the second class of materials, i.e., plasticizers and additive in coal blends, coal tar, HDPE sourced from waste plastic bottles, and bio-oil derived from fast pyrolysis of woody biomass were considered. These were intended as plasticizers of lignin-derived hydro chars and/or as additives to enhance coal fluidity. In parallel, alternative raw materials to be incorporated in coal briquettes were evaluated including waste sawdust from pine from multiple batches, oak and chestnut, residues from hydrothermal carbonization of biomass wastes, and pine Kraft lignin. Binder selection was intentionally broad reflecting both industrial by-products and renewable/waste streams. Coal tar, coal tar sludge, sugar cane molasses, paraffin, and a lignin-based

waste were considered for briquette preparation. Several binders and by-product streams relevant to coking plant integration were also selected such as waste ion-exchange resins, thermolyzed waste plastics, sugar beet molasses, waste tars/oils from coking plants, i.e., ammonia saturator waste tar and waste wash oil, and brown coal from the Turów mine. Surfactant selection necessary for the densification route was performed with commercial suppliers and screened through material safety data sheets to ensure compatibility with coke ovens, by-product plants, water courses and waste disposal, as well as downstream BF operation. Seven surfactants were selected spanning anionic, non-ionic and amphoteric chemistries. One of the primary drivers considered was to identify options that were more chemically and environmentally benign than the oils currently used in industrial blends.

All these materials were accurately characterized by combining proximate and elemental analyses, TGA, and inorganic characterization including XRF to compare alternative materials with conventional coking coals and to identify properties relevant to blend behavior and coke quality. In particular, high temperature rheometry, ^{1}H NMR (Nuclear Magnetic Resonance) and solid-state ^{13}C NMR were used to characterize Kraft lignin and several biomass residues, while proximate, elemental and TGA were applied to raw materials and blends to understand their devolatilization behavior, coke yield and ash chemistry. Surfactants were also examined in detail to determine their physical and chemical compatibility with industrial coke-making practice. The analysis confirmed that lignin had high oxygen content, i.e., 30-40 wt.%, and moderate C content around 60 wt.%, while hydro chars showed increased C and reduced oxygen after processing. Biomass materials exhibited variable compositions with sugar beet roots showing high volatile matter while woody biomasses had lower volatiles and higher lignin fractions. The rheological behavior of lignin showed clear differences. Dewatered lignin started to soften at a lower temperature, i.e., around 140 °C, while alkali and pine Kraft lignin started to soften at 160 °C. Furthermore, dewatered lignin exhibited its minimum viscosity at approximately 200 °C whereas the other two reached their minimum near 220 °C. A second minimum viscosity was observed for all types of lignin at 350-360 °C. Concerning fluidity, it decreased with increasing minimum viscosity and the overall fluidity development followed the order of pine Kraft and dewatered lignin with alkali lignin showing the lowest fluidity. Biomass materials behaved very differently with sugar beet roots becoming fully fluid at around 180 °C due to their molasses content, while eucalyptus wood, olive stones and olive cake developed only small amounts of fluid material and underwent more extensive structural collapse. High-temperature ^{1}H NMR confirmed that only sugar beet roots and lignin generated fully fluid phases while HDPE, coal tar and bio-oil were fluid due to their inherently aliphatic or liquid nature. Their plasticizing power for coal decreased in the sequence coal tar, HDPE and bio-oil. TGA demonstrated that lignin and coal tar sludge offered the highest coke yields among the alternative raw materials. When coals were blended with sawdust or other additives, the devolatilization events occurred at the same temperatures observed for the individual components, and comparisons between calculated and experimental yields confirmed the absence of synergistic effects during co-pyrolysis. Similar behavior was found in briquettes where interactions between constituents were negligible. The surfactants selected covered anionic, non-ionic and amphoteric chemistries and displayed compositions far more benign than industrial oils typically used with very low Na and S contents. Their chemical properties and performance in preliminary coal-blend tests were sufficiently favorable that no further surfactant screening was required. Industrial coal blends

supplied by two plants were successfully replicated through controlled crushing, enabling laboratory-scale flowability and bulk-density studies to be reliably compared with industrial practice.

The next step focused on maximizing the renewable C content through thermal processing. Hydrous pyrolysis and torrefaction were considered to increase renewable C incorporation. Hydrous pyrolysis experiments were conducted on the different types of lignin and on selected biomasses at temperatures from 200 to 300 °C with reaction times varying from 30 minutes to several hours. The process aimed to increase C content, reduce oxygen, and improve the coal-like character of the materials through controlled decarboxylation and dehydration reactions under subcritical water conditions. The hydrous pyrolysis of Kraft lignin at 250 °C for 1-2 hours yielded hydro chars with C content increased to 65-75 wt.% from the original 60 wt.%, while oxygen content decreased from 30-35 wt.% to around 20-25 wt.%. Volatile matter was reduced, and fixed C increased, bringing the hydro chars closer to low-rank coal characteristics. However, the hydro chars remained substantially different from medium- and high-volatile coking coals in terms of their thermoplastic behavior and caking properties. Biomass hydrous pyrolysis followed a similar trend with sugar beet roots producing hydro chars with enhanced C content but also with a retained high reactivity due to their residual carbohydrate structures. Eucalyptus and olive materials yielded hydro chars with improved heating values but limited thermoplastic development. The ash content of biomass-derived hydro chars remained a concern, particularly for olive cake, which showed elevated alkali and alkaline earth metal concentrations that could affect coke quality and BF performance. Torrefaction of sawdust was performed at 250-300 °C in inert atmosphere to evaluate an alternative upgrading pathway. Torrefied sawdust showed mass losses of 20-40 % depending on temperature and residence time with corresponding increases in C content and calorific value. However, like the hydro chars, torrefied biomass did not develop the thermoplastic properties characteristic of coking coals thus limiting their direct use as a coal substitute.

The plasticizing additives, i.e., coal tar, HDPE, bio-oil, were tested in combination with lignin-derived hydro chars to determine whether they could enhance fluidity and coking behavior. Coal tar proved to be the most effective creating fluid phases that could partially compensate for the lack of inherent plasticity in hydro chars. HDPE showed moderate plasticizing effect at higher temperatures above 400 °C when its thermal decomposition generated aliphatic fluid phases. Bio-oil had limited effectiveness due to its high oxygen content and the tendency to undergo repolymerization reactions during heating which reduced rather than enhanced fluidity in some cases. Blending trials with coal demonstrated that hydro chars and torrefied materials could be incorporated up to 5 wt.% in coal blends without severe deterioration of coking properties, provided that plasticizers like coal tar were also added. Coke quality declined at higher incorporation rates, i.e., 10-15 wt.%, unless compensatory measures were taken, such as increasing the proportion of high-fluidity coals in the blend or adding larger amounts of plasticizing agents. The fundamental limitation was that thermal processing alone did not transform biomass-derived materials into true coking coal equivalents, but rather it produced upgraded solid fuels that required careful integration into coal-based systems.

The next goal of the project was to increase coal charge bulk density which was attempted through densification techniques such as chemical densification with surfactants and mechanical densification

through briquetting. The surfactant route aimed to enhance particle packing and reduce inter-particle friction during charging while briquetting sought to create dense, compacted coal forms that could be blended with loose coal to increase overall charge density. Surfactant trials were conducted using the seven selected formulations and surfactants were applied to coal blends at concentrations ranging from 0.005 to 0.05 wt.% with the coal moisture adjusted to 8-10 wt.% to facilitate dispersion. Bulk density measurements were performed using standardized tapping procedures and flowability was assessed through angle of repose and flow-through-orifice tests. The results demonstrated that selected surfactants could increase bulk density by 30-50 kg/m^3 when applied at rates of 0.01-0.02 wt.%. This performance was comparable to or slightly better than conventional industrial oils used at 0.03-0.05 wt.%, indicating superior effectiveness on a per-unit-addition basis. The surfactants also improved coal flowability by reducing bridging and hang-up issues during charging. Importantly, the chemical analyses confirmed that surfactants had negligible Na content <0.1 wt.% and very low S <0.5 wt.%, making them compatible with downstream BF requirements and environmental constraints. Pilot-scale carbonization tests of surfactant-treated coal blends showed that coke quality remained acceptable when surfactant levels were kept within the optimum range of 0.01-0.02 wt.%. Cold strength indices were maintained or showed only minor variations compared to untreated reference coals as well as hot strength (CSR). IGP increased modestly, typically 5-10 kPa, due to the higher bulk density, but remained well within acceptable limits for most oven designs. The surfactant route was therefore validated as a low-risk, relatively low-cost method for achieving moderate bulk density increases without compromising coke quality or requiring capital investment in new equipment.

Briquetting trials were conducted using different binder systems and process parameters. The general approach involved pre-drying of coal to 3-5 wt.% moisture to improve binder distribution and reduce steam generation during carbonization, mixing binder at coal: binder ratios between 90:10 and 95:5, compacting the mixture in roller presses or piston presses to form briquettes and sizing/screening the briquettes to achieve uniform dimensions. The optimal briquette geometry identified through the trials was approximately 5 cm^3 volume with roughly 2 × 2 × 1.5 cm dimensions and mass around 10-12 g. Smaller briquettes with 2-3 cm^3 volume were easier to integrate into coal charges without segregation but offered lower bulk density benefits. Larger briquettes with volume >10 cm^3 achieved higher bulk densities but were prone to segregation during charging and generated excessive localized pressures during carbonization. The 5 cm^3 briquettes represented a practical compromise. Coal tar and coal tar sludge emerged as the most effective binders from both a technical and economic perspective. Addition rates of 8-12 wt.% of these binders provided sufficient mechanical strength for handling and charging while maintaining acceptable coke quality. Furthermore, they were available as by-products from coking operations thus reducing net cost. Sugar cane molasses and sugar beet molasses required higher addition rates of 12-15 wt.% to achieve comparable briquette strength but produced cokes with slightly lower CSR values likely due to the introduction of additional oxygen functionalities that increased reactivity.

Thermolyzed waste plastics and waste ion-exchange resins showed promising technical performance, with thermolyzed waste plastics briquettes producing high-quality coke in some trials. However, its cost of 300 €/t and the limited availability of ion-exchange resins made these binders economically unattractive for large-scale implementation. Brown coal from Turów mine proved to be an

economically favorable binder due to its low cost 40 €/t and reasonable binding performance at 15-20 wt.% addition though coke quality was somewhat lower than with coal tar binders. Particle size distribution of the coal used for briquetting was found to be critical with fine coal <1 mm providing better binder distribution and stronger briquettes but increased risks of excessive pressure during carbonization. Coarser coal of 1-3 mm produced more permeable briquette structures that better accommodated volatile release reducing pressure buildup.

The optimal approach used a bimodal distribution with approximately 60-70 % of fine coal and 30-40% of coarser material. Biomass incorporation in briquettes was explored using sawdust, BIOC, i.e., a residue of hydrothermal carbonization of biomass wastes, and lignin-derived materials. Sawdust could be included up to 10 wt.% in briquettes bound with coal tar without catastrophic quality loss, though CSR typically decreased by 5-10 %. Coke quality deteriorated significantly at 15-20 wt.% sawdust and BIOC showed similar behavior. The primary mechanism of quality reduction appeared to be increased porosity and reactivity in the final coke stemming from biomass volatile-rich nature and residual oxygen content. The bulk density increases achieved through briquetting was substantial with blends containing 20 wt.% briquettes showing bulk density improvements of 60-100 kg/m^3 compared to loose coal charges. Bulk densities increased by 90-130 kg/m^3 at 30 wt.% briquette addition, but carbonization pressure concerns became more pronounced. The trials recommended limiting briquette content to approximately 20 wt.% as a practical maximum for typical oven designs, with potential for higher percentages in ovens specifically designed for higher-pressure operation.

The next phase of the project was dedicated to the study of carbonization behavior and to the assessment of coke quality to evaluate how alternative materials, plasticizers, surfactants, and briquetting strategies may affect them. The analysis was performed through pilot-scale trials using a moveable-wall oven (MWO) able to provide detailed wall pressure profiles during carbonization. Larger-scale trials with 300 kg charges with comprehensive gas pressure monitoring and coke quality assessment were also performed. IGP measurements confirmed the correlation between bulk density and maximum pressure with typical IGP increase of 15-25 kPa for every 50 kg/m^3 increase in bulk density depending on coal blend properties and carbonization conditions. Surfactant-treated blends with bulk density increases of 30-40 kg/m^3 showed IGP increments of 10-15 kPa but remaining well below the 35-40 kPa threshold considered safe for older oven designs. Briquette additions at 20 wt.% generated IGP increases of 20-30 kPa approaching or slightly exceeding typical operational limits in some trials. The timing of pressure development was also influenced by charge preparation methods. Surfactant-treated charges showed pressure profiles similar to untreated coals with maximum pressure occurring at bulk temperatures around 450-500 °C. Briquette-containing charges sometimes exhibited earlier pressure maxima at 430-470 °C and more rapid pressure rise rates attributed to the fine particle structure within briquettes and their higher initial density. This necessitated careful attention to heating rates and potential adjustment of carbonization schedules to avoid excessive pressure buildup. Wall pressure measurements in the MWO indicated that pressure distribution was relatively uniform across oven width for surfactant-treated charges and for briquette charges when briquettes were well-distributed. However, when briquettes segregated during charging localized pressure hotspots were observed. This reinforced the importance of briquette size control and charging procedures to ensure homogeneous distribution.

Cold strength assessment showed that surfactant additions at recommended levels had minimal impact on coke strength. M40 values for surfactant-treated charges were typically within ± 2 % of reference values, and I10 indices showed similar stability. This confirmed that surfactants functioned primarily as physical processing aids without significantly altering coal carbonization chemistry or coke microstructure. Briquette-containing charges produced cokes with cold strength properties that depended strongly on binder type and briquette content. Coal tar-bound briquettes at 20 wt.% addition maintained M40 values above 85 % in most trials comparable to all-coal charges. Molasses-bound briquettes showed somewhat lower M40 around 82-86%, while brown coal-bound briquettes exhibited the widest variation of 78-87% depending on brown coal properties and addition rate. Biomass-containing briquettes showed reduced cold strength with M40 typically 80-84%, particularly those with sawdust >10 wt.% likely due to increased macro porosity introduced by biomass decomposition. Hot strength properties were more sensitive to alternative materials with CRI increasing when biomass or oxygen-rich binders were used thus reflecting the introduction of reactive C structures and residual catalytic ash species. CSR consequently decreased with the magnitude of decrease correlating with biomass/oxygen content. Coal tar-bound briquettes without biomass maintained CSR values above 60 % which were considered acceptable for most BF operations. Biomass-containing briquettes, i.e., 10 wt% sawdust in briquette formulation, showed CSR reductions to 55-58 % thus approaching the lower limit of acceptability. Hydro char and torrefied material additions tested at 3-5 wt.% in coal blends produced cokes with intermediate properties. Coke quality was acceptable when co-added with plasticizers, i.e., coal tar or HDPE, though CSR was typically 2-4 % lower than all coal cokes. Hydro char additions above 5 wt.% led to more significant CSR reductions, i.e., 5-8 %, without plasticizers due to poor integration of the hydro char particles into the plastic coal mass during carbonization.

Coke microstructure analysis using optical microscopy revealed that surfactant-treated cokes had microstructures essentially identical to untreated references, confirming the minimal chemical impact of surfactants. Briquette-derived coke regions showed finer mosaic textures when fine-grained coal and appropriate binders were used, consistent with the higher compaction and smaller particle sizes. Biomass-containing regions displayed increased porosity with pore sizes in the 10-50 µm range, explaining the reactivity and strength reductions observed in performance testing.

The last step of the project was devoted to industrial feasibility and economic evaluation assessing the industrial implementation potential of the developed technologies. The assessment considered capital expenditure (CAPEX), operational expenditure (OPEX), environmental compliance, and integration with existing plant infrastructure. The Best Available Techniques (BAT) reference document for iron and steel production was reviewed to ensure alignment with regulatory requirements. BAT emphasized minimizing dust emissions via optimal coal blend composition especially through moisture control, and the reuse of wastes produced such tars, organic wastes, sludge, solid residues. Charge preparation techniques such as briquetting, pre-drying and oiling were not explicitly prescribed in BAT but they could be applied provided they satisfied environmental requirements, while coke yield and quality remain overriding operational requirements.

The economic analysis showed the effective cost of coke produced using surfactants was competitive with conventional oils although unit costs of surfactant were higher than conventional oils thanks to the lower addition rates required. Bulk density increases of 35-45 kg/m^3 could be achieved at 0.02 wt.% addition with surfactant costs of approximately 500-530 €/t while conventional oils achieved similar density increases with 0.04-0.05 wt.% addition with costs around 450-500 €/t. Therefore, surfactants were competitive on a cost-per-tonne-coke and their superior environmental profile with lower toxicity and easier handling provided additional non-quantified benefits. Implementation costs for surfactant use were minimal since existing oil spraying systems could be adapted with minor modifications requiring investment of approximately 5,000-10,000 € for dosing equipment updates. The low CAPEX and immediate applicability made surfactants particularly attractive for plants facing restrictions on conventional oil use or seeking incremental productivity improvements without major infrastructure changes.

For briquetting, economic feasibility varied substantially depending on binder choice and plant-specific conditions. Considering an annual production capacity of 1 Mtons of coke, brown coal at 40-45 €/t emerged as the most economically attractive binder with estimated payback period of 8-10 years assuming 20 wt.% briquette addition and no productivity increase. If the higher bulk density enabled a 5 % production increase payback period would be reduced to 6-7 years. Considering waste wash oil from coking plant by-product recovery system, this solution would be economically favorable with essentially zero or negative cost as it displaced waste disposal, but the availability was limited to approximately 2,000-3,000 tons annually, sufficient for only 2-3% of total coal throughput. Sugar beet molasses at 150-180 €/t could be profitable if production increases were realized but were economically marginal under baseline scenarios without productivity gains. Thermolyzed waste plastics at ~300 €/t showed good technical performance but were not economically viable under assessed market conditions. CAPEX for briquetting installation was estimated at approximately 20 M€ for a complete system including coal pre-drying equipment, binder storage and dosing, briquetting presses roller-type with a 100-150 t/h capacity, cooling and screening systems, and integration with existing coal handling infrastructure. OPEX were projected at 3-4 M€ covering energy for pre-drying and compaction, maintenance, labor, and binder costs.

A detailed feasibility study was conducted at Voestalpine coke facility examining practical aspects of integrating a briquetting plant with an existing coal preparation system. The study confirmed technical viability but identified significant space constraints. Building height requirements up to 25 m for the conveyor head presented additional civil engineering challenges at the site constrained. The voestalpine study highlighted that CAPEX and OPEX sensitivities varied strongly with local conditions. Key parameters included purchased coke price, coal blend price, binder costs and plant ability to absorb higher carbonization pressures without oven modifications. The analysis concluded that briquetting implementation must be evaluated case-by-case. The technology should be framed as a strategic option to increase coke production and minimize purchased coke rather than a universally applicable solution.

Environmental aspects of coal tar use as a binder received particular attention due to its polycyclic aromatic hydrocarbon (PAH) content. Its use as briquetting binder was permitted but required strict containment during handling, comprehensive gas extraction during briquette production and

carbonization, and post-combustion treatment of extracted gases to destroy PAHs. Workplace exposure limits must be rigorously monitored and controlled. Despite these requirements, coal tar remained the preferred binder in many scenarios due to its technical performance, availability as a by-product, and established handling protocols at coking plants. In contrast, surfactants were found to be significantly more benign from environmental and occupational health perspectives. The selected surfactants posed minimal inhalation or skin contact risks, were biodegradable or readily treatable in wastewater systems, and introduced negligible contaminant loads to coke oven gas or by-product streams. This made surfactants particularly attractive for plants operating under stringent environmental permits or in regions with strict occupational exposure regulations.

ALTERAMA allowed to obtain a set of plant-relevant decision rules that connect additive/binder selection, dosing, and charge preparation methods to operational constraints. These rules are listed below.

For surfactant-based densification, the use anionic or non-ionic surfactants at 0.01-0.02 wt.% addition allowed to achieve bulk density increases of 30-50 kg/m^3 and ensured low levels of Na <0.1 wt.% and S <0.5 wt.% to avoid downstream contamination. IGP increases were 10-15 kPa and oven design can accommodate this modest pressure rise. No significant changes to coke quality were anticipated at recommended dosages and implementation requires minimal capital investment with the adaptation of oil dosing systems. This route was particularly suitable for plants with oiling restrictions or seeking modest productivity gains without major infrastructure changes. From a TRL perspective, the surfactant route appeared particularly attractive for near-term implementation where plants face restrictions on conventional oiling or where modest bulk density increases were required without new capital equipment. The evidence base supports that selected surfactants can deliver bulk density increases comparable to oiling while remaining relatively benign in terms of coke quality and carbonization pressure. The main engineering requirement is to tailor additive dosing to the pressure limits and wall strength of the specific battery.

For briquetting-based densification, the target briquette size recommended was 5 cm^3 to balance bulk density improvement against segregation and pressure risks. Pre-dry coal to 3-5 wt.% moisture before briquetting to improve binder distribution and reduce steam-related pressure was recommended as well as the use of coal tar or coal tar sludge as primary binder at 8-12 wt.% for optimal balance of strength, coke quality, and economics. Briquette content must be limited to 20 wt.% of total charge to maintain IGP within typical oven limits and the control of coal particle size distribution in briquettes was also necessary (60-70% <1 mm, 30-40% 1-3 mm) to balance strength and permeability. Finally, uniform briquette distribution during charging must be ensured to avoid localized pressure hotspots. Briquetting remains the higher-impact densification approach but was constrained by segregation control, infrastructure footprint, and coking pressure management and these parameters must be considered as a pragmatic balance between productivity gains and pressure risk. Successful implementation required significant capital investment, space availability, and organizational commitment to maintain quality control in briquette production and charging operations.

For biomass incorporation, the direct addition of raw biomass to coal blends should be limited to ≤2 wt.% to avoid excessive pressure and quality deterioration. Biomass could be included at higher levels

up to 10 wt.% within briquettes if coal tar or similar strong binder is used but expect CSR reductions of 5-10 %. Hydrocars and torrefied biomass could substitute raw biomass at slightly higher rates of 3-5 wt.% in blends and 10-15 wt.% in briquettes but still required careful quality monitoring. Biomass ash content and composition must be also assessed to ensure compatibility with BF requirements. Regarding renewable C incorporation, hydrous pyrolysis and torrefaction provide technically informative pathways but did not automatically create drop-in coking-coal analogues. The most robust near-term pathway was therefore the use of small-percentage of renewable or waste-derived materials while maintaining coke quality indices and protecting coke oven walls. Longer-term deployment would require further engineering to manage ash/metal content, porosity and reactivity of biocokes, and to ensure consistent supply chains and favorable economics.

The project demonstrated that alternative binders, surfactants and partial briquetting strategies can enhance coke production efficiency, environmental performance and operational flexibility. However, their industrial implementation must be evaluated case by case, considering local plant conditions, environmental regulations, and market dynamics. No single solution was universally optimal and ALTERAMA results provided a toolkit of proven technologies that could be tailored to specific circumstances. Viable pathways for increasing coking charge bulk density, reducing dependence on high-quality coking coals, and incorporating renewable or waste-derived materials into industrial cokemaking were addressed. Surfactant-based densification offers a low-risk, low-investment route to modest productivity gains with minimal environmental and quality impacts. Briquetting provides larger productivity improvements but requires substantial capital investment and careful process control. Renewable carbon incorporation remains at an early stage of industrial readiness, suitable for niche applications or minor blend adjustments, but not yet for large-scale coal substitution.

2.2.18 GREENEAF2: Biochar for a sustainable EAF steel production (44)

The project was coordinated by RINA-CSM with Ferriere Nord, Georgsmarienhütte, Imperial College, Stahl- und Walzwerk Marienhütte, and RWTH participating as partners in the consortium. The project started on the 1st of July 2014 and lasted almost three years, ending on the 30th of June 2016. The overall project cost 2.01 M€ and the EU contributed 1.00 M€, i.e., almost 50 % of the budget.

The previous GREENEAF project described in section 2.2.7 demonstrated the feasibility of using char from biomass as substitute of coal into the EAF. The GREENEAF2 project aimed to transform char use in EAF into standard practice. Considering this, the issues analyzed in experimental tests were dedicated to both charging in the bucket and injection. Concerning bucket charging, the higher reactivity of char respect to coal needed to be controlled and a briquetting stage was identified as a possible solution. Proper material selection and operating practice adjustment were also necessary. Concerning injection, proper injection system was studied to avoid dispersion of char into the off gas, to maximize penetration and reaction inside the slag layer and promote slag foaming. The effects of char use on productivity, costs, environmental emissions, materials handling and storage were also considered to make char utilization a standard and applicable practice. LCA study allowed to evaluate the impact of biomass use on the environment.

For char and briquettes production, providers of biochar char from biomass were identified to get materials for preliminary laboratory analysis and industrial trials. Laboratory characterization of raw

materials both pulverized and pelletized was carried out in terms of physical and chemical properties with TGA and CO_2-reactivity tests results being compared to those related to fossil coals, i.e., petrol coke and anthracite, as reference. A broad collection of materials was analyzed and was taken as representative of all that could be available on the market with relevant C content and heating value. Residue from gasification such as dust produced after thermochemical gasification process of wood chips with low ash content, high C-content, and low volatiles were considered. Char from thermal pyrolysis such as husk and pyrolyzed wood charcoal with medium ash content, high C-content, and low volatiles were included. Torrefied biomass thermally treated at temperatures lower than 300-350°C and materials from hydrothermal conversion which were highly reactive, with high volatile matter content were characterized. Virgin ligneous biomass with C content of about 50 %, low fixed C, and low humidity, biomass residues from paper production such as paper fibber sludge high ash content, low C-content, and middle volatiles and biomass residues from agriculture with C content of about 50 %, low fixed C, and high humidity were also assessed.

Tests performed through TGA and in wire mesh reactor underlined a clear separation between samples in terms of volatile compounds amount with chars from Andritz (torrefied biomass), Torrcoal (torrefied biomass), Cleancoal (hydrothermal conversion) and Palm Kernel Shell (virgin ligneous biomass) displaying a significantly higher volatile fraction compared to Futuris (residue from gasification), Carbon Terra (char from thermal pyrolysis) and Padovani (char from thermal pyrolysis) ones. These features were observed in the high weight fraction remaining in TGA experiments before switching the atmosphere to air as well as in the higher char yields in wire mesh reactor experiments. Futuris and Carbon Terra char showed a behavior like Padovani char which was already used in the previous GreenEAF project. These materials had also strong similarities with fossil coals and could be used as charge materials without significant modification of the operating practice. Limitation in their use could arise only from the low mechanical stability of the briquettes which could cause dispersion of dusts during handling and basket charging thus causing the starting of ignition phenomena. A further limitation factor could be the cost. The use of the other materials, Andritz, Torrcoal, and Palm Kernel Shell would require the adjustment of the operating practice due to volatilization at relatively low temperatures. The Cleancoal and AVA_CO_2 materials produced with hydrothermal conversion processes were very reactive and showed ignition at low temperature therefore they were not used for industrial trials. Although paper production residues could be used as limestone substitute, their C content and heating values were very low therefore industrial tests with this material were not performed.

The indications deriving from laboratory characterization can be summarized as follows. Residues from gasification and char from thermal pyrolysis displayed similar behavior to high temperature pyrolyzed biomass. TG and melting tests confirmed strong similarities to fossil coal behavior as charge material thus ensuring their potential utilization without significant impact on EAF operating practice in case of basket charging. Torrefied biomass displayed an intermediate reactivity between char from thermal pyrolysis and biomass itself with fast release of volatiles below 400 °C. Weight loss was observed at higher temperatures but with reduced rate. In case of basket charging, steel carburization was about half compared to fossil coal according to laboratory results. Hydrothermal conversion materials had a reactivity comparable with biomass itself and were not used in industrial tests due to problems outlined during handling even at laboratory level such as rapid ignition with air at temperatures below 200 °C. Virgin ligneous biomass displayed lower heating values with a fast release of volatiles, i.e., hydrocarbons and hydrogen. A positive foaming behavior and good handling properties were observed at laboratory scale. Paper production residues were characterized by low C content and low heating value and may

be useful to partially replace CaO but were not included in industrial trials. Finally, residues from cultivation were characterized by lower heating values and fast release of volatiles (hydrocarbons and hydrogen), but injection trials would be necessary to clarify if volatile emissions were suitable to promote foaming and FeO slag reduction. A difficulty in handling was also observed.

Laboratory simulation of the foaming behavior with biochar were carried out to define an injection methodology in terms of particle size, gas flow rate, proper mix of char, etc., able to promote efficiently foaming. Preliminary industrial injection trials showed a low tendency to promote slag foaming of char and biochar while biomass seemed more effective in promoting this phenomenon. The latter determined also rising panel temperature thus suggesting that a blend of biomass and pulverized coal could be a good compromise. Longer trials were necessary for final assessment and to check the reliability of preliminary results. Ferriere Nord performed charging experimental campaign, Marienhütte carried out injection trials and Georgsmarienhütte assessed both solutions. In all cases, short preliminary tests were done to set the operating practice and subsequent longer testing campaign were performed to validate biochar use.

Concerning charging tests, preliminary results allowed to optimize the operating practice and to make a first rough evaluation of the variation occurring in process parameters. Torrcoal char was charged in quantity variable between 500 and 1000 kg during the first trials at Ferriere Nord and no significant variation of operating parameters were recorded. Long term trials permitted to validate char utilization and estimate possible energy savings. The industrial charge trials at Georgsmarienhütte with Palm Kernel Shell did not show any negative impact on steel or slag quality or furnace operation. The surplus of material charged was reduced from 80 % in the first campaigns to about 20 % for the last campaign and still no detrimental effects were observed despite the differences between anthracite and Palm Kernel Shell in terms of fixed C and volatiles content. The Palm Kernel Shell and anthracite mix campaign showed a significant reduction of more than 6 % in the specific electric energy input without any negative effects on other characteristic process data. The trials also showed differences in off gas formation and temperature in accordance with Palm Kernel Shell higher amount of volatiles. Furthermore, the use of Palm Kernel Shell shifted oxygen consumption from lance to post combustion oxygen. Tests carried out by Ferriere Nord did not show significant variation of the main operating index of the furnace, i.e. consumption, productivity, steel analysis, power on time. Operating problems resulting from material dispersion and ignition during the charging step were solved using a mechanically stable briquette and with optimized basket charging practice. Contrary to Georgsmarienhütte trials, electricity saving was not observed. This was ascribed to the different oxygen injection facilities of the two steel shops. Georgsmarienhütte furnace was equipped with diffusors which promoted the combustion and post combustion in the freeboard space, while the lance injection at Ferriere Nord case was purposely designed to promote slag foaming but was less effective in energy transfer to the steel bath.

Char and biomass injection trials were performed considering also mixing with fossil coal and inert. The industrial tests indicated a pour foamy behavior ascribed to the combination of two factors, i.e., the lower reactivity of biochar with FeO compared to fossil anthracite and the lower density of biochar which decreased the penetration capacity into the slag. The lower reactivity with FeO also caused most of the materials to be transported by off-gas stream. Blends wit h anthracite and material pressing were tested to increase material density and promote foaming reactions, but the results were unsuccessful. Injection trials with virgin biomass were able to ensure slag foaming even if the trials were discontinued. In case of biomass, the higher presence of hydrogen formed during thermal

decomposition probably improved the FeO reaction and/or acted as activator of these reactions. This could explain the partial positive results obtained with Palm Kernel Shell even if the global evaluation of foaming results was not satisfactory.

The environmental impact of biochar use during EAF steelmaking was investigated by LCA study which was divided into four phases. The first phase concerned the definition of goal and scope by defining the system, system boundary and the complexity of the study. The second phase concerned the collection of process input and output data contained in the defined system boundary to obtain a LCI. The third step concerned the transfer of the collected data into environmental impacts to compare different life cycle stages with each other or compare different studies by standardization and weighting processes. This step was defined as life cycle impact assessment (LCIA). The last phase was dedicated to interpretation which illustrated and totalized the results of LCI and/or LCIA phase and referred to the defined aims from the goal and scope definition phase. LCIA showed the feasibility of using biogenic C during electric steelmaking processes with a calculated high potential CO_2 savings of about 20 %. Furthermore, productivity and oxygen consumption were a little lower for the industrial test of Ferriere Nord using Torrcoal whereas there were the same power-on time and electric consumption. The use of Palm Kernel Shell during the industrial tests of Georgsmarienhütte had no negative consequences for molten steel, slag or process control. The reduction concerning the specific electric energy consumption showed that the carbon footprint of the steel production in EAF could be reduced by substituting fossil coal with biochar. The mixed campaign with 50 % fossil carbon and 50 % biogenic carbon showed the lowest specific CO_2 emissions with a decrease of 13.31 % compared to the standard scenario. Despite this, the industrial long-term trials with Palm Kernel Shell displayed a different reaction behavior of the biogenic C carriers with the biochar displaying a significant higher reactivity than fossil carbon which led to a high average amount of CO and CO_2 in the off gas. The possible energy saving deriving from EAF post combustion reactions has been observed during industrial trials.

The feasibility study for on-site char production was carried out considering the utilization of torrefied biomass purposely produced considering local availability of large amount of biomass such as the large amount of agricultural residues available near Ferriere Nord. Part of this biomass could be potentially used to produce char from torrefaction for steelmaking purposes. A biomass torrefaction plant was dimensioned according to steel plant needs. In particular, the study was tailored on Ferriere Nord needs, but results could be easily adapted to other steel factories. The torrefaction plant schematized in Figure 15 was composed by various treatment stages. The first one was the collection of biomasses with subsequent grinding and homogenization followed by a drying stage where the biomass was dried using the heat from hot gases in a conveyor belt closed into a tunnel. After drying, torrefaction phase was included to thermally treat the biomass in a rotating drum with hot gas having a temperature in the range of 250-350 °C. The production of the hot gases stream occurred thanks to a boiler heated up by the syngas from the torrefaction drum and from the gas developed in a second reactor where an amount of residual biomass was burnt. A briquetting stage to compact material by pressure to obtain a final product having a size according to final destination and a density of about 600 kg/m^3 was also considered. Torrefied biomass had a market price at the time of the project in the range of 250-350 €/t therefore a first estimation of both CAPEX and OPEX for char production from torrefaction was performed to estimate the char cost resulting from this solution. Biomass cost must be also considered to estimate char cost since the cost resulting from purchasing (if due), collection and transportation could vary from very low price of 10 €/t accounting only for the cost for pick and

transportation nearby the steel factory with distance lower than 100 km up to 80 €/t. The results of this estimation are summarized in Figure 16.

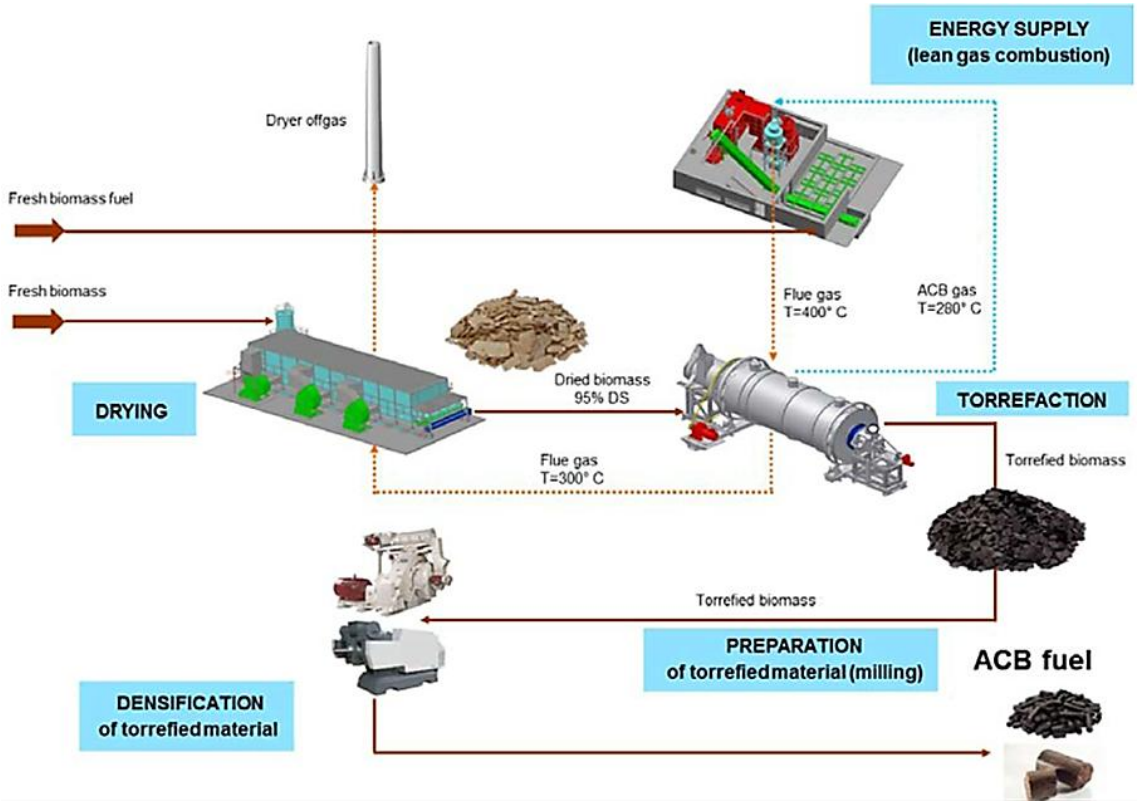

Figure 15: Schematization of the dimensioned torrefaction plant

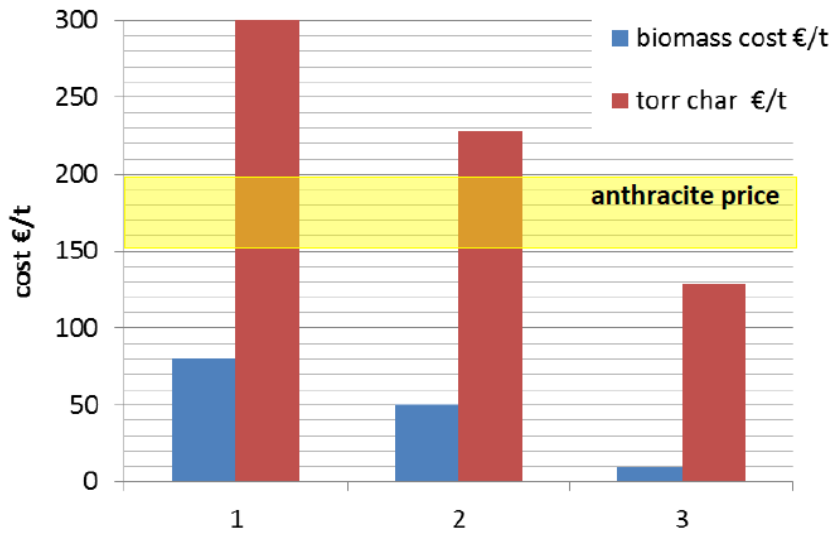

Figure 16: Simulation of biochar price assuming onsite production and three different prices for biomass

The overall economic evaluation of char use as fossil coal should account also for other components, i.e., CO_2 savings and electricity consumption. Regarding the trend of CO_2 price at the time of the project, it could be stated that the techno economical evaluation was mainly affected by electricity price. Tests outlined energy saving up to 6 % obtained with biomass utilization. This allowed to evaluate a global economic figure related to biochar utilization for a hypothetic steel plant. The data were estimated as follows: a substitution ration of 1.5 char/anthracite , a price range for biochar in between 120 and 300 €/ton, electricity savings from 0 to 6 %, average electricity cost of 0.15 €/kWh, 1 t of anthracite used per heat at cost of 170 €/t and 450 kWh/t the specific energy consumption. The results of this calculation are summarized in Figure 17. The calculation indicated that in the case of the lower price of char and with current level of CO_2 quotation, costs of biochar and fossil coal were equivalent while savings respect the standard situation were possible with electricity reduction consumption higher than 3 %.

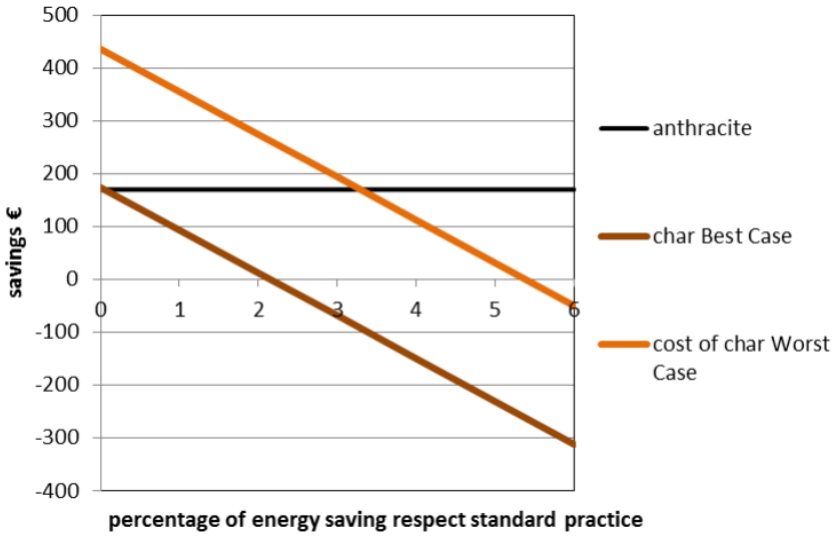

Figure 17: Comparison of costs of anthracite and char

The previous GREENEAF project demonstrated the feasibility of using char from biomass, as substitute of coal into EAF. The objective of the present project was to make char use a standard practice. At first, a deep characterization of various biomass derived carbonaceous materials, and virgin biomass was performed through TGA and CO2-reactivity to better understand the behavior of the selected material in case of char charging procedures. Then, industrial trials were carried out and allowed to conclude that not only gasification reactivity but also grain size distribution and bulk density influenced the required slag foaming behavior during char injection into EAF. The use of char as charge material was successful with little variations on the charging practices necessary ensuring standard operating parameters in terms of steel and slag quality and productivity. Actually, an energy saving of 6 % was measured when a mix coal/biomass was charged in the first basket of the furnace equipped with oxygen diffusors. The use of injected biomass presented some drawbacks since pour foaming was observed probably due to low biochar density which reduced the penetration of the jet into the slag layer and due to the reduced reactivity of the biochar with iron oxide. The techno-economical evaluation showed that in case of utilization of low-grade biomass a price comparable with fossil material was

obtained. Also, in case of substitution ration char/anthracite of 1.5 char utilization could be economically convenient in case of energy savings. In conclusion, char use could be a standard practice as charge material, while a global re-design of the injection system was necessary to be injected as coal substitute.

2.2.19 RIMFOAM: Recycling of industrial and municipal waste as slag foaming agent in EAF (45)

The project was coordinated by Swerea Mefos, with Arcerloemittal, CSM, Feralpi Siderurgica, HÖGANÄS participating as partners in the consortium. The project started on the 1st of July 2014 and lasted almost three years, ending on the 30th of June 2017. The overall project cost 2.3 M€ and the EU contributed 1.38 M€, i.e., almost 60 % of the budget.

The primary objective of the RIMFOAM project was to partially replace C and oxygen with industrial and/or municipal waste, e.g., ASR, rubber tires, plastics, biomass waste and by-products, EAF dust and mill scale, for slag foaming in EAF. In particular, the goal was to explore cost and energy effective alternative slag foaming agents while maintaining or improving the slag foaming intensity, preserving the liquid steel quality and keeping emissions at a low level. Furthermore, the project intended to explore the combined use of C containing waste materials with oxygen-rich residues, e.g., EAF dust and mill-scale, since co-injection of EAF dust/coal and charging of mill-scale agglomerates in EAF were known technologies to recover valuable metallic contents (Fe, Cr, Ni, Mo, Mn). A potential positive effect of co-injection with polymer and bio-mass waste instead of coal was a higher reduction degree and reaction rate of oxides in the slag, i.e., FeO and MnO, due to higher hydrogen content in the generated gas. This would improve the utilization of valuable metals in rich oxygen residuals. The use of all the above-mentioned substitute materials for both coal and oxygen were associated with technical challenges in EAF. In general, the proposed materials were readily available on the market in a variety of fractions and qualities. Hence, one general challenge was to find suitable commercial or internal and to define needs for further pre-treatment.

The RIMFOAM project set some quantifiable objectives such as at least 20 % substitution of injected carbon, i.e., about 1 kg/ton steel, with an optimum amount of C containing wastes to obtain optimal slag foaming efficiency. The second objective targeted a 5 % substitution of injected oxygen, i.e., about 1 Nm3/ton steel, with corresponding amount of metal oxide containing waste, i.e., about 12 kg/ton steel assuming 50 % FeO in waste. Further targets were the reduction of electrical energy consumption by 4 %, i.e., about 20 kWh/ton steel, thanks to a more efficient slag foaming and an increase in the yield of metallic oxides in oxidic wastes by 30 % by more efficient and faster reduction compared to coal injection. Finally, a reduction of steel scrap or scrap substitutes like DRI and hot briquettes was targeted with about 0.4 %, i.e., 4 kg/ton steel of valuable metals in oxidic waste. For example, assuming a 12 kg/ton steel increased use of oxidic waste with 50 % FeO and 80 % yield of Fe to steel. The partial use of waste resources instead of costly metallurgical coal and oxygen should bring estimated savings of 1 € / ton liquid steel.

The first part of project activities was focused on the characterization of waste materials that could potentially replace primary slag foaming agents in EAF. The materials investigated included both C and

oxygen-rich waste as well as pre-treated materials, material blends and ASR. Specific material parameters such as chemical composition, ash content and volatility needed to be evaluated to determine if a waste material was suitable for injection into an EAF for slag foaming purpose and to make sure that the chemistry of steelmaking was not affected. Particle size distribution played an important role since different injection devices were characterized by different demands. For example, Swerea criteria for its equipment was that particles < 2mm were suitable for injection whereas additions of particles > 2mm to the EAF needed agglomeration before charging. On the contrary, ArcelorMittal injection equipment could tolerate particles <8mm. Another important feature to consider was density since it could be challenging to blend materials if their densities differed excessively since they could separate.

Concerning C content, biomass materials showed similar results with about 40-45 % C which was significantly lower than anthracite with 50.8-79.8 % for the dry material. The different plastic waste displayed a C content in the range of 80 %. Hydrogen content was higher for all alternative waste materials as expected with anthracite displaying 0.7 % H for the dry sample while waste materials reported values between 5.5-7.6 % H. Values of 13 % H were achieved with PE (Polyethylene) and XLPE (Cross-Linked Polyethylene) plastic. Shredded plastic waste also contained significantly higher amounts of halogens than other materials while rubber and Petrit-T had higher S content than other materials. Rubber also had higher levels of Pb, Cd, Co, Cu and Zn. The Cu levels of all plastics and wood materials were higher than for anthracite and Zn levels of all waste materials were higher than for anthracite, except for PE (XLPE, XLPE), olive kernels and Petrit T. Twelve different oxidic wastes from steel industry and one oxidic waste from incineration of municipal waste were also identified and characterized including Petrit-T, oversized metal powder, EAF dust, BF dust, BF sludge, BOF dust, BOF sludge, three different kinds of mill scale, metal hydroxide sludge and grinding chips. These could be suitable for co-injection with C and/or hydrogen sources for a slag foaming purpose in EAF.

Further characterization concerned particle size distribution and density, whose measurements were performed by manual sieving and weighing of a known volume of each material, and full mineral analysis including moisture and Loss on Ignition (LOI, i.e., a measure of the volatile components in a sample. The analysis assumes that Si, Al, Ca, Fe, K, Mg, Mn, Na, P and Ti were oxidized which was not necessarily true. Indeed, some of the oxidic waste materials had a negative LOI which was an indication of oxidation during heating. BF-sludge, two of the mill scales, metal hydroxide sludge and grinding chips were not possible to sieve since they formed pellet-like agglomerates due to moisture or presence of other liquid in the samples. Therefore, they would need some pre-treatment, e.g. drying, to be used as a slag forming agents. As expected, dust and sludges were characterized by high Zn content as well as high S content were identified in materials from ore-based iron making. Cr content of the grinding chips was high and could be beneficial during stainless steel production. However, careful consideration was necessary when choosing oxidic waste depending on the specific EAF chemistry for the plant and for different steel grades as well as the thermodynamic impact of injecting oxidic wastes, since the reaction was endothermic and requires energy.

ASR was a highly heterogeneous mixture of residual ferrous and non-ferrous metals (5–23 %), plastics (20–49 %), rubber (3–38 %), textile and fiber material (4–45 %), wood (2–5 %), and glass (2–18 %). The

exact composition and physical properties depended mainly on shredder input, shredder equipment, and post-shredder separation processes. The heterogeneity of the material with varying levels of contamination, e.g., Cl, heavy metals, PCDD/Fs (Polychlorinated Dibenzo-p-Dioxins/Dibenzofurans), moisture content, ash content and calorific value constituted a considerable challenge to select or design an appropriate treatment process for ASR. However, two representative types were identified and selected for further investigation, i.e., a light fraction and a heavy fraction. ASR characterization showed that the light fraction had a high content of carbon-based materials such as plastic, rubber, textile and PUR foam reaching around 90 % while the metal content was about 4 %. Concerning the heavy fraction, plastic content was lower around 42 % while metal content was around 16 %. A major part of both fractions constituted volatile matter, i.e., 72 % for the light fraction and 84.8 % for the heavy fraction, while fixed C content was in the range of 3-5 % for both ASR fractions. Furthermore, the weight loss rate for light and heavy fractions in air and nitrogen were the same thus confirming that the fluff combustion occurred through mass transfer of volatile matter from particles to the surrounding and combustion of volatile material.

Theoretical calculations based on heat and mass balances for different material combinations were carried out to find suitable materials for the pilot and industrial trials together with an identification of the environmental and economic constraints. An existing EAF model was updated to consider the use of non-standard materials such as waste material blends, ASR and plastic residues. The mathematical model was calibrated with these materials using the results of the pilot experiment carried out to test the influence of the various C-based materials in EAF. The model was set up and validated for each steel plant furnace. The results of the model showed that the calculated steel composition was in line with the observed results after tapping for the pilot trial at Swewrea. However, there were small differences observed mainly due to the model overestimating the FeO content in the slag. The model calculated the tapping temperature correctly with 70 % of the heats being in the range of ±12 °C.

Preliminary experimental trials were used to calibrate the model for Feralpi EAF where 100 kg of anthracite was substituted with 450 kg of ASR. The calibrated model permitted the calculation of the trend of the EAF process parameters as a function of the amount of ASR charged, i.e., from 450 to 900kg. These results showed a negligible increase of elements that could influence steel quality such as S, Cu, P, Sn, as well as a negligible increase in NOx emission. The results also showed a slight reduction in production cost that was only indicative due to the variability of ASR pre-treatment price for production of the briquettes and the cost of ASR disposal. However, the model calculation showed that the use of ASR reduced heat costs. Finally, the model results also showed limiting factors in ASR use regarding off-gas temperature and reduction of EAF productivity. For the model calculations of Höganäs EAF, it was decided to use the same model parameters determined from the trials at Swerea since the mix of materials was similar. A comparison of model calculations between the reference case without injection and injection of C, Petrit-T as C injection substitution and EAF dust as reducible materials for Fe recovery from the slag showed that all cases simulated were compatible with possible production conditions in the industrial trials. Similar to the model calculations of Höganäs EAF model parameters from the trials at Swerea was also used for the calculations of ArcelorMittal EAF. A comparison of the use of only anthracite injection with 85 % C and the injection of a mixture of anthracite with rubbers, i.e., 75 % C and 7 % H, showed no vast differences.

Simulations of new materials charging in the different EAFs involved in the project were performed. The data was collected in a database where not only the characteristics of the inlet material, e.g., scrap, hot metal etc., but also the operative practices were reported to select a representative plan for the three industrial EAFs. The model results showed that the use of these materials in substitution of anthracite influenced not only steel and slag composition but also off-gas composition and temperature. At this phase, S and Cu contents in the steel were selected as limiting factors. The calibrated iCSMelt model allowed to determine boundary amount of the new blend of materials to guarantee that S and Cu did not increase from the reference level with more than 10 ppm for S and 50 ppm for Cu. The calculation of pilot trial material mixtures was performed without boundary conditions for the individual materials. Calculations were based on the hypothesis that all C, H and Zn in the injected/charged waste materials replacing anthracite and oxygen would form CO, H2 and Zn, and that these gases will have the same foaming efficiency of the gases generated from anthracite injection. The replacement rate of anthracite and oxygen was calculated based on the difference in gas generation ratio of anthracite and waste blend and the content of oxygen bound to reducible oxides in the waste blend. The replacement ratios were set to fulfil project objectives, but also with higher replacement ratios to determine a maximum amount of replacement in the mixtures. Material mixtures for various degrees of replacement of carbon, hydrogen and oxide-containing wastes could be calculated for the plant trials at Swerea. However, no material mixtures were calculated for the ArcelorMittal trials. Instead, the waste materials were injected through co-injection, and the flow of reference material and waste material was changed throughout the trials.

An activity was performed on pre-treatment methods to make the materials adapted for charging or injection into EAF. One objective was the identification of suitable particle sizes and shapes of the materials for injection purposes while other objectives were the identification of drying methods and the development of briquetting/pelletizing of materials. PU plastics proved to be unsuitable for injection since they compressed to a cake, and it was not possible to keep them fluid. EAF dust displayed similar problems connected with compression, but they could still be injected if mixed with anthracite. Pre-treatment of BF sludge by Tornado cyclone drying appeared to be a suitable way to turn Zn containing waste from BF steelmaking route into a usable slag foaming agent in EAF steelmaking. Rubber granules seemed to be suitable for C and H containing waste for replacing anthracite. The physical properties of PE/XLPE plastics made them unsuitable for injection due to the uneven particle shape and to the particle size distribution which could not be guaranteed. This fact may cause problems with clogging in material dispenser. It was also noticed that it was necessary to agglomerate ASR to charge the material into EAF with the scrape basket. Two main methods were available to compact this type of material, i.e., briquetting and hot extrusion, and both of them were found suitable for the compaction of ASR light fraction. Concerning briquetting, an adequate quantity of material was produced at CSM laboratory considering three different compositions containing different amount of ASR, iron scale, CaO (pure or in mixture with white slag), binders (molasses or lignin sulphate) and water. The results obtained proved that the light fraction of ASR could be briquetted by using the appropriate addition of binders including also by-products present in the steel plant such a ladle slag and iron scale, but it required a pre-treatment to eliminate the coarse fraction and the metals. Moreover, ASR content in the briquettes should not exceed 17-20 % since a further

increase would reduce the mechanical properties of the briquettes. Besides briquetting, hot extrusion at 150-250 °C of the ASR was carried out and ferrous and aluminum residues were obtained from the process. The results showed that the light fraction of ASR must be pre-treated eliminating metal residues and coarse fractions such as gravel and electronic components to be extruded. It must be also considered that ASR was classified as waste and its use must be authorized by the Italian local authorities. For this reason, it was mandatory for Feralpi to get the temporary authorization to use this material, classified as waste, as reductant agent in EAF to perform plant trials with the briquettes.

Moving to the pilot trials at ArcelorMittal, the material blends were decided according to the degree of replacement of anthracite and oxygen. ArcelorMittal decided to use different injection devices to inject both carbonaceous residues and anthracite simultaneously instead of pre-mixing. This approach would limit the risk of using a pre-mix blend where segregation due to size or density differences between coal and residues may occur thus leading to uncontrolled variations of coal and residue. The co-injection solution was also much more flexible regarding the proportion of coal and residue injected that could be changed to optimize slag foaming phenomena. Furthermore, only carbonaceous residues were assessed by ArcelorMittal. In their industrial plant, coal injection rate for slag foaming was around 10t/h in a furnace of 150 t of liquid steel capacity leading to a coal injection rate of 66 kg/h/t of liquid steel. This meant that 400 kg/h were necessary for their pilot furnace with a 6-t capacity which gave an injection flow rate of 6.66 kg/min. AMMR selected seven residues to test based on chemical and physical criteria. These materials include plastic fines from a plastic recycling company, fine rubber powder from end-of-life tires grinding, wood sawdust pellets, petroleum coke, a fraction of shredder residue extruded from Feralpi and two shredder residue fractions extracted with the Sicon technology. According to the trial plan, the replacement ratio of anthracite varied from 10 to 30%. Di/Dt measurements of the three electrodes of the pilot EAF were combined with sound measurements during the trials. Indeed, the current stability Di/Dt of the three electrodes during injection allowed to determine the foaming intensity combined with noise measurements and visual inspection. Noise measurements achieved during trials was not clear, but visual observations performed by the operators were obvious and confirmed when the best slag foaming was obtained. The current stability also provided applicable information on the foaming intensity. Besides these measurements, pollutants were measured by an external company LECES. Due to bag filter inefficiency, some other pollutants were found with relatively high concentrations such as Pb, Zn and dioxins. The concentration of organic pollutants measured during those trials could also be higher than those obtained during industrial heats, because at pilot scale only one heat was performed per day and therefore it was not easy to have a post-combustion chamber at high temperature, especially at the beginning of the heat.

The results showed that most injected materials had limited impact on liquid steel quality except tire rubber fines, Shredder Residue Sicon 1, petroleum coke and the Shredder residue Feralpi which brought some S. Furthermore, Shredder Residue Sicon 1 and the Shredder Residue Feralpi brought some Cu. Finally, no slag foaming was obtained during fine polyolefin injection. Only a lot of dark fumes and burning plastic smell were obtained. This phenomenon was such important that the fume collection system of the pilot EAF was saturated and many fumes went out of the furnace. The shredder residue prepared by Feralpi showed roughly the same behavior: no slag foaming, a lot of dark

fumes and a lot of VOC in the fumes at the chimney. The best material regarding slag foaming were the tire rubber fines, the Shredder Residue fraction Sicon 2, the petroleum coke and the wood pellets.

At Swerea, seven different material mixtures consisting of both carbonaceous residues and oxygen containing material were blended using four different materials in preparation of the injection trials. The materials blended were anthracite, rubber, Petrit T and EAF dust and the replacement degree of anthracite varied from 10-80 % while the replacement degree of oxygen varied between 0-10 % for the different material mixes. The most promising material mixes for injection and charging were selected for pilot trials. First, the materials were tested off-line by dry injection outside the furnace together with laboratory tests of briquettes/pellets. The purpose of the off-line tests was to confirm that the prepared materials had the correct physical properties required for charging and non-clogging injections at the appropriate flow rate used for the trials. After evaluation of the off-line tests, pre-treatment methods were adjusted, and unsuitable materials were excluded. Besides the development and control of the injection system, it was also essential to validate the feasibility of the injection scheme at pilot scale. Measurement of foaming efficiency, environmental impact and effect on steel quality were also crucial objectives. The test at Swerea aimed to establish the injectability of the different blends prepared for the pilot trials. Two different feeding rates were examined, i.e., 3-5 kg/min for the pilot trials and 20-30 kg/min for the plant trials. Two dispensers with different feeding systems were used for the two feeding rates. A dispenser with a ball sector valve for high feeding rates and a dispenser with a roto-feeder was used for low feeding rates. Swerea performed 15 slag foaming trials with six different material mixtures containing anthracite, rubber Petrit-t and EAF-dust. During the trials, the replacement ratio of anthracite varied from 20 to 50%, and the replacement oxygen ratio varied from 2 to 10 % for the different material mixes. Sound, electric with Rogowski coil and dioxin measurement of the waste gas was completed for the trials. Environmental measurements were performed for four heats to analyze dioxins, PCB (Polychlorinated Biphenyls) and PAH. Slag foaming intensity was visually evaluated on a scale from 1-5. Signal treatment for the Rogowski coil measurements was developed, and the total harmonic distortion (THD) was calculated. Evaluation of THD for the injection period together with the visually observed slag foaming intensity showed that THD could be used to evaluated changes in foaming intensity, but it was yet impossible to quantify the foaming. Unfortunately, the only foaming intensity obtained was from visual inspection and the results showed that good foaming was obtained for most of the material mixes.

The results showed that slag volume increased more when Petrit-T was used since it contained CaO and SiO2. Furthermore, an increase in the S content of steel was detected when Petrit-T or rubber was used in the mixes as C source for foaming. The mass balance calculations showed that the S increase in the steel samples was directly proportional to the amount of S in the injection material. The S content in the slag decreased for most heats, but not enough to even out the increase in the metal phase. One hypothesis was that the reduction potential would be higher if hydrogen-containing material was used to replace some of the C used for the creation of gas in the slag during foaming. This increased reduction potential would facilitate the reduction of oxides from the oxidic compounds in the slag and/or the oxygen containing materials that were injected to replace the oxygen gas. However, there was no correlation between the change in FeO in the slag and the amount of hydrogen injected. Results from the pilot trials were analyzed and material was prepared for industrial trials. All

material mixtures tested during the pilot trial could be used as slag foaming agent. The limiting factor was S increase in steel. It was difficult to determine a factor for the S increase in the metal phase based on the results from the pilot trial when scaling up the experiment to plant trials since the Höganäs EAF furnace was likely to behave differently than the pilot furnace with slag removal from the furnace to a greater extent. However, when calculating material blends and material flow for the plant trial it was assumed that the levels of S in the injection materials would be in the same range as in the pilot trial, i.e. all S from the material will end up in steel.

Plant trials were performed at the three industrial partners of the project Höganäs, ArcelorMittal and Feralpi aiming at validating the technical and economic feasibility of partial replacement of coal with waste/coal blends involving both injection and charging of agglomerates. Höganäs prepared and executed the full-scale trials in its EAF, i.e., an AC furnace with a capacity of 60 tones, which used anthracite as C source for carburization and slag foaming combined with oxygen injection. During the trials, the existing anthracite and oxygen injection system was used with the addition of Swerea injection vessel. A total of 17 heats were performed with two heats acting a reference with only anthracite and oxygen gas. Material mixtures consisting of anthracite, EAF dust, Petrit-T and granulated rubber were used during the trials. The mixtures were calculated based on project objectives but also with respect to the results from the pilot trials to avoid risk for S increase in the steel. The Höganäs trials showed that it was possible to inject EAF-dust, rubber and Petrit-T together with anthracite and keep good foaming at least qualitatively. However, it was intricate to quantify the effect of the different injection materials on slag foaming. Injected material blends containing EAF dust and rubber showed promising results for both S content in the steel and foaming capabilities. These results could form the basis for industrial implementation in the future. However, Höganäs decided not to go forward with the injection investigations due to the non-conclusive results regarding the S content in the steel. In any case, the results were judged to be promising and could form the basis for more activities in the future.

ArcelorMittal performed the plant trials in their twin shell DC furnace with a capacity of 155 tones equipped with four burners with lancing oxygen, two burners with post-combustion, three sidewall carbon injections and one fifth lime hole feeding through the roof. Five different residues were tested, i.e., EAF fine rubber powder (0-1 mm), coarse rubber powder (1-4 mm), sawdust pellets, shredder residue fraction obtained with Sicon technology and petroleum coke. Partial injection of the first four residuals was accomplished with arc stability and sound measurements. Both Sicon shredder residue fraction and coarse rubber powder from end-of-life tires performed similarly to coal injection as slag foaming agents. No measurements of arc stability and sound during were accomplished for the long-time trial with petroleum coke, but the furnace operators concluded that it had roughly the same behavior as coal with a replacement ratio of 1.

The industrial trials of ASR utilization charge material have been carried out at Feralpis 105 tonnes EAF. The plant trials were divided into two phases, i.e., a preliminary experimental trial and a long-term experimental campaign. The plant trials performed in Feralpi showed that the ASR after proper treatments of post shredder and agglomeration could be charged into the EAF. ASR did not modify the main EAF process parameters such as electric energy consumption, methane consumption etc. not

the addition of ASR briquette in the range of 450-900 kg per heat did not increase bath carburization. Furthermore, the amount of dust did not vary with ASR use but a slight increase of PAH compounds was detected due to the aromatic compounds contained in the ASR mix, and the dioxin level and heavy metal concentration in the off gas was not affected.

From the results from the plant trials, it was evident that partial substitution of C and oxygen with industrial and/or municipal waste was a viable option from a technical viewpoint. Of course, many of these waste materials needed pretreatment before being added to the EAF. This was especially true for ASR where agglomeration was needed. Some problems were also identified in quantifying the foaming intensity during injection trials of this type of materials. Results show that injected material blends containing EAF dust and rubber gave promising results for both S content in the steel and foaming capabilities. It was also clear that both Sicon shredder residue fraction and coarse rubber powder from EoL tires performed similarly to coal injection as slag foaming agents. Finally, it was most encouraging with the results from the long-time trial with petroleum coke where the furnace operators concluded that it had roughly the same behavior as coal with a replacement ratio of 1 to 1.

The environmental assessment showed that the environmental impact of the off gas was probably more related to process parameters than the material in the slag foaming agents in the range of replacement that was evaluated. Some increases were measured with full replacement on the environmental impact, e.g., dust, PCDD/F, CO and VOC. The slight increase of PAH compounds was due to the aromatic compounds contained in the ASR mix. The presence of aromatic was confirmed by the small increase of PCB. The dioxin level and heavy metal concentration in the off gas was not affected.

2.2.20 ACTISLAG: New Activation Routes for Early Strength Development of Granulated Blast Furnace Slag (46)

The project was coordinated by ArcelorMittal with Ecocem Materials, FEhS, Technische Universitet Clausthal (TUC), Centre National de la Recherche Scientifique (CNRS), Universite Paul Sabatier Toulouse III participating as partners in the consortium. The project started on the 1st of July 2017 and lasted four years, ending on the 30th June 2021. The overall project cost 2.88 M€ and EU contributed 1.72 M€, i.e., almost 60 % of the budget.

The focus of the Actislag project was to enhance the early reactivity and strength development of ground granulated blast furnace slag (GGBS) which was a major industrial by-product of ironmaking used as a supplementary cementitious material. The project investigated how both slag intrinsic factors, e.g., chemical composition and glass structure, and external activation strategies, e.g., thermal treatment and chemical activators, influenced slag hydration processes and early mechanical performance. A key ambition was to develop a second generation GGBS able to replace up to 80 % of cement in a blend while achieving early strength gains comparable to conventional cements with much lower slag content.

Detailed studies were carried out at both micro and nano scales to link slag composition and process history to its reactivity in cementitious systems. This included exploring both upstream modifications

to the slag during melting and granulation and downstream methods involving activators and curing conditions after slag production (47; 48). The experimental campaign started with the characterization of 16 different samples of industrial slag which led to the selection of 7 slag types for a further in-depth structural characterization including structural organization and thermal history of GBFS (49). The glass structure and hydration mechanisms were also investigated. The polymerization degree of the vitreous GGBS network was estimated from compositional data and electroneutrality assumptions providing a rapid but simplified overview of the glass structure. However, this approach relied on several assumptions regarding the structural role of constituent elements, the distribution of non-bridging oxygens, and the homogeneity of the material. Spectroscopic techniques such as Raman and solid-state NMR offered deeper structural insight, even if their application to industrial slags resulted challenging and required careful spectral acquisition, deconvolution, and interpretation, particularly due to the influence of Al–O–Si bonds (50). Furthermore, dissolution test and calorimetric measurements from literature enabled rapid evaluation of slag reactivity. In particular, the results of the R3 (Rilem)-protocol, i.e., a 24-hour heat release test, correlated well with the 2 days compressive strength of standard mortars typically used for evaluation using 75 wt.% of GGBS (51).

Around 160 modifications were performed to test the effect of major and minor components since small changes in quantity proved to have a big impact on reactivity. For example, alkali metals, alkaline earth metals and Al_2O_3 displayed a positive effect without drastic changes while TiO_2 and SiO_2, or ZrO_2, V_2O_5, Cr_2O_3 had a negative effect (47)Errore. L'origine riferimento non è stata trovata.. The cooling history of GBS was investigated using calorimetric measurements in the glass transition region combined with high-temperature viscometry analyses. The industrial slag examined was characterized by a median particle size of 700 µm and a predominantly glassy structure and it exhibited a high energetic state marked by a fictive temperature about 160 °C above the glass transition temperature under equilibrium conditions. By applying established viscosity models and linking quench rate to shear viscosity at the fictive temperature, the formation conditions were estimated to correspond to a shear viscosity of ~$10^{5.9}$ Pa·s and a cooling rate of 10^5 K/s which was consistent with wet granulation by water-jet quenching. These findings highlighted the strong influence of cooling rate on the GBS structural state and emphasized the importance of reporting both cooling rate and fictive temperature when assessing slag reactivity (52). Complementary thermal analyses, including DSC, thermogravimetry, and evolved gas analysis (EGA), were used to evaluate the effect of high-energy mechanical milling on the structural state of GBFS. Mechanically activated slag exhibited a markedly increased exothermic heat release below the glass transition temperature which intensified with milling duration and was significantly higher than unmilled materials one. This low-temperature energy release was ascribed to the relaxation of surface-related structural defects generated during milling in contrast to the bulk structural relaxation observed in hyper quenched glasses. The results indicate that mechanical milling induced substantial rejuvenation of the GBS glass network due to its low network connectivity, and suggest potential implications for enhancing cementitious reactivity, pending validation at industrial milling scales (53) .

Systematic testing of different GGBS with different activators and different Portland cements were tested. Hydration of industrial GBS samples, modified GBS samples and model glasses were tested with different high precision tools, i.e., solid state NMR, XRD, SEM-EDX, synchrotron facilities, and

X-ray tomography, to study the mechanisms behind the positive effect of alkali metals, alkaline earth metals, and Al_2O_3 and the negative effect of TiO_2. The reduction in cementitious reactivity observed in Ti-containing systems was attributed to an increased stabilization of the glass network as well as to the development of a Ti-enriched surface layer which acted as a passivating barrier Errore. L'origine riferimento non è stata trovata. (54). The use of $CaCl_2$ as accelerating admixture to improve the early-age performance of blended cements with high levels of GGBS was also investigated. Blends containing up 70 wt.% GGBS were characterized through compressive strength test, porosity measurements, calorimetry, ultrasonic wave propagation, and in-situ XRD, with inert quartz used as a reference to isolate the contribution of slag hydration. The addition of $CaCl_2$ promoted an earlier onset and higher rate of GGBS hydration which coincided with the formation of AFm phases and resulted in increased heat release, faster microstructural development, and significantly higher compressive strength during the first 7 days. These improvements were associated with accelerated pore refinement, while long-term compressive strength remained comparable to systems without $CaCl_2$ (55).

The project outcomes provided new insights into how glass structure, cooling rates, particle size, and chemical activation affect hydration and strength development of GGBS in cement ultimately creating pathways to tailor slag for improved early performance in concrete and mortar applications. ActiSlag contributed valuable knowledge toward increasing the utilization of slag in construction materials, supporting both environmental goals and competitiveness in the European steel and cement sectors while fostering industrial symbiosis. The work demonstrated the applicability of rapid testing methodologies to a wide range of GGBS, extending their use beyond the limited cases previously reported. After the modifications cooling rates were investigated which showed that different grain sizes have different cooling rates and that slower cooling has a negative effect on the hydraulic properties of the slag. The approach enabled estimation of slag cooling rates for the assessment of advanced quenching technologies aimed at enhancing reactivity and can be transferred to other steel slags, e.g., EAF slag. In addition, the systematic combination of slags and activators, supported by model glass studies and microtomography, provided improved insight into key parameters controlling phase evolution and cementitious performance.

2.2.21 FINES2EAF: Cement-free brick production technology for the use of primary and secondary raw material fines in EAF steelmaking (56)

The project was coordinated by RWTH with University of Oulu, Montanuniversität Leoben, Max Aicher Umwelt, Marienhütte, Sidenor, Politecnico di Milano and MFG (Metall-und Ferrolegierungsgesellschaft) participating as partners in the consortium. The project started on the 1st of July 2017 and lasts almost four years, ending on the 30th of June 2021. The overall project cost 1.62 M€ and the EU contributed 975 k€, i.e., almost 60 % of the budget.

In 2017, it was estimated that steel-making activities produced about 80 Mtonnes of by-products and waste in Europe and more than 10 Mtonnes were sent to disposal. The Fines2EAF project tried to address this waste of resources and land area and to increase the value of steelmaking fines residues by promoting internal recycling and their reuse in the form of cement-free bricks. In particular, an

innovative process to produce cement-free bricks with primary and secondary raw material fines, alternative binder systems and a hydraulic stamp was developed. The bricks produced must possess sufficient cold compression strength for low-abrasion handling and sufficient reduction behavior and metallurgical performance to be self-reducing bricks. All these features could be ensured only through a deep and clear understanding of bricks manufacturing and use. The project proved that the production of cement-free bricks by stamp press was a valuable option to process a wide range of fine residue materials arising in lower amounts at EAF steel plants in an economic way. The benefit of this strategy was fourfold since it promoted an improved utilization of residues, an internal recovery of metals, the reduction of the number of materials to be dumped and a consistent saving of natural resources such as limestone and dolomite. All these benefits clearly ensured an improved carbon footprint of steel production and an enhancement of the use of primary raw material fines and the recycling of secondary raw material fines.

The first part of the project was devoted to the sampling and characterization of the residues materials from steel plants and from other industrial sectors. In particular, an inventory with the physical and chemical characteristics of primary and secondary raw materials was accurately compiled including also information on the amounts and current use of those materials. The physical characterization included the determination of moisture content, bulk and true density, grain size distribution, and melting/softening behavior by hot stage microscope. The chemical characterization included elemental analysis by XRF, determination of carbonate amounts, specification of fractions and phases by SEM-BSE (Back Scattered Electron) and SEM-EDS analysis, determination of weight loss and/or volatiles and phase transformations by TG-DSC analysis, phase determination by XRD analysis and for specific samples analysis for the iron oxides and metallic Fe content. Based on the inventory, the most appropriate materials for the microwave pre-treatment process and for the development of the recipe for lab-scale brick production were selected. The microwave pre-treatment was developed to reduce the amount of Zn, Pb and volatiles since microwaves take the form of electromagnetic energy and can penetrate deep into the sample ensuring a volumetric heating providing a heating method substantially different from conventional ones where the sample is heated from outside inward. Considering this, the results obtained were compared with conventional furnace treatment ones. Microwave heating was able to ensure a similar de-zincing of EAF dust, but it was reached at lower bulk temperature and with a higher Zn purity of the dust removed. Indeed, the chemical composition of EAF dust after microwave heating indicated a Zn reduction of 53.5 % after 10 minutes at 1000 W and an increase in heating time up to 20 minutes ensured an increased Zn removal up to 90.4 %. In addition, the overall Pb, Cl and alkaline contents in the residue were reduced with Pb being decreased from 0.85 to 0.27 wt.%, Cl from 1.27 to 0.28 wt.%. and K_2O from 0.86 to 0.08 wt.%. A variation in material heating behavior was also observed according to the chemical composition. In particular, EAF dust reached 630 °C and the sample of water treatment sludge reached 723 °C after being exposed to microwave power of 1000 W for 5 minutes. Both materials displayed high microwave absorbing properties thanks to the presence of C and iron oxides which are classified as excellent microwave absorbers (57). Different recipes were developed according to the materials available and their suitable application in the steel plant. The recipe developed for Max Aicher Umwelt and Marienhütte was focused on CaO and MgO containing materials to produce synthetic slag former bricks while the recipe developed for

Sidenor focused on the use of oxy-cutting fines, metallic Fe containing grinding sludge and fines collected at the belt conveyors. The lab-scale production of the brick was conveniently optimized by considering different binders, e.g., sodium silicate, polyethylenglycol (PEG), carboxymethylcellulose (CMC), starch, molasses, copolymer binders, etc., as well as different agglomeration parameters such as pressing force, pressing time, drying conditions, etc. In addition to the different binding systems and agglomeration parameters, the effect of additives such as $CaCO_3$, bentonite, SiO_2, and fibers from paper recycling was also tested to increase for example the strength of the produced agglomerates. The preliminary agglomeration tests were performed with very fine and dry FeMnC filter dust with a C-based binder. Two series of agglomerates were produced with 4 wt.% binder (series A) and without binder (series B) as shown in Figure 18. The latter was characterized by a conspicuous number of cracks. The two classes of agglomerates were subjected to drop tests by dropping the sample three times from a height of 2.5 m and this procedure caused the complete destruction of the samples of series B while the samples of series A only showed a weight loss of about 1.5 % (Figure 18.C).

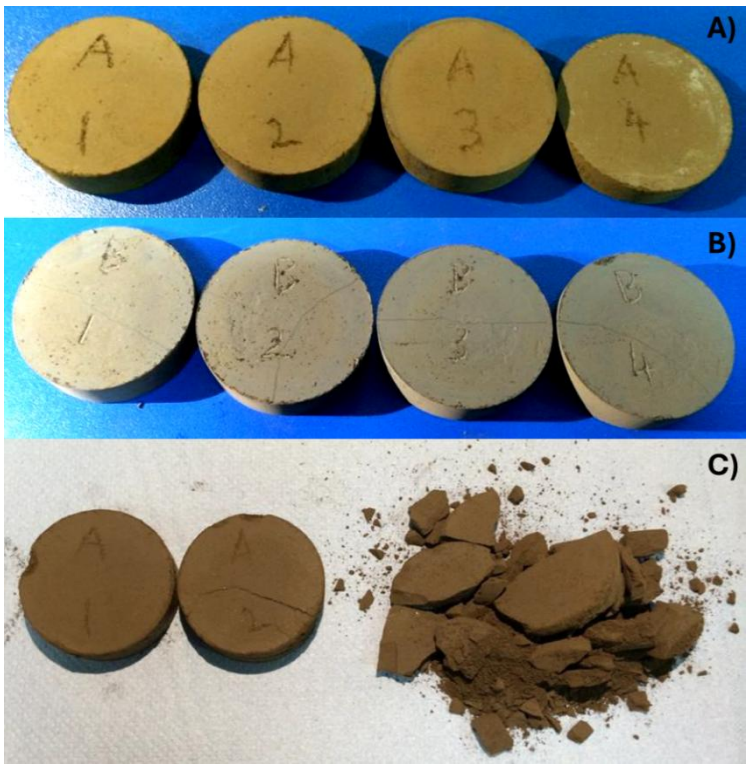

Figure 18: FeMnC filter dust agglomerates with (A), without (B) binder and samples of series A and B after the drop test (C) (57)

The second part of the project was dedicated to the high-temperature testing of the most promising recipes as well as the pilot-scale production of the optimum solution for the subsequent industrial trials. The thermal behavior of the bricks was investigated by optical dilatometry, by TGA-MS, by melting and dissolution trials up to technical scale melting experiments and the work was finalized by

an evaluation of the metallurgical performance of the tested recipes. Some preliminary results on the thermal and reduction behavior of five different briquettes recipes whose composition is reported in Table 19 were obtained through TGA-MS in Ar atmosphere reaching temperatures up to 1600 °C. All briquettes employed starch as binders and recycled fibers from paper production to increase strength. Some residues from TGA-MS analysis were characterized through optical microscopy, SEM, EDS and XRD.

Table 19: Recipes of five different briquettes whose thermal and reducing behavior were investigated through TGA-MS (58)

	A	B	C	D	E
Grinding Sludge	-	-	46.0	-	-
Belt Conveyer Fines	-	63.4	-	-	-
Oxy-Cutting Fines	36.2	-	33.8	-	-
Combustion Chamber Dust	35.9	-	-	-	-
Injection coal	15.6	-	10.2	-	8.4
Ladle Furnace Slag	-	-	-	55.2	-
Spent Refractory	-	-	-	27.5	-
FMC	-	-	-	-	69.7
$Ca(OH)_2$	-	-	-	-	2.4
Type 3 Fibers	0.9	0.7	0.9	0.8	1.0
Starch Type 6501	4.0	4.8	9.2	8.3	6.9
H_2O Addition	7.4	31.1	-	8.3	11.7

The thermal behavior of recipe A displayed a strong H_2O signal starting from 100 °C because of moisture evaporation and a second strong peak at 310 °C persisting up to 570 °C resulting from starch binder and fibers decomposition. It also indicated the elimination of the chemically bound water. The signal then progressively deteriorated up to 670 ° C, indicating a small amount of bound water still leaving the sample. The decomposition of fibers and starch was confirmed by the strong emission peaks corresponding to the release of CO and CO_2 detected at around 288 °C. A further decrease in mass at 700 and 950 °C was observed likely due to the reduction of hematite and magnetite, respectively. The results deduced from TGA-MS analysis were confirmed by SEM and XRD analysis of the residues since most of the briquette was converted into metallic material with Fe displaying the typical microstructure of cast-iron with a pearlitic matrix surrounded by primary cementite and graphite flakes. The non-metallic residue consisted mainly of unreduced iron oxides, especially wüstite, and from unburned C. Recipe B consisted mainly of conveyer belt fines which in turn consisted mainly of CaO, i.e., > 90 wt.%, which is very stable at high temperatures and cannot be reduced by C at the testing temperature range. The water added during the briquette production, i.e., 31.1 %, left the sample during the initial stage of the heat together with other volatiles. Again, the release of CO and CO_2 at 250 °C was ascribed to the decomposition of starch and fibers whereas the mass drop starting at 400 °C was ascribed to the release of chemically bound water. The second sharp decrease in mass occurring from 600 to 800 °C was ascribed to the decomposition of residual $CaCO_3$ as it was

accompanied by significant peaks of CO and CO_2. Recipe E consisted mainly of FMC, i.e., 69.7 wt.%, and a significant amount of added water, i.e., 11.7 wt.%. The latter was again released between 100 and 535 °C and the mass loss observed was further sustained at around 250 °C by the decomposition of starch and fibers. Briquettes reduction took place in different steps. The first sign of reduction was detected at 533 °C with a sharp CO_2 peak. The second one occurred at 680 °C with both CO and CO_2 peaks and a steep mass loss and finally a high temperature reduction from 1200 to 1600 °C with the briquette experiencing a mass loss higher than 20 % accompanied by a strong release of CO. The analysis of the residue displayed a small fraction of metallic Mn resulting from the reduction of MnO, but the main product resulting from the thermal test was Mn5SiC which is a typical product of carbothermic reduction of manganese ores. Finally, the analysis of recipe C consisting mainly of grinding sludge and oxy-cutting fines, i.e., iron and iron oxides, and injection carbon displayed again the typical peaks of water removal from 100 to 400 °C and a small mass change near 250 °C accompanied by CO and CO_2 peaks resulting from fibers and starch decomposition. Besides them, a continuous mass loss accompanied by CO and CO_2 emission was detected from 700 °C which indicates that C was utilized to reduce iron oxides from hematite to metallic iron. The mass loss became steeper at 1100 °C thus suggesting a further iron oxide reduction.

Besides TGA-MS tests, some preliminary pilot scale trials were performed to determine the dissolution behavior of agglomerated steel mill residues in an EAF-furnace environment. The trials were performed using a DC-EAF and using the slag obtained from the remelting of typical slag provided from the steel partners as heating element since it was the component with the highest electric resistance. The first trial employed 15 kg of slag,17 kg of steel and 0.9 kg of briquettes type D whereas the second one used 10 kg of slag, 40 kg of steel and 10 kg of briquettes type C. The change in the chemical analysis of steel and slag phases was determined to evaluate process performance. A total of 19.6 kg of ferrous alloy was tapped after trial 1 and the mass increase was due to the partial reduction of iron oxide from the slag and the dissolution of the charged briquettes. The chemical analysis of the steel and slag phases before and after briquettes introduction revealed no significant influence on both of them, a rapid and good dissolution of the briquettes was observed, and this proved the feasibility of substituting CaO additives with the briquettes which was the main objective of the experiment. A total of 48 kg of ferrous alloy was tapped after trial 2 and the 8kg mass increase was due to the partial reduction of iron oxide from the slag and the dissolution of the charged briquettes. Again, the chemical analysis of the ferrous alloy was not significantly influenced by the charging of the briquettes whereas the chemical composition of the slag reported a drop in basicity, a decrease in iron oxide content and an increase in MgO due to the charging of the briquettes. The experiment displayed again a good dissolution behavior of the briquettes although the ratio of charged material compared to the pre-molten slag and iron alloy was probably higher than it would be in an industrial application.

Based on the high-temperature testing, the optimum final recipes for pilot-scale brick production were defined and around 81 tons of bricks were produced and delivered to the steel shop. The following industrial trials in EAF were performed at Max Aicher Umwelt, Marienhütte and Sidenor and included an extensive investigation on the quality of the resulting EAF slag. In particular, the steel plants performed 7 campaigns with a total amount of 66 heats. The latter demonstrated that the use of cement-free residue bricks could ensure the substitution of lime and dolomite together with the

recovery of Fe without any negative influence on furnace operation, steel or slag quality. The project was concluded by a techno-economic and ecological evaluation including the development of plant concepts for brick production with and without pre-processing of the residues. The overall cost of brick production calculated was in the range of 60-105 €/t brick which was mainly due to the need of pre-processing and the amount and cost of the binder. These costs were offset by the costs for primary lime and dolomite as well as the cost of landfilling. The ecological evaluation was based on LCA and was compared to the current reference. The substitution of burned lime by recycled slag formers showed a higher reduction of the global warming potential than the substitution of scrap by metal bearing residues.

2.2.22 ECOSLAG: Eco-friendly steelmaking slag solidification with energy recovery to produce a high-quality slag product for a sustainable recycling (59) (60)

The project was coordinated by FEhS with Max Aicher Umwelt Gmbh, Sidenor, CIC EnergiGUNE (Fundacion Centro de Investigacion Cooperativa de Energias Alternativas Fundacion), RINA-CSM, A.C.P., Swerim, SFTec Oy, and Tenaris Dalmine, participating as partners in the consortium. The project started on the 1st of June 2018 and lasted almost four years, ending on 31st May 2022. The overall project cost 2.52 M€ and the EU contributed 1.4 M€, i.e., almost 60 % of the budget.

Steelmaking generates substantial quantities of slag, which retains a significant thermal energy content at the point of production. BOF, EAF and LF slag carry approximately 1.5 GJ of heat per ton each, i.e., 417 kWh/t, at tapping temperatures. Nearly all this energy is dissipated to the environment during uncontrolled air or water cooling in open slag yards in conventional practice. The ECOSLAG project aimed to find an integrated solution for heat recovery from steelmaking slag while still obtaining high value slag product for external use. The project tested three distinct heat recovery concepts and two associated slag treatment approaches in laboratory, semi-industrial and industrial scales. The first concept included the recycling of hot, solidified LF slag back into EAF as a lime substitute using a sandwich charging structure. The second approach considered the dry air granulation of LF slag at the tapping point to produce a vitreous high-value secondary raw material. The last concept focused on the recovery of heat from BOF slag through the RecHeat convective heat exchanger system with downstream material drying via a ModHeat dryer. Additionally, thermoelectric generator (TEG) panels and air-cooled refractory and pipe-to-pipe panels were tested to quantify the potential for electricity generation and hot-air production directly from slag pit radiation and conduction.

Before committing to physical construction of heat recovery hardware, the project used CFD modelling to optimize device geometry and operating parameters (61). For the RecHeat system, the model tracked both a structure-heating stage during which the metallic body of the apparatus absorbed conductive and radiative energy from the poured slag, and a heat-exchanging stage during which ambient air drawn through internal channels absorbed the stored thermal energy. These modelling results directly informed the structural redesign of the RecHeat prototype and guided the choice of operating conditions for subsequent physical tests. For the LF slag tundish, the CFD model characterized the evolution of temperature within a mixed steel/slag charge over a 2,200-second

cooling window, revealing important spatial gradients that governed the timing and safety of the sandwich charging operation. The model results confirmed that the minimum safe handling temperature of around 200 °C, below which LF slag begins to disintegrate by hydration, could be reliably identified and used to define the operational window for sandwich transfer.

Different tests were conducted at the laboratory scale to prepare for industrial trials and to validate the heat recovery concept from different means. Small-scale tundish cooling experiments using LF slag were conducted by heating it to 1600°C and pouring it into a pre-heated refractory-lined tundish. The slag cooled to approximately 100 °C within half an hour and no disintegration was observed upon removal consistently with the expectation that rapid cooling suppresses the phase transformations responsible for self-pulverization. Bench-test of a TEG panel at laboratory scale before industrial trials confirmed the functionality of both the cooling water circuit and the electrical acquisition system.

Two semi-industrial RecHeat tests with 6.7 tons and 5.9 tons of BOF slag were performed by pouring the slag onto the redesigned heat exchanger structure. Heat recovery efficiency was evaluated relatively to a theoretical slag energy content of 1.5 GJ/t and reached 33.3 % over the effective drying window, i.e., the period during which outlet air temperature exceeded 80 °C, in the second semi-industrial test with 814 kWh of energy recovered over a contact window of 3 hours 20 minutes. The structure tolerated the thermal and mechanical loading of the slag without damage, providing a positive proof-of-concept for scale-up.

EAF slag was used in extensive series of heat recovery experiments using a 1 m^3 packed-bed air test loop instrumented with 35 thermocouples at nine positions across five levels. Three heat transfer fluids were investigated, i.e., air, water and steam. Thermal efficiencies up to 96 % were obtained using air when slag initial temperature was 200 °C. This value fell to 83 % at slag initial temperature of 500 °C due to the poor thermal conductivity of slag and surface heat losses. A maximum cooling power of 30 kW was recorded under reproduced conditions. Efficiency was lower and equal to 76 % when using water as heat transfer fluid compared to air at the same initial temperature. Despite this, the recovered power was approximately seven times higher thus reflecting the superior thermal capacity of water and the potential benefit of faster pit throughput. Steam experiments were abandoned after commissioning tests revealed irresolvable pressure management difficulties with the available vessel design. Importantly, the experimental data validated the CFD models to within an average error of around 3 % thus confirming the predictive capability of the modelling framework.

Industrial testing was conducted in parallel across the three primary technologies investigated in ECOSLAG. Four sandwich structures were produced by collecting LF slag and residual steel from two to three heats into a refractory-lined tundish allowing the material to solidify and then tilting the tundish to release the intact sandwich for crane transport to EAF. All four sandwiches were successfully charged into the EAF without incident. Analysis of the resulting EAF slag showed no negative impact on slag composition or quality from the LF slag addition. The heat potential calculations indicated that at a realistic transfer temperature of 1000 °C with all 30 kt/y of LF slag produced at the site could theoretically contribute up to 14,324 MWh per year of recoverable thermal energy if continuously recharged to EAF.

Five dry air granulation campaigns were conducted each processing approximately 3000 kg of LF slag per heat at a gas-to-slag ratio of approximately 1.5 kg(air)/kg(slag) achieved with a 55-kW fan at 25,000 Nm^3/h. The chemical composition across all five campaigns was highly consistent with average values of CaO around 54.75 wt.%, Al_2O_3 18.05 wt.%, SiO_2 8.18 wt.% thus confirming process stability. Magnetic fraction separation from the granulated material yielded metallic Fe contents of 31 wt.% for carbon steel and 37.4 wt.% for high-alloy steel demonstrating the potential for metal recovery alongside slag valorization. An image-analysis-based intelligent control system was developed and validated against all identified granulation scenarios, though full automation awaited integration with plant process control infrastructure.

TEG panels installed at the slag pit generated 82 W of electrical power immediately upon first slag tapping with panel surface temperature at approximately 110 °C and cooling water at 18 °C. A subsequent peak of 110 W was recorded before the signal cable was damaged by contact with hot material. The available temperature data and polynomial extrapolation allowed to estimate that the panel was able to produce approximately 300 W at a panel temperature of 200 °C and 500 W at 250 °C. The total electrical energy generated by a single 0.7 m^2 panel in 24 hours was estimated at 1.2 kWh/day equivalent to approximately one fifth of the charge needed for a small electric city car. An array of 35 panels, covering a 5×5 m^2 area above the slag pit, was projected to produce 42 kWh/day equivalent to an 11.5 kW photovoltaic installation. The refractory and pipe-to-pipe panels demonstrated outlet air temperatures of 34 °C and 50 °C during testing, respectively. Scaled to full slag pit coverage 84 m^2 of refractory panels on the lateral walls and 40 m^2 of pipe-to-pipe panels on the pit floor provided a combined system which could deliver approximately 197 kW of hot air at 400 °C, sufficient to preheat approximately 2000 kg of ferroalloys per heat to a maximum of 240 °C displacing around 355 MWh/year of electrical energy per machine.

Two industrial-scale RecHeat tests were performed. In the first test, 5 tonnes of BOF slag were poured over the modified heat exchanger achieving an efficiency of 34.5 % over the effective 3-hour drying window recovering 720 kWh. In the second test, 10.9 tonnes of slag were used and the ModHeat dryer was also operated in this test drying wet sawdust as a demonstration of the full chain. Despite a 30 % reduction in air volume flow due to shared fan operation with the dryer, the test confirmed that drying is technically feasible and that the recovered heat output is sufficient for continuous industrial drying operations. BOF slag samples collected after RecHeat cooling showed mineralogy dominated by larnite with β-Ca_2SiO_4 at 30–45 wt.% and brownmillerite/srebrodolskite with $Ca_2(Al,Fe)_2O_5$ at 20–30 wt.% with no tricalcium silicate identified, i.e., the phase principally responsible for BOF slag self-disintegration during aging.

The project carried out detailed techno-economic analyses for each technology stream to establish commercial viability under realistic operating conditions. For the LF slag sandwich concept, direct electricity savings from EAF operation were not detectable across four trials due to the natural variability of EAF energy demand. Despite this, cost-benefit modelling identified two quantifiable savings streams namely avoided landfilling costs with approximately 50 €/t of LF slag and substitution of dolomitic lime with costs of 100 €/t at a 2:1 LF slag-to-lime substitution ratio. The savings would reach 3 M€ in the best-case scenario where all 15 kt/y of LF slag are recharged. This value decreased

to 800 k€ in a moderate case of 8 kt/y. For LF slag dry air granulation, the economic evaluation was based on payback time analysis across slag valorization price scenarios from 10 to 60 €/t and CAPEX scenarios of 2, 3 and 4 M€. Payback periods ranged from 1 to 4.5 years even under conservative assumptions, thus establishing air granulation as the most commercially compelling technology tested in the project. For the RecHeat system evaluated on a stand-alone heat recovery basis, the net cash flow analysis returned 236770 €/year and a net present value (NPV) of 525,100 € over a five-year lifecycle, with a payback time of 2.3 years. The break-even energy value was calculated at 17.2 €/MWh, which the project identified as a useful threshold for comparing slag heat recovery against alternative heat sources. For another industrial case with a total investment of 392800 €, the economic assessment showed an NPV of 414340 € and a payback period of 2.7 years based on current slag handling conditions. Improvements to initial slag bed temperature management raising from 150 to 300°C were projected to more than triple the NPV to 3.28 M€ and reduce payback to 1.3 years. The pipe-to-pipe and refractory panel system was the approach found not to offer economic viability under current conditions with a CAPEX of 1.85 M€ and OPEX of 380 k€/year yielding payback periods of 6–9 years depending on electricity price assumptions.

The ECOSLAG project successfully demonstrated that meaningful heat and material recovery from steelmaking slag is technically achievable across multiple process routes and plant configurations. All three primary heat recovery concepts, i.e., LF slag sandwich recharging to EAF, dry air granulation, and the RecHeat air-cooled heat exchanger, were validated at industrial or near-industrial scale with consistent slag quality outcomes and no adverse impacts on downstream slag applications. The project established a credible and evidence-based roadmap for reducing the thermal footprint of European steelmaking through the valorization of slag waste heat contributing directly to the decarbonization and circular economy objectives of the sector.

2.2.23 E-CO-Ladle Brick: Ecological and Economical waste management of the ladle refractory bricks by implementing circular economy criteria (62)

The project was coordinated by Sidenor with Tecnalia, FGF (Forschungsgemeinschaft Feuerfest) and 2.0 LCA Consultants participating as partners in the consortium. The project started on the 1st of June 2019 and lasts almost three and a half years, ending on the 30th of November 2022. The overall project cost 1.28 M€ and the EU contributed 768 k€, i.e., 60 % of the budget.

Ladle refractory wastes are mainly landfilled by EU steelworks thus lacking in systematic and integral solutions for their management. Considering this, the E-CO-LadleBrick project aimed to achieve innovative waste management for worn ladle bricks by implementing circular economy approaches based on a 4R model, i.e., reduce, reuse, remanufacture and recycle. In particular, the project targeted ladle refractory wastes reduction through appropriate monitoring system able to estimate the real degree of refractory consumption, i.e., the remaining thickness. In particular, a 3D laser scanner technique with an accuracy higher than 10 mm was coupled with machine learning models and regression analysis. The reduce-part of the project was the most time-consuming, but also the one with the bigger potential gain because the higher the reduction of bricks consumption the lower the

need to follow the other 3 Rs pathways. Concerning the reuse/remanufacturing and recycling of ladle refractory bricks, the best solution to valorize the worn bricks was identified by implementing a data-based decision algorithm which accounted for all benefits and restrictions. The final optimized application came from an expert decision tree accompanied by the corresponding LCA studies.

The first part of the project was devoted to data collection and to develop the structure of the decision tree. In particular, the industrial starting point for ladles information was assessed, the initial calibration and set up of the procedure for the 3D laser scanner measurement was performed, the data needed for the advance modelling through machine learning were identified, the procedures to remove worn refractory bricks from ladles so that their basic grade could be easily identified was defined and the process and other relevant data for LCA analysis were also determined. The analysis of refractories consumption was performed in Sidenor accounting for refractory aspects such as their basic grade, the applications where they were used, their format, the incorporation mode, the replacement frequency, the operating conditions, amounts and costs. Most of the refractory consumed in the ladles where MgO-C bricks which were sent to an external valorization agent before the project. Considering this, the identification of a new valorization alternative was fundamental to promote the reuse and remanufacture stages. New procedures for the selective removal of MgO-C and alumina spent bricks during the demolition of the ladle were established. This step was supported by FGF which performed laboratory tests such as cold crushing strength, apparent porosity, etc. to characterize the refractory waste and identify their potential reuse. The optimization of ladle life and of the wear lining thickness were possible thanks to industrial trials performed with the 3D laser equipment. In particular, 2 ladles were monitored during their entire life after identifying and conditioning the measurement areas, i.e., one for the ladles in hot conditions and another one in cold conditions, after preparing a laser measurement plan and selecting the reference system. The values obtained were then treated and refined to be exploited in the machine learning model. For the environmental and economic evaluation of the results obtained, LCA and LCC were conducted analyzing at first the departure situation to estimate its impact compared to the one at the end of the project.

The second half of the project was dedicated to the industrial laser measurements which lasted 3 months with more than 500 heats and whose procedure is schematized in Figure 19. The analysis of the measured thickness data revealed different wear rates in the ladle depending on the zone considered and distinguishing 4 main areas, i.e., nozzle side transition, nozzle side wall, porous plug side transition, porous plug side wall. The data coming from the laser measurements and the historical data of the remaining brick thickness which was measured manually in cold conditions during the reparation were combined with the operational parameters monitored during the refining process and were used to construct the Machine Learning Model (63). Five different predictive models were developed to estimate the remaining useful life of the refractory and the four wear rates in the four different areas of maximum degradation. The laser industrial trials and the machine learning model allowed to decrease of 3.5 % the MgO-C waste generated in the ladles, and of 7 % the consumption of new refractories. Parallelly, 35 new applications were identified for the reuse, remanufacture and recycle of ladle refractory wastes and the technical requirements of these applications were identified and included in the decision algorithm together with their environmental and economic impact. Two decision algorithms were developed, i.e., one for magnesia and one for alumina based refractory wastes.

The LCA and LCC studies carried out comparing the scenarios before and after the project, showed that the total annual life cycle costs were reduced by 1 M€ and GHG emissions and non-renewable energy demand was reduced by 19 %. The cost reduction estimated was ascribed both to the reduce-phase which allowed to reduce the ladle refractory purchased for replacement, but also to the reuse, remanufacture or recycle phases which provide a significant economic benefit thanks to the reduction of landfill costs and the incoming of possible gains in each of the valorization alternatives.

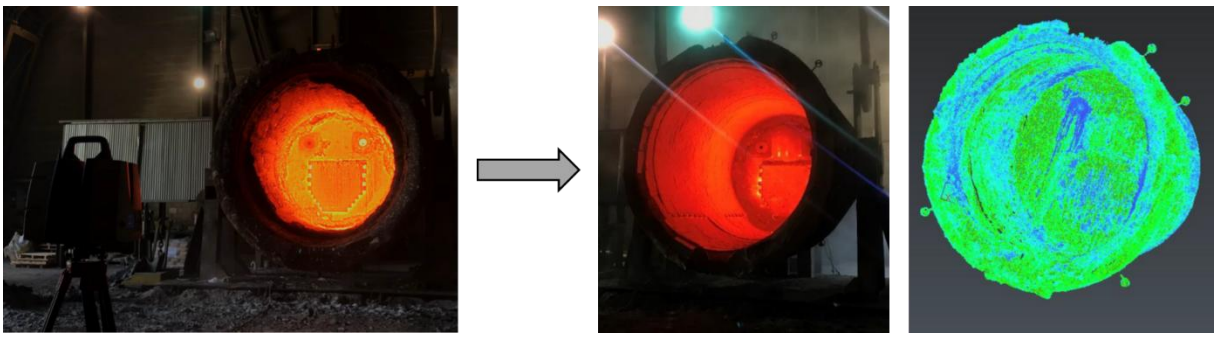

Figure 19: Example of the procedure followed and of the results obtained with the ladle refractory thickness measurement through laser

Some examples of potential reuse of LF wear lining were the construction of a MgO-C lining pre-wall in EAF, as lining for an emergency ladle and as ladle tapping spout. Some examples of potential remanufacture were the replacement of usual mixture made of dolomite lime and magnesia used in EAF, the construction of channels in the ground to prevent water or other fluids from going to the pits, lining of the refining and bloom cooling pits, and support of the tundish lids in the continuous casting pavements.

2.2.24 SLAGREUS: Reuse of slags from integrated steelmaking (64; 65)

The project was coordinated by BFI with voestalpine Stahl, K1-MET, University of Oulu and FEhS participating as partners in the consortium. The project started on the 1st of June 2019 and lasted almost three years and nine months, ending on the 28th of February 2023. The overall project cost 1.23 M€ and EU contributed 740 k€, i.e., almost 60 % of the budget.

The SlagReus project was a follow up of the PSP-BOF project. BOF slag is typically characterized by 20–25 wt.% of Fe total in standard heats, however this material cannot be freely recycled back into steelmaking processes due to its P content. Indeed, BOF slag carries P_2O_5 concentrations of 1.1–1.4 wt.% and the reintroduction of this P into BF or BOF increases the dephosphorization load, extends treatment times, and can compromise the quality of the resulting steel. Consequently, large quantities of BOF slag are deposited in landfills or used in low-value applications such as road construction, representing a significant loss of Fe and Ca values to the steel industry. SlagReus central premise was that BOF slag is not a homogeneous waste material but a mixture of discrete mineral phases with distinct chemical and physical properties that can be exploited after separation. The two primary

phases of interest are Fe-bearing phases principally wüstite FeO and magnetite Fe_3O_4, and calcium silicate phases rich in dicalcium silicate (C2S) which carry the majority of P. If these phases can be effectively separated, the Fe-rich fraction can be recycled internally as a substitute for iron ore in sintering, while the Ca- and P-rich fraction can be directed to external applications in the cement or fertilizer industries.

The first stage of the SlagReus process focused on primary Fe enrichment by liquid-phase segregation exploiting the differences in density between mineral phases while the slag remains in the liquid or partially molten state. Calcium silicate phases tended to float toward the surface, while Fe-bearing phases tended to settle toward the bottom when BOF slag were slowly cooled. This gravitational segregation produced a Fe-enriched lower layer and a Ca- and P-enriched upper layer which could be separately recovered. Three industrial trials were conducted. In the first trial, a Fe-rich slag batch with 25.2 wt.% of Fe total was held in its pot for two hours for partial solidification. The solidified Ca-rich top layer was 30–40 % of total mass and was discharged before the remaining Fe-enriched liquid was poured into a 3×3 m slag pit compartment together with a Fe-poor slag characterized by a 20.1 wt.% of Fe total. Approximately 70 kg of oxygen was injected via a lance to promote mixing and homogenization and a 100 kg sample with a Fe total of 24.1 wt.% was excavated after one week of slow cooling. The subsequent trials used slag pots and open pit compartments with and without oxygen injection. The industrial trials established several important conclusions. Segregation was driven primarily by slag viscosity which in turn was governed by Fe content of the input slag. Higher Fe-content reduced viscosity and improved phase mobility during cooling. Mixing a Fe-rich fraction with a Fe-poor slag to extend the recoverable volume was found to be counterproductive as the dilution effect outweighed any viscosity benefit. Oxygen injection into the liquid slag slightly enhanced segregation by reducing viscosity through temperature increase but achieved only incomplete FeO oxidation to Fe_2O_3 and added significant operational complexity. Pouring slag directly into a single prepared compartment in the pit was identified as the most practical industrial approach, avoiding the logistic complications of slag pot handling. Slow cooling of the pit content over several days was confirmed to produce crystal sizes adequate for subsequent liberation.

After solidification and primary separation, the Fe-enriched solid slag fraction must be comminuted to liberate individual mineral phases before magnetic separation. Microwave irradiation was investigated as a pre-treatment step to reduce grinding energy demand and improve liberation quality thus enhancing comminution and oxidation. Laboratory and pilot-scale trials confirmed crack formation and oxidation in treated samples. Microwave treatment of primary Fe-enriched samples reduced Bond work index from 23.4 kWh/t of untreated samples to approximately 20 kWh/t of samples treated for 7 minutes at 3.33 W/g. Treatments beyond 7 minutes yielded no further crack propagation and risked surface sintering. Higher specific power intensities achieved equivalent reductions in shorter times but with lower energy efficiency per unit of improvement. A key finding was that conventional solid-state oxidation by heating in ambient air produced substantially higher magnetite contents and stronger magnetic susceptibility than microwave irradiation alone. Considering the additional energy consumed by microwave treatment, the overall energy balance favored conventional solid-state oxidation as primary route to magnetic enhancement, with microwave treatment offering complementary value primarily for crack-induced grindability improvement. Industrial-scale microwave equipment specifically

engineered for BOF slag chemistry and does not yet exist commercially and represents an open development need.

Effective magnetic separation of Fe and Ca silicate phases required slag grinding to a particle size at or below the typical crystal grain size thus targeting 80 % of material passing 100 µm. Grinding was evaluated using ball mills and vertical roller mills (VRM) at laboratory and pilot scale. Closed-circuit operation was essential to avoid overgrinding which would generate large quantities of sub-10 µm fines difficult to separate magnetically and characterized by reduced hydraulic properties of the non-magnetic fraction intended for cement applications. Grinding to 100 % passing 100 µm was demonstrated as achievable with both mill types, confirming process feasibility across a range of equipment configurations.

Three separator configurations were evaluated for dry magnetic separation namely a laboratory oscillating Davis tube, a prototype airstream high-gradient matrix separator, and industrial-format low-intensity drum separators and permanent magnet drums. For non-oxidized slag processed through the Davis tube, η values for Fe were in the range of 1–6 % reflecting the predominantly paramagnetic character of wüstite and the associated difficulty of low-gradient separation. The air-stream matrix separator achieved η values for Fe up to 9–10 % surpassing Davis tube result even for microwave pre-treated samples thanks to its high-gradient field configuration and its capacity to process finer particles below 56 µm where mineral liberation is more complete. Oxidized samples processed through Low Intensity Magnetic Separation (LIMS) achieved η values for Fe 40–50 times higher than the corresponding non-oxidized material, because conversion of wüstite to magnetite shifted the material from paramagnetic to ferromagnetic behavior. This made standard low-intensity drum separation, the dominant technology in industrial mineral processing and fully effective. For non-oxidized material, high-field devices were required, with magnetic yields at 60 A reaching 57–63 %. The recommended end-to-end secondary enrichment process is therefore jaw crushing of slow-cooled Fe-enriched slag to below 5 mm, solid-state oxidation in ambient air utilizing residual slag heat, closed-circuit VRM grinding to below 100 µm with integrated air classification, and LIMS. Dry magnetic separation in any configuration produced a magnetic product enriched in Fe, MgO, and MnO with reduced P, Ca, and Si, meeting the compositional requirements for reintroduction into the sinter mix as an iron ore substitute.

Sinter pot tests were conducted to validate the compatibility of the processed Fe-enriched BOF slag concentrate with the existing sintering operation. The magnetic products of two slag samples were added to the standard sinter mix at rates of 4.4–5.9 wt.%, alongside two replicate reference tests without BOF slag addition. Chemical analysis of the produced sinter confirmed that Fe, CaO, SiO_2, and MnO concentrations were essentially unaffected by the addition. The sole constraint on recyclable volume is P. Based on annual P_2O_5 input limit for the sinter plant and an annual sinter output of 2.5 Mio t/a, the maximum addition of the processed BOF slag fraction was estimated at approximately 90-120 kt/year, requiring time-scheduled additions during periods when P from other raw materials is below its maximum permitted level.

Concerning the external valorization of P-rich non-magnetic fraction, three external application pathways were investigated. The fraction was enriched in CaO with 40–52 wt.%, SiO_2 with 10–17

wt.%, and P_2O_5 with 1.0–1.8 wt.%, with reduced Fe_2O_3 content compared to the input slag. The first application concerned the partial substitution of raw meals in clinker production. The comparison of the non-magnetic fraction elemental oxide distribution against the target ordinary Portland Cement clinker composition indicated a theoretical raw meal substitution potential up to 15–24 wt.%. Substitution at this level could displace approximately 8–12 wt.% of limestone and 2–4.5 wt.% of silica sand per unit mass of clinker produced. In practice, total Cr concentrations of 1600–2326 mg/kg in the slag products which convert almost entirely to water-soluble Cr(VI) under the oxidizing conditions of a rotary kiln, reduced the substitution rate, subject to site-specific input Cr limits. This remained the only technically viable external application pathway identified in the project.

The second application regarded the use as reactive cement constituent. Mortar prisms were prepared by blending non-magnetic slag fractions with CEM I 42.5 R standard cement in a 1:1 ratio and cured for 2, 7, 28, and 91 days. Processed fractions achieved compressive strengths of 21–28.6 MPa at 28 days significantly below the EN 196 minimum of 42.5 MPa required for classification as a reactive constituent. Heat of hydration measurements confirmed low hydraulic reactivity across all samples, attributable to P incorporation into C2S crystal lattice positions.

The third pathway addressed the feasibility as agricultural lime fertilizer. The P-rich fractions were assessed against the EU Fertilizer Regulation EU 2019/1009 and Commission Delegated Regulation EU 2022/973. P availability was uniformly high with citric acid extraction achieving recovery yields of 96–100 % of total P_2O_5 across all samples indicating that the P bound predominantly in larnite and C2S phases is readily plant-available. The sum of CaO and MgO was equal to 40–55 wt.% and basic reactivity values above 30 wt.% thus confirm adequate liming capacity. Toxic elements Cd, Hg, and Tl were consistently below analytical detection limits, and Cr(VI) was below 1 mg/kg in all non-intensively oxidized samples. However, total Cr concentrations of 1,600–2,326 mg/kg and V concentrations of 638–951 mg/kg exceeded the regulatory upper limits rendering the material non-compliant for CE-marked fertilizer products under current European legislation despite its otherwise favorable agronomic profile.

The SlagReus project successfully developed, tested, and validated a technically coherent multi-stage process concept for the selective enrichment of Fe from BOF steelmaking slag and the valorization of the resulting product fractions across laboratory, and industrial scales. The process chain comprising slag pre-selection by Fe content, gravity-driven segregation during slow cooling in an open pit compartment, solid-state oxidation in ambient air utilizing residual slag heat, closed-circuit vertical roller mill grinding with integrated air classification to below 100 µm, and low-intensity drum magnetic separation proved to be technically feasible and compatible with existing steelmaking infrastructure without the need for complex liquid-state handling or oxygen injection. Sinter pot tests confirmed that the Fe-enriched magnetic concentrate can be reintroduced into the sintering process without adverse effects on sinter quality or plant productivity. It was estimated an internal recycling potential of approximately 70,000 t/year of processed slag substituting 35,000 t of iron ore annually and delivering estimated savings of around 4 M€ per year. For the complementary Ca-rich non-magnetic fraction, the project identified partial raw meal substitution in clinker production as the sole currently viable external application, constrained in practice by Cr content limits. Use as a reactive cement constituent

was excluded due to insufficient hydraulic activity attributable to P-inhibited C2S hydration, while the otherwise agronomically promising fertilizer application is currently blocked by Cr and V concentrations exceeding regulatory thresholds.

2.2.25 TACOS: Towards A zero CO2 Sintering

The project was coordinated by CRM with ArcelorMittal, Tata Steel, RINA Consulting – CSM, and AST participating as partners in the consortium. The project started on the 1st of June 2019 and lasted almost four years, ending on the 30th of June 2023. The overall project cost 3.46 M€ and EU contributed 2.06 M€, i.e., almost 60 % of the budget.

The primary aim of the TACOS project was to identify a disruptive solution to drastically reduce CO_2 and other pollutants emissions at sinter plant. This goal was pursued by investigating different pathways, i.e., waste gas recirculation and alternative heat input. Alternative solid fuels with or without pre-treatment were considered as well as combustible gases for injection at strand surface combined with waste gas recirculation. High temperature fumes produced in the external combustion chamber were also evaluated. The impact of these solutions on sintering process performance and emissions was assessed through mathematical and DEM (Discrete Element modelling) modelling, lab trials, sinter pot trials and industrial measuring campaigns and trials. These solutions proved to have a significant impact on BF process, therefore a special focus was placed on their impact on sinter quality especially on its vertical segregation and on BF performances.

The project started with the study of alternative solid fuels to partially replace the solid fuels normally used in the sintering process, i.e., coke breeze and anthracite. Various coal and coke qualities, different biomass types, distinct by-products and residues were considered and some of them were also industrially used at sinter plant. These alternative solid fuels were studied in terms of sufficient quantity availability by performing market analysis and in terms of main physical properties for sintering thanks to a preliminary characterization of chemical and combustion properties. Indeed, ignition temperature must be able to ensure a homogeneous flame front, the reactivity should be tailored to ensure the correct propagation speed to the flame front and the ash content should be low enough since undesired residues would remain in the final sinter. Some of these alternative fuels also underwent different pyrolysis treatments, e.g., gasification, torrefaction, hydrothermal conversion, etc., to test the impact of these processes on their properties. The key candidates were then used by CSM for laboratory sintering trials in batch heating furnace including also gas analysis. Furthermore, a wide range of alternative solid fuels was also tested at the pilot scale through pot trials. In particular, pyrolyzed eucalyptus proved that it was possible to reduce fossil solid fuel usage, i.e., replacement rate, up to 60 % without degrading sinter quality and increasing productivity up to 17 %. A decrease of 50 % in CO_2 emissions and of 75 % in NO_x emissions was also detected. Despite the excellent results, it must be considered that the lower fixed carbon content of this alternative fuel led to an overall increase in solid fuel consumption. The sintering and environmental performance obtained were used to select the most suitable solid fuel to perform industrial trial at ArcelorMittal sinter strand using to replace 10 % of the mix solid fuel. Pyrolyzed olive pits were selected due to their high availability of 100 tonnes and since the pot trials highlighted a CO_2 emissions reduction of 7 % with constant productivity. These excellent results were confirmed by the industrial trials where both sinter quality, e.g., cold and hot

sinter strength, and BF quality requirements were met and a CO_2 emissions reduction of 7 % without any issue was detected. The environmental analysis of these trials showed that the use of a higher amount of alternative solid fuels was prevented by the high volatile matter of the fuel which caused excessively high VOC emissions incompatible with the electrical filter used to remove the dust from sinter fumes, i.e., increase from 40 mg/Nm^3 to 90 mg/Nm^3. An additional pretreatment of the alternative solid fuel could potentially solve this issue.

The effect of using an alternative fuel source on the preparation of the solid fuel for sintering was evaluated by sampling sinter mix every 3 hours to conduct granulometry and humidity analysis. The results showed that the introduction of the alternative fuel source in the solid fuel blend causes an increase in humidity of the sinter feed from 3.8 to 5.6 % while the D50 of the sinter feed was not impacted. This allowed to infer that the alternative solid fuel had no negative impact on the granulation process. As a result, the CO_2 mitigation achieved was declared as 10 % for a replacement of 10 % of standard solid fuel with alternative solid fuel. SO_x and NO_x were also monitored at ArcelorMittal stack during industrial trials, and they were strongly linked to the input of S and N brought to the sinter feed by the solid fuel. The replacement of standard solid fuel by alternative solid fuel therefore impacted the emission of these pollutants. SO_x emissions displayed a linear correlation with positive trend with solid fuel consumption directly linked to S input with the fuel. On the other hand, increasing solid consumption determined a clear decrease of NO_x emissions. This was counterintuitive since N input into the sinter feed increased with solid fuel rate. It was also noted that the application of 10 % of alternative fuel had a significant influence on NO_X emissions at the sinter plant is significant.

The second part of the project focused on the evaluation of different process modifications to improve sintering performance, i.e., high bed heights, waste gas recirculation with gaseous fuel injection, and use of hot fumes to replace part of the solid fuel. Concerning the first approach, i.e., high bed heights operations, some benefits were observed in previous studies working with a greater bed height to minimize energy consumption during sintering. Indeed, an average solid fuel saving of 0.5 kg/t sinter could be obtained by increasing bed depth by 1 cm to improve heat exchanges between the upper and lower parts of the process. These results were validated by several research works both at lab and industrial scale in a range of 30-70 cm of total bed depth. However, industrial application was limited by the decrease in production linked to very high pressure drops along the bed. In the framework of TACOS many different solutions were developed to face this issue. A DEM model for the charging system of the strand was developed to allow high bed height operations for optimized heat utilization and CO_2 emission mitigation at industrial strands. The model was also validated using lab tests and was used for the optimization of the mix charging on an industrial sinter strand. In addition, a sinter mix sampling system on an industrial pallet car to collect the mix at an industrial strand was also developed and tested. Furthermore, pressure drops were mitigated at the pot scale by increasing the burnt lime content in the mix to improve granulation and hot permeability. Vertical segregation of solid fuel or Fe^{++} was also assessed to mitigate pressure drops, but the only significant pressure drop improvement came from burnt lime use.

The second approach concerned waste gas recirculation which consisted in recirculating part of the off gas from the sinter process to replace process input air. The waste gas heat and low oxygen content

created favorable conditions for sinter quality and to achieve an equivalent quality at lower solid fuel input. Many different lay-out were available and they could be divided into two main categories, i.e., non-selective recirculation where a part of total fumes was recirculated after mixing and selective WGR recirculation where selected pollutants were mitigated by recirculating the waste gas from specific sections of the strand. Despite existing industrial applications, the impact of waste gas recirculation on vertical quality heterogeneity was not analyzed in depth and the sintering process needed to be reoptimized to consider this layout variation. In the framework of TACOS, pot trials at different oxygen levels with non-selective layout were performed according to the scheme shown in Figure 20. The results proved that this solution could provide up to a15 % reduction of solid fuel with a correct optimization of the sinter parameters. The industrial measurements and simulations showed that waste gas recirculation increased the sintering level of the layers that underwent the flame front while waste gas flows through the bed could increase quality heterogeneity in specific layouts. There was potential for optimization by increasing the ignition power to re-equilibrate the sintering level over the depth. During industrial measuring campaigns, different measurements were performed to fit CRM sintering model to the specific plants and configuration. Furthermore, sinter was sampled from pallet cars removed from industrial cars in different configurations to study quality heterogeneity.

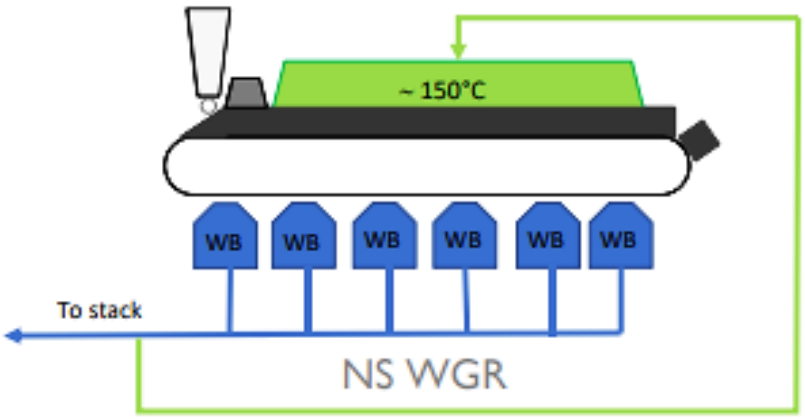

Figure 20: Nonselective waste gas recirculation (NS WGR) configuration

In typical European sinter strands, the top layers were of lower quality than bottom ones due to accumulation of heat over the course of the sintering process. One way to mitigate this effect was injecting combustible gas over the strand promoted their flowing through the top layer and their ignition when they reached the flame front thus releasing heat where it was most needed according to the scheme shown in Figure 21. This solution would allow to valorize biofuel-based gases leading also to potential solid fuel savings up to 10 %.

Another way to mitigate the lower quality of the top layers due to accumulation of heat over the course of the sintering process was the injection of hot fumes over the early sections of the strand according to Figure 22, i.e., VeLoSint layout. Despite the potential of lowering CO2 emissions, hot fumes sintering was not widely used in the steel industry. A high number of simulations and pot trials

were performed to study it and to find the configuration which allowed higher solid fuels savings. The key configuration selected was then used to perform a pot trial using only alternative solid fuel to replace all the fossil solid fuel in the mix sent to the combustion chamber. In particular, pot trials and simulations using the sintering model showed that injecting hot air transporting 60 % of standard ignition heat would allow solid fuel saving up to 35 % and CO_2 emissions reduction up to 31 % depending on the alternative fuel used. A specific layout called 2-phase VeLoSint shown in Figure 23 involved recirculating waste gas towards a combustion chamber fueled with alternative fuels then reinjecting the output gas over the strand at two different temperatures. This improvement was linked to both the additional heat input and the lower oxygen content of the gas compared to air. The combination of this layout with alternative solid fuel allowed to achieve an acceptable sintering level at 0 % fossil solid fuel in the mix but resulted in excessive VOC emissions. The impact of all solutions on BF operations was studied via lab and pilot trials and revealed that no negative impact can be expected.

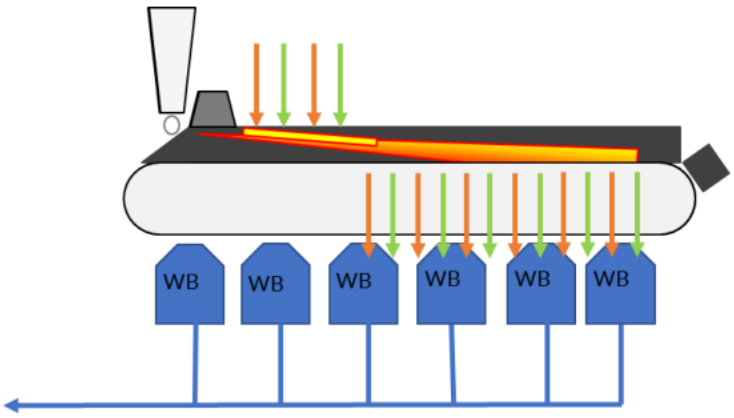

Figure 21: Fuel Gas injection configuration

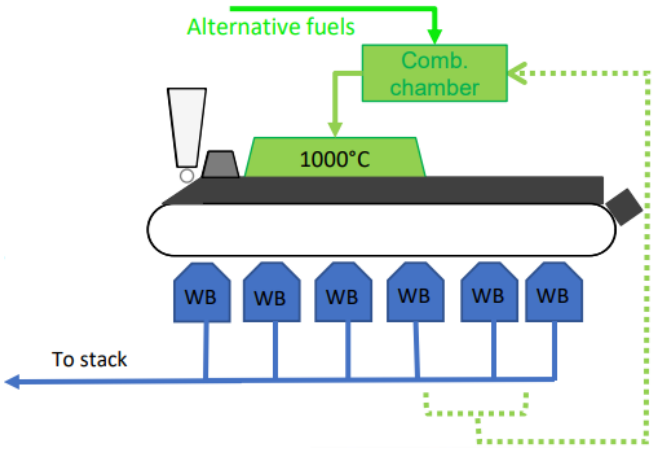

Figure 22: Hot fumes injection –VeLoSint process

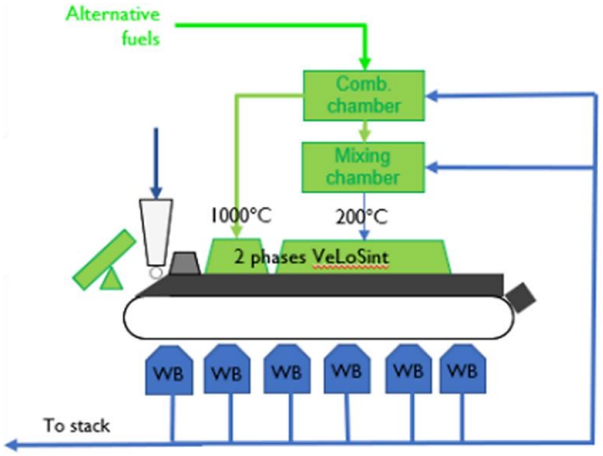

Figure 23: 2-phase VeLoSint layout

2.2.26 iSlag: Optimising slag reuse and recycling in electric steelmaking at optimum metallurgical performance through on-line characterization devices and intelligent decision support system

The project was coordinated by SSSA, with Dalmine, Sidenor, RINA-CSM, BFI, FEhS, Tenova, Acciaierie di Calvisano, and DEW, participating as partners in the consortium. The project started on the 1st of July 2020 and lasted 4 years ending on the 30th of June 2024. The overall project cost 2.82 M€ and the EU contributed 1.69 M€, i.e., almost 60 % of the budget.

The iSlag project aimed at improving slag valorisation from electric steelmaking route by improving slag conditioning, exploring new recycling paths, and facilitating the implementation of industrial symbiosis practices. To this aim, a novel intelligent system integrating innovative measurement devices was developed to characterize liquid and solid slag in a real industrial context through modelling and simulation tools to assess EAF and LF slags compositions and amounts. Two kinds of models were considered, developed and extended, i.e., an off-line physical-based models to support the analysis of the recycling paths and an on-line computationally efficient models based on analytical and data-driven approaches, e.g., heuristic, Artificial Intelligence (AI)-based and hybrid models, to be implemented at the plants to support slag conditioning to improve metallurgical performance and reusability. The exploitation of different systems at different industrial sites, e.g., on-site physical-based (LIBS and deterministic model) or based on electrical impedance sensor and analytical/data-driven approaches, e.g., (heuristic, AI-based and hybrid), aimed at identifying the most suitable recycling paths for each slag slot. These systems provided information on slag features exploited by decision support systems. In this regard, a flexible and ergonomic interface was developed and validated allowing a straightforward access and interpretation of all information provided by the devices and by the models. Its aim was to support operators and plant managers to the optimal valorisation of the slag inside and outside the steelmaking process. The investigated solutions were validated in different case studies related to industrial partners and were customizable and transferable across the whole European steel sector.

The preliminary analysis of requirements, definition of specifications, collection of samples and data aimed to set up an inventory of the available plant and process data to be exploited for model and

simulation developments. Furthermore, it aimed to collect and analyse slag samples from the involved industrial plants and define specifications for the devices aiming the fast on-line characterization of slag both at liquid and solid state and for decision support. These specifications were related to solutions for fast on-line characterization of liquid slag, LIBS analyser for solid slag, decision support concepts. Slag samples were collected at DEW and Calvisano both from EAF and LF at the liquid state for laboratory measurements at BFI for impedance sensor. Further samples were collected at Tenaris and Sidenor for measurement with the novel LIBS system by Tenova. FEHS performed all chemical and mineral composition analyses.

Focusing on the fast slag characterization in the liquid state, it aimed at developing and testing an impedance slag sensor for fast determination of basic liquid slag parameters. It also aimed at developing and testing a camera-based device for fast determination of liquid slag viscosity by image processing techniques. Lab scale trials based on real slags were performed at BFI in a high temperature lab furnace to develop and calibre the impedance slag sensor. Preliminary trials were dedicated to measurements in aqueous KCl solution and molten KCl to establish measurement dependency on immersion depth and check behaviour in hot environment. Furthermore, cable influence and optimal cable length was assessed. Laboratory trials were conducted on EAF slag from Calvisano and LF slag from DEW. EAF slag determined an excessive foaming at the graphite probe thus preventing reproducible measurement conditions therefore a second inert steel tube impedance sensor prototype was built. Considering this issue, crucible material selection was also critical especially for EAF slag and many crucible materials was tested. The results showed the available correlation function for electric conductivity and LF slag basicity B2=CaO/SiO_2 as well as a clear correlation of electric conductivity and slag basicity. Camera and objective were selected based on position, distance from ladle and resulting field of view to develop and calibrate the imaging system for a fast determination of liquid slag viscosity. In this regard, the visual camera and system were installed at DEW and the software was developed for acquisition of video sequences and translation of the motion detection into a characteristic value describing the slag viscous appearance.

Concerning the impedance slag sensor for industrial scale measurements, campaigns at DEW LF were carried out with 3 impedance sensor prototypes, and 1 campaign was conducted at Calvisano EAF slag pot. Results showed a good correlation of electric conductivity and slag basicity for both EAF and LF slag, but the impedance sensor was unsuitable for industrial deployment at Calvisano due to lack of reliable calibration at lab scale, long time required for sampling and need to modify the manipulator for slag sampling. Consequently, a fast slag analysis system was tested to obtain real-time analysis of EAF and LF slag. Results showed that the accuracy of the slag composition measurement was good for the variability and needed process monitoring in Calvisano. In addition, the system was used on site, and its exploitation was included in the decision support concept supporting slag conditioning and real time monitoring, and correction of EAF and LF processes.

A novel LIBS-based slag characterization device was developed and preliminary tested to fast characterise slag in the solid state. LIBS allowed fast characterization of both steel and slag samples with the same device. Tenova LIBS System consisting of a high energy 1064 nm laser able to ablate oxides and surface contaminants, was used. Advanced software analysis of the generated spectrum

provided elemental concentration measurements of the core metal. Laboratory tests focused on model training using a comprehensive dataset derived from slag samples as well as on performance testing where the prototype was subjected to various test conditions to ensure maintaining high accuracy across different slag compositions. Sample from Sidenor and Tenaris were of varying size, and the sample holder of the LIBS equipment was modified to fit all the samples. Sample analysis was carried out for Fe, Si, Al, Ca, Mg, Mn, Cr, Ti, V. A theoretical study was conducted to identify the spectral lines of interest for the chosen elements. Results showed good model performance for all elements. Advanced machine learning algorithm and Calibration Free LIBS were developed to improve LIBS software. SVM-based predictive models were refined to handle large datasets and ensure accurate element concentration predictions across varying slag compositions to enhance the data processing. The Calibration-Free Routine was further developed to reduce the need for frequent recalibrations, ensuring the system could operate reliably over extended periods in an industrial environment.

An inventory of the considered slag recycling paths inside and outside the steel sector as a function of slag features was developed to foster slag recycling paths for IS. A further objective consisted in formalising constraints and practical weight functions to valorise each of the identified recycling path and in developing practical criteria to select the recycling paths based on slag features. A recycling inventory was developed for EAF slag and LF slag use in Europe and specifically in Germany, Italy and Spain. Constraints such as environmental behaviour of the slag, chemical composition, physical values and grain size were categorised and selected to manage slag utilization. Furthermore, a series of objective categories were preliminary identified to be minimised or maximized to formalise objective functions and practical criteria to select the most suitable recycling paths. The objective categories considered were amount of slag reused, cost of landfilling slag outside the steelwork, cost of slag internal storage, cost of slag processing, cost of slag transportation to landfill, cost of slag transportation to slag processor, cost of slag transportation to sales point, capacity to alternate slag to meet market demand in terms of environmental behaviour, capacity to alternate slag to meet market demand in terms of physical behaviour, current political climate with respect to slag storage or utilization, opportunities for slag utilization and to recycle slag internally, savings due to internal recycling, revenue from sale of slag. Existing off-line simulation models to be used to support the analysis of the recycling paths were adapted and updated. Additionally, computationally efficient models exploiting data coming from the process and from the novel devices for fast on-line characterization of the slag were developed. Calvisano and CSM developed models for the evaluation of slag adequacy in both EAF and LF based on its chemical composition and temperature, while SSSA adapted and upgraded an available off-line flowsheet model of electric steelmaking to represent Sidenor production process and to allow a better simulation of produced slag. These models were used in different ways. SSSA used data provided by Sidenor to estimate solid slag amount and oxide contents based on process inputs and parameters. These data underwent a pre-processing stage to remove unreliable data and select most relevant variables. In particular, results concerned slag composition and dynamic modelling for scraps yield estimation at Tenaris Dalmine and adapted model for on-line estimation of slag amount and composition during LF treatment (BFI, DEW). Preliminary off-line test and validation of the on-line models to be used for decision support included process modelling to support slag conditioning practices at AdC, estimation of solid slag amount and oxide contents based on process inputs and

parameters, Echo-State Neural Networks, estimation of LF slag features, i.e. Mass balance (MB), Deep Multi-Layer Perceptron (DMLP), Hybridnet (HNET), Limited HNET (with MB only for Al2O3, TiO2, SiO2).

Concerning decision support concepts and systems helping the plant personnel in the implementation of smart slag conditioning practices and optimal slag handling and reuse, decision schemes guiding slag conditioning practices were developed and implemented. Four distinct steps were considered to estimate slag viscosity via video sequence image analysis. These steps concerned the images recorded at LF during non-heating periods when the lid was open. Phase 1 feature detection and motion tracking to obtain key features of the slag and track the main movements. Phase 2 frame-by-frame analysis to analyse consecutive frames to capture the dynamics of the tracked features. Phase 3 bar graph visualization which allowed to visualize the results of the analysis through bar graphs. Phase 4 waterfall diagram visualization to have a comprehensive view of the evolution over time. In addition, the standalone calculation tool to support steel and slag corrections suggested the most appropriate corrections based on thermochemical data by using FactSage to model the interactions between steel and slag thus ensuring optimal steel quality and facilitating slag reuse. For example, LF process involved several steps and specific material inputs such as crude liquid steel sourced from the EAF containing up to 1000 ppm O and 300 ppm S thus requiring deoxidation and desulphurization and influencing slag composition. Indeed, deoxidation could be performed via addition of Mn as FeMn, Si as FeSi and Al as metal while desulphurization was guided via CaO addition. The output targeted was a refined liquid steel with O<50 ppm and S <100 ppm with a slag without precipitated solids. Database creation involved calculating all combinations of input parameters, i.e., almost 720,000 possible combinations and calculations. The results were sorted by temperature, initial O_2 concentration, and additions of Mn, Al, Si, and CaO. The optimization strategy minimized costs and CO_2 emissions by considering the following costs and revenues: slag storage, transportation to treatment plants and/or selling locations, treatments, revenues for slags selling. Finally, ergonomic end-user interfaces for the different components were developed. Concerning iSlag decision support system, the webapp run in a local server and it was reachable through any common web browser. As the uploaded data was shown in editable tables, the user could change dynamically the data inside the application.

For industrial validation and transferability, extensive industrial tests of the developed devices and of the decision support system were performed. In addition, guidelines for the application of the developed tools throughout EU steel sector were developed. Concerning the impedance sensor measurements at LF (DEW), results showed that used impedance sensor prototypes had problems with internal electrical connections. In addition, measured electric conductivity was too low < 0.002 S/cm while the expected value of slags being between 0.1 and 1 S/cm. Consequently, it was not possible to calculate slag basicity via the calibration function from the lab trials. Due to handling issues with previous prototypes new, lightweight sensor prototypes comparable to single-use temperature or electromagnetic field sensors were built and used. Concerning slag viscosity estimation via video sequence image processing, results showed that the comparison of the mean characteristic of amplitude and frequency of the angle for 2 melts with suspected higher viscosity and 2 melts with lower viscosity did not reveal clear differences. This could be due to similar viscosities of the heats or to narrow view to the melt bath surface. Consequently, many more videos and motion data were

needed to draw final conclusions. Concerning industrial tests of the devices for fast solid slag characterization and assessment, LIBS-based system results showed that system validation performed at the industrial sites and errors were less than 1% of the absolute values. Concerning the industrial tests of the decision support system at Acciaierie Calvisano, three application cases were considered: 1) Evaluation of the status of steel oxidation at arrival to LF and of slag carryover from EAF tapping 2) Detection of low MgO content in EAF and LF slag that could lead to high refractory erosion 3) Determination of necessary additions for deoxidation, desulfurization, steel composition corrections to be performed in Ladle at EAF Tapping.

Finally, the economic analysis concerned monitoring system for liquid slag together with the advisory system which targeted adjustment of amount, composition and viscosity of the ladle slag leading to -15 % CaO additions and targeted also shorter treatment time with lower temperature losses achieving a reduction of -25 sec/heat. Concerning, Tenova LIBS System a reduction of the lime addition between 1 and 5 % and an increase in Fe yield was achieved. Concerning the economic analysis of the decision support concept at Calvisano, the first application case reported a shorter LF treatment time of 3-5 min/treat, i.e., 5-10 % of time saved, and an improper slag conditions due to carryover identified in 50% of cases thus allowing to save 5-10 % additions. For the second application case, potential reduction of refractory erosion of 1-2 % in EAF and 2-3 % in LF were obtained. Finally, for the last application case a reduction of additions at tapping of 32-71 % depending on oxygen activity and treatment time.

2.2.27 OnlyPlastic: EAF working with polymers derived from plastic residue in substitution of fossil fuel (66)

The project was coordinated by RINA Consulting-CSM, while Tenova, Feralpi Siderurgica, I.Blu and Strane Innovation participated as partners in the consortium. The project started on the 1st of September 2020 and lasted 3 years, ending on the 31st August 2023. The overall project cost 2.06 M€ and the EU contributed 1.03 M€, i.e., almost 50 % of the budget.

European steelmakers are increasingly seeking alternatives to fossil carbon sources. BF already used granulated polymers derived from plastic residues as secondary reducing agent when the project was proposed while their use in EAF was limited to lump material charged in buckets. Tests showed several advantages over other alternative C sources such higher heating value and C content, greater material availability, compatibility with existing plastic recycling systems, and the existence of a dedicated technical standard (UNI 10667-17) that classifies them as product rather than waste. The OnlyPlastic project aimed to completely replace fossil carbon sources both injected and charged in the Feralpi Lonato EAF with densified polymers from plastic residues. The project included the development of handling and transport prototypes, bucket charging systems, a customized injection system compliant with UNI 10667-17, evaluation of plastic blends with other materials, and optimization of operating practices to enable optimal their use as secondary reducing agent.

The project began with the sampling and characterization of the C materials normally injected in Feralpi EAF, e.g., injected and charged coal, and the polymers available from the recycling of industrial residue

and post-consumer material. The analyses included proximate and ultimate analysis, heating value, ash content, Cl and S content, density, and grain size distribution, with additional parameters from UNI 10667-17 to enable comparison with secondary reducing agent. The results showed that the charged coal had 74 % of particles larger than 31.5 mm whereas the injected coal presented 58 % of particles in the 8–3.35 mm size range. The plastic waste used originated from I.Blu sorting plants and consisted of post-consumer plastic residues classified under CER (Catalogo Europeo dei Rifiuti) code. Three samples were collected, namely Flake 1, Flake 2, i.e., granular injection material, and chips charging material. The results showed full compliance with UNI 10667-17 requirements. The mixed plastic content was inferred to be higher than 80 % based on the nature of the input stream, a total carbon content between 70-80 %, hydrogen content between 10-13%, and an ash content of approximately 4 %. Minor differences were observed between injection and charging materials in terms of density, moisture, carbon, oxygen and Pb content. Grain size analysis of the flake material indicated that about 96 % of the particles were between 2-8 mm with more than 65 % in the 4–6 mm range. TGA and dissolution tests were also performed. TGA was conducted in air with a heating rate of 300 °C/h on three plastic and two coal samples. Plastic samples showed comparable behavior and a more rapid mass loss compared to coal in agreement with proximate analysis results. Dissolution tests with molten steel were conducted to characterize the reactivity of the materials at high temperature and specifically their capability to dissolve into molten steel versus material devolatilization. The tests were conducted in an induction furnace using 3.5 kg of iron with an initial C content of approximately 5 ppm and about 5 g of material under an Ar atmosphere. Flake samples, compacted into briquettes, were immersed in molten steel for about 10 seconds, producing limited steel projections and sustained flames, while chips and coal were charged from the top. Post-test steel analyses allowed the determination of dissolution time, carbon pick-up and carburization efficiency which are summarized in Table 20. The selection of materials for injection and charging in EAF was based on particle size, shape, density and chemical composition in accordance with UNI 10667-17. Compared to coal, plastic materials showed a higher H content and a lower C content. This implied that similar or lower quantities of plastic may be sufficient to achieve slag foaming due to enhanced gas generation, while higher quantities may be required to maintain the same C input to the steel bath. The presence of hydrogen promoted endothermic reactions with slag oxides thus leading to local temperature reductions and changes in slag viscosity that could positively affect slag foaming behavior.

Table 20: Dissolution test results

Sample	Dissolution time (s)	C in steel (%)	Carburization efficiency (%)
Injected coal	68	0.008	7
Charged coal	75	0.03	25
Flake 1	85	0.015	12
Flake 2	94	0.018	14
Chips	51	0.005	6

The work proceeded with the implementation of process modifications aimed at obtaining optimal plastic grains and chips suitable for use in different EAF configurations, for both injection systems and basket charging, in compliance with the technical specification of UNI 10667-17. After a testing and adjustment phase of the production process conducted by I.Blu, a satisfactory level of plastic quality was achieved. The activities focused primarily on flake quality for EAF injection. Through several technical interventions during both the sorting phase and the recycling process, the separation process was enhanced to reduce Cl content and other sensitive parameters to acceptable levels. The material density was increased to approximately 370 g/cm^3 thus improving its suitability for EAF injection. Grain size distribution was also optimized by minimizing the fraction below 2 mm and concentrating about 65 % of the material in the 4–6 mm size range.

In the following stages, the production of non-biogenic SCC focused on the material for injection, following Feralpi decision to prioritize the development of the injection device and postpone experimentation with basket charging of chips. The first production of flakes supported the installation and preliminary testing of the new injection system for polymers used as reducing agents in the EAF process. The design of a new injection system constituted an important part of the study aimed at promoting reducing process and slag foaming into EAF. The analysis began with CFD simulations conducted on the current pulverized coal injector which coupled oxygen and solid coal injection in a single device mounted on the furnace wall. This configuration increased the velocity of the solid phase using a supersonic oxygen lance above the injector. Four different penetration scenarios were identified depending on system geometry, lance design, solid particle properties, and process steps, with the main difference being whether the supersonic oxygen jet and solid particles meet before reaching the slag surface or inside the slag layer. Two injection points in Feralpi EAF were analyzed and for both of them the injection concept relied on coupling the solid material with a supersonic oxygen jet. The injection points considered are shown in Figure 24. In the first injection point, the coupling followed a conventional layout with the supersonic oxygen lance positioned above the solid injector while in the second injection point the interaction between the solid particles and the oxygen jet occurred on a horizontal plane with a single coal injector installed near a coupled injector supplying supersonic oxygen and lime with the supersonic oxygen jet of injection point 3 being aligned on the same horizontal plane as the solid injection from injection point 2 thus enabling side coupling between the streams. CFD simulations indicated that in both cases the jets met near slag surface thus corresponding to a soft penetration scenario. The penetration distance of supersonic oxygen in the slag was always greater than slag thickness thus showing that it could reach the molten metal interface under all conditions of slag foaming. Comparisons of solid particle penetration revealed that coal consistently reached the slag-molten metal interface whereas plastic showed limited penetration often below or close to slag surface thus indicating that single-injector plastic may not be efficient under industrial conditions.

Based on the positive results obtained with the coupled injection configuration, a series of preliminary industrial trials of plastic injection from injection point 1 were carried out using dedicated experimental facilities to define a baseline for evaluating the performance of the new plastic injector. The trials were performed with a pilot system operating with a single injection point and an injected plastic amount ranging between 100 and 180 kg/heat. The experimental campaign included both SCC charging in the

basket and SCC injection into EAF using preliminary pilot devices, and the results were systematically compared with those obtained under standard coal injection practice. Several operating configurations were tested and are summarized in Table 21. The effectiveness of SCC in promoting slag foaming was assessed through the analysis of data provided by the acoustic sensor and evaluating the trend of the Acoustic Cover Index (ACI) during different heats operated with coal or SCC. The experimental results showed that the configuration with plastic flake injection combined with coal basket charging (Test 5) provided the best overall performance achieving full substitution of injected coal while maintaining good arc coverage efficiency. Conversely, the use of SCC in basket charging exhibited issues related to reaction regularity and stability with performance not comparable to those obtained with standard carbonaceous materials. Indeed, a low level of steel carburization was observed when C in the basket was substituted with plastic. In all tested configurations, no critical issues were detected in the off-gas system, either in terms of temperature or gas composition. The preliminary results demonstrated that SCC injection represented a more reliable and controllable approach for EAF operation. For this reason, SCC injection into EAF was identified as the priority development path. Despite the use of a non-optimized lance and relatively limited injected quantities of 100–180 kg/heat, encouraging results were obtained with the pilot system operating at injection point 1 thus confirming satisfactory EAF performance, effective arc coverage by foaming slag, good system reliability and maintenance behavior, and compatibility with long-term industrial operation and standard production practices.

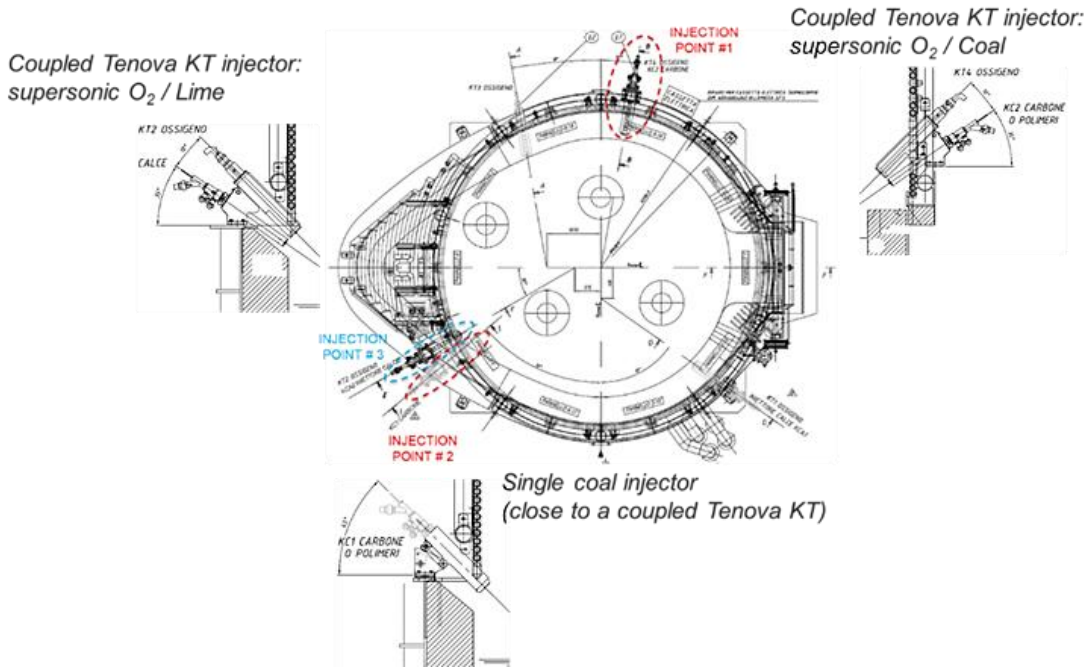

Figure 24: Sketch of Feralpi EAF with oxygen/solid material injection point. Injection point 1 and 2 were the ones used for coal/plastic injection while injection point 3 was the oxygen-lime injector coupled on the horizontal plane with injection point 2

Table 21: Trials to test SCC behavior in EAF

Test Number	Configuration
1	Only SCC injection (Flake)
2	SCC injection (Flake) coupled with SCC basket charge (Chips)
3	SCC (Chips) basket charging in EAF coupled with coal injection
4	Only SCC charged in basket (Chips)
5	SCC (Flake) injection coupled with coal basket charged

CFD analyses on the current pulverized coal injector showed that an effective use of SRA required coupling the solid jet with a supersonic oxygen jet to achieve sufficient penetration into the slag. However, the installation of conventional vertically coupled injectors was not always technically feasible or economically viable therefore a new injector concept was developed to enhance the performance of a single lance while preserving the solid–supersonic oxygen coupling mechanism. The new solution was based on a modification of the injection point 2 configuration where the KCA2 lance dedicated to lime was disabled and the existing KC1 was replaced by a new injector capable of delivering two solid streams within a single device. The original and optimized configurations considered are summarized in Table 22. In this configuration, the coupling between the solid material and the supersonic oxygen jet occurred on the horizontal plane rather than on the vertical one thus exploiting a side-coupling interaction. The injector was equipped with an external shrouding to increase operational flexibility and improve injection efficiency of small solid particles. This design offered several advantages. The injector was very compact and could be easily installed on existing EAFs with minimal modifications to the water-cooled panels thus facilitating the retrofit of current coal injection systems with polymer injection technology. In addition, the dual solid-material capability within a single injector represented a significant innovation in terms of material selection and process control enabling the simultaneous injection of materials with opposite thermal behavior such as lime and plastic. CFD simulations of the new injector indicated that the shrouding air effectively limited the spreading of the solid jets, maintaining their coherence even close to the liquid bath. At the same time, the shrouding contributed to the acceleration of solid particles with a particularly strong effect on the lower jet typically associated with lime injection. Thanks to these optimizations, the new injector generated a sufficiently strong and coherent jet to reach and interact with the nearby supersonic oxygen stream achieving an effective coupled oxygen–solid configuration. This approach resulted in a more flexible and robust injection solution allowing greater freedom in the positioning of the SCC injector relative to the supersonic oxygen lance.

Table 22:Material streams for the different injectors of injection point 2 for the two configurations analyzed

	Original Configuration	Optimized Configuration
KT2	Oxygen	Oxygen
KCA2	Lime	Off
KC1	Polymer	Lime+Polymer

Following the positive results obtained during the preliminary tests, the design of the new pneumatic system for polymer injection into the EAF was defined. The installation was based on two injection points and included a new storage system with automatic charging, two dedicated tanks with independent propulsion systems, i.e., one for each injection point, two pneumatic transportation lines, and new pressure and flow-rate measurement devices equipped with regulation valves. A dedicated control software was developed to allow flexible and independent regulation of each injection lance according to EAF process evolution and the different basket phases. The system was designed to handle polymer flakes with a particle size between 4-8 mm, transported pneumatically. The total installed power of the system was 20 kW with an air supply pressure of 6 dynamic bar and an air consumption of approximately 700 Nm^3/h. The overall purpose of the plant was the storage, handling, transportation, and controlled injection of SCC into EAF. Polymer was stored in a silo located outside the EAF shop and specifically designed for pneumatic conveying. Material extraction from the silo was carried out by two augers each feeding one injection line. The polymer was then pneumatically conveyed through underground pipelines to the two lances installed on the EAF. Both material mass flow rate and carrier gas flow were continuously measured and controlled to ensure stable and repeatable injection conditions. After the injector concepts were defined, the design was completed with full construction details, and two injectors were manufactured and integrated with the pneumatic system specifically developed for industrial application.

The realization and installation of the system at Feralpi plant followed a structured sequence of activities. A preliminary layout of the tank and propulsion unit was defined, after which the civil works were carried out. Foundations were constructed as the first step, and a dedicated tunnel was built to connect the polymer storage silo with the melting shop. This tunnel was designed to house the SCC transport pipelines and to allow easy inspection and maintenance. Subsequently, the steel structures required to support the storage and propulsion systems were installed. The propulsion system developed by Feralpi was positioned and connected to the compressed air network and to the electrical power supply. All components of the pneumatic injection system were managed by dedicated control software. During EAF operation, the operator could request the injection of a defined quantity of polymer, and the software automatically managed all system actions required to convey and inject the material into the furnace. A dedicated LED panel was installed on the control desk providing a graphical overview of the system components and generating alarms in the event of clogging or malfunction to improve operability and monitoring.

In normal EAF operation at Feralpi, a few hundred kilograms of C were typically charged per heat through the basket. Although the OnlyPlastic project initially included both injection and basket charging of alternative reducing agents, early industrial tests showed that polymer injection using the newly developed system was sufficient to fully replace the coal normally used in production. Nevertheless, additional tests were performed to evaluate whether charging polymer chips into the scrap basket could provide further benefits during the melting phase. Preliminary trials were carried out by defining different operating scenarios with particular focus on those involving plastic chips charged in the basket. In these tests, chips were charged into the first basket by placing a big bag of

about 290 kg in the middle of the scrap load. Each heat consisted of two scrap baskets charged into the EAF. In the reference scenario, polymer flakes were injected in quantities and with injection times equivalent to the standard coal injection practice while no coal was either injected or charged in the basket. The tests were conducted in collaboration with I.Blu. The effect of chips charged in the basket on slag foaming was evaluated using the acoustic monitoring system installed at Feralpi. This system processes the acoustic signal generated by the electric arc to calculate the ACI, which is used to assess the effectiveness of arc coverage by foamy slag during refining. The comparison between normalized ACI values for heats with and without chips charged in the basket showed lower ACI values when chips were present thus indicating an improvement in arc coverage and slag foaming behavior. During the same trials, dust concentration at the stack outlet of the off-gas duct was monitored and showed no significant variation compared to standard production conditions. Despite these positive indications on slag foaming, the trials also highlighted drawbacks related to process stability and overall operational management when polymer chips were charged in the basket. In addition, the results confirmed that the presence of reducing agents in the basket, whether coal or chips, did not provide significant advantages for EAF process under Feralpi operating conditions. Consequently, the optimal and final industrial configuration was defined as a process based exclusively on polymer injection without any reducing agent charged in the basket. This configuration represented the new standard production practice adopted by Feralpi within the OnlyPlastic approach. Since coal basket charging was no longer part of the production process and the total coal demand was replaced by SCC injection, the implementation of a dedicated plant for polymer chips basket charging was deemed unnecessary and was therefore excluded from the project scope under standard process conditions.

The final part of the study consisted of long-term industrial trials. The main objective was to validate the new injection system and evaluate its performance under extended industrial operating conditions. Following preliminary trials that tested both polymer injection and basket charging, Feralpi decided to focus exclusively on injection, promoting the complete substitution of coal with polymer injected through the newly developed system. Several aspects were considered to define an optimal injection practice including slag foaming, oxide reduction, energy consumption, off-gas temperature, and composition, using the standard coal injection practice as a reference. Standard coal injection at Feralpi was performed at two opposing injection points with pulverized coal (1–3 mm), manually controlled by the operator during the refining phase. The start of injection depended on the occurrence of an uncovered arc and increased noise in the furnace, resulting in low repeatability and potential delayed response. Standard practice involved injecting 100–250 kg of coal depending on arc coverage, with excessive coal potentially causing over-foaming, slag volume increase, and higher energy consumption (>300 kg/heat). These limitations could also distort the ACI because coal was injected only when the arc was uncovered producing counterintuitive monitoring results.

Feralpi combined production expertise with EAF process simulation to evaluate the new polymer injection practice. The simulator dynamically models mass and energy balances of the heat, including steel, slag, and off-gas composition and temperatures, to predict arc coverage, oxidation, and overall process performance. Using this approach, new operating practices were compared with reference coal injection scenarios. Simulation considered different production conditions including variations in energy prices and scrap quality and allowed the development of a flexible automatic polymer injection

system. The new practice extended injection to first, second, and third basket melting to ensure sufficient polymer mass for oxide reduction. Simulations indicated that polymer injection needed to approximately double the injected mass relative to coal to achieve similar steel bath C content and maintain off-gas temperatures within acceptable limits, i.e., 950–1000 °C. Three long-term industrial trials were conducted. The first used the Tenova standard injector under the OnlyPlastic approach, fully substituting coal with polymer injection, demonstrating the feasibility and reliability of this configuration. The second trial combined polymer injection with 200–300 kg of coal charged in the basket to maintain acceptable steel C content under low-carbon scrap conditions. The third trial employed a new Tenova injector developed within the project, confirming the feasibility of the OnlyPlastic practice and validating the new injector performance. These trials assessed polymer use as a foaming agent through ACI monitoring, identified potential weaknesses in the injection system, and evaluated EAF process performance. Long-term trial data demonstrated that polymer injection did not significantly alter EAF process parameters and confirmed that both the OnlyPlastic approach and polymer plus coal basket scenarios produced comparable results. ACI values remained within acceptable limits ≤ 1, indicating effective arc coverage. Slag quality analysis showed comparable Fe_2O_3 content in the OnlyPlastic and coal-injected scenarios with lower Cr_2O_3 in polymer-only trials, confirming no detrimental effect on oxide reduction. Off-gas monitoring over 8-h periods during a 3-day campaign showed that polymer injection slightly increased off-gas temperature, i.e., maximum 605 °C at the quenching tower inlet, relative to coal, remaining below the 700 °C threshold, with variability influenced by refining duration, injection rates, oxygen flow, electrical power, and scrap quality.

Several operational difficulties arose during the industrial tests, including the introduction of the new polymer material into established coal practices, clogging due to the plastic behavior of SCC when excess material accumulated in pipelines, and erosion in bends and branches of the transport lines due to the abrasive nature of SRA. These issues were addressed by installing reinforcements and modifying the pipeline layout. Adjustments were also made to the off-gas suction to prevent polymer extraction issues, and wear in the new Tenova injector was resolved through a redesigned durable configuration. Finally, a techno-economic evaluation was carried out comparing costs of the previous standard practice with coal injection and basket charging against the OnlyPlastic approach with polymer injection. Considering two periods and factors such as electrical energy, metallic losses, oxygen, gas, lime, carbon in basket, coal and polymer usage, and CO_2 emissions costs, results showed a cost reduction of 1.6 % in 2019 and 1.8 % in 2023 using polymers. Despite an overall increase in production costs in 2023 due to energy and material price rises (~84 %), polymer use reduced per-heat costs due to lower raw material costs and reduced CO_2 emissions.

2.2.28 BIOCODE: BIOmass for COkemaking DEcarbonization

The project was coordinated by Acciaierie d'Italia (AdI) with TKS, Paul Wurth and RINA-CSM participating as partners in the consortium. The project started on the 1st of July 2023 and lasts almost three and a half years. The overall project cost 5.09 M€ and the EU contributed 2.54 M€, i.e., almost half of the budget.

The decarbonization of the steel industry is one of the most urgent challenges faced by Europe in the transition towards climate neutrality since it is responsible for about 7 % of global CO_2 emissions and remains among the most carbon-intensive industrial branches. In Europe, steel production accounted for 139 Mt in 2020 representing 7.6 % of global output and contributing nearly 4 % of all EU GHG and 23% of emissions from the manufacturing industry. Among the different production routes, the BF–BOF pathway is still predominant in Europe, and it relies heavily on metallurgical coke which serves both as structural element within the BF burden and as the main source of C and reducing potential. On average, 350–400 kg of coke is required per ton of hot metal and the production of 1 ton of coke requires about 1.2–1.6 tons of coal. It appears evident that coke making is one of the major contributors to direct CO_2 emissions in integrated steel plants and the reduction on fossil coal dependence within coke making is a critical step to lower the carbon footprint of primary steelmaking. A possible solution was identified in the use of biomass as a C-neutral substitute for fossil coal. This route fits within the process integration pathway as it can be implemented within existing infrastructures without radically altering the BF–BOF route. The direct integration of biomass into coke making was not widely demonstrated in Europe, mainly due to challenges linked to biomass availability, variability, and its effect on coke quality therefore the BioCoDe project was conceived to address this gap. BioCoDe aims to partially replace fossil coal with biomass-derived C sources, e.g., biomass and biochar, up to 10 % on an industrial scale while maintaining the metallurgical quality of coke. This substitution rate is expected to result in a significant reduction of fossil-based CO_2 emissions from coke making, paving the way for further upscaling in the medium-long term. BioCoDe also aligns with circular economy principles, by valorizing locally available agro-forestry residues that would otherwise be underutilized or disposed of.

BioCoDe fosters a direct synergy between the agricultural and steelmaking sectors, with a focus on regional biomass resources. For instance, olive pruning produces more than 1.16 Mtons of residues annually in southern Italy, while vine wood and straw are abundant by-products of viticulture and cereal cultivation. By creating demand for these residues, BioCoDe promotes local supply chains, reduces transportation costs and emissions, and strengthens the link between rural and industrial economies. Ultimately, BioCoDe aims to demonstrate that biomass substitution in coke making is technically feasible, environmentally beneficial, and economically viable, provided that appropriate pretreatment and blending strategies are adopted. Project outcomes are expected to lay the foundation for a new European circular value chain in which agricultural residues become a strategic raw material for steel decarbonization while enhancing resource efficiency and industrial resilience.

The project follows a multi-level experimental approach. At first, selection and characterization of biomasses was performed with a strong focus on Mediterranean availability near the Taranto steel plant such as olive pruning residues, vine wood, straw, pallet and packaging wood, and olive pomace. After that, thermal pretreatment of biomass via torrefaction and carbonization was investigated to enhance the fixed C content and reduce the volatile matter thus improving compatibility with coke making blends. The produced biochar was conveniently characterized considering parameters such as proximate and ultimate composition, calorific value, ash chemistry, and plasticity behavior. After that, pilot-scale coke making tests in a 300 kg movable wall oven at AdI were foreseen trying to simulate industrial heating and pressure conditions. Industrial demonstration trials at the Taranto coking plant

were also foreseen to validate the process at TRL 7. Process monitoring was also digitalized through integration of Paul Wurth Distillation Process Module with the experimental ovens and the full-scale coke battery. Finally environmental, economic and regulatory assessment, including LCA and the identification of enablers and barriers for biomass adoption in the steel sector were considered.

Concerning the first step of the project, i.e., biomass selection and sourcing, it was performed considering three main criteria, i.e., local abundance, physical and chemical suitability and circular economy relevance. Local abundance is fundamental since residues must be generated in significant quantities close to the steelmaking site to minimize logistics and transport emissions. Physical and chemical suitability are also crucial and entails the evaluation of moisture content, ash yield, and potential to generate fixed C comparable to metallurgical coal as main screening parameters. Finally, preference was given to agro-industrial residues with limited alternative uses in a circular economy relevance perspective. Ten main biomass categories were identified in the Mediterranean area, particularly in Apulia, i.e., olive pruning residues (branches and trunks), vine wood, straw, pallet wood, packaging boxes (plywood and chipboard), pine, eucalyptus, and olive pomace. Quantitative availability was estimated at several hundred ktons per year with olive pruning alone producing more than 1 Mt/y.

The biomasses were subjected to mechanical pretreatment to ensure consistent heating during pyrolysis and improved mixing with coking coals. Biomass samples were chipped, dried, and milled to obtain homogeneous particle sizes <5 mm. Torrefaction was conducted at 220–300 °C under inert conditions to reduce moisture from 10–20 wt.% to values <5 wt.% and to partially remove hemicellulose to increases hydrophobicity. The pyrolysis experiments and developed an experimental pyrolysis line for detailed biochar studies. The line included a horizontal tubular furnace with six resistive heating zones for controlled heating up to 900 °C, a inert gas flow (N_2 or Ar) to purge oxygen and transport evolved gases, a condensation train with a cooled expansion chamber for heavy tars followed by six bubblers with isopropanol at +20 to –5 °C for light tar collection, an activated carbon filters for volatile organics and a gas bags for collection of non-condensable gases (CO, CO_2, H_2, CH_4). The measured outputs were mass balances of biochar, tar and gas yields, gas composition through gas chromatography, Tar and biochar characterization and energy balances enabling estimation of thermal efficiency and potential for heat recovery. These experiments provide critical insight into the correlation between process parameters such as temperature, residence time and heating rate and final biochar quality, supporting the optimization of pretreatment for coke making applications. Weight loss during torrefaction ranged between 20–30 %, depending on the biomass type. Carbonization or mild pyrolysis was performed at 400–600 °C to convert biomasses into biochar with a higher fixed C content. Higher weight losses around 60–70 % were observed leading to solid yields of 30–40 % by mass. Fixed C content increased significantly up to values >70 wt.% approaching values typical of metallurgical coals. The biomasses and the resulting biochars were characterized through proximate and ultimate analysis to evaluate moisture, volatile matter, ash, fixed carbon as well as C, H, O, N, S according to ASTM standard. Calorific value HHV and LHV using bomb calorimetry were also investigated. The results showed that raw biomasses had higher volatile matter around 65–80 wt.% and lower fixed carbon around 10–20 wt.% which make them unsuitable for direct coke making. After carbonization, volatile content decreased below 20 wt.%, while fixed carbon rose significantly. Concerning ash chemistry, XRF revealed that certain biomasses such as straw and olive pomace

contained high levels of alkali and alkaline earth oxides, e.g., K_2O, CaO, MgO, as well as undesirable elements like P and S which can influence coke reactivity and BF performance. Packaging-derived biomasses showed higher SiO_2 and Al_2O_3 due to adhesives and fillers. TGA allowed to investigate the thermal degradation behavior of the samples between 30–900 °C at controlled heating rates. Distinct decomposition zones were observed with hemicellulose degrading at 200–300 °C, cellulose at 300–400 °C and lignin gradually degrading up to 600 °C. Comparison of torrefied vs. carbonized samples confirmed improved thermal stability and higher residual char yield. These campaigns achieved biochar yield around 25-40 % depending on biomass type and temperature. Gas fractions were rich in CO, CO_2, H_2, and light hydrocarbons. Tar composition showed a mixture of oxygenated compounds, phenolics, and polyaromatics. Initial analyses showed that optimized pyrolysis conditions were moderate heating rates and temperatures of 500–550 °C to maximize char yield while limiting excessive tar formation. RINA-CSM results provide fundamental data on biomass-to-biochar conversion, bridging the gap between laboratory analysis and future pilot and industrial implementation.

After preliminary laboratory tests, pilot and industrial campaigns were planned. AdI coordinated the case studies in Taranto focusing on the integration of local biomass resources into industrial coking blends. Pilot oven trials are foreseen in a 300 kg electrically heated movable wall coke oven. This setup reproduces industrial heating rates and wall pressure conditions, enabling controlled studies on coal/biomass blends. Charging temperature, internal gas pressure, and raw gas composition were continuously monitored. Focusing on coke blends, further tests were performed through Gieseler plastometer and Audibert-Arnu dilatometry. Gieseler plastometer allowed to study coking blend fluidity assessing softening, maximum fluidity, and re solidification. Biomass additions generally reduced maximum fluidity, but torrefaction and carbonization mitigated this effect. Audibert-Arnu dilatometry analyzed volume changes of coal blends. Biomass lowered dilation, but pretreated biochar behaved more compatibly. Fluidity test showed that the addition of 3 % raw biomass drastically reduced fluidity while torrefied and carbonized forms mitigated this effect with carbonized samples performing the best. Dilation tests displayed similar trends with raw biomass addition, reducing dilation significantly, whereas carbonized samples maintained more acceptable values. AdI results underlined that raw biomass was unsuitable for direct addition, but properly carbonized biochar shows promising behavior for subsequent pilot and industrial trials. Further tests were undertaken from TKS which tested coal–biomass blends using its standard industrial coking blend representing a lower fluidity baseline compared to the AdI blend. Tests for 10 % substitution in the industrial blend were performed, and the impact of biomass was more severe with reductions in plastic range and maximum fluidity. Nevertheless, torrefied and carbonized biomasses showed acceptable behavior at substitution rates up to 10 %. TKS also modeled coke yield estimation and highlighted that torrefied olive trunks and carbonized pallet wood produced the most favorable results. Finally, the study of volatilization behavior through TGA confirmed that carbonized biomasses exhibited decomposition patterns more aligned with coal, thus reducing incompatibility during carbonization. These results confirmed that pretreatment was critical to ensure compatibility in low fluidity blends such as those used in Germany. Industrial trials are also foreseen in coke oven at Taranto plant using blends containing up to 10 % biochar to validate the process at TRL 7 and ensure that CSR and CRI remain within acceptable ranges.

Paul Wurth Distillation Process Module was integrated into both pilot and industrial ovens. This Level-2 automation tool monitors raw gas temperature profiles, detects the "ready-to-push" condition, and provides real-time data analytics for process optimization. Comparative analysis demonstrated the capability of the tool to detect differences in devolatilization behavior due to biomass/biochar addition. This digital tool is expected to play a crucial role during upcoming pilot and industrial trials, ensuring consistent monitoring and operator support. This represents a key enabling technology for scaling biomass substitution from laboratory to industrial demonstration.

The BioCoDe project provides one of the first systematic attempts to integrate biomass and biochar into the coke making process at industrially relevant scales. The findings so far highlighted both the potential benefits and the critical challenges of this approach. Laboratory analyses confirmed that raw biomasses are not suitable for direct addition into coal blends, mainly due to their high volatile content, low fixed C, and disruptive effects on coal plasticity. However, thermal pretreatments such as torrefaction and, more effectively, carbonization significantly improved the quality of the biochar derived with fixed carbon levels above 70 wt.% and reduced volatile matter which brought biochar properties closer to those of coking coals thus making substitution feasible up to 10% in blends. Gieseler and Audibert-Arnu tests demonstrated that pretreated biomass mitigates the loss of fluidity and dilation, though complete equivalence with fossil coals was not achieved. These results suggest that careful selection of biomass and pretreatment severity are essential to preserve coke quality. From a sustainability perspective, the substitution of fossil coal with biomass offers a direct reduction of fossil CO_2 emissions. By valorizing local agro-industrial residues, BioCoDe contributes to a regional circular economy, reducing waste management issues and creating a new supply chain that links agriculture and heavy industry. Nevertheless, several barriers remain such as variability of feedstocks and seasonal availability, logistic constraints for collection, drying, and transportation, regulatory frameworks that are still under development for large-scale biomass integration into steel processes.

2.2.29 BIORECAST: BIObased REsidues Conversion to Advanced fuels for sustainable STeel production

The project was coordinated by Politecnico di Torino with CSM, RE-CORD (Renewable Energy Consortium for Research and Demonstration), Sidenor, Acciaierie di Calvisano, HTT Engineering, and WIP Renewable Energy participating as partners in the consortium. The project started on the 1st of November 2023 and lasts almost three and a half years. The overall project cost 2.36 M€ and the EU contributed 1.42 M€, i.e., almost 60 % of the budget.

The BioRECAST project proposes a disruptive and circular solution for steelmaking decarbonization through slow pyrolysis of wet biowaste streams and the simultaneous recovery of critical raw materials. It aims to develop a new model to transform low-grade residues into high-quality bio coal and bioenergy suitable for EAF steelmaking by proposing an integrated Pyro-EAF concept where a slow-pyrolysis system able to convert biowastes into bio coal and pyro gases is linked with an EAF steelmaking plant. This would enable the substitution of fossil coal with high-quality bio coal, as well as the use of the produced pyro gases as a renewable fuel for burners. Furthermore, P-bearing

inorganic fractions could be recovered through acid leaching and repurposed while waste-heat from EAF off-gas system could be recirculated to power pyrolysis.

The first step of the project included a comprehensive characterisation of eight biowaste streams, i.e., civil and industrial sludge, OFMSW (Organic Fraction of Municipal Solid Waste), agricultural residues, digestate and green waste. Their proximate, ultimate and inorganic compositions were analysed, enabling the identification of four suitable candidates for slow-pyrolysis. The first residue was the agricultural digestate (ADG) which represented a residue of the anaerobic digestion of plants, largely available in Europe, and characterized by a very low market value even lower than woody biomass. The second residue was an agricultural waste (AGW), i.e., olive pruning, which represented the best quality material for high quality bio coal production. The third residue was OFMSW which demonstrated a reduced inorganics content and a valuable quality as precursor of bio coal as well as a negative cost. Finally, sewage sludge (SS) was selected given the high availability and the high disposal cost, represents a strategic residue to be valorised for EU, but the high concentration of P required to perform chemical leaching, as part of the integrated process. These residues were subjected to an extensive laboratory campaign of 48 pyrolysis tests, exploring temperatures between 450 and 650 °C and residence times up to 120 minutes. Temperature emerged as the dominant factor governing solid yields and carbon quality, as confirmed by Van Krevelen evolution and TGA results. Residence time had negligible influence within the tested ranges. Based on these results, slow pyrolysis was scaled up using two pilot units, i.e., the SPYRO auger reactor (3–5 kg/h) and the PYROK rotary kiln (100 kg/h), and the feedstocks were processed under real operating conditions. The resulting mass yields ranged from 31 to 51% depending on ash content and the energy balances demonstrated that 33–45% of the original energy was retained in the biochar fraction. Pilot-scale acid leaching was implemented using nitric acid under controlled conditions to upgrade the raw biochar into metallurgically suitable bio coal. The treatment significantly improved chemical quality reducing ash by 32–56 %, raising carbon to 66–70 wt.% and achieving P removal efficiencies between 91–100 %. Extraction analyses showed nearly complete removal of alkali and alkaline-earth metals, while silicates remained largely unaltered, explaining why sludge-derived bio coal could not reach the required carbon content. Mineralogical changes observed via SEM and XRD confirmed reduced calcite, sylvite and phosphate phases, and clarified variations in ash morphology. The overall results are summarized in Table 23 (67) (68).

Table 23: Fixed C, volatiles and ashes content of the four biowastes selected for the pilot campaign

	Volatiles (%, db)	Ashes (%, db)	Fixed C (%, db)
OFMSW	18.7	18.4	62.9
SS	19.3	39.5	41.2
AGD	18.5	15.8	65.7
AGW	16.7	16.9	66.4

Large-scale production using the 100 kg/h PYROK unit validated process scalability, producing hundreds of kilograms of bio coal from SS and AGW streams. These materials were then supplied to downstream metallurgical trials. Laboratory-scale carburisation tests were conducted by adding bio coal pellets to molten Fe at 1600 °C simulating EAF conditions and the main results are summarized in Table 24. Carburisation performance depended strongly on fixed carbon content and ash fraction. OFMSW and straw-derived bio coal achieved yields of 69.2 and 55.4%, while digestate and sludge underperformed with yields <45 %. Blends with anthracite (70:30) significantly improved results, pushing straw blends to 75.7 % yield. These findings demonstrated the feasibility of using upgraded biomaterials as partial or full substitutes for fossil carbon.

Table 24 :Main test conditions and outcomes of the laboratory-scale carburization tests performed with the four bio coals and their mixtures with anthracite

	OFMSW	ADG	Straw	Sludge	70 straw+30 anthracite	70 sludge+30 anthracite
Mass Fe (g)	150	150	150	150	150	150
Carburization target (%)	3	3	3	3	3	3
Stoichiometric C to add (g)	4.5	4.5	4.5	4.5	4.5	4.5
C fix in biomaterial (%)	63.4	64.2	65	42	77.5	66
Biomaterial stoichiometric to add (g)	7.1	7.0	6.9	10.7	8.9	11.4
Added biomaterial (g)	10.1	10.0	9.9	15.3	9.9	15.3
Yield carburization (%)	69.2	41.4	55.4	35.1	75.7	60.2

Concerning industrial trials, a complete 40-tonne storage and injection system was commissioned at Acciaierie di Calvisano including two injection points near the slag door and the eccentric bottom tapping. Preliminary polymer-injection trials were carried out to calibrate flowability, slag foaming performance and arc-covering indicators. At SIDENOR, pellet format was selected as the most operationally viable although fragility and rolling behaviour were noted as challenges awaiting further optimisation.

BioRECAST also advanced the utilisation of pyro gases produced during slow pyrolysis since HTT redesigned a burner to prevent condensation and tar-induced clogging, allowing reliable pyro gas combustion at high temperature. The burner integrated separate passages for pyro gas and natural gas and will undergo CFD validation at RINA-CSM before fabrication. To maximise the circularity of the Pyro-EAF concept, a detailed heat-integration study was undertaken to identify viable waste-heat sources within the EAF. Literature and industrial data confirmed that off-gases reaching average temperatures above 540 °C constitute the only suitable heat source, whereas slag and other thermal streams were excluded due to temperature, layout constraints or insufficient energy availability. A rotary-kiln reactor with external heating was selected as the most appropriate design for heat recovery

and preliminary sizing was conducted based on a median coal consumption of 16 kg/t steel. The early foundation laid through pyrolysis testing, chemical upgrading, carburisation trials, industrial system preparation, burner engineering and heat-integration assessments has unified BioRECAST scientific and industrial progress into a cohesive technological pathway.

2.2.30 BIORESTEEL: Valorisation of wet biomass residues for sustainable steel production with efficient nutrient recycling

The project was coordinated by Swerim with SSAB, RWTH, Ingelia, Ferriere Nord, RINA-CSM, KTH (Kungliga Tekniska högskolan), Celsa, O.R.I. Martin and Universitat Politecnica de Valencia participating as partners in the consortium. The project started on the 1st of October 2023 and should last almost three and a half years. The overall project cost 3.42 M€ and the EU contributed 2.05 M€, i.e., almost 60 % of the budget.

The BioReSteel project addresses the key challenge to replace fossil carbon sources in EAF steelmaking with sustainable and biogenic alternatives by valorizing wet biomass residues and converting them into high-quality hydro char. The project develops a circular and low-carbon solution for the metallurgical industry enabling the simultaneous recovery of P for fertilizer production. In particular, the project aims to develop, validate, and demonstrate a fully integrated concept in which hydro char derived from locally available wet biogenic residues replace fossil coal and natural gas in EAF. The process further promotes the recovery of P thus contributing to both decarbonization and circular economy objectives of the European Union. The BioReSteel process integrates several steps to transform biogenic residues into a metallurgically suitable and environmentally beneficial material. The first step includes feedstock selection to identify the most suitable biomass residues focusing on waste availability, low ash, and stable P content. After selection, the following step concerns hydro char production, i.e., the conversion of the feedstock via hydrothermal carbonization, at Ingelia facilities. A secondary thermal treatment, i.e., pyrolytic upgrading, is performed to increase fixed carbon and heating value. The following step includes P removal and recovery through a chemical extraction to transform an impurity for steelmaking into a valuable fertilizer precursor. Finally, metallurgical validation of the obtained hydro char is performed through the production of bio-briquettes in laboratory, pilot, and industrial EAF trials to assess carburization, slag foaming, and process efficiency.

Concerning feedstock selection, several biomass residues were investigated and subjected to the hydro char treatment including green waste, OFMSW, digestate, and olive pomace. The main results of the analysis are reported in Table 25. It was demonstrated that olive pomace hydro char offered the best compromise between low ash content around 8 wt.%, stable P content, and consistent quality. Green waste was kept as secondary reference, while OFMSW and digestate were excluded due to the high ash and P contents. The hydro char obtained was then subjected to pyrolysis between 200-600 °C to increase the fixed carbon. This goal was achieved as confirmed by the data reported in Table 26 where an increase of fixed carbon from 25% to 65% and a decrease of volatiles from 65 to 18 % was observed. These results were also accompanied by a solid yield decreased from 80 to 50 % identifying an optimal operating range at 300–400 °C, providing a balance between carbon content and yield. The main outcomes of this first step of the project identified olive pomace as the optimal feedstock and 300-

400 °C as the optimal pyrolysis temperature. Concerning P extraction, it was demonstrated that a nitric acid treatment could remove over 95 % of P and 60–70 % of ash from hydro char. P concentration dropped below 0.05 wt.% thus meeting the requirements for metallurgical use. The extracted phosphorus can be precipitated and reused as fertilizer, achieving a fully circular valorization of the biogenic residues.

Table 25: Ash and P content of the four biowastes considered

	Ash Content (wt.%)	P (wt.%)
Green Waste	12–18	0.25
OFMSW	>20	>0.4
Olive Pomace	7–9	0.2
Digestate	>15	>0.5

Table 26: Main characteristic of hydro char after being treated through pyrolysis at 400 and 600 °C

	Untreated Hydro char	Pyrolyzed (400°C)	Pyrolyzed (600°C)
Fixed Carbon (wt.%)	25	55–60	65
Volatile Matter (wt.%)	65	30	18
HHV (MJ/kg)	18–19	22–23	24
Solid Yield (%)	80	75	50

The next step of the project concerned the development of the briquettes and Swerim optimized the recipes for hydrocar-based briquettes using mill scale and two types of binders, i.e., an organic binder B2 and a composite B1. The main results are summarized in Table 27. The organic binder allowed to achieve a superior strength and the optimal composition included 15–25 % of hydro char and 4% organic binder resulting in compressive strengths above 250 kg/cm^2 and densities between 3.0–4.6 g/cm^3. Scale-up using a Komarek roller press confirmed industrial feasibility with stable production at 300–500 kg/h and minimal disintegration. The briquettes produced were exploited for slag foaming and carburization tests at the laboratory scale and the results obtained are summarized in

Table 28. They showed pristine hydro char induced a rapid initial slag foaming due to its high volatile content while pyrolyzed hydro char provided sustained foaming and higher metallization rates. The tests confirmed that pyrolyzed briquettes enhanced reduction and carburization, while pristine briquettes optimized slag foaming height thus proving their complementary behavior.

Table 27: Main characteristic of the briquettes produced with the hydro char and the different binders

	Hydrochar (%)	Binder (%)	CCS (kg/cm^2)	Density (g/cm^3)	Drop Test Loss (%)
B1 – 10% HC	10	4	180	3.1	5.2
B2 – 15% HC	15	4	250	3.9	2.1
B2 – 25% HC	25	4	260	4.3	1.5

Table 28: Main outcomes resulting from slag foaming and carburization tests performed with both pristine and pyrolyzed hydro char

	$C_{fix}/OFeO_x$	Reduction Degree (%)	Metallization Degree (%)	Density (kg/m^3)
Pristine	0.20	12	26	2950
Pyrolyzed	0.45	50	61	3000

RINA-CSM conducted pre-industrial tests in a vacuum induction furnace using both hydro char pellets and briquettes blended with mill scale. The tests evaluated carburization efficiency and FeO reduction behavior. Initial results demonstrated that hydro char can effectively carburize molten steel, producing ingots comparable to anthracite-based references. When mixed with mill scale, the hydro char briquettes showed partial reduction of FeO, with potential for optimization by adjusting hydro char-to-oxide ratios. In conclusion, hydro char acts as an effective carburizing and reducing agent and C and S contents in the final metal were within EAF operational ranges.

2.2.31 ZINCVAL: Valorisation of low zinc-containing residues

The project was coordinated by SWERIM with RINA-CSM, CRM, TATA STEEL, LINDE, ADI, O.R.I. Martin participating as partners in the consortium. The project started on the 30st of September 2023 and it is currently in progress. The overall project cost 3 M€ and the EU contributed with 1.81 M€, i.e., almost 60 % of the budget.

The ZincVal project addresses a long-standing challenge in the steel industry, i.e., the limited recyclability of Fe-bearing residues due to the high presence of Zn. Dust and sludge generated in BF, BOF and EAF often contain Zn levels excessively high for direct recycling in steelmaking, yet too low and contaminated to be economically treated by conventional Zn producers. As a result, valuable Fe units and C are lost while steelmakers face additional costs related to safe storage, landfilling and environmental compliance. ZincVal aims to develop and validate technological solutions enabling the removal of Zn from steelmaking residues and the production of Fe-rich secondary materials that can be recycled back into the steel production cycle. In doing so, the project supports EU objectives on

circular economy, resource efficiency and decarbonization of the steel sector, while also offering flexibility to both the steel and Zn industries in terms of feedstock selection.

The overall objective of ZincVal is to secure high raw-material efficiency by extracting additional value from existing residue streams produced in current and future steelmaking routes. Specifically, the project focuses on developing technologies for the treatment and separation of low-Zn residues to produce Zn-rich fractions suitable for further upgrading or direct use in Zn production and Fe-rich fractions which can be safely reintroduced into steelmaking processes. The different recycling routes starting from relatively low TRLs were also assessed in terms of environmental impact, energy consumption, CO_2 emissions and cost-effectiveness, to identify the most sustainable solutions for industrial implementation. To achieve these goals, ZincVal combines physical separation, pyrometallurgical and hydrometallurgical approaches, supported by comprehensive material characterization and process modelling.

A key foundation of the project is the detailed physical, chemical and mineralogical characterization of steelmaking residues. Multiple residue types, including BF and BOF sludge, and EAF dust, were analyzed to support the selection and optimization of appropriate treatment routes. In the first phase, AdI and RINA-CSM performed an in-depth characterization of six different residue matrices. Results showed that BF sludge presented a strong enrichment in Zn in its finest particle fractions thus making it particularly suitable for hydro cyclone-based separation. To ensure consistency and robustness of analytical data, the consortium carried out a Round Robin analysis, involving samples from three steel plants, i.e., Tata Steel, AdI and O.R.I. Martin. Partner laboratories independently performed standardized chemical and mineralogical analyses, after which the results were compared and jointly evaluated. This exercise strengthened confidence in the datasets and provided a harmonized analytical basis for the upcoming experimental trials.

Within ZincVal, hydro cyclone separation plays a central role as a physical treatment method for upgrading Zn-bearing sludges. RINA-CSM is responsible for the design and optimization of hydro cyclone units using CFD, supported by experimental data from literature and from the material characterization phase. A modular physical hydro cyclone model, manufactured in transparent Perspex, was constructed to study the effects of geometry, flow rate and outlet configuration on separation efficiency. Thanks to its modularity, the system allows systematic investigation of key parameters influencing particle classification and Zn enrichment. An experimental campaign is currently in progress testing 30–50 kg batches of sludge and analyzing the resulting fractions in terms of particle size distribution, Zn content and mineralogical.

Parallelly to physical separation, ZincVal investigates several pyrometallurgical technologies for an efficient Zn removal and metal recovery. CRM and Tata Steel are jointly advancing a dual-kiln (rotary kiln) technology, operating under reducing conditions. The process enables effective separation of Pb and Cd from Zn, while producing partially metallized ferrous residues with high Fe metallization. These residues can potentially be charged directly into a BF or a smelter. Laboratory-scale trials are being followed by pilot-scale demonstrations, with systematic evaluation of Zn and Pb separation efficiency and Fe metallization degree. To support future trials, CRM is also upgrading its rotary kiln, including partial electrification and improved dust capture systems.

Another key technology under evaluation is OXYFINES developed by Linde Gas. This process treats Zn-bearing dust and sludge using an oxygen-fuel burner, reducing zinc oxides with C present in the feed. Pilot trials in previous projects achieved Zn separation rates of up to 97 % from BF sludge. Within ZincVal, an OXYFINES campaign is planned to focus on further Zn removal and enrichment in the off-gas dust to reach Zn contents suitable for direct use in Zn production. The remaining Fe-rich melt can be reused in steelmaking.

In addition, RINA-CSM and ORI Martin are developing routes for the agglomeration of EAF dust using briquetting techniques. The objective is to produce stable agglomerates with Zn contents above the threshold typically required by Zn refiners, i.e., around 20 %, enabling improved downstream valorization. To minimize CO_2 emissions, biochar is being used as renewable reducing agent. Mechanical strength, i.e., drop tests, and melting behavior are being assessed through laboratory and pilot-scale tests, with initial results considered promising.

3. Further EU driven initiatives which fostered IS in the steel industry: 3rd to 6th FP and Horizon programs

Framework Programs (FP) for Research and Technological Development are funding programs created by the EU Commission to support and foster research. This funding scheme began in 1984 with FP1 until 1987 which provided a budget of 3.8 billion €, FP2 from 1987 to 1991 with 5.4 billion €, FP3 from 1990 to 1994 with 6.6 billion €, FP4 from 1994 to 1998 with 13.2 billion €, FP5 from 1998 to 2002 with 15.0 billion €, FP6 from 2002 to 2006 with 16.3 billion €, and FP7 from 2007 to 2013 with 50.5 billion €. Starting from 2014, the funding programs were named Horizon with Horizon 2020 from 2014 to 2020 providing 77 billion €, and Horizon Europe from 2021 to 2027 ensuring 95.5 billion €. The framework programs consist of three main research areas called pillars. The first pillar called "Excellent Science" focuses on basic science, the second pillar called "Industrial Leadership" aims to find ways to modernize European industries, and the third pillar called "Societal challenges" funds potential solutions to social and economic problems with the goal of implementing solutions rather than technology development.

3.1 FP3-FP4-FP5-FP6

3.1.1 FP3 - Recycling of zinc and lead containing dusts from the electric arc furnace (69)

The project was coordinated by TKS with Det Danske Stalvalsevaerk AS (DDS) and Forschungsgemeinschaft Eisenhuttenschl participating as partners in the consortium. The project started on the 1st of January 1993 and lasted almost three years, ending on the 31st of December 1995. EU contributed 1.2 M€ to the project.

Scraps recovered in EAF are often contaminated by elements from alloying and surface corrosion protection. Some of these contaminating elements, e.g., Zn and Pb, are characterized by a high vapor pressure and are transferred to dust after being vaporized. At the time of the project, EAF steelmaking produced almost 15-20 kg of dust per ton of steel with variable Zn and Pb content depending on the type of scrap used. In particular, Zn content varies from 10 to 30 % and Pb content from 0.2 to 4 % in EAF dust. These high concentrations encouraged the steel industry to develop efficient processes to recover these valuable metals since the presence of Fe and alkalis made impossible the direct use of EAF dust in the Zn production process. For this reason, Fe must be separated and Zn concentrated in a separate process. The most common concentration method was the rotary kiln process, i.e., the Waelz process, which was characterized by limited economic efficiency as the expenditure and the price of the dust depended on the Zn content. Indeed, Zn content in the dust must be at least 16 % and only minimum Zn concentrations of 24 % proved to yield profit. Considering this, it was of primary interest for steelmakers to provide dust with the highest Zn content to transform dust delivery from an expenditure into a profit. This could be achieved by selecting scrap with a high Zn content, but this method was limited by the quality of the scrap available and of the steel being produced. A far more interesting option was EAF dust recycling into the furnace to enrich the Zn content in the dust thanks to its high vapor pressure. This solution allowed to recover Fe from the dust because its non-volatile compounds could be dissolved in the slag and to increase the Zn and Pb contents in the dust by evaporation.

The trials were performed in the EAF steel shops of TKS and DDS and proved that dust recycling by melt injection was able to increase the Zn level in the dust by an amount equivalent to the Zn injected. An average Zn increase of 10 % was achieved by recycling about 60 % of the total dust. TKS EAF was characterized by a 140-t capacity and a normal tap to tap time of 80 minutes. It was used to produce a great variety of materials from special steels to high-alloy stainless steels. All exhaust gases from the different steel manufacturing units were funneled to the same collecting system, mixed and transported to the gas cleaning unit with two bag filter houses. The dust was then collected from the gas cleaning unit and subjected to further treatments, e.g., pelletization, for the subsequent shipping to non-ferrous smelters for Zn and Pb recovery. Analogous procedure was performed by DDS which was mainly devoted to low-alloy carbon steels production with two EAFs with a capacity of 110 t.

The experimental injection equipment used at TKS consisted of a control unit, a screw conveyor to transport the dust out of the filter dust bunker, a coal-bunker endowed with a fluidization equipment to mix coal and dust to improve the pneumatic support of the filter, a pressure vessel conveyor with a fluidization equipment to transport the dust and coal mixture to the daily dust bunker by means of a pipeline, and a pressure vessel conveyor with a fluidization equipment to transport the dust and coal mixture into the EAF by means of a lance. The equipment was progressively redesigned to face all the issues resulting from the handling and recycling of bigger amounts of filter dust. The main modifications concerned an additional fluidization equipment in the filter dust bunker to improve the outgoing dust stream, the introduction of a lump cutter to transform agglomerated dust into lumps smaller than 10 mm to facilitate dust transportation, an additional fluidization equipment in the daily dust bunker to improve the outgoing dust stream, an additional air dryer unit to avoid dust blockage in the pneumatic transportation system. DDS experimental injection plant for dust recycling consisted of a storage

bunker where the dust transported by the chain conveyor was mixed with C to ensure optimized conditions for injection and for metal oxides reduction before the dust was brought to the injection system. The mixture of dust and carbon (8-12 %) was injected into the furnace with a rate of 150 kg/minute using a lance. In both cases, injection was performed during the heating period to ensure dust dissolution in the molten steel/slag system. The idea was to inject for every heat a dust quantity equivalent to the average amount that would have been produced without injection to exclude spoiling of the steel quality. The results of the campaign were verified by an analysis of both steel and slag as well as of the injected and produced dust. Slag quality was also checked regarding its potential reuse as construction material.

After performing preliminary injection tests necessary to determine the relevant process parameters and operational techniques, experimental injection tests were planned. Steelmaking practices proved that only a single period of 10 minutes was available to perform dust injection during the melting process. Almost 2.5 tons of dust must be injected within this period to achieve the targeted dust production of 15 and 20 kg per ton of steel. This entailed a feed rate of 200 kg/minute even if the actual feed rates used during the trials were between 80 and 150 kg/min. One of the goals of the campaign was to get more information on how to inject the dust into the molten slag or directly into the phase boundary between steel and slag. This goal was achieved by using the lance manipulator which allowed to inject the dust into the steel/slag phase boundary thus ensuring dust dissolution in the slag and its partial reduction in the steel melt. There was no evidence that the injected dust was directly dragged and conveyed into the exhaust gas system. The chemical composition of the dust in terms of Zn and Pb content was evaluated throughout different melts and for increasing injection times. It was observed that Zn concentration significantly increased after injection started with enrichment between 4 and 6 wt.%, i.e., from almost 24.5 wt.% to more than 30 wt.%, after about 40 minutes. These outcomes were interesting considering that the economic efficiency and feasibility of dust recycling strongly depended on the average Zn concentration in the dust which in turn was directly correlated to the amount of recycled dust.

The project allowed to identify many other important outcomes and to draw some important conclusions. First of all, the increase in Zn concentration was the main aspect to tailor and improve and even though no Zn-coated scrap was charged values up to 34 wt.% were achieved. A second major outcome was the significant reduction in total dust achieved through dust recycling. Dry dust decreased from almost 17 to almost 12.5 kg/ton of liquid steel at TKS from January 1994 to December 1996. A third aspect concerned the additional energy consumption necessary to melt the dust and to reduce Zn compounds. Theoretical calculations reported an additional energy consumption of 680 kWh per ton of dust with a 34 wt.% of ZnO, but in real operating conditions it was observed that there were other factors affecting energy consumption, e.g., amount and quality of scrap, input temperature, alloys, additives, etc., and it was not possible to determine any additional energy consumption due to dust recycling. It was also observed that the concentration of Pb, Na and K in the dust increased by increasing the Zn content in the dust. Finally, the reaction of injected dust with steel, slag and the co-injected C determined a certain dissolution of Zn in the liquid steel. In particular, it was observed that the amount of Zn dissolved in the steel depended on Fe concentration in the slag and that higher values of Fe in the slag allowed to decrease Zn ratio between the steel and the slag.

Furthermore, Zn concentration in the steel was never so significant to influence product quality and its value could be easily decreased to 50 ppm using vacuum treatment in secondary steelmaking. Finally, some conclusions were also drawn about slag quality. No problems related to slag foaming were observed and the recycling procedure did not seem to affect slag properties regarding their feasibility as construction material. The experimental phase was too short to investigate the influence of a higher FeO content in the slag on the wear resistance of the refractory.

Overall, it can be concluded that the increase in Zn and Pb content of the dust met expectations, allowing to reduce the overall amount of dust to be shipped to a non-ferrous smelter thus ensuring less transport and processing costs. Therefore, pneumatic dust recycling can be considered as positive on the cost reduction in EAF steel making.

3.1.2 FP4 - A new treatment process to recover magnetite, zinc and lead from iron and steel making dusts and sludges (70)

The project was coordinated by EcoMetal with Insitute of Geotechnics of Slovak Acadymy of Sciences, the Research Institute Vitkovice and TecMinho (Associaçao Universidade Empresa P/o Desenvolvimento) participating as partners in the consortium. The project started on the 1st of September 1997 and lasted slightly more than two years, ending on the 30th of November 1999. The EU contributed 224.50 k€ to the project budget.

The hazardous and ecotoxic nature of steelmaking dust and sludge was mainly ascribed to the presence of heavy metals, e.g., Zn, Pb and Cd, in forms that were easily leachable by water or slightly acidic or alkaline media. In particular, the high mobility of heavy metals could be responsible for relevant environmental impacts when disposed of in controlled landfills. For this reason, the present project aimed at developing new processes to recover these valuable metals and products from steelmaking dust and sludge, assessing both technical and economic aspects.

At first a pre-treatment stage was foreseen to ensure alkalis and Cl removal through dust water leaching fundamental for the further treatment of dust to recover metals. After that, two different procedures were considered. The first procedure was developed exploiting the reduction of Zn and Pb oxides to perform a subsequent separation by vaporization and by physical means such a magnetic separation to recover magnetite. The remaining iron oxides, which were partially reduced, were re-oxidized by controlled means to produce magnetite which was again enriched by magnetic separation. The second treatment procedure developed consisted in a full oxidation of all iron phases to Fe (III) followed by a controlled reduction until important amount of magnetite were produced and could be easily separated through magnetic separation. The final residue consisted of concentrated amounts of Pb and Zn and was treated by hydrometallurgical means employing NH_4Cl.

The campaign focused on 12 different residues coming from different iron and steel shops, i.e., BOF dust, BOF sludge and BOF mud, LS sludge and EAF dust. The results of the chemical analysis reported higher average values of Zn and Pb in EAF dust, i.e., around 17 and 3.5 %, respectively, compared to BOF residues where Zn varied around 2.5, 1.6 and 5.2 % in sludge, dust and mud and Pb varied around 0.5, 0.85 and 1.0 % in sludge, dust and mud. On the contrary, BOF residues were richer in Fe with 63,

46 and 53 % in sludge, dust and mud compared to the 28.5 % of EAF dust. The results of ecotoxicity tests performed according to DIN 38414 and TCLP (Toxicity Characteristic Leaching Procedure) confirmed the ecotoxic nature of the residues due to the high amount of dissolved Pb. Residues washing behavior was investigated by mixing them with water at 110 °C and agitating them with a speed of 1100 rpm for 24 hours. The chemical analysis of the resulting water was performed by AAS while the one of residual dust by XRF. The results highlighted high degrees of Cl removal which were fundamental for the further treatment of the dust to recover Zn, ferrites and Pb by pyro or hydrometallurgical methods. Also, an important part of Pb was dissolved in water. This allowed the partial removal of this heavy metal from the residues but made necessary the identification of a suitable wastewater treatment to eliminate it from the pre-treatment water. Precipitation with H_2SO_4 or Na_2SO_4 was identified as potential strategy to remove more than 90 % of Pb ensuring a final content in the water around 0.4 g/l. Further wastewater treatments were foreseen to remove alkalis and Cl such as concentration and evaporation which cost was estimated around 45 €/m^3 of solution. The self-reduction roasting of pre-treated dust and sludge was also investigated performing the treatment with C and gas mixtures of CH_4+CO_2 and determining parameters such as residence time, temperature, C amount and degree of recovery of volatile metals and iron oxides. The experiments with desulphurized coal as reducing agent demonstrated an efficiency of dry filtering for Cd, Pb and Zn higher than 98.5 %.

3.1.3 FP4 - Economical, technical and ecological utilisation of treated steel slag in civil engineering of high-quality demands (71)

The project was coordinated by FEhS with Dillinger Hütte, Arbed, BRRC (Belgian Road Research Center), CRM, Cockerill Sambre, DSU (Gesellschaft für Dienstleistungen und Umwelttechnik mbH & Co.), AGC (ex Glaverbel) (Asahi Glass Company), Luleå University of Technology, Sidmar, Stiftelsen für Metallugisk Forskning, VITO (Vlaamse Instelling voor Technologisch Onderzoek), VoestAlpine Stahl and Will Klausmann Betonsteinwerk participating as partners in the consortium. The project started on the 1st of August 1997 and lasted almost three years, ending on the 31st of July 2000.

The present project was a great example of industrial symbiosis between the steel and the construction sector where the potential reuse of steel slag as civil engineer materials was addressed from economical, technical and environmental perspectives. The relevance of the project was confirmed by the involvement of important partners from both the steel, e.g., Dillinger Hütte, Arbed, Cockerill Sambre, Voestalpine, and construction, e.g., BRRC and Will Klausmann Betonsteinwerk, sectors. The project evaluated different routes to treat steel slag and ensure their compliance with the environmental demands imposed by the European legislation. In particular, the target of the project was to treat steel slag with various residues from steelmaking and other industries to improve their volume stability and to provide further steps towards the zero-waste target. Some of the treatment methods investigated were also transferred into operational practice.

The main issue connected with the use of carbon steelmaking slags as construction material was their poor volume stability. In light of this, different solutions were assessed to solve this problem. The first proposal tried to exploit internal recycling in the steelmaking with a view at minimizing also the

residues to be used in other fields. In particular, the Zn content in BOF dust was too high to ensure dust recycling into BF, but it was also too low for an efficient and economic viable recovery of Zn. For this reason, Voestalpine investigated the recycling of BOF dust into the converter itself to increase the Zn content in the dust up to amounts suitable for recovery. The effect on steel and slag quality was also evaluated. The results proved that BOF dust recycling into BOF vessel allowed Zn and all other volatile elements vaporization and transportation into the gas thus ensuring the desired dust enrichment. The poor stirring during BOF processes also ensured that all Zn introduced with the dust briquettes was vaporized thus preserving steel quality. Slag quality and properties fulfilled all the demands for the application as aggregates for road construction. The higher Fe contents in the slag allowed to bind the free lime into calcium ferrites thus increasing slag volume stability. These results were extremely interesting for all European steel producers and their processors for the slag being a further step to produce steel with minimum of residues.

A second approach was proposed in Germany where the treatment of liquid BOF slag with sand and oxygen injection was investigated. Indeed, BOF slag were characterized by good mechanical and environmental properties but also by an insufficient volume stability caused by the free lime content which tended to react with water or humidity causing an increase in aggregates volume. This volumetric change jeopardized slag integrity thus preventing its use in construction and building applications. The treatment proposed improved slag volume stability by binding the free lime into stable phases thanks to the presence of the SiO_2-rich sand. The procedure was expected to provide also a reduction in the free MgO. The good results obtained fostered the implementation of this treatment in a real process in one of the steelworks and could be easily extended to all steelworks interested in treating their slag. Overall, the slag treated in this way was characterized by a higher quality which allowed its application in fields with high quality demands, e.g., aggregates for road construction and asphalt layers or as additive for civil engineering concrete, which could not be fulfilled by other residues or wastes. Furthermore, this would allow to save dump space and natural resources.

A further treatment was investigated in Belgium and Luxembourg by Sidmar and CRM where liquid steel slag weas treated with glass cullet and oxygen to introduce SiO_2-rich materials and bind the free lime as it was done in Germany with sand. In the first test runs, glass cullet addition was limited to 750 kg, and it proved to be insufficient to bind the free lime. Therefore, additional tests with increasing content up to 2000-3000 kg were planned after the project to achieve the targeted slag volume stability. Indeed, this solution was of great interest not only because glass cullet was cheaper than sand, but also because industrial symbiosis principles would extend simultaneously to three partners, i.e., steel, construction and glass industries, providing strong environmental benefits. Moreover, the identification of this alternative recycling route for glass cullet was fundamental as it could not be recycled into the glass furnace since it did not fulfil the specifications on the raw material.

The evaluation of the technical feasibility of the processes showed that it was possible to produce volume stable steel slags with good technical properties fulfilling the demands of European and national standards. Some exceptions were noticed for the glass cullet route where the slag produced fulfilled only the environmental requirements but were characterized by a non-satisfactory volume stability thus requiring further improvement. The slags fulfilling all technological and environmental

requirements were tested for different applications such as armor stones on embankments in waterway construction, aggregates in road construction, aggregates in low noise asphalt layers on roads, aggregates for lean concrete in road construction as well as for concrete paving stones. Test fields were also constructed to demonstrate their excellent properties under actual conditions.

The potential use of other iron and steelmaking residues such as dusts from BF operations, e.g. casting bay degassing, sinter plant, BF sludges, dust from ladle degassing and dust from coal combustion, as filling mixtures for mining shafts was also investigated. After testing these mixtures in laboratory, the most promising ones were tested in lysimeter test fields but after one year the results gave unexpected outcomes thus requiring further investigations.

3.1.4 FP5 - A new metallurgical route for the on-line conversion of by-products into valuable mineral and metallic products with a reduction of CO_2 emissions (72)

The project was coordinated by CRM with ALZ, Basse Sambre E.R.I., Cometsambre, Institute of Chemical Processing of Coal in Zabrze (ICPC), Lafarge, Profilarbed, Usinor and Voestalpine Industrieanlagenbau participating as partners in the consortium. The project started on the 1st of January 2001 and lasted almost three years and nine months, ending on the 30th of September 2004. The overall project cost 4.6 M€ and the EU contributed 2.3 M€, i.e., half of the budget.

The project consortium was composed by steel industries, scrap metal (SME) and car dismantling companies, cement industries, coal-based power plants in Eastern Europe and steel engineering companies and all of them had as common goal the identification of a suitable way to recycle and reuse solid by-products from the different industrial sectors to reduce the amount of wastes to be landfilled. The by-products of primary interest for the project were steelmaking slags and dusts, residues from scrap conditioning and car dismantling, fly ash from coal fired power plants and bottom ash from urban incinerators. Other by-products from the steel industry which could be possibly included in the blend were BF dust and sludge, mill scales and sludges, dust from rolling plants, etc.

To reach the primary goal of the project, the consortium designed an original Zero waste (ZEWA) process which was an on-line metallurgical treatment based on a clean fusion-reduction technology. This process allowed the conversion of these adequately mixed by-products into valuable mineral and metallic materials. The metallic products, e.g., hot metal, could be recovered and re-used in the steel industry while the mineral components with a targeted chemical composition, e.g., hydraulic binders, could be used by the cement industry providing a viable substitute to Portland clinker and allowing to reduce CO_2 emissions by 25 %. In light of this, the ZEWA process had the big merit to foster the conservation of energy, raw materials, and lands used to bury the solid residues, but also to reduce the CO_2 emissions (73) (74). A schematization of the ZEWA smelting reduction process is provided in Figure 25.

The project provided a scaling up opportunity for the smelting reduction process already developed by CRM, FEhS and MEFOS in the framework of the ECSC project called IPBM and described in section 2.1.2. In particular, it focused on the design and erection of a dedicated ZEWA pilot plant at Vitkovice

steelworks to evaluate its performance during the pilot test campaign and to provide the basis for the final industrial scale up and commercialization.

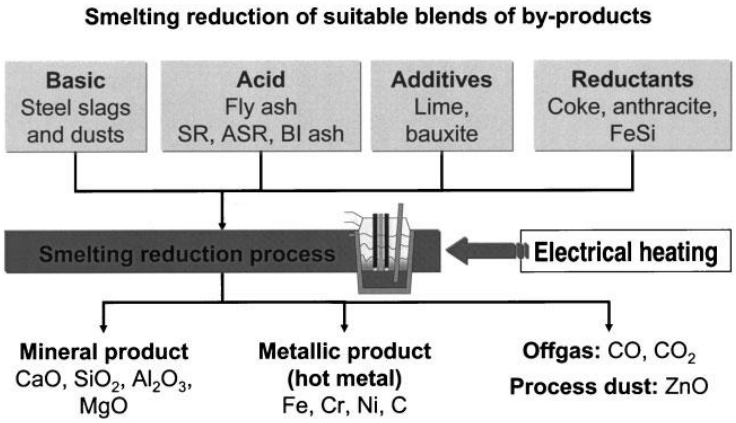

Figure 25: Brief schematization of ZEWA process including input materials and output products (73)

The technology selected for the ZEWA smelting reduction process was an electrical heated LF equipped with channels for top charging of liquid steelmaking slag and coarse solid materials, e.g., solid slag, into the foamy slag bath, and with a deep pneumatic lance for powder materials injection into the hot metal, e.g., steelmaking dusts, fly ash and reductants, as schematized in Figure 26. The ladle was also equipped with a bottom stirring system to enhance mixing and reaction kinetics, and with a post-combustion lance to recover heat through the combustion of the CO resulting from the reduction reactions. The latter were possible thanks to the reductants, e.g., coke, anthracite or coal, added to the blend of residue materials. The ladle was also endowed with a temperature and sampling manipulator for process control and with a camera for internal furnace operations monitoring. ZEWA process proved to be very flexible ensuring the charging of both liquid and solid materials and allowing to reduce material pretreatment costs not requiring pelletization or briquetting. Furthermore, it was very efficient in lowering dust emissions and energy consumption thanks to the thick foamy slag which exerted a filtering effect and reduced thermal losses by radiation from the arc and the metal bath.

Focusing on the output products obtained by the ZEWA process, they can be grouped in hot metal, mineral and dust products. Process dust was characterized by a high Zn content and was recovered in the off-gas filtering system. The main marketable products in the hot metal were Cr, Ni, Mn and Mo, but it required reprocessing prior to recycling in the converter due to the high P content. Finally, mineral products were targeted to be suitable for Portland clinker substitution in cement production or as metallurgical powders for steel refining in secondary metallurgy. As the main elements constituting the final slag were CaO, SiO_2 and Al_2O_3, the final composition necessary to comply with the requirements of the desired product could be tailored and adjusted by opportune selection of the input materials. Indeed, Portland clinker substitute could be obtained by mixing acidic, e.g., fly ash or scrap, and basic, i.e., steelmaking slag and dust, input materials whereas metallurgical powders could be obtained by processing steelmaking slag and dust with the addition of low-cost ferrous bauxite.

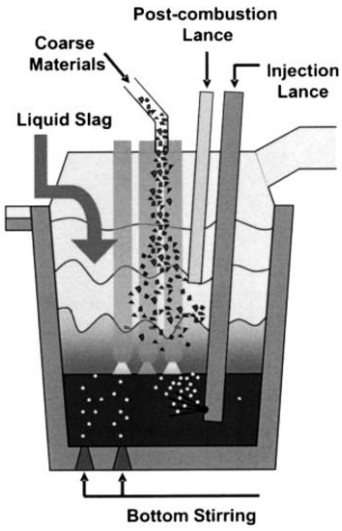

Figure 26: Schematization of the LF ZEWA reactor

The pilot plant was designed, erected and operated by Voestalpine in the foundry of the Vitkovice Steelworks in Ostrava where the ladle was erected beside an existing EAF to exploit the available 12 MVA power supply and the fume-extraction system. The ladle was characterized by an average diameter of 2.25 m and a height of 2.8 m providing an equivalent capacity of 55 t of liquid steel. The pilot test program consisted of 11 campaigns for a total of 70 heats which were performed with an average amount of 15 tonnes of hot metal and 3 to 5 tons of slags. The overall control of the metallurgical operations was good accurate with proper slag foaming and good reduction provided that the characterization of the charged residue materials was. The results connected with the use of different carbon-based reductants proved that coke breeze provided higher C yield whereas coal provided a higher foaming and stirring capability due to its greater content of volatiles.

The quality of the product obtained was also investigated. Concerning hot metal, the reduction of Ni was almost complete and the one of Fe and Cr was very high around 98 and 95%, respectively. Furthermore, Mn reduction was at an intermediate level around 20–75% depending on process conditions whereas Si one was quite poor. As previously mentioned, an issue to assess concerned the P transfer to the hot metal which was quite high and around 80 %. This caused a P content up to 2 % in the hot metal due to the P_2O_5 content in the converter slag and fly ash. This value was excessively high for most applications and for direct recycling thus making necessary a final dephosphorization step. Mineral products were generally produced according to the defined target compositions necessary for the specific final application thanks to an adequate preliminary characterization of the charged residue materials and an efficient control of blending and charging. The target composition for clinker substitutes was defined by Lafrange according to the typical compositions of European granulated BF slag, i.e., 44 % CaO, 34 % SiO_2, 10-15% Al_2O_3, MgO < 8 %. Regarding hydraulic properties, high glassy contents were achieved both with dry and wet slag granulators and good reactivity indices were measured with results comparable to industrial BF slag ones. A final crucial aspect to address was Cr content in the slag which must be minimized by providing a high reduction degree to maximize

its content in the hot metal. Indeed, leachable Cr content must be lower than 2 ppm to comply with European regulations for cements and ensure product commercialization. To this aim, higher reduction levels were obtained, when necessary, by adding small amounts of FeSi to further promote Cr recovery. This practice allowed to reduce the total Cr content of the slag to 0.5–1 %. All these tests indicated that synthetic slags from ZEWA process were like industrial granulated BF slag and no technical obstacles to their use as Portland cement clinker were observed. The target composition for metallurgical powders was defined by ProfilArbed which tested these products in an industrial secondary metallurgy facility. Very good desulphurization results were achieved and the technical and economical evaluation provided very high value to the products, i.e., 75-90 €/t of powder. Concerning the dust collected in the off gas, their content was quite low thanks to the effective filter action exerted by the thick foamy slag, and it was a potentially valuable product thanks to a high content of Zn and Pb with 50–70% equivalent ZnO despite the low content of these elements in the input material.

The economic aspects were also analyzed, assessing the economic viability of different options using both stainless and carbon steelmaking residues. Concerning stainless steel residues, all options considered demonstrated a good economic viability with payback time of 2.6, 1.9, 1.3 and 1.0 years for production of clinker substitute and aggregate for construction using all byproducts or only dusts, scales and sludges with no slag input, respectively. The treatment of slag charged at the solid state required higher electric energy input and larger ZEWA plant dimensions thus entailing higher payback time even because the recovery of Cr and Ni was quite low to provide compensation. In this perspective, the best economics were for treatment of dust, scales and sludges alone. It must be also noticed that the production of cement clinker substitute would require a slag granulation plant which would further increase the investment costs making the payback time of this solution higher. This was even more true considering the relatively low price of granulated slags and the rather low output. In the case of carbon steelmaking plants, the total quantity of generated residue materials was much higher than in stainless steelmaking plants therefore the economic viability depended much more on the prices for treatment solutions or landfill costs. Considering the low credit for slag processing, the most feasible solution from an economic perspective was again the one with no slag input with payback periods under 3 years. The CO_2 emission reduction was another important aspect for the ZEWA process, especially for carbon steelmaking with specific emissions of 840 kg CO_2 per tonne of hot metal which were about half of the corresponding emission from an integrated carbon steelmaking plant. A reduction of CO_2 emissions of about 230 kg per tonne of recycled residue materials would be obtained in a plant where the BF throughput would be reduced because of ZEWA hot metal recycling. Finally, if the CO_2 saving at the cement plant due to the substitution of clinker was considered, 900 kg of CO_2 savings per ton of recycled residue materials were achieved.

In conclusion, the project demonstrated the technical and economic feasibility of processing various residue materials from carbon and stainless steelmaking operations. Two mineral products were produced in accordance with the targeted figures, i.e., hydraulic binder for cement production and metallurgical powder for desulphurization practices in secondary metallurgy. Both products showed good suitability for industrial use with hydraulic binder displaying comparable properties to reference industrial BF slag and metallurgical powder being a high value product. Attractive economic figures for the ZEWA treatment of stainless-steel residues were calculated which indicated a short payback time.

3.1.5 FP5 – REZIN: Elimination of zinc ferrite

The project was coordinated by MEFOS with ENGITEC, Ferriere Nord and IVL Swedish Environmental Research Institute participating as partners in the consortium. The project started on the 1st of April 2002 and lasted almost three years, ending on the 31st of March 2005. The overall project cost 1.65 M€ and the EU contributed 830 k€, i.e., half of the budget.

Zn Recovery from EAF dust was dominated by the Waelz process since EAF dust was classified as hazardous waste in the early 80's. Despite the dominance of this process, consortium partners understood the primary importance of identifying more environmentally friendly processes for Zn reclamation from EAF dust. In light of this, the present project tried to develop a new method to transform the no leachable zinc ferrite contained into EAF dust in a leachable zinc oxide. This method could be combined with two other suggested methods for pre-treatment in the steel plant using excess heat. The solutions proposed were quite promising, especially considering that many alternative processes were already suggested and tested before REZIN project but none of them found commercial application. All these failures resulted from the high content of halide, i.e., Cl and F, in the case of pyrometallurgical solutions and the low Zn leaching yield resulting from the high ZnO fraction in EAF dust existing in the form of zinc ferrite, i.e., $(ZnO)(Fe_2O_3)$, in the case of hydrometallurgical solutions.

The first concept developed in the project was the use of a low temperature hydrometallurgical treatment to recover zinc ferrite from EAF dust with lime to transform it into leachable ZnO. In particular, the reaction of $(ZnO)(Fe_2O_3)$ with CaO according to $2CaO + (ZnO)(Fe_2O_3) = ZnO_{Free} + Ca_2Fe_2O_5$ allowed the complete elimination of zinc ferrite as also confirmed by both XRD and SEM analysis. Furthermore, the production of leachable ZnO led to high yields using the novel EZINC process plus a residue that could be converted in Fe and a saleable slag by melting. The hydrometallurgical route for Zn recovery displayed several advantages compared to the pyrometallurgical one thanks to low temperature operations, lower energy consumption and a high flexibility (75) (76).

Two further concepts were developed considering two different recycling pathways which were based on the following reduction reaction $ZnO(Fe_2O_3)+C=Fe_{met}+ CO/CO_2+ ZnO_{free}$ to achieve ZnO separation from zinc ferrite. The first solution proposed the recirculation of EAF dust by injecting it into the slag foam during the refining period. The dust generated during injection was then collected in a bypass filter and a high Zn content dust with Waelz quality was obtained. This solution was tested both at the pilot and full scale, but the high Zn grade dust achieved in the pilot tests, i.e., 70 % of Zn and only 2-3 % Fe, could not be confirmed in the full-scale test. The second solution proposed entailed the use of an on-line monitoring system for the continuous analysis of dust composition to ensure an efficient separation of the low and high Zn dust. Also, this solution proved to have a positive effect on the steel plant. The dust pre-treated with both recycling routes were again combined with a leaching step using the EZINC process and the leaching of pretreated samples showed a great increase of Zn recovery yield with bypass filter dust displaying values over 90 %. It appears evident the positive economic impact that this result would have on a full-scale steel plant (76) (75).

A preliminary life cycle analysis was also performed during the project displaying significant potential savings in CO_2 emissions, energy consumption and costs compared to the conventional routes at the time of the project. In particular, a potential energy saving of in the order of 3000 - 7000 MJ/ton EAF dust was registered.

3.1.6 FP6 – REDILP: Recycling of EAF dust by an integrated leach-grinding process

The project was coordinated by Relux with Eco-Transfer, ZOZ, Aqua-Biocarbon, Partneris, Instytut Metali Nieżelaznych w Gliwicach. Oddział w Legnicy, OVGU (Otto von Guericke University Magdeburg), IGAS (Innovative Gesellschaft fur Analytishen Service und Handel) and University of Miskolc participating as partners in the consortium. The project started on the 1st of November 2004 and lasted almost two and a half years, ending on the 30th of April 2007. The overall project cost 1.99 M€ and the EU contributed 1.29 M€, i.e., 65 % of the budget.

The well-established practice of recycling waste metallic scraps as raw material to produce steel by coupling together mini mills and EAFs has always been characterized by the main drawback of producing large quantity of dust. The latter was mainly composed of Zn, Fe and other non-ferrous volatile metals which evaporated during scrap melting and condensate as airborne particles which must be removed by the flue gas through gas cleaning system. At the time of the project almost 500 kton of EAF dust were produced each year in Europe and this value raised up to almost 1.3 Mton nowadays. These dusts were mainly characterized by high Zn and Fe, as well as significant Pb content and the Zn content was forecasted to increase due to steel galvanization, i.e., a corrosion protection method resulting in a protective Zn layer, of out sorted vehicles and other obsolete goods. The EAF dust recycling methods available at the beginning of 2000s, e.g., pyrometallurgical process such Waelz process, were characterized by extremely high energy consumption thus significantly contributing to GHGs emissions and global warming. Furthermore, there was the risk to produce dioxins and there were approximately 70 % of residues slags that must be disposed in landfills as hazardous waste.

Considering this background, the REDILP project aimed to develop a hydrometallurgical "cold" process to recycle EAF dusts to reduce the environmental impact and the GHG emissions of the process while ensuring the removal of heavy metals such as Pb from the dust, the recovery of valuable materials such as ZnO and Fe-rich materials which could be reused as input material in BF. Furthermore, the remaining inert materials were aimed to be repurposed as construction materials. The main idea of the project was to combine mass transfer in an aqueous medium with a mechanical impact to enhance and activate solubilization. This goal was achieved by combining simultaneously mechanical grinding with a high selective leaching which allowed to dissolve the dust and to form a solution from which each specific metal could be removed by selective precipitation. This process was designed to ensure the treatment not only of easy-to-leach zinc-bearing components like zincite but also of more difficult-to-leach phases like ferrites. The results obtained proved the efficiency of the problem allowing a recovery of 98 % of Zn and Pb. Furthermore, the ZnO produced was uncontaminated with Fe thanks to the highly selectivity of the leaching process. Further advantages of

the proposed route were the almost waste free process, CO_2 emission minimization, and no environmental risks resulting from potential dioxins emissions. After laboratory campaigns aimed at process optimization, a prototype plant was constructed to demonstrate the successful Zn recovery.

The first step of the project concerned the collection and characterization of various EAF dust, i.e., 12 samples, from different steel mills in distinct countries. Dust characterization included particle size distribution, density and specific surface by BET (Brunauer-Emmett-Teller) analysis, morphology observation wit SEM and EDS, phase analysis by XRD, chemical composition, and determination of solubility in different solvents. The main components of all samples were Fe, Zn and Pb with values ranging from 20.4-37.1 %, 8.5-37.5% and 0.27-7.2 %, respectively. Concerning phase distribution, the main component was franklinite which ranged from 24 to 57 % and it is quite difficult to leachate. The second main component was zincite which ranged between 1.5 and 29 % leading to ratio of franklinite-to-zincite between 1.31 and 21.0. The specific surface measured by BET was of primary importance for the leaching process and the values obtained ranged from 2.58 up to 11.83 m^2/g.

Another fundamental step concerned the design and build up of the test system envisaged by the project at a laboratory scale by OVGU. In particular, a stirred batch reactor, a stirred ball mill and a colloid mill were selected for the leach grinding process and a batch reactor system was selected for the precipitation process as shown by the PI flowcharts in Figure 27. In particular, the precipitation reactor system consisted of a 2.5 l glass reactor resistant to pressure, a gas stirring device with a rotation speed of 0-1400 rpm, a thermostat for cooling and heating from -10 to 120 °C, a pump-balance combination for the dosage of liquids, a mass flow controller for the CO_2 stream from 0-10 l/min, sensors for temperature, conductivity and pH-value and a control and measurement system for the acquisition of the experimental data.

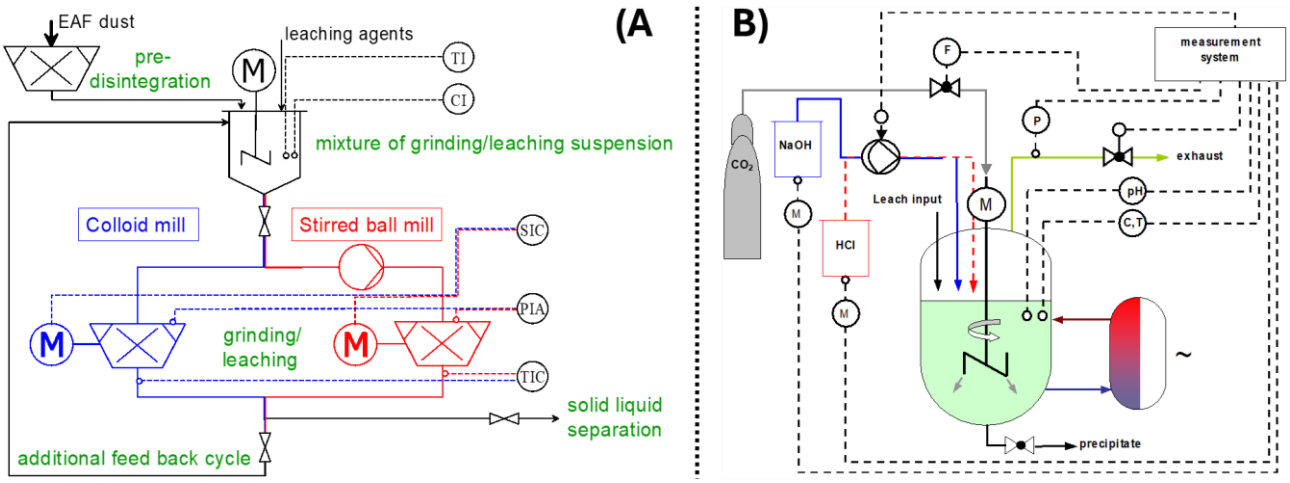

Figure 27: PI-flowcharts for the leach grinding (A) and precipitation (B) processes

Further attempts were made at University of Miskolc where a special vertical stirred-media mill was designed and developed to assess the effect of high energy impact on the leachability of EAF dust to further enhance ferrites solubility. The tests were performed on samples characterized by a Fe content around 23 %, a Zn content around 42 % and a Pb content around 2 % mainly portioned in franklinite, i.e., 38 %, and zincite, i.e., 29 %, using the same conditions exploited by OVGU in terms of circumferential speed, residence time and temperature. The results obtained were slightly better than those obtained with other types of mills, but yet comparable.

After developing the test system, it was necessary to optimize the parameters of the alkaline leach-grinding process. The tertiary amine of zinc $Zn(NH_3)_4^{2+}$ was identified as the most stable Zn soluble specie and the amount of ammonia species necessary to obtain it was given by the stoichiometric ratio $Zn:NH_3=1:4$. The first leach grinding trials at OVGU were performed with the colloid mill system and the influence of the main leaching, i.e., temperature and residence time, grinding, i.e., milling gap between rotor and stator and rotor circumferential velocity, and suspension parameters, i.e., the mass content of EAF dust and the molar ratio between $(NH_4)_2CO_3$ and NH_3 at the reagents input, were analysed. The results proved that it was possible to obtain an initial separation of Zn and Pb already at the integrated leaching and grinding step because temperatures above 50 °C allowed for Zn selective leaching with Pb recovery being below 8 % and leachate consisting mainly of pure Zn. This effect was further exacerbated using high levels of ammonia hydroxide, i.e., NH_4OH, and low levels of ammonium carbonate, i.e., $(NH_4)_2CO_3$. It was observed that Zn and Pb recovery could be significantly enhanced using integrated leaching and grinding (ILG) because the same or a higher recovery than pure leaching could be achieved applying a shorter residence time. In particular, a 60 % of Zn recovery could be reached after 15 minutes whereas longer residence times mainly influenced Pb recovery leading to a Zn recovery of just 65 % in 60 minutes. A multi-step process was suggested to enhance Zn recovery by coupling a pre-leaching step to an integrated leaching and grinding step to achieve an 88 % Zn recovery. Similar outcomes were reported by leach-grinding experiments performed at Miskolc University where a 60.9 % Zn recovery was achieved after 30 minutes using a circumferential speed of 10 m/s and a temperature of 80 °C. These results were ascribed to BET specific surface behaviour as a function of operating temperature. At room temperature, BET specific surface increased as a function of residence time and circumferential speed if the mass transfer was poor. At higher temperatures, BET specific surface was directly proportional to mass transfer which in turn was strongly influenced by the thermal energy input, i.e., operating temperature. Therefore, it was concluded that operating temperature was the main factor controlling the mass transfer rate, but also circumferential speed could play an important role to promote mass transfer at lower test temperatures.

Once optimized the leaching step, the fractionised precipitation of Zn and Pb was assessed. Different precipitation methods, e.g., thermal precipitation and chemical precipitation with HCl, NaOH, Na_2CO_3, and CO_2, were investigated and the best results were obtained with CO_2 which ensured a Zn recovery of 99 % when applying a 3-step process at 5 °C. The 3 steps were necessary as a single step of 1 hour was able to ensure a Zn recovery of only 40 % while a recovery of 99 % was achieved with 3 steps of 1 hour. Concerning the CO_2 input, it ranged between 1 and 5 L/min, i.e., specific CO_2 flow of 0.032 and 0.373 L/g solution, and it was observed that higher CO_2 dosages were able to reduce the time to start precipitation. The highest CO_2 input was selected together with a pH lower than 9.

The latter was the best compromise between reaction activation and amount of reagent needed. Indeed, pH value was decreased until carbonate precipitation started but the higher the pH value used the lower the CO_2 needed. Another important process parameter considered was the ammonia content, i.e., mass ratio ammonium carbonate to solution R_{AC}, and a value of 0.16 was selected as low $(NH_4)_2CO_3$ ratio leads to a high Zn selectivity in the process. Before the final precipitation step to obtain a nearly pure $ZnCO_3$ product, a cementation pretreatment of the leachate was investigated. At first, Pb cementation was performed in 2 steps of 20 minutes working at 15-30 °C with a circumferential speed stirrer of 2.1 m/s and a Zn powder concentration of 4 g/L leach allowing to achieve an almost 100 % Pb recovery. A second cementation phase was dedicated to Fe cementation, and it was performed at temperatures higher than 50 °C using more than 3 steps of 10 minutes, a Zn powder concentration of 4 g/L leach and a circumferential speed stirrer of 2.1 m/s, but in this case the recovery was quite low and equal to 27.9 %. An increasing number of cementation steps or a better solid liquid separation with a membrane filter was suggested to improve Fe removal.

The last step of this recovery path was $ZnCO_3$ calcination which was investigated through DTA and DSC. A first mass loss corresponding to $Zn(OH)_2$ decomposition was observed at 140 °C followed by a second mass loss at 200 °C resulting from $ZnCO_3$ decomposition into ZnO. This allowed to conclude that the calcination thermal treatment should have been performed at a constant temperature of 250 °C and a dust separation system should have been included if air convection flow was envisaged for humidity and CO_2 removal.

Considering the outcome obtained, additional work was performed in the direction of Zn electrolytic separation from the solution obtained during EAF dusts leaching by $(NH_4)_2CO_3$. All electrolyses were conducted at room temperature using ammonium carbonate solution containing Zn, NH_4^+, Fe, Pb, Cu, Sn, and Cl as electrolyte. The first test displayed a strong adhesion between the Zn deposit and the Al cathode for this reason the next tests were performed with a Ti cathode which provided an easier stripping of Zn. Concerning the anodes, acid-resistant steel anodes were used, but cathode deposit displayed a poor quality, i.e., corrugations, dendrites and black colour, regardless of the current density and only Zn and Al content met the standard requirements while the other impurities were high above the levels allowed. For this reason, electrolyte cleaning by cementation with Zn dust was performed for 2 hours at room temperature using 5 g of Zn for each litre of cleaned solution. Since the appearance of the Zn deposit obtained from the purified solution was still not satisfactory, some bone glue was added to the electrolyte. In this case, the main problem concerned the Fe and Cu contents which exceeded the threshold values provided by the standard. The reason was attributed to the use of the steel anodes. For this reason, a further series of tests was performed using graphite anodes to eliminate the potential influence of steel. The first electrolysis was performed with no additives to electrolyte, and the appearance of the Zn deposit was not satisfactory, so bone glue was added to the electrolyte in the next test, and this addition significantly improved the appearance of the obtained cathode deposit. The concentration of all components, i.e., Zn, Cu, Fe and Sn, decreased leading to Zn with a purity of level Z4-Z5.

After all the laboratory scale work performed, a final process was univocally designed as shown in Figure 28.A and a pilot plant coupling leaching dust by stirring with electrolysis was developed as shown

in Figure 28.B. This final solution replaced the original REDILP process planned with should have included successive leaching and precipitation processes.

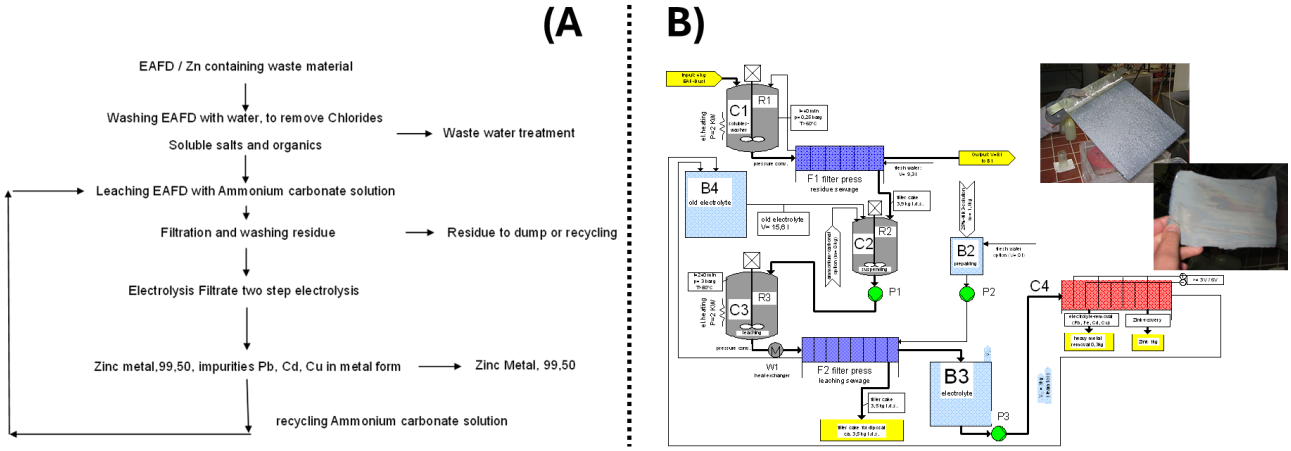

Figure 28: Final design of the REDILP process (A) and relative schematization of its PI (B)

3.2 Horizon 2020 and Horizon Europe

3.2.1 FISSAC: Fostering industrial symbiosis for a sustainable resource intensive industry across the extended construction value chain (77)

The project was coordinated by ACCIONA Construcción, with ACR+ (Association of Cities and Regions for Sustainable Resource Management), UNE (Asociación Española de Normalización), CSIC, AKG Gazbeton, BEFESA, British Glass Manufacturers Confederation, RISE CBI Betonginstitutet, RINA Consulting, RINA Consulting-CSM, Ekodenge, Fundación Agustín de Betancourt, Fenix TNT, Feralpi Siderurgica, Geonardo, Glass Technology Services, Ingenieurbüro Trinius, Hifab, Keraben Grupo, OVAM (Openbare Vlaamse Afvalstoffenmaatschappij), RINA Services, RISE (Research Institutes of Sweden), Símbiosy. Simbiosi Industrial, Türkiye Çimento Sanayicileri Birliği Derneği, Tecnalia, Vannplastic, Specialist Building Products, participating as partners in the consortium. The project started on the 1st of September 2015 and lasted almost five years, ending on the 29th of February 2020. The overall project cost 11.2 M€ and the EU contributed 8.89 M€, i.e., about 80 % of the budget.

The FISSAC project aimed to develop and demonstrate a new paradigm built on an innovative industrial symbiosis model towards a zero-waste approach in the resource intensive industries of the construction value chain, tackling harmonized technological and non-technological requirements, leading to material closed-loop processes and moving to a circular economy approach. A methodology and a software platform were developed to implement the innovative industrial symbiosis model in a feasible scenario of industrial symbiosis synergies between industries, i.e., steelmaking, aluminum, natural stone, chemical, demolition and construction sectors, and stakeholders in the extended construction value chain. The software guided how to overcome technical barriers and non-technical barriers, as well as standardization concerns to implement and replicate industrial symbiosis in a local/regional dimension in other regions and other value chains symbiosis scenarios. FISSAC demonstrated the applicability of the model as well as the effectiveness of the innovative processes, services and products at different levels. The first one level was the manufacturing processes where it was demonstrated how closed loop recycling processes could transform waste into valuable secondary raw materials by manufacturing novel products at industrial scale. The second level concerned product validation with demonstration of the eco-design of eco-innovative construction products such as new Eco-Cement and Green Concrete, innovative ceramic tiles and Rubber Wood Plastic Composites in pre-industrial processes under a life cycle approach. Furthermore, a demonstration at real scale in different case studies of the application and the technical performance of the products was performed. The last level was the FISSAC model with the demonstration of the software platform and replicability assessment of the model through living lab concept.

FISSAC partners manufactured at industrial scale innovative eco-cement and concrete, ceramic wall tiles, and rubber-wood-polymer composites for decking, cladding and fencing. The eco-cement was also used to make novel green precast concrete elements such as pavement and Jersey walls or barriers to separate lanes of traffic. These products were obtained using different types of secondary raw materials and techniques based on eco-design concepts that include life cycle considerations from procurement, manufacture and use to disposal. Among the materials reclaimed there were industrial ladle and EAF slag, glass and ceramic waste, Al waste, marble slurry, used tires and recycled or virgin

wood and plastics as shown in Figure 29. Eco-cements, green concrete and autoclaved aerated concrete blocks/panels were manufactured with secondary raw materials from the upgraded valorization of steel, glass, aluminum and ceramic industrial waste, i.e., autoclaved aerated concrete wall blocks were produced from ceramic waste and furnace slags. Innovative ceramic tiles were manufactured with secondary raw materials from the upgraded valorization of aluminum and natural stone industrial waste while rubber wood plastic composites were manufactured with secondary raw materials from the upgraded valorization of rubber, plastic & wood industries. Five different case studies showcased how the new solutions developed could be implemented as summarized in Figure 30. Running in parallel, several living labs took place in different countries, focusing also on non-technical barriers and social acceptance as key factors needed to implement symbiotic processes. The focus of FISSAC is ensuring sustainability of their circular economy concept by accounting for environmental, economic and social factors. The implementation of the new solutions for Eco Cement and Green Concrete, innovative ceramic tiles and rubber wood-plastic composites were done in nine different demonstration case studies, i.e., living labs, four being at pre-industrial scale and five being at real scale and all working in a real-life context with a user-centric approach. The living lab leaders engaged actors from the construction industry value chain to identify appropriate challenges related to industrial symbiosis in their regions. Through purposely designed meetings their collaborative knowledge and experience was then used to understand how these challenges could be addressed.

Focusing on the steelmaking sector, the main by-products considered in the project were slags. In total, 45.3 Mtonnes of ferrous slags were generated in 2010 with 4.2 Mtonnes coming from air cooled BF slag, 19.3 Mtonnes from granulated BF slag, 10.5 Mtonnes from BOF, 8.5 Mtonnes from EAF and 2.8 Mtonnes from secondary metallurgy. It was clear the need to identify new high-grade applications to achieve a successful valorization of these wastes which may be limited by both inadequate technical performance as well as by their environmental behavior. Indeed, several studies indicated that the leaching behavior and mechanical properties of alkaline materials such as steelmaking slags may be affected by accelerated carbonation treatment. Focusing on EAF and ladle slag, the use of EAF slag in the manufacture of concrete and its contribution in the manufacture of cement thanks to its iron oxides content was considered, but some unresolved issues surrounding its physical and chemical durability in structural applications needed to be addressed. Therefore, different route of treatment for steel slag such as granulation and carbonation processes were envisaged since they could help addressing both the inadequate particle size and the low volumetric stability. The project targets in the steelwork contest were the execution and validation of up-scaled pilot reactors at industrial environments for accelerated carbonation/aging of EAF steel slags to catalyze the aging process and improve the quality of the byproducts, the development of combined carbonation and granulation processes at industrial scale to enhance EAF slag quality as aggregates for use in concrete and exploring the potential applications of ladle furnace slag as novel supplementary cementitious admixture in cement and concrete manufacturing. Experimental results indicated that ladle slag fines showed significant cementitious property in the presence of an alkaline activator. The potential cementitious property of ladle slag fines increases with their fineness regardless of some differences in their mineral composition.

Figure 29: Secondary raw materials reclaimed in the framework of the FISSAC project and the resulting innovative materials and construction products produced

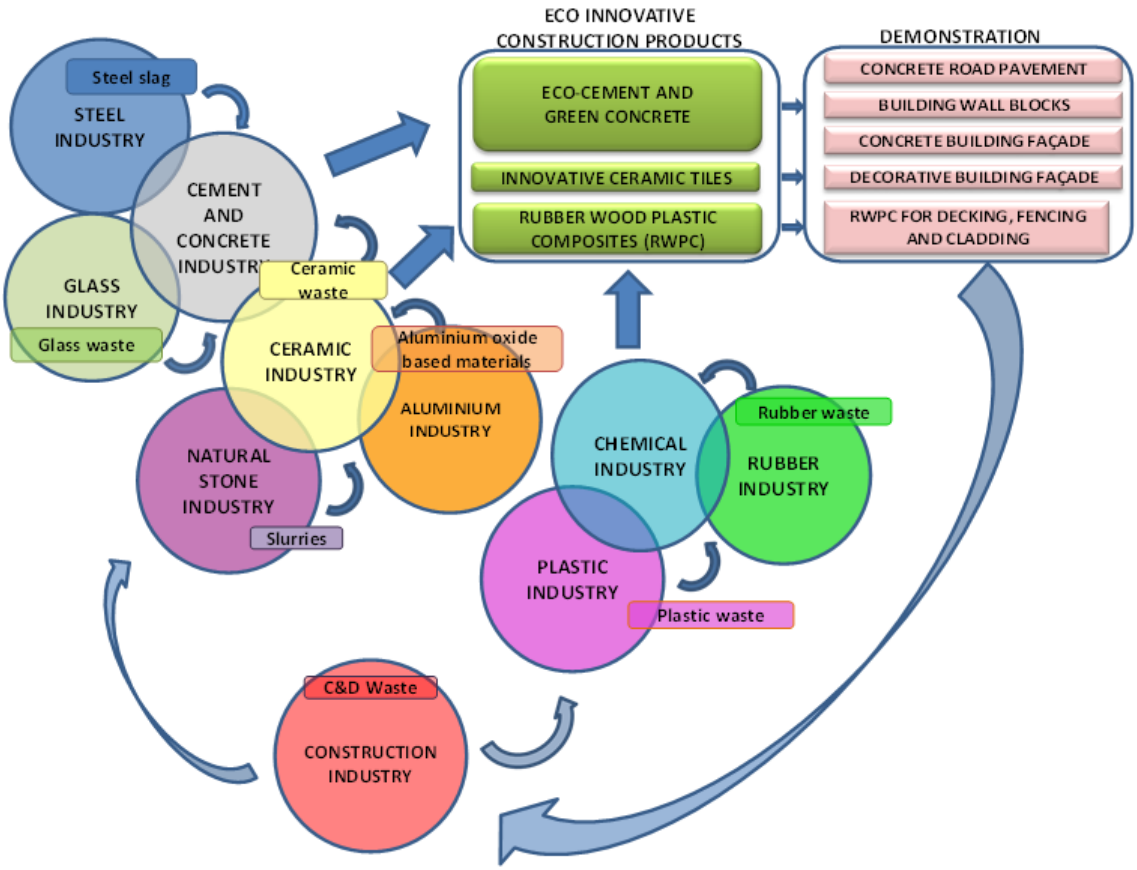

Figure 30: FISSAC concept

The principal symbiotic materials obtained by valorizing steel slags were Eco-Cements and Green Concrete. Eco-Cements was obtained using two different routes for synthesis. The first one was a belite-yeelemite based cements produced by using Al saline slags, glass waste, ceramic waste and ladle furnace slag within the raw meal. Compared to ordinary Portland cements, the new cements displayed lower CO_2 footprint up to 10 %, lowed embodied energy cements and high resistance to sulfate attack. The second route considered blended cement using ladle slag, glass and ceramic waste materials as mineral additives in Portland cement. The main advantage of this route was lowering the clinker content in the blended cement thus reducing the environmental impacts. Concerning green concrete formulations, both ready mix concrete and autoclaved aerated concrete blocks containing upgraded EAF and ladle furnace steel slags aggregates were obtained. In particular, the mix concrete was obtained using EAF slag as aggregates and the eco-cement with ceramic, ladle slags and glass as mineral additives whereas the autoclaved aerated concrete blocks were obtained from EAF slag, ladle slag and ceramic waste. Characterization and quality control, workability and behavior study, mechanical performance and durability in several phases have been accomplished. Figure 31 shows an example of precast pavement elements obtained using the blended eco-cement produced as cement base and EAF slags as coarse aggregates.

Figure 31: Precast Concrete Elements

3.2.2 RESLAG: Turning waste from steel industry into a valuable low-cost feedstock for energy intensive industry (78)

The project was coordinated by CIC EnergiGUNE with ArcerlorMittal, DLR (Deutsches Zentrum für Luft- und Raumfahrt), Azterlan, ETH Zurich (Eidgenössische Technische Hochschule), Imperial College of Science Technology and Medicine, FAU Erlangen-Nürnberg (Friedrich-Alexander-Universität), CEA (Commissariat à l'Énergie Atomique et aux Énergies Alternatives), HLG Management, ENEA (Agenzia nazionale per le nuove tecnologie, l'energia e lo sviluppo economico sostenibile), Teknologian tutkimuskeskus VTT, Tapojarvi, Alostom, Fraunhofer-Gesellschaft zur Förderung der angewandten Forschung, Life Cycle Engineering (LCE), MASEN (Moroccan Agency for Sustainable Energy), Zabala, Novargi, Hasten Ventures, Renotceh, and Fundacion CENER participating as partners in the consortium. The project started on the 1st of September 2015 and lasted almost four years, ending on

the 31st of July 2019. The overall project cost 9.54 M€ and the EU contributed 8.02 M€, i.e., almost 85 % of the budget.

The RESLAG project was primary focused on the valorization of steel slag which are the main by-product of the steelmaking sector. Indeed, 21.8 Mt of steel slags were generated in Europe in 2010 and only 76 % of them was recycled in construction and building applications, e.g., as aggregates for construction or as road materials, while the remaining 24 % was landfilled, i.e., 2.9 Mt, or self-stored i.e., 2.3 Mt. Considering this, the RESLAG process aimed to assess other industrial sectors able to make an effective use of this 2.9 Mt/y of landfilled slag if properly supported by the right technologies in the perspective of reducing the severe environmental impact resulting from this practice. In particular, the project proposed four innovative applications for slag valorization which led to four pilots as shown in the cross sectorial approach schematized in Figure 32. Pilot 1 considered the use of slag as feedstock for the recovery and extraction of non-ferrous high added value metals, e.g., Cu, Cr, Ni, Zn, Mn, which could become an attractive resource of raw critical metals, i.e., between 0.1-3 %. In particular, a new selective hydrometallurgical methodology was developed to provide an experimental demonstration of this technology. The second and third pilot envisaged the use of steelmaking slags as thermal energy storage (TES) materials for heat recovery in the steel industry (Pilot 2) as 30-40 % of the energy consumed is normally lost as waste heat and discharged into the atmosphere, and to increase dispatchability of concentrated solar power (CSP) plant electricity (Pilot 3). In particular, the application of low-cost TES system based on steel slag would allow to recover the heat from EAF off gases providing around 15 % of the primary energy while their use for CSP applications would allow to replace the traditional molten salt TES solution which was limited to a temperature range of 290-550 °C with steel slag with temperatures above 600 °C. The last pilot considered the use of slag as aggregates for the manufacturing of refractory ceramic compounds allowing the substitution of at least 20 % of virgin materials for castable refractories (Pilot 4). This would ensure a reduction of energy consumption of approximately 1.3 MWh/ton associated with the use of in-situ sintering castables rather than fired refractories. This would also result in a decrease of around 40 % of the corresponding CO_2 emissions. The research performed revealed that pilot 4 was the most promising solution as the entire amount of annually produced European FeCr-slag, usually valorized in road construction and substructures and in asphalt and concrete coatings, could be consumed in the refractory sector. The main components of this FeCr slag are SiO_2, MgO and Al_2O_3 with small amounts of CaO, Cr and Fe oxides. Project results also proved that the proposed solutions could provide further environmental benefits such as CO_2 saving and elimination of negative impacts associated with mining for both valuable metals and ceramics. Furthermore, up to 970 kt/y of CO_2 emissions could be saved through CSP applications and at least 71 kg/ton of steel from heat recovery.

The first step of the project concerned the identification of the technical requirements of each pilot process, i.e., pilot 2, 3 and 4, and the related final product together with the modelling and optimization of the process itself and the related pebbles sizes with CFD, FEA and Thermo-Calc tools. Based on these results and on the preliminary characterization performed on the raw slags to determine their properties, the specification of slag pebbles for the different applications were fixed and conspicuous amounts were produced for pilot plants 2 and 3. In particular, the mechanical conformation route was

selected for pilot 2 and 7 tons of slag were produced while sintering was chosen for pilot 3 and 10 tons of slag were produced.

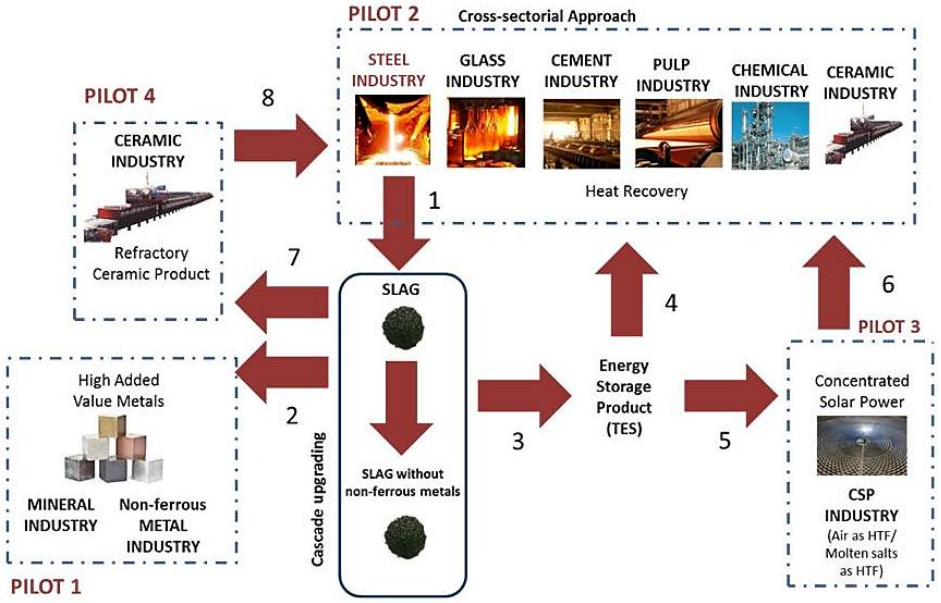

Figure 32: Overall schematization of the cross-sectorial approach used in the RESLAG project

The second part of the project was devoted to the design, construction, test and validation of the four pilot prototypes. A pilot plant based on simulated moving bed technology was constructed at CEA laboratories to demonstrate the feasibility of pilot 1 solution, i.e., the recovery of high added value metals from slag. In particular, a multistep process combining both physical and chemical treatments was developed and optimized allowing to obtain a high efficiency in rare earth recovery both in terms of yield and purity. The feasibility of pilot 2 for waste heat recovery through steel slag used as TES was assessed by constructing a pilot plant at ArcelorMittal steelworks in Sestao. The experimental campaign performed demonstrated the good thermal and mechanical properties of slag particles over various heating and cooling cycles and the design of the heat exchanger was identified as the key point to optimize heat recovery from EAF. As previously reported, this system should ensure a heat recovery potential of around 15 % of the total waste heat and this translates into 9.2 GWh/year/EAF. CICenergyGUNE specified that the pilot plant was also a demonstrator of a low-cost thermal energy storage system reaching an incomparable system storage cost of 5€/kWh.

Concerning pilot 3 to demonstrate the potential of steel slag as TES material for CSP applications, two different pilot plants were constructed. The first one was built at DLR facilities in Stuttgart using air as heat transfer fluid (HTF) while the second one was erected at ENEA laboratories in Casaccia using molten salts as HTF. The work performed at DLR confirmed the viability of using slag as TES material for CSP applications using air as HTF thanks to the cyclic thermal and mechanical tests used to determine slag resistance and inner insulation options. Analogously, tests at ENEA confirmed that

sintered slag pebbles were compatible with solar salt thus proving to be suitable TES material for packed-bed TES systems in CSP plants using molten salts as HTF.

Focusing on DLR solution, air was selected as HTF to be heated in the receiver, generate steam and therefore electricity thanks to its high conversion temperature and for the high solar-to-electric efficiency potential. It was used in conjunction with slag pebbles selected as TES materials fundamental to face the reduced energy output occurring when the sun sets or is blocked by clouds. Indeed, a suitable heat storage technology identified was the regenerator storage based on directly heated solid media applicable at temperatures higher than 1000 °C where slag exploitation as inventory materials would offer significant cost reduction. For the successful introduction of this technology into the market, regenerator storage in combination with slag-pebbles as inventory needed further investigations to ensure an efficient and scalable solution for heat storage. Considering this, both slag pebble characterization and investigation of the thermomechanical behavior of slag were performed. Slag pebbles were tested under operation conditions to ensure the most accurate data input for the thermo-mechanical calculations. Concerning slag characterization, part of the slag was subjected to compression tests whereas another part was subjected to hydration/oven tests, i.e., cyclic tests in hot humid atmosphere, before undergoing compression tests. A total of 16 cycles was performed employing a humidity of 50 %, a heating and cooling rate of 5 K/min passing from 200 to 800 °C and applying a holding time of 1 hour at the minimum and maximum temperatures. Samples were periodically weighed before the first cycle and after the 1 th, 2 th, 4 th, 8 th and 16th cycle to determine possible changes in the material resulting from hydration. No significant changes in weight were detected for the cubic samples whereas a significant weight increase was observed for powder samples due to the higher specific surface which made material changes much faster. The compression tests highlighted a very irregular compression strength regardless of the hydration test and no significant changes of strength were seen after hydration. Concerning thermo-mechanical calculations, DEM was exploited to model each particle as an independent physical object and to estimate the thermomechanical stresses arising during thermal cycling due to the thermal expansion of slag pebbles. This aspect is fundamental considering that these dilation phenomena determine an increase in contact forces between pebbles thus increasing the risk of damage for the single pebble. Furthermore, the pressure exerted on the container walls rises thus making its evaluation necessary when dimensioning the container. Considering this, DEM was used to estimate the inter-particle forces resulting from the thermomechanical stresses which were then used in FEM to determine the compressive and tensile stresses of the single particles. The assessment of thermomechanical stresses and forces was split into a static non-thermal portion and a thermally induced portion. The static mechanical portion was estimated with the Jannsen equation and after applying it as a uniaxial pressure the DEM model was restrained in all spatial directions. After that, thermal induced loads were applied since the particles movement was restricted by the restraining walls, and their size started to increase due to heating. This clearly caused a rise in inter-particle contact force. It must be considered that this procedure emulates what happens on the bottom of a large-scale packed bed where the individual particles are almost completely inhibited to rearrange due to the weight of the overlying bed but overestimates the forces of the packed bed in the upper regions where particles are less constrained. In light of this, all results with this method must be evaluated as the worst-case scenario. The results of the modelling

activity highlighted that contact forces correlate in a nonlinear way with the temperature spread of the packed bed and that they strongly depend on particle size with larger particles exerting higher contact forces. Despite this, they produce similar pressure on the containing walls. Furthermore, the particle-particle tensile stresses were investigated, and it was concluded that higher particle contact forces for larger particles are compensated by larger contact areas (79).

The last pilot scenario was assessed by building a pilot plant for the manufacturing of refractory bricks using steel slag as aggregate at Renotech laboratories in Turku. This activity provided a valuable property data bank with the properties of slag containing refractory castables against commercial refractory materials and had as main goal the development of a pilot scale processing route for refractory castables with maximal utilization of secondary raw materials to reduce the final cost of the product. Preliminary studies performed used calcium aluminate cement as binder, FeCr slag with a 0-4 mm diameter as aggregates, and JV slag and silica fume powder as fines to manufacture the castables. Their cold crushing strength, bulk density, apparent density, porosity, thermal expansion, specific heat capacity and thermal conductivity results were compared with the ones of the commercial castable provided by Calderys to establish a direct comparison of performance. Three castable recipes were investigated after curing and drying the specimens with a heat treatment at 1200 °C for 3 hours. In particular, the recipes produced were made with 1) 82 wt.% FeCr slag, and 18 wt.% of binder 2) 74 wt.% FeCr slag, 8 wt.% of JV slag and 18 wt.% of binder 3) 78 wt.% FeCr slag, 4 wt.% of micro silica and 18 wt.% of binder. The results of cold crushing strength reported comparable cold compressive strength values of 70-90 MPa for the three recipes which, however, were lower than the 130 MPa of commercial reference probably due to the higher open porosity which ranged between 18 and 22 % against the 16 % of the commercial reference. The Archimedes principle also reported bulk density values of the three recipes comparable to the commercial reference material. Comparable low values were obtained also for the thermal expansion coefficient measured up to 1100 °C which ranged between 8.1 and 8.5 × 10^{-6} 1/K for the three recipes and was equal to 6.8 × 10^{-6} 1/K for the commercial solution. Finally, good thermal insulating properties in terms of thermal conductivity, thermal diffusivity and heat capacity were observed for all three recipes showing values even below that of reference material thanks to the slightly higher porosity. These preliminary results confirmed the potential feasibility of FeCr slag use as raw material for refractory production and led to a final selected recipe formulas containing 80 % slag with comparable properties to commercial reference.

3.2.3 STEELANOL: Production of sustainable, advanced bio-ethANOL through an innovative gas-fermentation process using exhaust gases emitted in the STEEL industry (80)

The project was coordinated by Areclormittal with Primetals, Lanzatech and E4tech participating as partners in the consortium. The project started on the 1st of May 2015 and ended on the 31st of March 2024. The overall project cost 14.5 M€ and the EU contributed 10.2 M€, i.e., almost 70 % of the budget.

The gaseous emissions resulting from BF and BOF are unavoidable residues from the steelmaking process. They are rich in CO, CO_2, and H_2 and are mainly used to produce electricity or are flared but

could be advantageously exploited to produce ethanol to reduce the reliance and usage of fossil fuel molecules and the related GHG emissions. In light of this, the STEELANOL project aimed at repurposing the exhaust gases emitted by the steel industry by using them as raw material to produce ethanol via an innovative gas fermentation process based on microorganisms. The ethanol produced can be then used as an eco-friendly vehicle fuel, in the production of plastics, as feedstock for pharmaceutics, cosmetics and cleaning products, as well as in the food and beverage industry. Indeed, several key players in the transportation sector, e.g., Boeing, Virgin Atlantic, Mitsui, expressed their strong interest in the project. The production of ethanol and bioethanol through this pathway would ensure a GHG impact 65 % lower compared to oil derived fuels. Figure 33.A shows a schematic representation of the main steps included in the STEELANOL process.

The project allowed to build the Europe first-ever commercial scale production facility able to provide approximately 64 ktons/year of ethanol from steelmaking waste gases. The 210 M€ flagship pilot plant was constructed at ArcelorMittal Europe steel plant in Ghent (Belgium) and is shown in Figure 33.B. Gas fermentation technology was supplied by LanzaTech and used microbes as biocatalysts to ferment the gases emitted from the steel plant into a bioreactor to convert CO and H_2 into ethanol with high productivity. The main idea behind the fermentation process was similar to that used to produce wine where microbes converted sugar into ethanol. In this case sugar was replaced by CO/CO_2 gases. The engineering works were performed by Primetals which provided its support on automation, key equipment and commissioning. Finally, E4Tech developed the LCA of the produced fuels to provide detailed insights on the environmental impact of the process. In particular, LCA studies indicated that STEELANOL technology had the potential to reduce GHG emissions by over 80 %. Indeed, STEELANOL was able to produce 64 ktonnes bioethanol/year which could be used to fuel half million cars with ethanol blended gasoline thus saving 135 ktonnes/year of CO_2 emissions in the transport sector. This clearly demonstrated the paramount added value of this technology which not only reduced the emissions at source decreasing ArcelorMittal direct carbon footprint but reduced also fossil fuels production emissions by providing commodity chemicals and fuels that would otherwise be made from oil. The building of the plant started in 2019, and ethanol production started at the end of 2023. The ramp-up to full capacity could enable the production of around 80 Mliters of ethanol per year by 2025 which was recognized as biofuel by EU DG (Directorate General) Climate and DG Energy.

By analyzing the process in more detail, BF waste gases were partially directed to the power plant for electricity production and partially conveyed to the gas treatment unit. The latter is based on the Pressure Swing Absorption (PSA) principle, i.e., a regenerative separation technology, to separate clean gas mixtures through the absorption of impurities on tailored absorbent material. This 2-step process consisting of both absorption and desorption allowed to obtain a pure product gas rich in CO and H_2 and without CO_2 which was planned to be liquified and storage in the next future according to CCSU (Carbon Capture Storage and Usage) principles. The purified product gas was sent to the bioreactor where the acetogenic bacteria efficiently converts it into valuable products, i.e., efficiency conversion of CO> 90 %. This type of bacteria is found normally in anaerobic environments such as digestive systems and deep sea thus elaborating CO and H_2 without oxygen. The mixture coming from the bioreactor contained ethanol, water, microbes, and nutrients and was preliminary treated to separate

wet ethanol from microbes, water and nutrients. The wet ethanol stream was sent to distillation to produce a 98 % dry ethanol whereas the water stream rich in microbes and nutrients was sent to the wastewater treatment unit which consists of a digester. The latter allows to recover 30 m^3/h of process water which could be reused in the bioreactor and to produce fertilizers, e.g., struviet, NH_4OH and biogas exploitable to produce power and heat.

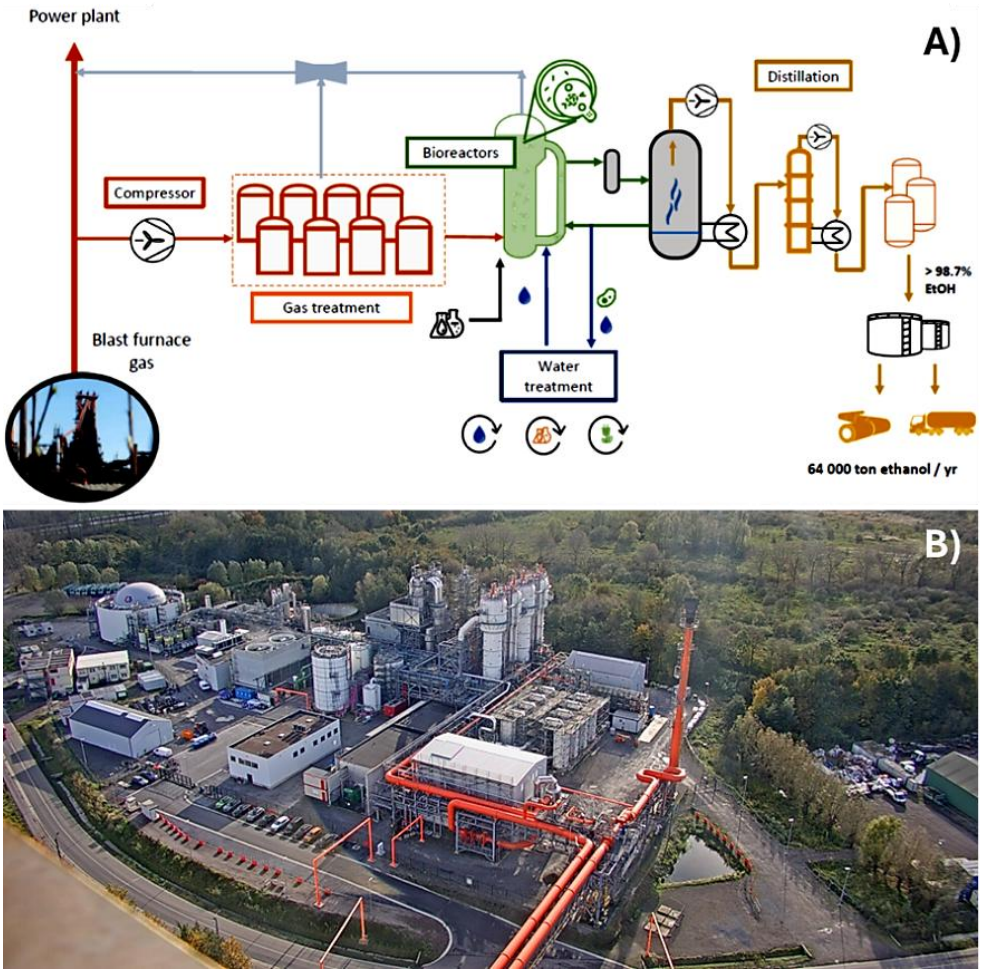

Figure 33: Scheme summarizing the main constituents of the STEELANOL process (A) and picture of the STEELANOL plant constructed at at ArcelorMittal steel plant in Ghent, Belgium (B).

3.2.4 CHROMIC: efficient mineral processing and Hydrometallurgical RecOvery of by-product Metals from low-grade metal containing secondary raw materials (81)

The project was coordinated by VITO with MEAM, Elektrowerk Weisweiler, ORBIX, FormicaBlu, ARCHE, Technicka Univerzita v Kosiciach (TUK), Helmholtz-Zentrum Dresden-Rossendorf (HZDR), BFI, FEhS, and Bureau de Recherches Geologiques et Minieres (BRGM) participating as partners in the

consortium. The project started on 1st of November 2016 and lasted almost four years, ending on the 31st of December 2020. The overall project cost 4.87 M€ and EU contributed the whole budget.

Metals play a vital role in European industry, yet a large share of supply is imported from outside the region. At the same time, Europe generates substantial quantities of industrial residues, e.g., slag, which can contain valuable metals. The CHROMIC project focused on the recovery of Cr, V, Nb, and Mo from slags produced during carbon steel, stainless steel, and ferrochrome manufacturing. These slags were predominantly used as construction aggregates or disposed of in landfills leading to the loss of the contained metals, typically present at levels of 2–7 % for Cr, 0.03–0.08 % for V, 0.02–0.06 % for Nb, and less than 0.01% for Mo. To this aim, CHROMIC developed a processing route that integrated pre-treatment steps including comminution and beneficiation, targeted leaching, metal separation, and reuse of the remaining matrix as construction material. The project was guided by economic, environmental, and risk evaluations to improve overall sustainability. A diagram showing the project objectives is shown in Figure 34.

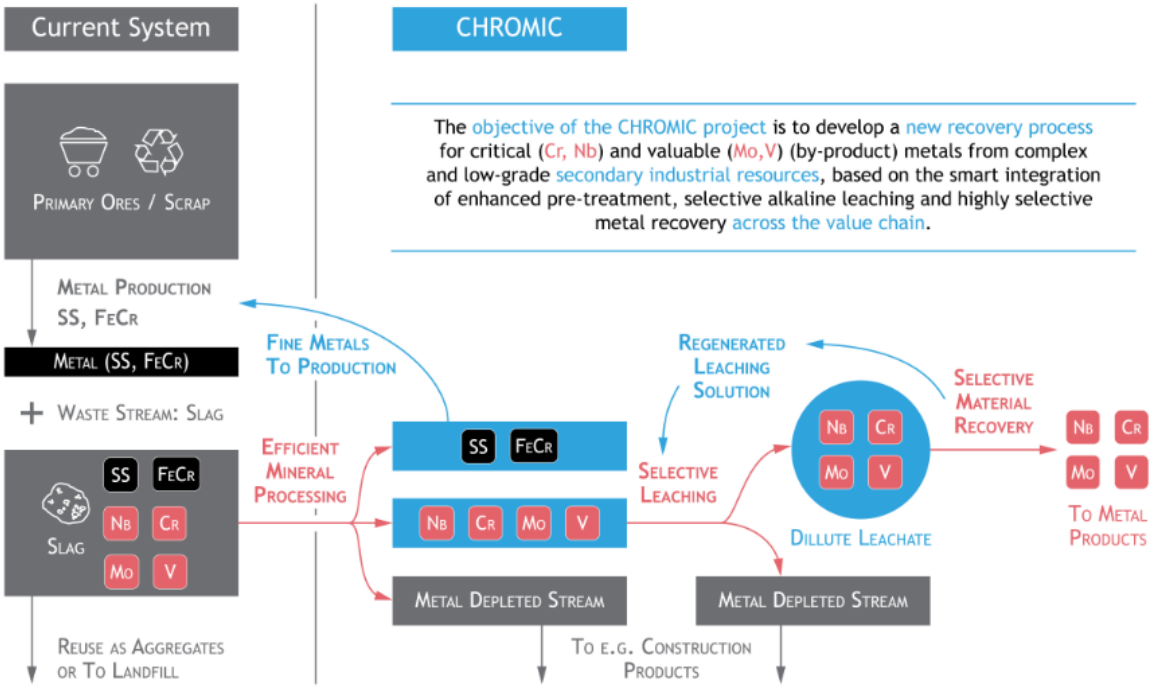

Figure 34: Diagram summarizing the main objectives of the CHROMIC project

The CHROMIC project started with mapping the metals and issues that could be encountered related to their recycling. For example, Cr chemicals are 100 % imported in EU since Cr salts and metals are potentially high value applications, but with limited demand in Europe. Nb is 100 % imported in EU from one dominant producer, making it difficult to enter this market, but less than 1% was recovered from scrap. Also, Mo is 100% imported in EU and it is needed for stainless steel making. V is 84% imported in EU, with need expected to increase in the future due to batteries (82). After an extensive

characterization of the slags in terms of chemical and mineral composition, SEM analysis and leaching, it was noticed that Cr-rich phases were relatively large with more than 40 % above 100 µm (83). Most of the tests investigated Cr or V and in some cases Mo as other elements were not found in concentrations in the slag high enough. Slag went also through physical pretreatment processes such as comminution, beneficiation and metal separation prior to be directed to thermal and chemical treatment to recover the targeted metals.

Focusing on the pretreatments, low magnetic separation of Fe-rich fraction from Fe-poor fraction was tried prior, but this was not successful due to very fine liberation size of the Fe and Cr bearing minerals, which prevented magnetic separation (84). In addition, up-concentration of Cr in the slags by magnetic and gravity separation was investigated and it was demonstrated that it was possible to concentrate Cr from 2.3 to 9 wt.% in stainless steel slag and from 3.1 to 11 wt.% in low carbon slag (85). After these pretreatments, conventional and microwave roasting treatment of the slag were elaborated assessing parameters such as slag type, grain size, temperature and additive amount. Leaching assisted by microwave or radio wave was investigated to increase the leaching concentrations of different metals, however both methods did not produce significant results compared to conventional roasting. The conditions of the latter were optimized for leaching Cr from the slag, but not for V or Mo. In particular, a Cr removal up to 100% was achieved for certain types of slags applying a 20 % NaOH addition and 1 hour roasting time which might have to be increased for other types of slagsErrore. L'origine riferimento non è stata trovata..

After the roasting face, extensive investigations were conducted to optimize the extraction of Cr and V from liquid solutions (synthetic and leachate produced from slag leaching). For example, liquid extraction was conducted at the laboratory scale to extract synthetic V prepared as a 2 g/L solution using V_2O_5 and 0.1 M NaOH, with an organic phase composed of Aliquat®336, i.e., 10 or 20 % of 1-octanol and 5 or 10 % of kerosene, to recover vanadate powders. This solution showed some potential but needed further investigation to disclose its full potential (86). After conventional roasting of slags with NaOH, the slags were leached and the leachate was investigated to extract Cr with electrocoagulation. By optimizing the pH to 6, 100 % of Cr could be removed after application of appropriate current intensities of 0.5 A for 140 min and of 0.1 A for 430 min (87)Errore. L'origine riferimento non è stata trovata.. Layered double hydroxides materials were also investigated to be used as sorption material with a very high selectivity for V over Cr and a high sorption capacity (up to 65 mg Cr/g) and were engineered to withstand the alkaline milieu in the leachates (88)Errore. L'origine riferimento non è stata trovata..

The main outcomes of the project highlighted that conventional roasting followed by water leaching enabled Cr extraction rates exceeding 95 %, while recoveries of V, Mo, and Nb remained below 10 %. The developed recovery processes achieved Cr yields above 95 % and produced Cr products with purities greater than 90 %. Figure 35 shows a diagram with the successful paths of CHROMIC technologies. Despite these successes, economic viability remained a key challenge and was highly dependent on the effective valorization of the processed residues. Targeted slags were used in construction before metal separation, as such no landfilling costs were avoided by separating metal from them which resulted in large share of fine liquid sludge. Additional research was required to

mitigate the risk of Cr(VI) leaching from the treated materials since slags before metal separation did not have issues with chromium leaching due to minerology of the slags. Fifteen other types of materials landfilled, with environmental issues or containing higher concentrations of metals which could be treated taking advantage of the CHROMIC technologies were also identified, i.e., V slags, chromite ore processing residues, Bayer liquor and sludge from Al industry, tailings, BOF slags, steel dusts and mill scale, fly ashes, petroleum residues (coke), metallurgical slags (Sn slags), galvanic waste, tannery waste materials and spent catalysts.

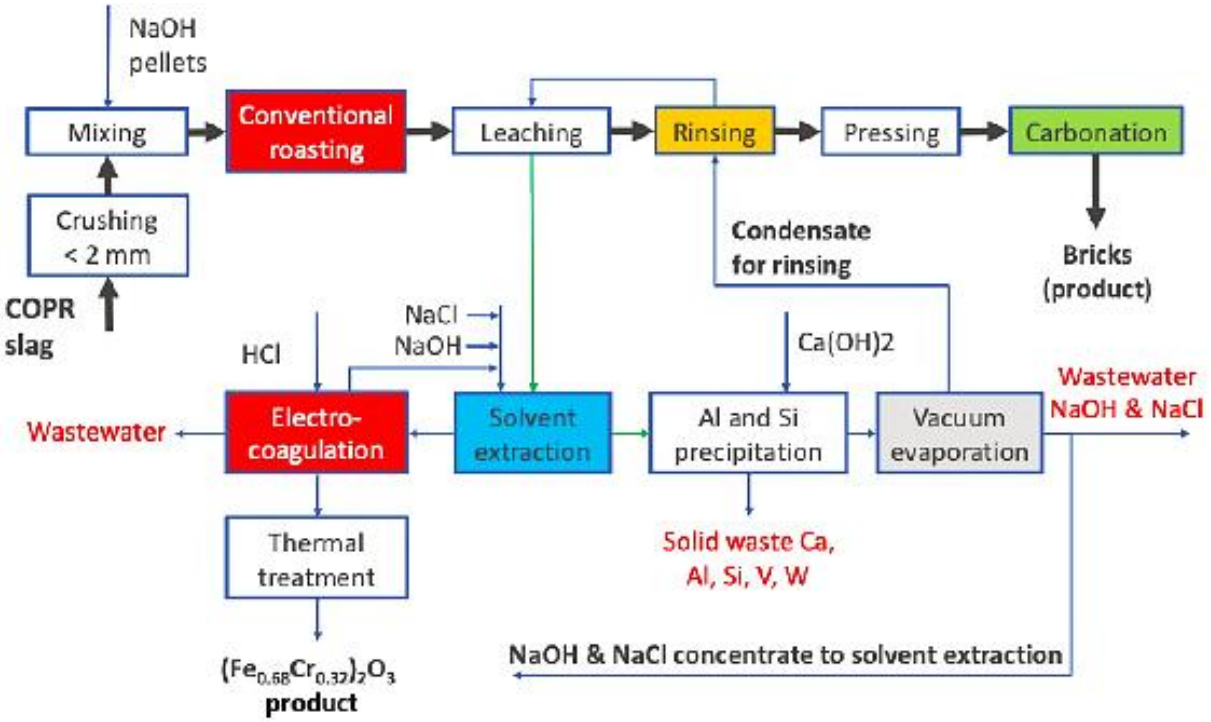

Figure 35: Integrated flow sheet with conventional roasting, solvent extraction and electrocoagulation for chromite ore processing residue slag.

3.2.5 FRESME: From residual steel gases to methanol (89)

The project was coordinated by i-deals Innovation & Technology Venturing Services, with NRG PALLAS, Swerim, CRI EHF, Kemijski inštitut, SSAB, Stena, Kisuma, Tata Steel, Array Industries, Politecnico di Milano and TNO (Nederlandse Organisatie voor toegepast-natuurwetenschappelijk Onderzoek) participating as partners in the consortium. The project started on the 1st of November 2016 and lasted almost four and a half years, ending on the 30th of June 2021. The overall project cost 11.4 M€ and the EU contributed with the whole budget.

Iron and steel industry are responsible for 8 % of world CO_2 emissions and the BF-BOF route is the main production route, accounting for nearly 60 % of the steel produced in Europe. Primary steel production emits around 1.7 tons of CO_2/ton of steel and CCUS can achieve significant CO_2 reduction and can be integrated within existing BF-BOF steel plants, although specific technologies need to be

demonstrated and favorable business cases need to be built. In this context, FReSMe aimed to demonstrate the feasibility of valorizing CO_2 and H_2 captured from BF gases by turning them into a versatile platform chemical and renewable fuel such as methanol. Moreover, other steel making residual gases such as BOF gas and Coke Oven gas could be suitable feedstock for methanol production using FReSMe technologies. The overall concept demonstrated was the methanol production from captured CO_2 and H_2 from BF gases plus additional H_2 produced through water electrolysis. The project used the existing equipment resulting from previous Horizon 2020 projects STEPWISE and MefCO2. STEPWISE focused on the efficient separation of H_2 and CO_2 from BF gases while MefCO2 targeted the synthesis of methanol from captured CO_2. In addition to the equipment from these projects, FReSMe pilot plant included supplemental H_2 production from an electrolyzer and an H_2/N_2 membrane separation unit. FReSMe successfully achieved three key goals which are the optimization of the technologies involved, their integration into a pilot plant and the end use demonstration of methanol as marine fuel. The main benefits derived from the project were an alternative valorization of the captured CO_2 from steel off-gases contributing to a more attractive business case around CCUS and a contribution to use greener methanol fuel.

The FReSMe system integrates SEWGS (Sorption Enhanced Water-Gas Shift), methanol synthesis, and electrolysis to convert steelmaking process gases rich in CO, CO_2, and H_2 into methanol while reducing CO_2 emissions. Therefore, FReSMe transforms these CO, CO_2, and H_2-rich gases into high-value methanol rather than using them for onsite power generation as done in conventional steel plants. A schematic representation of the FReSMe method is provided in Figure 36. The process included a process gas collection station to convey the by-product gases to the SEWGS treatment unit where steam is added to convert CO to CO_2 and H_2 in the pre-shift step and then SEWGS further converts remaining CO and separates two main streams, i.e., a high-purity CO_2 stream (almost 95 %) and a H_2/N_2-rich stream. After that, there is the methanol synthesis unit where CO_2 and H_2 are combined at a molar ratio of about 3:1 to produce methanol followed by distillation to chemical grade. Further units available are the electrolyzer to provide additional H_2 for methanol synthesis and to co-produce O_2 for steelmaking, e.g., for oxy-fuel combustion or BF enrichment, a CO_2 capture and storage station to compress the surplus CO_2 and sent it to pipeline for storage and an energy integration system to recover the heat from SEWGS and methanol units. This concept differs significantly from the reference system representing the state-of-the-art of conventional technology shown in Figure 37 consisting of two different parts the steel plant with power plant and a stand-alone natural gas-based methanol plant. In this case, methanol production was based on a large-scale natural gas-based plant (almost 2500 t/day), using a two-step reforming process with a pre-reformer converting heavier hydrocarbons to methane and CO/CO_2 and a following steam reforming unit to produce syngas ($CO + H_2$) adjusted for methanol synthesis. Methanol is purified via distillation. Concerning the power plant of the reference scheme, steel plant uses gas turbine combined cycle power plant burning process gases for onsite electricity and two possible variants exist. The first one without CO_2 capture and one with amine-based CO_2 capture from power plant flue. Even with capture, the steel plant still emits significant CO_2, and capture requires additional steam and energy.

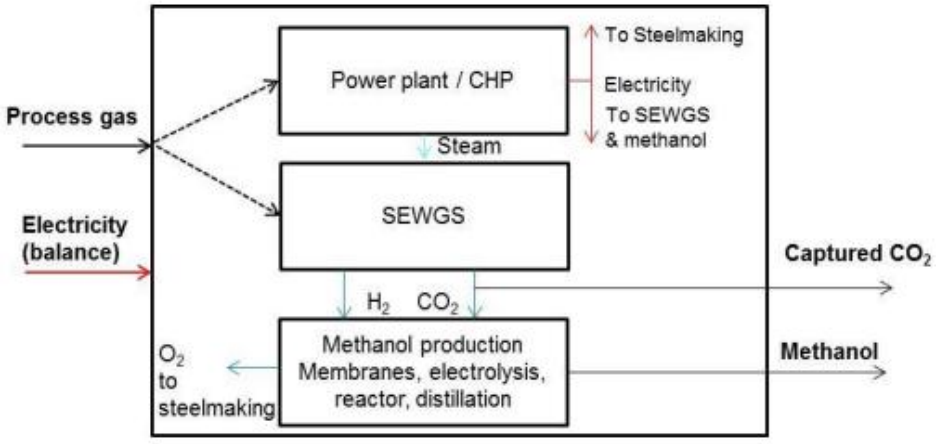

Figure 36: Schematic diagram of the FReSME method

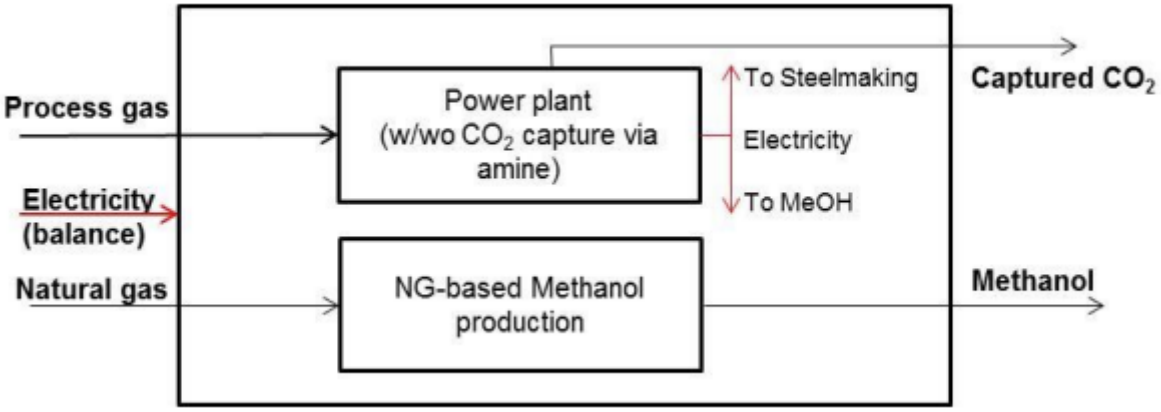

Figure 37: Schematic diagram of the reference process

Two main cases were considered for the FReSMe system to evaluate electrolysis and total system energy demand for variable methanol production rates. Case 1 did not include any captured CO_2 with the process gas currently fed to power production being partially or totally diverted to methanol production with all CO_2 in the diverted stream being converted to methanol. In Case 2, all excess gas was sent to SEWGS, the onsite power plant was eliminated, and CO_2 capture and storage infrastructure was available. Case 1 allowed for modification of the power plant to produce steam and electricity through a CHP (Combined Heat and Power) plant which improved the net energy use of the process gas. However, as methanol production increased the input of process gas to the CHP was reduced. Depending on availability of renewable energy the methanol production rate could be varied. CO_2 avoidance was relatively low and thus energy intensive per ton CO_2-avoided relative to Case 2. Overall avoidance can reach about 50 % relative to reference system without capture. Net emissions from electricity needed to be below about 190 g/kWh up to a production rate of 150 kg MeOH/t HRC (Hot rolled coil) for net reduction in CO2 emissions. Case 2 shifted all available process gas not used in the steelworks providing more H_2 to methanol production and lowering the electricity use for

electrolysis. It also eliminated the need for onsite power plant. It required access to CO_2 capture infrastructure or other applications of captured CO_2. CO2 avoidance could reach 39 % relative to reference system with capture.

Going more into detail, process gases were used for power generation in a gas turbine combined cycle plant and methanol production relies entirely on natural gas in the reference system without capture. Steel plant emissions were from 2046 kg CO_2/ ton HRC with no capture measures. Natural gas-based methanol consumed about 30.4 GJ/t MeOH, used about 275 kWh/t MeOH, and emitted about 388 kg CO_2/t MeOH. Overall, this system is highly energy and C-intensive and could not exploit the value of steel plant process gases. In the reference system with capture, the steel plant used amine-based capture for power plant flue gas capturing about 423 kg CO_2/t HRC, but significant direct emissions remained and the capture process imposed an energy penalty reducing power plant efficiency to around 37 %. Natural gas-based methanol energy used, and emissions remain unchanged with about 30.4 GJ/t MeOH, electricity about 275 kWh/t MeOH, and CO_2 emissions about 388 kg/t MeOH. Overall, even with capture, mitigation potential was limited, and the system lacks flexibility.

Part or all of the excess process gas was diverted to SEWGS, producing CO_2 and H_2 in Case 1. Hydrogen was used for methanol synthesis, while CO_2 was either converted or vented. Under this configuration, methanol production could reach 696 kg per ton of HRC with a maximum CO_2 avoidance of about 53 % compared to the reference system without capture. Additional energy per ton of methanol was approximately 2.6–10 GJ which was far lower than the conventional natural gas-based methanol route with 30 GJ/t MeOH. Electricity via hydrogen electrolysis was predominant in additional energy for production methanol from process gas. At low production rates <150 kg/t HRC, the system achieved optimal efficiency and offered high flexibility to adapt to renewable power availability. The breakeven electricity emission threshold was about 192 g CO_2/kWh thus meaning net CO_2 reduction was only possible when grid emissions were below this level.

In Case 2, all excess process gas was processed through SEWGS with CO_2 partly converted to methanol and the remainder compressed for storage. Methanol output was about 388 kg/t HRC, with CO_2 capture matching the reference system (423 kg/t HRC). CO_2 avoidance was around 39 % compared to the reference system with capture. Since the onsite power plant was eliminated, the system relied entirely on imported electricity, but the breakeven emission threshold for electricity was relaxed to 390 g CO_2/kWh allowing net CO_2 reduction even under relatively C-intensive power conditions. Further integration options, such as processing all BF gas and recycling the H_2/N_2-rich stream for steel plant combustion could push CO_2 avoidance close to 80 % approaching near-complete decarbonization.

FReSMe significantly outperformed the conventional route in energy efficiency and CO_2 reduction. Case 1 achieved up to 53 % CO_2 avoidance while Case 2 achieved about 39 %. Further integration by shifting and capturing CO_2 from all BF and BOF gas and using part of the H2/N2- rich stream from SEWGS for combustion applications in the steelworks and the remainder to methanol production could decarbonize the overall system to near 80 %. In contrast, the reference system remained highly energy and C-intensive even with capture and its mitigation potential was far below that of FReSMe. FReSMe also reduced energy consumption per ton of methanol by about 70 %.

FReSMe methanol was successfully used to power a roll-on/roll-off cargo ship connecting Gothenburg in Sweden and Kiel in Germany demonstrating that CO2 can be recycled and contribute to a reduction in fossil fuel demand and emissions. The versatility of SEWGS is now being demonstrated by producing ammonia from BF gas, and the process is ready for scale up. The project has reaffirmed the ability of circularity and industrial symbiosis to contribute to decarbonization of an important part of the economy.

The EU-funded FReSMe project addressed two major emission sources: steelmaking and shipping. Steel production accounted for about 5 % of EU CO_2 emissions and 8 % globally, while shipping contributed around 3 % worldwide. FReSMe demonstrated an innovative integration of existing processes to achieve significant decarbonization without building new plants. The project applied SEWGS technology for CO_2 capture and H_2 production in dealing with steelmaking emission. This hydrogen was combined with renewable H_2 from electrolysis and reacted with captured CO_2 in an emissions-to-liquids unit to produce low-carbon methanol. Methanol, a clean-burning fuel, was successfully used to power a cargo ship between Gothenburg and Kiel proving its potential to reduce fossil fuel demand in shipping. FReSMe delivered a flexible methanol production process using BF gas, tested in four operational modes: electrolyzer-only, high turndown, maximum capacity, and BFG-only mode—demonstrating adaptability beyond the original scope. Over 25 tons of methanol were produced meeting IMPCA standards and used as marine fuel in 2021. Additional achievements include catalyst development, multi-scale process optimization, impurity impact studies, novel sorbent testing, and SEWGS cycle design improvements. A full LCA and techno-economic analysis confirmed the feasibility of valorizing residual steel gases for methanol production, setting the foundation for CCUS deployment in steelmaking and enabling a decarbonization pathway compatible with existing plants.

3.2.6 Recyclatrack: 100% recovery and RECYCLing of construction vehicle crAwler TRACKs into constituent rubber and steel for sustainable raw material supply (90)

The project was coordinated by Aquablast and started on the 1st of March 2016 and lasted 3 months ending on the 31st of May 2016. The overall project cost 71,43 k€ and the EU contributed 50 k€, i.e., almost 70 % of the budget.

Aquablast is a company developing ultra-high pressure (UHP) waterjet technology with operating pressures up to 90,000 psi for steel and concrete surface preparation and cutting. Aquablast tried to enrich the portfolio of its product by introducing UHP water techniques to the recycling industry by developing the Recyclatrack © process to recover and recycle end-of-life rubber crawler tracks from civil, military and agricultural fields. Recyclatrack © is a patent-protected process which exploits low volumes of water to recover steel and high-grade ferrous scrap and rubber granulates from end-of-life vehicle crawler tracks to achieve 100 % recycling of a waste stream which until that moment was not treated with any practical or sustainable solution. The UHP waterjets were able to separate the rubber from the steel and the water used was also recycled leading to a green process.

The development of this environmentally attractive recycling process was fundamental considering the regulatory pressure and the progressive closure of landfills which strongly limited the options for track disposal. Furthermore, it proved to be quite urgent considering that a rise in crawler track usage in 2020 was estimated and it would result in 12 Mtonnes of high-grade steel and 5 Mtonnes of re-processable rubber. Extensive work was performed examining the demographics of waste tracks worldwide and research on the recovered products confirmed demand for rubber powders as fillers in rubber manufacturing processes which does not require any post-processing. A schematization of the key points of the process, i.e., the plant, the recycled products and the component to recycle, is reported in Figure 38.

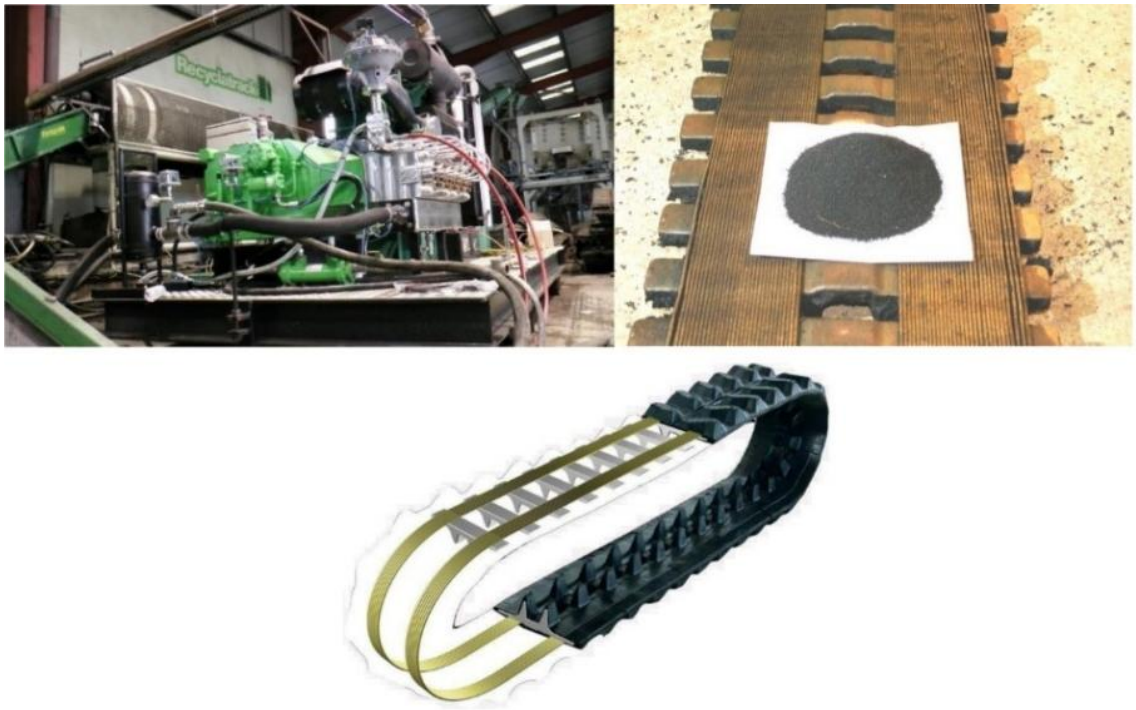

Figure 38: Recyclatrack © process plant, recycled products, i.e., the steel components and rubber powders and schematization of the crawler track component to recycle.

3.2.7 Carbon4PUR: Turning industrial waste gases (mixed CO/CO2 streams) into intermediates for polyurethane plastics for rigid foams/building insulation and coatings (91)

The project was coordinated by Covestro with Recticel, Megara Resins, Universiteit Gent, Universiteit Leiden, DECHEMA (Deutsche Gesellschaft für chemisches Apparatewesen), TU Berlin (Technical University), CEA, ArcelorMittal, South Pole, Grand Port Maritime de Marseille, RWTH, PNO Consultants, and Imperial College participating as partners in the consortium. The project started on the 1st of October 2017 and lasts almost three and a half years, ending on the 31st of March 2021. The overall project cost 7.76 M€ and the EU contributed 7.76 M€, i.e., the full budget.

The strong need of the EU process industry to become less dependent on fossils as C source and to reduce GHG emissions laid the foundations for the Carbon4PUR project which tried to address these two challenges by converting the waste flue gas streams rich in CO/CO_2 resulting from energy-intensive industries, e.g., steel industry, into valuable intermediates for consumer products, e.g., C sources for the chemical industry. In particular, the project tried to develop an innovative process able to convert directly the chemical flue gases resulting from a steel company into polyurethane products while eliminating the need for costly physical separation methods. This approach would allow to reduce significantly the carbon footprint while providing substantial economic savings exploring industrial symbiosis between steel and chemical industry. The consortium tried to investigate how the CO and CO_2 contained in BF gases could be used as carbon source for polyols which are key intermediate components for polyurethane which is largely exploited as insulation material and as coating and is normally derived from crude oil. The overall concept of the project is summarized in Figure 39.

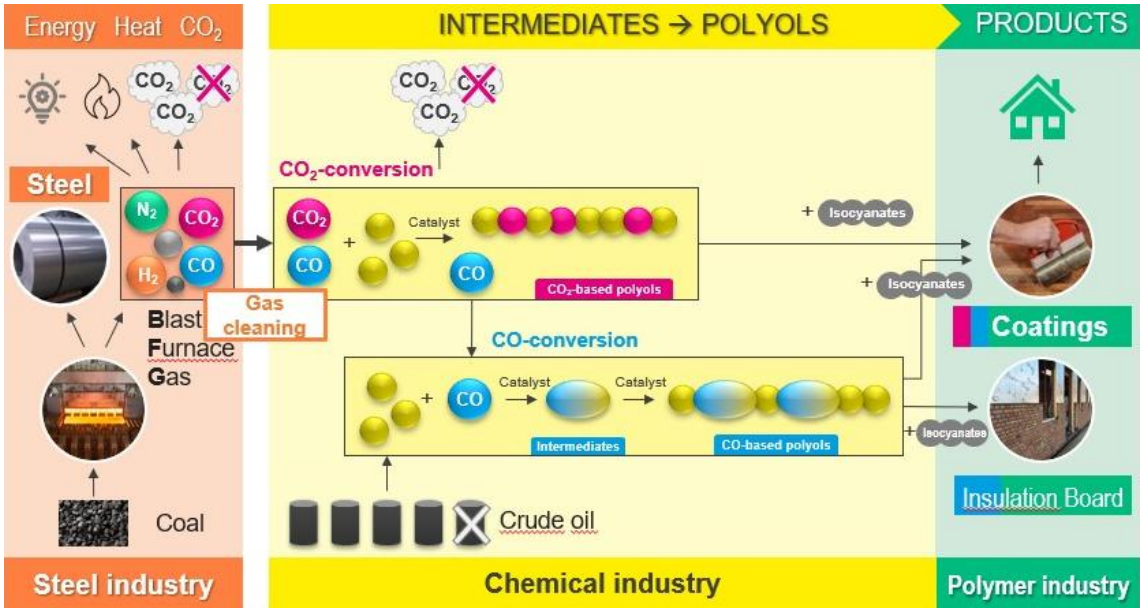

Figure 39: Main CO and CO_2 technologies analyzed and developed within the Carbon4PUR project

University of Gent investigated and developed a single-step catalytic process and a two-step chemical looping process for the conditioning of steel mill gases. The catalytic process was compatible with the treatment of both steel and Acheson process gases and required approximately 90 % of CO/CO_2 with more CO_2 than CO being more beneficial. This process allowed to tolerate CH_4 and other impurities, but the presence of inerts ends up in output stream. The chemical looping process was more versatile being compatible with the gases resulting from the Acheson process, with biogas before and after combustion, with pyrolysis gas after partial combustion eventually mixed with CO_2, with refineries after partial combustion, with steam crackers after partial combustion, with steel gases and with cement/lime kiln when mixed with natural gas and after removing O_2. This process needed at least 30-

40 % of CO_2 and reductants, i.e., CH_4, H_2, CO, which must be at least equal to CO_2. CO is not required but if present the CO_2 percentage can be lowered. This selective catalytic oxidation process was evaluated in a non-adiabatic lab-scale reactor and then successfully upscaled and validated to a semi-industrial scale at Arcelor Mittal Gent with real BF gases. Furthermore, a novel catalyst able to produce new polyols using CO was identified and developed at a laboratory scale by Covestro, CEA and RWTH for the ring-expansion carbonylation of epoxides, i.e., a one-step method which employs a catalyst to insert CO into an epoxide ring. Succinic anhydride was identified as the most appropriate intermediate in the CO conversion step and was successfully applied in polyol synthesis. Furthermore, the feasibility of using gas mixtures of CO and CO_2 for the new CO-conversion and the established CO_2-technology was also demonstrated. These conclusions allowed to proceed with the next step where different polyol recipes were developed and upscaled, and the most promising ones were optimized on a kg-scale for initial lab trials at Recticel and Megara. Recticel produced polyisocyanurate (PIR) rigid foams which are thermoset materials used for insulation boards while Megara Resins incorporated the new polyols into waterborne polyurethane dispersions for wood coatings. In particular, it synthesized and characterized several formulations of waterborne polyurethane dispersions with both CO and CO_2 deriving polyols optimizing their properties to fulfill the requirements of wood coatings.

Focusing on Recticel, it carried out various laboratory hand-mix trials using nine different CO-based polyols produced by Covestro and partially replacing the reference polyols in the mixture. In this first phase, the formulations were tested to optimize both the concentration of Carbon4PUR polyols in the formulation as well as the quantities of other formulation components such as surfactant, catalyst and blowing agent. These preliminary results demonstrated that a substitution up to 70 % of standard polyols with Carbon4PUR ones was possible but higher surfactant levels were necessary to obtain insulation boards with technical specifications comparable to market reference. After the preliminary laboratory hand-mix trials, semi-industrial trials were performed by selecting two different polyols, i.e., polyol based on succinic anhydride – ethylene oxide (PEGSAEO) chemistry and polyol based on succinic anhydride – glycol (PEGSA) chemistry. The results demonstrated that PEGSAEO systems were characterized by substantial mixing problems when processed under semi-industrial conditions thus resulting in non-homogeneous foams while PEGSA based systems were more promising in terms of processing, but some key properties of the resulting foams, e.g., thermal conductivity, were not in line with the reference system. Even if not all the properties were met, it was still possible to produce insulation boards by using Carbon4PUR polyols as 70% replacement of the standard polyol system. After this first semi-industrial trial the compatibility of the PEGSA polyol system was improved and optimized by Covestro by adding a stabilizer additive. This modified PEGSA polyol system was then tested at the laboratory scale to verify that the properties of the resulting foams fulfilled the requirements. After that the PEGSA modified system was produced on a large scale to perform again semi-industrial trials to produce rigid PIR insulation boards. At this stage, two different Carbon4PUR polyol concentrations as replacement of the standard polyol system were tested, i.e., 60 and 70 %, and the formulation was adapted by increasing the surfactant levels to overcome mixing issues. The adapted formulation was substantially better in terms of mixing compared to previous trials on pilot scale. Concerning insulation board properties, mechanical properties, i.e., compression and tensile strength, fire resistance, dimensional stability and stability under extreme conditions, thermal conductivity on

both short and long term and water absorption were investigated to verify whether the EN (European Standard) requirements were fulfilled. Both Carbon4PUR formulations, i.e., 60 and 70 % replacement, displayed properties comparable to the reference system ones in terms of water absorption, thermal conductivity on both short and long term, fire resistance, tensile strength and dimensional stability. On the contrary, they displayed slightly lower compression values which were in any case above the one required by EN specifications. The 70 % Carbon4PUR formulation also displayed slightly worse properties in terms of dimensional stability under extreme conditions, but again they were higher than the one required by EN. All these results allowed to conclude that the properties resulting from the use of Carbon4PUR polyol in rigid foam application were extremely promising.

The project also included some environmental considerations thanks to the LCA performed by Universiteit Leiden which considered three different Carbon4PUR scenarios, i.e., BF gases converted to CO-based polyol, BF gases sequentially converted into CO_2-based and CO-based polyols and BF gases converted parallelly into CO_2-based and CO-based polyols, and compared them with the baseline LCA performed on conventionally produced polyol/PUR and steel mill gas treatment by ArcelorMittal. An industrial scale of 50 kt/y of CO-based polyol was considered to perform the study and the following impact categories were considered: 1) Climate change, 2) Ecosystem quality, freshwater and terrestrial acidification, 3) Ecosystem quality, freshwater ecotoxicity, 4) Ecosystem quality, freshwater eutrophication, 5) Ecosystem quality, marine eutrophication, 6) Ecosystem quality, terrestrial eutrophication, 7) Human health, carcinogenic effects, 8) Human health, ionizing radiation, 9) Human health, non-carcinogenic effects, 10) Human health, ozone layer depletion, 11) Human health, photochemical ozone creation, 12) Resources, fossil resources, 13) Resources, minerals and metals. All three scenarios showed improvements in environmental performance of the Carbon4PUR system compared to the conventional one and the comparison of the three scenarios allowed to conclude that scenario 3 was the most promising. This scenario assumes yearly production levels of 50 kt of CO-based polyol and about ~110 kt of CO_2-based polyols and was expected to reduce impacts between 4-15 % for most impact categories with the only exception of ionizing radiation (-0.5%). Furthermore, it may result in GHG savings up to 90 kt CO_2-equivalents per year, i.e., 10 %, compared to the conventional system. The comparison of the different scenarios also allowed to draw some economic conclusions proving that CO_2 and CO-based polyols could be produced more efficiently by using pure gas streams since additional inert gas increased the overall flow rates and the necessary process pressures thus reflecting in higher energy demands and increasing amount of assets.

3.2.8 TORERO: TORrefying wood with Ethanol as a Renewable Output: large-scale demonstration (92)

The project was coordinated by ArcelorMittal with C-Shift, Chalmers tekniska högskola, Renewi, Joanneum Research Forschungsgesellschaft, Perpetual Next Biocarbon International, and Universität Graz participating as partners in the consortium. The project started on the 1st of May 2017 and lasts almost seven and a half years, ending on the 31st of December 2024. The overall project cost 18.09 M€ and the EU contributed 11.47 M€, i.e., almost 67 % of the budget.

The integration of biomasses within the BF route demonstrated great potential for the partial substitution of coke both as fuel and as reductant thanks to the relatively low ash and S content as well as the low number of harmful and undesired components for the metallurgical products, e.g., K and Na. In particular, the substitution of pulverized coke with biomasses at tuyere injection proved to be the most promising option. Woody biomasses need to be transformed and upgraded through torrefaction and pyrolysis processes to reach chemical and physical properties similar to coal which allows their use in BF. Furthermore, the energy contained in torrefaction by-product can be used to provide the heat necessary to run the reactor and the drying process.

Considering this, the Torero project developed a cost effective and energy efficient technology which allowed to exploit wood waste feedstock into a fully integrated large-scale functional steel mill and to repurpose BF off gases to produce bioethanol. The latter technology was developed in the framework of the Horizon 2020 STEELANOL project discussed in section 3.2.3. The Torero concept is summarized in Figure 40.A and was articulated in different steps. It started with the collection of waste wood and its processing through shredding and pollutants removal to reach the specifications required for torrefaction. After this first phase, shredded waste wood was dried, sieved and sent to torrefaction to produce bio-coal which was then grinded before being transported to BF where it replaced fossil powdered coal for injection. The carbon monoxide resulting from the exhaust gases of BF was sent to a bioreactor to be microbially fermented to produce bioethanol. Torero project focused primarily on waste wood, i.e., demolition wood and waste furniture, since it was an untapped resource with no attractive applications for recycling that would otherwise be incinerated. Despite this, the technology developed was open ended and other stakeholders may decide to replicate the same concept by exploiting other biomass feedstocks or by producing other types of fuels. Furthermore, Torero provides an add-on technology which can be conveniently used to upgrade existing facilities of the steel sector.

The torrefaction process is a thermochemical process which occurred at high temperatures up to 350 °C in oxygen-free environment and allows to convert bio-residuals and biomasses into bio coal by decreasing the water and volatile content and increasing the energy density and carbon content. Focusing on the optimization of this process, the effect of temperature was investigated, and it was observed that torrefaction temperatures higher than 300 °C were able to provide higher C content in the bio coal, i.e., 60-70 wt.%, but caused a decrease in yield and a decrease in the energy yield of the bio coal itself. On the other hand, torrefaction temperatures in the range of 280-300 °C provide a lower C content in the bio coal, i.e., 50-60 wt.%, but ensured a higher bio coal yield and a higher energy yield of the bio coal itself. The torrefaction technology was developed by the consortium partner TorrCoal which is a Perpetual Next Company and acted as technology provider for the Torero pilot plant built at ArcerloMittal together with STEELANOL one.

The pilot plant shown in Figure 40.B was commissioned at the end of 2023 and the first batches of bio coal were produced from waste wood but the ramp up to full capacity was achieved only in 2024 with 37.5 ktonnes biocoal/ reactor/ year. Production was expected to reach 50 ktonnes/ reactor/ year after an appropriate plant and technological optimization which would translate into a decrease of 150 ktonnes of CO_2 released into the atmosphere per year. Moreover, the fermentation process of BF off

gases would allow to produce 80 Ml of biofuel which would further contribute to the reduction of GHG emissions. Around 200 t of bio-coal was used in ArcelorMittal BF using a ratio of 9 % of bio-carbon and 91% of standard pulverized coal and no significant problems were detected during the test. Finally, the business case of the Torero project also showed that compared with the first-generation production based on cellulosic bioethanol, OPEX was 1/3 lower while keeping constant the CAPEX.

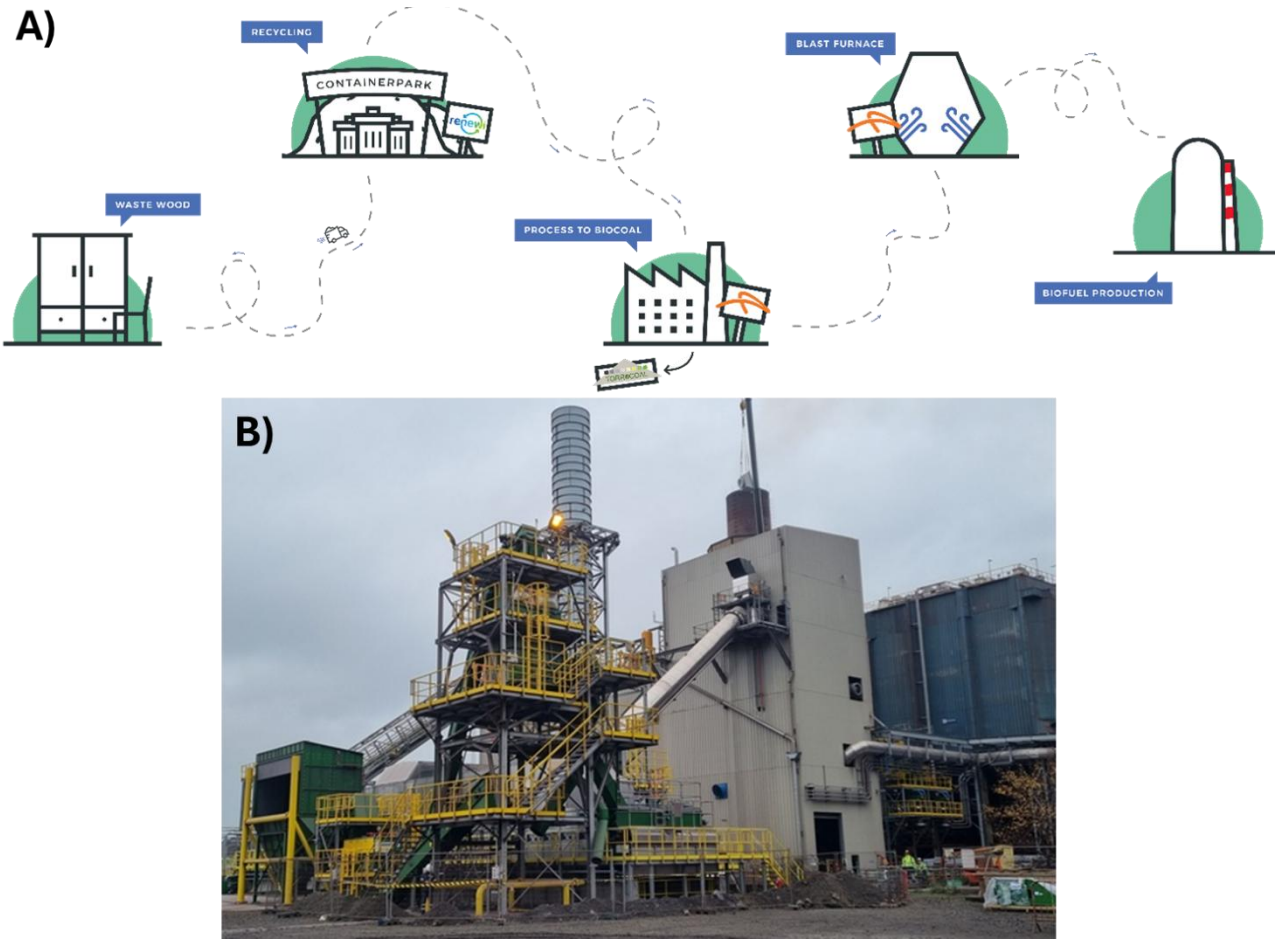

Figure 40: Schematization of the Torero workflow (A) and Torero plant built at ArcelorMittal (B)

3.2.9 POLYINSPIRE: Demonstration of Innovative Technologies towards a more efficient and sustainable plastic recycling (93)

The project was coordinated by CIRCE, while Repsol Quimica, Arkema, Novamont, Nurel, Kordsa, Ioniqa Technologies, Kemijski inštitut-National Institute of Chemistry (NIC), Fricke und Mallah Microwave Technology, TU/e, Fundacion AITIIP, Bada Hispanaplast, Maier, RINA-CSM, Ferriere Nord, I.BLU, HTT, CPPE d.o.o., Fonden Dansk Standard, European Plastics Converters (EuPC), IKMIB (İstanbul Kimyevi Maddeler ve Mamulleri İhracatçıları Birliği) participating as partners in the consortium. The project started on the 1st of September 2018 and lasted almost five years, ending on

the 28th of February 2023. The overall project cost 9.81 M€ and the EU contributed 7.94 M€, i.e., about 80 % of the budget.

The growing plastic pollution must be mainly ascribed to low recycling rate resulting from the heterogeneous nature of plastics. Existing sorting and waste management systems cannot separate plastic blends and composites. In light of this, the POLYNSPIRE project aimed to increase the recycling and valorization rates of plastic-containing waste by demonstrating cost-effective and sustainable solutions to improve energy and resource efficiency. POLYNSPIRE sought to demonstrate a comprehensive set of innovative, cost-effective and sustainable solutions to improve the recycling processes of post-consumer and post-industrial plastic containing materials. Project activities were developed according to three pillars, i.e., chemical recycling to recover plastic monomers and valuable fillers, mechanical recycling to enhance the quality of the recycled plastics and valorization of low-grade plastics for use in the steel industry. Chemical recycling was selected as suitable path to recover plastic monomers and valuable fillers such as carbon and glass fibers relying on microwaves-assisted organic chemistry and smart magnetic catalysts. Advanced additivities were investigated for mechanical recycling processes to enhance recycled plastics quality by using vitrimers, high-energy radiation and compatibilization additives. Finally, valorization of plastic waste as carbon source in EAF for steel industry was considered. The degree of demonstration achieved for the three innovation pathways was different. TRL7 was achieved in the framework of the steel sector where between 25-50 % of fossil coal was replaced by plastic product. Same TRL was achieved by the improvement of properties of mechanically recycled products where recycling test using industrial plastic injectors were implemented. Concerning chemical recycling, polynSPIRE worked within TRL 5-6. An intermediate reactor with assisted microwave heating was built and tested and trials were performed thus reaching TRL 6. In the case of innovation assisted by solvent-assisted modified monomer, TRL5 was obtained since the operational environment and the developed process were proved on the lab scale, and the design of the equipment suitable for large scale was made. In particular, progresses were made in understanding the catalytic activity in the relevant depolymerizations step.

The project focused on three types of plastic materials, i.e., Polyamide (PA), PU foams and polyolefins. Regarding PA value chain, the hypothetical scaled-up processes would allow to reduce the environmental impacts of the monomers obtained since the microwave assisted recycling of PA66 and the use of recycled monomers would reduce the impact of PA66 manufacturing between 3.1 and 3.5 t CO2 eq/t PA66 and between 0.2 to 0,3 t oil eq/t PA66. In this framework, CO2 emissions would be reduced between 57 to 69% and fossil resources between 10 to 30%. Considering the mechanical recycling of PA6 through gamma irradiation, it could reduce CO2 emissions by around 43 %, i.e., 3.4 t CO2 eq/t PA6, and fossil resources around 72 %, i.e., 2.7 t oil eq/t PA6. Concerning polyurethane value chain, the hypothetical scaled-up processes would also reduce the environmental impacts compared to virgin polyurethane foams. Polyols obtained through chemical recycling of PU foam with both microwaves and solvent-assisted modified routes would be less pollutant than virgin polyols reducing CO2 emissions of between 11 and 19%, i.e., 0.6 to 1 t CO2 eq/t PU foam, and fossil fuels between 10 and 30 %, i.e., 0.3 to 0.6 t oil eq/t PU foam. Mechanical recycling of PU foam through vitrimers could reduce the CO2 emissions by around 84 %, i.e., 4.6 t CO2 eq/t PU, and fossil resources around 89 %, i.e., 1.7 t oil eq/t PU. Finally, regarding the valorization of plastic wastes in steel industry,

the partial substitution of hard coal by plastic grains allowed the reduction of the impacts of the steel manufacturing process, determining a reduction of at least 30 % of fossil carbon sources, i.e., 2,4 kg oil eq/t steel, and of 7 kg CO_2 eq/t steel in CO_2 equivalent emissions.

POLYNSPIRE project provided significant improvement in chemical depolymerization of PA and PU assisted by microwaves developing, building and testing an intermediate scale reactor. Specific simulations of the microwave heating process were completed to evaluate the power needs of an industrial recycling process, and the design of industrial reactor was also developed. Material and safety requirements and know-how for future industrial scale have been generated. Processes for chemical recycling of PU and PA assisted by solvent-assisted modified monomers were developed and progresses were made in understanding the catalytic activity in the relevant depolymerization processes. These progresses were proven on the lab scale with post-industrial waste feedstock. These application tests provided useful guidance on how to further develop this technology, and the final detailed engineering of the pilot plant was completed. Mechanical recycling processes were also validated with advanced mechanical recycling processes and use of vitrimers to recycle PU foams through the application of standard plastic processing technologies. Validation at semi-industrial level of gamma rays as an external energy source for the generation of crosslinking and the implementation of gamma rays treated materials in injection molding was achieved. Development of an industrial methodology for the application of gamma rays in plastic materials was achieved as well. PolynSPIRE also contributed to validate the use of plastic residues as C substitute in the EAF steel manufacturing. Plastic grains were studied for this application and a new injector in EAF was designed and commissioned. Real industrial scale tests proved the successful substitution of 30 % of coal in every operation. As transversal activities developed to evaluate the project results, LCA and LCC methodologies were created and applied to evaluate the impact of each technology developed. Also, an exploration of the data collected for the recycling processes was conducted and different machine learning models were trained to estimate the environmental impacts depending on the selected operating conditions.

3.2.10 C2FUEL: Carbon Captured Fuel and Energy Carriers for an Intensified Steel Off-Gases based Electricity Generation in a Smarter Industrial Ecosystem (94)

The project was coordinated by Engie with DTU (Danmarks Tekniske Universitet), TU/e (Technische Universiteit Eindhoven), CNRS, Université de Lorraine, Fundacion Tecnalia, DENS (Dutch Energy Solutions), Elcogen, BTD (Breuer Technical Development), Ayming, and Benkei participating as partners in the consortium. The project started on the 1st of June 2019 and lasts almost three and a half years, ending on the 30th of November 2023. The overall project cost 4.13 M€ and the EU contributed 3.99 M€, i.e., almost 97 % of the budget.

The C2FUEL project tried to provide new viable decarbonization pathways for hard-to-abate sectors while preserving profitable business models by developing energy-efficient, economically competitive and environmentally friendly CCU technologies for CO_2 conversion. In particular, the project aimed to create an interaction between carbon intensive industries, power production and local economies

by demonstrating at an industrially relevant scale the capture of CO_2 from industrial off gases and its conversion into formic acid (FA) and dimethylether (DME) as chemical energy carriers by combining it with green hydrogen generated by high temperature water electrolysis. The e-fuels obtained were meant to be dedicated to local use thus providing solutions for hard to abate mobility sectors or decentralized electricity production. The concept was demonstrated in Dunkirk (France) between the DK6 combined cycle power plant, i.e., a natural gas-fired combined cycle power plant, Arcelor Mittal steel factory and Dunkirk harbor using the CO_2 contained in the BF gas which was selectively removed and combined with the green hydrogen generated by electrolysis. This allowed to simultaneously reuse the CO_2 emission from steelmaking and the electricity surplus in the Dunkirk area while improving the operational and environmental performance of the DK6 combined cycle. This circular approach could help mitigate up to 2.4 Mt of CO_2 per year.

The C2FUEL project aimed to integrate 3 technologies, i.e., CO_2 capture, H_2 production by electrolysis and DME or FA production. Focusing on the first technology, i.e., CO_2 capture, membrane contactors proved to intensify the capture processes allowing to reduce installation CAPEX. In light of this, a TRL5 pilot was installed in DK6 and succeeded in the 2000 h long-duration tests performed with real BF gases ensuring CO_2 absorption, production and outlet purity matching the required specifications. The validation of the technology selected allowed to move to a TRL6 pilot. The latter was constructed and validated on-site and permitted to provide 1 Nm^3/h of CO_2 in a real industrial environment. Considering the extreme harshness of BF gases, the knowledge acquired on pre and post treatment technologies was fundamental to achieve scalable CO_2 capture technologies with promising perspectives for membrane contactors application for CO_2 capture in other fields such as coal, natural gas power plants and cement. BF gas pretreatment and CCU units of C2FUEL are summarized in Figure 41. A small fraction of BF gases flowing in the main pipeline was diverted and sent to the pretreatment section for cleaning. The gas resulting from pretreatment must be characterized by a pressure between 200 and 500 mbar, a temperature of 45 °C and a humidity lower than 6 % before entering the membrane module. After that, BF gases entered the membrane absorption module where they came in contact with the solvent, i.e., monoethanolamine (MEA), to ensure CO_2 transfer from the gas to the liquid phase. The gas resulting from the membrane contactor must be characterized by a pressure of 1 atm, a temperature lower than 20 °C and a humidity lower than 3 %. This module was followed by a stripping process in a distillation unit where water vapor resulting from the partial evaporation of the solvent in the reboiler encountered the CO_2-rich solvent ensuring CO_2 stripping. Any further entrained water in the gas stream was then separated into the downstream condenser before CO_2 compression and storage at 45 barg.

The BF gases pretreatment was characterized by many different steps. At first, BF gases were transported from the main pipeline to the pretreatment section through a tap and an electrically heated tube to maintain gas temperature at 55 °C and avoid temperature drop and condensation along the pipe. The pipeline was characterized by a diameter of at least 20 mm to avoid excessive pressure drops and was made of an anti-static material to avoid deposition and adhesion of charged dust on the walls which could clog the line as well as risk of electrostatic spark inside the line. The first unit of the pretreatment section was a dust filtering unit with HEPA (High Efficiency Particulate Air) filters to remove dust particles greater than 0.3 µm and was followed by a gas blower to compensate pressure

drops and control the flowrate. The second unit consisted of a condensate mitigation step to remove condensate by coupling a chiller with a separator. In this step, BF gases were cooled from 55 to 45 °C using a gas-liquid heat exchanger and using industrial cooling water. After this step, the gas passed through a reheater and was sent to the acid gas removal unit to eliminate S components, e.g., SO_2, COS, H_2S, via adsorption on activated carbon. This step was crucial since H_2S is a direct competitor of CO_2 for chemical solvent absorption and is able to regenerate along with CO_2 downstream thus leading to catalyst poisoning in the DME reactor. COS can hydrolyze CO_2 in the presence of a weak base like MEA and to form H_2S and CO_2 but is also able to react directly with MEA forming a heat-stable species and degrading solvent performance. Finally, SO_2 can form heat-stable salt with the chemical solvent thus impacting its long-term performance. An additional adsorption unit could be foreseen after CO_2 regenerator to properly mitigate risk if the adsorption beds in the pre-treatment line were ineffective. The downstream CO_2 to send to the compressor can admit an absolute humidity lower than 3 % therefore a dehydration unit with silica gel as solid desiccant, a separator unit and a cold trap combined with a cryocooler were foreseen before the final compression stage.

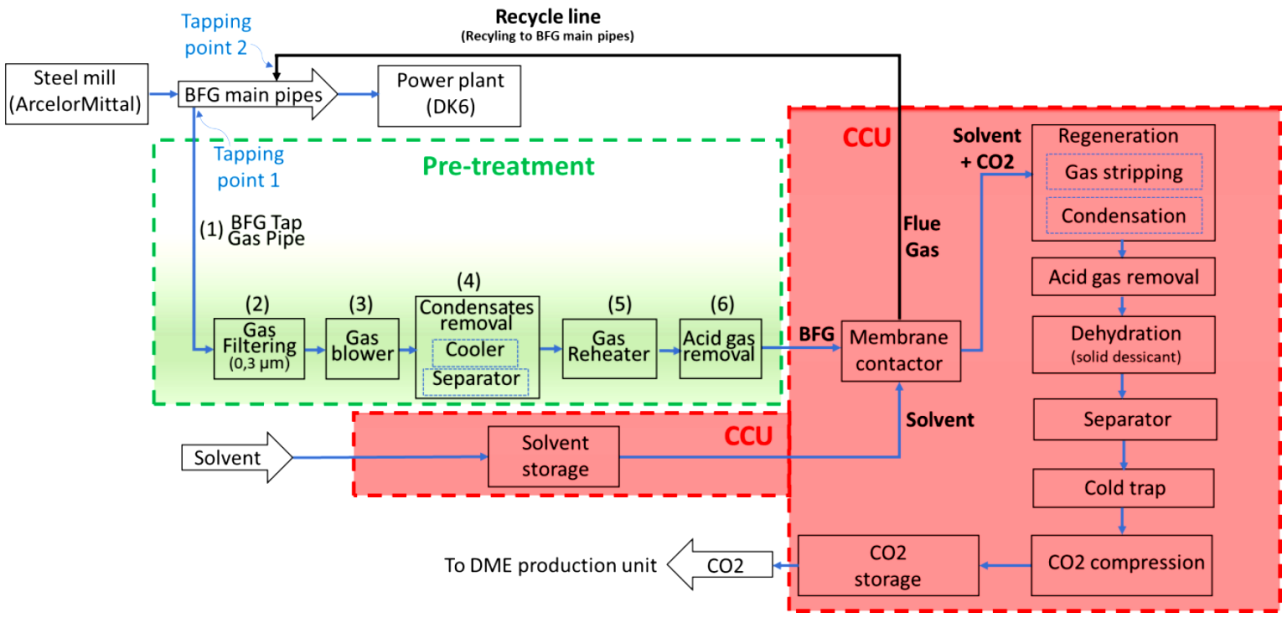

Figure 41: Block diagram summarizing the BF gases pretreatment and the CO_2 capture units of the C2FUEL project

Regarding the development of the Solid Oxide Electrolysis Cells (SOEC) for the high temperature electrolysis, their testing reported remarkable specific consumption of 2.6 kWh/Nm^3 H_2 at 15 bar while the long-term testing of 2200 h and the dynamic testing of both cells and stacks reported promising results. All these results led to the construction of a complete electrolyzer unit able to produce 1Nm^3/h of H_2 at 40 bar upon validation. At first, the influence of operating conditions such as temperature, inlet gas composition, steam utilization and current density on cells performance and durability was investigated to map out the most suitable operational window and to identify the

parameters which affected cells lifetime. Increasing operating temperatures were beneficial for SOEC performance thanks to faster kinetics and lower resistance while increasing CO_2 concentrations proved to be detrimental due to the slower kinetic of CO_2 electrolysis. The effect of temperature on durability was investigated by testing the cells at 650, 700 and 750 °C for 1200 hours. A strong effect of temperature on cell degradation was observed with higher temperatures determining lower degradation rates, i.e., 633 mV/kh at 650 °C and 174 mV/kh at 750 °C. Cells operating at 700 and 750 °C displayed similar degradation behavior with a slow degradation rate in the first 300 hours followed by an acceleration in the 300-600 hours range and a final degradation rates around 100mV/kh in the last 200 hours. Another important factor promoting SOEC degradation was the presence of impurities such as S and Si species in the inlet gas stream since they can poison the Ni catalyst in the fuel electrode. For this reason, fuel gas streams need to be cleaned with a gas cleaning filter filled with commercial gas clean powders to eliminate such impurities. Two tests with and without gas cleaning filter were performed at 700 °C with a 10 % H_2 + 90 % H_2O flow being supplied to the fuel electrode and air being supplied to the oxygen electrode. The cell tested without gas cleaning exhibited a fast initial degradation followed by a linear long-term degradation while the cell with gas cleaning showed a degradation levelling off after the initial degradation step. The overall and last 200 hours degradation rates were 370 and 260 mV/kh with no gas cleaning and 264 and 109 when applying gas cleaning. The effect of current density was investigated setting values of -0.5 and -0.75 A/cm^2. Higher current density resulted in a higher overall degradation rate, i.e., 341mV/kh against 264 mV/kh, but a lower degradation rate in the last 200 hours, i.e., 44 mV/kh against 109 mV/kh, thus indicating that higher current densities may accelerate cell initial degradation potentially reaching a steady state in a shorter time. The effect of steam utilization on cell degradation was also investigated performing tests at 700 °C with a 10% H_2 + 90% H_2O stream being supplied to the fuel electrode and air being supplied to the oxygen electrode under a current density of -0.5A/cm^2. A reduction in steam utilization allowed to decrease the overall degradation, i.e., 264 mV/kh for 56 % steam utilization, 160 mV/kh for 40 % steam utilization and 147 mV/kh for 28 % steam utilization, but a steady state with almost no degradation in the 400 hours was reached for the 40 % steam utilization test while a linear degradation in the last 400 hours was observed in the cell tested at 28 % utilization. Finally, the effect of fuel electrode inlet gas composition on cell durability was investigated performing the tests at 700 °C and with -0.5 A/cm^2 current density. Three inlet gas composition considered were 10% H_2 + 90% H_2O for steam electrolysis, 10% H_2 + 45% H_2O +45% CO_2 for CO-electrolysis and 10% CO + 90% CO_2 for CO_2 electrolysis. The starting voltage was similar for steam and CO-electrolysis, but slightly higher values were observed for CO_2 electrolysis since more energy was required to split CO_2. Despite this, CO_2 electrolysis displayed a linear degradation rate with the lowest overall degradation, i.e., 52 mV/kh, and CO-electrolysis exhibited a fast initial degradation rate in the first 200 hours and a linear degradation afterwards which led to the highest overall degradation, i.e., 310 mV/kh.

An advantage of high temperature SOEC over other electrolysis technologies is the capability of converting the CO_2 captured from different sources into high purity CO. Despite this, it must be considered that the impurities in the fuel gas stream are a big issue for SOEC durability and deep cleaning of CO_2 for high impurity is an expensive process therefore it is fundamental to understand the S tolerance concentration limits. Considering this, the influence of CO_2 impurities in BF gases on

SOEC durability was investigated and the S tolerance window for CO_2 electrolysis was identified. In particular, the effect of different H_2S concentrations was assessed performing tests at 700 °C, applying a current density of 0.5 A/cm^2 and a gas composition of 10% CO + 90% CO_2 to the fuel electrode and air to the oxygen electrode. H_2S concentrations lower than 0.09 ppm displayed a degradation behavior similar to the condition without H_2S in the gas stream, but noticeable signs of degradation were detected when H_2S concentration reached values above 0.045 ppm. This degradation was irreversible since no changes were observed after reducing the H_2S concentration. It was concluded that H_2S concentration should be controlled below 0.045 ppm for SOEC to be stable under CO_2 electrolysis.

The influence of oxygen electrode sweep gas on SOEC performance and durability was also assessed since most of the previous studies focused only on fuel electrode. This is of primary importance since O_2 is produced during electrolysis and purging with another gas such as CO_2 could reduce its concentration in the oxygen electrode exhaust gases thus improving safety. Furthermore, this solution could provide a hot oxygen enriched gas that could be directly used in oxy-combustion processes to replace air and eliminate N_2 dilution. Durability tests were performed at 700 °C, applying a current density of -0.5 A/cm^2 and a 10% H_2 + 90% H_2O gas to the fuel electrode. The tests operated for steam electrolysis with air, no gas and CO_2 supplied to the oxygen electrode showed that no extra degradation occurred on the cell without sweep gas, i.e., overall degradation of 264 mV/kh with air and 238 mV/kh with no gas purge, and a slightly lower degradation rate was observed in the last 200 h due to the presence of impurities in the purged air. A higher degradation rate was detected on the cell with CO_2 as oxygen electrode sweep gas, i.e., 464 mV/kh, due to the surface absorption of CO_2 on oxygen electrode which blocked the active reaction site for oxygen evolution. H_2O was omitted from this study since a strong detrimental effect on the cell was detected together with conspicuous energy loss associated with H_2O evaporation at inlet and condensation at the outlet.

Most SOEC operate under ambient pressure, but the use of higher pressures would reduce energy consumption producing pressured H_2. Indeed, pressurization by evaporating liquid water is less energy intensive than pressurizing the produced gas with an improvement of 3-4 % in global efficiency. Considering this, the effect of pressure on SOEC performance and durability was investigated up to values of 15 bar. Increasing pressures had a beneficial effect on cell performance reducing cell area specific resistance. This improvement was overtaken by the increase in open-circuit voltage when current density became lower than 0.8 A/cm^2. Long term tests were performed at a temperature of 700 °C, a current density of 0.375 A/cm^2, with a gas composition of 10% H_2 + 90% H_2O applied to the fuel electrode. The increased pressure was responsible for a fast initial cell voltage increase in the first 300 hours which stabilized afterwards. The impedance analysis revealed that the initial degradation was caused by the increase of cell polarization resistance, which was mainly due to fuel electrode degradation. The overall degradation behavior was like the tests performed at 1bar.

After this huge preliminary characterization of SOEC, the effect of a 5000-hour long term operation under relevant conditions was evaluated to study the occurring degradation mechanism since commercial SOEC generally requires a stable operation for at least five years. Long-term tests were performed at 700 °C and ambient pressure applying a current density of 0.5 A/cm^2, a gas composition of 50% H_2 + 50% H_2O to the fuel electrode and air to the oxygen electrode. Despite a high initial

degradation rate in the first 900 hours with a voltage increase from 1090 to 1330 mV and a degradation rate of 263mV/kh, the cell exhibited nearly zero degradation over the last 4000 hours with a cell voltage stabilization around 1330 mV for the rest of the test. SEM analysis underlined a decrease in cell porosity passing from the fuel gas inlet to the outlet thus confirming the degradation of the fuel electrode.

Another crucial point in the project was DME production and the higher performance of membrane reactors over classical packed-bed reactors was demonstrated thanks to a new generation of carbon membranes which allowed to exceed the conversion rates previously reported in literature. The carbon membranes were first tested in a lab-scale reactor and were then prepared and characterized for the TRL6 production pilot. The experimental lab-scale activity included the comparison of the performance of a packed bed membrane reactor (PBMR) based on carbon molecular sieve membranes with the ones of a conventional packed bed reactor (PBR) for the one-step conversion of CO_2 to DME using a bifunctional catalyst, i.e., a physical mixture of a $CuO/ZnO/Al_2O_3$ catalyst and a HZSM-5 zeolite using a mass ratio of 1. The catalytic tests were performed in a stainless-steel reactor with a diameter of 28.5 mm and a length of 150 mm loaded with 0.25 g of catalyst and 0.75 g of SiC placed in the outer space and characterized by a particle size of 50–125 μm. SiC was necessary to ensure isothermal operations thanks to its good thermal conductivity and to prevent sintering. The reactor presented a top flange for the connection with the membrane tube and was heated via an external jacket. It was also placed in an electric oven to preheat the feed lines. The reaction mixture was analyzed with a compact gas chromatograph. PBR experiments were performed with the same configuration and packing procedure just replacing the membrane with a stainless-steel tube of the same size. Reaction tests were performed in a temperature range of 200–260 °C and a pressure of 40 bar. The feed was a mixture of H_2, CO_2 and N_2 with a H_2/CO_2 molar ratio of 3 or 5 and a GHSV (gas hourly space velocity) ranging from 400 to 2600 $Nl/kg_{cat}h$. A sweep gas ratio ranging from 1 to 5 was also used and reaction performance was evaluated in terms of CO_2 conversion, product yield and selectivity.

DME, methanol and CO yields displayed an increase with temperature when working at 40 bar and with a feed composition of $CO_2/H_2/N_2$ = 3/9/1. Crossover behavior was observed for DME and CO yields at 220 °C with DME yield being higher than CO one for temperatures < 220 °C while for temperatures >220 °C the situation was reversed. The same trend repeated at all H_2:CO_2 ratios with increasing H_2 concentration affecting positively CO_2 conversion and DME selectivity thus shifting the crossover point towards higher temperatures. The further conversion of methanol and DME to olefins on the HSZM-5 zeolite was excluded given the absence of any other C species thus proving the absence of any side reaction. The product yield measured at 250 °C within 40 hours did not show any significant change thus indicating that in these conditions and timespan catalyst deactivation was negligible. PBMR outperformed PBR in most experimental conditions in the one-step CO_2 conversion to DME. In particular, CO_2 conversion proved to be 35-40 % higher and DME yield 16-27 % higher when applying a sweep gas ratio of 1. The benefits were higher at lower GHSV since these conditions approach thermodynamic equilibrium and water formation was more severe making its removal via the membrane more effective. Nevertheless, PBMR improved CO formation more than DME one with an improvement of 75 % in CO yield and of only 27 % in DME yield. This was ascribed to the strong removal of methanol from the reaction zone which limited its conversion into DME. Indeed, methanol

was removed as much as water while CO and DME removal was similar. Better membrane performance and the recirculation of the permeated methanol in the sweep gas would prevent this problem. Larger sweep gas-to-feed ratios increased reaction performance in terms of CO_2 conversion and product yield thanks to a better water removal, i.e., almost 80 % at sweep gas-to-feed ratios of 5. Nevertheless, alongside the removal of water, a considerably amount of all products was removed thus leading to a greater improvement in CO yield, i.e., 122 %, than DME yield, i.e., only 66 %. Finally, temperatures higher than 200 °C proved to improve the WGS (Water Gas Shift) reaction more than DME synthesis leading to a lower DME yield with PBMR than PBR at 260 °C due to significant loss of methanol. Indeed, product removal achieved almost 98–99 % for all species because at higher temperature the reaction rate is very fast (95). DME production intensification through CO_2 hydrogenation could enable both CAPEX and OPEX decrease while reducing CO_2 emissions leading e-DME and by extension e-methanol to competitivity with fossil DME and methanol.

More complex was the scenario for FA production which was investigated in the framework of WP4 where many different catalysts were tested and different experimental apparatus and kinetic studies were performed. The first step was the identification and development of a catalyst able to convert CO_2 into formic acid. Pd and Au were the most popular active metals for the direct hydrogenation route, i.e., $CO_2 + H_2 \rightleftarrows HCOOH$ and $HCOOH + base \rightleftarrows [HCOOH{\cdot}base]$, investigated in literature and their catalytic performance was strongly dependent on the support material used. In particular, Pd performed better with hydrophobic C-based support while Au performed better with hydrophilic support such as Al_2O_3 and TiO_2. The support material is fundamental to increase the number of active sites thanks to a fine dispersion of the active metal, to increase the stability of the catalyst by preventing sintering of the active metal and can alter the electronic structure of the catalyst enhancing its activity. A lab-scale experimental campaign was performed using a commercially available Au/TiO_2 catalyst to study the reaction kinetics using different extraction bases. The gaseous feed consisted of H_2 and CO_2 while the liquid feed consisted of different tertiary amine bases to achieve in-situ extraction of formic acid, lower its activity within the reaction mixture thus shifting its equilibrium and increasing the conversion. The major benefit of this process was the almost negligible reaction time for adduct formation which resulted in an almost instantaneous equilibrium shift. The study focused only on tertiary amines able to create ionic and hydrogen bonds with the formic acid since primary and secondary amines bind covalently with formic acid forming a carbamate that cannot be thermally separated thus complicating the separation process. The use of high-boiling amines was also encouraged to obtain virtually pure formic acid through an amine-exchange method which ensures the formation of salt which can then be decomposed in formic acid and the high-boiling base through distillation. A good solution was identified in trialkyl amines. The main disadvantage of this approach is that the use of this base as the only reactant/solvent did not result in observable reaction due to amine protonation which does not supply sufficient reaction enthalpy. The use of polar hydrogen-bonding solvents such as diols may solve this problem. Several tertiary alkylamines with increasing hydrocarbon chain lengths and with both symmetrical asymmetrical hydrocarbon tails were investigated to gain more insight into the formation of the tertiary alkylamine/formic acid adducts. The results obtained with four different symmetrical trialkylamines, i.e., triethylamine, tributylamine, trihexylamine and triocylamine, showed that formic acid-trialkylamine system exhibited phase separation with the

formation of two distinct layers independently on the hydrocarbon chain length. The upper layer consisted of trialkylamine not binding formic acid while the bottom layer consisted of the adduct phase. A homogeneous mixture was obtained when the molar stoichiometry of FA and trialkylamine was above 1.5. No phase separation was observed for methoxylated/ ethoxylated/propoxylated tertiary amines at any molar stoichiometry, but it was found that the molar stoichiometry of the FA:amine was reduced from 1.5 to 1 thus meaning that these amines can bind less formic acid.

Once completed these preliminary tests on ammines alone, the testing of amine extractants and the produced catalysts was performed. The adduct proved to be nearly insoluble in pure amine leading to a biphasic tertiary alkylamine/formic acid system causing a significant degradation of reaction performance and a negligible conversion. Indeed, adduct inability to dissolve in the non-binding amine resulted in catalyst pores reaching equilibrium readily thus making the system unable to refresh the reagents. The addition of a polar solvent determined an improvement in the performance thanks to the formation of a monophasic system independently of formic acid molar ratio. The addition of a solvent also caused a decrease in formic acid binding capacity with the binding stoichiometry being reduced from 1.5 to 1 molecule of formic acid. 1-decanol was selected as solvent thanks to its high boiling point which should result in an easier removal of the solvent after reaction. Solvent inclusion determined a significant increase in formic acid concentration. Besides the addition of a solvent, biphasic system formation could also be inhibited using ethoxylated/propoxylated amines. The experiment performed using such amines led to significant increase in formic acid yield compared to pure triethylamine. After establishing the protocol for a monophasic reaction mixture with 1-decanol, catalyst stability was investigated by reusing it over a time span of 31 operational days and no significant performance decrease was detected.

The use of different amines was studied by exploiting the principle of microscopic reversibility which allowed to use FA decomposition as model reaction for FA formation. The concept of microscopic reversibility for catalysis states that catalysts are equally good in increasing the forward and backward reaction rate to ensure that reaction equilibrium remains undisturbed. Herein, tertiary amines with superior performance for the backward reaction should theoretically also perform well for the forward reaction. Therefore, the amines were screened by investigating their catalytic performance on FA adduct decomposition. The reactant mixture contained a 1:1 molar ratio of formic acid to triethylamine and a 1:6 volume ratio of triethylamine to decanol to form pure adducts and prevent the presence of pure FA. The reactant mixture was mixed with the catalyst and heated to a constant temperature. The results showed that an increase in hydrocarbon chain length caused a reduction in reaction speeds due to steric hindrance. An asymmetrical amine was used to further investigate this aspect since this configuration ensured a smaller volume of the amine while still providing high boiling point. The results showed that FA decomposition became significantly faster by decreasing the volume occupied by the tertiary amine. As previously discussed, a possible way to avoid solvent use entailed the employment of tertiary amines containing OH-groups. It was found out that hydrocarbon chain length played a less pronounced effect when using alkylamines containing OH-groups than in the case of regular trialkylamines. This would allow to avoid the use of solvents within the reactor while still applying amines having a significantly higher boiling point than FA. Lastly, the performance of OH-group containing amine was compared to the triethylamine used in literature and the performance of the

OH-containing amine and triehtylamine was equal at lower temperatures, while at higher temperatures the triethylamine resulted in higher reaction speeds. Despite the huge amount of data gathered, the catalytic performance during hydrogenation proved to be significantly lower than expected.

Concerning the electrocatalytic reduction of CO_2 to formic acid, it is characterized by the main advantage of operating at ambient pressure and temperature providing also a tradeoff between high faradaic efficiency and high current density. Process selectivity depends on many parameters, e.g., pressure, potential and current density, pH, electrolyte type and concentration, electrode material and morphology and aqueous or non-aqueous solvent, which need to be tailored as a function of the catalyst to optimize the charge transfer and CO_2 diffusion. The most promising catalytic active and selective metals reported in literature were Sn, In, Bi and Co with efficiencies up to 90 %. Among them, In and Bi were selected in the present project since they provided high faradaic efficiency. Furthermore, gas diffusion electrodes (GDE) were studied to optimize the three-phase boundary dynamics where gaseous CO_2 and liquid water were reduced at the solid catalyst surface to formate overcoming CO_2 diffusion limitations through the electrolyte. The catalysts investigated were In_2O_3, ZrO_2- In_2O_3, CeO_2- In_2O_3, Co- In_2O_3, Pd- In_2O_3, Cu- In_2O_3, Ni- In_2O_3, Bi_2O_3 and In-Bi-oxide and were synthesized through flame spray pyrolysis with a size around 5 nm because particles lower than 10 nm contain a high degree of undercoordinated surface atoms which are more active in catalytic reactions. These catalysts were then dispersed in an ink with a Nafion binder, and high surface area conductive C particles to be deposited on GDE and study their electrochemical properties in a flow cell. The effect of C content in the catalyst ink was investigated, and it was observed that increasing C content from 20 to 40 wt.% did not have any significant impact on catalyst activity, but removing C totally had a detrimental effect on the faradaic efficiency. This indicated that the dispersion of catalyst particles over a C particles framework led to a better diffusion of CO_2 on the catalyst surface and to a better conductivity of electrons to the catalyst particles. The results obtained with both In and Bi metal oxide nanoparticles showed excellent efficiencies for CO_2 reduction to formate at industrially relevant current densities. Pure Bi_2O_3 and In_2O_3 displayed very high efficiencies up to 90 % with Bi_2O_3 performing slightly better and at lower overpotential. Doping In_2O_3 with Co, Cu, Pd, CeO2 or ZrO2 did not lead to any improvement in efficiency while the combination of Bi and In decreased the faradaic efficiency. Based on these results, further investigation was mainly devoted to In_2O_3 and Bi_2O_3. The effect of different binder content was also investigated since it influenced GDE conductivity and porosity as well as catalyst stability against sintering. Five different weight ratios of catalyst and C particles to Nafion binder were investigated and a ratio of catalyst particles, C particles and Nafion binder equal to 5:5:3 allowed to obtain the largest efficiency towards formate as well as the largest applied potential. A trade-off between required potential and achieved faradic efficiency was necessary in GDE design for industrial applications depending on cost analysis of the whole process. Once completed GDE optimization, the other process parameters to maximize CO_2 reduction through electrolysis were assessed. Above a CO_2 gas flow of 5 ml/min, i.e. 3 times the CO_2 conversion, the faradic efficiency did not depend on gas flow anymore. Concerning the electrolyte flow, a small increase in faradic efficiency was observed between 25 and 50 ml/min while no further increase was observed above these values. Based on these results, the ratio between liquid and gas flow proved to be more important than the actual value of the gas flow. Indeed, sufficient electrolyte was necessary between

the GDE and the membrane to ensure water at the catalyst as well as good conductivity. Additionally, enough CO_2 was necessary at the catalyst surface without decreasing the conductivity by overfilling the catholyte chamber with gas bubbles. Based on these trends, a 10 ml/min CO_2 flowrate and a 75 ml/min electrolyte flowrate were selected for the 1 cm^2 cell configuration. pH exerted a large influence on faradic efficiency and moving from a pH of 7.5 to a pH of 1, there was almost no formation of formic acid due to the lowered thermodynamic barrier for hydrogen evolution which made water reduction completely replace CO_2 reduction. Analogously, an increase of pH from 7.5 to 10 caused a decrease in faradic efficiency due to the conversion of CO_2 into carbonates rather than into formate. Therefore, the use of highly alkaline solutions caused the consumption of CO_2 and salts without leading to the formation of the desired products. Based on these results, a neutral pH of 7.5 was suggested. Temperature was varied between 25 and 60 °C and a decrease in faradic efficiency was observed for increasing temperatures because CO_2 reduction to formic acid is a slightly exothermic reaction. Furthermore, an increase in temperature determines a decrease in CO_2 solubility by a factor of 3 which may be responsible for a small liquid film depleted of CO_2 at catalyst surface. The effect of pressure was also studied, increasing its value from 1.0 to 2.0 bar and a small increase in faradic efficiency was observed probably due to a change in CO_2 concentration close to the catalyst. The change in faradic efficiency for both pressure and temperature variations was quite small in the order of 5 %. The optimal process parameters for electrochemical CO_2 reduction were neutral media, ambient pressure and temperature.

The C2FUEL project also included some technological innovations related to the two final products considered to cover the whole value chain. In particular, 200 hours DME combustion tests were performed to demonstrate the feasibility of this e-fuel on a diesel-adapted engine with competitive efficiency and promising emissions. Furthermore, the technical feasibility of a FA-to-Power genset was demonstrated in outdoor conditions thanks to the design and building of a first prototype which allowed the construction and validation of a new genset in another project with a net output power of 25 kW.

3.2.11 RETROFEED: Implementation of a smart RETROfitting framework in the process industry towards its operation with variable, biobased and circular FEEDstock (96)

The project was coordinated by CIRCE (Centro de investigacion de recursos y consumos energeticos), with AIMEN (Asociación de Investigación Metalúrgica del Noroeste), Instytut Energetyki, IVL Svenska Miljöinstitutet, EEIP (Energy Efficiency in Industrial Processes), Geonardo, ODYS, OPTIT, Torrecid, SECIL, ASAŞ, Ferriere Nord, Fertiberia, Sistem Teknik, RINA Consulting - CSM, HTT Engineering, and Silcotub participating as partners in the consortium. The project started on the 1st of November 2019 and lasted almost four years, ending on the 31st of October 2023. The overall project cost 15.5 M€ and the EU contributed 9.9 M€, i.e., about 65 % of the budget.

The main objective of the RETROFEED project was to enable the use of an increasingly variable, bio-based and circular feedstock in process industries through the retrofitting of core equipment and the implementation of an advanced monitoring and control system. It would also provide support to plant

operators by means of a decision support systems covering the production chain. This approach was demonstrated in five resource and energy intensive sectors, i.e., ceramic, cement, aluminum, steel, and agrochemical, with the potential to reach an average increase of 22 % in resource efficiency and 19 % in energy efficiency with a consequent reduction in costs and GHG emissions of 9.3 M€ and 135 kton CO_2, respectively. The project aimed to develop a methodology to support retrofitting in resource and energy intensive industries complemented by a decision support system able to perform a diagnosis of the impact in the process of different retrofitting solutions so plant managers and operators could decide on the most suitable retrofitting action for their companies. This decision support system remained operative after the modification of the process so it could ease the operation of the process under the increased variability of feedstock by analyzing a set of key indicators defined within RETROFEED over the production chain for this purpose. RETROFEED not only enabled technological advances in the technologies and demonstrators involved but also contributed to the development of new standards, regulations, training programs, adaptation and certification of industrial processes thus facilitating the replication of the project results within the EU industry.

To achieve the objective of the project, RETROFEED developed a digital twin of the core process equipment for all demo sites to characterize the behavior of the equipment and analyze the impact of several retrofitting scenarios and the modification of the process conditions without affecting the product quality. The project demonstrated that the solutions proposed increased the amount of waste and recycled material that could be feed into the processes of ASAŞ, Torrecid and Fertiberia. Furthermore, it boosted the use of bio-based materials to reduce their fossil fuel reliance in SECIL, Ferriere Nord and Silcotub. It also allowed to improve the existing control systems in the plant by acting in two levels. The first one concerned the design of new control loops and the second one the design of the control commands on the new actuators to allow a more precise and rapid response. A holistic decision support system tool was developed by integrating the advanced models developed for each demonstrator to fully exploit the information provided about the process energy and material flows and overall performances. Finally, a replication methodology was prepared and an analysis of technical and non-technical barriers, policy recommendations, an environmental framework and a capacity building program to ensure a proper transfer of the project outcomes was performed. RETROFEED aimed at providing industries with strategies and engineering tools to help them meet their sustainability goals. A preliminary estimation of the impacts of the retrofitting activities was 20 % increases in resource and energy utilization efficiencies, and average reductions GHGs and fossil-based sources reliance of 30 and 20 %, respectively, resulting in mean operating expenses savings of 30 % and likewise, mean productivity increases of 20 %.

Many different achievements were accomplished for each demo case. Concerning Torrecid, both the digital twin and decision support system were tested and validated. Furthermore, the retrofitted heat recuperator was installed and validated by melting 9 different frits in the retrofitted furnace and the results highlighted an improved high temperature recuperator. The digital twin and decision support system were tested also in SECIL as well as the satellite burners. The latter were installed and tested together with the related sensors, allowing to use higher rates of refuse derived fuel. In ASAŞ, the digital twin and decision support system were tested and validated while the oxygen lance was designed and constructed together with the O_2 level measurement system and the delacquering system with

the related control system. The activity performed at Ferriere Nord and Silcotub included again the testing of the digital twin and decision support system and were accompanied by the design and construction of the innovative burner by HTT and the CFD simulations by CSM. Feasibility study of waste heat utilization was also performed. In Fertiberia, detailed engineering of the novel reactor and the preparation for the relative commissioning was accompanied by pilot plant tests and digital twin and decision support system testing. The correct performance of the RETROFEED solutions proposed in each demo sites were fine-tuned, and their replicability potential was analyzed.

A set of performance indicators were defined and their values assigned prior to and after retrofitting. For Torrecid, the retrofitting actions increased energy and material savings through the optimization of fuel usage, air thermal conditions for combustion, drying, and regulation of water flows. Moreover, a 4-to-6-fold reduction of material waste during the time between load changes was achieved, leading to an increment in furnace productivity. Moving to SECIL, the optimization of combustion performance through modelling and enhancement of the monitoring and control system, together with the integration of a new drying frits strategy decreased the emissions generation during frits manufacturing. The retrofitting solutions promoted a reduction of CO_2 emissions through fossil fuel switching for biobased counterparts attempting to substitute between 60 and 80 % of the thermal energy required for calcination. At the same time, a reduction of at least 5 % of the specific energy consumption was expected through a greater degree of control over kiln thermal conditions. Moreover, the new strategies led to an increment of energy efficiency without altering the product quality and productivity. The improvement of the monitoring and control system allowed a faster response over the system when variable feedstock was introduced, optimizing clinker production. In ASAS, the share of scraps to be used for smelting was expected to experience roughly a 50 % increase, reducing primary Al consumption. This substitution together with the modifications of the delacquering unit significantly affected the energy toll of the process. The new conditions required about 15 times less energy than current practices. In addition, the new O_2 injector and the new sensors ensured more efficient combustion and emissions generation conditions to maintain product quality and exert greater control over the exhaust gas composition. The retrofitting actions in Ferriere Nord reduced GHG emissions thanks to the more sustainable feedstock incorporated, integrating circular economy concepts and bio-based sources. The degree of substitution of the traditional feedstocks was the maximum admissible by the process without altering productivity or product quality. Similarly, the main results expected in Silcotub were related to raw materials reclamation from waste containing lime, C and Fe. This way, the landfilling residues and costs were minimized together with capital expenses associated with feedstock purchasing. Fertiberia gained greater raw material supply flexibility after retrofitting thus providing higher feedstock autonomy. This approach also led to a reduction in indirect and direct costs with modifications attempting to substitute at least 10 % of the currently employed P sources, simultaneously cutting back on costs since prices of the alternative feedstocks were estimated at roughly half the value corresponding to their conventional counterparts. P recovery was also in line with EU objectives under the Action Plan on Circular Economy, to secure reliable access to Critical Raw Materials. Energy resources were positively affected through the process of retrofitting, since the heat generating reaction to be incorporated in the fertilizer production line, had an energy yield 3 times greater than the currently employed pathway. New sensors were implemented in the system to

accomplish an improved performance of the plant under the new conditions and avoid negatively influencing the amount of rejected product.

The final impacts of the project included an increase of 23 % in resources efficiency, of 8 % in energy efficiency and of 17 % in productivity together with a reduction of 8 % in GHG emissions, of 23 % in the utilization of fossil resources and of 3 % in OPEX. Modelling and simulation through the development of digital twin and decision support system implemented increased helped to improve control capabilities and overall plant performance. Sensors & control system created improved monitoring of the plant conditions. A more sustainable use of feedstock was achieved with Torrecid reducing feedstock waste, SECIL increasing the use of refuse derived fuel, ASAŞ increasing scrap used, Ferriere Nord and Silcotub using plastic byproducts as new feedstock and Fertiberia using ashes as P alternative.

3.2.12 CORALIS: Creation Of new value chain Relations through novel Approaches facilitating Long-term Industrial Symbiosis (97)

The project was coordinated by CIRCE with Fertiberia, Quimica del Estroncio (QSr), INCRO, AZCATEC Tecnologia e Ingenieria, RISE, WA3RM, Regenergy Kullabygden, Linkopings Universitet, Hoganas, RINA-Consulting CSM, Confindustria Brescia, ORI Martin, Raffmetal, Fonderia di Torbole, Feralpi Siderurgica, SIDENOR Aceros Especiales, Energieinstitut an der Johannes Kepler Universitat Linz, LAT Nitrogen Linz, Borealis Polyolefine, Voestalpine Stahl, K1-MET, TUPRAS (Turkiye Petrol Rafinerileri Anonim Sirketi), IMMIB (Istanbul Maden Ve Metaller Ihracatci Birlkleri), ICCS (Erevnitiko Panepistimiako Institouto Systimaton Epikoinonion kai Ypologiston), EEIP, RINA-Consulting, SSSA, White Research, European Aluminium, IMA-Europe (Industrial Minerals Association-Europe) participating as partners in the consortium. The project started on the 1st of October 2020 and lasted almost four and a half years, ending on the 31st of March 2025. The overall project cost 22.5 M€ and the EU contributed 17.9 M€, i.e., almost 80 % of the budget.

The 4-year Horizon 2020 CORALIS was designed as a demonstration project and addressed the key challenge of implementing real Industrial Symbiosis solutions. In particular, the project tackled the three main barriers which normally slow down and hinder IS: technical, economic, and managerial. CORALIS aimed to decarbonize resource and energy intensive sector value chain through the implementation of viable IS solutions by combining innovative technologies with new business strategies. CORALIS also aimed to deepen the understanding of IS performance, strengthen the IS facilitator role and develop monitoring and data-sharing tools, enhance IS sustainability via improved business models and economic methods, implement novel IS value chains in real settings, and promote IS through awareness, stakeholder cooperation, and contributions to standardization and policy. CORALIS allowed to build three demonstration sites and three follower sites across different industrial sectors which allowed to generate practical knowledge to support future IS initiatives thus promoting resource and energy efficiency and contributing to environmental, economic, and social sustainability. The first demo site was the Escombreras Lighthouse in Spain which was developed to readapt the fertilizer production process of KNO_3, $Ca(NO_3)_2$, $Mg(NO_3)_2$, $Sr(NO_3)_2$, $SrCO_3$, $(NH_4)_2SO_4$ and NH_4NO_3 in QSr by replacing imported raw material such as HCl and $CaCO_3$ utilizing the CO_2

produced from surrounding industries and reducing wastewater discharge and water consumption. The second demo site was the Frövi Lighthouse in Sweden which aimed to bring into full operation a full-scale 10-hectare greenhouse supplied with low temperature waste heat from a pulp and paper mill. The demo site allowed to demonstrate the physical feasibility of the industrial symbiosis, as well as the business feasibility between the parties involved including the anchor industry, the enabling intermediary WA3RM, the greenhouse grower, financers and the local community. The last demo case was the Brescia Lighthouse in Italy which involved ORI Martin, Raffmetal, Fonderia di Torbole and Feralpi Siderurgica, i.e., two steelworks, a cast iron industry and an aluminum producer.

This demo case was the one of main interest for the present document purposes being the one focused on the iron and steel sector. In particular, the main aim of the demo site was to enable the recovery of industrial materials to be used as alternative feedstock to reduce the landfilling ratio considering that the companies involved were landfilling about 50 % of the metal powder, oxides and other industrial waste with high metallic content before the CORALIS project. The initial objective was to implement technologies which should have enabled the 100 % recovery of these wastes by exchanging them among the companies involved to achieve a reduction in pig iron and Al consumption up to 10,000 and 500 t/year, respectively. To this end, the residues produced in the four companies were treated with four new technologies to recover metal introduced in the companies to demonstrate the feasibility of the collaborative scheme for transforming industrial residues into raw materials for others or, eventually, recycled internally. Furthermore, the interaction with rural communities was fostered to analyze bioresources that could replace carbon fractions in these companies. The overall collaborative scheme to ensure the correct valorization of the industrial waste through the exchange between the four industries is shown in Figure 42.

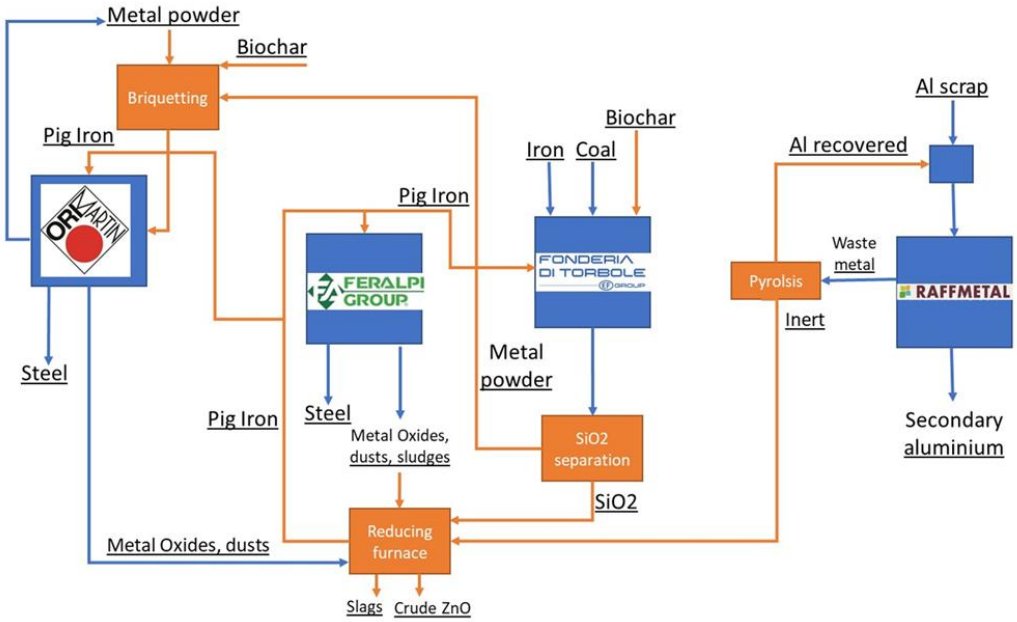

Figure 42: Schematization of the collaborative scheme for industrial waste exchange and valorization between the four companies

Going more into detail, Ori Martin set up a process for the internal recovery of waste, e.g., scales, sludges, and metal residues, which could easily incorporate similar residues generated by external steelmakers or other manufacturing lines. The process was based on the installation of a briquetting unit to produce briquettes with suitable composition and, in a future prospective, metal residues could be collected also from local metal producers and manufacturing, e.g., recovered metal powder for pig iron and steel production. In particular, the briquetting unit installed at ORI Martin to recover the metal powder was characterized by 12000 t/y productivity. Concerning Torbole, the industry started to design an industrial process to separate fine metals and silica, i.e., SiO_2, from sand blasting operations because both fractions could be conveniently reused despite containing a certain percentage of the other components. In particular, the 3000 ton/y separation unit installed at Torbole allowed to obtain metal powder as alternative raw material and SiO_2 as reducing agent. In addition, some preliminary analysis was performed to evaluate the potential substitution of fossil-based carbon with biochar to carburize the melt bath, but many issues were identified and need to be faced before potential industrialization of this practice. Moving to Feralpi, the company developed a process based on a reducing furnace of 40000 t/y to recover the metal fractions from residual oxides, dust and sludges that enable the substitution of pig iron, and scrap. Feralpi with the support of the external partner Epiros developed a process for the ferroalloy production and the recovery of metal oxides. Finally, Raffmetal performed a deep experimental campaign both at the laboratory and pilot scale to develop an innovative pyrolysis unit that treats internal residue for the heat generation and the recovery of residual Al not oxidated. In particular, the pyrolysis unit is an energy self-sustained pyrolysis unit of 2000 t/y which allows the recovery of Al and the provision of the solid inert residue as reducing agent. The results obtained from the Brescia lighthouse demonstrated the feasibility of synergies at regional level for waste landfilling prevention and metallic or oxide residues valorization. Potentially reusable residues were generated not only inside the Brescia IS, but also by small local producers and a suitable collection of materials can be the next step to improve the IS realization. Indeed, evident economic and environmental benefits clearly emerged during the project such as the use of recyclable materials, e.g., metals, slags, sludges, ashes, the reduction of waste disposal, the slight reduction in the use of virgin materials.

The first conclusion which can be drawn from the Brescia demo case concerns the volumes and the characteristics of the collected waste which are very variable thus making necessary a more accurate standardization to ensure the development of a future symbiosis on the industrial scale. Furthermore, it was observed that it is fundamental that all partners in the IS start at the same TRL (Technology Readiness Level) because strong differences in the knowledge of the adopted technologies or process can become a bottleneck for the completion of the whole symbiosis. Furthermore, it was observed that the presence of a facilitator in the regional consortium was fundamental to drive synergistic opportunities. Indeed, the facilitator, i.e., RINA-CSM, helped to deliver more rapid progress with respect to a project leader which often undertakes ongoing business as usual commitments.

3.2.13 INITIATE: Innovative industrial transformation of the steel and chemical industries of Europe (98)

The project was coordinated by TNO, with ArcelorMittal, CO2 Value Europe, Johnson Matthey, Kisuma Chemicals, KT Tech, Politecnico di Milano, Radboud Universiteit, SSAB, Stamicarbon and Swerim participating as partners in the consortium. The project started on the 1st of November 2020 and lasts almost five and a half years, ending on the 30th of April 2026. The overall project cost 25.11 M€ and the EU contributed 21.3 M€, i.e., almost 85 % of the budget.

The INITIATE project aims to advance the implementation of circular economy, industrial symbiosis and CCU by re-using residual steel gases as a resource for a cross-sectorial, more efficient and less wasteful manufacture of urea at a significantly reduced carbon footprint. Based on the prior experience of the STEPWISE and FRESME projects, INITIATE aims to achieve a positive business case while proving reductions in primary energy intensity, carbon footprint, primary raw material intensity, waste generation, etc. Both steel and fertilizer markets are growing in the decades while they are facing the urgent need to transform into CO_2 neutral sectors since they are responsible for 30 % of industrial C emission and more than 4% of annual global GDP (Gross Domestic Product). The INITIATE industrial symbiosis approach schematized in Figure 43 aims to directly contribute to reduce emission, energy and raw material use since carbon capture, re-use and storage are sustained by generating added value products such as NH_3 and urea. The project targeted a 30 % decrease in primary energy use, a 40 % decrease in raw material demand and up to 90 % reduction in direct CO_2 emissions as shown in the graphs reported in Figure 44. Additional benefits are the provision of grid balancing services through flexible use of green H_2 and by proving CO_2 for circular use, accelerating the transition towards locally closed loop and integrated renewable energy systems.

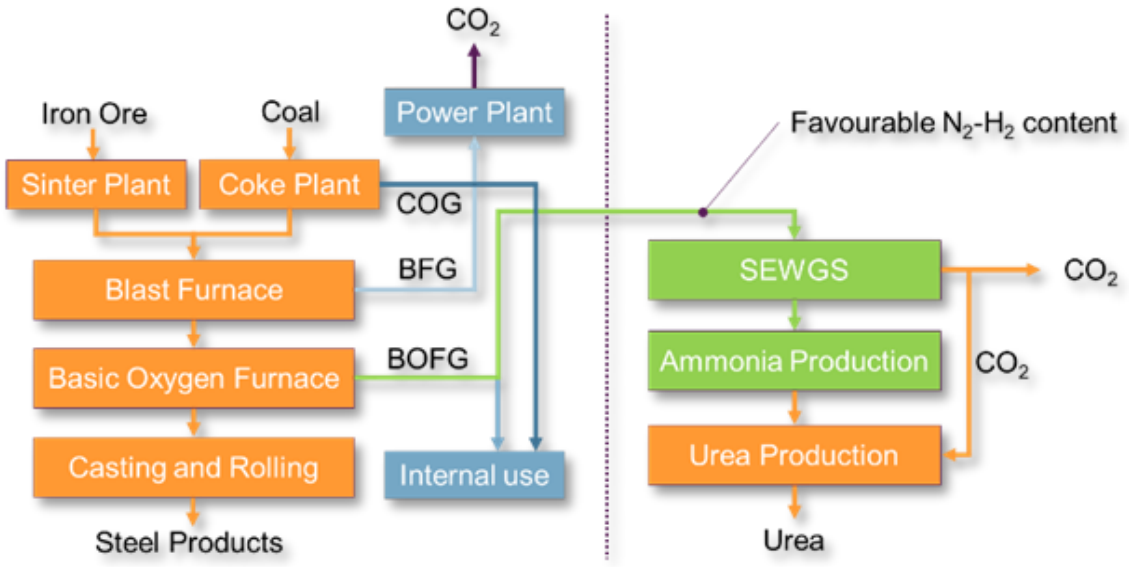

Figure 43: Schematization of the industrial symbiotic approach proposed by the INITIATE project

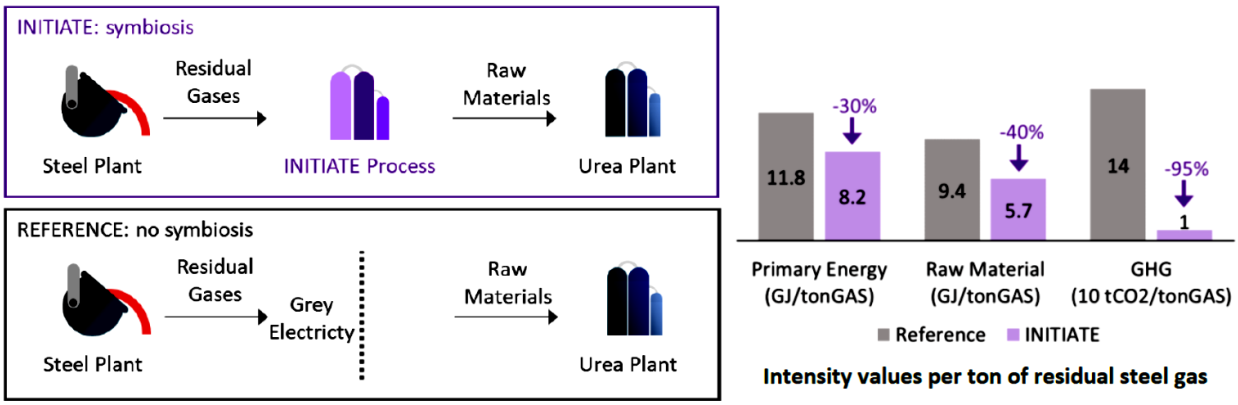

Figure 44: Comparison between INITIATE approach and reference process.

The INITIATE project takes all necessary steps to provide the basis for the roll-out of a first commercial size demonstrator of 50 kt/y of urea produced from BOF gases. The operational reliability of the technological innovations is demonstrated in a pilot plant at TRL7. Additionally, the energy, economic and environmental advantages are assessed via the verification of the KPIs of the concept and comparing them with a base case without CO2 removal and a reference case that use amine-based CO2 removal technology. Furthermore, a bankable design of the First-Of-A-Kind (FOAK) commercial plant is made to convert BOF gases to AdBlue® and/or another NH3 based product. The development of a long-term implementation plan ensures successful implementation beyond the FOAK plant. The synergies on local and European scale are identified considering industrial infrastructures and other symbiotic systems. As part of the implementation plan, stakeholder alignment is required and licensing strategies are developed to ensure successful future deployment.

The project included many steps to prepare for the final pre-design of a FOAK at the end of the project. The project started with the lab-scale validation and selection of the functional materials taking BOF gases dynamics and typical contaminant types and levels into account. Besides pilot demonstration, this allows transferability of the concept to other locations and other qualities of steel gasses. A dynamic digital twin was also developed to replicate the INITIATE concept to other sites. The digital twin includes a model to learn BOF gases dynamics and specific composition. The functional materials were produced using industrial scale facilities. Two key technologies will be validated in the pilot plant at TRL-7 which are the SEWGS process shown in Figure 45 and the sub-stoichiometric NH_3 conversion loop.

The techno-economic assessment performed compared the small-scale INITIATE implementation using BOF gases for NH_3/urea production at 224 t_{NH3}/d and the large-scale INITIATE implementation using BF and BOF gases at 1500 t_{NH3}/d with their base and reference cases. The base and reference cases represent the individual industries without and with conventional carbon capture and storage implemented, respectively. Concerning the emissions, Figure 46 summarizes the CO_2 avoidance and SPECCA (Specific primary energy consumption per unit of CO_2) for reference and INITIATE cases as a function of the electricity CO_2 footprint. Indeed, INITIATE provides strong benefits in terms of primary energy savings when electricity with a CO_2 footprint below 200 kg_{CO2}/MWh is imported.

SPECCA as low as 2.5 GJ/t_{CO2} means that both primary energy consumptions and CO_2 emissions are reduced. The environmental assessment shows that INITIATE reduces the climate change impacts from 2.4 t_{CO2}/t_{HRC} for a plant producing 3.1 Mt/y HRC steel and 0.49 Mt/y urea, down to 1.06 t_{CO2}/t_{HRC} assuming the 2030 scenario to be further reduced to 0.805 t_{CO2}/t_{HRC} in the 2050 scenario. Similarly, the INITIATE symbiosis reduces ecosystem damage and human health damage by 40 % and by 20 % compared to conventional steel production, respectively.

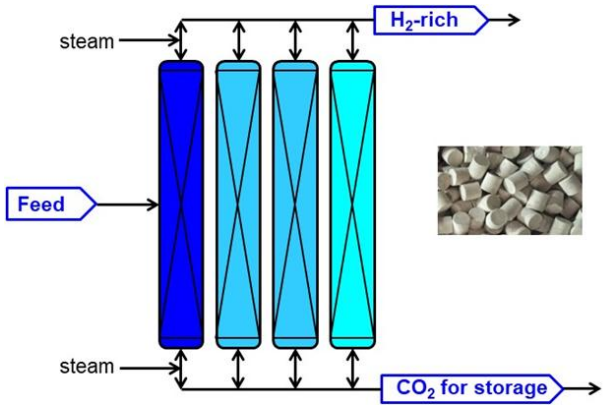

Figure 45: Schematic diagram of SEWGS process

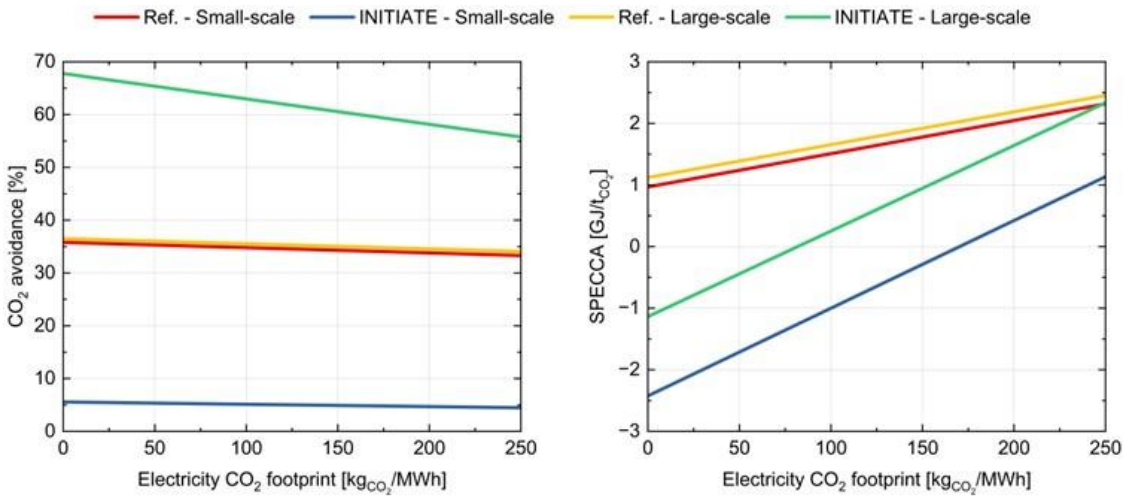

Figure 46: CO_2 avoidance and SPECCA for reference and INITIATE cases as a function of the electricity CO_2 footprint.

The economic assessment whose results are summarized in Figure 47 shows that the symbiosis case using only BOF gases is always more convenient than the reference case regardless the assumed cost of electricity and natural gas. Cost of CO_2 avoided could be negative for natural gas prices above 100 €/MWh. When considering both BF and BOF as gases for the symbiosis, INITIATE is more convenient

at electricity prices around 50 €/MWh with cost of CO_2 avoided below 80 €/t_{CO2}. The lower the electricity price the more convenient the concept.

As part of the long-term implementation plan the key costs, benefits and uncertainties were analysed and the main results are reported in Figure 48. The business case is positive as the benefits are potentially larger than the costs although the uncertainties in the costs and benefits are rather large. On the main uncertain key cost does not relate to the implementation of the SEWGS technology, but to the costs for CO_2 transport and storage. The large uncertainties in the benefits relate to ETS (Emissions Trading System) pricing of the CO_2 related to the BF and BOF gases use and the prevented natural gas consumption that is related to the conventional NH_3/urea. Moreover, the uncertainty of increased benefits due to CO_2 pricing and prevented natural gas use in the future scenarios outweighs the uncertainty of transport and storage costs. It is therefore expected that when CO_2 transport and storage develops in time, their costs decrease, while the ETS CO_2 pricing and natural gas pricing increases, leading to an even higher net benefit. It is observed that all main uncertainties depend on the development of legislation, guidelines and norms. A very important factor is the CO_2 price once the free allowances are reduced to 0 towards 2034.

In conclusion, the INITIATE concept eliminates a substantial amount of natural gas feedstock for NH_3/urea production by utilizing the steel gases, even when accounting natural gas imports to compensate the steel production energy requirements. It allows room for renewable energy penetration, and the concept allows flexibility to the grid via dynamic H_2 addition to the C-rich BF gas by electrolyzer systems, while the NH3 product can be dynamically stored. The captured CO_2 is partially reused for urea production while the remaining CO_2 is intended for other re-use cases or for sequestration. The digital twin, together with the understanding of the type and levels of impurities in the steel gases and their abatement options ensure the replication potential of the concept. Accordingly, the concept takes the future shift from the BF-BOF route towards the DRI/EAF-BOF route into account.

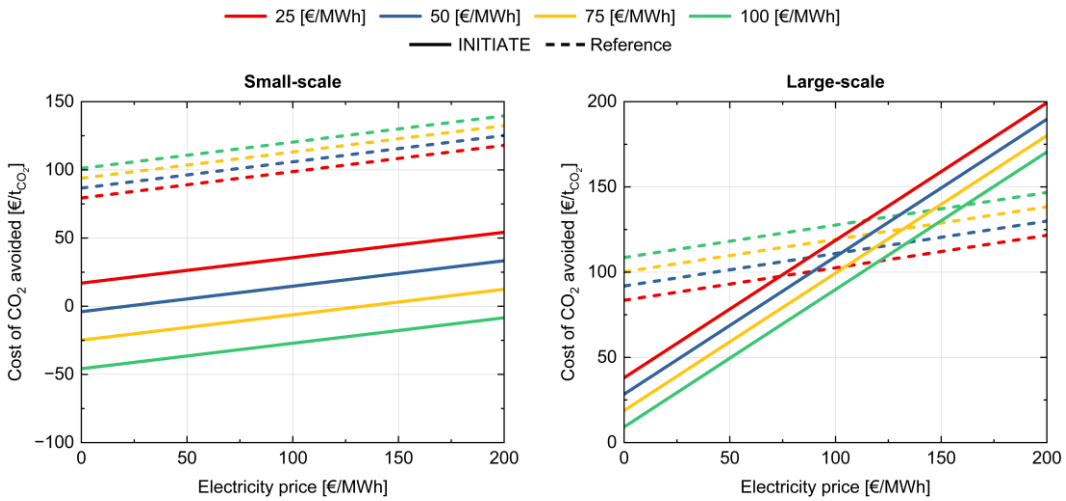

Figure 47: Cost of CO_2 avoided for reference and INITIATE cases as a function of the electricity and natural gas prices

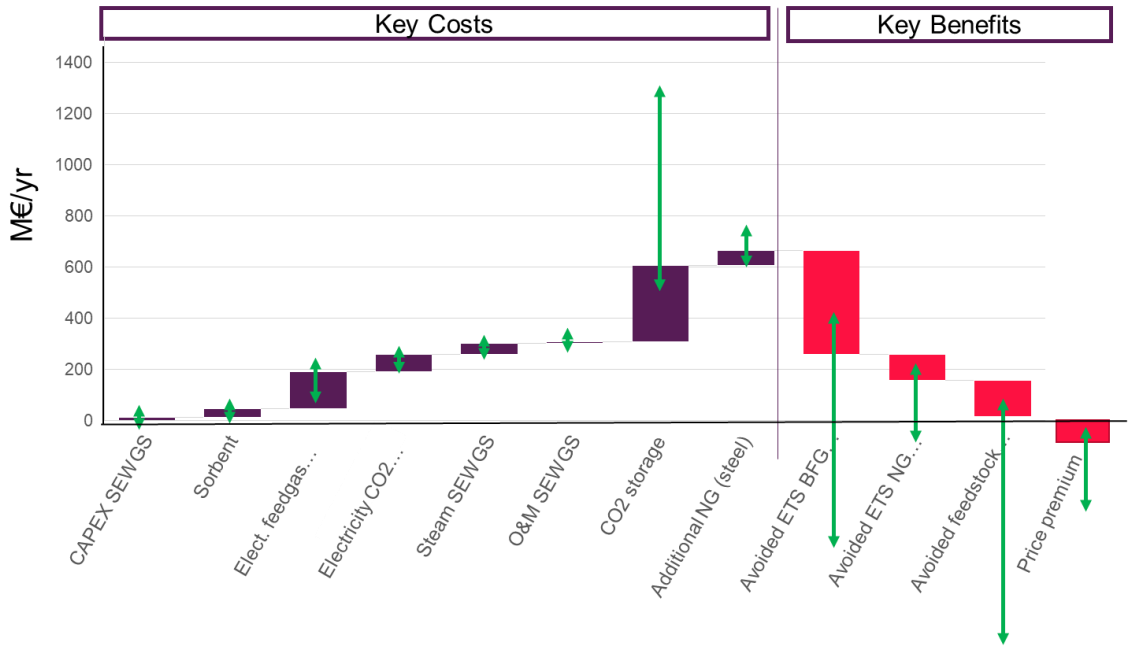

Figure 48: Overview of the key costs and key benefits for the implementation of the INITIATE concept.

3.2.14 REVaMP: Retrofitting Equipment for Efficient Use of Variable Feedstock in Metal Making Processes

The project was coordinated by BFI with Narodowe Centrum Badań Jądrowych (NCBJ), zastawny henryk Wojciech, Ośrodek techniki jądrowej-Polon, Fraunhofer-Gesellschaft, LSA - Laser Analytical Systems & Automation, Arcelormittal, Sidenor, Eurecat, Grupal Art, Fundacion Azterlan, GHI Hornos Industriales, Refineria de Aluminio, RWTH, Fundacion Cartif and Exide Technoogies participating as partners in the consortium. The project started on the 1st of January 2020 and lasts almost four years, ending on the 31st of December 2023. The overall project cost 9.9 M€ and the EU contributed 7.93 M€, i.e., almost 80 % of the budget.

The global metal recycling industry was estimated at 250 billion€ in 2020 and displayed an unprecedented growing rate thanks to increasing circular economy awareness and to the need of metal manufacturers to reduce the environmental footprint. European metal production plants need to be retrofitted with appropriate sensors for scrap analysis and furnace operation to meet this growing demand and to face the increasing variability in feedstock quality. The REVaMP project tried to address this challenge by developing and applying new retrofitting technologies including high-tech sensors for metal scrap characterization, new process control and decision support tools to improve the selection of feedstock in terms of both material and energy efficiency. In particular, the high-tech sensors developed within the REVaMP project enabled the analysis of metal scrap in the bulk form for the first time thus ensuring their correct processing to achieve high quality products with less materials and energy. In particular, in-line sensors based on prompt gamma neutron activation analysis (PGNAA) and

LIBS were used for bulk analysis of metal scraps in large containers, e.g., trucks. The latter coupled with appropriate statistical method allowed a comprehensive characterization of the scrap types in use enabling industries to use cheaper low-quality scrap while maintaining product quality thus also reducing the reliance on primary raw materials.

The technologies developed included a smart LIBS sensor system and two different set-ups of a neutron sensor to characterize metal scrap in terms of chemical composition in steel, Al and Pb plants leading to the establishment of three use cases, i.e., EAF steel making based on scarps, Al refining and Pb recycling, at five plants. A smart LIBS sensor for the surface chemical analysis of metal scrap was tested on site on Al scrap and Pb recycling material transported on a conveyor belt and on steel scrap in large containers. It was successful providing accurate results on the composition for most relevant elements. Analogously, a truck sensor using a switchable neutron generator was applied to the bulk analysis of different steel scraps in large containers showing promising results in the analysis of relevant elements. Furthermore, a large sample neutron activation sensor based on the PGNAA principle was applied for bulk analysis of Al chips transported through a pipe and it displayed good accuracy for most relevant elements. In the framework of the aluminum use case, a multi-measurement system called Alu-Q® and a preheating system were also developed. The Alu-Q® system was designed to determine simultaneously the quality of liquid Al alloys with respect to material density, inclusions and mechanical analysis while the preheating system was supposed to use waste derived fuels and was installed at an instrumented pilot rotary furnace in an Al refining plant, but scrap preheating trials were performed based on natural gas just to evaluate the energy saving potential. Furthermore, a software tool for feedstock characterization was developed and applied for optimization of the charge material mix together with a model-based monitoring system to supervise the process and detect anomalies. Finally, the control systems to optimize the processes for energy and material efficient metal production were industrially applied and tested.

The three use cases which applied the optimal charge mix tool and the model-based control system achieved a reduction in energy consumption, emissions, material use, and the cost related to the materials. For example, the consumption of natural gas in the melting furnace for Al refining was reduced by 15 % thus leading to a reduction of 5 % in CO_2 emissions while the overall CO_2 of Al refining decreased around 2 %. The CO_2 emissions reached values of 5.9 % for electric steelmaking and of 8.7 % for Pb production. Furthermore, a reduction in the costs of pure Al alloy consumption around 3-18 % and an improvement in resource efficiency of 10 % were observed. The latter was lower around 5 % for the Pb sector and of just 1 % for steelmaking. An optimized selection of lead bullion in the Pb recycling sector allowed to save about 1 tonne/year. In the framework of the Al use case a scrap preheating system was also developed as pilot plant. Finally, an economic and ecological evaluation of the retrofitting solutions benefits was performed together with a cross-sectorial transferability analysis. Indeed, the greatest merit of most of the developed retrofitting technologies was that they could be easily adapted and applied in other energy intensive industries that exploit secondary raw materials as feedstock. The economic analysis highlighted that all use cases were characterized by a payback period of the retrofitting solutions well below 5 years. Furthermore, reduced OPEX costs and increased productivity were guaranteed by the increased use of low-quality scrap allowing to achieve saving values of 2.47 €/t for oxygen steelmaking, 5.46 €/t for Pb production

and 14.64 €/ t for electric steelmaking. For Al refining OPEX savings lie around 2 %. Grupal Art experienced a decrease of 13.7 % in gas consumption (Nm^3/t), 13.3 % in energy consumption (kWh/t), 8.3 % in oxygen consumption (Nm^3/t), 22.6 % in Cu consumption (kg/t), 11.2 % in Ti consumption (kg/t) and 15.1 % in Ni consumption (kg/t). Concerning Refial, it was estimated that the operational cost by ton of alloy ENAC 46000 would decrease from 13.34€/t to 10.67€/t with the new retrofitting solution.

A first fundamental step for the project concerned the assessment of the variability in material and energy feedstock for the different use cases to identify potential challenges for retrofitting. Traditional and alternative input materials and energy feedstocks for steel, Al and Pb furnaces were analyzed pointing out elements of interest such as tramp elements and valuable alloying elements and establishing metal refining/alloying requirements such as micro addition. Focusing on steelmaking, both electric steelmaking at Sidenor and oxygen steelmaking at ArcelorMittal were addressed. The assessment of feedstock variability at Sidenor focused on steel scrap from three different origins, i.e., post-consumer scrap, pre-consumer scrap and internal recovery such as rolling mills. Post consumer scrap derives mainly from old industrial buildings, obsolete machinery, railway, car and naval scrap, while pre-consumer scrap derives mainly from all those industries that use steel as raw material in their manufacturing process and is usually very clean, characterized by a lower variability and by higher costs. Other charge materials available in the market are pig iron from BF and high briquetted iron. Pig iron has a high C content and a considerable amount of Si which requires higher oxygen consumption during melting and an early charge into the furnace to avoid longer processing times for complete decarburization. High briquetted iron is characterized by a very low residual content, but it tends to break and originate fines which results in a lower yield. The chemical composition of 11 steel grades was analyzed considering both alloying and tramp elements. Focusing on alloying elements, Mn is the alloying element most used besides C since it provides significant hardening by solid solution and greatly improves hardenability. Its low price compared to other alloying elements makes it less economically interesting for charge optimization. Another important alloying element is Cr thanks to its hardenability properties and secondary hardening by carbides formation. Its economic value is much higher than Mn one but is lower than Ni one. The latter allows to increase toughness and to reduce cracks and quenching distortions. Differently from Cr and Mn, it is not oxidized during EAF process, but its high price makes necessary a good characterization on the internal recovery from the scrap. The latter alloying element to consider is Mo which exerts a stronger effect in improving hardenability than Cr and Ni. It is commonly used for case hardening steel grades and quenching and tempering grades and has a higher price than Cr and Ni. Moving to tramp elements, Cu is one of the most important elements to control when designing the scrap mix to be fed in EAF since all Cu introduced in the process cannot be removed from the steel. Although its content is lower than Cu, Sn comes with scrap as common protective layer and causes hot shortness defects. S is normally considered detrimental due to its low solubility in the steel which leads to the formation of sulfides with low melting point and embrittlement effect at high temperature. It can be removed in the secondary metallurgical process, but an optimization of its amount in the scrap charge may allow to increase productivity reducing the time required for desulphurization. P is another detrimental element which can be removed only under the oxidizing conditions provided during the refining stage at EAF. Another

fundamental point to consider is the metallic yield obtained depending on the steel grade considered since Fe and other elements such as Cr can be lost in exhaust dust and slag.

Moving to oxygen steelmaking at ArcelorMittal, the scrap types used could be grouped into the three groups already defined for Sidenor, i.e., post-consumer scrap, pre-consumer scrap and internal recoveries, but in contrast to electric steelmaking in oxygen steelmaking only 20 % of scraps is charged into the BOF converter. In this case, scrap mix optimization was dedicated to maximize the amount of post-consumed scrap thanks to their lower price while limiting the amounts of tramp elements by adding pre-consumer scrap and internal recoveries. The chemical composition of 18 scrap type was analyzed considering the 8 elements already considered for Sidenor. The post-consumer scrap types displayed the highest contamination with Cu and Sn. Cu, Cr, Ni, Mo and Sn must be strictly limited already in the phase of charge mix selection since they cannot be sufficiently or not at all removed from the steel during the processes. This is particularly important for Cu, Cr and Ni since they have the highest variability in post-consumer scrap types.

Concerning the analysis of Al feedstock variability, it was performed by Grupal Art which is specialized in recycling and treating Al chips to obtain Al ingots of different alloys. Concerning the element to monitor, Si was the least concerning one since all the casting alloys produced by Grupal Art had at least 5 % Si. Cu is another common alloying element in Al alloys, and it is common to find high concentration in the chip feedstock, but its level must be accurately controlled since many alloys produced by Grupal Art did not require it. Similarly, Mg is commonly used in wrought alloys, but it was present in much lower levels in the casting alloys produced by Grupal Art until becoming an impurity in some cases. Same conclusion can be drawn for Pb which is used in some wrought Al alloys at levels around 0.5 % to improve machinability, but it was regarded as an impurity in all the casting alloys produced by Grupal Art and must keep below 0.05-0.35 %. Ti is typically used as grain refiner at concentrations below 0.15 % in both wrought and casting alloys and it was not a big concern as most of Grupal Art alloys accepted levels up to 0.2 or 0.25 %, but efficient tailoring of the scrap may allow some cost reduction. Mn and Zn are commonly used in some wrought and casting alloys, but they are considered as impurities in all other alloys, therefore their levels must be controlled to use Mn and Zn rich feedstock to produce those Al alloys that required them. Fe is always considered as an impurity playing a detrimental effect on the ductility of the alloy and can be present in the Al chips feedstock due to the machining tools used to treat them which are made in steel. It is critical for high-grade Al alloys to keep Fe levels below 0.5 % and in some cases even below 0.15 %. Finally, Cr is considered an impurity in most of the casting alloys, but it is used in some wrought alloys to limit grain growth and improve corrosion resistance, but it was classified as an impurity for all casting alloys produced by Grupal Art therefore its level should be kept as low as possible. The knowledge of chips feedstock chemical composition was fundamental to use them in the most effective and convenient manner for their daily production, and it must be as accurate as possible to ensure the lowest possible level of impurities.

The Al use case was further developed by the analysis performed by Refial, i.e., an aluminum refinery which supplies Al from secondary smelting. The refining process at REFIAL consisted in two melting tilting rotary furnaces and two holding furnaces of reverberatory type. A new step including scrap

preheating before charging into the melting furnace was proposed and the preheater was supposed to work with a Waste Derived Fuel (WDF) combustor, a heat exchanger and a heated scrap charging system. A polymeric fraction of ASR was planned to be used as fuel for the scrap preheating system since this waste stream was not recovered and was landfilled. The reason for including a preheating scrap system was the reduction of the melting time and the increase in energy efficiency as well as the removal of moisture from the scrap before loading into the furnace to avoid explosions. Considering this, Refial performed both the characterization of scrap feedstock as Grupal Art as well as the characterization and preparation of waste streams as potential WDF for scrap-preheating together with their analysis of variability. Concerning scrap variability, the key grades of scrap used were from waste electrical and electronic equipment and EoL vehicles which were characterized by different chemical composition and alloying elements. The key elements to be detected were Si, Cu, Fe, Mn, Mg, Zn, Cr, Ni, Pb, Sn and Ti as seen for Grupal Art. Si reduces the melting temperature of casting Al alloys and improves fluidity and it was one of the main alloying elements used by Refial requiring strict control of its content. Refial also produced Al-Cu alloys with typical Cu contents between 1 and 5 % to increase strength and facilitate precipitation hardening while risking to reduce ductility and corrosion resistance. Mn increases strength through solution strengthening and improves strain hardening while not appreciably reducing ductility or corrosion resistance and the maximum quantity admitted in REFIAL alloy was < 1% in all cases. Mg increases strength through solid solution strengthening and improves strain hardening ability. Its limit in the alloys produced by Refial was < 2%. Zn substantially increases strength and permits precipitation hardening and the maximum level allowed in the alloys produced by Refial goes from 0.07 to 3 %. Finally, Fe proved to be again the most common impurity which must be strictly controlled. The metallic yield of most scrap types was high and between 75-90 %.

Concerning ASR, two fractions were selected for the analysis, i.e., a polymeric fraction of light ASR with a Low Calorific Value (LCV) of 22 MJ/kg and a polymeric fraction of heavy ASR with a LCV of 24 MJ/kg, since the net calorific value of both streams was high enough to be considered for preparation of WDF. The characterization of the polymeric fractions of ASR included the analysis of material composition, Cl content and dissolved organic matter (DOM). The heavy fraction displayed a higher content of plastics and a lower content of fines compared to the light fraction and both of them were characterized by a near to zero proportion of metals. The Cl analysis highlighted high content for both streams, but bigger values were observed for the light fraction. Analogously, three times higher values of DOM were detected in the light fraction compared to the heavy fraction. In light of the high net calorific value, of the higher quantity generated, of the lower Cl content and DOM, the polymeric fraction of heavy ASR was selected for WDF production and treatment trials including crushing and sieving for size reduction and halogen content reduction by eliminating pieces with high halogen content using RX technology were performed. Crushing was performed in a knife mill and the selected treatment included crushing (25 mm) and sieving (>15 mm) because it provided sufficient conditions to feed the material to the next step of the treatment. The elimination of pieces with halogen content using RX technology led almost to a 40 % material rejection due to a halogen content higher than 1 % while more than 60 % of the input was prepared to be tested as a fuel containing a median Cl content of 0.5 %. The accepted sample consisted of 75 % of plastics, 5 % of wood, 1.5 % of textiles and less

than 1% of foam. The analysis of these streams with X-Ray technology reported the absence of Bi, Se, As, Hg and Au in all streams. A Cl content in the range of 500-1000 ppm was observed in plastics while its amount became very low in the other streams. Fe, Cl and Zn were the main elements detected in wood while Fe, Ba, Zn, Ti and small quantities of Pb were the main elements detected in textile and foam material. The cost for conditioning the heavy fractions of ASR would amount to 6.70 €/t considering an energy of 45.3 kWh/t, a productive capacity of 1.79 t/h and maintenance (2.77 €/t). The performance of the WDF was assessed by determining its high and low heating values and by studying its thermal degradation behavior in inert and oxidative atmospheres at various heating rates through TGA and DSC to define the range of temperatures for combustion, the evolved gases, char yield and reactivity, and ash melting behavior. The need and conditions of a post-combustion step to destroy persistent organic pollutants in combustion gases to comply with air emissions limits were also investigated. The results of the proximate analysis for the heavy fractions of ASR reported a LHV of 26.26 MJ/kg and a Higher Heating Value (HHV) of 27.94 MJ/kg. Thermal analysis by TGA was performed to study the thermal degradation of the samples in air in a temperature range from 25 to 950 °C. Three thermal decomposition stages were detected from 250 to 450 °C with the highest mass loss, from 450 up to 600 °C and from 600 to 725 °C. LOI was also measured at various temperatures, i.e., every 50 °C from 250 to 850 °C, and a trend coincident with TGA results was observed.

The use of WDF in combustion processes in dedicated plants may have several technical and environmental limitations due to formation of residual solid waste and to air emissions and those aspects must be considered for the correct design of burner and the definition of the operative conditions of the pre-heating system. Considering this, WDF combustion performance was investigated studying the composition of combustion and post-combustion gases and solid waste after performing a set of combustion and post-combustion experiments operating at different ratios of WDF/air/O_2 and continuously measuring the temperature. The first set of experiments was performed to select the optimal operating conditions in terms of temperature and WDF/air ratios in the combustor to achieve the most complete combustion and stable reaction. It was concluded that WDF needed to be heated from 250 to 550 °C at low heating rates while air flow started, and that the residence time of evolved gases should be increased to allow for combustion reaction in the gas phase before venting. These results seemed also to underline a WDF combustion behavior following the two-step conversion process of combustion of biomass, municipal solid waste or coal in a grate furnace with a first step of heterogeneous gasification of the solid fuel which was pyrolyzed and gasified, and a second homogeneous combustion in the gas phase when burnout of the pyrolytic decomposition and gasification products takes place. This reaction should be considered when designing the scrap pre-heating system to allow for enough residence time of volatilized products in the combustion chamber. The second set of experiments was dedicated to evaluate the completeness of combustion at different temperatures and different O_2 contents in the airflow. The results reported HCl concentration in the flue gas recurrently out of range thus highlighting the paramount importance of incorporating flue gas cleaning systems to comply with emission limits and avoid equipment corrosion problems. Concerning the analysis of combustion of solid waste, i.e., bottom ash, it was fundamental to check if it shows hazardous properties or if the content of certain substances exceed limit values. The C content proved to be always below 3 wt.% with lower carbonaceous residues observed in the ashes of the combustion

processes performed with O_2 and enriched air. The contents of heavy metals, e.g., Ba, Se, Mo, Zn, Sb, As, Cd, Cu, Cr, Hg, Ni and Pb, and of some inorganic anions, e.g., sulphate, chloride and fluoride, displayed average concentrations which met limit values set as criteria for acceptance of non-hazardous waste in landfills.

The last use case concerned the Pb industry and required again the characterization of Pb feedstock and the analysis of scrap variability. The main source of Pb scrap for recycling was acid batteries used mainly in cars, i.e., 85 %, but also in emergency power supply, traffic lights, telephones etc. They represented over 90 % of the Pb available for recycling. Other Pb scrap sources for recycling included sheaths from telephone and power cable, lead pipe sheet, automobile and truck wheel weights, fishing weights, printing metals, ammunition, nodes, residues, dross, sludges and dust. The EXIDE plant used mainly two different sources of raw materials, i.e., 70 % from an external supplier and 30 % from an internal supplier. The external supplier provided mainly paste and some metallic components while mixed battery elements were provided to a lower extent. The internal supplier provided almost 90 % of used batteries and 10% of rejects from EXIDE battery production plants which resulted in 20 % of pastes and 70 % of metallic. The laboratory analysis reported a Pb content around 92 % for metallic and of 72 % for paste and a moisture content around 1 % for metallic and around 7.3 % for paste. The amount of Pb in the scrap metal was not the only parameter of interest since the knowledge of the content of each Pb compounds, e.g., oxides and sulfates, could help to determine the number of fluxes necessary for thermodynamic reactions to take place optimally. Indeed, the feedstocks to send to the rotary kiln were Pb-bearing materials, flux and reductant components, e.g., coke and anthracite. Among the Pb bearing materials there were metallic Pb which could be alloyed with other elements, e.g., Sb, or include other impurities such as Cu, Zn, Cd and S, Pb paste consisting mainly of $PbSO_4$, PbO_2 and PbO, and dross from the bullion refining stage composed of Pb oxides, metallic Pb and Pb compounds with Sb. The main slag former was Fe which acted as S collector and could be added as iron or steel production residues. Further fluxes to reduce the melting temperature and viscosity of the slag were Na_2CO_3 and soda. The amount of flux and reducing agent must be carefully controlled since a lack of flux would prevent trapping all S leading to the release of large quantity of sulfur oxides while a lack of reducing agent would prevent the whole conversion of Pb oxides. An excess C may also trap a portion of Fe that was in the form of FeS or FeO leading to metallic iron or Fe_3C which are solid and increase the viscosity of the slag making the process poorer in recovery of the bullion. Other elements such as Sb, As, Sn, Cu, Bi, Ag, Ni, Se, Te, Al, Fe and Zn can be found in batteries and other types of scrap. Generally, Ag and Bi are not removed because the quantities do not justify the costs of removal while the other elements are eliminated in the refining process to obtain pure Pb and Pb-Sb and Pb-Ca alloys according to the final required properties.

3.2.15 H2STEEL: Green H2 and circular bio-coal from biowaste for cost-competitive sustainable Steel (99)

The project was coordinated by Politecnico di Torino with RE-CORD, Universiteit Leiden, I3P (Società per la Gestione dell'Incubatore d'Impresa del Politecnico di Torino), Contactica and ArcelorMittal and Imperial College participating as partners in the consortium. The project started on the 1st of June

2022 and lasts almost four years, ending on the 31st of March 2026. The overall project cost 2.37 M€ and the EU contributed 2.37 M€, i.e., the full budget.

The H2STEEL project aims to support the green transition and decarbonization of the steel sector by proposing an innovative and disruptive solution to convert biowastes and biomethane into green hydrogen, carbon, and critical inorganic raw materials, e.g., inorganic P-rich fertilizers, through a new catalyzed pyrolysis combined with chemical leaching. Indeed, steel is traditionally produced in BF where coal is used for combustion purposes, for minerals smelting and for metal oxides reduction thus resulting in huge CO_2 emissions which could be conveniently reduced by replacing coal with natural gas or better with green hydrogen generated from renewable energy.

The production of green hydrogen necessarily implies the development of economically feasible routes with costs comparable with the traditional processes, therefore the H2STEEL project attempts to develop a disruptive hydrogen production route via biomethane catalytic cracking through a new waste-derived catalyst. This solution allows to work with a carbon neutral solution sequestering also CO_2 in the form of a carbonaceous solid, i.e. bio coal, which can be then reused in steelmaking processes and ensures the use of a cost-effective catalyst which is sourced from wastes and is resistant to contaminants and temperature. Basically, H2STEEL has the main goal to create a ground-breaking competitive solution for sustainable green hydrogen and bio coal production from circular biowaste streams. The proposed solution would ensure a full valorization of the nutrients and carbon contained in the digested biowaste streams which are nowadays underexploited. Indeed, digestate from anaerobic digestion of plants is characterized by relevant concentration of C and macro-nutrients, but has a limited market demand whereas digestate from anaerobic digestion of urban biowaste and agricultural residues can be adopted to produce soil conditioners, but the presence of heavy metals and other contaminants can prevent their application in the soil. Finally, digested sludges derived from both civil and industrial wastewater treatment are not feasible for agriculture due to contamination risks according to EU regulations.

The pyrolysis of biomethane is performed in a proof-of-concept reactor which was designed ad-hoc and consists of a bio coal bed made from cheap pre-carbonized biowastes which are very resistant to temperature and contaminants. Once new solid C is generated as a consequence of methane cracking, it deposits on the bio coal catalyst surface thus reducing its performance. This requires the introduction of a new bio coal catalyst in the reactor while the spent bio coal is removed and used in steelmaking as a substitute of fossil coke thus generating a net GHG reduction. The continuous renewal of the catalyst is feasible thanks to its low cost and to the market value of the spent catalyst furthermore, the avoidance of catalysts regeneration allows to avoid the release of CO_2 resulting from this step.

The identification of suitable biowastes streams was carried out and four different streams were selected depending on their annual production volume, chemical composition, disposal cost, availability, and inorganic compound content. Their preliminary characterization in terms of chemical and physical properties was performed through TGA, i.e., determination of ash, moisture and volatiles content, MP-AES (Microwave Plasma Atomic Emission Spectroscopy), i.e., determination of inorganic elements, CHN analysis for the estimation of C, H, N and finally bomb calorimeter to estimate HHV. Based on

the results obtained from the characterization of the biowaste streams, biochar was produced and upgraded at lab scale for the identification of the optimal process parameters. The preliminary pyrolysis at lab scale was performed at mild temperature, considering different residence time and using a heating rate of 20 °C/min. The biochar obtained was characterized again through TGA and MP-AES in terms of ash, moisture and volatiles content, inorganic elements, and CHN. The type and concentration of inorganics, and volatile matter were determinant in the selection of the raw biochar to be upgraded by chemical leaching since P, Ca and other micronutrients were crucial for the application of the leaching process, as well as metals for biomethane cracking. Parallelly, preliminary laboratory-scale methane pyrolysis tests were performed to identify the best operating conditions in terms of temperature, reagent flow, velocity, etc., to maximize the conversion of biomethane into hydrogen.

The classification of bio waste according to Eurostat includes paper and cardboard wastes, wood wastes, animal and mixed food, Municipal Solid Wastes (MSW) and common sludges. Three biowaste categories were considered in the preliminary characterization performed by RE-CORD, i.e., wastewater treatment sludge, urban biowaste, agricultural waste. Civil and industrial sludge are the results of wastewater treatment to remove pollutants such as organic substances, nutrients, e.g., N, P and K, and hazardous substances, e.g., pathogen microorganisms, mutagens, carcinogenic and teratogens, from the wastewaters of domestic, urban and industrial origin. The acknowledgment of the long-term effects of wastewater constituents on human health led to the definition of more restrictive discharge limits which resulted in higher removal efficiencies of water pollutants and in the production of higher sludge volumes. Eurostat reported a production of sludge in EU around 9-13.EU of million of dry tons per year with 9-9.5 million tons of dry substance per year resulting only from civil sludge. Sewage and industrial sludge disposal represent around 50 % of wastewater plant costs since landfilling and incineration are the most common disposal solutions when disposal in agriculture is forbidden due to dangerous biological and chemical pollution. These are expensive practices with costs from 120 to 250 €/t of sludge. In light of this and of the technical drawbacks of sludge incineration such as the relatively low calorific value and the high ashes content as well as the scarce social acceptance of incinerators installation from population, the investigation of alternative disposal pathways is highly encouraged. The relevance of sludge as source of C and raw materials depends on the composition of its dry matter, i.e., its solid content, which varies depending on the section of the wastewater treatment plant which produced it. In particular, dry matter ranges from around 0.5-1.5% for secondary sludge to 6 % for primary sludge. Primary, secondary and tertiary sludges are usually mixed and dewatered by centrifugation and after centrifugation the dry matter content rises to around 25-30 %. Urban biowaste are mainly biodegradable garden and park waste, food and kitchen waste from households, restaurants, etc. and the identification of suitable recycling pathways is crucial for reaching the new recycling targets defined in 2018 which include a recycling of at least 55 % by 2025, 60 % by 2030 and 65 % by 2035. These are quite huge numbers considering that between 118 and 138 million tons of biowaste are produced annually across EU and that currently only about 40 % is effectively recycled into high-quality compost and digestate whereas the majority is disposed through landfilling (24 %) or incineration (27 %). Moreover, anaerobic digestion of biowaste is still covering a small fraction of biowaste treatment plants with a production of only 11.7 Mtons of compost and about 4.8 Mtons of digested, but these data are estimated to increase in the next years. The treatment

of urban biowaste is less expensive than sewage or industrial sludge one with a cost of 80-100 €/t. This must be ascribed to the lower water content, the higher capability to produce biomethane, and its organic fraction containing less contaminants thus making it usable with other wastes to produce compost. However, compost demand is low and a large fraction of collected urban biowaste does not fulfill compost quality requirements therefore it must be disposed in landfill or incinerated.

Based on the biowaste streams identified above, RE-CORD characterized 8 different samples: industrial sludge from food industry (ISL1), industrial sludge from pharmaceutical industry (ISL2), mixed urban biowaste digestate (DBW1), urban biowaste digestate (DBW2), ash-rich civil sewage sludge (CSL1), conventional civil sewage sludge (CSL2), and two different types of agricultural digestate (AGD 1 and 2). Moisture content was estimated through TGA by heating the samples at 105 °C and by air fluxing until constant weight of the material is reached, ash content was calculated on a dry basis as wt.% after complete combustion of the organic compounds performed at a temperature of 550 or 710 °C in oxygen atmosphere, and volatiles were defined on a dry basis as the wt.% loss after heating of the dry sample in absence of air by nitrogen fluxing to 600 °C. Fixed carbon represents the recalcitrant fraction of total carbon that is non-volatile and is determined indirectly subtracting ashes and volatiles percentage from total mass on a dry basis. To identify C, H and N content of the material, it was combusted at high temperature in a CHN analyzer so that carbon is converted into CO_2, hydrogen into H_2O, and nitrogen into N_2. The mineral fraction of the biowaste, e.g., B, P, Si, was characterized by MP-AES after mineralizing the sample using a solution of H_2O_2 and HNO_3 to remove organic compound and to dissolve inorganics. Finally, HHV was measured by a bomb calorimeter by burning a certain amount of the specimen in a pure oxygen atmosphere and registering the heat released by the combustion reaction.

The proximate and ultimate analysis as well as the macro and micro elemental analysis of the eight biowastes selected is summarized in Table 29. These results were useful to identify the classes of biowastes more appropriate for the H2STEEL project purposes to be employed in the following part of the experimental campaign, i.e., slow pyrolysis. Among the industrial sludge, the one from the food industry was selected as the most appropriate since it is certainly of biological origin whereas the one from the pharmaceutical plant is derived from a process where the organic matter contained in the wastewater is derived from a pharmaceutical production process thus not necessarily of biological origin. Concerning the digested urban biowaste, the one with the lower ash content of about 26 %, i.e., DW2, was selected because it ensured reduced concentration of Fe and Al and a higher C content. Indeed, DWB1 displays the typical characteristics of digested sewage sludge with high ash contents around 39 % and high amounts of Al and Fe deriving from iron and aluminum chloride used as flocculating agents. Among the civil sewage sludge, CSL2 from Piedmont was selected whereas CSL1 from Tuscany was rejected due to a higher ash content around 50 % against the 33 % of CSL2 which consequently entails a higher C content. Finally, AGD2 was selected among the two agricultural digestants using again as main decision guideline the ash and the fixed C content. Indeed, AGD2 displays a higher fixed C content of 21.4 % against the 16.6 % of AGD1 and a lower ash content of 10 % against the 15 % of AGD1.

Table 29: Proximate and ultimate analysis and macro and micro elemental analysis of the eight biowastes considered

Parameter	Unit	ISL1	ISL2	DBW1	DBW2	CSL1	CSL2	AGD1	AGD2
Moisture	% a.r.	8.2	33.8	80.2	74.8	73.9	9.9	73.3	84.2
Dry matter	% a.r.	91.8	66.2	19.8	25.2	26.1	90.1	26.7	15.8
Ashes 550 °C	% d.b.	20.7	26.0	39.1	25.6	49.3	33.6	15.0	10.0
Ashes 710 °C	% d.b.	63.1	26.0	36.7	21.4	48.5	33.1	14.4	9.9
Volatiles	% d.b.	63.1	66.7	52.6	63.6	46.0	58.9	68.4	68.5
Fixed C	% d.b.	16.2	7.3	8.3	10.8	4.7	7.5	16.6	21.4
C	% d.b.	43.0	39.5	32.4	38.2	23.6	35.7	44.4	45.7
H	% d.b.	5.2	5.7	4.0	4.6	4.0	4.9	5.3	5.4
N	% d.b.	7.5	7.0	2.9	1.3	3.8	5.8	1.4	2.2
S	% d.b.	0.9	2.3	0.5	0.4	0.8	1.5	0.5	0.17
Cl	% d.b.	0.4	0.11	0.7	0.67	0.05	0.04	0.64	0.35
LHV	MJ/kg d.b.	16.6	16.9	11.6	14.3	9.5	14.8	16.4	17.3
Al	mg/kg d.b.	7575	4730	12115	4778	40574	23944	713	119
B	mg/kg d.b	-	-	325	174	6	b.d.l.	b.d.l.	b.d.l.
Ba	mg/kg d.b.	122	44	b.d.l.	2	784	280	13	6
Ca	mg/kg d.b.	30240	42802	62790	50555	23550	28746	21330	4808
Cd	mg/kg d.b.	b.d.l.	b.d.l.	b.d.l.	b.d.l.	b.d.l.	b.d.l.	b.d.l.	b.d.l.
Co	mg/kg d.b.	2	b.d.l.	b.d.l.	b.d.l.	b.d.l.	b.d.l.	b.d.l.	b.d.l.
Cr	mg/kg d.b.	22	46	98	b.d.l.	77	152	9	4
Cu	mg/kg d.b.	11	67	114	19	702	292	38	4
Fe	mg/kg d.b.	504	51777	42853	4757	15763	49537	2498	1068
K	mg/kg d.b.	3630	2034	15289	2027	6055	3161	21803	23473
Li	mg/kg d.b.	7	1	16	5	20	6	1	b.d.l.
Mg	mg/kg d.b.	2571	2324	5598	7858	5792	6539	4246	2930
Mn	mg/kg d.b.	238	455	738	501	358	285	189	97
Mo	mg/kg d.b.	b.d.l.	b.d.l.	b.d.l.	b.d.l.	b.d.l.	b.d.l.	b.d.l.	b.d.l.
Na	mg/kg d.b.	8600	1638	5920	14101	842	1194	6318	329
Ni	mg/kg d.b.	9	b.d.l.	35	b.d.l.	96	b.d.l.	b.d.l.	b.d.l.
P	mg/kg d.b.	11838	20043	16913	8755	37498	28176	8725	7188
Pb	mg/kg d.b.	b.d.l.	16	59	b.d.l.	61	b.d.l.	b.d.l.	b.d.l.
Si	mg/kg d.b.	795	1576	-	-	-	-	-	-
Ti	mg/kg d.b.	5863	26	177	104	277	244	18	3
V	mg/kg d.b.	b.d.l.	2	14	b.d.l.	34	12	3	b.d.l.
Zn	mg/kg d.b.	93	416	293	179	453	830	189	67

Laboratory scale pyrolysis tests were performed via TGA by setting the appropriate operating parameters and collecting the resulting char for further analysis. Different temperatures and residence times were considered applying a heating rate of 20 °C/min. ISL2 and CSL2 were tested at 450 and 550 °C for 30 and 60 minutes while DBW2 and AGD2 were tested at 500 and 600 °C for 30 and 60 minutes. Furthermore, all biowastes were treated at 700 °C for 30 minutes. This was necessary since

700 °C is the minimum temperature for catalytic methane cracking but higher pyrolysis temperatures were not considered since H2STEEL process includes an intermediate chemical leaching step for char upgrading and nutrients, i.e., P and Ca, extraction whose solubility and the resulting extraction performance decreases with increasing pyrolysis temperature. The different temperature ranges were selected due to the higher volatility of sludge compared to digestate. The results obtained highlighted a decrease in char mass yield from 45.7 to 40.5 % for industrial sludge due to increasing operating temperatures whereas no evident effect was detected for the residence time. Analogous results were observed for digested urban biowaste with a mass yield decrease from 43.5 to 41.5 %, for civil sewage sludge with a mass yield decrease from 48.5 to 44.5% and for agricultural digestate with a mass yield decrease from 34.1 to 30.6 % with increasing operating temperatures. For agricultural digestate the devolatilization of the feedstock proved to be influenced also by the retention time. The mass yield of the slow pyrolysis test performed at 700 °C highlighted a higher mass yield for those materials characterized by a higher ash content with agricultural digestate reporting the lowest yield of 31.5 %, and civil sewage sludge the higher yield of 41.9 %.

A comparison of the biochar obtained to select the most promising materials for the H2STEEL process was performed considering the C content, char stability (molar H/C ratio), ash content at 710 °C and the content of P, Fe, and Al at 710 °C. Concerning the C content, it tended to decrease slightly for increasing operating temperatures due to the high ash concentration in the processed materials and it reached a maximum value with agricultural digestate pyrolyzed at 600 °C and a minimum value with civil sewage sludge at 550 °C. Concerning biochar stability at high temperatures, this property is fundamental to ensure the suitability as catalysts during methane cracking as well as bio coals in steelmaking. It was estimated as the hydrogen on carbon molar ratio since this parameter indicates the volatility of the material and consequently its reactivity at high temperatures. Clearly, the lowest H/C ratio was achieved at 700 °C for almost all processed materials except for agricultural digestate which displayed the best stability at 600 °C after 60 minutes. In conclusion a pyrolysis temperature of 450 °C could be too low to produce a good quality char from for civil and industrial sludge feasible as catalyst, while 550°C is recommended. For urban biowaste digestate and agricultural digestate 600 °C could be suitable. The comparison of the ash content of the different biochar produced underlined the great difference between sludges and digestates. Indeed, the ash content in the biochar produced from sludge was 50 % higher even after the pyrolysis at 450 °C. Finally, P, Fe and Al concentration in the biochar ash were analyzed. These three elements were investigated since P is highly valuable in agriculture, being commercialized at more than 1.5 €/kg and is harmful to steelmaking thus making its extraction from char recommended. Fe is considered a high value catalyst enhancing methane cracking process thus being beneficial when using the biochar as catalyst in methane pyrolysis reactor and Al is also a high value element which could be extracted being also harmful during the methane catalytic process. Industrial sludge contains the highest concentration of Fe and P probably due to the use of iron chloride in the wastewater treatment process, as it is also high in civil sewage sludge. Therefore, both biochar obtained from sludge were of potential high quality given the high P and Fe content.

In conclusion, industrial sludge presented interesting characteristics with high value elements to be valorized in agriculture (P) and as catalyst in the methane pyrolysis process (Fe) despite the high ash content. Civil sludge presented a high volatility and high concentration of ashes containing high amounts

of Al_2O_3 and SiO_2 both useless for the process and difficult to extract. In light of this, biochar from civil sludge could be critical to produce a metallurgical grade bio coal. Among the digestates, urban biowaste digestate displayed a quality not high enough quality for the H2STEEL process due to limited P, Fe, and C content and the high concentration of ash whereas agricultural digestates displayed interesting composition in terms of total C content and low ash concentration despite the reduced amount of P.

Beyond the technical results, some studies on the real potential contribution of hydrogen produced from biomasses by methane pyrolysis to the European de fossilization targets with some highlights on the resulting environmental benefits for the metallurgy sector were also released. Considering a scenario where steel is produced using the DRI-EAF route, 6 Mtons of green hydrogen/year should be produced to correctly supply the chain, but the actual scenario would allow to cover only 4.14 % of this demand starting from biomethane pyrolysis. A better outcome was foreseen for 2030 where methane pyrolysis should cover 56.6 % of the total demand, but full coverage was envisaged only for 2050 when the 6 Mtons would be achieved with only 48 % of the available biomethane. The CO_2 emissions associated with the production of 1 ton of liquid steel were further analyzed by comparing the results obtained for green hydrogen production through methane pyrolysis with the ones achievable through electrolysis and also comparing the use of green hydrogen with the use of natural gas in DRI-EAF route. This analysis confirmed that biomethane pyrolysis route is the best choice for reducing CO_2 emissions both in the nowadays and 2030 scenarios. Indeed, the use of natural gas in DRI entails emissions of 974 $kgCO_2$/ton liquid steel in the actual scenario and 843.2 $kgCO_2$/ton liquid steel in 2030 scenario which are significantly lower than the 600 $kgCO_2$/ton liquid steel for the actual scenario and the 350 $kgCO_2$/ton liquid steel for the 2030 scenario estimated when using biomethane pyrolysis. This must be ascribed to CO_2 emissions released from biomethane which are considered biogenic. The pyrolysis route is also advantageous compared to electrolysis since the electricity consumption for hydrogen production in the first case is significantly lower than for electrolysis thus resulting in emission differences of 466 $kgCO_2$/ton liquid steel and 228.6 $kgCO_2$/ton liquid steel for the current and 2030 scenarios, respectively. This proved that biomethane pyrolysis can be an interesting decarbonization option for the steel sector which provides a carbon-neutral pathway for hydrogen production together with the production of a solid carbon by-product. The demand for hydrogen is very high as well as the corresponding volumes of biomethane required which is currently not available. However, the stable legal and political framework both at European and national levels are strongly increasing the biomethane market uptake and investments. Best practices already established in countries with mature biomethane market, e.g., Italy, should be spread in other countries, in terms of technological, regulatory and financing know-how (100).

Further studies explored the potential production of low-carbon hydrogen from biobased processes and their contribution to EU hydrogen goals for 2030 and 2050 considering a renewable hydrogen production of 10 Mtons by 2030. In particular, the study tried to assess whether biomass-derived hydrogen could serve as viable and substantial component of hydrogen production complementing more established methods such as electrolysis powered by renewable electricity. The study assessed the main hydrogen production pathways from biomass including both thermochemical and biological methods putting emphasis on hydrogen yield, production costs, and TRLs. The study also considered

the availability of biomass resources and potential production scenarios for 2030 and 2050. Thermochemical processes displayed higher biomass conversion with an average hydrogen yield of 53.96 gH_2/kg biomass compared to biological processes with an average hydrogen yield of 20.36 gH_2/kg biomass. Among the thermochemical processes, pyrolysis showed the most promising results with an average yield of 65.44 gH_2/kg biomass and a maximum yield of 148 gH_2/kg biomass. It is important to highlight that most of the gasification studies were at a laboratory scale and omitted often the water gas shift stage after the gasification thus limiting the final hydrogen production. Among biological processes, the hybrid configuration of dark and photo fermentation reached the highest conversion value with an average of 37.27 gH_2/kg biomass. From an energy efficiency perspective, thermochemical processes outperformed again biological methods with energy efficiencies of 0.43−0.7 for wood gasification compared to 0.01−0.1 for photo fermentation, 0.1−0.25 for dark fermentation and 0.27 for integrated processes of dark and photo fermentation. Further literature studies reported efficiencies of 0.35−0.5 for biomass pyrolysis, 0.01 for photo fermentation, and 0.6−0.8 for gasification. This must be ascribed to the fact that biological processes operate under milder conditions and require less energy input but exhibit also lower conversion rates thus necessitating considerable energy for plant operation and resulting in a reduced overall efficiency. Concerning TRL analysis, water electrolysis showed a very high TRL of 9 whereas biobased processes presented a wider range of TRLs with gasification being the most advanced with a TRL between 8 and 9. Pyrolysis showed lower TRL values with a range between 6 and 9, strongly depending on the configuration adopted. Biomethane pyrolysis TRL ranged between 3 and 8, including industrial scaled technologies such as plasma pyrolysis but also less mature configurations, like catalytic pyrolysis. Finally, biological processes displayed the lowest TRLs between 3 and 5 facing challenges such as optimization of microbial activity and handling feedstock variability. The analysis also included increasing shares of available biomass for energy purposes, ranging between 310.6 and 836.6 Mt of dry matter by 2030, and reaching a hydrogen yield of over 16 Mt in the best-case scenario (101).

3.2.16 HEPHAESTUS: Heavy and Extractive industry wastes PHAsingout through ESG Tailings Upcycling Synergy (102)

The project was coordinated by RINA Consulting with CSM, Ethnicon Metsovion Polytechnion, LARCO GMMSA (GENIKI METALLEUTIKI KAI METALLOURGIKI ANONIMI ETAIRIA), ADMIRIS (Advanced Minerals and Recycling Industrial Solutions), Metlen Energy & Metals, KU (Katholieke Universiteit) Leuven, AIT Europa Engineering, Engitec Technologies and AST participating as partners in the consortium. The project started on the 1st of June 2022 and lasts almost four and a half years, ending on the 30th of November 2026. The overall project cost 16.0 M€ and the EU contributed 11.9 M€, i.e., almost 75 % of the budget.

EAF steelmaking accounts for over 40% of crude steel production in Europe and generates substantial amounts of residues such as dust, slag, and sludge. Among these, EAF and AOD dust are particularly problematic. Classified as hazardous waste under the European Waste Catalogue due to their high content of Zn, Pb, and other heavy metals, these residues are often landfilled or exported outside the EU for treatment. Such practices result in economic losses, environmental burdens, and strategic

dependency on external markets for critical raw materials like Zn. At the same time, the steel industry is facing growing pressure to decarbonize in line with the European Green Deal and the 2050 climate neutrality targets. New technological solutions are needed to simultaneously address resource efficiency, waste minimization, and CO_2 reduction, while fostering the creation of novel circular value chains. The HEPHAESTUS project aims to demonstrate a circular, near-zero wastes and carbon-reduced steelmaking route by integrating multiple innovative technologies into a coherent industrial ecosystem. Its approach combines pyrometallurgical, hydrometallurgical, and CCU processes to fully valorize EAF/AOD dusts, slag, and associated by-products.

The project focuses on three main technological pillars. The first one is the CleanTech EAF which is a 5 MVA demonstration furnace designed to improve energy efficiency, enable flexible use of alternative reductants, and reduce CO_2 intensity. The second one is a fiber drawing unit dedicated to transform treated slags into high-value mineral fibers and wool products suitable for thermal and acoustic insulation. The last one concerns the EZINEX® process by Engitec which is a hydrometallurgical technology to recover high-purity Zn metal and zinc oxide from EAF/AOD dusts, closing the loop for non-ferrous elements. Two complementary technologies were also integrated. The first one is a CCU solution to convert CO_2-rich furnace off-gases into methanol and was validated through a demonstrator at Metlen in Greece while the second one is a hydrometallurgical leaching process developed by KU Leuven for selective recovery of Zn and Fe fractions from steelmaking dusts through ammonia-ammonium carbonate (AAC) and methanesulfonic acid (MSA). The expected outcomes of the project include a recovery of Zn and Fe higher than 90 % from EAF and AOD dusts, the production of mineral fibers as a sustainable alternative to commercial glass or stone wool, the substitution of fossil carbon with alternative reducing agents, lowering the CO_2 footprint of EAF operation and the conversion of captured CO_2 into methanol, creating a valuable feedstock for the chemical sector.

By integrating these technological pathways, HEPHAESTUS aims to demonstrate that circular, residue-free, and carbon-reduced steelmaking is not only technically feasible but also economically and environmentally advantageous. The project is expected to deliver validated pilot-scale solutions, market analyses, and policy recommendations, paving the way for replication across the European steel sector and contributing to EU strategic autonomy in critical raw materials.

The methodological approach of the project was designed to validate a set of complementary technologies for the valorization of EAF and AOD residues under industrially relevant conditions. It combined resource mapping, process modelling, pilot and demonstrator design, and sustainability assessment, ensuring coherent progression from laboratory scale to pilot implementation. The first activity focused on the systematic mapping of residues from European steelmaking plants and the collection and analysis of data from industrial sites across the consortium. This included both EAF and AOD dusts as well as other waste streams from mining and metallurgical operations that could be treated within the HEPHAESTUS framework. Residues were characterized in terms of chemical composition using XRF, ICP and wet chemical analysis with emphasis on Zn, Fe, Pb, and Cr, of mineralogical phases determined by XRD to assess zincite, franklinite, and ferrite content, of particle size distribution and morphology through sieving and SEM-EDS, and moisture and oil content particularly relevant for sludges. This mapping allowed the creation of a database that quantified the

annual availability of residues and provided the baseline for selecting suitable feedstocks for the CleanTech EAF, EZINEX®, and hydrometallurgical units.

A second methodological pillar was the use of predictive models to anticipate the behavior of residues in different technological pathways. RINA-CSM developed thermodynamic and thermo-chemical models of slag chemistry and EAF operation focusing on parameters such as slag viscosity, foaming, and thermal balances. These models guided the design of the fiber drawing unit by predicting which slag chemistries could yield stable glass-forming phases suitable for mineral wool production. KU Leuven concentrated on hydrometallurgical recovery building models for the AAC and MSA processes. These simulations identified the operating windows for maximum Zn extraction, selective Fe precipitation, and minimized reagent consumption. Laboratory leaching tests on real EAF and AOD dust were conducted to validate the predictive models, providing kinetic data and solid–liquid separation behavior. Ethnicon Metsovion Polytechnion and Metlen focused on the CCU pathway with process modelling assessing the techno-economic feasibility of converting CO_2-rich off-gases from the EAF into methanol. Catalytic reactor modelling combined with gas composition analysis, was used to design the Greek demonstrator and identify optimal syngas ratios.

The project also advanced the engineering design of pilot and demonstration plants. AIT, Engitec, and RINA-CSM prepared the demonstrator site integrating the CleanTech EAF, the slag fiber drawing line, and the EZINEX® process. The furnace design included a modified off-gas capture system, slag tapping points for fiber drawing, and improved power supply for flexible operation. The fiber drawing line was dimensioned based on slag viscosity ranges predicted by modelling and validated by laboratory melting tests. Engitec led the adaptation of the EZINEX® process, a proprietary hydrometallurgical technology for selective Zn recovery. Pilot-scale design included leaching reactors, electrowinning cells, and solid residue management systems. Parallel work at KU Leuven optimized AAC and MSA processes, with parameters fed back to Engitec for integration into the pilot setup.

In Greece, Ethnicon Metsovion Polytechnion and Metlen prepared the demonstration of the CCU process. This involved the design of a syngas conditioning unit, catalytic methanol synthesis reactor, and product purification system. The demonstrator was dimensioned to handle CO_2-rich gas streams from EAF off-gases, providing real validation of C valorization at steel plant conditions. All pilot activities were supported by extensive laboratory characterization. This included microstructural and mechanical testing of fibers produced from treated slags, metallurgical analysis of Fe-rich residues, and purity determination of recovered zinc oxide and Zn metal. The use of standardized protocols such as ASTM and ISO ensured comparability across partners.

Optimization was carried out in iterative cycles starting from modelling predicted behavior under given operating parameters, passing through laboratory validation which provided empirical data and concluding with the pilot design which was adjusted accordingly. This loop was applied consistently across the CleanTech EAF, EZINEX®, AAC/MSA, and CCU processes. Finally, the methodology integrated an economic and environmental perspective. RINA Consulting defined the framework for LCA and LCC covering each technological pathway. These analyses considered CO_2 reductions, material substitution, waste avoidance, and potential revenues from Zn, Fe, fibers, and methanol. A market analysis complemented sustainability work, mapping the potential demand for circular products

such as mineral fibers and secondary Zn up to 2030. Through this multi-layered methodology, encompassing resource mapping, modelling, engineering, validation, and sustainability analysis, HEPHAESTUS lays the groundwork for a holistic demonstration of circular, carbon-reduced steelmaking.

RINA-CSM coordinated much of the modelling and process integration activities. A major result was the development of thermodynamic models of slag behavior which allowed the prediction of viscosity ranges suitable for fiber drawing. These models confirmed that certain EAF and AOD slags after appropriate conditioning, can form glassy phases comparable to commercial mineral wool feedstocks. RINA also carried out detailed mass and energy balances for the CleanTech EAF and slag fiber drawing units, identifying optimal operational parameters to reduce energy demand while maximizing slag valorization. RINA Consulting expanded the scope of the project through a market study for circular products. The analysis highlighted strong growth opportunities for secondary Zn which is projected to face increasing demand from the battery and galvanizing sectors, and for mineral fibers, particularly in insulation markets aligned with EU renovation strategies. The study also mapped regulatory drivers and potential barriers to market entry providing essential guidance for exploitation pathways.

KU Leuven worked on hydrometallurgical processes producing substantial advances in the selective recovery of Zn and Fe from EAF dust. Predictive models of the AAC and MSA processes were validated through laboratory experiments. Results demonstrated that Zn extraction yields above 90 % could be achieved under optimized conditions, while Fe could be selectively precipitated and recovered for further use. Process optimization revealed that operating parameters such as temperature, pH, and reagent dosage strongly influence separation efficiency. For instance, the AAC process provided higher Zn selectivity, whereas MSA showed advantages in reducing overall chemical consumption. These insights are critical for scaling up the processes and integrating them into Engitec pilot design.

Engitec in collaboration with AIT advanced the design of the EZINEX® pilot plant. Engineering studies defined the operational envelope for Zn recovery from EAF and AOD dust by adapting laboratory findings from KU Leuven to a pilot configuration. Detailed layouts for leaching reactors, electrowinning cells, and solid residue management units were completed, ensuring compatibility with the Italian demonstration site. AIT contributed to the integrated pilot plant design for the Italian demonstrator, combining the CleanTech EAF, slag fiber drawing unit, and EZINEX®. Their work produced the executive design for installation, including material flow diagrams, energy integration schemes, and safety assessments. These results provide the foundation for physical implementation of the pilot units.

The Greek partners concentrated on the CCU process performing techno-economic analyses of CO_2 conversion to methanol, combining reactor modelling with assessments of off-gas composition from EAF operation. Results demonstrated the technical feasibility of integrating CCU with steelmaking off gases if syngas ratios are adjusted to match catalytic requirements. Metlen contributed practical expertise from its metallurgical operations and prepared the site for hosting the CCU demonstrator. Preliminary integration studies confirmed that off-gas capture, conditioning, and catalytic conversion could be installed without disrupting existing industrial activities. This work paves the way for validating CO_2-to-methanol pathways at industrially relevant scale.

ADMIRIS played a central role in resource mapping since their surveys quantified the annual generation of EAF and AOD dust across the consortium and analyzed their chemical variability. Results showed that Zn content typically ranged between 15–35 wt.% with significant variations depending on furnace operation and scrap mix. Complementary mapping of non-ferrous residues identified additional feedstocks, such as Ni slag and stainless-steel dusts which could expand the applicability of HEPHAESTUS technologies. This mapping provides the empirical basis for scaling technologies and assessing their replication potential in other regions of Europe. LARCO contributed Ni-containing residues which were characterized for potential integration into the CleanTech furnace. These materials showed distinct behavior compared to C steel dust, requiring tailored operating conditions for smelting and reduction. Other industrial partners supported the collection of representative residue samples and provided operational data for modelling and design activities.

The HEPHAESTUS project represents a comprehensive attempt to establish a circular, near-zero waste route for EAF-based steelmaking by combining pyrometallurgical, hydrometallurgical, and carbon capture technologies. The results obtained so far demonstrate the technical feasibility of the proposed solutions, while also revealing the critical challenges that must be addressed before full industrial deployment. Laboratory and modelling activities confirmed that EAF and AOD dust can be effectively treated using hydrometallurgical and electrochemical processes. KU Leuven optimization of AAC and MSA leaching routes demonstrated Zn recovery yields above 90 %, with selective precipitation of iron oxides that can be reused as secondary feedstock. Engitec adaptation of the EZINEX® process further validated the potential for industrial-scale Zn recovery aligning well with the requirements of European galvanizing and battery sectors. RINA-CSM thermodynamic modelling established that conditioned slags could achieve the viscosity and chemical composition required for fiber drawing. This finding supports the viability of producing mineral fibers and wool products as high-value outputs from slag, reducing reliance on natural basalt or other virgin materials. Parallel mass and energy balances for the CleanTech EAF identified operational strategies to improve energy efficiency and reduce CO_2 intensity, providing a robust baseline for the Italian demonstrator. In Greece, it was demonstrated through process modelling that CO_2-rich furnace off-gases could be converted into methanol at pilot scale, if syngas composition is carefully controlled. This pathway offers a direct link between steelmaking and the chemical industry, enabling carbon capture and valorization rather than storage or release. Each partner delivered critical building blocks for the integrated system. KU Leuven advanced hydrometallurgical science, proving that selective leaching and separation can be scaled up. Engitec and AIT translated these laboratory results into a pilot-ready EZINEX® plant design. Ethnicon Metsovion Polytechnion and METLEN bridged steelmaking with CCU technology, while LARCO and other industrial partners supplied critical feedstocks and operational data.

Despite these achievements, several issues remain open. The variability of dust composition among plants and even within single sites requires flexible process control and potentially pre-blending strategies. The energy intensity of CleanTech EAF operation, particularly when integrating off-gas capture and slag conditioning, poses challenges for economic viability. On the hydrometallurgical side, the cost and sustainability of reagents in AAC and MSA processes must be optimized to ensure competitiveness with existing dust management practices. For CCT methanol synthesis, the integration of catalytic units with fluctuating EAF gas streams remains technically complex, especially

given the intermittency of steel production cycles. If these challenges can be overcome, the environmental benefits are substantial. HEPHAESTUS technologies collectively aim to recover more than 90 % of Zn and Fe from EAF and AOD dust drastically reducing landfill disposal of hazardous residues. The production of mineral fibers from slag provides a sustainable alternative to commercial insulation materials, contributing to EU energy efficiency targets in the construction sector. The conversion of CO_2 into methanol offers not only a GHG mitigation strategy but also a pathway to produce a valuable chemical feedstock fostering cross-sectoral synergies.

From an economic perspective, the recovery of secondary Zn and high-value fibers can offset operational costs, while methanol production has the potential to open new revenue streams. Market analyses indicate strong demand growth in all three product categories, Zn, mineral fibers, and methanol aligned with European policy priorities. The next steps for HEPHAESTUS involved the installation and validation of pilot and demonstration units. In Italy, the CleanTech EAF, fiber formation line, and EZINEX® process will be integrated and tested with real residues. In Greece, the CCT demonstrator will validate CO_2-to-methanol conversion at industrially relevant scale. HEPHAESTUS has shown that a multi-technology approach, combining pyrometallurgy, hydrometallurgy, and carbon valorization, can unlock the circular potential of EAF and AOD residues. While scale-up challenges remain, the project is on track to deliver a replicable model for residue-free, carbon-reduced steelmaking. Its outcomes will support European strategic autonomy in critical raw materials, reduce environmental burdens, and create new circular markets for fibers, zinc, and methanol.

3.2.17 RecHycle: Recycling renewable hydrogen for climate neutrality (103)

The project was coordinated by Areclormittal with Joanneum Research Forschungsgesellschat, Università Politecnica delle Marche, CNRS, University of Bordeaux and IRT Antoine de Saint Exupéry participating as partners in the consortium. The project started on the 1st of June 2022 and lasts almost four and half years, ending on the 30th of November 2026. The overall project cost 28.4 M€ and the EU contributed 6.2 M€, i.e., almost 20 % of the budget.

Hydrogen produced from renewable energy is climate friendly being one of the potential paths to help EU achieving climate neutrality. The RecHycle project aims to implement a gas hub able to mix metallurgic gases produced on site with/without external green hydrogen sources. The mixing will be balanced using predictive software tools and adding natural gas to ensure a secure mix. The mixed gas will be then fed into BF as substitute to coke and pulverized coal and in the future in DRI furnaces for the sustainable production of green steel. The project represents a cost-efficient solution to decrease carbon emissions starting a new symbiosis between the steel industry, chemical industry and renewable energy sources, e.g., wind or solar to obtain green electricity or hydrogen, and contributing to the transition towards circular economy where waste products are valorized to the maximum of their potential. The main challenges to be addressed are the dynamic optimization of gas mixtures and flows, the minimization of the risks connected to material embrittlement due to hydrogen, ceramic feed-inlet tuyere within the furnaces, the quality of the produced steel and the future material scrap streams of the DRI.

The development and integration of the gas-hub and its auxiliaries was divided into three steps. The first step is dedicated to verify the correct functioning of all systems and processes through cold and hot commissioning and to improve the operation in terms of equipment wear, maintenance requirements, safety aspects, etc. The second phase consists of an industrial measurement campaign which targets the characterization and specification of the metallurgic gases, load and energy demand requirements, the balancing of the gas hub with natural gas, and injection into BF with subsequent monitoring of its operations. Finally, the demonstration will be concluded by a 2-year campaign in which the stability and continuity of the process will be evaluated as well as the quantity and quality of the mixed metallurgic gases. During this phase, system performance will be evaluated from the end-user point of view, but also from the authorities, recycler, product, and technology provider point of view. The operation should be safe, techno-economically viable and within environmental and health standards.

A real-time software protocol was developed to connect the energy management system with dispatch tools, supported by a dashboard displaying multi-day forecasts of coke oven gas production and usage to help BF operators anticipating flaring risks. Ceramic tuyere design was refined through modelling and feasibility tests were done and geometry was verified via scanning to rule out faults.

It must be considered that the use of hydrogen imposes relevant material challenges in metallic components because it can infiltrate and position at the border of the grains where it accumulates and expands promoting cracks, or it can react with the metallic material creating hydrides brittle formation. In both cases, the phenomena can be grouped as hydrogen embrittlement which is a detrimental effect which leads to material weakening and premature failure. The latter could be extremely dangerous in installations such as hydrogen-driven steel making because hydrogen is extremely flammable and could cause tragic explosions. Considering that the RecHycle project aims to develop a hydrogen-driven steel-making prototype plant which will include a supply system to transport hydrogen to BF, it is of paramount importance the analysis of H2 effect on metallic piping and BF elements.

The evaluation of hydrogen embrittlement included a first step where an analysis of the components exposed to H2 was performed. The level of impact that it has on their correct functioning was determined. Since not all materials or components are equally affected by hydrogen embrittlement, the first step is fundamental to select the critical components of the pipeline which supplies H2 to BF. After that an accurate screening of the materials used to make these components was carried out and an in-depth study of the impact of hydrogen on their properties was performed to determine if they are prone to hydrogen embrittlement and therefore to degradation of their functionality. Both these preliminary studies should lead to the definition of an accurate material testing campaign to determine these effects physically and chemically. The first step in this sense included the definition of the main properties which can reveal the hypothetical hydrogen embrittlement while the second step included the identification of an appropriate way to measure these properties in a constrained experimental facility, i.e., the definition of an accurate test procedure. After performing the tests, a fourth step should include the proposition of protective measures to improve component resistance to embrittlement, e.g., coatings, and/or the identification of other more suitable materials.

Concerning the first step, H2 storage elements are not of interest for the present project purposes since the main H2 supplier will be an independently located electrolyzer. Therefore, the attention was focused on all elements which transfer hydrogen to the furnaces, i.e., the pipes of pipeline and the final blow lances. Furthermore, it was considered that these components are exposed to both cold and hot temperatures, i.e., from room temperature to 1000 °C, thus making necessary the evaluation of different scenarios. The area of the components affected by hydrogen at high temperatures are mainly made of two types of HT Ni alloys, i.e., 57 % Ni/22 % Cr and 70-75 % Ni/14-18 % Cr, while the cold end is made of Sandvik Avesta, i.e., a specialized stainless steel. The testing of these materials was conveniently organized in four parts. First, materials were exposed to H2 for 48 hours both at room temperature and at elevated temperature, i.e., 1000 °C, to simulate in lab conditions the exposure of the pipes to 100 % hydrogen at the cold end and exposure of the lances at the hot end. After that mechanical testing of the exposed and non-exposed material was performed to comparatively evaluate the effect of embrittlement through fatigue tests since fatigue behavior tends to decrease because of hydrogen embrittlement. Metallurgical observations through SEM were also exploited to spot the reasons for embrittlement in terms of metallurgical transformations. Concerning the origin of the material to be tested, the initial idea was to use the real unused components from ArcelorMittal to make the samples, but a problem occurred since the samples obtained were not perfectly flat and mechanical flattening introduced excessive plastic deformation and microstructural change. In light of this, flat materials made with the two Ni alloys of interest were purchased from Goodfellow and compared with the one from the real components. Concerning the first Nickel alloy, the analysis revealed the same phase with γ matrix phase and no γ', γ'' or δ phase for both Good Fellow and ArcelorMittal components. Despite this, it was observed that Goodfellow material was characterized by a relevant number of pores formed during manufacturing process and present throughout the whole bulk of the material. Concerning the second Ni alloy, the overall W percentage proved to be the same for both Goodfellow and Arcelor Mittal components whereas the grain size of Goodfellow was bigger, i.e., >100 μm, than Arcelor Mittal.

Concerning the dynamic properties of the materials exposed and unexposed, hydrogen embrittlement was calculated as the ratio of the cycles withstood by the material after H2 cycling and the ones without H2 exposure. The first alloy, i.e., Inconel 600, was tested with the range of loads 350 and 550 MPa, starting at the mid-value of 450 MPa while the second alloy, i.e., Haynes230, was tested with the range of loads 700 and 500 MPa, starting at the mid-value of 600 MPa. It was concluded that their dynamic mechanical properties were not affected by a 48-h hydrogen exposure, and this will be further confirmed by metallurgical and fracture analysis. Indeed, Inconel 600 did not display any significant variation in terms of chemical composition, microstructure, i.e., γ phase with Cr-rich scattered carbides being the main phase, and grain size, i.e., >50 μm, both at room and high temperatures after H2 exposure thus indicating no hydride or further carbide formation within the material. The absence of intergranular and intragranular carbides may be a reason for the material not being affected by hydrogen infiltration. Indeed, hydrogen embrittlement occurs often at carbide inclusions as these are defects within the material. Analogously, Haynes230 did not display any significant variation in terms of chemical composition, microstructure, i.e., tungsten rich precipitates remained evenly scattered throughout the material, and grain size, i.e., from 50 – 200 μm, both at room and high temperatures

after H2 exposure. In conclusion, none of the material displayed relevant embrittlement and microstructural change on both room and high temperature after charging and testing which indicates their resistance to the phenomena of cracking or hydride formation.

3.2.18 ReMFra: REcovering Metals and Mineral FRAction from steelmaking residues (104)

The project is coordinated by Tenaris with Tenova, RINA Consulting-CSM, ESTEP, K1-MET, Voestalpine, Montanuniversität Leoben, FEhS, TKS, Tata Steel and Celsa participating as partners in the consortium. The project started on the 1st of December 2022 and lasts almost three and a half years, ending on the 31st of May 2026. The overall project cost 6.76 M€ and the EU contributed 4.64 M€, i.e., almost 70 % of the budget.

The European steel sector is a cornerstone of modern industry producing more than 150 Mtonnes of crude steel annually and supporting key value chains in manufacturing, construction, and energy. However, steelmaking is also one of the most resource and emission-intensive industrial activities generating several Mtonnes of by-products and residues, e.g., dusts, scales, sludges, and slags, each year which remain largely underutilized. Currently, a significant share of these residues is disposed in landfills representing both an environmental liability and a waste of valuable secondary raw materials that could replace virgin inputs. This challenge can be addressed only through new technologies to combine resource efficiency, circular economy, and decarbonization objectives and the ReMFra project aims to provide exactly such a solution. Its main objective is the development and validation of a highly efficient pyrometallurgical melting and reduction process at industrial scale able to recover metals and minerals from a broad range of steelmaking residues. By recovering valuable metals from residues, the project reduces the need for virgin raw materials, minimizes landfill disposal, and contributes to lowering the overall CO_2 footprint of steelmaking. The use of secondary C sources, e.g., waste polymers, as reducing agents further enhances the sustainability profile of the process. Ultimately, ReMFra is expected to deliver a flexible and replicable solution for steel plants across Europe.

The project focuses on two complementary demonstration technologies. The first one is a plasma reactor dedicated to coarse residues such as mill scale, sludges, and slags where the plasma unit operates as high-temperature smelting and reduction furnace producing pig iron, iron-rich oxide fractions, and an inert slag suitable for further valorization. The second one is the RecoDust solution developed by K1-MET which targets fine-grained dust, e.g., EAF, BOF, BF dust, and micro-granulates, which employs a flash reactor with pneumatic conveying of residues using reducing gases, enabling the separation of ZnO and recovery of Fe-rich fractions. By integrating these two processes, ReMFra aims to reach a residue recycling rate over 80 % with metal and mineral recovery efficiencies exceeding 90 %. The outputs of the system include pig iron directly reusable in steelmaking, concentrated ZnO which represents an economically valuable by-product for the non-ferrous industry, iron-rich oxides substituting primary iron ore and inert slag, suitable for applications in construction and other sectors. A schematization of the overall ReMFra concept is provided in Figure 49.

A plasma reactor operates through collisions between gas molecules and electrons generating excited and highly unstable ionic species with high energy. Electrical energy is supplied via graphite/tungsten electrodes which create an electric arc. Plasma operation typically begins after flame stabilisation under an Ar flux. It is widely accepted that applying plasma technology to the steel industry would lead to lower costs and a smaller environmental impact, given that a higher calorific power can be obtained using the same reducing agent. This technology could also be applied to recover iron from steelworks waste, reducing resource recovery costs. The process is suitable for various feeds such as slag, dust, and sludge from steel production, as well as streams containing heavy metals (V, Mn, Co) and silicon-based materials. More sustainable reducing agents like biomass, waste plastics, and hydrogen could also be used. The reactor operates at temperatures up to 2000 °C with minimal energy consumption, producing iron for direct reuse in steelmaking and mineral-rich slag that could be used in cement production. The temperature of the reactor walls is monitored and cooled by water circuits at both the bottom where the charge melts and top where the flame forms. A simplified scheme of the plasma reactor is shown in Figure 50.

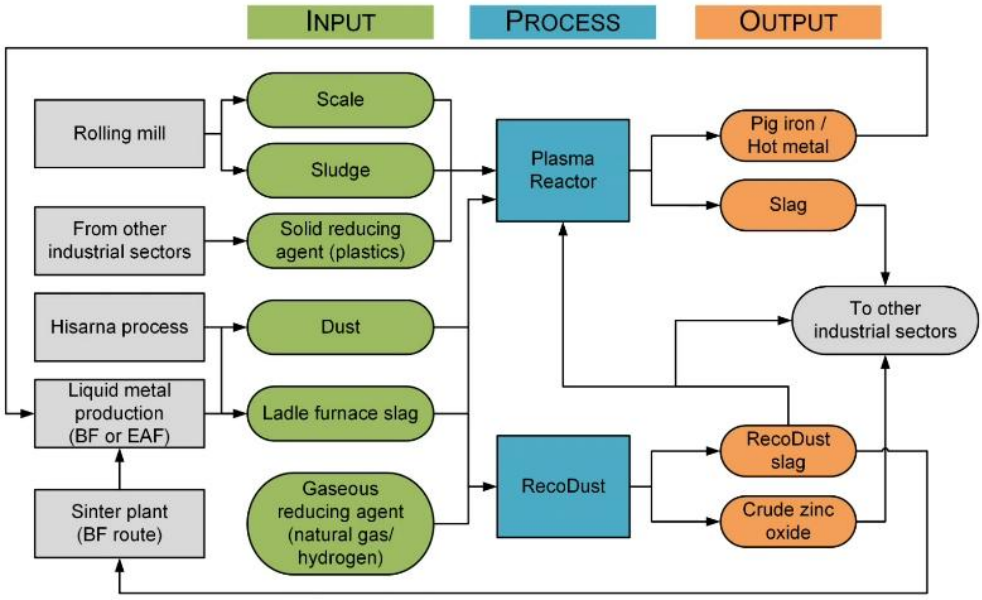

Figure 49: Schematization of the ReMFra project (105)

The RecoDust technology is dedicated for the use of steel mill dusts like from BOF, EAF or the HIsarna pilot plant and the related pilot plant is shown in Figure 51. The dusty feedstock is filled into the storage tank and after an inertization is brought pneumatically with natural gas as conveying media to the burner. Slagging happens in the flash-reactor using an air excess ratio below one. This low reducing atmosphere reduces Zn and gaseous Zn is brought via the off-gas to the converter where the post-combustion of the unburned substance and its reoxidation takes place. After further quenching, a bag filter cleans the off-gas and crude zinc oxide can be separated. The non-volatile components are

separated as an oxidic phase. The RecoDust slag in the flash-reactor can be tapped discontinuously. Due to the low reducing atmosphere, no metallic fraction is formed out.

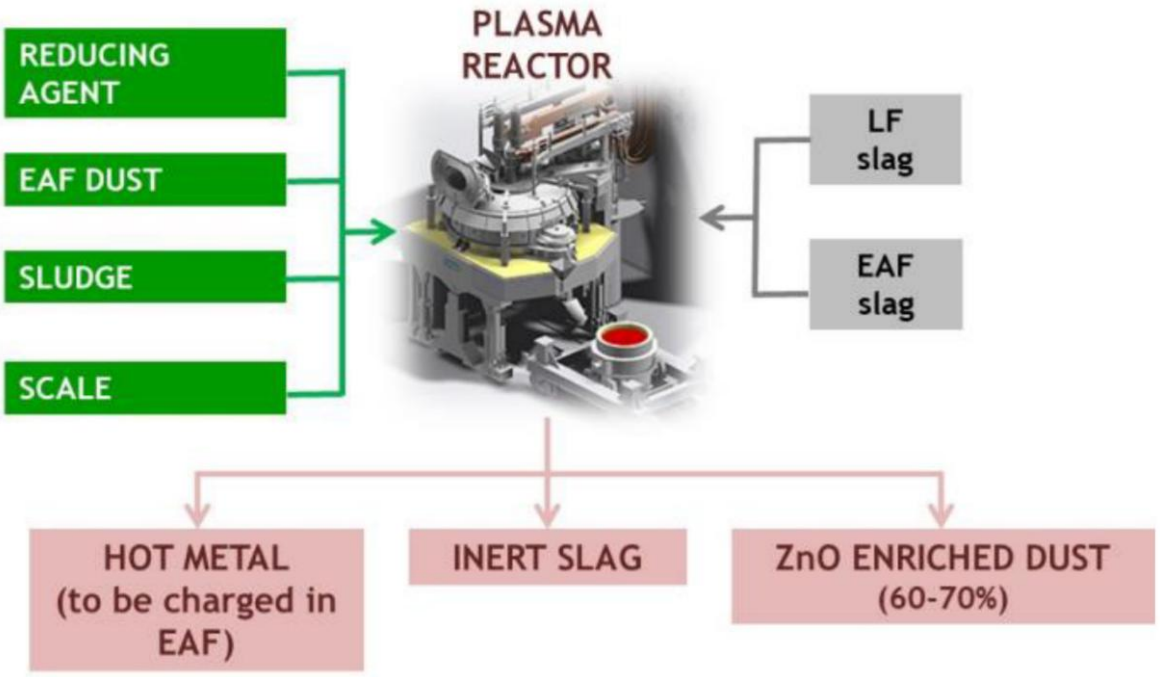

Figure 50: Simplified scheme of the plasma reactor-based pyrometallurgical process, including the input and output streams (106)

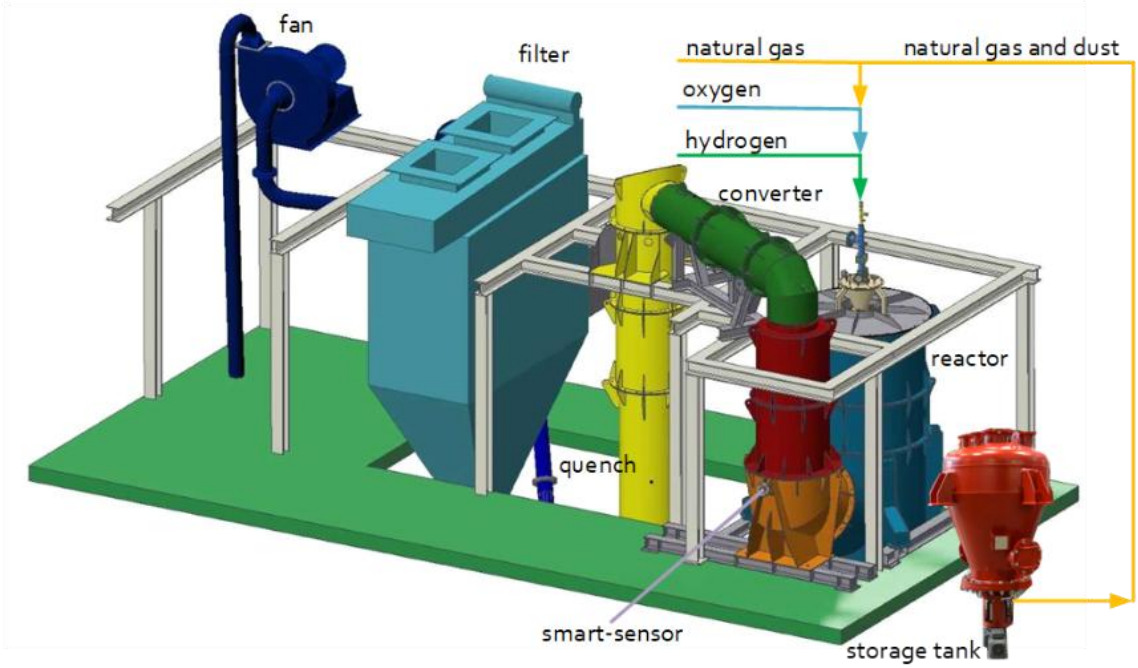

Figure 51: RecoDust pilot plant established at the Chair of Thermal Processing Technology (107)

A distinctive feature of the ReMFra concept is its focus on industrial-scale validation. Indeed, laboratory and pilot studies have long demonstrated the technical potential of pyrometallurgical residue treatment, but large-scale implementation remained limited due to challenges such as feedstock variability, energy consumption, and process integration. ReMFra directly addresses these barriers by adapting existing metallurgical infrastructure. In particular, the Tenaris Dalmine ladle furnace was modified to host the plasma-based smelting reduction process while an industrial RecoDust plant, including dust feeding, flash reactor configuration, ZnO collection, and energy recovery concepts were designed and engineered. By combining plasma and RecoDust technologies, the project demonstrates that full valorization of steelmaking residues is technically feasible, environmentally beneficial, and economically viable. The outcomes will not only validate the demonstrators but also contribute to the development of new industrial standards, training programs, and regulatory frameworks, paving the way for widespread adoption of residue recycling in the steel industry. In parallel, extensive thermodynamic modelling, CFD simulations, and material testing were performed to define briquette recipes, evaluate melting behavior, and optimize off-gas management. These activities were essential for ensuring that the plasma and RecoDust systems operate safely and efficiently without disrupting normal steel production.

A fundamental step of the project was the identification and classification of steelmaking residues suitable for processing in the two demonstrator units, i.e., the plasma reactor for coarse fractions and the RecoDust system for fine dust. Residue data were collected and compiled into a dedicated database integrating information from industrial partners Tenaris, TKS, Tata Steel, Voestalpine, and Celsa. Four main categories were selected which are slags from EAF, BOF and ladle, scales from rolling mill which are rich in FeO/Fe_3O_4, sludges from wet dust removal systems containing fine oxides and oil residues, and dusts from EAF, BOF, and BF. Each residue stream was characterized by chemical composition through XRF and ICP, by moisture, particle size distribution, and LOI, to determine the suitability for pyrometallurgical reduction.

After this preliminary characterization, residues destined for plasma reactor required agglomeration into briquettes to ensure proper handling, mechanical stability, and efficient smelting reduction. In light of this, RINA-CSM defined different briquette recipes using scale, sludge, and slag as base fraction combined with carbonaceous reductants and binders. Conventional anthracite as benchmark and I.BLU polymer wastes as alternative secondary carbon sources to reduce CO_2 footprint were tested as reducing agents. Concerning the binders, molasses, lime, and water were added to improve green strength and reducibility and the recipes tested were both binary, i.e., 75 % scale and 25 % reductant, and ternary mixtures. Drop tests were performed to evaluate briquette mechanical strength and resistance to handling and the optimal recipe was selected based on density, durability, and Fe/C ratio ensuring suitability for plasma furnace charging. Laboratory-scale melting trials were also conducted in controlled conditions to evaluate metallic yield, i.e., wt.% metal recovered, C content in pig iron, i.e., carburization, slag composition in terms of basicity and residual Fe and finally Zn distribution, i.e., concentrated ZnO versus slag. The comparison between binary mixture with 75 % scale and 25 % of anthracite or I.BLU-based extrudates indicated high metallic yields in both cases, though carburization remained lower for polymer-based recipes. As previously disclosed, RecoDust targeted fine-grained dust and included a pre-treatment step with sieving to adjust grain size distribution, drying to reduce

moisture content and prevent blockages in pneumatic transport and pneumatic conveying trials to assess dust fluidity and optimize injection conditions. Different dust samples from Voestalpine BOF, Tenaris EAF dust, TKS BOF, and Tata steel micro granulates were tested with a heating microscope and in lab-scale setups to determine melting range and reduction potential.

Concerning process modelling and simulations, thermodynamic modelling of briquette smelting in the plasma furnace was performed by RINA-CSM evaluating mass and energy balances, predicted slag/metal ratios, expected metal yield and C pick-up and off-gas composition, i.e., CO, CO_2, H_2. Three briquette recipes were simulated at 5 and 10 t/h feed rates, providing data for reactor sizing and ladle volume requirements. Tenova performed CFD analyses with ANSYS Fluent to model gas flow, temperature distribution, and heat flux in the plasma reactor and off-gas duct. This analysis optimized reactor geometry and identified potential hotspots or areas of incomplete combustion. K1-MET and Montanuniversität Leoben contributed to the design of the RecoDust Flash-Reactor and their modelling efforts included fluid dynamics of dust injection, residence time optimization which must be long enough for Zn volatilization, post-combustion zone design for ZnO recovery and heat recovery concepts during gas quenching.

Concerning plant design and modifications, Tenova developed the basic and detailed engineering for adapting the ladle furnace at Tenaris to host the plasma smelting reduction process. The modifications included the installation of two new silos and vibro-feeders for briquette feeding, adaptation of ladle refractory lining to withstand high-temperature reducing conditions, integration of plasma torches and off-gas extraction system and automation and control upgrades to allow dual operation both conventional and ReMFra process. For the RecoDust demonstrator, K1-MET and Voestalpine led the engineering of a demonstration plant with a throughput of 1000 kg/h. The key features were an adapted pneumatic conveying system using reducing gas, a flash reactor with optimized geometry for dust melting, ZnO collection unit and quenching system with heat recovery and refractory design for extended lifetime under aggressive dust conditions.

Focusing on the main results of the project, Tenaris Dalmine hosted the plasma reactor demonstrator and provided residues such as EAF dusts, scales, and slags. The briquetting trials performed using their own feedstocks and employing briquettes with 75 % of scale and 25 % of anthracite/I.Blu polymer wastes displayed high metallic yields and good mechanical stability although carburization remained lower when using I-Blu polymers compared to anthracite. Initial smelting tests confirmed high metallic yield in all cases with slightly higher performance for anthracite-based briquettes. The slags obtained were chemically stable though adjustments in basicity were necessary. Tenova led the basic and detailed design and engineering of the plasma reactor demonstrator together with a tailored control system for monitoring plasma power input, off-gas composition, and slag foaming behavior and ensure allow safe and efficient dual operation of the ladle furnace. Their CFD simulations to simulate gas flow, temperature fields, and heat fluxes in the reactor and off-gas duct indicated stable thermal profiles and effective gas extraction, with optimization of burner positioning and flue gas cooling. RINA-CSM contributed to feedstock characterization and process modelling. In particular, residue classification was developed and a residue database with full chemical, mineralogical, and physical data was created and served as the basis for recipe formulation. Thermodynamic modelling simulating three briquette

recipes at 5 and 10 t/h feeding rates predicted metal yield between 75–90 % depending on recipe, slag volume and composition including maximum foaming behavior and off-gas composition with CO up to 40 vol.%. Energy balances demonstrated that operating at ~5 t/h minimizes specific energy consumption while 10 t/h operation increases throughput but requires higher plasma power. Results also indicated that polymer-based briquettes could partially replace fossil reductants, but supplementary C addition was required to reach target carburization.

K1-MET and Montanuniversität Leoben coordinated the development of the RecoDust demonstrator for fine-grained residues. Lab-scale trials with dust samples from Voestalpine, TKS, Tata, and Dalmine in a heating microscope under inert conditions displayed significantly varying melting ranges. BOF dust from TKS displayed high melting temperatures while EAF dust from Tenaris showed excessively high melting range suggesting the need for blending with BOF dust. The RecoDust flash reactor with 1000 kg/h throughput was engineered and the pneumatic conveying tests confirmed that most residues could be fed with minor pre-treatment. In particular, Voestalpine BOF dust was suitable after sieving with a stable melting behavior, TKS BOF dust required both drying and sieving and displayed melting range higher than expected requiring blending with other residues, Celsa provided EAF-based residues and Tata Steel provided micro granulates which could potentially be used in RecoDust, but pneumatic conveying trials are still needed. Furthermore, the reactor was designed with a post-combustion zone for Zn volatilization and a quenching system for ZnO capture coupled with energy recovery solutions. More than 20 RecoDust trials with different feedstocks were done and one exemplificative trial is described in Table 1Table 30. It reports the total iron (Fe_{tot}), iron reduction degree (Fe_{Rd}), the iron metallisation degree (Fe_{MD}) and the Zn content.

Table 30: Fe and Zn of the feedstock and both RecoDust products, the RDS and the CZO

Substance	Feedstock	RecoDust Slag	Crude Zinc Oxide
Fe_{tot}	46.1	48.41	7.94
Zn	18.1	0.22	69.10
Fe_{RD}	31.09	25.73	17.46
Fe_{MD}	22.77	0.04	17.46

The main element of the feedstock is iron with Fe_{tot} values > 46 %, the Fe_{RD} shows that nearby 10 % is metallic iron. Due to the high Fe_{RD}, hematite is the main substance accounting for more than 34 %. The Zn content of this feedstock, i.e., a BOF dust, is >18 %. The first product of the RecoDust process, i.e., the slag, has higher Fe_{tot} content than the feedstock due to the evaporation of volatile components. The Fe_{MD} is due to the very low with 0.04 % gas atmosphere in the Flash-Reactor. The Fe_{RD} of about 26 % shows that the main component is wüstite with nearby 50 %. The Zn content of 0.22 % is very low compared to the 10% content in the feedstock. Most of the Zn is collected in the second RecoDust product, i.e., the crude zinc oxide, having a content of 69.1 % present as zinc oxide. Fe_{tot} of nearby 8 % is representing the carry-over, i.e., the non-volatile components which are brought via the off gas to the bag filter. Via optimisation of the Flash-Reactor geometry in combination with the burner design

should be able to reduce this amount of Fe_{RD}. There is still a little bit metallic iron, which means that it is not oxidised in the Flash-Reactor or in the converter.

The results obtained so far demonstrated both the technical feasibility and the strategic value of integrating advanced pyrometallurgical processes for residue valorization. The plasma reactor route validated through briquetting trials and thermodynamic modelling proved to be capable of converting coarse steelmaking residues into valuable outputs such as pig iron, Fe-rich oxides, and inert slag. High metallic yields of 75–90 % were achieved with both anthracite and polymer-based briquettes though carburization levels remained a critical parameter. Further optimization of reductant type and ratio is required to meet metallurgical specifications, especially for pig iron C content. The RecoDust route confirmed its ability to treat fine-grained residues. Zn volatilization and recovery are technically achievable at the designed throughput of ~1000 kg/h, though some feedstocks require blending to optimize melting ranges. Despite encouraging progress, several challenges remain before full industrial demonstration can be achieved. The first one is feedstock variability since chemical composition and physical properties of residues differ significantly among plants requiring flexible recipes and blending strategies. The second concern attains to carburization control since alternative reductants such as polymers reduce CO_2 footprint but limit C dissolution in pig iron, necessitating careful balancing with fossil reductants. Operational integration is another challenge since modifications to industrial furnaces must minimize impact on standard production, delaying implementation and increasing engineering complexity. If successfully demonstrated, ReMFra will deliver substantial environmental advantages with recycling of steelmaking residues >80 % thus drastically reducing landfill disposal, reduction of CO_2 emissions through the use of secondary C sources and energy recovery, substitution of primary Fe ore with iron-rich oxides thus cutting dependency on virgin raw materials and production of concentrated ZnO as a marketable by-product for the non-ferrous industry. Economically, the recovery of ZnO and pig iron represents a revenue stream that could offset operational costs, while inert slags can find applications in the construction sector.

The next project phases will include industrial trials at Tenaris plasma reactor industrial testing briquette recipes under real production conditions, ramp up of the RecoDust demonstration plant validating fine dust processing and ZnO recover, LCA and techno-economic assessment quantifying environmental benefits and cost-effectiveness, standardization and policy integration, fostering regulatory acceptance and future replication across European steel plants. ReMFra has demonstrated that a combined Plasma/RecoDust approach can close the loop on steelmaking residues, transforming what is today considered waste into valuable secondary resources.

3.2.19 Carbon4Minerals: Transforming CO2 into added-value construction products (108)

The project was coordinated by VITO with Heidelberg Materials, ArcelorMittal, Etex Services, Vandersanden Steenfabrieken, RWTH, Fenix TNT, NTNU (Norges teknisk-naturvitenskapelige universitet), TCKI (Stichting Technisch Centrum voor de Keramische Industrie), SINTEF, Carbonoro Products, Konlechner Davide, and Carbon Upcycling Technologies participating as partners in the consortium. The project started on the 1st of January 2023 and lasts almost four years, ending on the

31st of December 2026. The overall project cost 20.3 M€ and the EU contributed 14.8 M€, i.e., almost 73 % of the budget.

The reduction of 40 % of GHG emission by 2030 and climate neutrality by 2050 are major challenges for energy intensive industries such as steel and cement ones. This green transition can be only partially assisted by renewable energies which can alleviate a significant part of GHG emissions but offer no solution for process-inherent emissions. Considering this, residual hard-to-abate CO_2 emissions need to be captured, processed, and recycled into new products to meet these targets while preserving sector competitiveness by developing less expensive carbon capture solutions. The Carbon4Minerals project aims to propose viable solutions to simultaneously use CO_2 from industrial flue gases in conjunction with current and future waste streams to release a stock of resources for innovative low C binders and construction materials. Indeed, the cement industry is looking for alternative materials to replace Portland clinker and reduce the huge amount of GHG resulting from limestone calcination while the green transition in steel production is decreasing the supply of low C resources commonly used for cement production such as BF slag and coal fly ash. A total of 8 industrial pilots summarized in Figure 52 were planned to be built within the project and to operate across the process value chain from CO_2 capture to cement production and low C construction products. It was foreseen that the development of innovative CO_2 capture technologies and their use in carbon-negative construction products should ensure a reduction by 80-135 % in CO_2 emissions compared to cement-based reference materials. Furthermore, this cross-sectorial approach has the potential to reduce European CO_2 emissions by 46 Mt/y, i.e., 10 % of EU process industry emissions, while safeguarding the competitiveness of the European industry.

Concerning CO_2 capture, two different technologies were considered and developed to reduce energy requirements and costs compared to state-of-the-art technologies. In particular, a 3rd generation liquid amine solvent solution (Pilot 2.a) which allows to obtain a CO_2 purity of 80-99 % with an energy consumption <2.4 GJ/tonne, and a porous structured sorbent material (Pilot 2.b) were considered. The preliminary results on the sorbent porous structure showed that a decrease of 5-10 times in pressure drops could be achieved compared to conventional packed beds and further optimization should ensure an increase in efficiency of the sorption/desorption cycles. Moving to the cement level, three different concepts were developed. The first concept was a carbonation clinker (Pilot 3.a) created by coupling steel slag and cement-based residues targeting savings of 200 kg CO_2/tonne. After optimizing the clinker mix at the laboratory scale, a pilot trial was performed, and more than 1 tonne of carbonation clinker was produced with the same performance obtained at the lab scale and capturing 150-200 kg CO_2/tonne. The second concept was a carbon-negative SCM made by CO_2-mediated mechanical activation of steel slags (Pilot 3.b). The last concept included the CO_2 beneficiation of recycled cement-based construction and demolition waste (Pilot 3.c). Finally, three low carbon construction products were proposed. The first concept (Pilot 4.a) concerned carbon-negative carbonation cured facing bricks and pavers produced by direct carbonation of steel slags. The pilot is already operative and is producing its standard mix products and many efforts are made to adapt the mix to BOF slag use. The second concept (Pilot 4.b) focused on precast carbonation cured products such as façade panels, and roof tiles made using the carbonation clinker and SCMs including eventually carbon fibers (Pilot 4.c).

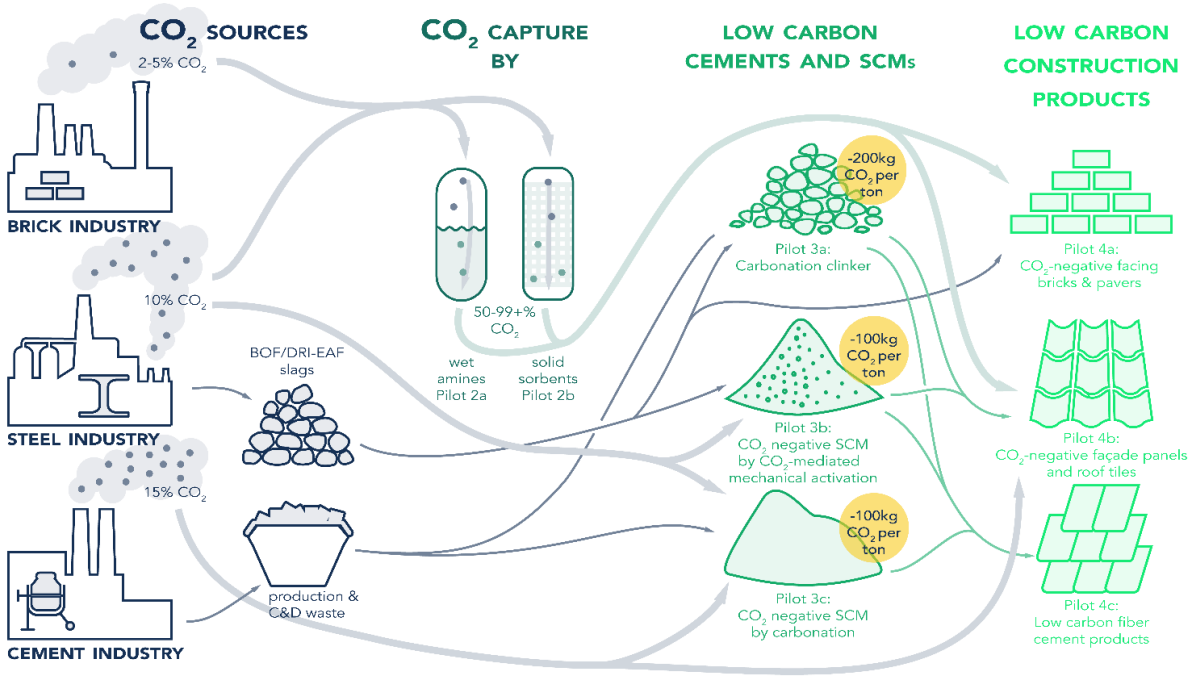

Figure 52: Representation of the Carbon4Minerals concept with the 8 industrial pilots foreseen

3.2.20 GreenHeatEAF: Gradual integration of REnewable non-fossil ENergy sources and modular HEATing technologies in EAF for progressive CO_2 decrease (109)

The GreeHeatEAF project was coordinated by SSSA with BFI, Swerim, Sidenor, Linde Sverige, ESTEP Plateforme Technologique Europeenne de l'Acier, 7 Steel Nordic Manufacturing, Celsa Opco, SA, Heidelberg Materials Cement Sverige, Hoganas Sweden and SSAB participating as partners in the consortium. The project started on the 1st of January 2023 and will end on the 31st of December 2026. The overall project cost 4.1 M€ and the EU contributed 3.56 M€, i.e., almost 85 % of the budget.

EAF represents the key technology to achieve the steelmaking decarbonisation since it is scrap-based, i.e., a circular economy process. In this context, the DRI-EAF route where EAF is fed with DRI to limit the contents of contaminants in liquid steel is expected to partially replace the steel production by BF-BOF therefore the GreenHeatEAF project aims at further increasing the key role of EAF. EAF route is the most important example for modular and hybrid heating, as already now partly combines electric arc heating with burner technologies. The project addressed the replacement of natural gas and other fossil energy sources with hydrogen in existing or re-vamped burners together with innovative technologies like CoJet burners. Further technologies to re-optimise the heating management with maximum heat recovery from off-gas and slag are explored by coupling pilot tests with digital applications. Decarbonisation of EAF route by feeding EAF with alternative Fe-bearing materials like DRI and hot briquetted iron and alternative non-fossil carbon sources was also investigated. Technologies to re-optimise the heating management with maximum heat recovery from off-gas and slag employing new sensor and soft-sensor concepts as well as extended digital twins are also developed. The extended CFD and flowsheet models, and monitoring and control tools must support

an analysis on how the different decarbonisation measures influence EAF and process chain to support upcoming decarbonisation investments and to enable the control of decarbonised hybrid heating with maximum energy efficiency. Trials in demonstration scale, e.g. in combustion- and EAF-demo plants, were combined with validations in industrial scale and digital optimisations. GreenHeatEAF supports the implementation and digitisation to accelerate the transition of the European steel industry to highly competitive energy-efficient decarbonised of the whole sector. GreenHeatEAF aims to demonstrate the integration of non-fossil fuels and renewable C-sources in EAF route to reduce CO_2 emissions and the dependence from fossil energy and C-sources markets combining pilot, on field and simulations. Furthermore, improvement of heat recovery solutions both from off-gases and slag, considering the features with the introduction of H_2 and/or biomass as well as different charge materials and modes are considered. Technologies for heat recovery are tested and optimized. By considering different business cases, the results transferability at industrial levels will be ensured.

The specific objectives of the project include the integration of non-fossil gases flows in EAF processes, including different charge materials and configurations in the context of GHG reduction and green transition of the steel sector. The project also targeted the development of modular regenerative and alternative heating technologies to improve the heat recovery from off-gases and to maximize slag latent heat exploitation for their valorisation. Furthermore, biomass/biochar exploitation for non-fossil energy intake in EAF will be also demonstrated together with the potential of coupling novel measurement techniques and optimised control strategies to exploit and facilitate the integration of novel non-fossil heat/energy sources and streams. GreenHeatEAF solutions will be also assessed in terms of CO_2 emissions and environmental impact considering the transition to C-lean steelmaking. Finally, different business case will be considered and developed. The overall concept of the GreenHeatEAF project is summarized in Figure 53.

Figure 53: GreenHeatEAF overall concept

The main results achieved so far include the design and construction of the scaled burner for demonstrating hydrogen enhanced combustion for EAF heating by using standard EAF burner as well as the demonstration of hydrogen use with CoJet-technology with different iron carriers in the pilot EAF at Swerim. CFD simulations to study hydrogen enhanced combustion were also performed and the data provided by Sidenor allowed to update the EAF dynamic process model of BFI and the EAF and secondary metallurgy stationary process model of SSSA. Another important result was achieved by performing trials on DRI and scrap feeding to modify EAF slag for the cement industry using additives, e.g., Al, FeSi, SiO_2, during tapping. The SSSA model was adapted to simulate hydrogen use in EAF burners in partial or total replacement of natural gas and to feed DRI and hot briquetted iron in EAF and perform preliminary simulations. Furthermore, one option to integrate renewable C-sources in EAF operations and avoid CO_2 emissions in the melting process of steel production is related to the substitution of fossil fuels by other renewable organic materials based on C like biomass and biochar. This material could directly substitute the anthracite and coal used during the process. By analysing and selecting the most suitable biomass and biochar to substitute fossil fuels in the EAF, industrial trials complemented by simulations with a dynamic process model for the EAF allowed to assess the influence of biomass/biochar on energy and material flows and chemical composition of the liquid steel. Market research on the available biochar and other renewable materials were carried out and the different industrial cases studies with their technical requirements were analysed to select the most adequate bio char available for the industrial trials. This activity was supported by the development of simulation analyses to determine the influence of these C-renewable materials on steelmaking processes and product. The first versions of flowsheet models related to two biomass upgrading processes, i.e., pyrolysis and torrefaction, was also developed and pilot/demo trials at Swerim using bio-carbon as injection coal, and industrial trials at Sidenor, Höganäs and Celsa were also performed. Finally, a new system to monitor gas heat basing on the specifically adapted Acoustic GAs-Measurement system (AGAM) system and other relevant process data was developed and the optimal position for the measurement to prepare the installation of the AGAM system was also identified. Initial impact plan and possible deployment opportunities were also developed.

Focusing on the use of SCCs, industrial trials substituting different C-sources during the melting process in the EAF were carried out, by introducing C to EAF in different shapes and ways. Concerning anthracite, it can be added in the scrap basket or through the 5th hole due to its higher size while foaming coal was added through injectors. One of the aims of performing both pilot and plant industrial trials within GreenHeatEAF is to explore the effect of different biomass/biochar on process stability as well as injection efficiency. However, a study of the features of the biomass that could affect most the operation in the EAF was carried out with each industrial partner studying the technical and conditioning requirements to be used distinguishing between the use cases and applications. In the case of Sidenor, two main applications were considered, i.e., substitution of anthracite introduced through the 5th hole and the substitution of the foaming coal injected through the cojets, demanding to obtain the same performance of current C materials. In Celsa Nordic, the biochar replaced the current C-bearing foaming agent while if Höganäs steel plants different requirements for biochar to be used in sponge iron and EAF processes were considered. At Swerim, some criteria were considered when injecting bio-carbon in pilot trials, e.g., max size for C particles of 3 mm, max moisture of 5 %,

fixed C over 90 % to be good for the process, ash and volatile content should be as low as possible, high density.

A market investigation was carried out to study the availability of biomass and biochar by contacting 20 companies specialised in biomass and identifying 24 different materials from 9 countries. Types and quantities of biomass and biochar available were analysed considering factors such as geographical location, source, composition, morphology, production processes and industrial process target. In addition, characteristics of biomass and biochar such as the calorific value, nutrient content, moisture levels, and stability, were also considered. Investigation on the characterization of biochar samples was conducted to assess the suitability of biochar from various sources for specific applications, to inform decision-making processes and promote the development of sustainable biochar production practices. Laboratory analyses were focused on contents of C, S, N, moisture, volatile, ash and HHV. In addition, analyses of the quality and chemical composition were carried out.

Investigations and statistical analysis of first Sidenor trials with the use of biochar at 5th hole were carried out. As far as the investigations with EAF route flowsheet stationary model are concerned, the flowsheet model was developed by SSSA in Aspen Plus V11 environment and adapted during GreenHeatEAF. It was used to perform scenario analyses and evaluate the effect of the substitution of fossil C sources used in EAF with alternative ones. They were complementary to the industrial tests, to extend the industrial trials and/or guiding them. The C-sources were considered in the flowsheet stationary model investigations. They correspond to the alternative C-sources having a content of Fixed C higher than 40 wt.% and only tires were outside these constraints. Biochar of the supplier CPL INDUSTRIES was considered the reference C-source. It was adopted by Sidenor in the preliminary industrial trials where it was used instead of anthracite at 5th hole for the starting of foaming slag formation. Three different scenarios were analysed through SSSA flowsheet model simulations. All scenario were carried out for 4 steel families, i.e., alloyed case hardening, alloyed Q&T, free Cutting, carbon case hardening. The simulation results were used to calculate the following KPIs consumption of electrical energy in EAF [kWh/tliquid_steel], CO_2 emissions of the EAF [kg/tliquid_steel], content of C and S in the tapped metal [w/w], metallic yield [kgmetal_material/tliquid_steel], EAF slag [kg/tliquid_steel]. In addition, secondary metallurgy was monitored.

For the first scenario some heats were simulated by reproducing the preliminary industrial trials at Sidenor which tested the substitution of a part of the whole fossil carbon used in EAF, i.e., anthracite fed at the 5th hole, with alternative carbon sources. The replacement corresponded to less than 15 % of the whole fossil C used. The first industrial tests only considered the use of Biochar supplied by CPL INDUSTRIES used as a reference in the simulations therefore, the simulations expanded the investigations by testing all the alternative C-sources considered. In addition, anthracite was considered as a source of C with the following features fixed C 84 wt.%, S 1wt.%, N 1.20 wt.%, H 5.21 wt.%, O 0.59 wt.%, moisture 6.00 wt.%, volatile 8.00 wt.%, ash 8.00 wt.% and HHV of 8250 kcal/kg. two different scenarios were considered in the simulation. The first scenario, i.e., scenario 1.a, considered the addition of an amount of C-material ensuring the same amount of fed fixed C through the 5th hole while the second case, i.e., scenario 1.b, considered the addition of an amount of C-material ensuring the same quantity of energy supplied through the 5th hole. The second scenario aimed at analysing the

effects of the content of the main compounds of biochar, i.e., C, S, moisture, on the considered KPIs. A partial substitution of fossil C-source, i.e., the one fed in the EAF through the 5th hole and corresponding to less than 15 % of the whole fossil carbon, was considered according to the preliminary industrial trials. The sensitivity analysis was carried out considering the reference biochar by changing respectively the content of fixed-C (scenario 2.a), S (scenario 2.b) and moisture (scenario 3.b) in the range of ±25%. The third scenario involved the replacement of the overall amount of fossil carbon used in EAF and considered two different alternatives. The first scenario, scenario 3.a, considered the addition of an amount of C-material ensuring the same amount of the overall fed fixed C while the second case, i.e., scenario 3.b, considered the addition of an amount of C-material ensuring the same quantity of energy supplied.

Sidenor performed first industrial trials with biochar material which should substitute anthracite addition via the 5th hole to start the slag foaming process. Trial data with biochar were analysed with statistical methods to investigate the possible effect on the chemical composition of critical elements like S and P, or on the consumptions of electrical energy, blown oxygen and C. Consequently, the results were compared with the heats produced under standard conditions and showed that the amount of biochar added via the 5th hole is almost the same as the anthracite added in standard production. No clear effect of biochar usage on the liquid steel composition at EAF tapping regarding S and P were found thus meaning that biochar use seems to have no critical effect on liquid steel quality. Concerning the amount of blowing coke, less C was used before biochar trials, but almost the same amount in the period after the trials. The statistical model considered the specific consumption of total and several individual ferrous materials, slag formers, burner gas, oxygen for blowing by lances and injectors as well as for post-combustion, temperature before tapping and tap-to-tap time. All consumption values were related to the tap weight. The calculated electrical energy demand was plotted versus the actual electrical energy consumption to assess the overall energetic performance. It was noted that the standard production after biochar trials had a slightly lower energetic performance than in the phases before. In addition, the trials with biochar were performed under better controlled conditions. Overall, the use of biochar instead of anthracite did not influence negatively the energetic and yield performance of Sidenor furnace resulting in a good achievement for green steel production.

Concerning the results obtained during the simulations and the sensitivity analyses, the results of stationary simulations included three simulated scenarios. Scenarios 1.a showed that tires provided the highest decrease of EAF electric energy. Due to the low amount of fixed C contained in tires, high tires amount was required to reach the desired fixed C fed and, consequently, higher chemical energy was provided also considering their significant HHV, i.e., 8938 kcal/kg. Anthracite increased CO_2 emissions while there was no clear correlation between C-bearing material and C content in tapped metal, but the variations were limited. In addition, tires led to highest S content in tapped metal due to their highest S content with respect to the other C-sources and their significant amount for ensuring the fed fixed C. Furthermore, small changes in terms of metallic efficiency without a clear correlation were detected and similar behaviour were observed for the different C-sources with respect to EAF slag amount. Only tires led to an evident decrease of EAF slag. Scenarios 1.b showed no clear general correlation between C-bearing material and EAF electric energy consumption and CO_2 emissions from

EAF were almost similar for all considered C-sources apart from anthracite which again led to the highest CO_2 emissions. The C content in tapped metal was lower when tires were used as alternative C-source probably due to their lowest fixed-C content and to low amount of tires fed for achieving the desired energy contribution because of their high HHV. No clear general correlation between C-bearing material and EAF metallic efficiency were detected. Finally, tires and anthracite led to a decrease and an increase of EAF slag, respectively.

Scenarios 2 concerned the sensitivity analyses carried out varying some features of biochar that was added at the 5th hole in Sidenor industrial trials. Scenarios 2.a showed almost linear behaviours of monitored parameters as a function of fixed-C content in the alternative C-source. Limited observed variations were achieved due to the small amount of fossil C substitution between about 5 and 13%. However, the increase of fixed-C content in biochar led to a decrease of EAF electric energy and to an increase of C content in the tapped metal. Slag amount was decreased with negligible changes in CO_2 emissions and in metallic yield. During simulations of Scenarios 2.b where the S content in biochar was varied, higher S content in biochar led to higher S content in tapped metal. The observed variations obviously were limited due to the small amount of fossil C substitution between about 5 and 13 %. Scenarios 2.c investigated the effects of moisture content in biochar referring to the behaviour of EAF electric energy and EAF slag. Small almost linear variations for EAF electric energy and EAF slag were observed with the variation of moisture content in biochar. In particular, the increase of moisture increased the request of energy due to its evaporation therefore, small amounts of moisture were preferable.

Scenarios 3 concerned the substitution of the whole fossil C used in EAF with biochar. For both sub scenarios, i.e., constant fixed-C fed and constant energy supplied with the alternative C-source, the following KPIs were monitored EAF Electric Energy, CO_2 emissions from EAF, C and S content in tapped metal, EAF metallic yield, Slag produced by EAF. The results showed that the complete substitution of fossil c keeping constant the fed fixed-C with biochar led to a significant decrease of CO_2 emissions and of S content in tapped metal as well as a decrease of EAF slag. Similar results were achieved scenarios 3.b. The main difference was due to free cutting family where the simulation was not converged. The possible reason was that for ensuring the energy previously supplied with fossil-C by using biochar meant adding a higher amount of biochar with respect to fossil-C because of its lower HHV. Therefore, more fixed-C was available, and this could lead to higher C content in free cutting steel not respecting its specifications.

The trial heats carried out at Sidenor on biochar usage were assessed with the dynamic EAF model of BFI and heats with biochar usage were compared to standard heats with anthracite addition. Results showed that C input by anthracite presented a higher increase in C content compared to biochar due to its slightly higher C content. Modelling accuracy was almost equal in both cases, showing that the use of biochar did not have a negative impact on the reproducibility of the process performance.

In conclusion, alternative C-sources did not affect always clearly the different monitored process parameters and only in some cases more evident behaviours could be observed. This was the case for instance of tires. In particular, its use seems leading to decrease electric energy and EAF slag, but highest S content and lowest C content in tapped metal. However, to understand the effect of their

partial usage together with anthracite and/or with other alternative non-fossil C-sources, more simulations should be performed. In addition, anthracite led to the highest CO_2 emissions. Overall, alternative C-materials in general did not negatively affect Sidenor process in terms of energy and yields nor product regarding C and S content, but can lead to significant CO_2 reduction, resulting in more sustainable production.

3.2.21 FlexoFibers: Unlocking the potential of second life steel fibers from tire waste for the construction industry (110)

The project was coordinated by FlexoFibers Europa and started on the 1st of March 2023 lasting 2 years and ending on the 28th of February 2025. The overall project cost was 3,56 M€ and the EU contributed 2,49 M€, i.e., almost 70 % of the budget.

The construction sector is facing the critical challenge to embrace circular economy principles to reduce its reliance on foreign material supplies and mitigate its substantial environmental impact characterized by a carbon footprint of 1.83 tons of CO_2 for every ton of virgin steel produced. The use of 600,000 tons of steel fibers for concrete reinforcement in Europe results in 1000 million tons of CO_2 emissions annually. An opportunity to face this challenge was identified in the 3.7 Mtons of end-of-life tires discarded every year, which could potentially provide over 600,000 tons of steel fibers, i.e., almost the current European demand. The FlexoFibers project arose from this opportunity and tried to support the development of a groundbreaking process to produce sustainable second-life steel fibers from end-of-life tires to support the demand for eco-friendly building materials. This would allow to reduce carbon emissions and resource consumption while promoting circular economy principles.

FlexoFibers Europa developed an innovative and proprietary production process for the recovery of high-quality steel wires from discarded tires to be reused within the construction industry. The resulting product is shown in Figure 54.A and is characterized by a small diameter of 0.25 mm, which allows the incorporation of numerous filaments per m^3 of reinforced concrete, and by high tensile strength and flexibility. The process allows a precise and strict control of fiber length thus preventing the occurrence of balling effects within the mixed concrete (Figure 54.B) and enhancing its resistance to flexo-traction and its permeability. Overall, the FlexoFibers process allows to obtain a high-impact resistant concrete with a reduced environmental footprint while fostering the use of sustainable materials into the construction sector and granting tire industry to enter circular economy.

Throughout the project, both the process and the product were improved and developed. In particular, the processing line and the operational processes were refined leading to a notable increase in the processing rate and to the successful engineering design and setup of a pre-industrial line. Furthermore, progress was made in the development of the software for automated control of the process and of an AI-based system (Artificial Intelligence) for quality control. From the product perspective, a range of innovative and market ready concrete-based prototypes for different applications, e.g., pavements and tunnel shotcrete, was created and their performance in terms of lifetime and durability was validated through a comprehensive field-testing program performed in collaboration with industrial customers. A rigorous laboratory testing campaign was also performed to identify product

specifications including dynamic and static load bearing to ensure compliance with EU standards. Based on these outcomes, technical datasheets for steel FlexoFibers will be developed, and efforts will be made to secure essential product certifications, such as CE (Conformité Européenne) marking.

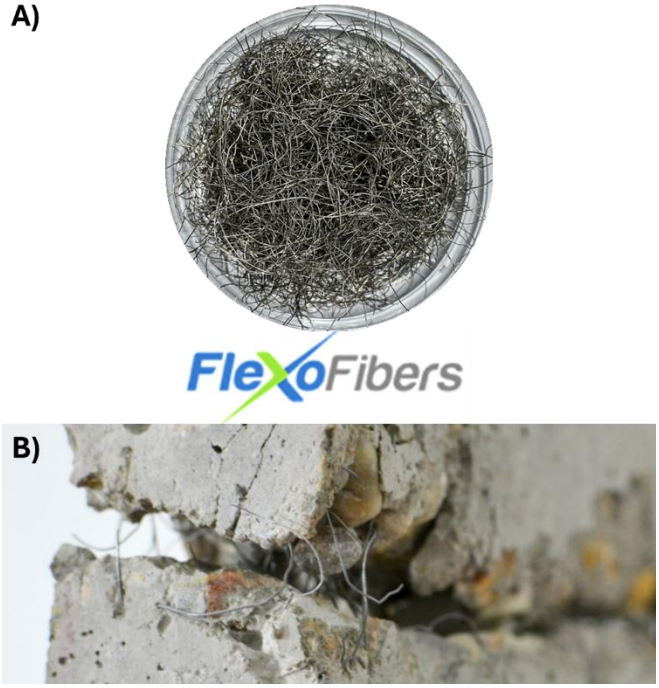

Figure 54: Sample of short steel FlexoFibers (A) and FlexoFibers embedded in the concrete matrix (B) (111)

3.2.22 RESURGENCE: Industrial Water Circularity: Reuse, Resource Recovery and Energy Efficiency for Greener Digitized EU Processes (112)

The project was coordinated by CETIM (Centro Tecnológico de Investigación Multisectorial) with The Navigator Company, RAIZ – Forest and Paper Research Institute, Organik Kimya, Celsa, Aqualia, Universidade do Porto, KTH, NUST (National University of Sciences & Technology), Sveučilište u Zagrebu, SSSA, Universidade Nova de Lisboa, Fundación tecnológica advantx, Aquaporin, Pozzi Leopoldo, Water Europe, ENCO, Strane Innovation and Central Solutions Limited participating as partners in the consortium. The project started on the 1st of December 2023 and lasts almost four years, ending on the 30th of November 2027. The overall project cost 9.22 M€ and EU contributed with the entire budget.

The RESURGENCE project is dedicated to improve the sustainability and efficiency of industrial water management. In particular, the project focuses on advancing circular water systems by integrating innovative, high-performance technologies that enable increased water recirculation, energy recovery, and the extraction of valuable feedstocks from wastewater streams. Through these solutions, RESURGENCE aims to reduce resource consumption and environmental impacts while supporting the transition toward more resilient and circular industrial processes. RESURGENCE is based on the

awareness that European industry is currently facing unprecedented challenges. Growing pressure on water resources, rising energy costs, the need to reduce emissions and waste, and remain competitive in a rapidly changing global market. In this context, RESURGENCE proposes a new paradigm, based on the concept of the circular economy applied to water, energy and materials, introducing innovative solutions that make industrial systems smarter, more sustainable and more resilient. The expected impacts of the project are manifold. From an environmental perspective, reducing water consumption, energy demand, and emissions contributes directly to mitigating climate change. Economically, industries that adopt circular approaches can lower operating costs, enhance competitiveness, and strengthen their resilience to resource price fluctuations. At a strategic level, the project supports Europe goals of achieving climate neutrality and driving the ecological transition, providing concrete examples of how innovation, sustainability, and digitalization can mutually reinforce one another.

The central element of the project is water, which is considered one of the most critical resources for many industrial sectors. The goal is not only to purify wastewater but also to transform it into a regenerated resource, ready for reuse in production processes. To this aim, innovative materials and technologies are being developed in terms of selective membranes, advanced biological processes, high-efficiency filtration systems, integrated solutions that reduce pollutants, recover heat and return high-quality water. In this way, overall freshwater consumption is drastically reduced, and the environmental impact of discharges is significantly decreased. The project also includes two important forms of recovery from wastewater, i.e., energy and resources. Wastewater is often rich in thermal energy and organic substances and their recovery through anaerobic processes, heat exchange, biogas production and other techniques allows them to be transformed into a resource. Similarly, many industrial processes produce waste containing valuable materials, e.g. nutrients, metals, biopolymers, that can be recovered and reintroduced into production cycles. This integrated approach not only reduces waste but also cuts costs and dependence on raw materials.

A key innovative component of RESURGENCE is digitalization. The project enables intelligent management of water and energy systems through advanced sensors, distributed monitoring systems, digital twin models, and data-driven models. In particular, digital twins reproduce real processes analyzing plant behavior, predicting anomalies, suggesting operational improvements, and enabling simulations and decisions. This integration of engineering, data and artificial intelligence permits a qualitative leap towards an industry capable of controlling and optimizing its consumption in real time.

The value of RESURGENCE is clear in its pilot cases which are full-scale laboratories located in various European countries. Each site represents a strategic industrial sector such as paper and pulp in Portugal which is highly dependent on water, chemicals in Turkey with complex and delicate processes, steel in Poland which is an energy and resource-intensive production, and finally, a model of urban-industrial symbiosis in Spain where cities and industry collaborate to share resources and infrastructure. These case studies permit to verify the effectiveness of technologies in real operating conditions, study their economic feasibility, measure their environmental impact and define replicable standards. Another distinctive feature of the project is replicability. RESURGENCE does not aim to create solutions that are only valid in pilot contexts, but to develop guidelines, models, digital tools and methodologies that

enable the large-scale dissemination of innovations. The creation of these hubs is a fundamental step in transforming the project into a driving force for European industrial transition.

Currently, the project has achieved substantial progress in both technological development and validation. A wide range of innovative solutions, including advanced membrane systems, electrochemical processes, selective adsorption materials, hybrid biological treatments, advanced oxidation technologies, and energy recovery concepts, were successfully tested on a laboratory scale using synthetic wastewater representative of the three targeted industrial sectors. In several cases, the systems were also preliminarily validated with real industrial wastewater. Across these tests, the technologies demonstrated strong potential in terms of water recovery, energy efficiency, selective solute separation, and pollutant degradation. Notable achievements include the development of nanostructured and biomimetic membranes with marked performance gains and reduced energy consumption, functionalized electrodes, MOF-based adsorbents, and biochar-based materials. Hybrid anaerobic membrane bioreactors and early-stage energy recovery approaches also showed meaningful improvements over the current state of the art.

In parallel, the project advanced its modelling and optimization activities by developing comprehensive physical and data-driven models tailored to the selected industrial processes. These models are being used for scenario analysis and to optimize energy, chemical, and material consumption. The results directly feed into the Decision Support Tool and support the first risk assessments. Significant steps were also taken in monitoring innovation. The consortium initiated the development of new hardware and software tools for water quality monitoring. These tools pave the way for more reliable process control and improved plant operation. Also, the study related to life cycle assessment (LCA) and cost analysis was started. The initial results compare RESURGENCE technologies with conventional solutions and provide insights into environmental and economic hotspots at laboratory scale, supporting future optimization and safe-by-design strategies for upscaling towards pilot implementation. The project also progressed in assessing circularity and cross-sector synergies. Preliminary evaluations identified potential reuse pathways and opportunities for industrial symbiosis, while tailored circularity metrics were applied at two partner sites to benchmark performance and identify improvement potentials.

3.2.23 Dust2Value: Pioneering Sustainable Recovery in Steelmaking: Hydrogen-Based Technology for Byproduct Management (113)

The project was coordinated by Montanuniversität Leoben with Befesa Steel, M.A.L. (Metallbau Anlagenservice – Leitungsbau), Politecnico di Milano, Georgsmarienhütte and InsPyro participating as partners in the consortium. The project started on the 1st of January 2024 and lasts almost three years, ending on the 31st of December 2026. The overall project cost 4.6 M€ and the EU contributed 4.6 M€, i.e., the full budget.

Zn-coated steel scraps in Europe are mainly recycled through EAF, but this circular activity is responsible for the generation of fine and hazardous dust which is rich in Zn and Fe. Each year, EU produces over 1.5 Mtonnes of this dust while 7–10 Mtonnes are produced globally. The main recycling

path is the Waelz process which relies strongly on coal and coke to recover Zn determining a significant carbon footprint and exacerbating environmental concerns. Furthermore, this process focuses only on Zn recovery thus resulting in the loss of other valuable metals especially Fe. This approach is not only inefficient in its use of resources but also causes a significant energy and climate footprint.

The Dust2Value project is addressing this challenge by introducing innovative hydrogen reduction technology that efficiently recovers all Zn while simultaneously producing an iron-rich material with a high metal content, i.e., DRI, that can be used as a substitute for scrap. This process is briefly summarized in Figure 55 and is able to enhance circularity in steelmaking and industrial symbiosis exchanges with Zn producers while slashing GHG emissions. The core of this innovative technology is a self-sustaining sealed loop that regenerates its own hydrogen. In particular, the hydrogen used to extract Zn and Fe from their oxide is sent in a counter-current flow in a kiln reactor and is then regenerated thanks to the Zn vapor which is captured and re-oxidized using steam in a cooler zone of the furnace. The ZnO fine particles formed exit the furnace via the off-gas stream and are recovered in bag-house filters serving as secondary Zn concentrate. This in-situ hydrogen regeneration is a key innovation which allows to drastically reduce the need for fresh hydrogen thus minimizing heat loss and improving both the climate and cost performance of the technology. Another important aspect of the process is that it does not require any agglomeration.

The Dust2Value project aims to establish a new European value chain for secondary raw materials thus strengthening EU strategic autonomy in critical materials like Zn and providing a high-quality recycled DRI for steelmakers. This circular solution allows to turn a costly waste stream into a revenue source while reducing landfill dependency. Furthermore, a widespread adoption of this technology has the potential to cut CO_2 emissions substantially compared to conventional treatment routes. Indeed, combined with internal heat recovery and lower operating temperatures the modelling of the present process indicates the potential to lower the energy demand for Zn recovery by 1/3 compared to conventional methods.

To reach these goals, the Dust2Value project has planned to build and operate a demonstrator plant to prove the effectiveness of the proposed technology using also different types of steel dust. The structural and thermal integrity of the design was already validated using advanced computer simulations and rigorous safety analyses to establish a safe and reliable operational framework ahead of construction. The entire process chain will be validated to ensure that the final products are able to meet the market quality standards. Furthermore, a sophisticated digital twin of the process will be developed to optimize the performance for industrial purposes and to deliver a full technical and economic blueprint for commercialization and industrial-scale deployment. The digital twin was fed with data resulting from laboratory experiments which measured the reaction speed allowing to create the first kinetics dataset for this specific process. This approach allows the predictive model to go beyond simple theory and to forecast the real-world rate of Zn extraction and Fe metallization inside the kiln to achieve precise control and high efficiency.

As previously mentioned, different types of steel dust will be tested in the pilot plant to prove the effectiveness of the proposed technology therefore the preliminary chemical and mineralogical

characterization of 15 representative dust samples produced in different EU countries was performed to provide the data necessary to transfer the process and reliably treat diverse real-world waste streams. Besides this, a simple and effective pre-treatment step was developed by washing the dust with water to remove harmful chlorides and halogenide that could compromise the process thus making more complex the downstream gas-cleaning or jeopardizing the final product quality.

Montanuniversitaet Leoben performed some preliminary studies to investigate the effect of operating temperature and gas composition on the reduction behavior of EAF dust during hydrogen-based processing (114). In particular, the effects of different reduction temperatures ranging from 900 and 1200 °C and different H_2/H_2O ratio in gas composition on reaction kinetics and microstructural evolution were evaluated. Quantitative relationships between reduction conditions and Zn recovery efficiency were established through TGA and subsequent material characterization thus providing practical guidelines for the process engineering of efficient hydrogen-based recovery of EAF dust. The EAF dust investigated was provided by Georgsmarienhütte and was characterized by a trimodal particle size distribution, i.e., D10=0.30 µm, D50=1.3 µm, and D99=20.0 µm, a specific BET surface area of 8.4 m^2/g and franklinite, zincite and halite as main mineralogical phases. The chemical analysis of the dust performed through XRF and ICP-MS highlighted a content of 26.2 % ZnO, 44.3 % Fe_2O_3, 3.5 % CaO, 1.8 % MgO, 1.0 % Al_2O_3, 3.5 % SiO_2, 3.0 % MnO, 1.0 Cr_2O_3, 4.6 % Na_2O, 0.7 % Cl, 0.2 % PbO, 0.4 % Cuo, 0.2 % P_2O_5, 0.4 % S, 2.0 % C_{tot}, 0.1 % Sn and 0.06 % Cd. Before performing TGA reduction analysis, EAF dust was dried at 105 °C for 24 h to remove moisture and was then compacted at 14 MPa using an electromechanical press to obtain a final diameter of 7.5 mm diameter, an height of 3.75 mm and a bulk density of 2.1 g/cm^3. Reduction tests through TGA were carried out by heating the samples with a rate of 25 °C/min up to 200 °C and of 40 °C/min up to the selected reducing temperature in a nitrogen atmosphere. The latter was kept also during the 15 minutes of homogenization and was then switched for 120 minutes to hydrogen to perform the reduction. Samples were subsequently cooled at 25 °C/min under inert conditions. Reaction kinetics were evaluated through numerical differentiation of the continuous mass loss data with respect to time thus providing instantaneous reaction rates throughout the reduction process.

TGA revealed that reduction proceeds by three mechanistic kinetic regimes. The first regime is surface-controlled and exists from 900 to 1100 °C where the kinetic of ZnO reduction is limited by thermodynamics. The second optimal reduction window was observed at 1150 °C whereas a solid-state diffusion limited regime was detected between 1150 and 1200 °C. EAF dust reduction proceeds through multiple simultaneous reactions each limited by thermodynamic requirements, especially regarding the H_2/H_2O ratio which changes with temperature thus creating distinct reaction patterns in different process conditions. As hydrogen penetrates from the surface inward, all reduction reactions progress concentrically and top down. The transformation of Fe_2O_3 to Fe_3O_4 occurs readily throughout the accessible sample volume thanks to its minimal H_2/H_2O ratio requirement <0.01 both at 900 and 1200 °C. Focusing on the 900 °C configuration, the subsequent reduction steps are characterized by different reactions occurring at different zones of decreasing depth. The conversion of Fe_3O_4 to FeO occurs when $H_2/H_2O > 0.4$ and forms the deepest reaction front enabling reduction across a substantial sample volume. The conversion of FeO to Fe occurs when $H_2/H_2O > 1.3$ and follows the previous one with a narrower reaction front and a smaller active reaction volume. Finally,

ZnO reduction requires the highest H_2/H_2O ratio>12.6 at pZn = 0.1 bar and establishes the most restricted reaction front width, resulting in the smallest active reaction volume and limiting the overall Zn removal rate despite occurring simultaneously with the iron oxide reductions. Considering the 1200 °C configuration, it transforms the reaction front architecture with Fe_2O_3 reduction maintaining its presence throughout the accessible sample volume and with a significant lower H_2/H_2O ratio required for ZnO reduction, i.e., 0.1 for a pZn of 0.1 bar, which matches also the thermodynamic conditions for Fe_3O_4 to FeO conversion. This enables ZnO and Fe_3O_4 reductions to proceed with similar depth thus creating an expanded reaction volume for Zn removal. Only the final FeO to Fe conversion requires a H_2/H_2O ratio > 1.8 which forms a more confined reaction zone. This enhances Zn removal rates at elevated temperatures. If higher temperatures initially foster the reduction process through expanded reaction zones and improved conversion rates, it must be also considered that sintering effects can occur between 1150 and 1200 °C thus establishing a critical upper temperature limit. Indeed, the collapse of structure microporous begins immediately at 1200 °C and significantly intensifies during FeO formation due to its lowest melting and sintering point among all iron oxides. This degradation of the microstructure changes the rate limiting mechanism from gas-phase diffusion through the macro and micropore to solid-state diffusion. Reaction rates displayed a decrease by two orders of magnitude due to particle sintering and micropore collapse. These findings reveal a critical trade-off between kinetic enhancement and structural degradation.

Microstructural evolution was also characterized by SEM providing direct evidence of structural changes evolution as a function of temperature. At 1100 °C, the microstructure consisted of fine-grained particles with a highly porous network of interconnected micropores with low ZnO concentration of 0.2 % which indicates minimal sintering and enables efficient gas diffusion pathways. A significant transition occurred at 1150 °C where pronounced sintering is observed leading to a denser structure through the coalescence of FeO and metallic iron and to a partial collapse of micropores which reduces the gas diffusion pathways. The most dramatic transformation appeared at 1200 °C when a complete micropore collapse was observed with only macropores being present in a fully dense material. This structural densification confirms the transition to a solid-state diffusion-limited regime thus explaining the steep decline in reaction rates despite more favorable thermodynamics at this temperature. The temperature of 1150 °C emerges as a threshold balancing optimal reduction kinetics with structural integrity before excessive densification. The experimental campaign also highlighted a significant influence of gas atmosphere composition in terms of H_2O/H_2 ratio since process efficiency is controlled by the H_2O generated during the reaction which creates local thermodynamic barriers. The effect of this parameter was investigated by varying H_2O/H_2 ratio between 0 and 1.2 at temperatures of 1000 and 1150 °C and two gas-related mechanisms controlling the reduction rate were identified. The first mechanism was H_2 concentration at reaction sites which determines collision frequency between H_2 molecules and metal oxides. The second mechanism concerned H_2O removal rate from the reaction sites which strongly influences the thermodynamic conditions locally because H_2O accumulation at reaction sites decreases locally the thermodynamic driving force thus limiting reaction front penetration and the overall reaction rate. In particular, mass loss displays an initial rapid reduction of hematite to magnetite and the decomposition of $ZnFe_2O_4$ to ZnO and magnetite at 1000 °C. After this preliminary step, H_2O/H_2 ratios up to 0.1 ensure a stable

rate to the subsequent reduction thus indicating chemical reaction control rather than macropore diffusion limitations whereas H_2O/H_2 ratios up to 0.4 causes a decrease in mass loss rates while maintaining the final reduction degree thus suggesting reduced kinetics due to H_2O accumulation in the pores. Finally, H_2O/H_2 ratios up to 0.6 determines a mass loss decrease thus indicating thermodynamic limitations that prevent complete FeO conversion to Fe.

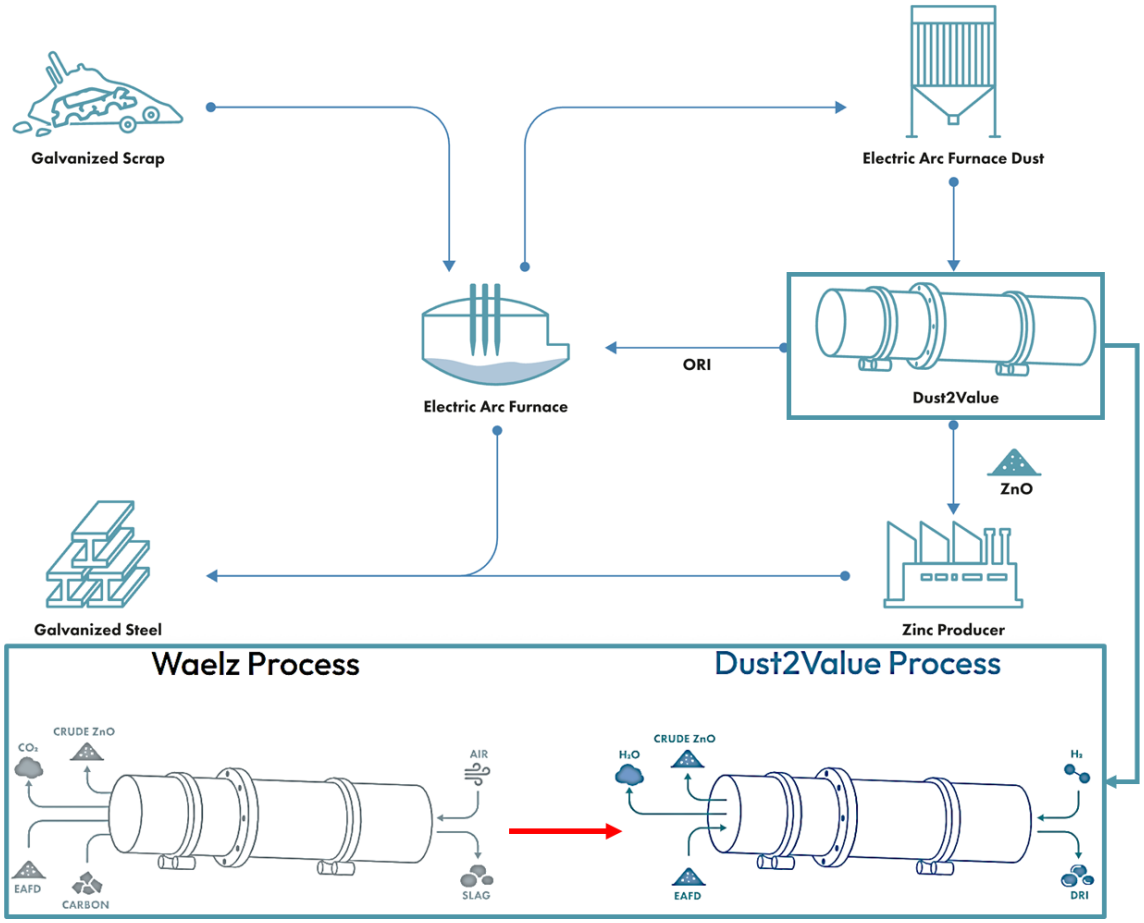

Figure 55: Flowsheet of the Dust2value project with some insights into the main inputs and outcomes of the Dust2Value process compared to the traditional Waelz process

3.2.24 H2PlasmaRed: Hydrogen Plasma Reduction for Steelmaking and Circular Economy (115)

The project was coordinated by Oulun yliopisto with Montanuniversität Leoben, K1-MET, Max-Planck-Institut, RWTH, Luxmet, KU Leuven, ESTEP (European Steel Technology Platform), Voestalpine, Swerim, Metso Metals, Aperam, and Universität Duisburg-Essen participating as partners in the consortium. The project started on the 1st of January 2024 and lasts almost four years, ending on the 31st of December 2027. The overall project cost 6.37 M€ and the EU contributed 5.99 M€, i.e., almost 95 % of the budget.

The main objective of the H2PlasmaRed project is to develop a green CO2-free steelmaking route based on H2-plasma technology while promoting a circular economy approach by valorizing industrial side streams to meet the targets of the European Green Deal for reducing CO2 emissions in the steel industry across Europe. In particular, the project aims to advance hydrogen plasma smelting reduction (HPSR) from TRL 5 to 7 by validating the technology in a pilot reactor of 100 kg at K1-MET and in a 5-ton DC EAF retrofitted for H_2 plasma at Swerim. HPSR combines melting and reduction in one step using a hydrogen arc since the ionized/atomized hydrogen species can provide high reduction kinetics while the arc supplies the heat for the endothermic reactions and the melting of the material. The industrial uptake was further fostered by integrated process control, modelling, LCA/LCC, and safety. Online characterization is based on optical emission spectroscopy and, where applicable, hyperspectral imaging while predictive models support control and scale-up. The project targeted a CO_2 reduction of 90–95 % compared to the BF–BOF route when powered by green H_2 and electricity. The side streams considered included EAF slags, stainless dusts, leach residues as well as various iron ores such as sinter, pellets, and lumps.

At first, two complementary laboratory campaigns were performed to investigate methodology and reproducibility by establishing a baseline in terms of operating windows and diagnostics. One campaign was performed in the HPSR laboratory reactor of the Max-Planck-Institut consisting of a manual electrode control without automated logging, using a Cu hearth filled with almost 15 g of samples and applying an atmosphere of Ar-10%H_2 at 900 mbar and a current of 100-300 A. The second campaign was in charge to the HPSR reactor of Montanuniversität Leoben consisting of an automated current/voltage logging, optical emission spectroscopy and off-gas mass spectroscopy. The tests were performed using up to 200 g of samples charged in a steel crucible and applying 3 L/min of Ar during pre-melt, 3/2 L/min Ar/H_2 during operation and a current of 90-160 A. Process times ranged between 2.5 and 60 minutes. In both cases, the materials investigated included sinter, iron ore fines, lumpy hematite iron ore, sideritic domestic ore, and leach residue and were analyzed through SEM and EDS, EPMA (Electron Probe Microanalyzer)-WDS (Wavelength-Dispersive Spectrometry) and XRD while LECO gases for C, O, N, S, H where relevant. The preliminary results obtained in terms of off-gas trends highlighted CO/CO_2 spikes during pre-melt due to calcination and decomposition and an H_2 uptake increases after full melting. Concerning arc stability, initial instabilities of 20–30 s were observed until full melt and magnetite proved to be slightly more stable than hematite. Geometry of the feed, e.g., powder or pellet, also proved to exert a critical influence on arc stability. The microstructural analysis highlighted that FeO is reduced to Fe across ores and side streams therefore the slag becomes depleted in FeO and enriched in $CaO/SiO_2/Al_2O_3$. Entrapped oxidic droplets were routinely observed in the metal. Increasing electrode distance allowed to reduce Fe evaporation and minimizes Fe entrapment in slag. In some trials, fayalite (Fe_2SiO_4) persisted in inter dendritic regions of slag until longer exposures.

Montanuniversität Leoben focused on process time optimization to improve the metallization of the pre reduced pellets. Pellets with three pre-reduction levels, i.e., none/low/high ≈0/35/65–73 % were considered. Pre-melt was performed under Ar for 7–11 min and then the atmosphere was switched to Ar/H_2 60/40, i.e., 3 L/min Ar + 2 L/min H_2. Frequent arc interruptions appeared with highly pre-reduced feed and crucible wall attack was also observed. Nevertheless, full metallization around

97–100 % was reached with shorter HPSR times as pre-reduction increased. Hydrogen injection marked higher reduction rates and hydrogen utilization decreased faster for pre-reduced feeds.

Universität Duisburg-Essen developed an experimental model system for process optimization. The model experiments allows to map spatial reduction potential of arc zones and to tune melt hydrodynamics for better metal/oxide separation. Short exposures on oxidized substrates resolved concentric reduction zones (I–IV). A motorized linear slide enabled steady low-current arcs (15–35 A) scanning across oxidized surfaces to imprint radial reduction profiles measurable by EDX. Concerning Cu crucible geometry, it could be either bowl, spherical or cup and it proved to affect turbulence and separation. Concerning pulsed arc control, square, trapezoid, and spike pulses were tested in Ar-10%H_2 on 50 g of 50 % pre reduced pellets and square pulses improved reduction per kWh by enabling slag floatation at low power and targeted reduction at high power.

H2PlasmaRed demonstrates a technically credible pathway to near-zero direct CO_2 ironmaking by HPSR in both standalone and retrofitted EAF configurations. Baseline laboratory evidence is establishing kinetics, diagnostics, and slag/metal chemistry. Optimization levers in terms of crucible geometry and pulsed power are being addressed to offer improved metal/oxide separation and energy efficiency. Pre-reduced feeds are being evaluated to reduce time-to-metallization, but the results obtained until now underlined a demand enhanced arc control.

3.2.25 HURRICANE: Sector-coupling hub for circular use of thermal and industrial waste (116)

The project was coordinated by ArcelorMittal with C-Shift, CRM, Vito, DBFZ (Deutsches Biomasseforschungszentrum gemeinnützige), Università Politecnica delle Marche, PDMFC (Projecto Desenvolvimento Manutenção Formação e Consultadoria), Gemeente Zelzate, Provincie Oost-Vlaanderen, FINAMIRT, Organisatie Broeders van Liefde, Warmtenet Zelzate, and Heaten Germany participating as partners in the consortium. The project started on the 1st of January 2024 and lasts almost three and a half years, ending on the 31st of December 2028. The overall project cost 19.09 M€ and the EU contributed 27.48 M€, i.e., almost 70 % of the budget.

Industrial sites worldwide are notorious for squandering huge amounts of energy, water, and raw materials and this inefficiency strongly contributes to resources depletion, environmental degradation and climate change. The HURRICANE project tries to address this resources inefficiency creating a sector-coupling circular hub centered around the steel manufacturer ArcelorMittal in Ghent to optimize resource usage and harness wasted industrial heat and water. This industrial symbiotic approach between ArcelorMittal and other industrial partners such as renewable energy producers, chemical producers, wastewater treatment, etc., fosters a multi-sectoral ecosystem. Furthermore, a 20 % reduction in energy, water, and raw materials was forecasted by developing and integrating novel heat recovery, i.e., heat exchangers, and upgrading, i.e., heat pumps, solutions from selected operations and coupling them with the internal and external off takers by means of a heat grid the project targets. Furthermore, the digital tools developed within the project will allow to assess aspects like broadening the district heating network, and adapting the heat demand profile of the buildings to better match

the intermittent of the waste heat. HURRICANE paves the way for replicable circular hubs across Europe.

3.2.26 ZHYRON: Valorisation of iron-rich & Zinc-containing steelmaking by-products via HYdrogen-based ReductiON (117)

The project was coordinated by CIRCE with ArcelorMittal, CRM, GreenIron H2, BFI, HydroMetal, and Fondazione ICONS participating as partners in the consortium. The project started on the 1st of January 2024 and lasts almost three years, ending on the 31st of December 2026. The overall project cost 4.53 M€ and the EU contributed with the full budget.

The EU steelmaking sector is facing the double challenge of managing and valorizing increasing amount of by-products especially those containing Zn while reducing the CO_2 emissions resulting from the current valorization processes strongly reliant on fossil fuels. Indeed, 50 Mtons of by-products materials are recycled every year and, therefore, 49 Mtons of CO_2 are emitted by the recycling processes which are also not efficient enough to valorize both Zn and Fe at the same time. In this framework, the ZHYRON project tried to propose an innovative solution by combining pyrometallurgical and hydrometallurgical stages using green H_2 as reducing agent to develop a sustainable valorization route for both Fe-rich and Zn-containing by-products endorsing circular economy practices and carbon emissions reduction in the steel industry. The ZHYRON project should guarantee the production of DRI to be recycled in EAF, ZnO rich concentrates to be marketed in the smelting industry and wastewater that is safe for its disposal or reuse. To achieve this goal, the ZHYRON project is addressing all stages of the process, i.e., conditioning of waste raw materials, H_2-based thermal reduction, wastewater treatment and valorization of Zn contained in the sludges. The combination of treatment techniques developed within the project will be transferable to other multiple secondary flows in the metal industry. Furthermore, the ZHYRON project aims to reduce the cost of Fe and Zn products by over 10 % and to lower the recycling energy used by 15–25 %.

The technical activities of the project started with the construction of a solid baseline to provide a comprehensive understanding of the characteristics of Fe-rich and Zn-containing steelmaking byproducts to select the most suitable candidates for further processing. In particular, by-products and agglomerates were characterized to identify the best techniques and the optimal parameters for cold agglomeration to be sure that cold agglomerates made from steelmaking byproducts were compliant with the physical and mechanical characteristics defined in the KPIs, e.g., 95 % of the cold agglomerates must be characterized by a dimension higher than 10 mm after 2 drops from 2 m. Other fundamental KPIs were the physical and chemical properties of the DRI produced from these cold-agglomerates necessary to meet EAF requirements, and which can provide further support in the selection of wastes and by-products and can be the most suitable for the recovery of metallic Fe and metal fractions. For example, cold agglomerates to be fed in EAF must be characterized by a moisture <1%, a cold compression strength >150 kgf/agglomerate, a metallization degree of 92-96 %, a total Fe content >90 % and a total metallic Fe >85 %, a S and P content lower than 0.02 and 0.05 %, a gangue content lower than 6 % and a size between 6 and 40 mm. Further KPIs were defined for ZnO concentrates according to the forecasted market applications, e.g., Zn smelting, ZnO concentrate as

filler or additive in the production of high value-added products, etc., and for the characteristics of the wastewater produced during the process to be recycled back or to be safely disposed to the environment. After the identification of the main KPIs, the sampling and physio-chemical characterization of six different steelmaking dusts and sludges by ArcelorMittal was performed to understand which wastes and by-products were the most suitable for the recovery of metallic Fe and other metal fractions. After this stage the attention was moved on the agglomeration process, two main pathways were investigated, i.e., cold agglomeration by stiff vacuum and roll-press briquetting, and lab-scale trials were performed to optimize the cold agglomeration parameters, the recipes, the moisture content, the amount and type of binder, etc. A thorough characterization e.g., crush test, drop test, tumble test, density, was performed before testing the materials in the GreenIron bell furnace at high hydrogen pressure and medium temperatures to be sure that the cold agglomerated materials could be successfully processed. Additionally, the hot reduction properties of the agglomerates were evaluated using a lab scale furnace and applying reduction conditions representative of some of GreenIron reduction process conditions.

After this preliminary phase, the activities were devoted to the optimization and development of the hydrogen thermal reduction at low temperature (550-650 °C) to produce DRI and demonstrate the recyclability of Zn-rich by-products through the Bell-type furnace provided by GreenIron. The effect of particle shape and size on process pressure and temperature is going to be studied and DRI quality is going to be assessed. Furthermore, DRI agglomerates will be tested in a smelting furnace for EAF suitability. The outcomes of these activities had a direct influence on the activities dedicated to the conditioning of wastewater and sludges to obtain high quality Zn and safe water. Lab-scale trials for Zn recovery from process condensate water deriving from the pilot plant of GreenIron were initiated and membrane distillation infrastructure was commissioned. All these technical activities were supported by environmental and economic impact assessment to validate the overall performance of the proposed solutions and guarantee its commercial upscaling and replication. The ZHYRON project will include 3 pilot sites. The first one will be a cold agglomeration pilot in Kumpla (Sweden) to validate this technology at a scale of 20 kg to work with targeted EAF dust, BOF fine sludge, DR sludge, pellet fines, and mill scales. The second pilot will be in Dusseldorf (Germany) and will be devoted to study the wastewater from the H_2-based thermal reduction process to integrate and validate a smart monitoring concept. Finally, a third pilot will interest Engis city in Belgium and will focus on Zn production.

4. Other funded projects which assessed IS in the steel industry

4.1 C-CED: Carbon Cycle Economy Demonstration

Carbon – Cycle Economy Demonstration (C-CED) is a flagship project where a sustainable and closed carbon cycle is being established by combining and demonstrating different CO_2 capture and utilization technologies. In the project, CO_2 from various sources is captured on a pilot scale and converted into valuable renewable methane through methanation. Methane is a C-containing energy carrier as well as a raw material and plays an important role in many industrial processes making its complete abandonment hardly conceivable nowadays even though CO_2 is often produced in these processes. Gaseous energy carriers characterized by a high energy density and by the existing infrastructure stand out as an excellent energy storage medium. At the same time, there are also industrial processes where CO_2 does not originate from fuels and CO_2 emissions are unavoidable. Based on these considerations, it is reasonable to establish a carbon cycle economy with seasonal large-volume storage facilities that provide the flexibility urgently needed for the switch to a renewable energy system.

The C-CED project is essentially working on two research areas. The first concerns the research and demonstration of CO_2 capture from real gases such as amine scrubbing for CO_2 capture from steel industry waste gases, CO_2 separation by membrane separation process, utilization of CO_2 contained in biogas and development of a novel Direct Air Capture (DAC) process. The second area concerns CO_2 utilization in methanation and demonstration will be carried out on bio electrochemical processes and flexibilization of geo-methanation from the Underground Sun Conversion project. In the C-CED project, the interaction of different technologies for the formation of a closed sustainable carbon cycle including the storage functions necessary for the energy system of the future is investigated for the first time as shown in Figure 56. The technical-scientific investigations are complemented by techno-economic analyses.

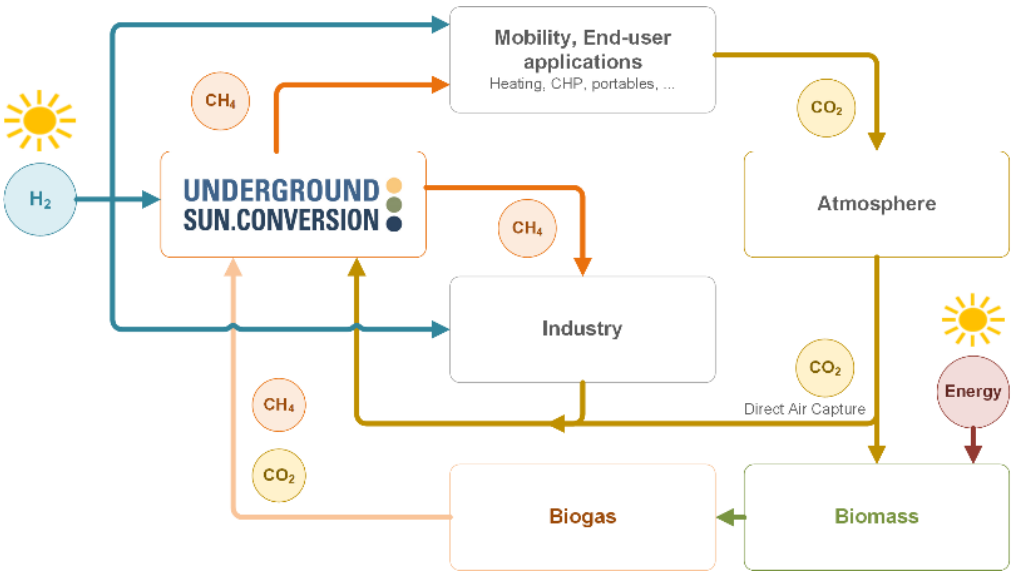

Figure 56: Carbon-Cycle Economy Demonstration

Focusing on the carbon capture in steel industry, iron and steel industries are responsible for more than 7 % of the global CO_2 emissions and it is crucial to minimize them (118). In particular, 2.32 tons of CO_2 per ton of steel are emitted from the BF route where carbon capture and storage and CCU could be promising technologies to reduce the CO_2-footprint. Amine-scrubbing is a well-known technology to capture CO_2 from industrial gas streams employing chemical absorption to bind CO_2 with an amine-based solvent. The most common amine-based solvent is aqueous monoethanolamine (MEA) thanks to its low cost, fast reaction kinetics, and thermal stability (119). Despite this, a major drawback of amine-scrubbing is the high energy consumption of the process therefore the reduction of energy consumption is one of the main objectives in amine-scrubbing plants research. In 2023, Voestalpine and K1-MET arranged the dismantling of an amine-scrubber pilot plant at coal-fired power plant Dürnrohr in Lower (Austria) and the re-erection at the power plant of the Voestalpine site in Linz to reuse existing infrastructure. This choice was made since the power plant which converts process gases from upstream processes, e.g., BF gas, coking gas, etc., into electrical energy is the largest emitter of CO_2 of the integrated steel mill. The goal of the pilot plant was to investigate and demonstrate amine scrubbing in the steel industry, optimize the process and provide CO_2 for downstream CCSU applications. Figure 57 shows a picture of the amine scrubber pilot plant at Voestalpine power plant in Linz and its principal flow sheet. As a special feature, the plant is equipped with two absorber columns which can be operated in series or individually thus enabling future operation with different amine-based solvents characterized by different CO_2-absorption kinetics. The pilot plant has a height of 20 m and is equipped with a compressor station to fill gas bottles/bundles with CO_2 to supply project partners for CCU applications. A blower transports the power plant CO_2-rich off-gas through a direct contact water cooler and a scrubber to remove undesired SO_2 to a minimum, i.e., <1 mg/Nm^3. Subsequently, the off-gas enters a packed bed absorber column at the bottom and contacts counter-currently with the liquid amine-based solvent. The solvent selectively reacts with CO_2 via chemical reactions while inert gas species, e.g., N_2, exit the absorber at the top.

The CO_2-rich solvent is then pumped to the desorber column where increased temperature and H_2O-steam drive reversible reactions and CO_2 is removed from the solvent. This regeneration step is the energy-intensive part of the process. The regenerated lean solvent is recycled to the absorption column and CO_2 exits the desorber at the top to the compressor station or into the atmosphere.

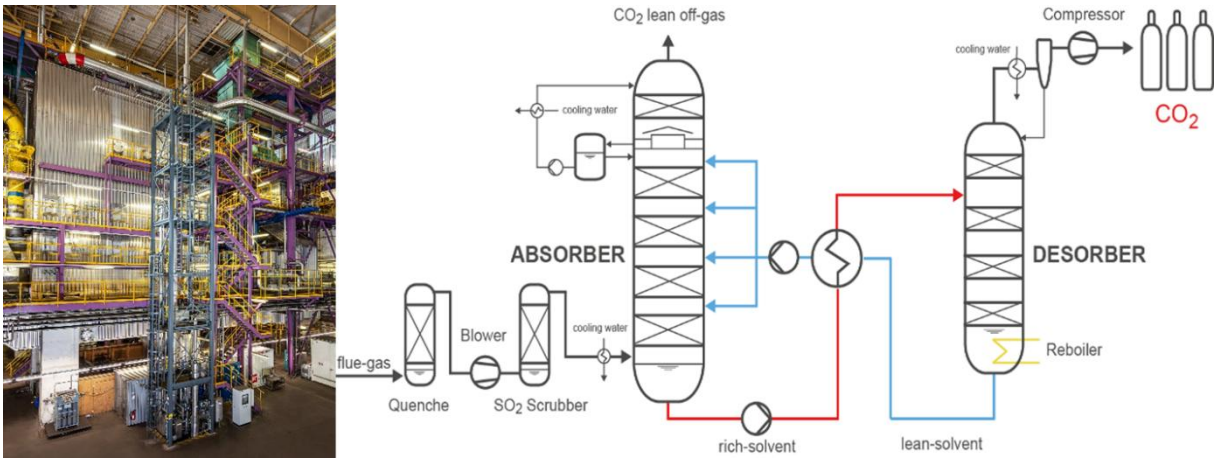

Figure 57: Amine scrubber at Voestalpine/K1-MET power plant (Linz) and principal flowsheet

A test campaign was carried out to optimize the amine scrubbing process with respect to CO_2-separation efficiency and energy consumption. Two characteristic numbers were defined to evaluate the process, i.e., the CO_2-separation efficiency η [%] which describes the ratio of captured CO_2 over the incoming CO_2 via the off-gas and the specific regeneration energy e [GJ/t CO_2] which describes the ratio of heat duty of the reboiler and the captured CO_2. The first parameter needs to me maximized while the second must be minimized. The most important process parameters varied during the tests were the power plant off-gas between 50 and 90 m^3/h, the power plant off-gas CO_2 between 17 and 27 vol.%, the reboiler heat duty between 17 and 30 kW, the liquid gas ratio between 4 and 7 l/m^3, the desorber pressure between 1.8 and 2.2 bara and the aqueous solvent with 30 wt.% of MEA. In particular, the CO_2-concentration of the power plant off-gas in the range of 17-27 vol.% (dry basis) was set by the power plant operation since the combustion of different gas mixtures, e.g., BF gas, coke oven gas, etc., resulted in various CO_2 concentrations and could not be influenced during the test campaigns. Another important parameter is the reboiler heat duty in the desorber which directly affects the amount of H_2O-steam in the desorber to drive out the CO_2 from the solvent with the limit of the electric heater being 30 kW. The L/G ratio [l/m^3] is also a very typical parameter for amine scrubbers. This parameter describes the ratio of lean-solvent flow at the absorber-top inlet and the off-gas flow at the absorber-bottom inlet (e.g., L/G=5 could be 350 l/h solvent flow and 70 m^3/h off-gas flow).

The results of the campaign in terms of separation efficiency and specific regeneration energy as a function of the heat duty of the reboiler, keeping constant the other parameters, are reported in Figure 58. An increase in the heat duty determines an increase in CO_2 separation efficiency while the specific

regeneration energy follows a different trend reaching a minimum at 90 % separation efficiency. Higher capture rates up to 98 % are therefore possible but an abrupt increase in the specific regeneration energy occurs thus making the process more energy intensive. Further test campaigns were performed at a constant separation efficiency, η, of 90 % and focused on the reduction of the specific regeneration energy. The main results are summarized in Figure 59. The solvent flow between absorber and desorber described by the L/G ratio proved to have a huge influence on the energy consumption of the capture process as proved by the left graph in Figure 59 which shows that the regeneration energy has an optimal range with L/G = 4.5 - 5.5 resulting in only 3.3 GJ/t CO_2. Another parameter which has huge influence on the regeneration energy is the concentration of CO2 in the off-gas as proved by the right graph in Figure 59 which shows how a higher CO_2-concentration in the off-gas resulted in significantly lower specific regeneration energies. The reason is that absorption/desorption reaction mechanisms can be described by a second order rate law (120) and high concentrations of CO_2 accelerate mass transport and chemical reactions. Again, the L/G ratio must be selected adequately to operate at optimum conditions.

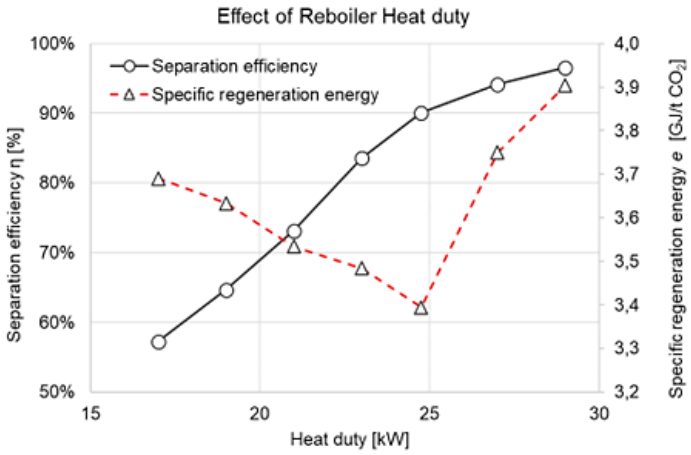

Figure 58: Heat duty variation, off-gas=70 m^3/h, CO2 off-gas=25 vol.%, L/G=5, pDES=1.8 bar, MEA

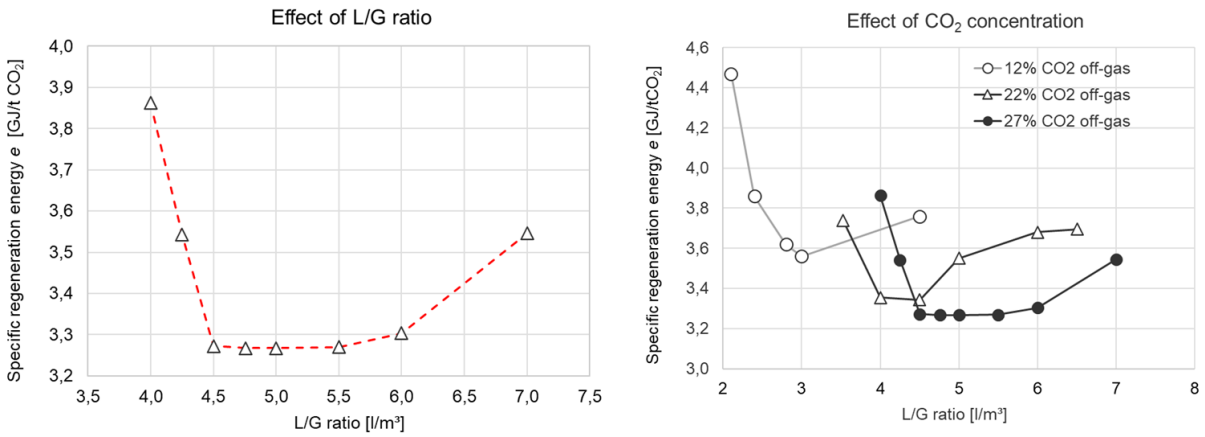

Figure 59: Effect of L/G variation and CO2-concentration on specific regeneration energy

In conclusion, carbon capture in steel industries was successfully demonstrated with an amine scrubbing pilot plant with a maximum capacity of about 800 kg/d. Optimization of the process was achieved and crucial process parameters that affect separation efficiency and specific regeneration energy were identified. The plant was operated with 30 wt.% MEA as solvent and it was shown that a separation efficiency of 90 % was the most feasible for the process. During parameter tests the specific regeneration energy could be lowered to about 3.3 GJ/tCO_2 and the liquid to gas ratio and CO_2 concentration of the flue gas could be determined as decisive factors with respect to plant efficiency. The liquid to gas ratio must be adapted to the CO_2 content of the flue gas source to reach a low specific regeneration energy while in general elevated CO_2 concentrations lead to a more efficient process.

4.2 USS2030: Underground Sun.Storage 2030

The Underground Sun Storage 2030 (USS 2030) project is the only one of its kind in the world and is developing a safe, seasonal and large-scale storage of renewable energy in the form of hydrogen in underground gas reservoirs. In particular, renewable solar energy is converted into green hydrogen in a climate-neutral way by means of electrolysis and stored in a pure form in former gas reservoirs. In addition, all partners involved in the project will gain valuable technical and economic knowledge for the development of a secure hydrogen supply. Until 2025, interdisciplinary technical-scientific investigations for the energy future will be carried out under real conditions at a small former gas reservoir in the municipality of Gampern (Upper Austria) under the leadership of RAG Austria. A customised research facility will be built for this purpose. These investigations will be complemented by the development of suitable processing technologies, the modelling of future energy scenarios, and techno-economic analyses.

The predecessor Underground Sun Storage projects already demonstrated that a hydrogen content up to 20 % could be stored in gas reservoirs in a well-tolerated manner while laboratory tests suggested that hydrogen content could also be increased to 100 %. Building on this information, the USS 2030 project is now moving to the real scale and is investigating the storage of pure hydrogen generated from solar and wind energy in former gas reservoirs as part of a field trial. The project is also investigating other aspects related to stored hydrogen such as the use of hydrogen as substitute for fossil natural gas, hydrogen direct use in energy-intensive industry and processing and utilisation of hydrogen with high purity according to the scheme shown in Figure 60. To be able to achieve the climate targets and a significant reduction in CO_2, reductions are needed in the entire energy sector. In addition, affordability and security of supply must be maintained. Without gaseous energy carriers and the associated storage capacities, the energy transition is not possible. The project is part of the energy showcase region WIVA P&G and an important step for the development of a secure hydrogen economy.

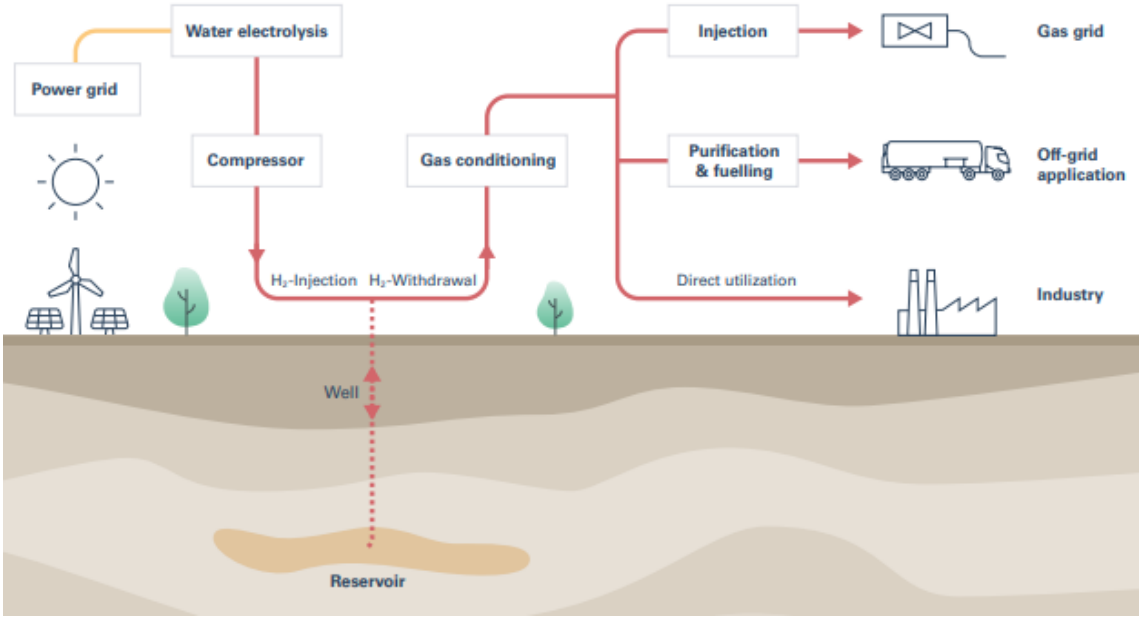

Figure 60: Schematization of the whole chain foreseen by the USS2030 project.

The plant facility resulting by the project is schematized in Figure 61 and consists of many different components. The first one is an electricity grid connection and transformer station (01) since the project aims at storing renewable electricity by converting it into a storable energy source. In particular, the renewable electricity is sourced from a nearby hydroelectric plant via the power grid and transformed to the required voltage level via a transformer. The second component is the electrolysis station (02) where hydrogen is generated from electric power. After cleaning the water through a reverse osmosis system, it is decomposed into hydrogen and oxygen by green electricity. The hydrogen is then transferred to the compressor while the oxygen is released as a by-product to the atmosphere. In this process a proton exchange membrane electrolysis is used. The electrolysis unit was characterized by an electrical connection power of 2 Mwe and by an efficiency of electricity to hydrogen of the whole plant of 72 %. Furthermore, it provided an output of 400 m^3/h with a transfer pressure of 30 bar. The third and fourth facilities consisted of a compressor unit (03) and of a well (04). The compressor unit was a piston compressor machine necessary to bring hydrogen to the required pressure to be able to be injected it into the reservoir. The well is equipped with appropriate safety features and has the role to manage the injection and withdrawal in batch operation. The fifth facility is a porous sandstone reservoir (05) with a field extension of 1.3 km × 0.75 km, a porosity of 16-25 %, a permeability of 18-25 mD, an initial reservoir pressure of 107 bar and is located at a depth below surface of 1091.61 m TVD. Indeed, millions of years ago natural gas reservoirs were created in the pores of the sandstone, which are sealed by more than 100 m thick clay layers. Here, large quantities of energy can be stored sustainably, safely and invisibly. In the project, the microbiological generation of renewable natural gas will be restarted, a process that took place exactly here millions of years ago. The sixth and seventh unites are a drying unit (06) and a gas quality measuring unit (07). The drying unit is fundamental since gas is absorbing moisture while contained in the subsurface

reservoir thus requiring drying before gas can be distributed into the downstream systems and the pipeline network. The gas quality measuring is another step in the processing of the gas extracted from the reservoir to be sure that its quality meets the high standards. The last two units are the hydrogen purification unit (08) where the hydrogen injected into the reservoir is prepared for the various utilization paths and the hydrogen pipeline (09).

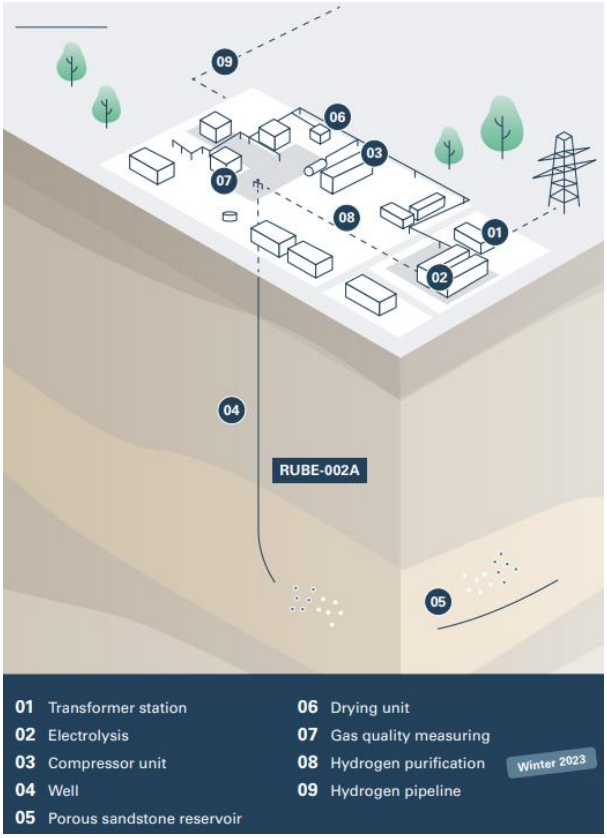

Figure 61: Overview of the plant facility foreseen by the project.

The project proved the possibility to convert the surplus solar power into hydrogen via electrolysis, and its storage in porous subsurface rock formations. Furthermore, the utilization of existing gas-storage infrastructure for hydrogen, enabling large volumes and supporting future vision of a hydrogen based seasonally balanced energy system was assessed. Technical feasibility under real conditions, including safe injection, storage and withdrawal cycles, and hydrogen quality meeting pipeline or industrial use standards were developed and insight into techno-economic, infrastructural, and operational aspects of hydrogen seasonal storage, contributing to the broader of decarbonisation of energy systems and increased security of supply during low-renewable seasons was evaluated. In conclusion, USS 2030 establishes that geological underground hydrogen storage is not only technically possible but also operationally viable, thus offering a promising pathway for large-scale renewable energy integration and seasonal balancing.

4.3 OSMET 3.0: Utilization of organic sludge in metal industry

Metal and pulp & paper industries use over 70 % of the total energy demand of the Swedish industrial sectors and they are facing tremendous challenges regarding the reduction of fossil CO_2 emissions and residues to landfills to achieve climate and environmental goals. Pulp & paper mills generate large amounts of organic and inorganic residues such as organic bio-sludge and fiber reject which contain up to 45 % C and could be used after pretreatment as biofuels for mitigating CO_2 emissions. However, there are few incentives to exploit their energy due to the need for sludge dewatering and/or energy intensive evaporation in the recovery boilers of pulp mills. The unused sludge in Sweden contains an unexploited energy resource up to 1 TWh/year. The main inorganic residues, i.e. fly ash, lime mud and calcined lime mud (secondary lime materials), account for almost ~400 kton/year, are rich in CaO and could be exploited as secondary lime materials with zero carbon footprint. Despite this, this type of waste is disposed of in landfills most of the time. Concerning also the metal industry, the most common fuels or reductants used are fossils, i.e., coal and coke, thus emitting large amounts of CO_2 from C that has not participated in the carbon cycle for a very long time. For instance, the BF at SSAB for hot metal production and the cupola furnace at Volvo for cast iron production use large amounts of fossil coal and coke. Furthermore, all metallurgical processes use lime or limestone as slag formers such as the EAF at Outokumpu for stainless steel production. The production of burnt lime from limestone in a limekiln requires energy and the CO_2 is emitted both from the fuel combustion and from the limestone calcination processes. If the valuable components, e.g., C and CaO, in the residues could be upgraded in a proper way and used in metallurgical processes, it could be expected that the consumption of fossil C and primary lime material would be reduced thus reducing the CO_2 emissions and the residues to landfills. For example, biomass energy is considered a renewable or sustainable energy carrier because of its closed C cycle. The synergy effects will facilitate the industrial clusters towards zero fossil CO_2 emissions and zero waste to landfill. Considering the current uncertain economic situation in the metal industries, proper utilization of pulp & paper residues might lead to positive economic potential. For instance, C from organic sludge streams generated at pulp & paper mills could be used as biofuels for mitigating CO_2 emissions. By estimation, an annual cost saving potential of 22-30 MSEK could be achieved for the metal industries, with a corresponding CO_2 emissions reduction of 175-270 kton/year.

The OSMET project aims to valorize pulp & paper residues for metallurgical application investigating the possibilities of briquettes making by use of organic sludge together with iron-oxide residues from a standard steel plant. Pre-trials were conducted to evaluate the feasibility of organic sludge briquettes for BF application as energy input and reductant material which could provide concrete basis for the continuation of the project. The industrial implementation of the proven concept will create great benefits for society from both economic and environmental perspectives. The new concept of OSMET 3.0 was first developed in OSMET 1.0 and dealt with the upgrade and maximization of the value chain of pulp & paper residues, i.e., the secondary lime material and organic sludge, for metallurgical applications in an industrial symbiosis perspective. This would contribute to mitigate climate change, minimize residues to landfills and save natural resources. This concept can be an effective way to assist the major industrial sectors to achieve sustainable development and meet the global goals set in 2030 Agenda. In OSMET 2.0, the concept developed in OSMET 1.0 we tested and evaluated through pilot

scale trials conducted by using the secondary lime materials from pulp & paper mills to partly replace the primary lime material. The trials were performed in EAF and AOD test-beds at Swerim. Test results showed possibilities to use the newly developed lime-briquettes in both EAF and AOD processes without any negative effects. By doing so, the amount of residues sent to landfills would be reduced. The use of secondary lime for metallurgical applications would also avoid the calcination process of limestone in which large quantities of CO_2 are emitted. It will also lead to protection of natural resources by decreasing the extraction of limestone at the mining sites.

Furthermore, hydrothermal carbonization was used to upgrade organic residues to produce hydro char and two short-term industrial trials were performed to test this type of biochar. One trial was performed at SSAB for the hot metal production and the other one at Volvo for cast iron production. In the case of SSAB, hydro char was top charged into BF in the form of bio-briquettes and 418 tons of hydro char briquettes were prepared and produced by SSAB. Compared to the reference period, no negative effects were noticed regarding the production rate, hot metal quality, amount and chemical composition of slag, or C and S content in dust and sludge. In the case of Volvo, the industrial trial was performed through hydro char injection with no negative impacts during the trials. Two different types of feedstocks were used for hydro char production, i.e., the organic sludge generated from pulp & paper mills and organic residues of green waste. Thus, it was proven that hydro char derived from various types of organic residues could be used for metallurgical applications. Based on the promising results obtained, the concept needs to be demonstrated by the next stage towards industrial implementations with validation via different trials, furthermore non-technical aspects needed to be taken into account to establish this cross-industry system, such as transportation of wastes, mapping of pulp & paper sludge suppliers and possible end-users, geographic locations of sludge upgrading plants, etc.

OSMET 3.0 aims precisely to verify the developed concept for upgrading and using residues generated from pulp & paper mills for metallurgical applications, towards industrial implementation. The first target expected to be achieved is the successful pilot trials of hydro char in EAF test-bed at Swerim. The pilot trials results will be compared with reference trials where anthracite is used while heat and mass balances for all trials will be performed and compared. A comparison will also be made with two types of wood char to prove hydro char suitability for EAF. The overall goal is development of a final concept to be tested by the industry. The second target of the project is a pilot trial of iron-powder hydro char in the induction furnace pilot at Höganäs. The metal and slag samples will be analyzed and compared with the reference cases in which anthracite and wood char are used. The third objective is the industrial trials of using the developed lime briquettes in EAF at Outokumpu. During EAF trials, steel, slag and dust will be sampled and analyzed and the results will be compared with the normal EAF operations for quality control. The overall goal is de-risking the final industrial implementation of the concept. The fourth goal of the project was the development of a business model canvas for a hydrothermal carbonization plant for hydro char production. The feasibility studies including process design, plant location, feed stocks, etc. will be discussed with several stakeholders. Finally, the project attempted to update the business model canvas and plan which is ready to implement for secondary lime for the metallurgical process.

The primary goal of the project is to develop a new type of briquette by using the organic sludge generated from the pulp & paper industry together with the iron-oxide residues from the steel plant. The C in the organic sludge can partially substitute fossil fuels, e.g., coal and coke, in the processes such as BF. However, organic sludge has high moisture and ash content which are major bottlenecks to produce briquettes with required metallurgical properties for BF application. Figure 62 summarizes the process of briquette production. Organic sludge was characterized physically and chemically with special focus on C and CaO content and the different types considered were prepared via different pretreatment technologies such as drying with a cyclone dryer. A briquetting machine was used for making briquettes with different recipes by mixing organic sludge, lime containing sludge and iron-oxides waste from the integrated steel plant. Cement was added as binder to enhance the briquette strength. The influences of C and CaO in organic sludge on the mechanical strength were evaluated by performing a drop tests procedure and the preliminary tests showed that upgraded organic sludge after cyclone dryer deteriorates briquette strength and therefore the amount of addable is limited.

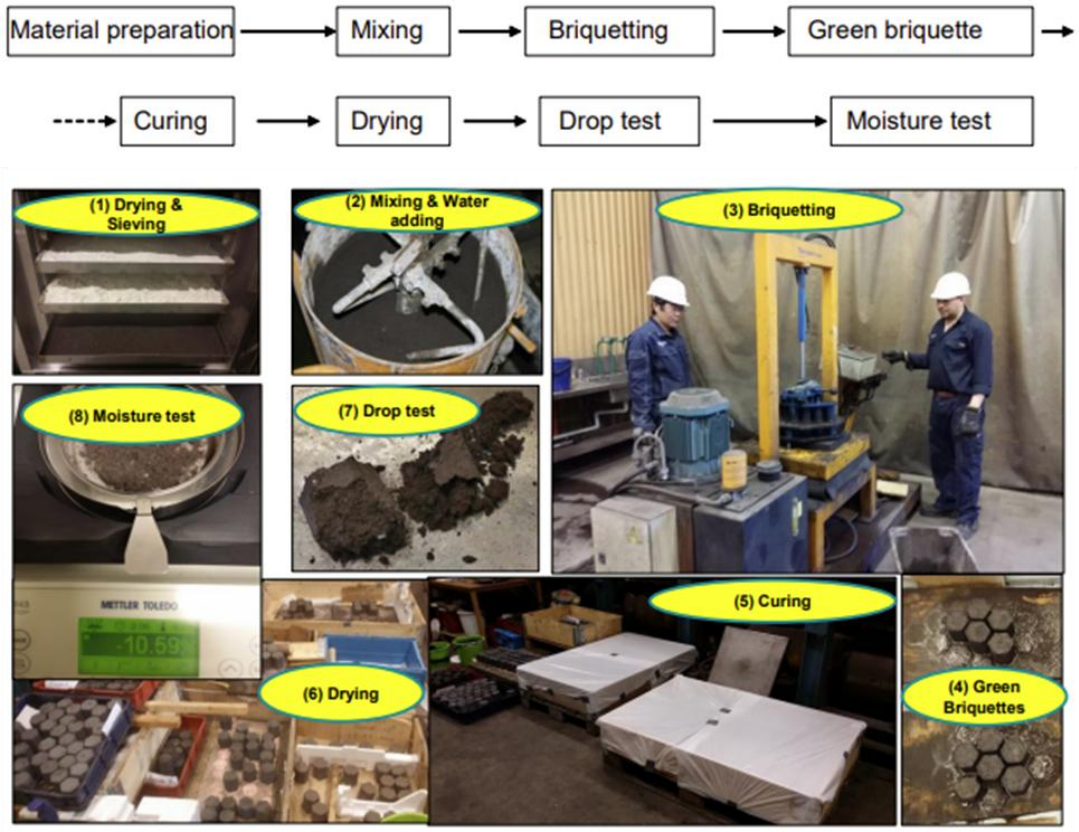

Figure 62: Schematic diagram of the procedures of briquettes production and the equipment used

Alterative upgrading methods need to be investigated, and hydrothermal carbonization is one promising solution for bio-sludge treatment according to the literature study. Indeed, it is performed in a pressurized and wet atmosphere and is particularly suitable for thermal treatment of wet materials

to enhance the drying properties and increase the effective moisture diffusivity of the sludge as shown in Figure 63. Therefore, to overcome the high moisture content, low C concentration, and poor mechanical properties of organic sludge, hydrothermal carbonization is applied under high-temperature, high-pressure and wet conditions. It breaks down cell structures, reduces moisture, and increases C content, producing hydro char with enhanced fixed C and heating value. This process solves the limitations of conventional drying and low briquette strength, enabling organic residues to serve as a viable C source. Hydro char is then optimized into briquettes or powder formulations to ensure mechanical integrity and high C yield under steelmaking conditions.

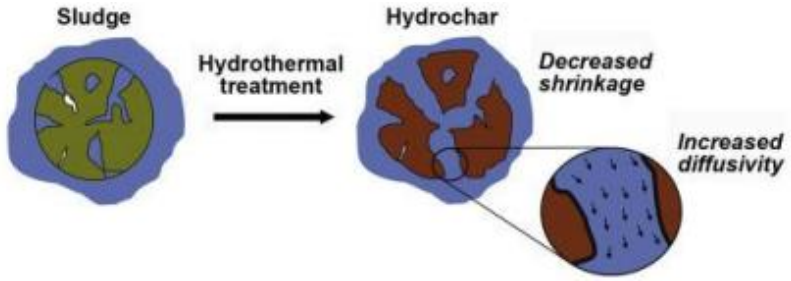

Figure 63: Effect of hydrothermal carbonization on organic sludge drying behavior

Secondary lime briquettes are developed from inorganic residues, e.g., fly ash, lime mud, which are in powder form and prone to dusting. The briquettes achieve sufficient cold and hot strength and slag-forming capability through recipe design and binder selection allowing them to replace quicklime in EAF and refining processes thus reducing CO_2 emissions from lime calcination. The use of AOD slag as binder was also considered. Comprehensive physical and chemical characterization was performed including C content, CaO content, ash, S and P levels, reduction behavior, melting properties, and mechanical strength. Hydro char is evaluated for fixed C ratio, heating value, and thermal stability, while secondary lime briquettes are tested for slag-forming ability and resistance to breakage under high temperatures.

The first step of the OSMET project concerned materials preparation and characterization. In particular, testing of briquetting and characterization of the mechanical strengths of burnt lime fly ash briquettes revealed key findings. Increasing fly ash content enhanced briquette drop test performance with 80-100 % fly ash resulting in less than 50 % weight loss after 7 drops. Heat treatment at 850 °C further reduced weight loss to under 20 %. However, prolonged exposure to moisture weakened the briquettes over time. Characterization of hydro char produced from lemon peels was compared to a charcoal used as bio reference material and anthracite used as fossil-reference material. Lemon peel hydro char displayed high volatile matter of 62 %, a medium heating value of 24 MJ/kg, and low fixed C of 32 %. Pyrolysis increased the C content to 84 % and the heating value to 29 MJ/kg but the levels of ash, S, and P remained high requiring further processing for steelmaking. Characterization in terms of density, mechanical strength, and surface morphologies of carburizing briquettes used in 15 kg induction furnace carburization trials at Höganäs was performed. Iron-hydro char briquettes

demonstrated strong mechanical properties higher than 16 MPa and weight loss lower than 5 % after 7 drops. Slow heating to 1600 °C resulted in higher carburization for iron-charcoal briquettes around 70-72% compared to iron-hydro char around 43-58%. However, direct charging favored iron-hydro char due to the weaker mechanical integrity and C losses of the charcoal briquettes.

After this preliminary characterization, the use of hydro char at the pilot-scale for validation was performed. Experiments with self-reducing briquettes were carried out analyzing hematite reduction using anthracite and hydro chars from lemon peels and rice husks. Pyrolyzed hydro char fully replaced anthracite at Cfix/O(FeOx) ≥ 0.9 while pristine hydro char had values ≥ 0.6. Volatiles achieved 12-35 % hematite reduction at 5°C/min in nitrogen. After that, a series of pilot trials were carried out at Swerim EAF in Luleå to test different carburizer materials through injection and top charge. A total of 18 melt trials were conducted using 18-8 stainless steel and various carbonaceous materials with anthracite employed as reference. For each trial test, the carbonaceous material was introduced as top charge and for some trials it was also injected into the molten steel. Two tests were conducted for each material at the same conditions to ensure reproducibility. It was found that hydro char materials could be added into EAF to replace anthracite via both top charging and injection as carburizing agents. Higher carburization yields were achieved by top-charging hydro char compared to the injection into the melt. P and S levels in the melt could be controlled within acceptable ranges for all three types of hydro char. Slag conditions obtained during the trials were favorable for the desulphurization, but not good for P removal. The strategy of adding hydro chars into EAF should consider the addition amount and the addition approach.

Another validation step concerned the use of secondary lime materials in industrial EAF trials through 72 trial heats covering 10 steel grades in EAF stainless steelmaking process at Outokumpu Stainless in Avesta. The results show that the increase of S in the steel was not an issue for any of the steel grades investigated with an average increase of 11.5 ppm. Moreover, the P-level in the steel was like the trials in reference heats. The increase of the P-content was 5.4 ppm on average and in none of the heats it was above the maximum level for the specific steel grade produced. Also, the slag basicity B2 was 0.01 units higher on average for the trial heats compared to the reference heats. The small difference in B2 between the trial heats and the reference heats indicated that the yield of the CaO in the fly ash briquettes and the primary lime to slag are very similar. The slag volume increased by 460 kg per heat on average which to a steel weight of 85 tonnes is about 6 kg/tonne crude steel. In addition, industrial trials were performed at Höganäs with the aim to replace burnt lime by the secondary lime of fly ash which was delivered from Essity. In total, 28 ton of fly ash was top charged into EAF.

After that, sustainability and system analysis were carried out and LCA was conducted to support and enhance knowledge of the processes developed in the project and the sustainability of the concept developed, in particular investigating its environmental aspects. The results showed that 1 ton of fly ash briquette, with 61.5 % of CaO could replace 0.64 ton of quicklime with 95.2 % of CaO. Higher quantities of fly ash briquette were needed to provide the same amount of CaO required for slag forming as quicklime, however, the climate impact was 13 times lower than quicklime. Hydro char could be used as C source to replace anthracite used for iron and steel industry. The results showed that 1 ton of hydro char could replace 0.23 ton of anthracite providing that both can provide 202 kg

of fixed C. The climate impact of producing and use hydro char for slag forming was 3 times lower compared to anthracite. The assessment of the feasibility of large-scale introduction of hydrothermal carbonization as enabler for industrial symbiosis between pulp and paper and iron and steel industry in Sweden from the combined perspective of national production potential and techno-economic performance was performed. Specific objectives were to identify national production potential and suitable locations for regional industrial symbiosis collaborations and assess the economic feasibility of using hydro char produced from pulp and paper bio sludge as coal replacement in the steel industry. The results indicate that hydro char production from Swedish pulp and paper mill sludge is feasible but not sufficient to meet the full demand of the steel industry EAFs. While integration with pulp mills shows some economic viability, overall feasibility depends heavily on energy efficiency and fossil fuel prices. Finally, a business model was developed focusing on exploring the potential of using biochar and secondary lime in the metal industry. Economic feasibility and identification of potential obstacles like market uncertainty and technical limitations were investigated. Key findings showed that biochar had potential as a fossil fuel replacement, though challenges remain in scaling up and ensuring market viability. Additionally, a matrix analysis was used to evaluate hindrances in the value chain with the market theme showing the most significant challenges. The work also covered gender equality in the business ecosystem and proposed further collaboration for industrial symbiosis.

In conclusion, the metal & steel and pulp & paper industries are two of the largest industrial sectors in Sweden each facing distinct challenges. Although accounting for only 15 % of the total energy use, the metal & steel industry is heavily reliant on fossil fuels leading to a disproportionate CO_2 emission of 60 %. In contrast, the pulp & paper industry is driven by bio-based materials and has a larger share of energy consumption but maintains a relatively low fossil CO_2 emission at just 6 %. However, both industries face a significant challenge in managing residues with approximately 1.5 Mtons generated annually. These residues containing valuable elements such as C and lime are partially utilized internally but often with low value, and a portion still ends up in landfills. The primary challenge is to valorize these residues and minimize landfill waste. The OSMET initiative aimed to connect these two sectors by upgrading and valorizing residues from the pulp & paper industry for metallurgical applications. This approach not only reduces the use of coal thus cutting fossil CO_2 emissions and conserving natural resources like coal and limestone, but also economically minimizes landfill waste, aligning with global sustainability goals.

4.4 CESAREF: Concerted European action on Sustainable Applications of REFractories (121)

The project was coordinated by CNRS (Centre National de la Recherche Scientifique) with Université de Liège, Montanuniversität Leoben, RWTH, TU Wien (Technischen Universität Wien), BAM (Bundesanstalt für Materialforschung), Elkem Silicon Products Development, Imerys Aluminates, Calderys Deutschland Gmbh, RHI Magnesita GmbH, Vesuvius Group, Saint Gobain CREE (Centre de Recherches et d'Etudes Europeen), Tata Steel Nederland Technology, Arcelormittal Maizières Research and Safran participating as partners in the consortium. Beyond these partners, ten more associated partners which received no funding from EU were included in the project, i.e., Université

de Limoges, ENSAM (École Supérieure Nationale d'Arts et Métiers), Universität Potsdam, FIRE (Federation for International Refractory Research and Education), Almatis GmbH, Pyrotek Scandinavia, Refratechnik Asia, Steuler-KCH GmbH, Hochschule Koblenz University of Applied Sciences and Seoul National Unviersity. The project started on the 1st of October 2022 and lasts almost four years, ending on the 30th of September 2026. The EU contributed with a financing of 4.1 M€ to the project.

The CESAREF project was devoted to the study of refractory materials with a special focus on assessing the critical challenges identified by the European Green Deal. Refractory materials play a crucial role in high-temperature and energy-intensive industries such as steelmaking which significantly contribute to global GHG emissions. Considering the great effort of this industrial sector to embrace more sustainable practices such as the transition towards hydrogen-based technologies, it is fundamental that the development of refractory materials grows hand in hand with this transformation to identify and propose new innovative solutions able to withstand new operational conditions while improving energy efficiency and reducing environmental impact.

The CESAREF project brought together academic and industrial partners with the common aim of training 15 PhD (Philosophiae Doctor) students to provide them with the knowledge and skills necessary to develop sustainable refractory solutions to contribute to the decarbonization of energy-intensive industries. The PhD candidates were selected to cover four key technological areas spread in different work packages (WPs): efficient use of mineral resources and recycling, i.e., WP1, microstructure design for increased sustainability, i.e., WP2, anticipation of hydrogen steelmaking requirements, i.e., WP3, and enhancement of energy efficiency and durability, i.e., WP4. The interdisciplinary nature of the project which combines materials science, engineering, and environmental assessment is evident. It aims at developing new methodologies for a more efficient use and recycling of resources as well as innovative environmental assessment tools for eco-design of refractory materials and at enhancing design and characterization routes for improved process and material sustainability.

WP1 "Efficient use of mineral resources and recycling" focused on promoting a sustainable use of mineral resources and recycling in the refractory industry exploiting LCA methodology which is nowadays a standard tool for environmental assessment. WP1 addresses the four main challenges associated with circular economy, i.e., feed the loop, design the loop, slow down the loop and close the loop, with 3 PhD thesis. The knowledge of accurate raw materials extraction procedures including secondary raw materials is fundamental to feed the loop in an accurate way to build robust inventory databases. Concerning the loop design phase, it is of primary importance to have access to relevant production routes for the different types of refractory, e.g., bricks and precast blocks, to optimize them in an eco-design perspective. The third phase, i.e., slowing down the loop, refers to the environmental footprint of the refractories once applied in the steel industry and is being assessed through the monitoring of several operating parameters with a view at reducing the environmental impact and costs associated with refractories for the steel industry. Finally, closing the loop means evaluating the different recycling routes and the associated environmental impacts. Considering the huge amount of data necessary to feed LCA models, the benefit resulting from a strong interconnection with industrial partners appears evident for WP1. This allows to create robust

databases on refractory raw materials to calculate the environmental impact, climate change and resource depletion connected with each refractory solution and will propose appropriate eco-design strategies.

WP2 "Microstructure design for increased sustainability" was structured with the primary idea of providing insights into the correlation between structure, microstructure and macroscopic properties both at room temperature and high temperatures, at the virgin state and after service for example after exposure to H_2 combustion atmospheres. Conventional experimental techniques like the ones usually employed in European large-scale facilities, e.g., synchrotron radiation sources, were selected to analyze material transformations and to better understand how microstructure can influence macroscopic properties, e.g., thermal expansion, thermal conductivity, Young's modulus. Stress-strain relationships and creep laws will be determined from tension and compression tests and work of fracture by wedge splitting tests to shed light also on the effects of thermal treatments on microcracks and stress distributions. Considering the huge number of materials to study, of microstructural and structural properties to investigate and the conspicuous numbers of techniques available, 7 PhD thesis were foreseen in WP2.

WP3 "Anticipation of Hydrogen Steel Making" tackled the challenges of hydrogen-based steelmaking and its effects on refractory materials by developing a thermochemical database for refractories used in hydrogen environments which will be the core of the steelmaking industry to reach emission free processes. The model should disclose how hydrogen exposure can alter refractories mechanical and thermophysical properties and their long-term behavior which will be dramatically affected by the drastic changes in the process conditions. The success of this WP is supported by 2 PhD thesis and is strongly dependent on the results of the extensive characterization performed in WP2 which forms its backbone.

WP4 "Energy efficiency and durability" was designed with the primary aim of leveraging advanced digital tools and methods to reduce heat losses in steel making process and prolong the useful lifetime of refractory linings and components. New monitoring sensors and methods aided by machine learning and data driven approaches were developed to track refractory performance and gather accurate real-time data to control the thermal state of ladles and the condition of the refractory lining. Furthermore, improved modelling techniques will be developed to simulate refractory systems thermal behavior, and they will be validated through experimental data gathered in industrial settings. Both monitoring and modelling activities will be transferred to the steelmaking process to provide a decision-making support tool to optimize refractory use and steel ladle management contributing to reduce energy consumption and improve sustainability.

In the framework of WP1, the three PhD thesis considered were "Documenting the upstream of refractories manufacturing to support LCA" by João Victor Menezes Cunha from University of Liège, "Comparison between production routes" by Sarah Badioli from University of Liège, and "Enhanced Value in Use of Refractories in Industrial systems, by developing Life Cycle Assessment methodologies" by MD Jubayed from University of Liège.

The first thesis was mainly dedicated to the feed the loop phase of LCA since one of the main challenges in implementing this technique within the refractory industry is the lack of availability of good quality data. In this perspective, the PhD project aimed to improve the knowledge about the production of refractory raw materials with a special focus on magnesia production to build a database for this material from mine to the kiln to support LCA. A description of the production routes available will be accompanied by an inventory with the main inputs and outputs of the processes, e.g., CO_2 emissions, energy consumption, etc. The project also aimed to address the problem of resource depletion within LCA by reviewing the Abiotic Depletion Potential (ADP) methodology. Finally, magnesia bricks recycling was investigated considering both benefits and challenges and the resulting eco-design recommendations. With a view at sustainability and circularity, the present project tried to provide a systemic vision of the whole life cycle from raw materials to EoL of magnesia refractories with a special focus on developing valid life cycle inventory (LCI) databases and models to feed LCA. If a better picture of the whole production chain is the final goal to help decision-making, conspicuous and reliable input data for LCA are required and this is not yet the case for the refractory sector. Indeed, the inconsistency and incompleteness of LCI refractory databases makes professionals prefer not to use them and trust on their own internal data. All these issues could be ascribed to the great variability of refractory products in terms of both composition and production processes. For example, RHI Magnesita, i.e., the global leader in refractories manufacturing, uses more than 6000 raw materials to produce more than 200,000 refractory products. One of the aspects considered by the PhD project was resource depletion since mineral resources are not renewable and refractories are exposed to harsh corrosive conditions during their service life which led to high dissipation rates. This clearly affects circularity and must be considered in LCA as virgin raw materials will always be needed. ADP is a method within LCA which accounts for the risk of elements depletion and is defined as the ratio between the annual extraction rate to the square of the assumed stock of a given element. The results are usually normalized by antimony data chosen arbitrarily as reference element. Despite the simplicity of the calculation, the determination of the assumed stocks can be extremely challenging especially when diverse potential sources and uses of the same element are present. The multiplicity of resources and functional minerals to define the stock for a given element can be faced by considering the overall crustal content which is the only reliable and stable base, but economic, geological and technological constraints must be also considered in the analysis. Indeed, different elements may have different origins, different types of mineralization thus varying the size, shape, and depth of the deposits. This generalization is also economically wrong since different elements may have different commercial added value not being able to afford the same extraction costs, e.g., gold vs limestone. Moreover, crustal content may be misleading if it is applied disregarding the minimum concentration that allows the processing of a given element with the actual technology. Therefore, general assumptions should be avoided, and the specificities of each element should be considered. Furthermore, anthropogenic stocks should be included in the ADP calculation considering the increasing stimuli for the implementation of circular economy principles and for material recycling. The estimate of these stocks requires individual studies on the main uses of a given element in the techno sphere and on the respective dissipation and production rates. Furthermore, alternative sources to crustal content should be considered to avoid supply shortages as in the case of magnesia. Natural magnesia is usually

produced from magnesite calcination, but developed countries without commercial magnesite resources typically produce synthetic magnesia from seawater, brine, or evaporitic deposits. The latter requires up to twice the energy needed in natural magnesia production due to the low Mg concentration in seawater, i.e., only 1290 ppm, therefore it is not environmentally advantageous but further extraction methods could be investigated and developed (122).

The second thesis in WP1 aimed to apply the three pillars of circular economy, i.e., design, slow down and close the loop, to investigate, model and quantify the environmental impact generated by the production and usage of refractory materials in the steelmaking through an LCA perspective. The main idea was to identify the most sustainable option for both producers and users by optimizing relevant production routes of several refractories from an eco-design perspective, by optimizing the environmental footprint of the refractories once applied in the steel industry, e.g., their energy efficiency, and finally integrating recycled materials in the production route. The first step of the project concerned the identification of the current state of the art of LCA on refractory materials which is relatively new and mostly unexplored to identify the actual gap of knowledge to fill. Once identified the refractories of interest for the steel sector, an analysis of the entire life cycle was performed including a full modelling of the main production routes, i.e., curing, sintering and fused casting. All this work aimed at enhancing both recyclability potential and eco-design by feeding the LCA database with data collection at the process level. Furthermore, the environmental impact resulting from the change in new refractories properties in steelmaking was also investigated and quantified. Two of the 70 refractory products used in steel industry were selected for analysis. In particular, two pairs of refractories used as linings in the most critical areas of the coupled DRP-EAF process were selected reminding the green steel goal and the emerging technology based on hydrogen (123).

The last PhD thesis of WP1 was similar to the previous two aiming at exploiting LCA to evaluate the environmental impact of MgO-C refractory bricks used as steel ladle lining. MgO-C bricks are produced from high purity fused magnesia and graphite with extremely energy-intensive production processes, e.g., sintering and fusion, characterized by high carbon footprint. Considering this, it is crucial to assess the life cycle environmental impact of these refractories to identify potential ecological hotspots and to develop strategies to reduce impact. A preliminary study was performed to compare the LCA of two different bricks produced in China and in Western Europe, i.e., Netherlands, respectively. A functional unit of 1 t of MgO-C bricks able to provide refractoriness as lining to a 1 m^2 area of a steel ladle in the slag line with a 178 mm thickness was considered in the study. The impact assessment method used was EF 3.0, the input LCI data were collected from both literature and industry and the output impact categories considered were climate change in terms of kg CO_{2eq}, acidification in terms of mole H^+_{eq}, Eutrophication of freshwater in terms of kg P_{eq} and use of fossil resource in terms of MJ. LCA was performed for both brick types using a cradle to gate approach including mining of ore, processing of raw materials, production of bricks, and transportation of bricks to the steel plant. For Netherlands bricks fused magnesia was outsourced from Australia while for China bricks it was locally produced. Furthermore, two scenarios were considered according to the source of electricity, i.e., scenario 1 used as baseline with electricity taken from the national grid mix of the respective country and scenario 2 where electricity was only from the hydroelectric plant. The

results proved that fused magnesia had the highest contribution to the overall impact in terms of climate change, eutrophication of freshwater and use of fossil resource displaying an impact up to 82 % for climate change applying scenario 1 to Chinese bricks. The second main contribution was often ascribed to Al in all impact categories even if transportation had a larger contribution than magnesia and Al in acidification in scenario 2 for both brick types. Concerning the comparison of the two brick types, European bricks performed better in climate change and acidification impact whereas Chinese bricks perform better in eutrophication and resource use. It was also demonstrated that hydroelectricity could significantly reduce the overall environmental impact by at least 50 % compared to the national grid electricity mix. (124) (125).

In the framework of WP2, the seven PhD thesis considered were "Use of metallurgical residues as potential raw materials for high performance refractory castables" by Mathilda Derensy from RWTH, "Characterization of refractory material properties after usage for recyclability determination" by Andrea Salerno from Université de Limoges, "Microstructure design of refractory castables for in use thermomechanical properties optimization" by Kwasi Boateng from Université de Limoges, "Microstructure dependence of local strain through in-situ micromechanical investigations" by Molla Ewnete, "Discrete Element Method to support microstructure design of refractories" by Harikeshava Ranganathan from Université de Limoges, "Influence of microstructure of refractory materials on the macroscopic mechanical behavior" by Michiel Smedes from Montanuniversität Leoben, and "Microstructure impact on refractory materials during In-Situ testing by means of X-Ray imaging methods" by Paula Campos De Oliveira from BAM.

The first thesis of WP2 focused on the recycling of metallurgical residues repurposed as raw materials to produce high-performance castable refractories in a ZEWA and climate neutrality perspective. Castable refractories are easier to produce and cheaper to install than conventional bricks and consist of large-sized aggregates up to 60-80 vol.% which are bonded together with a finer binder phase which is traditionally calcium aluminate cement (CAC). Its initial content was decreased from 15-30 % up to 1-2.5 % to reduce the water content and attain lower porosity and improved mechanical strength. Ultra-low cement castables with 0.2-1.0% of CAC and cement-free castables with CaO <0.20 % were developed for their faster dry out, the favorable heating properties and the superior corrosion resistance from metal and slags at the expenses of mechanical properties. The decrease of CAC usage in refractory aimed also at reducing the environmental impact since the production of 1 tonne of cement generates approximately 1.2 tonnes of CO_{2eq} emissions, i.e., 1 % of global CO_2 emissions. Considering this background, the research work focused on reusing steelmaking V-bearing slag as new value-added binder into high alumina castable refractories as this type of slag account for more than 60 % of the world production. The attention was focused on BOF slags as they are characterized by high amount of Al_2O_3 as well as a high lime content which makes it suitable for binding application. This type of slag is also characterized by the presence of V which is normally added for specific applications to strength the steel at very low level, i.e., <1 wt.%. Considering this, the present study addressed the use of V slag in high alumina refractory castable formulations to obtain high performance. The experimental campaign exploited two different types of V slags from BOF characterized by a

particle median grain size of 11–20 μm as binding agents. These slags were characterized by an Al_2O_3 content of 74 and 68.5 %, a CaO content of 6 and 25 %, and a MgO content of 16 and 3 %, respectively. Furthermore, ultrafine tabular alumina and reactive alumina with a grain size <1 μm were selected as aggregates. The refractories were prepared applying an overall binder amount of 5 % and gradually substituting 0, 2.5, and 5 wt.% of commercial CAC with the two different types of slags. After mixing all components, the castables were poured into the molds, were cured in a wet chamber, i.e., relative humidity >90 %, at room temperature for 24 hours. The samples were further cured in these conditions 24 hours after demolding and this procedure was followed by curing in a dryer oven at 100 °C for 24 hours and by sintering in an electric furnace at 1500 °C. The mechanical behavior of these refractories was investigated, and the results were compared with those of traditional CAC binder. Uniaxial compression tests for cold crushing strength (CCS) determination and resonant frequency damping analysis for Young's modulus, shear modulus and Poisson's ratio determination were performed. XRD and SEM analysis were performed to support the morphological characterization of these materials while bulk density and apparent porosity were evaluated according to Archimedes' principle and true density was obtained with a helium pycnometer. Heating microscopy was also used to determine the dimensional changes as a function of temperature while information on sintering, swelling and melting was derived from dilatometry. Finally, the flowability of the different recipes using a fixed water content of 5 wt.% was determined after 10, 20, and 30 minutes from water addition. The low content of vanadium oxide in the slag did not allow to detect any crystalline phase related to them by XRD but spinel phases such as $(Mg(Al,V)_2O_4)$ were identified in the slag richer in V as also confirmed by EDS analysis. Furthermore, the thermal analysis proved that the presence of V in the spinel structure played a marginal effect on the expansion behavior of the grain. The absence of free vanadium oxide entrapped in other oxides such as alumina, calcium, and magnesia, reduces the hazardous risks related to V slag management and disposal. The sintering temperature of V-rich slag was identified around 1550 °C while the one of the less V-rich slag was around 1470 °C. Regarding the self-flow properties, similar values were observed for the reference CAC and their mixtures with both V-bearing slags whereas lower flow values were observed when using the two slags alone probably due to the lower specific surface area of the slags compared to cement which led to decreased dispersion of the castables. Considering the absolute values, self-flow must range between 80–110 % of the base diameter to meet the criteria for a self-flow castable and the mixes containing 5 wt.% of slag did not meet this requirement thus not being qualifiable as self-flowable. All castable refractories displayed comparable true density values around 3.95 g/cm^3, but the introduction of slag tended to increase porosity decreasing the bulk density. These results are strongly related to the flow values since the lower rheological properties detected for slag samples are indicative of a poorer packing of the materials which resulted in a higher apparent porosity and a smaller bulk density of the hardened sample. Furthermore, refractories containing V-slag are characterized by fewer hydrates due to the combination of CAC and slag resulting in a decrease in the bonding between the grains which in turn results in a porous and less dense ceramic with lower mechanical resistance. Concerning the mechanical behavior, a significant decrease in CCS was observed when adding slag to the binder due to the attenuation of the hydrate bonding effect of CAC and to the smaller number of hydrates formed which resulted in lower mechanical resistance. Furthermore, a direct correlation between the decrease

in CCS of the castables containing slag and their increase in apparent porosity was observed. Despite this, refractory with 2.5 wt.% of slag displayed an acceptable level of CCS for practical applications. A good compatibility between the binder and the aggregates was also detected in samples containing a combination of slags and cements after firing at 1500 °C. In particular, refractories containing 2.5 wt.% of slag showed a CCS in the range of 71–116 MPa while refractories containing 5 wt.% of slag fell into the range of 53–68 MPa. Concerning the Young's and shear modulus data, reference samples were characterized by values of 135 and 60 GPa, respectively. A decrease of these parameters to 100 and 50 GPa was detected when incorporating the slag richer in V at 2.5 wt.% while no significant deviations were observed between 2.5 and 5 wt.% of slag thus indicating that adding more slag does not affect further the microstructure in terms of elastic and shear modulus. Indeed, these mechanical properties are microstructure-dependent, and the V-bearing phases observed around the alumina grains are not well embedded with the coarse grains thus influencing the interactions between the binder and the aggregates. Analogous results were observed for flexural strength with the highest values of 38-42 MPa being achieved by the reference samples and the lowest values around 15 MPa being achieved by refractories with 5 wt.% of slag. It was concluded that the microstructure and the mechanical properties obtained with the samples containing 2.5 wt.% of slag are a promising sustainable alternative as refractory lining considering also that the hazardous risk related to V presence in the slags did not represent an issue as it is not present in free vanadium oxide phase, but is entrapped with other oxides to form a spinel phase reducing the risk associated with disposal and management of V-bearing slag (126). The PhD work assessed also further recycling routes such as the mineral processing route of grog aggregates and its transfer into the formulation of castables for metallurgical application as well as the investigation of advanced and sustainable V extraction routes from metallurgical residues.

The second PhD thesis in the framework of WP2 aimed to provide an insight into the variation of specific key properties, e.g., thermal conductivity, thermal expansion, Young's modulus fracture energy, etc., of refractory materials during operative conditions for the determination of their recyclability. These mesoscale aging studies may allow to quantify after various using cycles the evolution of the properties of interest compared with the pre-use state contributing to the definition of an appropriate Finite Element Models (FEM) to predict the operative and post-operative conditions of the refractory materials and their lifetime. Furthermore, the coupling of numerical and empirical characterization may allow to define the potential recyclability and the most convenient recycling routes of refractories. This project aims to contribute to the EU Green Deal circular economy growth by ensuring a well-managed EoL of materials in terms of collection and treatment to provide better recycling and reuse practices and greater inputs in materials supply. This approach is fundamental considering that worldwide refractory production is nearly 40 Mtons/year with strong fluctuations determined by the steel industry which is responsible for more than half of the total demand. Indeed, steelmaking replaces almost 40 % of the total refractories every year during the operational period. However, it is important to distinguish between recycling practices, i.e., closed-loop and open-loop, to be able to maximize the intrinsic value and potentiality of the waste. For example, the properties of the waste are close to those of the primary raw materials in the closed-loop case, therefore it is possible to reprocess the materials and reintroduce them in the same circle of production. In the open-loop case, the material experiences a significant change in its properties due to the operating conditions which make it

substantially different from the primary raw materials. In this frame, the waste must be repurposed for other applications as potential substitute of other materials. The closed-loop option has the potential to keep the value and functionality of the materials as constant as possible and must be preferred to the open-loop one. To this aim, two possible strategies can be considered and combined to provide good practices to repress open-loop recycling generating strong incentives and interest in the closed-loop circularity of refractories. The first strategy consisted in the replacement of a certain amount of virgin raw material in the novel formulation with a portion of the recycling one whose quantity varies depending on the number of lifecycles to which the waste was subjected since the operative lifetime of refractories can range from hours to several months depending on their role. A critical threshold of 20 % of non-novel raw materials in the formulation was reported in many studies to ensure the maintenance of high performance in the final material therefore the amount of recycled raw materials added to the formulation decreases drastically by increasing the number of life cycles. The second strategy is based on downscaling the waste materials to overcome the needs for constant high purity and performance therefore by increasing the impurities, i.e., the number of life cycles, the application in less performing refractories will occur. Besides waste hierarchy and value-based concept, a functionality and purity classification must be always considered since the purity of a refractory material is strongly related to its performance. Chemicals like calcium ovide, iron oxides and silica can significantly affect refractory properties due to the formation of low melting phases, high volume variations, incompatibility with slag or molten metal, etc. thus reducing material service lifetime. At the same time, the formation of high thermal and corrosion resistant chemicals like spinels or structural reinforces, e.g., nano whiskers, can improve the durability and the performance of the refractory. There are two main issues that still hinder the spread of these solutions. The first one is the lack of information in terms of simulation on the thermodynamic evolution of the system during the in-use conditions even if some computational software like FactSage® is being developed throughout the years to overcome this problem. The second issue concerns the complex mechanical response of refractory materials which is difficult to determine due to their nonlinear behavior deriving from their heterogeneous nature, the multi-phase composition and the great variety of interactions among the molten metal. Considering this, reliable investigations at the meso- and macroscale of refractories system must be performed through computational methods such as FEM to obtain further and accurate information on thermal and mechanical properties evolution during operative conditions. This is one of the objectives of the PhD project which aims at developing an experimentally validated thermomechanical model with ABAQUS® software to predict the evolution of refractories properties, e.g., Young's module, thermal dilatation and conductivity, etc., during thermal cycling of typical high temperature processes. The results obtained from the mathematical model will be compared with empirical results at different temperatures, e.g., thermal dilatation measurements, crush, Brazilian, and triaxial tests. Once validated, the model will be exploited as supporting tool in combination with compositional models to foreseen phases and chemicals in the spent refractories, and multi criteria decision approaches based on machine learning to develop a methodology to predict the reuse and recyclability of the various refractory materials. The PhD project focused its effort on tundish linings, e.g., isostatically pressed materials such as Al_2O_3/C and ZrO_2/C and insulating boards such as Vermiculite. A crucial priority to enhance the performance of the products and to tackle the

prevention step of circularity is the identification of the pivotal properties and simulation through the proper yielding function. Indeed, many yield functions have been developed to explain the plastic behavior and consequent failure of various material classes, e.g., Mohr-Coulomb, Tresca, von Mises, and Drucker-Prager, but most of them were characterized by some drawbacks such as requiring the evaluation of the shear and tensile yield stresses to define the ranges of applicability or approximating material properties as homogeneous. The alternative yield criterion proposed by Bigoni and Piccolroaz (127) is considered more suitable. It is a modulable criterion based on a phenomenological yield function which is directly obtained from the interpolation of experimental data. It is extremely valuable in predicting the mechanical behavior also of ceramic materials sensitive to pressure. Experimental and numerical modeling alone are not sufficient to predict refractory material failure since it can vary significantly due to the heterogeneous nature, the complex geometry, and the strong variety of stresses occurring. Different failure mechanisms can arise in the material for the same application as a result of fatigue phenomena which appear in the form of preferential cracks propagation paths, damage saturation, cracks coalescence and interlocking, and grains relocation mechanisms. The turning point is the connection of these energy dissipation mechanisms with the key thermomechanical properties of the material to define its lifetime by adopting a Failure Mode, Effects, and Criticality Analysis (FMECA) strategy to assess the operativity and reliability of a product through inductive reasoning. The analysis consists in the identification of the modes in which a product can fail, in the evaluation of the consequences of such failures on product operativity and on the overall system, and finally in the definition of criticality and severity levels for each of the individuated failures. This approach could enable a more rigorous and statistical treatment of failure analysis allowing to incorporate fatigue effect in the investigation. This strategy allows a quantitative analysis by estimating the criticality number of each i-th failure mode which is defined as: $C_i=\alpha_i\beta\lambda_n t$. The failure mode ratio α_i is the probability that the product will fail in the i-type mode, is given as a percentage of the total observed failures and is statistically derived. The condition probability, β, of operational failure represents the probability that the identified failure mode will cause the product failure due to the ageing or degradation of the key properties related to the identified i-type failure mode. The component failure rate, λ_n, represents the number of particular n-parts of the product which are subjected to the i-type failure mechanism and t corresponds to the total operational time the product has been utilized. Afterwards, a severity classification of the operational conditions is built by taking advantage of the numerical modeling already performed as FEM outputs can provide maps of stresses, strains, pressures, etc. Comparing the output fields with the experimental properties of the material prior usage, it is possible to classify the severity in four categories: negligible, marginal, critical, and catastrophic (128).

The third thesis from WP2 attempts to improve refractory castables microstructure to increase both sustainability and thermomechanical performance. The work focused on different formulations of alumina spinel refractory castables proposing new designs by considering the nature of the aggregates as well as the arrangement of the calcium aluminate phases network. Indeed, alumina-spinel based refractories are excellent furnace and ladle linings thanks to high refractoriness and low thermal conductivity which ensure heat losses reduction and increased energy savings as well as superior corrosion and slag penetration resistance which allows to produce clean steel with low or no C pick up. The alumina-spinel containing refractories, i.e., pre-formed refractories, investigated are preferred

to in-situ ones because they can ensure high hot strength and volumetric stability at high temperatures. Two types of alumina aggregate were considered in the work, i.e., tabular alumina and white fused alumina, both produced starting from bauxite ores but differing for the processing route, i.e., sintering against electrofusion, which is responsible for the different morphology and porosity. The significant amount of evenly distributed closed pores is thought to be responsible for the improved thermal shock resistance of tabular alumina compared to castables containing white fused alumina. The main physical properties of tabular and white fused alumina aggregates, i.e., apparent density, open porosity and water absorption, were determined using Archimedes method. Tabular alumina was characterized by a blocky shape with an apparent density of 3.6 g/cm^3, an open porosity of 4.3 %, and a water absorption of 1.2 %. White fused alumina was characterized by an angular shape with an apparent density of 3.5 g/cm^3, an open porosity of 9.9 %, and a water absorption of 3.7 %. The morphological characterization with SEM confirmed that tabular alumina aggregates are denser with many small pores distributed throughout the microstructure with more rounded grains whereas white fused alumina aggregates were characterized by dense grains with straight-edged shapes and larger pores of different sizes and shapes. The grain sizes were also evaluated, and white alumina reported an average grain size 10 times higher than tabular alumina aggregates. The mineralogical XRD analysis underlined mainly the presence of α-Al_2O_3, i.e., around 94 %, with little amounts of β-Al_2O_3, i.e., around 4-5 %, in both alumina aggregate types. Three different sets of formulations were considered: tabular alumina and white fused alumina-spinel castables, tabular alumina and white fused alumina-spinel micro-castables to disclose the effects of fine aggregates on the thermomechanical behavior and pure alumina systems of tabular alumina and white fused alumina castables to describe the effect of castables without sintered spinel. All formulations contained also CAC binder, reactive alumina, dispersant and water. All formulations were cured at 20 °C and 100 % RH (Relative Humidity) for 48 h, dried at 110 °C for 24 h and then fired at 5 °C/min up to 1100, 1300 and 1500 °C for 6 h. Concerning alumina-spinel castables, 3-point bending tests were performed to measure the modulus of rupture after curing, drying and firing while thermal shock tests were carried out on pre-fired samples at 1500 °C for 6 h by applying five heating and cooling cycles. Samples were placed in the furnace already heated at 950 °C for 2 h and were then removed to be air-cooled to room temperature. For each cycle, the damage induced by the thermal cycling was evaluated by elastic modulus measurements via frequency resonance at room temperature while modulus of rupture tests allowed to evaluate the residual strength. The apparent porosity of castables made with tabular alumina was lower than the one of castables made with white fused alumina probably due to the inherent higher porosity of the aggregate. Furthermore, an increase in porosity for increasing temperature, i.e., at drying and firing temperatures, was observed for both castable configurations. Concerning the mechanical response, modulus of rupture proved to be comparable up to 1300 °C between the two configurations, but tabular alumina-spinel castables displayed a higher modulus at 1500 °C probably thanks to the less porous microstructure. For thermal shock, both castable configurations displayed a progressive loss in the modulus of elasticity after thermal shock cycles but tabular alumina castables displayed a higher elastic modulus and a higher residual elastic modulus whereas white fused alumina castables exhibited a lower modulus of rupture but a higher residual modulus of rupture of about 50 % after five thermal cycles (129). For all six castable configurations, the evolution of Young's modulus with temperature was used to investigate

thermomechanical behavior. The castables were exposed to two thermal cycles. The first cycle showed how phase transformations can influence the stiffness of the castables while the second cycle allowed studying the potential crack-healing and crack-opening of the previously fired castables. Acoustic emission accompanied all thermal cycles providing information in terms of damage occurrence by monitoring the microcracks developed in the refractory during cooling. The results of alumina spinel castables highlighted very high elastic modulus around 140 GPa after drying at 110 °C at the beginning of the Young's modulus measurements while a strong decrease up to about half of the initial value was registered at 400 °C due to the dehydration of the cementitious phases. No further changes were observed from 400 to 1100 °C despite the formations of calcium monoaluminate phase at 950 °C. A recovery of elastic modulus was observed between 1100 and 1300 °C thanks to the formation of calcium dialuminate phase which is accompanied by an expansive effect which stiffens the microstructure. Analogously an increase in elastic modulus from 1300 to 1500 °C was observed thanks to the formation of calcium hexaluminate phases which strengthen the microstructure. If the first cycle heating curves of the two refractories are quite comparable, significant differences were detected in the cooling curves. Tabular alumina castables displayed a gradual increase in the elastic modulus until the end of cooling while white fused alumina displayed this trend only until 650 °C and afterwards a gradual decreasing trend until the end of cooling. This entailed that tabular alumina castables end up with a higher stiffness compared to white fused alumina. A second thermal cycle was applied to study castables behavior after sintering. Tabular alumina castables displayed a gradual and linear decrease from room to high temperatures and a gradual increase during cooling. Furthermore, a small hysteresis curve was observed, and it was attributed to crack healing during heating by viscous phases and crack opening during cooling due to the coefficient of thermal expansion mismatch between the matrix and the aggregate phases. A more significant hysteresis was recorded for white fused alumina castables which exhibited a higher coefficient of thermal expansion mismatch between the aggregates and the matrix inducing intense microcracks into the system when cooled. Acoustic emissions corroborated these conclusions reporting fewer acoustic emissions for tabular alumina castables compared to white fused alumina castables. Regarding alumina-spinel micro-castables, curves comparable in shape with the ones of the respective castable formulations were obtained during the first heating cycle due to the similar microstructural changes occurring within the systems. The only difference was observed during the cooling stage as both micro castables displayed a gradual increase in elastic modulus towards the end of cooling. After the second thermal cycle, both micro castables did not show any sign of hysteresis in the curves thus meaning that the amount of microcracks developed is relatively low and not significant to impact Young's moduli. This is confirmed by acoustic emission experiments where lower acoustic emissions were recorded in both micro castable systems compared to the respective castable formulations. Also, pure alumina castables displayed curves during the first thermal treatment up to 1500 °C with similar shapes as recorded in all castables due to the various phase transitions. The second thermal treatment followed an almost linear curve during heating and cooling for pure tabular alumina castables whereas a significant hysteresis loop was formed during heating and cooling of white fused alumina castables. Again, acoustic emissions recorded lower values for the first and second thermal cycles in tabular alumina compared to white fused alumina (130).

The fifth thesis from WP2 was focused on the development of a numerical tool to correlate the thermomechanical properties and microstructure of refractories by using a discrete element method (DEM) to be then integrated in the free software GranOO. The developed model aims to guide the controlled introduction of microcracks into the refractory to improve their thermal shock resistance. Indeed, the presence of numerous microcracks within the microstructure can promote a nonlinear macroscopic mechanical response which improves thermal shock resistance. In this perspective, the modelling activity plays a major role considering the complexity of the relationship between microstructure and macroscopic thermomechanical properties and the need for a deeper understanding to enable the use of microcrack engineering for commercial production. DEM is an explicit technique which represents bodies as discrete particles and characterized as rigid elements in the 3D domain. These particles interact together according to contact interaction laws which state that microscale interactions result in emergent properties that can be measured on the macroscale as an apparent property. For example, rheological models, e.g., the spring model, can be selected to describe these interactions. For these reasons, DEM offers significant potential for modeling microstructures with numerous discontinuities, such as inclusions, cracks, debonding, and porosity in refractory microstructures. The current study used polyhedral discrete elements to investigate this relationship whose translation and rotation are described through Newton's laws. Furthermore, the phases were assumed to be chemically inert and the presences of interphases negligible. DEM is extremely useful to perform quasi-brittle analysis with Multiphysics and multiscale simulations allowing to preserve the realistic nature of the phenomena. Finally, it is able to model multiple cracks nucleation, propagation, branching and failure while keeping a good computational efficiency compared to the time consuming FEM. The reference material chosen for the modelling activity was polycrystalline aluminum titanate, Al_2TiO_5, because the numerous microcracks in its microstructure are responsible for a low thermal expansion, a high thermal shock resistance and promotes a significant quasi-brittle behavior in tension. These microcracks are the result of the anisotropic thermal expansion coefficients of the individual grains which generate internal stress during the cooling stage right after sintering. The simulation was performed with GranOO an opensource discrete element workbench using as input data the local properties of each aluminum titanate grain at 1200 °C. Each crystal is modeled as a polyhedral discrete element of random size with random orientation. The model is imposed with the elastic brittle law and local failure criteria (Mode I). The model selected to describe element interactions is the lattice spring model which is an advanced contact model able to deal directly with continuous mechanical properties, e.g., stress and strain, and allows the direct introduction thermomechanical properties, such as Young's modulus, Poisson's ratio, and coefficient of thermal expansion. This introduction is possible only if the interaction surfaces between the discrete elements are equivalent to a continuum medium without voids and this is achievable with the plane-sweeping algorithm Voronoi tessellation. The polyhedral discrete elements resulting from Vornoi tessellation were connected using contacts generated by a Delaunay tessellation, therefore the process to generate the DEM model with lattice spring model involved a dual tessellation. The simulation was developed to be able of handling also anisotropic thermal expansion thanks to the inclusion of periodic boundary conditions which allow to eliminate boundary surfaces. Indeed, periodic boundary conditions introduce an infinite cohesive media using a finite periodic cell to replicate the microstructure exploiting the

potential periodicity of the microstructure. The thermomechanical simulation was then split into two steps. The first one concerned the cooling process of the sample from 1200 to 900 °C when some microcracks are initiated and propagated due to the anisotropic thermal expansion of the crystals. The second step exploited the numerical sample with microcracks obtained in the first step to perform a uniaxial tensile test to monitor material macroscopic mechanical response in terms of strain versus stress evolution. Microcracked numerical sample exhibited a sharp nonlinear mechanical response under tension when cooled from 1200 to 900 °C and this trend continued even after further cooling to 600 °C. On the contrary, no microcracked numerical sample exhibited the typical brittle mechanical response. These outcomes strongly support the claim that microcracks network strongly influences the thermomechanical properties of Al_2TiO_5 refractories. The model will be validated with experimental results resulting from the other PhD thesis from the CESAREF consortium (131) (132).

In the framework of WP3, the two PhD thesis considered were "Influence of H2 containing atmospheres on the thermo-mechanical behavior of refractories" by Cristian Bohorquez Moreno from Montanuniversität Leoben, and "Changes of microstructure and thermal properties of refractory castables in H_2 combustion atmospheres" by Milena Gomes from RWTH.

Part of the work performed in the first PhD Thesis of WP3 was devoted to the investigation of the effects of H_2 on a burnt phosphate bonded high alumina refractory which is a material potentially used in DR reactors thanks to the superior corrosion resistance of Al_2O_3 against hydrogen. Although preliminary studies already proved that H_2 can strongly influence refractories thermomechanical properties, e.g., Young's modulus and compressive strength, most of them were performed from 1100 and 1800 °C to accelerate the kinetics while limited research is available for temperatures around 900 °C which better resembles the conditions of direct reduction. Indeed, 900 °C was established as the optimal value for iron ore reduction in terms of energy consumption and reduction balance. The proposed study tried to fill this gap of knowledge investigating the effect of hydrogen on an industrial-grade phosphate-bonded alumina refractory focusing on the effects of duration exposure on the microstructure and temperature dependent evolution of the Young's modulus. The refractory selected was characterized by a density of 2.66 g/cm^3, a porosity of 20 % and a chemical composition with an Al_2O_3 content of 75 %, a SiO_2 content of 21.4 % and a P_2O_5 content of 1.1 %. The refractory specimens were continuously purged with hydrogen at 900 °C for 16 and 48 h and were then tested in compression after being heated to 900 °C for 1 h. Young's modulus was determined by the impulse excitation technique employing a heating rate of 5 °C/min from 25 to 1300 °C. The preliminary morphological characterization highlighted an increase in glassy phase surrounding mullite and an increase in mullite aspect ratio after samples exposure to hydrogen which resulted in the formation of microcracks. Furthermore, EDS analyses underlined a migration of Na, K and P from mullite and corundum toward the glassy phase after H_2 exposure and this effect was progressively more pronounced for increasing exposure hours. The exposure is also responsible for an alteration of the crystalline phases with corundum and glassy phase content increasing at the expense of mullite. This phase change was ascribed to the complex phase dynamics because Na, K and P compounds which are characterized by notably high partial pressure and are sensitive to reduction by hydrogen at 900 °C tend to migrate towards the glassy phase modifying the activity of SiO_2 and Al_2O_3 in the glassy phase. SiO_2 activity in the glassy phase decreases thus reducing the stability of Si-rich mullites which tend to

enrich in Al_2O_3 and providing SiO_2 to the glassy phase. Concerning the formation of microcracks, they must be ascribed to the cooling phase where the variations in thermal expansion coefficients among the different phases led to microcrack formation. Indeed, the glassy phase is characterized by a lower thermal expansion coefficient than corundum and Al-rich mullites therefore the grains underwent compressive stress, while the glassy matrix experienced tensile stress thus leading to the formation of microcracks throughout the matrix. Focusing on the evolution of Young's modulus with temperature, the unexposed material exhibited values of 28.7 GPa at room temperature reaching 59.1 GPa at 1160 °C during heating. Upon cooling, Young Modulus displayed a maximum of 63.1 GPa at 833 ◦C, returning to approximately 30.6 GPa at room temperature after two thermal cycles. For unexposed samples, the overall response of Young's modulus to temperature was described dividing the curves in 15 regions. The first region from room temperature to 750 °C reported an increase of Young's modulus due to material thermal expansion and potential microcracks closing, then in the second region from 750 to 850 °C constant values were observed resulting in a plateau region for the curve. In the third region from 850 to 1100 °C, Young's modulus increased again since the formation of liquid phases alters curve shape. In particular, the damping increased approaching the theoretical onset of liquid phase formation at 970 °C. After that a sharp drop in Young's modulus was detected in the fourth region from 1100 to 1300 °C due to increasing liquid glassy phase. When starting the cooling from 1300 to 1000 °C the fifth region was identified, the beginning of solidification of the glassy phase caused an increase of Young's modulus which decreases as microcracks open. The sixth and seventh region concern the further cooling from 1000 to 700 °C where a slight and steady Young's modulus increase was recorded due to cracks closing and glassy phase solidification, and from 700 to 50 °C where a reduction of the Young's modulus was observed due to the formation of microcracks resulting from thermal expansion differences. The other regions were observed during the second cycle with region 8 occurring between 50 and 750 °C where Young's modulus increase was observed similarly to the behavior to the first cycle and region 9 occurring between 750 and 850 °C where a plateau similar to region 2 was observed. Some differences were observed in region 10 from 850 to 1000 °C where a rapid Young's modulus increase higher than the first cycle was observed due to the transition of the glassy phase to liquid. Young's modulus increase due to crack closure was observed also in region 11 from 1000 to 1100 °C whereas a significant drop was observed between 1100 and 1300 °C in region 12 due to a significant increase in the liquid phase. The last three regions, i.e., 13, 14 and 15, concern the cooling regions and displayed a behavior like regions 5, 6 and 7 indicating solidification, constant Young's modulus behavior, and material crack opening during cooling. After assessing the response of the untreated samples, the effects of hydrogen exposure on refractories mechanical properties were investigated considering two different exposure periods of 16 and 48 h. In both cases, a noticeable reduction in Young's modulus at room temperature was observed compared to unexposed samples. In particular, the 16 h exposed samples exhibited a Young's modulus of 23.8 GPa at room temperature reaching a peak of 61.1 GPa at 1130 °C during the first heating cycle. Before the onset of the second heating cycle, Young's modulus at room temperature was 35.8 GPa. The sample exposed for 48 h exhibited a similar trend with a Young's modulus of 22.4 GPa at room temperature reaching a peak of 59.2 GPa during the first heating cycle at 1158 °C. Before the second heating cycle started, Young's modulus value dropped to 36.1 GPa at room temperature. More information was obtained from high

temperature compressive tests at 900 °C which highlighted a progressive decrease in compressive strength and maximum strain for increasing hydrogen exposure times. These differences are a consequence of the microstructural changes arising in the material such as the increase in the glassy phase amount at 900 °C which promotes softening of the structure thus suggesting that the compressive behavior at evaluated temperature is not dominated by microcracks but by intergranular weakening (133).

Also, the second thesis from WP3 was devoted to evaluate the corrosion resistance to H_2 atmosphere of different castable refractories assessing also the effects on the microstructural and thermal properties. The work was focused on DRI plants and on the effect that a 100 % H_2 atmosphere for iron ore reduction could have on refractory lining since previous studies proved that H_2 can permeate through refractories and reduce ceramic oxides under certain process conditions. SiO2-containing materials were reported as being extremely susceptible to H_2 attack since their reaction leads to the formation of volatile SiO as main product. The latter can also cause clogging, fouling and product contamination problems upon cooling. On the contrary, alumina proved to be extremely performing since its reaction with H_2 takes place only at very high temperatures, i.e., higher than 1800 °C. Considering that there is a lack of studies on the behavior of refractories under H_2 atmospheres, the PhD thesis aimed to investigate the effects of H_2 exposure on refractory bricks with different Al_2O_3 and SiO_2 contents using different atmospheres, i.e., 100 % H_2, 98 % H_2 with 2 % CO and 98 % H_2 with 2 % CO_2, at temperatures of 1000, 1200 and 1400 °C for 200 h. Six different commercial bricks were investigated and their chemical composition is summarized in Table 31. In particular, the D series of bricks concerned dense refractories whereas the L series concerned lightweight insulating bricks.

Table 31: Main oxide contained in the chemical composition of the bricks under investigation

	Al_2O_3 (wt.%)	SiO_2 (wt.%)	Fe_2O_3 (wt.%)	TiO_2 (wt.%)	P_2O_5 (wt.%)	Bulk density (g/cm^3)
D1	43.1	52.0	1.38	1.48	0.45	2.23
D2	59.4	38.6	0.98	0.34	0.04	2.52
D3	90.4	6.59	0.30	0.11	1.66	3.09
L1	40.2	54.2	1.85	0.76	0.08	0.51
L2	65.8	32.0	0.70	0.24	0.07	0.94
L3	90.0	9.23	0.25	0.15	0.00	1.40

The first outcomes from the trials performed with 100 % H_2 concerned the color change experience by all bricks at all temperatures caused by the reduction of iron oxides as shown in Figure 1. The original white, beige or earthy color always transformed into a light/dark grey one. This change was also accompanied by a loss of weight of the bricks since the reduction of ceramic oxides by H_2 generated gas-phase products. Low and almost negligible weight losses were observed at 1000 °C while they became more significant at 1200 °C being between 2-5 % for the D series and between 2-15 % for the L series. The corrosion became even more severe at 1400 °C when L1 bricks experienced a mass loss of 30 %. The comparison between the different brick types clearly highlighted that weight

loss was much more significant for lightweight refractories than for dense ones proving that reaction kinetics depended on mass transport and that H_2 permeated more easily in the less dense structure as well as reaction products left more readily the interior of the sample. It was also observed for both dense and lightweight bricks that the higher the SiO_2 content the higher the weight loss while an increase in Al_2O_3 ensured a superior corrosion resistance. This conclusion was further confirmed by chemical analysis which underlined a depletion of SiO_2 after reaction with H_2 while Al_2O_3 content increased not reacting with H_2 in these conditions. The onset of SiO_2 reduction by H_2 was identified between 1000 and 1200 °C because the small weight losses measured at 1000 °C could not be linked to the volatilization of SiO_2. The best performance was achieved with the denser brick with the highest Al_2O_3 and lowest SiO_2 content. The analysis of the microstructure revealed the presence of small droplets with a diameter up to 1 µm for all exposed samples starting from 1000 °C and intensifying with higher temperatures. These beads were made of Fe alloyed with small amounts of P and Si thus proving that P_2O_5 impurities were also reduced causing a depletion of this oxide in the matrix. SEM analyses also revealed the effects of SiO_2 reduction on refractories microstructure highlighting a decomposition of the glassy phase and in the most severe cases also an attack of the mullite structure. Concerning the trials performed with a 2 % of CO and CO_2 in the atmosphere, none of them seemed to exert an appreciable effect on refractory weight loss. It can be concluded that refractory lining in high-temperature applications with H_2-bearing atmospheres must be characterized by a high density and a low SiO_2 content with Al_2O_3 being a suitable candidate. Furthermore, phosphate binders can be easily reduced by H_2 being therefore discouraged as well as the glassy phase content which must be kept low being more susceptible to H_2 attack (134).

In the framework of WP4, the three PhD thesis considered were "Sensoring material performance in use, and monitoring using machine learning" by Amit Kumar Gope from Université de Limoges, "Smart Factory: Predicting thermal behavior of steel ladles with advanced digital methods for improving the thermal efficiency" by Fatemeh Azizi from TU Wien, and "Smart Factory: Enhancing energy efficiency in steel making through advanced digital technologies" by Victor Ruela from TU Wien.

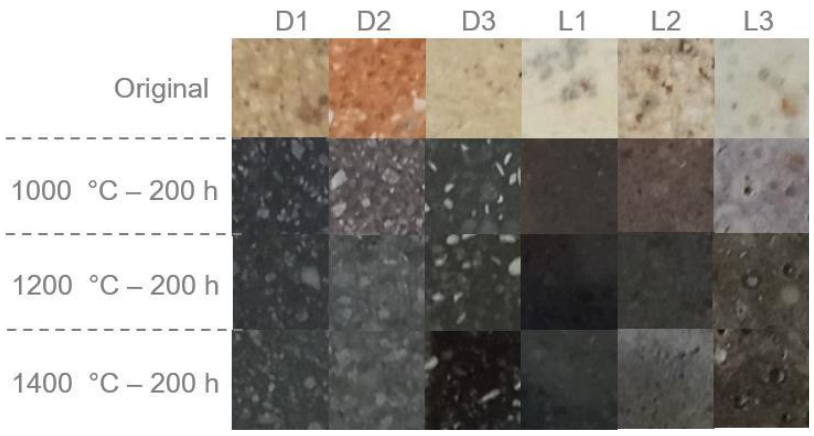

Figure 64: Color change experienced by the bricks after 100% H_2 exposure at different temperatures (134)

The first PhD thesis in the framework of WP4 aims to predict the changes occurring in refractories properties during their operations to be able of assessing their potential for reuse extending the lifespan and reducing costs. Data on thermal properties and mechanical behavior of refractory components will be collected through non-destructive techniques and will be used to train machine learning networks. Before implementation in the field, a pertinent monitoring technique must be identified and developed at a laboratory scale and various NDT (Non-Destructive Technique) will be tested to this aim. Furthermore, an accurate machine learning and deep learning model for refractory thermochemical and mechanical properties prediction based on NDT outcomes must be selected preparing properly also the dataset. Once developed the machine learning tool, it will allow to detect and assess the characteristics of refractory materials and to develop an accurate decision-making numerical model to evaluate the reusability and recyclability of refractory components. Decision-making will be based on the 4Rs approach, i.e., Reduce, Reuse, Recycle, and Replace, of the material under consideration.

4.5 ZEUS: Zero emissions through sector coupling

Different CO_2 emission reduction pathways are being investigated within the project ZEUS "Zero Emissions through Sector coupling" including green H_2 production and carbon capture of unavoidable CO_2 emissions. An amine scrubber is employed within an integrated steel mill as well as a membrane separation technology in the cement industry to evaluate potential carbon capture strategies. While carbon capture technologies reduce emissions at its source, transforming the captured CO_2 into valuable products is crucial to close the carbon loop. ZEUS focuses on catalytic methanation with particular emphasis on the development of novel catalysts and reactor designs. In addition, syngas (CO + H_2) and formic acid (CH_2O_2) are produced via CO_2 electrolysis to demonstrate the technological potential and provide a basis for scalability. All pilot plants within the ZEUS project are operated under real industrial conditions to ensure practical relevance and scalability of the tested technologies. The goal of ZEUS is to develop a cross-sectoral demonstration of a climate-neutral process chain - from the production and processing of green hydrogen under fluctuating process conditions to the separation of CO_2 from industrial exhaust gases and the conversion into valuable products. The processes are all being operated under real conditions at TRL 7 to accelerate the transfer into practice.

Focusing on the steel sector, an amine scrubber pilot plant with a capacity of 800 kg/day was used to capture CO_2 from the industrial off gas of an integrated steel mill power plant. Different solvents were tested to minimize the regeneration energy required and to minimize solvent degradation. Two different solvents were compared, i.e., MEA and activated methyldiethanolamine (aMDEA). Preliminary results from solvent comparison showed that process parameters such as the liquid to gas ratio must be significantly altered to achieve feasible operations using aMDEA. Indeed, the liquid-to-gas ratio, i.e., the ratio between the volumetric flow of the liquid solvent and the volumetric gas flow of the off-gas, needed to be about twice when using aMEA compared to MEA to reach a separation efficiency of 90%. A comparison of the specific regeneration energy of both solvents also revealed that aMDEA required 10 % less energy than MEA. The results are summarized in Figure 65 which shows that the regeneration energy for aMDEA is around 3.3 GJ/tCO_2 while the energy needed for MEA is 3.7 GJ/tCO_2.

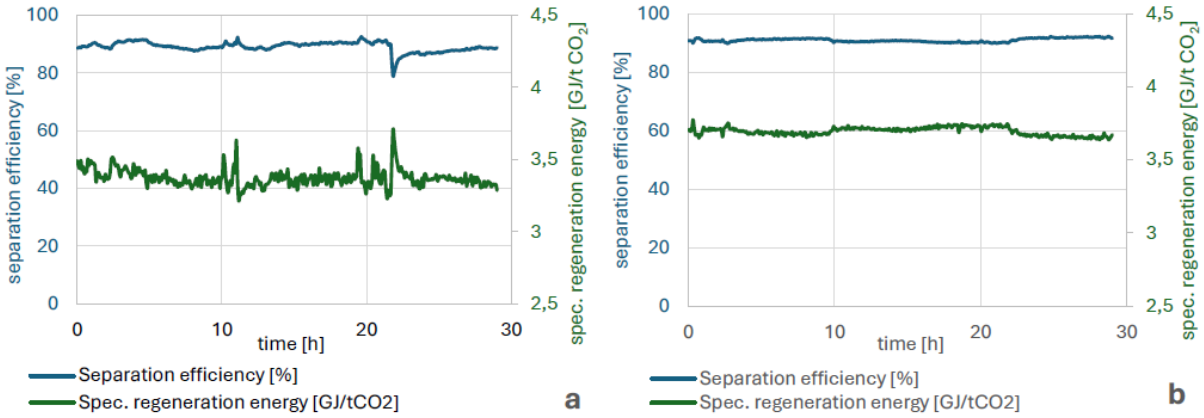

Figure 65: Comparison of specific regeneration energy with aMDEA (a) and MEA (b) at 90 % separation efficiency

Moving to the cement industry, a 500 kg/day CO_2 membrane separation unit was installed enabling a direct comparison of this technology with the amine scrubber. Therein, the flue gas passes through a cylindrical membrane module containing spiral-wound membranes to separate CO_2 from the off-gas. The aim of the separation unit is to optimize the separation efficiency, long-term stability and energy input. The captured CO_2 was then converted into formic acid, by an in-house-developed electrolysis cell, shown in Figure 66.

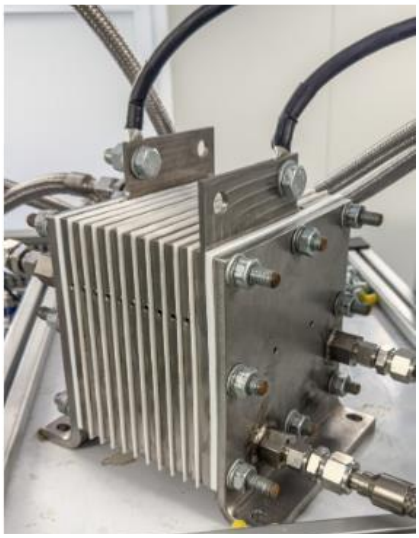

Figure 66: Close-up of the electrolytic cell for CO_2 conversion into formic acid

Furthermore, an existing pilot plant for catalytic methanation was operated under real industrial conditions using captured CO_2 from the amine scrubber and H_2 from the 6 MW proton exchange membrane electrolyzer. The exothermic reaction ($CO_2 + 4\ H_2 \rightarrow CH_4 + 2\ H_2O\ \Delta H0 = -165$ kJ/mol)

is controlled by an oil bath. Around 10 Nm^3/h of synthetic natural gas was produced, and it was fed directly into the power plant gas injection system thus closing the internal carbon cycle. Preliminary experiments were conducted to investigate methanation reactions, demonstrating the influence of pressure and temperature on its performance as shown in Figure 67. In addition, the durability of the catalyst was evaluated, under steady operation and dynamic feed gas flow rate.

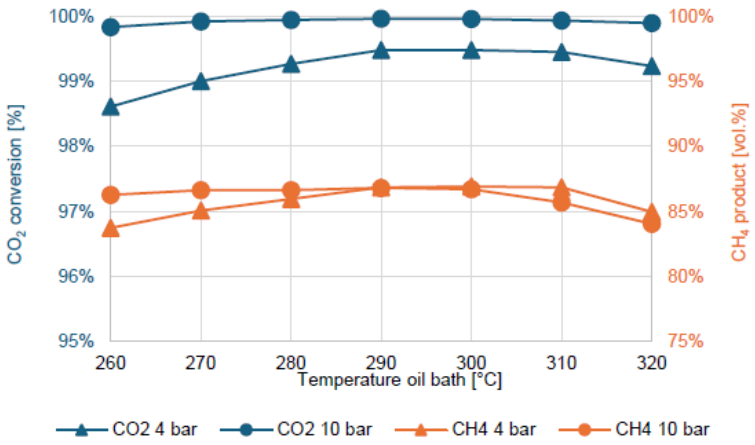

Figure 67: CO_2 conversion and CH_4 production rate as a function of oil bath temperature at 4 and 10 bar.

For the electrochemical conversion of CO_2 to syngas, new catalysts and electrodes were developed and tested in zero-gap cells. The aim of the experiments was to achieve the highest possible CO_2 conversion rate, selectivity (Faraday efficiency) and long-term stability. Additionally, a pilot plant for syngas production is planned to be erected in the environment of a steel industry to demonstrate the technical feasibility and scalability under industrial conditions. Laboratory tests of CO_2 from the amine scrubber, which was captured by two different solvents (MEA and aMDEA) were conducted to select an appropriate absorbent for CO_2 supply for pilot plant testing. To bring the project to a conclusion, use cases, scale-up and roll-out scenarios for large-scale applications of the demonstrated CCU process chains were developed. This is based on an evaluation of energy/chemical efficiency and total costs. To this aim, a techno-economic analysis was conducted for each technology, incorporating elements such as market dynamics, technological learning, and the scaling up of systems.

In conclusion, ZEUS enables to convert CO_2 emissions from challenges into opportunities via developing a carbon cycle. In the future, sector coupling will be essential. The chemical industry like the methanol, urea, olefines will need C as a feedstock. ZEUS develops scenarios to convert CO_2 into a valuable carbon source.

5. Main takeaways of actual IS scenarios and technologies

CE and IS are two of the measures that the European Green Deal is promoting to reach climate neutrality by 2050. Both concepts foster a more sustainable management of materials and resources to replace virgin raw materials and reduce the dependence on critical materials thus resulting in CO_2 emissions mitigation. Compared to the traditional linear model of economy, CE promotes continuous reuse, repair, and recycling of materials, leading to lower consumption rate of natural resources and lower waste generation decreasing the overall environmental impact. In this perspective, IS represents a practical solution where the wastes or by-products generated by one industry become a resource and a feedstock for another promoting environmental sustainability and economic efficiency. Despite the great potential of this approach, many companies still lack awareness of IS, due to different barriers, including environmental, economic, technical, regulatory, organizational, social, and cultural ones. Among them, technological barriers are certainly a major factor since innovative technologies must be identified, investigated and developed to high TRLs to upgrade waste resources in the value chain and transform them into a usable form.

The present deliverable was envisaged as an accompanying measure to collect and summarize all the main technological solutions and achievements obtained in the framework of EU funded projects dedicated to the implementation of IS in the steel sector. The deliverable aims to spread the main outcomes obtained and to promote their implementation in new potential IS scenarios concerning the steel industry but also other energy intensive sectors such as cement and glass ones. Hereinafter, the main technical solutions achieved were summarized by dividing them according to the main upstream, i.e., biogenic and non-biogenic SCCs and scraps, and downstream, i.e., slag, dust, sludge, off gas and refractories, solutions investigated.

5.1 Upstream solutions

5.1.1 Secondary Carbon Carriers (SCCs)

Secondary Carbon Carriers (SCCs) are defined as alternative carbon materials used in heavy industries such as steelmaking to replace fossil fuels and reduce the reliance on coal and coke thus potentially lowering emissions and representing a compelling upstream solution for decarbonization. In the steelmaking sector, they can act as reducing agents, carburizing agents, chemical energy providers, and foaming agent according to the targeted application. SCCs can be divided into two main categories

biogenic and non-biogenic. Biogenic SCCs are processed organic materials derived from biomass such as biochar, torrefied biomass, and hydro char which allowed to reduce net carbon emissions by using C that was recently sequestered from the atmosphere. Non-biogenic SCCs are alternative carbon materials derived from waste streams such as packaging plastics wastes, ASR and tires which aim to promote circular economy and decarbonization by preventing new fossil fuel extraction and releasing C that was sequestered for a long period. As proved by the many projects on this topic revised and reported above, the use of SCCs in iron and steelmaking is a powerful solution to decarbonize its upstream and for this reason their feasibility for many different steelmaking processes was investigated. In particular, SCCs could be conveniently exploited in BF and EAF through injections at the tuyeres or through briquettes charging, but also in sinter and coking plants. According to the envisaged application, the selection of the most appropriate SCCs requires the correct evaluation of their key characteristics since the ideal carrier depends both on the specific process and the desired role.

One of the most crucial properties is the fixed C content, i.e., the non-volatile C, which must be as high as possible to reduce iron oxides, act as carburizing agent and provide chemical energy to the system serving as a primary heat generator during combustion. Three other important properties are the moisture, oxygen and ash content which must be kept as low as possible. Indeed, high moisture contents may cause storage issues due to agglomeration in the silos, but also transportation issues resulting from tuyeres clogging. Furthermore, high moisture contents may be responsible for a decrease in energy efficiency since water is characterized by a high heat capacity and requires high thermal energy amounts to be volatilized. Concerning the ash content, it must be kept as low as possible since it does not provide C and can contaminate both steel quality and slag properties thus also influencing the process. Indeed, a modification of slag chemical composition may lead to an increase in viscosity which may affect the refining process and the resulting steel quality and may also hinder foaming thus jeopardizing arc coverage and reduce process efficiency. In this perspective, the input of harmful elements such as P, S and Cl must be also minimized to avoid steel contamination or noxious emissions in the off gases. Concerning volatile matter content, this parameter must be carefully controlled since higher values may be appreciated in EAF providing a good slag foaming but may be undesired and detrimental in BF/BOF as well as in coke making due to gas evolution issues.

Besides chemical features, physical properties must be also considered. Particle size and density as well as mechanical strength and wear resistance may affect handling, charging, permeability in furnaces, reaction rates, bath penetration thus being fundamental to optimize the process. Specific surface area is another key aspect to consider since it concerns both flammability and reactivity. Indeed, flammability must be reduced as much as possible to avoid fire and explosion risks and ensure safe operations in the steel shop whereas reactivity must be sufficiently good to ensure quick reactions and energy release, when necessary, e.g., slag foaming or iron oxide reduction. The calorific value that SCC can provide is also fundamental since high values contribute to the chemical energy of the process thus reducing, for example, electric consumption in EAF. Two further aspects which must be considered are material availability since enough SCC must be allocable to sustain the production chain without competing with other industrial sectors, and SCC cost to maintain the economic viability of the process.

5.1.1.1 Biogenic SCCs: biomass, biochar, hydro char

The use of biogenic SCCs in different steelmaking processes has undoubtably a great potential as proved by the 12 projects dedicated to the topic. In particular, 5 projects focused on the use of biogenic SCCs in EAF, 3 projects on their use in BF, 2 projects on their use in sintering, and 2 further projects on their use in coke making.

Biomasses pretreatment is undoubtably a fundamental step to ensure the desired fixed carbon, moisture, volatile matter, ash and harmful elements, e.g., P, S and Cl, content, and provide the highest performance in each of the aforementioned processes. For example, project 2.2.29 proposed a slow pyrolysis treatment in a Pyrok rotary klin to produce a bio coal which was then leached with nitric acid to remove P. This would allow to obtain high-quality bio-coal for steelmaking together with a P-rich by product, spendable as fertilizer or as liming agent in agriculture. The preliminary results of the carburization tests proved the feasibility of the bio coal obtained from OFMW and straw while the one obtained from SS and AGD needed to be blended with anthracite. Another interesting, coupled pretreatment process was addressed in project 2.2.30 where hydrothermal carbonization followed by pyrolysis at 300-400 °C was performed to increase fixed C and reduce volatile at the expenses of yield. The hydro char obtained was again subjected to leaching to remove ash and P to be reused as fertilizers. Different biomasses were tested but the best results were obtained with olive pomace. Furthermore, carburization and slag foaming tests demonstrated that pyrolyzed briquettes enhanced reduction and carburization, while pristine briquettes optimized slag foaming height thus proving their complementary behavior.

Focusing on biogenic SCCs use in EAF, projects 2.2.7 and 2.2.18 focused on the partial or total substitution of coal with charcoal and biochar produced from biomass pyrolysis, in particular project 2.2.7 targeted both pilot and industrial trials while project 2.2.18 tried to transform char use in EAF in standard practice. The projects considered two different feeding strategies, i.e., charging and injection. Concerning the charging feeding options, char reactivity was a fundamental issue to address to avoid burning during charging. Considering that reactivity was strongly dependent on surface area, volatile content and powder dispersion, a briquetting pre-treatment was proposed as solution. The industrial trials proved that this solution was successful with just little variations on the charging practices to ensure standard operating parameters in terms of productivity and steel and slag quality. Actually, an energy saving of 6 % was measured when a mix of coal and biogenic SCC was charged in the first basket of the furnace equipped with oxygen diffusors. More complex was the scenario for EAF injection solution since some trials showed a good foaming behavior of the slag while others were not satisfactory. This variability in the results was ascribed to the low density of the biochar which reduced the penetration of the jet into the slag layer and to its reduced reactivity with iron oxide. The solutions proposed were an improvement of the injection system to ensure char injection below the slag level, and the application of a suitable additive to increase char/slag wettability thus promoting char reaction with iron oxide.

The use of biogenic SCC in BF was also widely investigated in projects 2.2.2, 2.2.9, 3.2.8, and 3.2.15. Project 2.2.9 attempted to reduce metallurgical coke usage in BF by substituting it with cold bonded C briquettes made with a variety of C-bearing materials such as coke breeze, coke dust, anthracite,

petroleum coke, lignite coke and charcoal. The study demonstrated that C-bricks produced from low-cost carbon materials such as coke breeze, coke dust and petroleum coke, using standard cement binders, could partially replace metallurgical coke in BF. Industrial trials also confirmed that vibration-compacted C-bricks met BF operational requirements with sufficient cold strength for handling and charging enabling coke substitution rates up to 10 % with economic benefits strongly dependent on coke market prices.

Project 2.2.2 mainly focused on charcoal evaluating its feasibility for injection at BF tuyeres and reporting a combustion behavior comparable or better than high-volatile pulverized coal. Furthermore, charcoal achieved high conversion degrees thanks to a highly porous structure and a large reactive surface area, and this was confirmed by the small-scale injection trials where charcoal achieved high conversion degrees in the tuyere and oxygen-rich raceway zone. It was also observed that conversion increased for both coal and charcoal with increasing O/C atomic ratio, but charcoal showed a flatter dependence thus reporting a lower sensitivity of conversion to oxygen availability. In the combustion pilot chamber, charcoal combustion efficiency reached 60 % similar to coal while average charcoal efficiency was around 18 % higher when accounting for lower injection rates. Carbon balance calculations showed that direct CO_2 emissions decreased up to 1.8 % when charcoal replaced coal. Furthermore, when charcoal was considered CO_2-neutral, total CO_2 input decreased by 36–45 % for full substitution of pulverized coal, depending on charcoal quality. This concept was further upgraded through a large-scale demonstrator at ArcelorMittal in 3.2.8 where wood waste feedstocks such as demolition wood and waste furniture were collected, processed through shredding and pollutants removal to reach the specifications required for torrefaction. Shredded wastes wood were dried, sieved and sent to torrefaction to produce bio-coal which was then grinded and transported to BF to replace fossil powdered coal for injection. The torrefaction process was performed at high temperatures up to 350 °C in an oxygen-free environment and allowed to convert bio-residuals and biomasses into bio coal by decreasing the water and volatile content and increasing the energy density and C content. Torrefaction temperatures higher than 300 °C were able to provide higher C content in the bio coal, i.e., 60-70 wt.%, but caused a decrease in yield and a decrease in the energy yield of the bio coal itself. The CO resulting from BF exhaust gases was then sent to a bioreactor to be microbially fermented to produce bioethanol. Finally, a disruptive solution was proposed in project 3.2.15 where biowastes and biomethane were attempted to be converted through a new catalyzed pyrolysis combined with chemical leaching into green hydrogen and C to be used in BF, and in critical inorganic raw materials, e.g., inorganic P-rich fertilizers, for agricultural purposes. The preliminary results at the laboratory scale on 8 different samples, i.e., industrial sludge from food industry and from pharmaceutical industry, mixed urban biowaste digestate, urban biowaste digestate, ash-rich civil sewage sludge, conventional civil sewage sludge, and two different types of agricultural digestate, disclosed some important information for the further development of the project. Sludge from food industry was selected as the most appropriate since it was certainly of biological origin whereas the one from pharmaceutical plant was derived from a process where organic matter was derived from pharmaceutical production thus not being necessarily of biological origin. Among digested urban biowastes, the one with the lower ash content was selected ensuring reduced concentration of Fe and Al and a higher C content. Among civil sewage sludges, Piedmont one was selected whereas Tuscany

one was rejected due to a higher ash content around 50 % against the 33 % of Piedmont one which consequently entailed a higher C content. Industrial sludge presented interesting characteristics with high value elements to be valorized in agriculture (P) and as catalyst in the methane pyrolysis process (Fe) despite the high ash content whereas civil sludge presented a high volatility and high concentration of ashes containing high amounts of Al_2O_3 and SiO_2 both useless for the process and difficult to extract. In light of this, biochar from civil sludge could be critical to produce a metallurgical grade bio coal. Among digestates, urban biowaste digestate displayed a quality not enough high for the H2STEEL process due to limited P, Fe, and C content and the high concentration of ash whereas agricultural digestates displayed interesting composition in terms of total C content and low ash concentration despite the reduced amount of P.

Moving to sinter plants, only two projects, i.e., 2.2.3 and 2.2.25, were dedicated to the topic. Project 2.2.3 investigated the use of pit olives at Tata steel characterized by lower S content and ash levels, higher P, CaO and MgO levels compared to coke breeze. The most promising results were obtained with the substitution of 15 % of C from coke breeze combined with a small additional coke input which led to the best compromise between productivity, cold strength and coke consumption. The results also demonstrated a high sensitivity of the sintering process to small variations in moisture content, ignition conditions and blend composition. Despite the generally positive trends, the overall performance of biomass remained below that of the base case indicating a C replacement factor <1 due to reduced combustion efficiency and lower bed temperatures. More sinter plant modifications were proposed in 2.2.25. At first, the use of alternative solid fuel at sinter strands at an industrial scale was investigated and VOC emissions were identified as the main limiting factor. A layout allowing to replace 35 % of the solid fuel with hot fumes, i.e., 2-phase VeLoSint, was also developed together with other layouts to replace lower quantities of solid fuel with fuel gas and waste gas. Each of these solutions allowed lower specific pollutants emissions. The combination of these layouts with alternative solid fuel allowed to achieve an acceptable sintering level at 0 % fossil solid fuel in the mix but resulted in excessive VOC emissions.

Finally, the use of biogenic SCCs for coke making was addressed in 2.2.2, 2.2.17 and 2.2.28. First attempts were carried out in 2.2.2 trying to incorporate charcoal obtained from pyrolyzed Brazilian eucalyptus and French hardwood fines into coal blends. The results demonstrated that charcoal impaired mechanical strength due to fluidity loss although acceptable fragmentation (I40) and abrasion (I10) resistance were maintained when charcoal was added to highly fluid blends. Furthermore, coke reactivity increased systematically with charcoal incorporation leading to a reduction of about 100 °C in the threshold temperature of the Boudouard reaction due to the intrinsic reactivity of charcoal and to its ash chemistry. This reduction in gasification temperature of 100 °C validated the reduction observed in TRZT. Sinter reduction kinetics remained acceptable down to 870 °C while some loss of shaft efficiency appeared at 750 °C requiring additional coke to compensate. Nevertheless, the net balance indicated a potential coke saving when TRZT was lowered with modelling predicting substantial reductions in coke consumption and CO_2 emissions at constant or near-constant shaft efficiency. Project 2.2.17 attempted the direct introduction of raw biomass to coal blends and proved that it should be limited to values ≤2 wt.% to avoid excessive pressure and quality deterioration. Biomass ash content and composition must be also assessed to ensure compatibility with BF requirements.

Higher biomass level up to 10 wt.% could be foreseen within briquettes if coal tar or similar strong binder were used at the expenses of CSR which would experience a reduction of 5-10 %. The study also showed that the use of hydro char or torrefied biomasses as raw biomass substitute would ensure slightly higher rates of 3-5 wt.% in blends and 10-15 wt.% in briquettes while still requiring careful quality monitoring. The topic was further examined in project 2.2.28 where pilot-scale and industrial demonstration trials are foreseen. In particular, pilot scale coke making tests were planned in a 300 kg movable wall oven at Adl to simulate industrial heating and pressure conditions while industrial trials at Taranto coking plant were also programmed to validate the process at TRL 7. The preliminary laboratory tests focused on various biomasses largely available in the Mediterranean area near the Taranto steel plant, i.e., olive pruning residues (branches and trunks), vine wood, straw, pallet wood, packaging boxes (plywood and chipboard), pine, eucalyptus, and olive pomace. They supported the results reported in 2.2.17 confirming that raw biomasses are not suitable for direct addition into coal blends due to their high volatile content, low fixed C, and disruptive effects on coal plasticity. Biomass thermal pretreatment via torrefaction and carbonization was therefore investigated to enhance fixed C content and reduce volatile matter to improve the compatibility with coke making blends. These pretreatments demonstrated to significantly improve biochar quality ensuring fixed C levels above 70 wt.% and reduced volatile matter thus bringing biochar properties close to those of coking coals and making its substitution feasible up to 10 % in blends. Gieseler and Audibert-Arnu tests also demonstrated that pretreated biomass mitigates the loss of fluidity and dilation, though complete equivalence with fossil coals was not achieved. These results suggest that careful selection of biomass and pretreatment severity are essential to preserve coke quality.

Project 2.2.7 also evaluated the possibility of using the syngas resulting from biomass pyrolysis as natural gas substitute in burners, but the simulations activity showed that syngas flames were characterized by a lower temperature than natural gas thus reflecting in a lower burner efficiency of 8-15 %. Possible solutions to overcome this drawback were identified in the use of burners with bigger sizes, in higher syngas flow rates and in modifying burner geometry to increase combustion efficiency. The latter solution was simulated and an increase in efficiency of about 10 % was estimated. The use of syngas in burners was further developed in 2.2.29 where a new burner was developed to prevent condensation and tar-induced clogging allowing reliable pyro gas combustion at high temperatures. The burner also integrated separate passages for pyro gas and natural gas. An overview of the projects dealing with the different technological solutions involving the use of biogenic SCCs is provided in Table 32.

Table 32: Summary of the main projects addressing each technological solution concerning biogenic SCC use

Technological Solution	Reference Projects
EAF Injection	[2.2.7], [2.2.18], [2.2.29], [3.2.20]
EAF Briquetting	[2.2.7], [2.2.18], [2.2.29], [2.2.30]
BF	[2.2.2], [2.2.9], [3.2.8], [3.2.15]
Sintering Plant	[2.2.3], [2.2.25]
Coke making	[2.2.2], [2.2.17], [2.2.28]
Syngas use in burners	[2.2.7], [2.2.29]

5.1.1.2 Non-biogenic SCCs: plastics, tires, ASR

The use of non-biogenic SCCs in different steelmaking processes was also widely addressed, focusing on three main sources, i.e., ASR, EoL pneumatic tires granules, and mixed plastics wastes mainly from packaging (polyolefins). Special attention was given to EAF injections applications as proved by 5 over 8 projects dedicated to the topic. An initial overview on the use of non-biogenic SCCs in EAF was provided in project 2.2.19 which aimed to explore cost and energy effective alternative slag foaming agents by partially replacing C and oxygen with both industrial and/or municipal waste, e.g., ASR, rubber tires, plastics, and by-products, e.g., EAF dust and mill scale, while maintaining or improving slag foaming intensity, preserving liquid steel quality and keeping emissions at a low level. The project also aimed to recover valuable metallic components (Fe, Cr, Ni, Mo, Mn) through the co injection of SCCs and metallic waste such as EAF dust and mill scale. ASR was a highly heterogeneous mixture of residual ferrous and non-ferrous metals (5–23 %), plastics (20–49 %), rubber (3–38 %), textile and fiber material (4–45 %), wood (2–5 %), and glass (2–18 %). Two representative types were identified, a light fraction and a heavy fraction with the light fraction being characterized by a high content of C-based materials such as plastic, rubber, textile and PUR foam reaching around 90 % while the metal content was about 4 %. The heavy fraction displayed a lower plastic content of 42 % while metal content was around 16 %. A major part of both fractions consisted of volatile matter, i.e., 72 % for the light fraction and 84.8 % for the heavy fraction, while fixed C was in the range of 3-5 %. The different plastic waste displayed a C content in the range of 80 % and H content higher than anthracite and ranging between 5.5-7.6 % with the highest values of 13 % achieved with PE and XLPE. ASR also contained significantly higher amounts of halogens while rubber displayed higher contents of S, Pb, Cd, Co, Cu and Zn. A specific activity was performed to investigate pre-treatment methods to make materials suitable for application into EAF focusing mainly on the identification of suitable particle sizes and shapes for injection purposes and the development of briquetting/pelletizing solutions for EAF charging. Concerning injections, PU plastics were unsuitable since they tended to compress into a cake and it was not possible to keep them fluid. The uneven particle shape and the typical particle size distribution of PE/XLPE plastics made also them unsuitable for injection since clogging in material dispenser may occur. On the contrary, the C and H contents in the rubber granules made them suitable for replacing anthracite. Moving to charging, ASR needed to be agglomerated to be charged into EAF with the scrape basket and the two main methods available, i.e., briquetting and hot extrusion, proved to be suitable for compacting ASR light fraction. ASR content in the briquettes should not exceed 17-20 % to maintain sufficient mechanical resistance of the briquette while metal residues and coarse fractions must be eliminated from ASR light fraction to make the material extrudable. Plant trials with co injection of EAF-dust and rubber demonstrated good foaming as well as promising results in terms of S content in the steel and foaming capabilities. Further trials with injection of Sicon shredder residue fraction and coarse rubber powder from EoL tires displayed similar performance to coal injection as slag foaming agents. Finally, ASR charging trials showed that proper ASR agglomeration made it suitable for EAF without modifying the main process parameters, e.g., electric energy consumption, methane consumption etc., nor increasing bath carburization.

A more focused study was provided in 3.2.9 and 2.2.27 where packaging plastic wastes injection in EAF was uniquely addressed. A substitution of 30 % of hard coal by plastic grains was investigated in project 3.2.9 through industrial scale tests which demonstrated this successful substitution in every operation. The concept was further dissected in 2.2.27 where a new co injection system for both plastic and lime was developed. Indeed, coal consistently reached the slag-molten metal interface with single-injector whereas usually plastic showed limited penetration often below or close to slag surface

thus not being efficient under industrial conditions. On the contrary the use of the new co-injection system in conjunction with supersonic oxygen lances ensured good penetration in slag and bath providing performance comparable with coal one and improved arc coverage capability. Indeed, the coupling between the solid material and the supersonic oxygen jet occurred on the horizontal plane thus exploiting a side-coupling interaction. The shrouding air of the new injector was able to effectively limit the spreading of the solid jets maintaining their coherence even close to the liquid bath contributing also to the acceleration of solid particles. Thanks to these optimizations, the new injector generated a sufficiently strong and coherent jet to reach and interact with the nearby supersonic oxygen stream achieving an effective coupled oxygen–solid configuration. The injector developed by Tenova was very compact and could be easily installed on existing EAFs with minimal modifications to the water-cooled panels thus facilitating the retrofit of current systems. Furthermore, the dual solid-material capability within a single injector represented a significant innovation in terms of material selection and process control enabling the simultaneous injection of materials with opposite thermal behavior such as lime and plastic. Long-term trial demonstrated that polymer injection did not significantly alter slag quality and EAF process parameters with ACI values remaining within acceptable limits thus indicating effective arc coverage. Several operational difficulties arose during the industrial tests including clogging resulting from the plastic behavior of SCC when excess material accumulated in pipelines, and erosion in bends and branches of the transport lines. These issues were addressed by installing reinforcements and modifying the pipeline layout. Adjustments were also made to the off-gas suction to prevent polymer extraction. Project 3.2.20 always focused on EAF injections providing constructive information on the use of EoL tires granules. The latter seemed to provide a decrease in electric energy consumption thanks to a high calorific value, but also higher S and lower C content in tapped metal. Overall, this alternative C-materials did not negatively affect the process in terms of energy and yields nor the product regarding C and S content but can lead to significant CO_2 reduction resulting in more sustainable production.

Moving to non-biogenic SCCs application in BF, project 2.2.2 evaluated the feasibility of mixed plastic waste from packaging recycling as suitable feedstock for the generation of reducing gases to be exploited in BF. To this aim, a two-step industrial concept including secondary raw materials gasification using recycled top gas as carrier and oxidant at first, and a subsequent conditioning and reforming at 1100 °C with the addition of natural gas to achieve the required quality, was evaluated by equilibrium calculations. This solution allows partial substitution of natural gas by secondary fuels and results in a CO_2 mitigation of about 43 kg/t DRI. Another attempt to exploit plastic wastes in BF was performed within project 2.1.14 devoted to hearth refractories protection by injection of TiO_2-materials to form a TiCN solid high melting scaffold. In particular, plastic waste was mixed with TiO_2-rich waste from chemical industry with high TiO_2 content, i.e., 75 wt.%, to act as additional reductants into the furnace, but the campaign underlined massive problems regarding conveyance mixture. Indeed, plastic waste formed woolen structures which caused choking of the conveying lines and nozzles together with bridging phenomena and arch formation in the hopper. Possible causes of these issues were plastic waste composition or a higher humidity of the agglomerated plastic. The trial proved that the injection of a mixture of plastic wastes and TiO_2-rich powder did not guarantee sufficient operational reliability thus requiring a separate injection of TiO_2-rich powder into BF hearth.

An attempt to exploit post-consumer plastic waste, e.g., polyolefins, PET and PS, as minor coke additives, was also made in 2.2.2. Their effect on coal blends thermoplastic properties was assessed and it was proved that they reduced the maximum fluidity. Different polyolefins caused similar and relatively moderate reductions whereas PET and PS determined a much stronger effects due to their

aromatic structure. Gray–King carbonization tests were also carried out. The results showed that polyolefins were mainly recovered as oils, waxes and light hydrocarbons contributing less than 0.6 % to the solid residue while PET behaved differently increasing both coke and gas yields reducing also coking pressure. Plastic wastes rich in PET and PS also increased coke reactivity while maintaining mechanical strength and porosity. Pilot-scale carbonization confirmed these trends with mixtures richer in PET reducing coking pressure while maintaining coke quality.

Project 2.2.11 was primarily dedicated to the development of an innovative preheating process to clean scrap surface and improve the recyclability of coated scrap (section 5.1.2) by using ASR and pneumatic tires as alternative fuel sources. At first, pre-treatment and refining methods to separate and treat energy containing waste streams were developed. The Volkswagen-SiCon modular process, i.e., an innovative technology to recycle EoL vehicles and transform complex shredder residues into valuable secondary raw materials, was adapted according to the requirement for separation of non-complex, e.g., tyres, and complex fractions, e.g., ASR and WEEE. After that, thermochemical conversion methods to transform these energy containing wastes into valuable resource and to generate suitable fuel for downstream preheating and surface rinsing application was investigated. Pyrolysis and gasification were studied to produce a suitable combustible syngas to be used as fuel in the preheating concepts while the remaining solid residue, e.g., inorganics and metals, could react with Cl entrapping it. An overview of the projects dealing with the different technological solutions involving the use of non-biogenic SCCs is provided in Table 33.

Table 33: Summary of the main projects addressing each technological solution concerning non biogenic SCC use

Technological Solution	Reference Projects
EAF Injection	[2.2.19], [2.2.27], [3.2.9], [3.2.11], [3.2.20]
EAF Briquetting	[2.2.19]
BF	[2.1.14], [2.2.2]
Coke making	[2.2.2]
Syngas production	[2.2.11]

5.1.2 Scrap

Every year, 630 Mtonnes of steel are recycled and this amount is much higher than glass, paper and plastic ones thus making steel the permanent material in a circular economy perspective with a worldwide recycling rate of 85 %. The unrecoverable part of the scrap in Europe is relatively low around 2 % since ferrous scrap recovery through magnetic methods or Eddy currents proved to be quite efficient. The recoverable part of the scrap is recycled as raw material in steel mills to produce new steel with BOF using almost 15 % of scrap in the charge and EAF exploiting almost 100 % of scrap in the charge. Actually, around 60 % of steel production in Europe is made from scrap and this has led to the development of a complete value chain for the valorization of scrap broadening the sources, quality and diversity of the ferrous scrap. Indeed, more than 3500 different types of commercial steel grades are available with a wide variety of chemical compositions in combination with the numerous collection and recycling pre-treatment routes which generate different scrap grades and qualities.

Different alloying elements like Mn, Si, Ni, Mo, V, P, S, can be added to tailor steel mechanical and physio-chemical properties while surface treatments such as galvanizing with Zn and tin plating can be applied to protect steel surface from corrosion. This alloying elements and metallic leftovers from coating layers may become impurities or tramp elements when used in steel products that do not require them. For example, scraps contamination with Cu prevents their use to produce new steel for structural applications since Cu reduces tensile strength and toughness. It must be also considered that some of them like Cu, Sn, Ni, Mo or Co cannot be completely removed from steel during recycling by using existing methods thus making necessary the addition of pure Fe to the molten steel to dilute them and minimize their harmful effects on the new steel. It appears that evident that the numerous sources and forms of scraps require the use of several sorting and preparation techniques to remove contaminants and non-metallic parts to ensure a good quality of the final scrap while recovering valuable metals. Furthermore, accurate control of scrap chemical composition may allow to better tailor the charging phase selecting the most suitable types to produce the steel grades of interest. All these aspects as well as the identification of new reuse applications were conveniently considered in different European projects trying to improve scrap circular economy value chain.

Focusing on scrap preparation and pretreatment, project 3.2.6 tried to make available steel scraps resulting from crawler tracks from civil, military and agricultural fields by applying UHP waterjet technology with operating pressures up to 90,000 psi to separate them from the rubber. The project aimed to exploit a waste stream which until that moment was not treated with any practical or sustainable solution ensuring also the reusability of the EoL rubber. The Recyclatrack © process allowed to recover steel and high-grade ferrous scrap and rubber granulates from end-of-life vehicle crawler tracks to achieve 100 % recycling using low volumes of water. A powerful solution was also proposed in 2.2.11 where a combined scrap preheating and surface cleaning process was developed to remove organic and metallic coatings from the scrap while reaching a high preheating degree. This would allow to obtain a scrap of higher quality while recovering valuable metals, e.g., Zn, in the gas phase. Indeed, a dedicated scrubber and recovery system was derived for the exhaust gases from the preheating system, and the recovery of valuables was performed exploiting the EZINEX process designed to recover valuables from the wet scrubber. The preheating system was also conceived to be fed with the combustible syngas produced through the thermochemical conversion of ASR and granulated tires waste through pyrolysis and gasification. The scrap preheating system was tested on the pilot scale and demonstrated good results and good potential. Another approach to implement IS scenarios focusing on steel products rather than on steelmaking processes was proposed in project 3.2.21 where FlexoFibers Europa developed an innovative and proprietary production process for the recovery of high-quality steel wires from discarded tires to be reused within the construction industry. The process allows a precise and strict control of fiber length thus preventing the occurrence of balling effects within the mixed concrete and enhancing its resistance to flexo-traction and its permeability.

The design and development of new pretreatment solutions is as important as the development of new sensor technologies for monitoring scrap chemical composition and select the most suitable ones according to the steel grades to produce. This was the goal of project 3.2.14 which aimed to develop a new smart LIBS sensor system and two different set-ups of a neutron sensor to characterize metal scrap in terms of chemical composition in steel, Al and Pb plants. Focusing on the steel sector, the

LIBS sensor was tested on site on steel scrap in large containers and it displayed a successful functioning providing accurate results on the composition for most relevant elements. Analogously, a truck sensor using a switchable neutron generator was applied to the bulk analysis of different steel scraps in large containers showing promising results in the analysis of relevant elements. The latter coupled with appropriate statistical method allowed a comprehensive characterization of the scrap types in use enabling industries to use cheaper low-quality scrap while maintaining product quality thus also reducing the reliance on primary raw materials.

5.2 Downstream solutions

5.2.1 Slag

Slags can be considered as queen among downstream wastes since almost 20.7 Mtons of BF slag and 16.3 Mtons of steelworks slag, i.e., 52.3 % BOF slag, 34.9 % EAF slag, and 12.6 % other types of slag such as ladle slag, were produced in Europe in 2018 (135). The need to identify efficient reuse and recycling pathways in an IS perspective for all these different types of slags to reduce landfill disposal, is confirmed by the fact that almost one third of the projects reported above was dedicated to this topic. An overview of the projects assessing the different technological solutions to reuse and recycle the different type of steelmaking slag is provided in Table 34.

Table 34: Summary of the main projects addressing each technological solution for each type of steelmaking slag, i.e., BF, BOF, EAF and ladle

Slag Type	Application	Projects
BF	Construction and Buildings	[2.1.9], [2.2.20]
	Fertilizers and liming agents	[2.1.12]
BOF	Internal Recycling	[2.2.16], [2.2.24]
	Construction and Buildings	[2.1.2], [2.1.9], [3.1.3], [3.2.19]
	Fertilizers and liming agents	[2.1.12], [2.2.12]
	Heat recovery, TES and TEG	[2.2.22]
	Other: wastewater treatment	[2.2.8]
	Other: sealing material	[2.1.8]
	Slag treatment	[2.2.16], [2.2.24], [3.2.4]
EAF	Construction and Buildings	[2.1.9], [3.2.1], [3.2.19]
	Heat recovery, TES and TEG	[3.2.2]
	Other: wastewater treatment	[2.2.8]
	Other: sealing material	[2.1.8]
	Slag treatment	[2.2.14], [3.2.4], [3.2.24]
Ladle	Internal Recycling	[2.1.10], [2.2.22]
	Construction and Buildings	[3.2.1]
	Fertilizers and liming agents	[2.1.12], [2.2.12]
	Other: sealing material	[2.1.8]
	Slag treatment	[2.2.22]

5.2.1.1 Internal reuse and recycling

The first and more intuitive route to undertake when possible is undoubtedly internal reuse and recycling within the steel plant. This solution proved to be particularly interesting for ladle slag which is classified as a high Ca material and whose recycling in EAF was deeply investigated in projects 2.1.10 and 2.2.22 to exploit its desulphurization potential. In particular, project 2.1.10 assessed the possibility to recycle LS in EAF both at the liquid and solid state. Liquid ladle slag recycling up to rates of 80 % proved to be beneficial to reduce primary resources and to exploit slag melting heat to achieve significant energy savings. The procedure did not increase the S content in steel nor induced significant modifications in EAF slag chemical and mineral composition and melting behaviour. The only small drawback was identified in EAF control with an increase of 2 minutes in the tap-to-tap time due to the power off time for LS recycling which resulted in a partial energy loss by heat radiation with additional power consumption ranged of 0-0.4 %. Solid LS recycling was investigated considering different recycling procedures like fines injection, pellets injection and big bags charging and investigating also potential mixture with spent refractories. These procedures demonstrated again a positive effect thus confirming the feasibility of recycling by both pneumatic injection and via big-bags ensuring a partial substitution of lime without detrimental effects on metallurgy. Positive results were obtained also in 2.2.22 where again hot solidified LS were recycled into EAF using a sandwich charging structure. LS and residual steel were collected into a refractory-lined tundish to solidify and were then transported to EAF. The analysis of the resulting EAF slag displayed no negative impact on slag composition and heat potential calculations indicated that a transfer temperature of 1000 °C and a 30 kt/y of LS recycling could theoretically contribute to 14,324 MWh/y of recoverable thermal.

The recover of CaO and MgO containing materials to produce synthetic slag former bricks through cement-free bricks was investigated also in 2.2.21. The bricks were produced using starch as binder and containing other residues like oxy-cutting fines, metallic Fe containing grinding sludge and fines collected at the belt conveyors. The project demonstrated that the use of cement-free residue bricks could ensure the substitution of lime and dolomite together with the recovery of Fe without any negative influence on furnace operation, steel or slag quality. The overall cost of brick production calculated was around 60-105 €/t brick and was offset by the costs for primary lime and dolomite as well as the cost of landfilling.

The internal recycling of BOF slag is hindered by the high P content which can cause P accumulation in steel thus affecting the final quality of the product. Projects 2.2.16 and 2.2.24 tried to solve this problem to recover the valuable content of Fe around 10–25 wt.% and the high levels of calcium oxide. In particular, project 2.2.16 first and 2.2.24 later tried to develop a technically coherent multi-stage process for the selective enrichment of Fe-rich and P-rich phases from BOF slag to create distinct material streams suitable for internal reuse and external applications. The process chain comprised slag pre-selection by Fe content, gravity-driven segregation during slow cooling in an open pit compartment, solid-state oxidation in ambient air utilizing residual slag heat, closed-circuit vertical roller mill grinding with integrated air classification to below 100 µm, and low-intensity drum magnetic separation. This pathway proved to be technically feasible and compatible with existing steelmaking infrastructure. The preliminary results at the laboratory scale on dry magnetic separation showed that grain with size <1 mm did not display any separation effect due to the metal sticking to the slag fraction

while fraction between 1 and 2 mm showed an effective decrease in metal Fe. Air sorting was also assessed but the separation obtained was low while wet-magnetic separation displayed a good separation rate with increased Fe yield in the Fe-rich fraction around 55 %. Fe yield increased to 77 % if the samples were produced with blown oxygen. Sinter pot tests confirmed that the Fe-enriched magnetic phase could be reintroduced into the sintering process without adverse effects on sinter quality or plant productivity. Its valorisation as sinter plant or BF burden component was evaluated positively thanks to its high CaO content around 40–50 % and the good FeO content around 16–20 % which ensured both fluxing and Fe units, partially replacing primary iron ore, manganese ore, and limestone. It was estimated an internal recycling potential of approximately 70,000 t/year of processed slag substituting 35000 t of iron ore annually and delivering estimated savings of around 4 M€ per year.

5.2.1.2 Construction and building applications

Besides internal reuse and recycling other external valorization options in an IS approach vision were considered namely applications in construction and buildings, in agriculture as fertilizers and liming agents, for thermal energy storage, for wastewater treatment and for refractories production. Focusing on the construction and building sector, BF slags are today perceived more as a co-product by the market rather than as a waste. There are two main types of marketed BF slag namely air-cooled and granulated ones. Air-cooled slag is hard and dense thus being suitable as construction aggregate while granulated slag forms sand-sized particles suitable for cementitious material. It was noticed that concretes incorporating granulated slag develop strength more slowly than Portland cement concretes but display better long-term strength and less heat release during hydration. The Slag Cement Association reported that the replacement of Portland with granulated BF slag cement in concrete can save up to 59 % of embodied CO_2 emissions and 42 % of embodied energy required to manufacture concrete and its constituent materials (136).

All these achievements were possible also thanks to projects like 2.1.9 which tried to complete and update existing data on slag environmental compatibility through laboratory and in situ experimental campaign and to develop computer-aided hydro dispersive model to rate the impact of steelmaking slags, i.e., GBF, BOF and EAF slags, on soils and groundwater for road construction. The modelling activity allowed to draw some important conclusion highlighting that the embankment configuration was the most disadvantageous infrastructure compared to road and highways and that crystalline aquifers were the most vulnerable type. Concerning the type of slag, BOF slag was the most disadvantageous one while GBF slag was the most promising generating the lower impact on groundwater. Some studies like 2.2.20 tried also to enhance the proneness of BF slag for construction applications trying to improve the early reactivity and the strength development of GBF. The addition of alkali metals, alkaline earth metals and Al_2O_3 displayed a positive effect without drastic changes while TiO_2 and SiO_2, or ZrO_2, V_2O_5, Cr_2O_3 exerted a negative effect. Furthermore, it was observed that mechanical milling induced substantial rejuvenation of the GBF slag glass network suggesting potential implications for enhancing cementitious reactivity pending validation at industrial milling scales. The addition of $CaCl_2$ promoted an earlier onset and a higher hydration rate which coincided with the formation of AFm phases resulting in increased heat release, faster microstructural development, and

higher compressive strength during the first 7 days. These improvements were associated with accelerated pore refinement while long-term compressive strength remained comparable to systems without $CaCl_2$.

The possibility to exploit BOF slag in roads and buildings construction was also widely investigated in projects 2.1.2, 3.1.3, and 3.1.4. Project 2.1.2 developed an IPBM process in a DC furnace with a hollow electrode to treat fine grained by-products generated within steel plants like BOF slags, EAF dust, BOF and BF-dust and mill scale ensuring a recovery of Zn >99 %, of Cr >95 %, of Ni=100%, of Fe >95 % and of V almost 80 % and the production of cement clinker from low V BOF-slags, and hydraulic binder. Analogously, project 3.1.4 developed a smelting reduction process in a ladle furnace using coke anthracite and FeSi as reducing agent to treat steel slag, dust, fly ash from coal plant, and bottom ash from urban incinerator to produce hot metal to be de phosphorated before recycling, mineral product for Portland cement substitution or as metallurgical powders. Finally, project 3.1.3 investigated the treatment of liquid BOF slag with sand and oxygen injection to improve its volume stability and ensure its application in fields with high quality demands, e.g., aggregates for road construction and asphalt layers or as additive for civil engineering concrete. The treatment allowed to bind the free lime to stable phases thanks to the presence of the SiO_2-rich sand. An attempt was also made using glass cullet and oxygen to introduce the SiO_2-rich materials and bind the free lime using a cheaper material than sand, but the results were not satisfying and need further investigation for potential feasibility.

EAF and ladle slag valorization in construction and building applications was also investigated in project 3.2.1 where the symbiotic materials Eco-Cements and Green Concrete were obtained through slag valorization. Eco-Cements were obtained using two different routes. The first solution was a belite-yeelemite based cements produced using Al saline slags, glass waste, ceramic waste and ladle furnace slag within the raw meal. The second route considered blended cement using ladle slag, glass and ceramic waste materials as mineral additives in Portland cement thus lowering the clinker content in the blended cement and reducing the environmental impacts. Ready mix concrete and autoclaved aerated concrete blocks containing upgraded EAF and ladle furnace slags aggregates were obtained with regards to Green Concrete formulations. The mix concrete was obtained using EAF slag as aggregates and the eco-cement with ceramic, ladle slags and glass as mineral additives whereas the autoclaved aerated concrete blocks were obtained from EAF slag, ladle slag and ceramic waste.

The latest and more disrupting solutions were proposed in project 3.2.19 which tried to couple the recycling of BOF and EAF slag with the capture and use of the CO_2 resulting from process off gases to produce construction materials. At first, the project focused on the development of two different CO_2 capture technologies, namely a porous structured sorbent material and a third-generation liquid amine solvent solution which allowed to obtain a CO_2 purity of 80-99 %. The captured CO_2 was then intended to be used for cement production, and three different concepts were developed. The first concept was a carbon-negative SCM made by CO_2-mediated mechanical activation of steel slags. The second concept concerned CO_2 beneficiation of recycled cement-based construction and demolition waste. The last concept regarded a carbonation clinker created coupling steel slag and cement-based residues. Clinker mixes were optimized at the laboratory and pilot scaled with carbonation clinker

produced with the same performance obtained at the lab scale. Three low carbon construction products were also proposed, i.e., carbon-negative carbonation cured facing bricks and pavers produced by direct carbonation of steel slags, and precast carbonation cured products such as façade panels, and roof tiles made using carbonation clinker and SCMs including eventually carbon fibers.

5.2.1.3 Fertilizers and liming agents

The feasibility of BF and steel slags, i.e., BOF and ladle slag, as fertilizers and liming agents was widely investigated in project 2.1.12 and 2.2.12. The preliminary results obtained in 2.1.12 demonstrated that fertilizers and liming materials produced from BF and steel slags can contribute significantly to a sustainable agriculture improving plant yields with no risk on soil, soil fertility, groundwater and health of men and animals. Soil enrichment in Cr and V seemed to have no negative effects on crop development and soil fertility. These outcomes were of primary importance considering that fine grained slags cannot be used in the building sector and dumping must be avoided. These outcomes were further confirmed and developed in 2.2.12 which focused mainly on BOF and ladle slag. It was demonstrated that Cr and V accumulation into soil occurred only after long periods of slag application and the risk for groundwater pollution was very low since these elements remained confined into the top 30 cm of soil even after 60 years of fertilization. Furthermore, no significant Cr and V uptake was observed in most crops. The project confirmed that slag as fertilizer was as beneficial in increasing crop yield as natural fertilizers.

5.2.1.4 Heat recovery and thermal energy storage (TES)

Slags proved to play a paramount role also in the energy sector displaying a huge potential for heat recovery and as thermoelectric generator (TEG) and thermal energy storage (TES) material. Project 2.2.22 dedicated to the recovery of heat from BOF slags as well as their exploitation to generate electricity while project 3.2.2 focused on the use of steel slag such as EAF slag as TES materials. Heat recovery from BOF slag was performed using the RecHeat convective heat exchanger system considering also downstream material drying via a ModHeat dryer. Two semi-industrial tests were performed and a heat recovery efficiency of 33 % was achieved with a theoretical slag energy content of 1.5 GJ/t. The structure tolerated the thermal and mechanical loading of the slag thus providing a positive proof-of-concept for scale-up. Two industrial tests were also performed and an efficiency of 34.5 % over the effective 3-hour drying window was obtained recovering 720 kWh. Tests with coupled RecHeat and ModHeat dryer systems were also carried out to dry wet sawdust. They confirmed the technical feasibility of drying since the heat recovered was sufficient for continuous industrial drying operations.

TEG panels and air-cooled refractory and pipe-to-pipe panels were also tested to quantify the potential for electricity generation and hot-air production directly from slag pit radiation and conduction. TEG panels installed at slag pit generated 82 W of electrical power upon slag tapping with panel surface temperature at approximately 110 °C and cooling water at 18 °C. It was estimated that the panel was able to produce approximately 300 W at a panel temperature of 200 °C and 500 W at 250 °C and that the total electrical energy generated by a single 0.7 m^2 panel in 24 hours was 1.2 kWh/day. Scaled

to full slag pit coverage 84 m^2 of refractory panels on the lateral walls and 40 m^2 of pipe-to-pipe panels on the pit floor provided a combined system which could deliver approximately 197 kW of hot air at 400 °C sufficient to preheat approximately 2000 kg of ferroalloys per heat to a maximum of 240 °C displacing around 355 MWh/year of electrical energy per machine.

Two different pilot solutions were considered for the use of steel slag as TES. The first one aimed at recovering heat from EAF off gases using low-cost TES system based on steel slag since 30-40 % of the energy consumed in the steel shop was normally lost and discharged into the atmosphere. This solution would provide around 15 % of primary energy as well as a low-cost TES system with an incomparable system storage cost of 5€/kWh. The key points to optimize heat recovery where good thermal and mechanical properties of slag particles over various heating and cooling cycles and an appropriate design of the heat exchanger. The second solution for the use of steel slag as TES aimed at increasing the dispatchability of CSP plant to replace traditional molten salt TES solution limited to a temperature range of 290-550 °C with steel slag with temperatures above 600 °C. Two different pilot plants were constructed, i.e., the first one at DLR facilities using air as HTF and the second one at ENEA using molten salts as HTF. The work performed at DLR confirmed the viability of slag as TES material for CSP applications using air as HTF thanks to the cyclic thermal and mechanical tests used to determine slag resistance. Tests at ENEA confirmed that sintered slag pebbles were compatible with solar salt thus being suitable for packed-bed TES systems in CSP plants using molten salts as HTF.

5.2.1.5 Other applications

Further interesting solutions for slag reuse and recycling were investigated like the one proposed in 2.2.8 where it was evaluated the possibility to apply EAF and BOF slag in small wastewater treatment plants to upgrade P removal. Two demonstration-scale filters were successfully built and operated in France and Germany proving that slag was able to remove P from wastewater in very different treatment environments without any environmental issues. It was also observed that P removal performance varied depending on the design and operation of the system, i.e., batch load, downflow, residence time, wastewater temperature and composition, which affected the rate of CaO-slag dissolution and hence calcium phosphate precipitation. The unique problem identified was the high outlet pH which could be easily solved using CO_2 injection. This solution is extremely interesting considering also the potential reuse of P-saturated slag as fertilizer which magnify the circular economy concept making an industrial by-product of steel industry a reactive material to remove P from wastewater and this wastewater treatment material a liming material and phosphate fertilizer in agriculture.

Another alternative route for slag recycling was proposed in 3.2.2 which investigated the feasibility of FeCr-slag as aggregates in the manufacturing of castable refractory compounds to substitute at least 20 % of virgin materials which would result in a decrease of around 40 % of CO_2 emissions. Preliminary studies were performed using calcium aluminate cement as binder, FeCr slag with a 0-4 mm diameter as aggregates, and JV slag and silica fume powder as fines for castables manufacturing. The recipes investigated displayed comparable cold compressive strength values around 70-90 MPa which were lower than the 130 MPa of commercial reference due to the higher open porosity of 18-22 % against

the 16 % of the commercial reference. Comparable low values were obtained also for thermal expansion and good thermal insulating properties in terms of thermal conductivity, thermal diffusivity and heat capacity were observed for all three recipes showing values even below that of reference material thanks to the higher porosity. These preliminary results confirmed the potential feasibility of FeCr slag use as raw material for refractory production and led to a final selected recipe formulas containing 80 % slag with comparable properties to commercial reference.

Supplementary applications field were evaluated in 2.1.2, 2.1.8 and 3.2.16 where slag feasibility as waste neutralization agent, sealing material, and insulating component was investigated. Project 2.1.2 studied a vitrification process in DC furnace with a hollow electrode to neutralize wastes such as Zn and Pb containing dust and sludges as well as spent noxious refractory, with liquid steel slags to obtain inert products for glass and ceramic industries. Project 2.1.8 evaluated the viability of LS, EAF and BOF slag as alternative sealings solutions obtained from silica gel amended EAF-slag system or with a mixture of LS and BF Sludge with 1:1 ratio. This new potential field of application entails economic and industrial benefits like the evident cost reduction of the sealing systems for in-house landfills by using own by-products and residual materials in substitution to clay. Project 3.2.16 aimed at transforming treated slags into high-value mineral fibers and wool products for thermal and acoustic insulation applications through fiber drawing as sustainable alternative to commercial glass or stone wool.

5.2.1.6 Slag treatments

Besides identifying new industrial sectors to implement IS scenarios, some projects dedicated to the investigation of potential physical and chemical treatments to recover valuable elements contained in the slags or to modify their composition and properties to make them more effective and compatible with the final application. Concerning the recovery of valuable elements, project 3.2.2 tried to extract non-ferrous high added value metals like Cu, Cr, Ni, Zn, Mn from slags using a new selective hydrometallurgical methodology. A multistep process combining physical and chemical treatments was developed to obtain high efficiency in rare earth recovery in terms of yield and purity. Another example is given by project 3.2.24 which aimed to advance hydrogen plasma smelting reduction (HPSR) from TRL 5 to 7. HPSR combines melting and reduction in one step using a hydrogen arc since the ionized hydrogen species can ensure high reduction kinetics while the arc supplies the heat for the endothermic reactions and the melting of the material. The project targeted the valorization of EAF steelmaking residues such as EAF slag and stainless-steel dust as well as various iron ores such as sinter, pellets, and lumps.

Considering the stream which addressed the treatment of slag to make them compatible with the final application, some important examples were already provided in section 5.2.1.1 where it was described the chain of treatments foreseen in projects 2.2.16 and 2.2.24 to decrease the P content in BOF slag and ensure the internal reuse of its Fe-rich phase. As previously explained, the projects allowed to develop a multi-stage process for the selective enrichment of Fe-rich and P-rich phases including slag pre-selection by Fe content, gravity-driven segregation during slow cooling, solid-state oxidation in ambient air utilizing residual slag heat, closed-circuit vertical roller mill grinding with integrated air

classification, and low-intensity drum magnetic separation. Potential applications for the non-magnetic fraction, i.e., the P-rich phase, were also envisaged like construction and buildings and fertilizers in agriculture. The suitability of the non-magnetic BOF slag fraction as SCM or clinker substitute was evaluated after wet magnetic separation, but it displayed a near-inert behaviour. Indeed, the slag fraction contributed in a negligible way to cementitious activity due to the pre-hydration experienced by the slag during the wet magnetic separation. This caused its reactive mineral phases to be consumed prior to cement test leaving a material with no residual hydraulic potential. The inhibition of C2S hydration due to the presence of P is another phenomenon which jeopardized material hydraulic activity in cement constituent. Regarding external valorisation in agriculture, greenhouse pot trials were conducted with sandy "Lavesum" soil and the P-enriched BOF slags were benchmarked against triple superphosphate, and rock phosphate. The BOF slags enriched with sewage sludge ash achieved equivalent yields and P uptake in spring rape compared to triple superphosphate and its neutralizing liming value was also confirmed. Despite these promising results, the agronomic application was blocked by Cr and V concentrations exceeding regulatory thresholds.

It appears evident that Cr is another fundamental element to control and its removal and recovery may extend the range of applications of slag. For example, project 2.2.14 tried to overcome the limited reuse of EAF slag resulting from the concerns over the leaching of potentially hazardous elements such as Cr, Mo, V, and others, often exceeding regulatory limits. The project investigated two slag treatment pathways one at the liquid phase and the after solidification. In the liquid phase, the focus was on modifying slag chemistry to foster the formation of stable mineral phases capable of immobilizing problematic elements before slag solidification. Post-solidification treatments were also studied and included controlled cooling strategies, mechanical processing, and washing techniques to remove or reduce the mobility of contaminants. Ba leaching was reduced by adding silica, e.g., sand, though care is needed to avoid increasing V leaching which could be decreased by adding ladle furnace slag thus increasing Ca content and alkalinity. Al oxide promoted the formation of stable spinel structures that effectively immobilized Cr achieving reductions of 70-90 % in leaching concentrations. Controlled slow cooling reduced the amorphous phase content by approximately 15–30 % enhancing mineral stability. The environmental performance of EAF slags was significantly improved through a combination of metallurgical control and targeted treatment processes, achieving up to 90 % reduction in Cr leaching, 60 % in Ba leaching, and 50 % in V leaching under optimized conditions. Mo and Se leaching could not be mitigated therefore the main option is controlling scrap input. Many efforts to recover Cr were also made in project 3.2.4 where the process developed to recover Cr allowed to achieve Cr yields above 95 % and Cr products with purities greater than 90 %. An initial pretreatment to concentrate Cr in the slag was performed through magnetic and gravity separation. It allowed to increase Cr content from 2.3 to 9 wt.% in stainless steel slag and from 3.1 to 11 wt.% in low carbon slag. Enriched slags were than subjected to conventional and microwave roasting treatments which consisted in heating the slag in a rotary kiln or muffle furnace after mixing them with sodium salts to convert metal compounds into soluble forms recoverable via leaching. Selective leaching was the last step and was performed with a 20 % NaOH addition and 1-hour or more roasting time allowing to obtain for some slag types a Cr removal up to 100 %. The conventional roasting followed by water leaching enabled Cr extraction rates exceeding 95 %, while recoveries of V, Mo, and Nb remained below 10 %.

The projects considered up to now were dedicated to the identification of suitable chemical and physical treatments to recover valuable elements and make slag compatible with the final applications while some other projects were more focused on plant-specific optimization and on the identification of best practices investigating the effect of these process modifications on slag quality. An example is given by project 2.2.4 where three plant-specific optimization routes were designed and. The first route focused on developing an EAF slag conditioning technique through the injection of CaC_2 mixtures as reductant to recover the oxidized Cr from slag. This route was effective for Cr recovery but introduced energy and leaching-related limitations since it altered slag structure thus increasing Cr leaching and making its application in construction and building more complex. Better were the results obtained with the other two approaches which yielded clear reductions in electrical energy and improvements in productivity. In particular, the first route developed an EAF slag conditioning technique through carbon/oxygen injection and FeSi addition to make the slag foamable and recover oxidized Cr from the slag reduction while the second route developed an EAF slag conditioning technique through the coherent-jet injection of Al granules as additive and as chemical heating technique to reduce electrical energy demand.

The last type of treatment considered was dry air granulation which was applied to LS at the tapping point in project 2.2.22. Five dry air granulation campaigns were conducted to produce a vitreous high-value secondary raw material characterized by an average composition of 54.8 wt.% CaO, 18.1 wt.% Al_2O_3, 8.2 wt.% SiO_2. Magnetic fraction separation from granulated material yielded metallic Fe contents of 31 wt.% for carbon steel and 37.4 wt.% for high-alloy steel demonstrating the potential for metal recovery alongside slag valorization.

5.2.1.7 Slag monitoring

From an operational perspective, the development of improved control and monitoring systems is crucial to ensure reliable and consistent data on material and energy flows to properly characterize by-products, manage variability and ensure stable quality. This topic was addressed in relation to slag quality in projects 2.1.10, 2.2.11, and 2.2.26. In particular, project 2.1.11 evaluated the feasibility of slag analysis by LIBS to solve measurement issues of liquid and solid slags in steel plants. LIBS proved to be a suitable online analytic solution to monitor slag chemical composition and the related environmental impact already during the process. In particular, the use of LIBS tried to reduce the Cr content providing economic benefits and ensuring slag feasibility for the construction sector. Cr control would also allow to tailor slag foaming as increasing Cr content determines an increase in slag viscosity. Project 2.2.10 dedicated to slag monitoring to improve deslagging operations through image-based analysis with process models and advisory/online control integration. A coupled CCD camera system with IR was used to carry out the experimental campaign and it was combined with rake position sensing. The online system continuously monitored purging gas flow, slag area and remaining slag amount during ladle deslagging of liquid steel after EAF tapping. The estimation of remaining slag amount relied on operator input for slag height since no online slag thickness measurements method were available, and full automation was limited by missing actuators for rake control. Despite these constraints, both implementations improved deslagging performance, enabled the definition of

optimized deslagging schemes, and provided a pathway towards reproducible operation and yield improvements through data-supported decision making. The implementation of this monitoring system allowed to reduce steel loss by 29 %. Finally, project 2.2.26 developed a novel intelligent system integrating innovative measurement devices to characterize liquid and solid slag with modelling and simulation tools to assess EAF and LF slags compositions and amounts. Two kinds of models were considered and developed namely an off-line physical-based models to support the analysis of the recycling paths and an on-line computationally efficient models based on analytical and data-driven approaches to be implemented at the plants to support slag conditioning to improve metallurgical performance and reusability. Different systems such as on-site physical-based systems, e.g., LIBS and deterministic model, or systems based on electrical impedance sensor and analytical/data-driven approaches were developed to identify the most suitable recycling paths for each slag slot.

5.2.2 Dust

BOF and EAF dust are considered as hazardous and polluting materials due to the presence of heavy metals such as Zn, Pb and Cd and every year almost 30 Mton of BOF dust and 10-15 Mton of EAF dust are produced by steel shops. Possible solutions for their management are landfilling which implies extremely high costs, or the use of the Waelz process to produce high-grade oxide with 60-70 % of Zn to be used in smelters. The latter solution relies strongly on coal and coke to recover Zn thus determining a significant carbon footprint and exacerbating environmental concerns. For all these reasons, many EU research projects were committed to develop new treatments, e.g., pyrometallurgical, hydrometallurgical, and pyro-hydrometallurgical, and new recycling routes, e.g., briquetting and injection, to recover valuable metals such as Zn and Pb to be sold to nonferrous industries as well as the lost Fe to be recycled in the still shop thus making dumping easier. Among the 22 projects identified on this topic, 8 were dedicated to pyrometallurgical treatments, 4 to hydrometallurgical treatments, 5 to combined pyro and hydrometallurgical treatments, 5 to briquetting, 4 to injection and 2 to recover in sinter plant. An overview of the projects dealing with the different technological solutions dedicated to the recovery of EAF, BF, BOF dust is provided in Table 35.

Table 35: Summary of the main projects addressing each technological solution

Technological Solution	Reference Projects
Pyrometallurgical Treatment	[2.1.5], [2.2.5], [2.2.31], [3.1.2], [3.1.4], [3.2.18], [3.2.23], [3.2.24]
Hydrometallurgical Treatment	[2.1.1], [3.1.5], [3.1.6], [3.2.16]
Pyro+ Hydrometallurgical Treatment	[2.1.5], [2.1.6], [2.2.1], [3.1.2], [3.2.26]
Briquetting	[2.1.3], [2.1.4], [2.1.13], [2.2.5], [2.2.21], [2.2.31]
Injection	[2.1.7], [2.2.6], [3.1.1], [3.1.5]
Sinter Plant	[2.1.13], [2.2.3]
Sensors and Monitoring	[2.1.3], [3.1.5]

5.2.2.1 Pyrometallurgical treatments

Focusing on the pyrometallurgical pathway, project 2.1.5 proposed three different thermal solution for dust treatment. The first attempt was made through the agglomerating of BOF and EAF dust and sludges with some reductants to produce briquettes and pellets to be subjected to a high temperature solid state process to volatilize Zn and Pb components which are separated as marketable by-products. The process produces also a solid residue with high metallic Fe content recyclable as DRI or scrap substitute. The general procedure in the rotary hearth furnace included an initial preheating at around 400-600°C for almost 20 minutes before heating to the maximum temperature of 1300 °C with dwell time of 20 minutes. A rapid cooling of 30 °C/min was also applied under a nitrogen atmosphere to limit or avoid reoxidation phenomena. The strong dependency of the process on operating temperature allowed to obtain a versatile route which ensured the treatment of many different dust and sludge mixtures. Despite the slightly lower metallization degree, briquettes performed better than pellets, ensuring a higher consistency in performance. Zn and Pb oxides reduction was also exploited in 3.1.2 where a separation by vaporization was performed after a pre-treatment to remove alkalis and Cl through water leaching. After separation through vaporization, a physical operation of magnetic separation was performed to recover magnetite. The remaining iron oxides, which were partially reduced, were re-oxidized by controlled means to produce magnetite which was again enriched by magnetic separation. A solution like the one of project 2.1.5 is being developed in the ongoing project 2.2.31 where dual-kiln technology operating under reducing conditions enables an effective separation of Pb and Cd from Zn, while producing partially metallized ferrous residues with high metallization degree potentially exploitable into a BF or a smelter. Project 3.2.23 also focused on the use of rotary kiln to treat EAF dust trying to further improve the environmental sustainability of the project and to reduce its carbon footprint by introducing hydrogen as reducing agent. The disruptive technology proposed consisted of a self-sustaining sealed loop that regenerates its own hydrogen. In particular, the hydrogen used to extract Zn and Fe from their oxide is sent in a counter-current flow in the kiln reactor and is then regenerated thanks to the Zn vapor which is captured and re-oxidized using steam in a cooler zone of the furnace. ZnO fine particles formed exit the furnace via the off-gas stream and are recovered in bag-house filters serving as secondary Zn concentrate. This in-situ hydrogen regeneration is a key innovation which allows to drastically reduce the need for fresh hydrogen thus minimizing heat loss and improving both the climate and cost performance of the technology.

The second pyrometallurgical process developed in project 2.1.5 was in a fluidized bed reactor to produce again a fraction with a higher Zn-content for reutilization in smelting plants and a fraction with a higher Fe-content for reutilization in hot metal and steel production. A pneumatic transportation reactor proved to be the most suitable reactor allowing to avoid long residence times of dust particles in the fluidized bed and related phenomena such as particles agglomeration. The results also demonstrated that residence time for an equivalent degree of dezincing could be further reduced applying higher temperatures and increasing CO/CO_2 ratio. The latter must be tailored once a selective reduction is targeted to avoid FeO_n components reduction to metallic iron while ensuring the full conversion of ZnO in Zn. The last pyrometallurgical solution proposed in 2.1.5 concerned EAF dust purification to improve Waelz process efficiency. After a preliminary washing to eliminate Cl and sulphates, EAF dust was pelletized after being agglomerated with other high Fe-content wastes

and calcinated with petroleum coke before undergoing thermal treatment. The latter guarantee the reduction and volatilization of Zn which was then further treated and depurated, while coke and iron fractions were recovered by pellets grinding and magnetic separation. A temperature of 1200 °C and a residence time of 2 hours ensured the production of a ZnO of greater quality together with high quality residues in the pellets characterized by enriched metallic iron which could be conveniently separated by fluorine residue through magnetic separation being fluorine accumulated in the nonmagnetic fraction together with Ca. The non-magnetic fraction could be then repurposed in clinker manufacturing processes, as forming part of the bituminous binder in the asphalt layer in road surfacing and as platform, bases and sub-bases in road construction.

Further interesting solutions were proposed in projects 3.1.4 and 2.2.31and 3.2.24. A technology called ZEWA reactor was proposed in project 3.1.4 to treat not only steel dust, but also steel slag and fly ashes from coal plant and urban incinerator thus targeting the Zero Waste goal for the steel industry. ZEWA reactor consisted in a ladle furnace equipped to carry out smelting reduction operation using coke, anthracite and FeSi as reducing agent to produce hot metal to be phosphorated before recycling, mineral product suitable as Portland cement substitution or as metallurgical powders and Zn enriched dust. Another compelling and alternative pathway is proposed in project 2.2.31 with an oxy-fines treatment of Zn-bearing dust and sludge using an oxygen-fuel burner to reduce zinc oxides with the C present in the feed ensuring Zn separation rates up to 97 % from BF sludge. The remaining Fe-rich melt can be reused in steelmaking. Project 3.2.24 tried to foster a green CO2-free steelmaking route based on H2-plasma technology while promoting the valorization of industrial side streams through the use of advance hydrogen plasma smelting reduction (HPSR). The latter combines melting and reduction in one step using a hydrogen arc since the ionized/atomized hydrogen species can provide high reduction kinetics while the arc supplies the heat for the endothermic reactions and the melting of the material.

Project 2.2.5 focused mainly on EAF stainless steel dust with RecoDust process consisting in a first flash-smelting of steel mill dust under oxidizing conditions to evaporate impurities like Pb, alkalis and halogens, and in a second ICBR step where the pre-melt containing Zn, Fe, Ni, V, W, Cr, Ca, Si, Al in oxidic form was reduced on the inductively heated coke bed. This allowed to collect Fe and other valuable alloying components in the hot metal, while Zn was separated into the off gases as a ZnO product. The reduction rate of Co, Mn, Ni, V, W and Cu was high and above 90 % allowing to obtain a slag almost free from heavy metals and characterized by a very good leaching behavior. The iron alloy produced was rich in C and displayed a high Cu content together with high amount of Cr, i.e., 10.2 %, and Mn, i.e., 7.6. This mixed composition made it difficult to use the Fe alloy as scrap substitute even for high alloyed steels although it contained a lot of expensive alloying elements. Concerning the treatment of off gases from the inductively heated coke bed reactor, a steam reforming process of Zn and CO in the off gases was selected so that the ZnO produced could be sold as valuable raw material to hydrometallurgical Zn winning, while the cold CO and H_2 rich gases from the reforming unit could be used as fuel in the Flash Reactor. The RecoDust route was readdressed also in project 3.2.18 where the pneumatic conveying of residues using reducing gases in the flash reactor confirmed its ability to treat fine-grained residues enabling the separation of ZnO and recovery of Fe-rich fractions. The project ensured Zn volatilization and recovery up to a designed throughput of ~1000 kg/h. The

RecoDust solution would allow to drastically reduce landfill disposal while ensuring the recovery of ZnO and pig iron which represents a revenue stream that could offset operational costs. Furthermore, the inert slag could find application in the construction sector.

5.2.2.2 Hydrometallurgical treatments

Beyond pyrometallurgical treatments, hydrometallurgy was also widely investigated in different EU funded projects as suitable pathway to recover and valorize steel dust. Project 2.1.1 dealt with the hydrometallurgical extraction through electrolysis of pure Zn from EAF dust at the cathode and of Pb and heavy metals in the form of cement. Beyond the non-ferrous metals readdressed to the non-ferrous alloy manufacturing sector, ferrous residues were also obtained and were recycled in EAF to recover Fe. After drying, mixing with reductants and converting everything into pellets, experimental trials in EAF demonstrated the feasibility of this solution since no process or product anomalies were remarked thus ensuring also an internal exploitation of the wastes in a circular economy perspective.

Project 3.1.5 introduced the EZINC process, i.e., EZINEX process, which is a proprietary hydrometallurgical process developed by Engitec Technologies in 1993. The low temperature hydrometallurgical treatment proposed aimed to recover the zinc ferrite from EAF dust with lime to transform it into leachable ZnO in the ammoniacal solution of ammonium chloride (NH_4Cl) according to the reaction $2CaO + (ZnO)(Fe_2O_3) = ZnO_{Free} + Ca_2Fe_2O_5$. This hydrometallurgical route displayed several advantages compared to the pyrometallurgical one thanks to low temperature operations, lower energy consumption and a high flexibility ensuring also the complete elimination of zinc ferrite and production of leachable ZnO with high yields. The process produced also a residue that could be converted in Fe and a saleable slag by melting. This process was further developed in 3.2.16 where the EZINEX® was employed. Parallelly a lab scale hydrometallurgical leaching process was developed by KU Leuven for selective recovery of Zn and Fe fractions through AAC and MSA.

Finally, project 3.1.6 tried to develop another hydrometallurgical cold process to recycle EAF dust by combining mass transfer in an aqueous medium with a mechanical impact to enhance and activate solubilization. This goal was achieved by combining simultaneously mechanical grinding with a high selective leaching which allowed to dissolve the dust and to form a solution from which each specific metal could be removed by selective precipitation or by electrolysis. Leaching results proved that it was possible to obtain an initial separation of Zn and Pb already at the integrated leaching and grinding step because temperatures above 50 °C allowed Zn selective extraction. This effect was further exacerbated using high levels of ammonia hydroxide, i.e., NH_4OH, and low levels of ammonium carbonate, i.e., $(NH_4)_2CO_3$. The project was successful since Zn and Pb recovery seemed to be significantly enhanced using integrated leaching and grinding and electrolysis was selected as final step of the final pilot plant rather than cementation.

5.2.2.3 Coupling of pyrometallurgical and hydrometallurgical treatments

If many interesting solutions were identified among the pyrometallurgical and hydrometallurgical pathways available, many projects tried to couple the advantages resulting from both by proposing combined pyro-hydrometallurgical solutions. Project 2.1.5 addressed the treatment of both BOF and EAF dust proposing a preliminary pyro-metallurgical treatment with a DC plasma-arc furnace and a further purification of the enriched ZnO and PbO fraction with hydrometallurgical and electrolysis treatments. A leaching pre-treatment with water was considered to decrease chlorides and it was followed by a leaching step with H_2SO_4 and a coagulation step with H_2O_2 to oxidize Fe^{+2} to Fe^{+3} and allow the precipitation of Fe^{+3} as iron hydroxide. The next step included Zn solution purification to remove Ni, Co, Cu, and Cd. The treatment was divided in a first stage at 60 °C where Zn powders were added to the leached solution to promote Cu and Cd complete and Ni partial precipitation, followed by filtration and by the second stage performed at 90 °C where $CuSO_4$ and Sb_2O_3 were added with excess of Zn powders to remove Ni, Co and Sb. The purified solution containing Zn was then subjected to electrolysis to recover Zn at th cathode. The results of this project were scale up to the pilot scale in project 2.1.6 where the pyrometallurgical treatment was performed in a single electrode electric arc DC furnace using snorkel feeding and a temperature lower than 1450 °C. The hydrometallurgical procedure remained the same with water washing at 50 °C to remove chlorines, fluorine and alkali, powder leaching with H_2SO_4 and residues rich in Pb, coagulation process for precipitation of $Fe(OH)_3$, cementation of Ni, Cu and Cd 90 °C with $CuSO_4$ and Sb-tartrate as catalysts, electrolysis. After the pilot tests, the concept was further expanded in project 2.2.1 where it was tried to achieve continuous hydrometallurgical treatment at industrial scale which was not achieved in the previous project. Both carbon and stainless-steel dust were considered with 360 t of stainless-steel dust from AST being treated in the plasma arc furnace to obtain 70 t of dry ZnO enriched dust and 100 t of carbon steel dust from ASO being treated at Wealz furnace to obtain almost 20 t of dry ZnO enriched dust. After the pyrometallurgical treatment, hydrometallurgical treatment was developed to reduce and control impurities. Chlorides and fluorides were decreased through water washing of the Zn enriched powders while sulfuric leaching aimed at dissolving the ZnO and zinc ferrite contained in ZnO enriched powders. The resulting suspension was pumped in the filter press to separate the filtered residue composed by $PbSO_4$, $CaSO_4$, Fe_2O_3, SiO_2, and Al_2O_3. The solution was then sent to the coagulant oxidation station to decrease Fe ions in the solution by oxidation from bivalent to trivalent form by means of H_2O_2 and the consequent precipitation as $Fe(OH)_3$. After that, a purification treatment was included to reduce Ni^{++}, Cd^{++} and Cu^{++} to metals and separate them from the solution as cement. The reducing agent selected was fine Zn metallic powder. After this last step, the solution was filtered and stored in tanks for subsequent electrolysis to deposit metallic Zn from the purified solution.

Two further combined solutions were proposed in projects 3.1.2 and 3.2.26. After an initial pretreatment stage to ensure alkalis and Cl removal through dust water leaching, project 3.1.2 proposed a full oxidation of all iron phases to Fe (III) followed by a controlled reduction to produce high amount of magnetite which could be easily separated through magnetic separation. The final residue consisted of concentrated amounts of Pb and Zn which was treated through hydrometallurgy employing NH_4Cl. Project 3.2.26 is an ongoing project which promotes the combination of

pyrometallurgical and hydrometallurgical stages using green H_2 as reducing agent to develop a sustainable valorization route for both Fe-rich and Zn-containing by-products. After a preliminary conditioning of the waste raw materials through agglomeration, a hydrogen based thermal reduction was envisaged followed by the treatment of the wastewater resulting from the H_2 reduction and by the valorization of the Zn contained in the sludges. The process should ensure the production of DRI to be recycled in EAF, ZnO rich concentrates to be marketed in the smelting industry and safe wastewater suitable for disposal or reuse.

5.2.2.4 Briquetting

Apart from the development of new treatments, EU projects dedicated also to the identification of new recycling routes and briquetting proved to be the most popular one. Project 2.1.3 dedicated to the recovery of BOF slurries through two agglomeration techniques, i.e., briquetting and extrusion. The results established that both techniques were useful to transform BOS slurry into hard and durable feedstock for recycling if a suitable moisture control was developed. Despite this, the moisture content of briquettes ensured a higher green strength and easier handleability of the product immediately after production thus making the commercialization of the briquetting route preferable. Furthermore, BOS slurry was mixed with EAF dust and mill scale to achieve the desired Zn content in the briquettes. Trial results showed that slurry diversion for in excess of 60% of the blowing period would be required to optimize the recovery of zinc early in the blow a slurry diversion for in excess of 60% of the blowing period would be required. Project 2.1.4 was entirely dedicated to the briquetting of self-reducing blends made of waste iron oxide mixtures including EAF dust, oily mill scale, and BF and BOF sludge contaminated with oil and grease. In particular, the project aimed to exploit low temperature briquetting to produce self-reducing briquettes to be fed in melting facilities such EAF and cupola furnace. The first attempt was made by blending mill scales, sludges and EAF dust with the reducing agent using molasses as binder. The results highlighted a better response in terms of metallization yield of the briquettes produced with finer grain materials. Furthermore, the addition of K_2CO_3 and Na_2CO_3 proved to be beneficial for metallization thanks to thermal decomposition at 850-900 °C of the carbonates into K_2O, Na_2O and CO_2 and to the following full conversion of CO_2 into CO at temperatures higher than 1000 °C in absence of O_2 according to Boudouard reaction. The industrial trials performed in EAF displayed good results with just a slight increase in electric energy consumption of 0.5 MWh per ton of briquettes loaded due to the supplementary energy necessary for iron oxide reduction in the briquette. Analogously, the percentage of Fe in the liquid slag did not increase significantly in comparison with the reference slag analyses thus proving that the C added to the briquette was sufficient for the reduction reaction. The idea of a cement free brick was recovered in project 2.2.21 where briquettes were produced using starch as binder. Briquettes included CaO and MgO containing materials to produce synthetic slag former bricks as well as oxy-cutting fines, metallic Fe containing grinding sludge and fines collected at the belt conveyors. A microwave preheating system was also developed to ensure a good de-zincing of EAF dust at lower bulk temperature compared to normal thermal treatment and with a higher Zn purity of the dust removed. The chemical composition of EAF dust after microwave heating indicated a Zn reduction of 53.5 % after 10 minutes at 1000 W. An increase in heating time up to 20 minutes ensured an increased Zn removal up to 90.4 %. The use

of cement-free residue bricks produced with starch as binder could ensure the substitution of lime and dolomite together with the recovery of Fe without any negative influence on furnace operation, steel or slag quality. The overall cost of brick production calculated was in the range of 60-105 €/t brick which was mainly due to the need for pre-processing and the amount and cost of the binder. These costs were offset by the costs for primary lime and dolomite as well as the cost of landfilling. A further step forward was made in project 2.2.31 where the briquettes of EAF dust, BF and BOF sludge and reducing agent were manufactured using biochar as renewable reducing agent to minimize CO_2 emissions. This project aimed to produce stable agglomerates with Zn contents above the threshold typically required by Zn refiners, i.e., around 20 %, enabling improved downstream valorization.

The second attempt in project 2.1.4 was made mixing BF and BOF dust and sludge with the reducing agent and using 20 wt.% of Portland cement as binder. The industrial trials in Cupola furnace were performed only with BF sludge and confirmed the feasibility of the recycling process. Similar work was performed in project 2.1.13 where briquetting of BF and BOF dust and mill scale was investigated to obtain a feedstock directly applicable in BF or in sinter plant. Briquetting was performed via vibration compacting press and the best mix investigated included 40 % mill scale, 30 % BF dust which provided part of the C for reduction, 10 % BOF dust and 20 % Portland cement. The BF trials performed using the briquettes as 10 % of the charge highlighted no significant influence on operating behavior, hot metal composition, slag composition and basicity and on BF dust analysis.

Some investigations were carried out also on EAF stainless steel dust in project 2.2.5 using vegetable binders. The optimal briquetting parameters identified were a water content < 3 % and a wheat content < 13 % which ensured a good durability for long time (> 3 months) if stored in a dry environment and the ability to remain at the slag/steel interface. The comparison of the different briquette utilization technologies, i.e., continuous injection and batchwise charging, in the pre-industrial test did not show significant differences from a chemical point of view. Also, energy consumption did not increase significantly, compared with standard melting procedure. It was suggested to introduce briquettes together with the second or/and third bucket so to have better melting conditions.

5.2.2.5 Injection

Another potential recycling route identified was injection which was addressed mainly with reference to EAF (projects 2.1.7, 3.1.1 and 3.1.5) and only to a lower extent to BF (project 2.2.6). The latter was mainly dedicated to the mixing of BF dust and sludge with pulverized coal in a fluidized bed to ensure a homogeneous mixture before proceeding with the injection at BF tuyeres. The use of Al_2O_3 refractories was advised to ensure sufficient abrasion resistance for conveying BF dust and refeed them into BF. Focusing on EAF, project 3.1.1 tried to implement EAF dust recycling into the furnace through injection to enrich the Zn content in the outgoing dust thanks to its high vapor pressure. This solution would allow to recover Fe from the dust thanks to its non-volatile compounds which dissolved in the slag, and to increase the Zn and Pb contents in the dust by evaporation. Zn concentration significantly increased after injection started with enrichment between 4 and 6 wt.%, i.e., from 24.5 wt.% to more than 30 wt.%. This solution also allowed to obtain a significant reduction in total dust amount from almost 17 to almost 12.5 kg/ton of liquid steel. The main drawback lied in the slightly higher energy

consumption necessary to melt the dust and to reduce Zn compounds while no problems related to slag foaming or slag properties were observed thus still ensuring their feasibility as construction material. This solution was also investigated in project 3.1.5 trying to promote ZnO separation from zinc ferrite following equation $ZnO(Fe_2O_3)+C=Fe_{met}+ CO/CO_2+ ZnO_{free}$. In particular, EAF dust was recirculated into EAF by injecting it into the slag foam during the refining period. The dust generated during injection was then collected in a bypass filter and a high Zn content dust with Waelz quality was obtained. This project also addressed a second recycling pathway which included the use of an on-line monitoring system for the continuous analysis of dust composition to ensure an efficient separation of the low and high Zn dust. The dust pre-treated with both recycling routes was again combined with a leaching step using the EZINC process. The leaching of pretreated samples showed a great increase of Zn recovery yield with bypass filter dust displaying values over 90 %. The injection recycling route was also applied to EAF stainless steel dust in project 2.1.7 to improve the recovery of alloying elements from both dust and slag by using reduction agents other than coal. Dust injection did not play any negative effect on chemical and mineralogical composition of tapped slag nor detrimental effects on the metallurgical process, but it was concluded that the reduction phase should be performed very shortly after the blowing of oxygen and the injection of dust to shorten the period with higher concentrations of Cr in the slag which resulted in a stiffer slag. The partial substitution of C with FeSi as reducing agent allowed to improve the recovery of Cr, Mn and Fe, but it was necessary to substitute the injection equipment due to sticking problems resulting from the unsuitable shape of the conveyor-screw. The project also aimed at developing an efficient slag foaming process to improve EAF productivity and increase dust valorization and this was attempted by creating a mixture of 70 % of dust and 30 % of carbon. The results were quite promising since arc voltage was usually decreased from 374 to 324 V during refining to avoid an increase in cooled panels temperature, but dust injection ensured a good slag foaming with a good thermal insulation allowing to keep constant the arc voltage at the highest level thus reducing the power-on time.

5.2.2.6 Recirculation in the sinter plant and online monitoring systems

The last recycling pathway considered concerned BF dust and their recirculation in the sinter plant which was addressed both in project 2.1.13 and project 2.2.3. In particular, project 2.1.13 showed that the recirculation of small amounts of recycling materials did not affect specific sinter productivity and could exert a positive effect on sinter quality in terms of strength, grain size distribution and return of fines thus confirming that the most efficient utilization of fine iron bearing recycling materials was still sintering. Nevertheless, an increase in specific emissions and an adverse alteration of sinter waste gas composition was observed depending on the composition of the recycled materials. Project 2.2.3 proposed a slight variation of the process by exploiting dust and sludge not as fine, but as briquettes in the sintering process. The results obtained were promising with clear benefits compared with untreated dust since a significantly higher C replacement factor close to 1 was achieved while untreated dust required additional C input. In conclusion, pelletizing proved to enhance C utilization stabilizing sinter operation with no negative effects on sinter chemistry or emissions.

Finally, project 2.1.3 was dedicated to the development of online monitoring system to measure dust concentrations in gas streams and improve the effectiveness of the waste gas cleaning system. In particular, a XRF hot end system was proposed to assist early slag formation to reduce iron fume losses allowing also to reduce lime fluxing with evident costs benefits. A XRF cold end was also investigated as useful process control tool for monitoring vessel emissions and composition to develop an effective slurry diversion route by monitoring Zn levels to indicate optimum time to divert slurry stream to maximize recycling potential of low-zinc slurry solids to a sinter plant.

5.2.3 Sludge and Mill Scale

Sludge and mill scale are two further steelmaking wastes characterized by high content of iron and other nonferrous metals worthy of recovering and valorization. Considering this, the investigation of potential routes for sludge and mill scale recycling often walked parallelly to dust one. The main routes investigated in the different projects are summarized in Table 36.

Table 36: Summary of the main projects addressing each technological solution.

Technological Solution	Residue Investigated	Reference Projects
Pyrometallurgical Treatment	Sludge, Mill scale	[2.2.31]
Pyro+ Hydrometallurgical Treatment	Sludge	[3.1.2], [3.2.26]
Briquetting	Sludge, Mill scale	[2.1.4], [2.1.13], [2.2.21], [3.2.18]
Injection	Sludge	[2.2.6]
Sinter Plant	Sludge	[2.1.13], [2.2.3]

5.2.3.1 Briquetting

The main pathway investigated for both sludge and mill scale was briquetting, which was addressed in four different projects, i.e. 2.1.4, 2.1.13, 2.2.21 and 3.2.18. Oily mill-scale and BF and BOF sludge contaminated with oil and grease were considered in project 2.1.4 to produce self-reducing briquettes at low temperatures to be fed in melting facilities such EAF and/or cupola furnace. The project exploited two different binders, i.e., molasses and Portland cement, as already anticipated in section 5.2.2. The solution with molasses as binder allowed to recover both mill scales and sludges by mixing them with the reducing agent, and with K_2CO_3 or Na_2CO_3 which improved metallization thanks to their thermal decomposition at 850-900 °C. The feasibility of this solution was confirmed by industrial trials in EAF which displayed good results without significant influence on process or product quality. The second approach with Portland cement as binder focused only on BF and BOF sludges and the industrial trials performed in cupola furnace confirmed the feasibility of the proposed solution. This solution was further analyzed in project 2.1.13 where BF dust and sludge and mill scale were briquetted via compacting press using again Portland cement as binder. The best mix proved to be the one with 40 % mill scale, 30 % BF dust, 10 % BOF dust and 20 % Portland cement with briquettes displaying good mechanical performance also after reduction tests. In this case, the trials were

performed in BF using 10 % of briquettes in the charge. The results were promising since no significant influence on operating behavior, on hot metal composition, slag composition and basicity and on BF dust analysis was detected. The idea of a cement free brick already embraced in project 2.1.4 with molasses was recovered in project 2.2.21 where briquettes were produced using starch as binder. Briquettes included CaO and MgO containing materials to produce synthetic slag former bricks as well as oxy-cutting fines, metallic Fe containing grinding sludge and fines collected at the belt conveyors. The use of the cement-free residue bricks could ensure the substitution of lime and dolomite together with the recovery of Fe without any negative influence on furnace operation, steel or slag quality. Sludge and mill scale briquetting proved to be necessary also for material recovery in smelting reduction furnace as demonstrated in project 3.2.18 where a plasma reactor operating as high-temperature smelting and reduction furnace was used to produce pig iron, iron-rich oxide fractions, and an inert slag suitable for further valorization. High metallic yields of 75–90 % were achieved with both anthracite and polymer-based briquettes though carburization levels remained a critical parameter. Further optimization of reductant type and ratio is required to meet metallurgical specifications, especially for pig iron C content.

5.2.3.2 Recirculation in the sinter plant

Another relevant pathway for sludge and mill scale recycling was identified in sinter plant which was addressed in projects 2.1.13 and 2.2.3. Projects 2.1.13 demonstrated that the recirculation of small amounts of recycling materials, e.g., BF dust, BF sludge and mill scale, into the sinter plant did not affect significantly sinter productivity and could rather exert a positive effect on sinter quality in terms of strength, grain size distribution and return of fines. Nevertheless, an increase in specific emissions and an adverse alteration of sinter waste gas composition was observed depending on the composition of the recycled materials. Some steps forward were made in project 2.2.3 where the attention was dedicated to dust and sludge trying to optimize sludge pre-processing. In particular, a full-scale pre-processing of BF sludge including hydro cyclone separation, dewatering in a chamber filter press and crushing of filter cake was implemented and allowed about 70 % of the sludge from BF to be recycled. The physical treatment of hydro cyclone separation to upgrade Zn-bearing sludges was also investigated in project 2.2.31 since BF sludge finest particle fractions presented a strong enrichment in Zn thus making it particularly suitable for hydro cyclone-based separation. Sludge recycling through injection was also assessed in project 2.2.6 where BF dust and sludge were mixed with pulverized coal to obtain a homogeneous mixture through fluidized bed to be injected into BF. A Tornado process to dry BF sludge before injection was also developed since variable moisture content proved to reduce BF heating efficiency. Preliminary trials with Tornado process showed that this technology allowed to obtain metallurgical sludge with 20–40% moisture at 40 °C and with an energy consumption of 0.7 kWh/kg of evaporated water. The process simultaneously dried, grinded, classified and modified particle shape improving transport and fluidization behavior.

5.2.3.3 Other recovery and recycling options

The recycling of sludge to recover not only its carbon fraction, but also valuable ferrous and nonferrous metals can pass also through thermal and hydrometallurgical treatments to obtain concentrated amounts of Pb and Zn marketable to smelting reduction industries. Besides the combined pyrometallurgical and hydrometallurgical treatment proposed in project 3.1.2 and 3.2.26 and already summarized in section 5.2.2, an interesting solution was proposed in project 2.2.31 where an oxygen-fuel burner was employed to treat Zn-bearing dust and sludge to reduce zinc oxides with the C present in the feed. This solution should ensure a Zn separation rate up to 97 % from BF sludge and the remaining Fe-rich melt can be reused in steelmaking.

If the recycling of steelmaking sludge is fundamental to recover the valuable metallic component contained inside, the exploitation of organic sludge from pulp and paper mill in steelmaking has clearly a great potential in an industrial symbiosis perspective as proposed in project 4.3. In particular, the project aimed at valorizing pulp & paper residues in metallurgical applications investigating the possibilities of briquetting them together with iron-oxide residues for application in EAF and BF as energy input and reductant material. Since organic sludge is characterized by high moisture and ash content to produce briquettes with metallurgical properties idoneous for BF application, different pretreatment technologies such as drying with a cyclone dryer were considered. Hydrothermal carbonization also proved to be a promising solution for bio-sludge treatment to overcome the high moisture content, low C concentration, and poor mechanical properties of organic sludge. This hydro char was then optimized into briquettes or powder formulations to ensure mechanical integrity and high C yield under steelmaking conditions. Concerning briquetting, different recipes were made by mixing organic sludge, lime containing sludge and iron-oxides waste using cement as binder to enhance strength. The use of hydro char at the pilot-scale for validation was performed. It was observed that it could be added into EAF to replace anthracite as carburizing agents via both top charging and injection, but higher carburization yields were achieved by top-charging compared to the injection into the melt. P and S levels in the melt could be controlled within acceptable ranges and the slag obtained provided favorable properties for the desulphurization, but not good for P removal.

5.2.4 Off gas

Global temperatures increased of about 1.1 °C from 1850 to 2023 with global warming being primarily driven by anthropogenic CO_2 emissions from hard to abate industrial processes and energy production. This led to the pressing need of limiting global temperature rise to well below 2 °C above pre-industrial levels as outlined in international climate agreements. This proved to be extremely challenging considering the actual strong reliance on fossil fuels, but CCUS technologies emerged as critical tools to reduce CO_2 emissions by capturing it directly from off gases and emission sources thus preventing its release into the atmosphere. After capture, CO_2 can be stored in deep geological formations, used to produce chemical, fuels or other products or to enhance oil recovery. It appears evident that the development of efficient and cost-effective capture technologies is of primary importance as well as the identification and advancement of suitable reuse pathways. Considering this, many EU projects

were dedicated to the evolution and improvement of CCS and CCUS technologies as well as to the identification and development of new products which could benefit of CO_2 as feedstock.

Focusing on carbon capture, some projects related to this topic and directly developed in the framework of steelmaking were financed from EU such as projects 4.1 and 4.5 focused on amine scrubbing, i.e., a well-known technology which exploits chemical absorption to bind CO_2 with an amine-based solvent. The most common amine-based solvent is aqueous MEA thanks to its low cost, fast reaction kinetics, and thermal stability. Carbon capture in steel industries was successfully demonstrated in project 4.1 through an amine scrubbing pilot plant whose functioning was optimized through the identification of crucial process parameters that affect separation efficiency and specific regeneration energy. The plant was operated with 30 wt.% of MEA as solvent achieving a separation efficiency of 90 %. During testing, the specific regeneration energy could be lowered to about 3.3 GJ/tCO_2 and the L/G ratio and CO_2 concentration of the flue gas were determined as decisive factors with respect to plant efficiency highlighting that L/G ratio must be adapted to CO_2 content of the flue gas to reach a low specific regeneration energy while elevated CO_2 concentrations lead to a more efficient process. This concept was assessed also in project 4.5 where an amine scrubber pilot plant used was used to capture CO_2 from the industrial off gas of an integrated steel mill power plant. Different solvents, i.e., MEA and aMDEA, were tested to minimize the energy regeneration required and to minimize solvent degradation. Furthermore, an existing pilot plant for catalytic methanation was operated under real industrial conditions using the CO_2 captured from the amine scrubber and the H_2 from the proton exchange membrane electrolyze to produce around 10 Nm^3/h of synthetic natural gas. The latter was fed directly into the power plant gas injection system closing the internal carbon cycle. Project 4.5 also investigated the use of a CO_2 membrane separation unit with reference to the cement industry, and its installation enabled a direct comparison with the amine scrubber. Flue gas passes through a cylindrical membrane module containing spiral-wound membranes to separate CO_2 from the off-gas and the captured CO_2 was converted into formic acid by an in-house electrolysis cell.

Besides its capture, CO_2 and off gases need to be conveniently repurposed as feedstock for new products to close the carbon loop and its application for the synthesis of fuels and chemicals was identified as a compelling solution. A breakthrough solution was proposed in project 3.2.3 where BF and BOF off gases were exploited to produce ethanol through an innovative gas fermentation process based on microbes used as biocatalyst. CO and H_2 were converted into ethanol using a bioreactor with high productivity. Part of the BF gases was conveyed to the PSA gas treatment unit to perform absorption and desorption operations and obtain a pure gas product rich in CO and H_2 without CO_2. The latter was planned to be liquified and storage according to CCSU. Purified CO and H_2 were sent to the bioreactor where the acetogenic bacteria efficiently converted them into valuable products. The mixture coming from the bioreactor contained ethanol, water, microbes, and nutrients and was preliminary treated to separate wet ethanol from microbes, water and nutrients. Wet ethanol was sent to distillation to produce a 98 % dry ethanol which can be used as vehicle fuel, in the production of plastics, as feedstock for pharmaceutics, cosmetics and cleaning products, as well as in the food and beverage industry. The water stream rich in microbes and nutrients was sent to the wastewater treatment unit which consisted of a digester which allowed to recover process water to be reused in

the bioreactor and to produce fertilizers, e.g., struviet, NH_4OH and biogas exploitable to produce power and heat. Another interesting concept to produce methanol from the CO_2 captured from BF gases and the H_2 produced through water electrolysis was proposed in project 3.2.5. The project applied SEWGS technology for CO_2 capture and H_2 production from steelmaking emissions. This hydrogen was combined with renewable H_2 from electrolysis and reacted with captured CO_2 in an emissions-to-liquids unit to produce low-carbon methanol, i.e., a clean-burning fuel, which was successfully used to power a cargo ship between Gothenburg and Kiel proving its potential to reduce fossil fuel demand in shipping. Methanol synthesis through the CO_2 emitted from EAF was also addressed in project 3.2.16 and was validated through a demonstrator at Metlen in Greece.

Besides ethanol and methanol, the synthesis of other important chemicals and fuels such as urea, DME, and formic acid by exploiting steelmaking off gases was largely investigated. Project 3.2.13 dedicated to ammonia and urea synthesis starting from BOF gases after treating them through SEWGS while project 3.2.10 focused on the synthesis of DME and formic acid starting from BF gases. After initial pretreatments with HEPA filter, condensate mitigators, acid gas removal unit to eliminate S components via adsorption on activated carbon, and dehydration unit, BF gases were conveyed to the membrane absorption module where they came in contact with the solvent to ensure CO_2 capture and transfer from the gas to the liquid phase. This module was followed by a stripping process in a distillation unit where the water vapor resulting from the partial evaporation of the solvent in the reboiler encountered the CO_2-rich solvent ensuring CO_2 stripping. The other reagent necessary for both DME and formic acid production was H_2 which was conveniently produced through high temperature electrolysis in SOEC. DME synthesis was investigated considering a packed bed membrane reactor based on carbon molecular sieve membranes using a bifunctional catalyst, i.e., physical mixture of a $CuO/ZnO/Al_2O_3$ catalyst and zeolite. Two different pathways were considered for formic acid production, i.e., catalysis in amines and electrocatalytic reduction. Concerning the catalyst, Pd catalyst performed better with hydrophobic C-based support while Au performed better with hydrophilic support such as Al_2O_3 and TiO_2. Concerning amines, the study focused only on tertiary amines able to create ionic and hydrogen bonds with formic acid since primary and secondary amines bind covalently thus forming a carbamate that cannot be thermally separated. Good results were obtained with trialkyl amines, but the use of this base as both reactant and solvent did not result in observable reaction due to amine protonation, but the use of polar hydrogen-bonding solvents such as diols may solve this problem. Despite this care and many other attentions considered, the catalytic performance during hydrogenation proved to be significantly lower than expected. Moving to electrocatalytic reduction of CO_2 to formic acid, the optimal process parameters included neutral media, ambient pressure and temperature. Different catalysts, e.g., In_2O_3, ZrO_2- In_2O_3, CeO_2- In_2O_3, Co- In_2O_3, Pd- In_2O_3, Cu- In_2O_3, Ni- In_2O_3, Bi_2O_3 and In-Bi-oxide, were synthesized through flame spray pyrolysis and were then dispersed in an ink with Nafion binder and high surface area conductive C particles to be deposited on GDE. Both In and Bi metal oxide nanoparticles showed excellent efficiencies for CO_2 reduction to formate at industrially relevant current densities. Pure Bi_2O_3 and In_2O_3 displayed very high efficiencies up to 90 % with Bi_2O_3 performing slightly better and at lower overpotential.

Fuels and chemicals are not the only products which can include CO_2 since polymers, and construction and building materials can need it as feedstock. Project 3.2.7 focused on the incorporation of CO_2 in PUR polymers developing a single-step catalytic process and a two-step chemical looping process for the conditioning of steel mill gases. This selective catalytic oxidation process was evaluated in a non-adiabatic lab-scale reactor and was successfully upscaled and validated to a semi-industrial scale. Furthermore, a novel catalyst to produce new polyols using CO was identified and developed for the ring-expansion carbonylation of epoxides. Succinic anhydride was identified as the most appropriate intermediate in the CO conversion step and was successfully applied in polyol synthesis. Furthermore, the feasibility of using gas mixtures of CO and CO_2 for the new CO-conversion and the established CO_2-technology was also demonstrated. Different polyol recipes were developed and upscaled. Recticel produced PIR rigid foams using CO based polyols for insulation boards while Megara Resins incorporated the new polyols from CO and CO_2 into waterborne polyurethane dispersions for wood coatings. Interesting results were also achieved in project 3.2.19 where CO_2 was destined to the production of construction and building materials. Two different CO_2 capture technologies were addressed, a 3rd generation liquid amine solvent solution to obtain a CO_2 purity of 80-99 % and a porous structured sorbent material. The CO_2 captured was then employed to produce different cement materials, in particular three different concepts were developed. The first concept concerned a carbonation of clinker created by coupling steel slag and cement-based residues. The second concept was a carbon-negative supplementary cementitious materials made by CO_2-mediated mechanical activation of steel slags. The last concept developed concerned CO_2 beneficiation of recycled cement-based construction and demolition waste. Besides cement products, three low carbon construction products were proposed, i.e., carbon-negative carbonation cured facing bricks and pavers produced by direct carbonation of steel slags and precast carbonation cured products such as façade panels, and roof tiles made using the carbonation clinker and SCMs including eventually carbon fibers.

5.2.5 Refractories

Refractory materials play a crucial role in high-temperature and energy-intensive industries such as steelmaking. Considering the huge effort of this industrial sector to embrace more sustainable practices, e.g., the transition towards H_2-based technologies, it is fundamental that the development of refractory materials grows hand in hand with this transformation to withstand new operational conditions while improving energy efficiency and reducing environmental impact. Furthermore, the identification of suitable reuse and recycling strategies is fundamental to reduce the pressure on landfills while valorizing the added value of these materials when they become a waste. One of the first projects dedicated to the topic was project 2.1.10 which investigated the possibility to recycle mixtures of fines resulting from ladle furnace slag and refractories into EAF both via big bags as fine and after pelletizing and by pneumatic injection after pelletizing. The idea arose from the awareness that these materials are characterized by high CaO and MgO concentrations thus ensuring a high metallurgical potential in primary steelmaking to solve S and P and replace part of the virgin material. The campaign demonstrated that a correct balancing of the mixtures ensured the feasibility of these recycling strategies demonstrating that a partial substitution of lime was possible without detrimental effects in

metallurgy. The project also demonstrated through an industrial scale validation that spent refractories characterized by high MgO contents were suitable substitute for olivine in BOF, BF, and sinter plant.

Project 2.1.10 was focused on the identification of suitable recycling pathways for refractories while project 2.2.23 was dedicated to the reduction of refractory waste with special attention to ladle refractories. An appropriate monitoring system was developed to estimate real degree of refractory consumption, i.e., the remaining thickness, in particular a 3D laser scanner technique with an accuracy higher than 10 mm was coupled with machine learning models and regression analysis. The analysis of the data from the measured thickness revealed different wear rates in the ladle depending on the zone considered distinguishing 4 main areas, i.e., nozzle side transition, nozzle side wall, porous plug side transition, porous plug side wall. Five different predictive models were developed to estimate the remaining useful life of the refractory and the four wear rates in the four different areas of maximum degradation. Laser industrial trials and machine learning models allowed to decrease of 3.5 % the MgO-C waste generated and of 7 % the consumption of new refractories. Two decision algorithms were developed, one for magnesia and one for alumina based refractory wastes.

A huge effort to support the research and innovation in the field of refractory materials was made in project 4.4 where academic and industrial partners had the common aim of training 15 PhD students to provide them with the knowledge and skills necessary to develop sustainable refractory solutions to contribute to the decarbonization of energy-intensive industries. The PhD candidates were selected to cover four key technological areas: efficient use of mineral resources and recycling, microstructure design for increased sustainability, anticipation of hydrogen steelmaking requirements, and enhancement of energy efficiency and durability. The first thesis aimed to feed the loop of LCA to overcome the lack of availability of data within refractory industry with a special focus on magnesia. The work included a description of the production routes available accompanied by an inventory with the main inputs and outputs of the processes. The problem of resource depletion within LCA was also addressed by reviewing the ADP methodology. Finally, magnesia bricks recycling was investigated considering both benefits and challenges and the resulting eco-design recommendations. A second thesis was dedicated to the application of the three pillars of circular economy, i.e., design, slow down and close the loop, to investigate the environmental impact generated by the production and usage of refractory materials in the steelmaking through an LCA perspective. The project aimed at identifying the most sustainable option for both producers and users by optimizing relevant production routes of several refractories in an eco-design perspective, by optimizing the environmental footprint of the refractories once applied in the steel industry and finally integrating recycled materials in the production route. The third thesis was devoted to the evaluation of the life cycle environmental impact of MgO-C refractory bricks used as steel ladle lining to identify potential ecological hotspots and develop strategies to reduce impact.

The fourth thesis focused on castable refractories easier to produce and cheaper to install than conventional bricks. They consist of large-sized aggregates up to 60-80 vol.% bonded together with a finer binder phase which is traditionally calcium aluminate cement and whose content was decreased from 15-30 % up to 1-2.5 % to reduce the water content and attain lower porosity and improved mechanical strength. This approach also allowed to reduce the environmental impact in terms of CO_2

emissions. The work focused on reusing steelmaking V-bearing slag, i.e., BOF slag, as new binder into high alumina castable refractories since they are characterized by high amount of Al_2O_3 and lime thus making it suitable for binding application. The microstructure and mechanical properties obtained with the samples containing 2.5 wt.% of slag in substitution of 2.5 wt.% of CAC were promising as alternative refractory lining. No issues related to the presence of V in the slags were detected since it was not present as free vanadium oxide phase but was entrapped with other oxides to form a spinel phase reducing the risk associated with disposal and management of V-bearing slag.

The fifth thesis investigated the variation of specific key properties, e.g., thermal conductivity, thermal expansion, Young's modulus, of refractory materials under operative conditions for the determination of their recyclability. The main idea was to quantify the evolution of the properties after various cycles compared with the pre-use state to define an appropriate FEM to predict the operative and post-operative conditions of refractory materials and their lifetime. Coupling numerical and empirical characterization should allow to define recyclability and the most convenient recycling routes, i.e., closed-loop and open-loop. If the properties of the waste are close to those of the primary raw materials it is possible to apply the closed-loop case and reprocess the material to reintroduce it in the same production circle. In the open-loop case, the material experiences a significant change in its properties due to the operating conditions thus becoming substantially different from the primary raw materials and needing to be repurposed for other applications as potential substitute of other materials. There are two main issues that still hinder the spread of these solutions. The first one is the lack of information on the thermodynamic evolution of the system during the in-use conditions while the second one concerns the complex mechanical response of refractory materials due to their nonlinear behavior deriving from their heterogeneous nature, the multi-phase composition and the great variety of interactions among the molten metal. Reliable investigations must be carried out through FEM to obtain further and accurate information on thermal and mechanical properties evolution during operative conditions. The PhD project aims exactly at developing an experimentally validated thermomechanical model to predict the evolution of refractories properties during thermal cycling of typical high temperature processes. The results from the mathematical model will be compared with empirical results at different temperatures. Once validated, the model will be exploited as supporting tool in combination with compositional models to foreseen phases and chemicals in the spent refractories, and multi criteria decision approaches based on machine learning to develop a methodology to predict the reuse and recyclability of the various refractory materials. The attention was focused on tundish linings, e.g., isostatically pressed materials Al_2O_3/C and ZrO_2/C and insulating boards such as Vermiculite.

The sixth thesis aimed at improving the microstructure of alumina spinel refractory castables to increase sustainability and thermomechanical performance. Two types of alumina aggregate were considered in the work, i.e., tabular alumina and white fused alumina, since the high amount of evenly distributed closed pores is responsible for the improved thermal shock resistance of tabular alumina compared to white fused alumina. Three different sets of formulations were considered: tabular alumina and white fused alumina-spinel castables, tabular alumina and white fused alumina-spinel micro-castables to disclose the effects of fine aggregates and pure alumina systems of tabular alumina and white fused alumina castables to describe the effect of castables without sintered spinel. The first

heating cycle of the two refractories was quite comparable, but significant differences were detected in the cooling phase with tabular alumina castables ending up with a higher stiffness than white fused alumina. A second thermal cycle was applied to study castables behavior after sintering. Tabular alumina castables displayed a gradual and linear decrease of stiffness from room to high temperatures and a gradual increase during cooling. A small hysteresis was also observed due to crack healing during heating by viscous phases and crack opening during cooling due to the mismatch in thermal expansion coefficient between the matrix and the aggregate. A more significant hysteresis was recorded for white fused alumina castables which exhibited a higher coefficient of thermal expansion mismatch between the aggregates and the matrix inducing intense microcracks into the system when cooled. Concerning micro castables, the only difference in behavior compared to reference materials was observed in the cooling stage where a gradual increase in elastic modulus towards the end of cooling was observed. After the second thermal cycle, both micro castables did not show any sign of hysteresis thus meaning that the number of microcracks developed is relatively low and not significant to impact Young's moduli.

The seventh thesis aimed to develop a numerical tool to correlate the thermomechanical properties and microstructure of refractories by using a discrete element method considering polycrystalline Al_2TiO_5 as reference material for the modelling activity. The developed model aims to guide the controlled introduction of microcracks into the refractory to improve their thermal shock resistance. Indeed, the presence of numerous microcracks within the microstructure can promote a nonlinear macroscopic mechanical response which improves thermal shock resistance. In this perspective, the modelling activity plays a major role enabling the use of microcrack engineering for commercial production.

The eighth and nineth thesis were dedicated to study the effect of H2-bearing atmospheres on refractories. Thesis number eight addressed the effects of H_2 on a burnt phosphate bonded high alumina refractory potentially used in DR reactors thanks to the superior corrosion resistance of Al_2O_3 against hydrogen. High temperature compressive tests at 900 °C highlighted a progressive decrease in compressive strength and maximum strain for increasing hydrogen exposure times due to the microstructural changes arising in the material such as the increase in the glassy phase amount at 900 °C which promotes softening of the structure. This suggests that the compressive behavior at evaluated temperature is not dominated by microcracks but by intergranular weakening. Thesis number nine focused on refractory lining for high-temperature applications with H_2-bearing atmospheres which must be characterized by high density to reduce H_2 diffusion and low SiO_2 content with Al_2O_3 being a suitable candidate. The study demonstrated that phosphate binders could be easily reduced by H_2 thus being discouraged as well as the glassy phase content which must be kept low being more susceptible to H_2 attack.

5.2.6 Others

Besides slag, dust, sludge, off gas and refractories, two other waste downstream of steelmaking processes where identified, i.e., heat and water. In general, waste heat is defined as unintended rejected heat from the plant which can be classified into three temperature levels, i.e., low-grade heat with

temperatures <100 °C, medium-grade heat with temperatures around 100–400 °C and high-grade heat with temperatures >400 °C. Waste heat recovery represents a great opportunity for reducing energy loss in energy intensive industries while simultaneously reducing their carbon footprint and associated GHG. High-grade waste heat can be recovered for high-efficiency applications including steam generation, preheating furnace combustion air to reduce fuel consumption, power generation, direct heating in manufacturing such as drying or smelting operations, high-temperature thermal energy storage to store excess heat for later use in intermittent processes. Medium-grade waste heat can also be exploited through direct reuse in industrial processes such as preheating combustion air, process fluid preheating, drying and evaporation, steam generation, and electricity generation. Low-grade waste heat is more complex to recover and is mainly dedicated to residential or commercial building heating, or drying biomasses or other products.

Considering the great value of this waste, some EU funded projects in the steelmaking sector focused on the topic such as project 3.2.20 which developed a novel ceramic recuperator for modular regenerative and alternative heating to increase in-process heat recovery from off-gases and maximize slag latent heat exploitation. The project also proposed a flexible distributed control solution based on model predictive control to manage the different heat sources and capacities in electric steelmaking. Waste heat recovery was also addressed in project 3.2.12 with not direct reference to the steelmaking sector, but demonstrating the transferability and cross sectoral nature of the solutions proposed. The pilot developed demonstrated the feasibility of recovering the low-grade waste heat and the CO_2 contained in the flue gases of a pulp and paper production facility in a nearby greenhouse. Indeed, the CO_2 contained in the waste gases could be exploited in the greenhouse application for plant enrichment. The need to use low-grade heat arouse from the previous sale of all higher-grade heat to district heat which is a widespread practice in Sweden. Heat recycling must be designed for a 45-55°C supply and 25°C return to achieve the required capacity. Harmful substances such as NO_x harmful to plants and CO harmful to humans must be removed to use the CO_2 from the pulp and paper plant.

Another important downstream source to consider is wastewater which was deeply investigated in project 3.2.22 where a wide range of innovative solutions, including advanced membrane systems such as nanostructured and biomimetic membranes, electrochemical processes with functionalized electrodes, selective adsorption materials such as MOF-based adsorbents, hybrid biological treatments, advanced oxidation technologies, and energy recovery concepts were tested on a laboratory scale using synthetic wastewater representative of the three targeted industrial sectors. These technologies demonstrated strong potential in terms of water recovery, energy efficiency, selective solute separation, and pollutant degradation. In parallel, the project advanced its modelling and optimization activities by developing comprehensive physical and data-driven models tailored to the selected industrial processes. These models can be used for scenario analysis and to optimize energy, chemical, and material consumption and its results directly feed into the decision support tool. Significant steps were also taken in monitoring innovation by developing new hardware and software tools for water quality monitoring which pave the way for more reliable process control and improved plant operation.

List of Figures

Figure 1: Hot end and cold end XRF traces, and scrubber pressure drops for two particular trials performed at Llanwern plant..... 17
Figure 2: Schematization of the test field (A) and practical example of the sealing layer deposition procedure. (16)..... 40
Figure 3: Soil profiles used in the 12 different test fields (16)..... 41
Figure 4: Schematic diagram of the instrumental set-up used with the Galilean telescope..... 60
Figure 5: Schematic diagram of the instrumental set-up used with fiber optics..... 62
Figure 6: Schematic diagram of the instrumental set-up used by University of Patras..... 64
Figure 7: Flow diagram of the hydrometallurgical treatment..... 92
Figure 8: Sequence of the slag-carbon-reaction with different carbonaceous materials as a function of temperature..... 127
Figure 9: Comparison of steel and slag analysis of standard and biochar charges measured at DEW..... 128
Figure 10: Calculated flame temperature for natural gas and syngas burning (A) and comparison of efficiency between syngas and natural gas (B)..... 130
Figure 11: Basket charging schedule used to perform experimental BF trial..... 140
Figure 12: Example of images from deslagging operations at Saarschmiede recorded with both a CCD camera and an IR camera..... 145
Figure 13: Strategy used by the image analysis software to estimate deslagging efficiency at Saarschmiede..... 146
Figure 14: Guidelines developed for EAF slag management..... 167
Figure 15: Schematization of the dimensioned torrefaction plant..... 188
Figure 16: Simulation of biochar price assuming onsite production and three different prices for biomass..... 188
Figure 17: Comparison of costs of anthracite and char..... 189
Figure 18: FeMnC filter dust agglomerates with (A), without (B) binder and samples of series A and B after the drop test (C) (57)..... 201
Figure 19: Example of the procedure followed and of the results obtained with the ladle refractory thickness measurement through laser..... 209
Figure 20: Nonselective waste gas recirculation (NS WGR) configuration..... 215
Figure 21: Fuel Gas injection configuration..... 216
Figure 22: Hot fumes injection –VeLoSint process..... 216
Figure 23: 2-phase VeLoSint layout..... 217
Figure 24: Sketch of Feralpi EAF with oxygen/solid material injection point. Injection point 1 and 2 were the ones used for coal/plastic injection while injection point 3 was the oxygen-lime injector coupled on the horizontal plane with injection point 2..... 224
Figure 25: Brief schematization of ZEWA process including input materials and output products (73)..... 247

Figure 26: Schematization of the LF ZEWA reactor 248
Figure 27: PI-flowcharts for the leach grinding (A) and precipitation (B) processes 252
Figure 28: Final design of the REDILP process (A) and relative schematization of its PI (B) 255
Figure 29: Secondary raw materials reclaimed in the framework of the FISSAC project and the resulting innovative materials and construction products produced 258
Figure 30: FISSAC concept 258
Figure 31: Precast Concrete Elements 259
Figure 32: Overall schematization of the cross-sectorial approach used in the RESLAG project 261
Figure 33: Scheme summarizing the main constituents of the STEELANOL process (A) and picture of the STEELANOL plant constructed at at ArcelorMittal steel plant in Ghent, Belgium (B). 265
Figure 34: Diagram summarizing the main objectives of the CHROMIC project 266
Figure 35: Integrated flow sheet with conventional roasting, solvent extraction and electrocoagulation for chromite ore processing residue slag. 268
Figure 36: Schematic diagram of the FReSME method 270
Figure 37: Schematic diagram of the reference process 270
Figure 38: Recyclatrack © process plant, recycled products, i.e., the steel components and rubber powders and schematization of the crawler track component to recycle. 273
Figure 39: Main CO and CO_2 technologies analyzed and developed within the Carbon4PUR project 274
Figure 40: Schematization of the Torero workflow (A) and Torero plant built at ArcelorMittal (B) 278
Figure 41: Block diagram summarizing the BF gases pretreatment and the CO_2 capture units of the C2FUEL project 282
Figure 42: Schematization of the collaborative scheme for industrial waste exchange and valorization between the four companies 293
Figure 43: Schematization of the industrial symbiotic approach proposed by the INITIATE project 295
Figure 44: Comparison between INITIATE approach and reference process. 296
Figure 45: Schematic diagram of SEWGS process 297
Figure 46: CO_2 avoidance and SPECCA for reference and INITIATE cases as a function of the electricity CO_2 footprint 297
Figure 47: Cost of CO_2 avoided for reference and INITIATE cases as a function of the electricity and natural gas prices 298
Figure 48: Overview of the key costs and key benefits for the implementation of the INITIATE concept. 299
Figure 49: Schematization of the ReMFra project (105) 321
Figure 50: Simplified scheme of the plasma reactor-based pyrometallurgical process, including the input and output streams (106) 322
Figure 51: RecoDust pilot plant established at the Chair of Thermal Processing Technology (107). 322
Figure 52: Representation of the Carbon4Minerals concept with the 8 industrial pilots foreseen. 328
Figure 53: GreenHeatEAF overall concept 329
Figure 54: Sample of short steel FlexoFibers (A) and FlexoFibers embedded in the concrete matrix (B) (111) 335

Figure 55: Flowsheet of the Dust2value project with some insights into the main inputs and outcomes of the Dust2Value process compared to the traditional Waelz process 341
Figure 56: Carbon-Cycle Economy Demonstration 347
Figure 57: Amine scrubber at Voestalpine/K1-MET power plant (Linz) and principal flowsheet 348
Figure 58: Heat duty variation, off-gas=70 m^3/h, CO2 off-gas=25 vol.%, L/G=5, pDES=1.8 bar, MEA 349
Figure 59: Effect of L/G variation and CO2-concentration on specific regeneration energy 349
Figure 60: Schematization of the whole chain foreseen by the USS2030 project. 351
Figure 61: Overview of the plant facility foreseen by the project. 352
Figure 62: Schematic diagram of the procedures of briquettes production and the equipment used 355
Figure 63: Effect of hydrothermal carbonization on organic sludge drying behavior 356
Figure 64: Color change experienced by the bricks after 100% H_2 exposure at different temperatures (134) 374
Figure 65: Comparison of specific regeneration energy with aMDEA (a) and MEA (b) at 90 % separation efficiency 376
Figure 66: Close-up of the electrolytic cell for CO_2 conversion into formic acid 376
Figure 67: CO_2 conversion and CH_4 production rate as a function of oil bath temperature at 4 and 10 bar. 377

List of Tables

Table 1: Configurations tested in the typical cases modelling 50
Table 2: Chemical analysis of the fertilizer used in Austrian Fields 71
Table 3: Composition of the mixtures used for the technical scale investigation expressed in wt.% . 75
Table 4: Composition of the blends and the reference materials considered in the preliminary campaign 87
Table 5: Reducing gas requirements 96
Table 6: Cost allocation example for the CaC_2 injection route at Acroni. 108
Table 7: Comparison of the standard practice with the practices of processes A, B and C at Gerdau Sidenor 109
Table 8: Comparison of the production cost (€/t liquid steel) of the standard practice with the cost of processes A, B and C at Gerdau Sidenor 109
Table 9: Chemical and physical properties of the char produced after test at 500°C for 700s of the four biomasses 125
Table 10: Composition (%) and LHV of the syngas produced as a function of temperature, for mischantus 125
Table 11: Main characteristics of the EAFs of the industrial partners participating to the project 128
Table 12: Main parameters for selecting slag for P removal in wastewater. 131
Table 13: Comparison of slag filter and coagulation-flocculation for P removal 135
Table 14: Physical and chemical properties of the different carbon materials considered 138
Table 15: Composition of the four recipes selected for the next step of the agglomeration trials... 139
Table 16: Average BF-data from DK for Reference periods and Trials 142
Table 17: Summary of Cr and V composition in soil before and after 3 years of fertilization. 157
Table 18: Average yield of selected crops after 3 years of fertilization (dt dry matter/ha) 158
Table 19: Recipes of five different briquettes whose thermal and reducing behavior were investigated through TGA-MS (58) 202
Table 20: Dissolution test results 222
Table 21: Trials to test SCC behavior in EAF 225
Table 22:Material streams for the different injectors of injection point 2 for the two configurations analyzed 225
Table 23: Fixed C, volatiles and ashes content of the four biowastes selected for the pilot campaign 233
Table 24 :Main test conditions and outcomes of the laboratory-scale carburization tests performed with the four bio coals and their mixtures with anthracite 234
Table 25: Ash and P content of the four biowastes considered 236
Table 26: Main characteristic of hydro char after being treated through pyrolysis at 400 and 600 °C 236
Table 27: Main characteristic of the briquettes produced with the hydro char and the different binders 237

Table 28: Main outcomes resulting from slag foaming and carburization tests performed with both pristine and pyrolyzed hydro char 237
Table 29: Proximate and ultimate analysis and macro and micro elemental analysis of the eight biowastes considered 309
Table 30: Fe and Zn of the feedstock and both RecoDust products, the RDS and the CZO 325
Table 31: Main oxide contained in the chemical composition of the bricks under investigation 373
Table 32: Summary of the main projects addressing each technological solution concerning biogenic SCC use 383
Table 33: Summary of the main projects addressing each technological solution concerning non biogenic SCC use 386
Table 34: Summary of the main projects addressing each technological solution for each type of steelmaking slag, i.e., BF, BOF, EAF and ladle 388
Table 35: Summary of the main projects addressing each technological solution 397
Table 36: Summary of the main projects addressing each technological solution. 405

List of acronyms and abbreviations

Acronym	Full Name
AAC	Ammonia-Ammonium Carbonate
AAS	Atomic Absorption Spectroscopy
ACI	Acoustic Cover Index
ACM	Alternative Carbon Material
ACR+	Association of Cities and Regions for Sustainable Resource Management
AdI	Acciaierie d'Italia
ADMIRIS	Advanced Minerals and Recycling Industrial Solutions
ADP	Abiotic Depletion Potential
AGAM	Acoustic GAs-Measurement
AGC	Asahi Glass Company
AGD	Agricultural Digestate
AGES	Österreichische Agentur für Gesundheit und Ernährungssicherheit GmbH
AGW	Agricultural Waste
AI	Artificial Intelligence
AIMEN	Asociación de Investigación Metalúrgica del Noroeste
aMDEA	activated Methyldiethanolamine
AOD	Argon Oxygen Decarburization
ARC	Austrian Research Centers
ASR	Automotive Shredder Residue
AST	Acciai Speciali Terni
AW	Available Soil Water
BAM	Bundesanstalt für Materialforschung
BAT	Best Available Techniques
BET	Brunauer-Emmett-Teller
BF	Blast Furnace
BFI	Verein Deutscher Eisenhüttenleute
B.I.	Basicity Index
BLW	Bundesamt und Forschungszentrum für Landwirtschaft
BOF	Basic Oxygen Furnace
BOS	Basic Oxygen Steel
BRGM	Bureau de Recherches Geologiques et Minieres
BRRC	Belgian Road Research Center
BSE	Back Scattered Electron
BTD	Breuer Technical Development

CAC	Calcium Aluminate Cement
CAPEX	Capital Expenditures
CCD	Charge-coupled device
CCS	Cold Crushing Strength
CCU	Carbon Capture & Usage
CCUS	Carbon Capture Usage and Storage
CE	Conformité Européenne
CEA	Commissariat à l'Énergie Atomique et aux Énergies Alternatives
CENIM	Centro Nacional de Investigaciones Metalúrgicas
CER	Catalogo Europeo dei Rifiuti
CETIM	Centro Tecnológico de Investigación Multisectorial
CFD	Computational Fluid Dynamics
CHP	Combined Heat and Power
CIC EnergiGUNE	Centro de Investigacion Cooperativa de Energias Alternativas
CIRCE	Centro de investigacion de recursos y consumos energeticos
CMC	Carboxymethylcellulose
CNRS	Centre National de la Recherche Scientifique
CPM	Condensable Particulate Matter
CREE	Centre de Recherches et d'Etudes Europeen
CRI	Coke Reactivity Index
CRM	Centre de Recherches Metallurgiques
CSIC	Consejo Superior de Investigaciones Científicas
CSM	Centro Sviluppo Materiali
CSP	Concentrated Solar Power
CSR	Post-reaction strength
DAC	Direct Air Capture
DBFZ	Deutsches Biomasseforschungszentrum gemeinnützige
DC	Direct Current
DDS	Det Danske Stalvalsevaerk
DECHEMA	Deutsche Gesellschaft für chemisches Apparatewesen
DEM	Discrete Element Method
DENS	Dutch Energy Solutions
DEW	Deutsche Edelstahlwerke
DG	Directorate General
DLR	Deutsches Zentrum für Luft- und Raumfahrt
DME	Dimethylether
DMLP	Deep Multi-Layer Perceptron
DOM	Dissolved Organic Matter
DRI	Direct Reduced Iron
DSC	Differential Scanning Calorimetry
DSF	Demonstration-Scale Filter
DSU	Gesellschaft für Dienstleistungen und Umwelttechnik mbH & Co.
DTA	Differential Thermal Analysis

DTG	Derivative Thermogravimetry
DTU	Danmarks Tekniske Universitet
EAF	Electric Arc Furnace
EBF	Electric Blast Furnace
ECSC	European Coal and Steel Community
EDXS	Energy Dispersive X-ray Spectrometry
EEIP	Energy Efficiency in Industrial Processes
EGA	Evolved Gas Analysis
EN	European Standards
ENEA	Agenzia nazionale per le nuove tecnologie, l'energia e lo sviluppo economico sostenibile
ENSAM	École Supérieure Nationale d'Arts et Métiers
EoL	End-of-Life
EPMA	Electron Probe MicroAnalyzer
ESTEP	European Steel Technology Platform
ETH	Eidgenössische Technische Hochschule
ETS	Emissions Trading System
EU	European Union
EuPC	European Plastics Converters
FA	Formic Acid
FAU	Friedrich-Alexander-Universität
FEhS	Forschungsgemainschaft Eisenhuttenschlacken
FEM	Finite Element Model
FENO	Ferriere Nord
FGF	Forschungsgemeinschaft Feuerfest
FIRE	Federation for International Refractory Research and Education
FMECA	Failure Mode, Effects, and Criticality Analysis
FOAK	First-Of-A-Kind
FP	Framework Program
FTC	Freezing/Thawing Cycles
GBFS	Granulated Blast Furnace Slag
GCL	Geosynthetic Clay Liner
GDE	Gas Diffusion Electrode
GDP	Gross Domestic Product
GGBS	Ground Granulated Blast furnace Slag
GHG	Greenhouse Gases
GHSV	Gas Hourly Space Velocity
GMMSA	GENIKI METALLEUTIKI KAI METALLOURGIKI ANONIMI ETAIRIA
GMSFEMWATER	Groundwater Modelling System – Finite Element Water
GWP	Global Warming Potential
HDPE	High-Density Polyethylene
HELP	Hydrologic Evaluation of Landfill Performance
HEPA	High Efficiency Particulate Air

HHV	Higher Heating Value
HNET	Hybridnet
HPSR	Hydrogen plasma smelting reduction
HRC	Hot Rolled Coil
HRTv	Void Hydraulic Retention Time
HTF	Heat Transfer Fluid
HZDR	Helmholtz-Zentrum Dresden-Rossendorf
I3P	Società per la Gestione dell'Incubatore d'Impresa del Politecnico di Torino
ICBR	Inductively heated Coke Bed Reactor
ICCS	Erevnitiko Panepistimiako Institouto Systimaton Epikoinonion kai Ypologiston
ICPC	Institute of Chemical Processing of Coal
ICP-MS	Inductively Coupled Plasma-Mass Spectrometry
ICP-OES	Inductively Coupled Plasma Optical Emission Spectroscopy
IGAS	Innovative Gesellschaft fur Analytishen Service und Handel
IGP	Internal Gas Pressure
IKMIB	İstanbul Kimyevi Maddeler ve Mamulleri İhracatçıları Birliği
ILG	Integrated Leaching and Grinding
IMA-Europe	Industrial Minerals Association-Europe
IMMIB	Istanbul Maden Ve Metaller Ihracatci Birlkleri
IPBM	In-Plant By-product Melting
IR	Infrared
IRSID	Institut de Recherches de la Siderurgie Francaise
IS	Industrial Symbiosis
ISQ	Instituto de Soldadura e Qualidade
KEP	Krupp Edelstahl Profile
KPI	Key Performance Indicator
KTH	Kungliga Tekniska högskolan
KU	Katholieke Universiteit
LCA	Life Cycle Assessment
LCC	Life Cycle Costing
LCE	Life Cycle Engineering
LCI	Life Cycle Inventory
LCIA	Life Cycle Impact Assessment
LCPC	Laboratoire central des ponts et chaussées
LCV	Low Calorific Value
LD	Linz-Donawitz
LDPE	Low-density polyethylene
LECES	Laboratoire D'Etude et de Controle de L'Environment Siderurgique
LF	Ladle Furnace
LHV	Lower Heating Value
LIBS	Laser-Induced-Breakdown-Spectroscopy
LKAB	Luossavaara-Kiirunavaara Aktiebolag
LLV	Leaching Limit Value

LOI	Loss on Ignition
L/S	Liquid/Solid
LS	Ladle Slag
M.A.L.	Metallbau Anlagenservice – Leitungsbau
MARTHE	Modélisation d'Aquifère par un maillage Rectangulaire en régime Transitoire pour le calcul Hydrodynamique des Ecoulements
MASEN	Moroccan Agency for Sustainable Energy
MEA	Monoethanolamine
MB	Mass Balance
MEFOS	Foundation for Metallurgical Research
MFG	Metall- und Ferrolegierungsgesellschaft
MISP	Modèle d'Impact sur les nappes Souterraines
MMHF	Model-Driven Mobile HMI Framework
MP-AES	Microwave Plasma Atomic Emission Spectroscopy
MPBO	Magnesium-rich Pelletized Blast Furnace Olivine
MSA	Methanesulfonic Acid
MSCA	Marie Skłodowska-Curie Actions
MSW	Municipal Solid Waste
MWO	Moveable-Wall Oven
NCBJ	Narodowe Centrum Badań Jądrowych
NDT	Non-Destructive Technique
NIC	Kemijski inštitut-National Institute of Chemistry
NMR	Nuclear magnetic resonance
NPV	Net Present Value
NS WGR	Nonselective waste gas recirculation
NTNU	Norges teknisk-naturvitenskapelige universitet
NUST	National University of Sciences & Technology
OFSM	Optical Foaming Slag Management System
OPEX	Operating Expenditure
OFMSW	Organic Fraction of Municipal Solid Waste
OVAM	Openbare Vlaamse Afvalstoffenmaatschappij
OVGU	Otto von Guericke University Magdeburg
PA	Polyamide
PAH	Polycyclic Aromatic Hydrocarbon
PBMR	Packed Bed Membrane Reactor
PBR	Packed Bed Reactor
PCB	Polychlorinated Biphenyls
PCDD/Fs	Polychlorinated Dibenzo-p-Dioxins/Dibenzofurans
PDMFC	Projecto Desenvolvimento Manutenção Formação e Consultadoria
PE	Polyethylene
PEG	Polyethylenglycol
PEGSA	Polyol based on succinic anhydride – glycol
PEGSAEO	Polyol based on succinic anhydride – ethylene oxide

PET	Polyethylene terephthalate
PGNAA	Prompt gamma neutron activation analysis
PhD	Philosophae Doctor
PI	Process Integration
PIR	Polyisocyanurate
PLC	Process Logic Control
PLEFFIC	PLuie EFFICace
PP	Polypropylene
PS	Polystyrene
PSA	Pressure Swing Absorption
PU	Polyurethane
PVC	Polyvinyl chloride
QSr	Quimica del Estroncio
RE-CORD	Renewable Energy Consortium for Research and Demonstration
RFCS	Research Fund for Coal and Steel
RH	Relative Humidity
RINA	Registro Italiano Navale
RISE	Research Institutes of Sweden
RSD	Relative Standard Deviation
RTD	Residence Time Distribution
RWTH	Rheinisch-Westfälische Technische Hochschule
SBR	Saturable-Bragg-Reflector
SCC	Secondary Carbon Carriers
SCM	Supplementary Cementitious Materials
SEM	Scanning Electron Microscope
SEWGS	Sorption Enhanced Water-Gas Shift
SME	Scrap Metal
SOEC	Solid Oxide Electrolysis Cells
SPECCA	Specific primary energy consumption per unit of CO_2
SS	Sewage Sludge
SSRR	Submerged Slag Revolving Reactor
SSSA	Scuola superiore di studi universitari e di perfezionamento Sant'Anna
STA	Simultaneous Thermal Analysis
SWIM	Soil Water Infiltration and Movement
TCKI	Stichting Technisch Centrum voor de Keramische Industrie
TCLP	Toxicity Characteristic Leaching Procedure
TecMinho	Associaçao Universidade Empresa P/o Desenvolvimento
TEG	ThermoElectric Generator
TES	Thermal Energy Storage
TGA	Thermogravimetric Analysis
THD	Total Harmonic Distortion
TKS	Thyssen-Krupp Stahl
TNO	Nederlandse Organisatie voor toegepast-natuurwetenschappelijk Onderzoek

TRL	Technology Readiness Level
TRZT	Thermal Reserve Zone Temperature
TTL	Transistor–Transistor Logic
TU	Technical University
TU/e	Technische Universiteit Eindhoven
TUC	Technische Universitet Clausthal
TUK	Technicka Univerzita v Kosiciach
TUPRAS	Turkiye Petrol Rafinerileri Anonim Sirketi
UHP	Ultra-High Pressure
UNE	Asociación Española de Normalización
USI	Ugine-Savoie Imphy
VASL	Voest-alpine Stahl Linz
VDEh	Verein Deutscher Eisenhüttenleute
VIM	Vacuum Induction Melting
VITO	Vlaamse Instelling voor Technologisch Onderzoek
VOC	Volatile Organic Carbon
VOD	Vacuum Oxygen Decarburization
VRM	Vertical Roller Mills
WDF	Waste Derived Fuel
WDS	Wavelength-Dispersive Spectrometry
WDX	Wavelength-dispersive X-ray
WEEE	Waste of Electrical and Electronic Equipment
WGS	Water Gas Shift
WP	Work Package
WWTP	WasteWater Treatment Plants
XLPE	Cross-Linked Polyethylene
XRD	X-ray Diffraction
XRF	X-ray Fluorescence
ZEWA	Zero Waste

References

1. E. Burström, G. Ye, J. Piret, T. Cimarelli, M. Kühn. *The in-plant by-product melting.* s.l. : European Commision, 2002. EUR 20068.

2. *Improvement of Continuous.* Riboud, P.V., et al. pages 859-866, s.l. : Fachberichte Hüttenpraxis Metallweiterverarbeitung, 1981, Vol. 19.

3. *Viscosity of Silicate Melts.* Urbain, G., et al. pages 139-141, s.l. : Trans. Brit. Ceramic Society, 1981, Vol. 80.

4. K.G. Ridgeway, S. Dye, P. Mink, A. Gritzan. *Improved cleaning of waste gases and recycling of BOF dusts.* s.l. : European Commision, 2002. EUR20286.

5. *Zur Bildung des braunen Rauches.* H. Popper, K.H. Schmitz, K. Schwerdtfeger, D. Reinisch,. 17 pp.55-60, s.l. : Stahl u. Eisen , 1981, Vol. 101 .

6. *Chemische Zusammensetzung, Entstehungsmechanismus und Bildungsrate von Konverterstaub.* E. Schurmann, A. Ploch, H.D. Pflipsen, U. Herwig. pp. 55-61, s.l. : Stahl u. Eisen, 1995, Vol. 6.

7. *Direktreduktion von Huttenwerksstauben* . K. Sugasawa, Y.Yamada, Osaka, O. S. Watanabe, K. Kato, K. M. Masuda, Kashima, Y. Sato, T.Kawabata. 24 pp. 1239-1245, s.l. : Stahl u. Eisen , 1976, Vol. 96.

8. P. Derungs (ProfilABRED), J. M. Brouhon (CRM), G. Harp (BFI). *Briquetting of self-reducing blendings of waste iron oxides mixture.* s.l. : European Commission, 2002.

9. *Selective Zinc Removal from Electric Arc Furnace (EAF) Dust by Using Microwave Heating.* Mamdouh Omran, Timo Fabritius, Eetu-Pekka Heikkinen. 331-340, s.l. : Journal of Sustainable Metallurgy, 2019, Vol. 5.

10. *Chemical and Physical Characteristics Affecting the Reduction Kinetics of Iron Oxide Pellets with Solid Carbon.* Ajersch, Frank. 137-144, s.l. : Canadian Metallurgical Quarterly, 1987, Vol. 26.

11. *Kinetics of Reduction of Composite Pellets Containing Iron Ore and Carbon.* Roberto José De Carvalho, Pedro Gutemberg Quariguasi Netto &José Carlos D'abreu. 217-225, s.l. : Canadian Metallurgical Quarterly, 1994, Vol. 33.

12. A. Coletta, F. G. Carcedo, K. Linsley, T. Bürgler, B. Kohl. *Development of technologies for treatment of dust and sludges containing zinc and lead to improve their recycle and reuse.* s.l. : European Communities, 2001. EUR 19474 EN.

13. A. Colletta, G. Brascugli, H. H. Ballewski, A. Artioli, M. Bianchiferri. *High-purity zinc and ferroalloy recovery from EAF dusts through a combined pyro-metallurgical treatment.* s.l. : European Communities, 2002. EUR 20505 EN.

14. H. Tavernier, C. Grisvard, H. P. Jung, P. Drissen. *Foaming of the slag and recycling of stainless steel dusts by injection into the electric arc furnace for stainless steels.* s.l. : European Communities, 2004. EUR 20926 EN.

15. *Viscosity of slags.* Mudersbach, D., Drissen, P.. Kühn, M., Geiseler, J. 3, s.l. : steel research, 2001, Vol. 72.

16. K. J. Arlt, N. Wolsfeld, G. Endemann. *Innovative use of iron- and steelmaking by-products for the sealing and securing of steel industry deposits.* s.l. : European Communities, 2005. EUR 21361 .

17. S. Gries, J. Chevalier. *Characterisation, modelling and validation of the impact of the iron and steelmaking slags used in road construction on groundwater.* s.l. : European Commission, 2006 . EUR 21630 EN.

18. A. Cores, P. Drissen, M. Kuehn, H. P. Jung, J. Mernitz, F. Richter, N. Veneri. *Efficient utilisation of raw materials used in secondary steelmaking as flux in steelmaking furnaces.* s.l. : EUROPEAN COMMISSION, 2005. EUR 21343 EN.

19. *Slag – Metal equilibrium during stainless steel melting.* McCoy, C. W., Langenberg, F. C. s.l. : Journal of Metal, 1964.

20. D. Senk, O. Wiens, K. Mavrommatis, L. F. Sancho, O. Rivas,N. Androutsopoulos, C. Galvao, J. J. Laserna, D. Papamantellos, C. Palangas, G. Angelopoulos. *In-situ, quick sensing system for measurements of critical components in steelmaking slags (Inquisss).* s.l. : EUROPEAN COMMISSION, 2007. EUR 22818 EN.

21. M. Kühn, H. Spiegel, F. A. Lopez, M. Rex, R. Erdmann. *Sustainable agriculture using blast furnace and steel slags as liming agents.* s.l. : European Commission, 2006. EUR 22033 EN.

22. G. Harp, S. Möhring, C. Hillmann, W. Bsirske. *Alternative processing of sinter plant recycling materials.* s.l. : European Commision, 2007. EUR 22974 EN.

23. B. Korthas, J. Hunger, V. Pschebezin, J. Adam, G. Harp,S. Kallio, R. Hurme, J.-O. Wikström, P. Hahlin, S. Wiedner, L. Di Sante, I. Gelli. *Hearth protection in blast furnace operation by injection of TiO2 materials.* s.l. : European Commision, 2007. EUR 22821 EN.

24. *Effect of titania on the Characteristics of Blast Furnace.* K. Datta, P.K. Sen, S.S. Gupta, A. Chatterjee. p.232-238, s.l. : Steel Research, 1993, Vol. 64.

25. *The practice of ilmenite application in the BF, A technical and economical review.* J.T Chao, J. Cook, A.E Grau. s.l. : Ironmaking conference proceedings, 1989. pp383-393.

26. *Fundamentals of titanium-rich scaffold formation in the blast furnace hearth.* D. Bergsma, R.J. Fruehan. Baltimore, USA : 60th Ironmaking Conf. Proc., 2001. p. 297/312.

27. Di Sante, L., et al. *Hydrometallurgical continuous treatment of ZnO-enriched powders for metal zinc.* s.l. : European Commision, 2008. EUR 22989.

28. Hanrot, F., et al. *Short term CO2 mitigation for steelmaking SHOCOM.* s.l. : European Commision, 2011. EUR 24989 EN.

29. Pietruck, R., et al. *Alternate carbon sources for sintering of iron ore (ACASOS).* s.l. : Eurpean Commision, 2013. EUR 25151.

30. Stubbe, G., et al. *Energy and productivity optimised EAF stainless steel making by adjusted slag foaming and chemical energy supply (EPOSS).* s.l. : European Commision , 2013. EUR 25082.

31. Stubbe, G., et al. *Upgrading and utilisation of residual iron oxide materials for hot metal production.* s.l. : European Commission, 2013. EUR 25081.

32. Sundqvist-Ökvist, L., et al. *Flexible injection of alternative carbon material into the blast furnace (Flexinject).* s.l. : European Commission , 2013. EUR 25909.

33. Bianco, L., et al. *Sustainable EAF steel production (GREENEAF).* s.l. : European Commission, 2013. EUR 26208.

34. Chazarenc, F., et al. *Using slag as sorbent to remove phosphorus from wastewater (Slasorb).* s.l. : European Commission, 2014. EUR 26412.

35. Pietruck, R., et al. *Innovative carbon products for substituting coke on BF operation (INNOCARB).* s.l. : European Commission, 2015. EUR 27121.

36. Köchner, H., et al. *Increased yield and enhanced steel quality by improved deslagging and slag conditioning (OPTDESLAG).* s.l. : European Commission, 2015.

37. Larsson,, M., et al. *Processes and technologies for environmentally friendly recovery and treatment of scrap (PROTECT).* s.l. : European Commission, 2015. EUR 27201.

38. Algermissen, D., et al. *Impact of long-term application of blast furnace and steel slags as liming materials on soil fertility, crop yields and plant health (SLAGFERTILISER).* s.l. : European Commission, 2017. EUR 28447.

39. Colla, V., et al. *Efficient use of resources in steel plant through process integration (Reffiplant).* s.l. : European Commission, 2017. EUR 28457.

40. Algermissen, D., et al. *Control of slag quality for utilisation in the construction industry (SLACON).* s.l. : European Commission, 2017. EUR 28460.

41. Colla, V., et al. *Environmental impact evaluation and effective management of resources in the EAF steelmaking (EIRES).* s.l. : European Commission, 2017. EUR 28916.

42. Magnusson, M., et al. *Removal of Phosphorus from BOF-slag (PSP-BOF).* s.l. : European Commission, 2018. EUR 29532.

43. Castro Díaz, M., et al. *Developing Uses of Alternative Raw Materials in Cokemaking (ALTERAMA).* s.l. : European Commission, 2018. EUR 29524.

44. Cirilli, F., et al. *BIOCHAR FOR A SUSTAINABLE EAF STEEL PRODUCTION (GREENEAF2).* s.l. : European Commission, 2018. EUR 29517.

45. Alexis, J., et al. *Recycling of industrial and municipal waste as slag foaming agent in EAF (RIMFOAM).* s.l. : European Commission, 2021. EUR 30852.

46. *Synopsis of RFCS Projects 2017 – 2020.* s.l. : European Commission, 2020.

47. *ACTISLAG 2nd periodic report* . 2021.

48. Ehrenberg, A. . *ACTISLAG: New Activation routes for early strength development of granulated Blast Furnace Slag.* s.l. : FEhS Institute Report 1/2023, 2022.

49. *The thermal history of granulated blast furnace siag and its impact on reactivity.* Ehrenberg, A., et al. s.l. : ZKG Cement Lime Gypsum, 2020, Vol. 4.

50. *Glass structure of industrial ground granulated blast furnace slags (GGBS) investigated by time-resolved Raman and NMR spectroscopies.* Blotevogel, S., et al. s.l. : Ceramics, 2021, Vol. 56. 10.1007/s10853-021-06446-4.

51. *Ability of the R3 test to evaluate differences in early age reactivity of 16 industrial ground granulated blast furnace slags (GGBS).* Blotevogel, S., et al. s.l. : Cement and Concrete Research, 2020, Vol. 130. 10.1016/j.cemconres.2020.105998.

52. *Cooling history of a wet-granulated blast furnace slag (GBS).* Pronina, N., et al. s.l. : Journal of Non-Crystalline Solids, 2018, Vol. 499. 10.1016/j.jnoncrysol.2018.07.054.

53. *Rejuvenation of granulated blast furnace slag (GBS) glass by ball milling.* Romero Sarcos, N., et al. s.l. : Journal of Non-Crystalline Solids, 2021, Vol. 556. 10.1016/j.jnoncrysol.2020.120557 .

54. *Titanium in GGBS-like calcium-magnesium-aluminosilicate glasses: Its role in the glass network, dissolution at alkaline pH and surface layer formation.* Blotevogel, S., et al. s.l. : Journal of Non-Crystalline Solids, 2022, Vol. 591. 10.1016/j.jnoncrysol.2022.121708.

55. *Experimental evidence for the acceleration of slag hydration in blended cements by the addition of CaCl2.".* Steger, L., et al. s.l. : Cement and Concrete Research, 2021, Vol. 149. 10.1016/j.cemconres.2021.106558.

56. Commision, European. Fines2EAF. *Cement-free brick production technology for the use of primary and secondary raw material fines in EAF steelmaking.* [Online] 05 19, 2025. [Cited: 12 19, 2025.] https://ec.europa.eu/info/funding-tenders/opportunities/portal/screen/opportunities/projects-details/31061225/754197/RFCS?order=DESC&pageNumber=2&pageSize=100&sortBy=es_SortDate&frameworkProgramme=31061225.

57. *DEVELOPING A NEW PROCESS TO AGGLOMERATE SECONDARY RAW MATERIAL FINES FOR RECYCLING IN THE ELECTRIC ARC FURNACE – THE FINES2EAF PROJECT.* Echterhof, T., et al. s.l. : CLEAN TECH 4 - The 4th European Conference on Clean Technologies in the Steel Industry, 2018.

58. *Investigation on the Chemical and Thermal Behavior of Recycling Agglomerates from EAF by-Products.* Willms, T., et al. 8309, s.l. : Applied Sciences, 2020, Vol. 10.

59. *ECOSLAG 1st periodic report.*

60. *ECOSLAG 2nd periodic report.*

61. *Towards Greener Industry: Modelling of Slag Heat Recovery.* Safavi Nick, R., et al. 1144, s.l. : Metals, 2021, Vol. 11 (7). 10.3390/met11071144.

62. Commision, European. E-CO-LadleBrick. *Ecological and Economical waste management of the ladle refractory bricks by implementing circular economy criteria.* [Online] 05 28, 2025. [Cited: 12 18, 2025.]

https://ec.europa.eu/info/funding-tenders/opportunities/portal/screen/opportunities/projects-details/31061225/847249/RFCS?order=DESC&pageNumber=1&pageSize=100&sortBy=es_SortDate&frameworkProgramme=31061225.

63. *REMAINING USEFUL LIFE AND WEAR ESTIMATION OF THE REFRACTORY.* Arostegi, M. and Manjarrés, D. FRANKFURT, GERMANY : UNITECR 2023, 2023.

64. *SLAGReuS 1st periodic report.*

65. *SLAGReuS 2nd periodic report.*

66. *Multi-material injection system to foster circularity: Valorization of recycled polymers from waste plastics in electric arc furnace.* Bissoli, M., et al. 103497, s.l. : Thermal Science and Engineering Progress, 2025, Vol. 61.

67. Salimbeni, A., et al. *D1.1 – Report on residual biomass characterization, biomass slow pyrolysis and biocoal quality.* 2024.

68. Salimbeni, A. and Pezzati, N. *D1.2 – Report on chemical leaching process performances and obtained biocoal quality at pilot scale.* 2025.

69. KRUPP Edelstahlprofile GmbH, Det Danske Stalvalsevaerk A/S, Forschungsgemeinschaft Eisenhuttenschlacken. *Rec:ycling of zinc and lead containing dust from the electric arc furnace.* s.l. : Europea Commision, 22.01.1997. BRE2.CT92.0116.

70. *A new treatment process to recover magnetite, zinc and lead from iron and steel making dusts and sludges.* A. Delalio, Z. Bajger, P. Balaz, F. Castro. Bilbao : Steel Research & Development on Environmental Issues, 1999.

71. Economical, technical and ecological utilisation of treated steel slag in civil engineering of high quality demands. *CORDIS - EU research results.* [Online] September 1, 2025. [Cited: October 28, 2025.] https://cordis.europa.eu/project/id/BRPR970446.

72. Commision, European. CORDIS - EU research results. *A new metallurgical route for the on-line conversion of by-products into valuable mineral and metallic products with a reduction of co2 emissions.* [Online] January 18, 2010. [Cited: October 29, 2025.] https://cordis.europa.eu/article/id/85288-recycling-waste-from-steel-making.

73. *ZEWA – metallurgical process for treatment of residues from steel industry and other industrial sectors to generate valuable products.* A. Fleischanderl, U. Gennari, A. Ilie. 6, s.l. : Ironmaking and Steelmaking, 2004, Vol. 31. 10.1179/irs.2004.31.6.444.

74. *ZEWA (Zero waste) process: a new way for co-processing steel slag.* F.P. Sorrentino, M. Gimenez. Montreal : 12th ICCC, 2007.

75. *Rezin - new ways to recover zinc from EAF dust.* G. Ye, E. Burström, M. Maccagni, L. Bianco, H. Stripple. 501-509, s.l. : Scanmet, International Conference on Process Development in Iron and Steelmaking, 2004, Vol. 2.

76. *Elimination of zinc ferrite for hydrometallurgical recovery of zinc from EAF dust.* G. Ye, E. Burström, M. Maccagni, L. Bianco, and H. Stripple. pp. 397–411, s.l. : TMS Fall Extraction and Processing Division: Sohn International Symposium, 2006, Vol. 6.

77. FISSAC. *FOSTERING INDUSTRIAL SYMBIOSIS FOR A SUSTAINABLE RESOURCE INTENSIVE INDUSTRY ACROSS THE EXTENDED CONSTRUCTION VALUE CHAIN.* [Online] European Commission, 09 06, 2024. [Cited: 12 12, 2025.]

78. COmmision, European. Turning waste from steel industry into a valuable low cost feedstock for energy intensive industry. [Online] May 22, 2024. [Cited: 12 05, 2025.] https://cordis.europa.eu/project/id/642067/reporting.

79. *Slag as inventory material for Thermal Energy Storage (TES): Material investigation and thermo-mechanical consideration* . Kruger, M., et al. 454-463, s.l. : Energy Procedia, 2018, Vol. 155.

80. Commision, European. Production of sustainable, advanced bio-ethANOL through an innovative gas-fermentation process using exhaust gases emitted in the STEEL industry. [Online] 11 11, 2025. [Cited: 12 05, 2025.] https://cordis.europa.eu/project/id/656437/reporting.

81. CHROMIC. *effiCient mineral processing and Hydrometallurgical RecOvery of by-product Metals from low-grade metal contaIning seCondary raw materials.* [Online] European Commission, 08 16, 2021. [Cited: 12 23, 2025.] https://cordis.europa.eu/project/id/730471/reporting.

82. *Rebound effects following technological advancement? The case of a global shock in ferrochrome supply.* Buyle , M., et al. 10, s.l. : Journal of Cleaner Production, 2023, Vol. 391. 10.1016/j.jclepro.2023.136264.

83. *Multi-Analytical Characterization of Slags to Determine the Chromium Concentration for a Possible Re-Extraction.* Horckmans, L., et al. 646, s.l. : Minerals, 2019, Vol. 9(10). 10.3390/min9100646.

84. *Characterization of a Chromium-Bearing Carbon Steel Electric Arc Furnace Slag after Magnetic Separation to Determine the Potential for Iron and Chromium Recovery.* Bru , K., et al. 1, s.l. : Minerals, 2022, Vol. 12. 10.3390/min12010047.

85. *Up-Concentration of Chromium in Stainless Steel Slag and Ferrochromium Slags by Magnetic and Gravity Separation.* Kukurugya, F., Nielsen, P. and Horckmans, L. 906, s.l. : Minerals, 2020, Vol. 10 (10). 10.3390/min10100906.

86. *Preparation of Volborthite by a Facile Synthetic Chemical Solvent Extraction Method.* Sánchez-Loredo , M.G., et al. 1977, s.l. : Nanomaterials, 2023, Vol. 13(13). 10.3390/nano13131977.

87. *Recovery of Chromium from Slags Leachates by Electrocoagulation and Solid Product Characterization.* Pikna, L., et al. 1593, s.l. : Metals, 2020, Vol. 10(12). 10.3390/met10121593.

88. *Development of monodisperse porous microspheres of MgAl-layered double hydroxide by droplet coagulation.* Seftel, E.M., et al. 1, s.l. : Powder Technology , 2021, Vol. 391. j.powtec.2021.06.021.

89. FReSME. *From residual steel gasses to methanol.* [Online] European Commission, 09 06, 2024. [Cited: 12 12, 2025.] https://cordis.europa.eu/project/id/727504.

90. 100% recovery and RECYCLing of construction vehicle crAwler TRACKs into constituent rubber and steel for sustainable raw material supply. [Online] February 10, 2022. [Cited: November 18, 2025.] https://cordis.europa.eu/project/id/719038/reporting.

91. Commision, European. Carbon4PUR. *Turning industrial waste gases (mixed CO/CO2 streams) into intermediates for polyurethane plastics for rigid foams/building insulation and coatings.* [Online] 06 28, 2023. [Cited: 12 15, 2025.] https://cordis.europa.eu/project/id/768919.

92. —. TORERO. *TORrefying wood with Ethanol as a Renewable Output: large-scale demonstration.* [Online] 11 11, 2025. [Cited: 12 15, 2025.] https://cordis.europa.eu/project/id/745810.

93. POLYNSPIRE. *Demonstration of Innovative Technologies towards a more Efficient and Sustainable Plastic Recycling.* [Online] 12 18, 2023. [Cited: 12 16, 2025.] https://cordis.europa.eu/project/id/820665.

94. Commision, European. C2FUEL. *Carbon Captured Fuel and Energy Carriers for an Intensified Steel Off-Gases based Electricity Generation in a Smarter Industrial Ecosystem.* [Online] 09 01, 2025. [Cited: 12 15, 2025.] https://cordis.europa.eu/project/id/838014.

95. *Experimental investigation of a packed bed membrane reactor for the direct conversion of CO2 to dimethyl ether.* Poto, S., et al. 102513, s.l. : Journal of CO2 Utilization, 2023, Vol. 23.

96. RETROFEED. *Implementation of a smart RETROfitting framework in the process industry towards its operation with variable, biobased and circular FEEDstock.* [Online] European Commission, 09 01, 2025. [Cited: 11 07, 2025.] https://cordis.europa.eu/project/id/869939.

97. [Online] Coralis, 2020. https://www.coralis-h2020.eu/.

98. INITIATE. *Innovative industrial transformation of the steel and chemical industries of Europe.* [Online] European Commission, 09 15, 2025. [Cited: 12 10, 2025.] https://cordis.europa.eu/project/id/958318.

99. Commision, European. H2STEEL. *Green H2 and circular bio-coal from biowaste for cost-competitive sustainable Steel.* [Online] 11 11, 2025. [Cited: 12 11, 2025.] https://cordis.europa.eu/project/id/101070741.

100. *The production of biogenic carbon and green hydrogen through biomethane pyrolysis: the environmental benefits for the metallurgy sector.* Negro, V., Riorda, A. and Chiaramonti, D. 012009, s.l. : Journal of Physics: Conference Series, 2024, Vol. 2893.

101. *Sustainable Hydrogen from Biomass: What Is Its Potential Contribution to the European Defossilization Targets?* Riorda, A., et al. 6412−6425, s.l. : Energy Fuels, 2025, Vol. 39.

102. HEPHAESTUS. *Heavy and Extractive industry wastes PHAsing out through ESG Tailings Upcycling Synergy.* [Online] European Commission, 03 11, 2025. [Cited: 12 07, 2025.] https://cordis.europa.eu/project/id/101058696.

103. Commision, European. RecHycle. *Recycling renewable hydrogen for climate neutrality.* [Online] 07 28, 2022. [Cited: 12 11, 2025.] https://cordis.europa.eu/project/id/101058692.

104. ReMFra. *REcovering Metals and Mineral FRAction from steelmaking residues.* [Online] European Commission, 01 16, 2026. [Cited: 01 19, 2026.] https://cordis.europa.eu/project/id/101058362/it.

105. *ReMFra: REcovering Metals and Mineral FRAction from steelmaking residues.* Doschek-Held, K. and Wolfgang, R. s.l. : Chair of Thermal Processing Technology, 2024. 580.

106. *Towards the Circularity of the EU Steel Industry: Modern Technologies for the Recycling of the Dusts and Recovery of Resources.* Simoni , M., et al. 233, s.l. : Metals, 2024, Vol. 14. 10.3390/met14020233.

107. *ReMFra – possibilities for residues from steel plants.* Reiter, W. and Simoni , M. s.l. : ESTEP 2023 annual event: -a-circular-economy-driven-by-the-european-steel, 2023.

108. Commision, European. Carbon4Minerals. *Transforming CO2 into added-value construction products.* [Online] 09 01, 2025. [Cited: 12 15, 2025.] https://cordis.europa.eu/project/id/101091870.

109. GreenHeatEAF. *Gradual integration of REnewable non-fossil ENergy sources and modular HEATing technologies in EAF for progressive CO2 decrease.* [Online] 11 03, 2025. [Cited: 12 16, 2025.] https://cordis.europa.eu/project/id/101092328/it.

110. Unlocking the potential of second life steel fibers from tire waste for the construction industry. [Online] November 3, 2025. [Cited: November 18, 2025.] https://cordis.europa.eu/project/id/190109136.

111. FlexoFibers. [Online] 2025. [Cited: 11 19, 2025.] https://flexofibers.com/.

112. RESURGENCE. *INDUSTRIAL WATER CIRCULARITY: REUSE, RESOURCE RECOVERY AND ENERGY EFFICIENCY FOR GREENER DIGITISED EU PROCESSES.* [Online] European Commission, 07 30, 2025. [Cited: 12 12, 2025.] https://cordis.europa.eu/project/id/101138097.

113. Commision, European. Dust2Value. *Pioneering Sustainable Recovery in Steelmaking: Hydrogen-Based Technology for Byproduct Management.* [Online] 09 01, 2025. [Cited: 12 12, 2025.] https://cordis.europa.eu/project/id/101138742.

114. *Impact of temperature and gas composition on hydrogen-based zinc recovery from electric arc furnace dust.* Leuchtenmüller, M. and Keuschnig, A. 434–439, s.l. : International Journal of Hydrogen Energy, 2025, Vol. 130.

115. H2PlasmaRed. *Hydrogen Plasma Reduction for Steelmaking and Circular Economy.* [Online] European Commission, 10 28, 2025. [Cited: 12 12, 2025.] https://cordis.europa.eu/project/id/101138228/reporting.

116. Commision, European. HURRICANE. *Sector-coupling hub for circular use of thermal and industrial waste.* [Online] 08 12, 2025. [Cited: 12 17, 2025.] https://cordis.europa.eu/project/id/101138494.

117. COmmision, European. ZHYRON. *Valorisation of iron-rich & Zinc-containing steelmaking by-products via HYdrogen-based ReductiON.* [Online] 08 11, 2025. [Cited: 12 23, 2025.] https://cordis.europa.eu/project/id/101138276.

118. Koolen, D. and Vidovic, D. *Greenhouse gas intensities of the Eu steel industry and its trading partners.* Luxembourg : Publications Offica of the European Union, 2022.

119. *Open-loop step responses for the MEA post-combustion capture process: Experimental results from the Esbjerg pilot plant.* Faber, R., et al. 1427-1434, s.l. : Energy Procedia, 2011, Vol. 4.

120. *Kinetics of carbon dioxide absorption and desorption in aqueous alkanolamine solutions using a novel hemispherical contactor-II: Experimental results and parameter estimation.* Jamal, A. 6590-6603, s.l. : Chemical Engineering Science, 2006, Vol. 61.

121. CESAREF: Concerted European action on Sustainable Applications of REFractories. [Online] [Cited: 11 6, 2025.] https://www.cesaref.eu/.

122. *Overview on LCA: Challenges and Opportunities for the Refractory Industry.* J. V. Menezes Cunha, E. Pirad, T. Drnek. Francfurt : Unified International Technical Conference on Refractories , 2023.

123. *Prospective LCA on the Design of New Refractories for a Greener Steelmaking Process.* S. Badioli, T. Champion, L. Roumiguier, M. Dargaud, A. Leonard. Dublin : SETAC Europe 33rd Annual Meeting, 2023.

124. *The Choice of Refractories for Steel Ladle Lining: a Life Cycle Perspective.* Md Jubayed, R. Siebring, A. Léonard. Dublin : SETAC Europe 33rd annual meeting, 2023.

125. *The Choice of Magnesia-Carbon Refractories for Steel Ladle Lining: a Life Cycle Perspective.* Md Jubayed, R. Siebring, A. Léonard. Lille : LCM2023: The11th International Conference on Life Cycle Management, 2023.

126. *New approach of recycling vanadium-bearing slags as a binder in high-alumina refractory castables application.* M. Derensy, T. Zanin, J.F. Bleck, T. Tonnesen, J. Gonzalez-Julian. e10242, s.l. : International Journal of Ceramic Engineering Science, 2025, Vol. 7.

127. *Yield criteria for quasibrittle and frictional materials.* D. Bigoni, A. Piccolroaz. pp. 2855-2878, s.l. : International Journal of Solids and Structures, 2004, Vol. 41.

128. *Insights on numerical models to predict potential recyclability of spent refractories from steel making industry.* A. Salerno, M. Piciccoa, L. Rebouillatc, N. Tessier-Doyenb, E. Thuneb, S. Romero Baiviera, M. Hugerb. Francfurt : Unified International Technical Conference on Refractories 2023 (UNITECR 2023), 2023.

129. *Microstructure Design of a More Sustainable Alumina-Spinel Refractory Castable.* K. A. Boateng, J.M. Auvray, C. Wöhrmeyer, N. Tessier-Doyen, E. Thune, M. Huger. Francfurt : Unified International Technical Conference on Refractories 2023 (UNITECR 2023), 2023.

130. *Influence of tabular and white fused alumina aggregates on Young'smodulus evolution versus temperature in refractory castables.* K.A. Boateng, R. P. Kaczmarek, J.-M. Auvray, C. Wohrmeyer, E. Thune, N. Tessier-Doyen, M. Huger. 117583, s.l. : Journal of the European Ceramic Society, 2025, Vol. 45.

131. *Discrete element modeling deepens understanding of microcracking phenomena in refractory materials.* H. Ranganathan, D. André, M. Huger, R. Soth, C. Wöhrmeyer. 2, s.l. : American Ceramic Society Bulletin, 2024, Vol. 103.

132. *A multiscale discrete element thermomechanical modeling approach of microcracking generated at high temperature by anisotropic thermal expansion in an elastic brittle polycrystalline ceramic material.* H.

Ranganathan, D. André, M. Mouiya, M. Huger, R. Soth, C. Wöhrmeyer. 111088, s.l. : Engineering Fracture Mechanics, 2025, Vol. 320.

133. *Hydrogen's influence on microstructure and Young's modulus evolution in a phosphate bonded alumina refractory.* C. D. Bohorquez, D. Gruber , K. Klima. 54862–54872, s.l. : Ceramics International, 2025, Vol. 51.

134. *Hydrogen-resistant refractories for direct reduced iron production.* M. R. Gomes, A. Ducastel, L. Konrad, T. Janssen, E. E. Ospino. Düsseldorf : METEC & 6th ESTAD, 2023.

135. *Roadmap for recycling practices and resource utilization in the.* Kieush, L., et al. 503, s.l. : Matériaux & Techniques, 2024, Vol. 112. 10.1051/mattech/2024026.

136. Association, Worldsteel. *Steel industry co-products.* 2021. https://worldsteel.org/wp-content/uploads/Fact-sheet-Steel-industry-co-products.pdf.